

**PhD Thesis**

**TOWARDS HIGHLY EFFICIENT LIGANDS  
FOR ASYMMETRIC HYDROGENATIONS: A  
COVALENT MODULAR APPROACH AND  
INVESTIGATIONS INTO BIO-INSPIRED  
SUPRAMOLECULAR STRATEGIES**

**Héctor Fernández Pérez**

**Supervised by Dr. Anton Vidal i Ferran  
(ICIQ-Universitat Rovira i Virgili)**

**Tarragona  
September 2009**



UNIVERSITAT ROVIRA I VIRGILI

UNIVERSITAT ROVIRA I VIRGLI

TOWARDS HIGHLY EFFICIENT LIGANDS FOR ASYMMETRIC HYDROGENATIONS: A COVALENT MODULAR APPROACH AND  
INVESTIGATIONS INTO BIOINSPIRED SUPRAMOLECULAR STRATEGIES

Héctor Fernández Pérez

ISBN:978-84-693-3385-3 /DL:T.994-2010

Dr. ANTON VIDAL i FERRAN, Group Leader in the Institute of Chemical Research of Catalonia (ICIQ) and Research Professor of the Catalan Institution for Research and Advanced Studies (ICREA),

CERTIFIED:

That the present research work entitled “Towards Highly Efficient Ligands for Asymmetric Hydrogenations: A Covalent Modular Approach and Investigations into Bio-Inspired Supramolecular Strategies” that Héctor Fernández Pérez presents to obtain the PhD degree in Chemistry, has been carried out under his supervision in the corresponding research group of the ICIQ.

Tarragona, September 2009

Dr. Anton Vidal i Ferran



UNIVERSITAT ROVIRA I VIRGILI

UNIVERSITAT ROVIRA I VIRGLI

TOWARDS HIGHLY EFFICIENT LIGANDS FOR ASYMMETRIC HYDROGENATIONS: A COVALENT MODULAR APPROACH AND INVESTIGATIONS INTO BIOINSPIRED SUPRAMOLECULAR STRATEGIES

Héctor Fernández Pérez

ISBN:978-84-693-3385-3 /DL:T.994-2010

*“La vida (Tesis) es aquello que te va sucediendo  
mientras tu te empeñas en hacer otros planes”*

*(John Winston Lennon)*

UNIVERSITAT ROVIRA I VIRGLI

TOWARDS HIGHLY EFFICIENT LIGANDS FOR ASYMMETRIC HYDROGENATIONS: A COVALENT MODULAR APPROACH AND  
INVESTIGATIONS INTO BIOINSPIRED SUPRAMOLECULAR STRATEGIES

Héctor Fernández Pérez

ISBN:978-84-693-3385-3 /DL:T.994-2010

*A mis padres, a mis hermanas  
y a M<sup>a</sup> Ángeles*

UNIVERSITAT ROVIRA I VIRGLI

TOWARDS HIGHLY EFFICIENT LIGANDS FOR ASYMMETRIC HYDROGENATIONS: A COVALENT MODULAR APPROACH AND  
INVESTIGATIONS INTO BIOINSPIRED SUPRAMOLECULAR STRATEGIES

Héctor Fernández Pérez

ISBN:978-84-693-3385-3 /DL:T.994-2010



Todas aquellas sensaciones que rodean el desarrollo de una Tesis Doctoral son muy difíciles de explicar en tan pocas palabras, pero si echo la vista para atrás, algo más de cuatro años (como pasa el tiempo!!) y veo el resultado final, creo que sin lugar a dudas puedo decir que mereció la pena, no sólo por todo aquello que he aprendido sino por la gente que me ha rodeado, unos más cerca y otros más lejos, y que han contribuido a que finalmente el sueño se hiciera realidad y a los que deseo expresar mi más sincero agradecimiento.

En primer lugar, deseo expresar mi agradecimiento a mi director de Tesis Dr. Anton Vidal i Ferran por la oportunidad que me ha brindado y su dedicación a lo largo del desarrollo de esta Tesis Doctoral. Gracias por tus consejos, tú apoyo y todo lo que he aprendido a tu lado, pero también por los buenos ratos que hemos pasado a lo largo de los duros momentos que supone la realización de la misma.

También, quería agradecer a todos los compañeros del laboratorio de los “*Vidalines*”, tanto de los actuales como de los que estuvieron. El buen ambiente hace más llevadera la ardua tarea que supone la investigación, de verdad muchas gracias a cada uno de vosotros, sobre todo a los iniciales que me acogieron de una manera excelente e hicieron menos duro todo aquello que supone alejarte de tu casa y tu familia.

No quisiera tampoco olvidarme de todas aquellas personas que he conocido en ICIQ, los “*Ballesteres*”, los “*Pericases*”, así como todas aquellas personas que forman parte del Área de Soporte a la Investigación (RMN, masas, rayos-X, síntesis en paralelo, etc...), gracias por vuestro granito de arena en esta Tesis Doctoral.

Finalmente, y de una manera muy especial, no puedo dejar la oportunidad de agradecer a mi familia todo el apoyo y fortaleza que me han dado a lo largo de este periodo. Muy especialmente a mis padres, a los que les debo lo que soy, gracias por enseñarme que todo esfuerzo tiene su recompensa, y este trabajo es

un claro ejemplo de ello. Como no, acordarme de mis hermanas, que a pesar de la distancia que nos separaba, siempre os he sentido muy cerca y habéis sido un buen ejemplo para mí.

De una manera muy especial, quiero agradecerle este trabajo a M<sup>a</sup> Ángeles, sin ti nada de esto hubiera sido posible, gracias por todos tus consejos, tus ánimos, por estar ahí en todos los momentos y fundamentalmente porque conocerte es lo mejor que me ha podido pasar en la vida, gracias de todo corazón.

Por último, el trabajo desarrollado en esta tesis doctoral ha sido posible gracias a la financiación de L'Institut Català d'Investigació Química (ICIQ), la Fundación Ramón Areces de una manera muy especial (por la concesión de una beca pre-doctoral), el Ministerio de Educación y Ciencia, la Agencia de Gestió d'Ajuts Universitaris y de Recerca (AGAUR) y se ha desarrollado en el marco de los proyectos CTQ2005-02193/BQU, CTQ2008-00950/BQU, *INTECAT* (CSD2006-0003) perteneciente al Programa Consolider Ingenio 2010 (CSD2006-0003), DURSI (Grant. No. 2005SGR225).



UNIVERSITAT ROVIRA I VIRGLI

TOWARDS HIGHLY EFFICIENT LIGANDS FOR ASYMMETRIC HYDROGENATIONS: A COVALENT MODULAR APPROACH AND  
INVESTIGATIONS INTO BIOINSPIRED SUPRAMOLECULAR STRATEGIES

Héctor Fernández Pérez

ISBN:978-84-693-3385-3 /DL:T.994-2010

## **CONTENTS**

UNIVERSITAT ROVIRA I VIRGLI

TOWARDS HIGHLY EFFICIENT LIGANDS FOR ASYMMETRIC HYDROGENATIONS: A COVALENT MODULAR APPROACH AND  
INVESTIGATIONS INTO BIOINSPIRED SUPRAMOLECULAR STRATEGIES

Héctor Fernández Pérez

ISBN:978-84-693-3385-3 /DL:T.994-2010

## CONTENTS

<b>INTRODUCTION</b> .....	1
<b>CHAPTER 1: MODULAR COVALENT APPROACH TO ASYMMETRIC CATALYSIS</b> .....	21
<b>LITERATURE PRECEDENT</b> .....	23
1.1 Literature Precedents.....	25
1.1.1 Phosphino alcohol ligands.....	27
1.1.2 Phosphino-Phosphinite ligands.....	32
1.1.3 Phosphine-Phosphite ligands.....	42
<b>RESULTS AND DISCUSSION</b> .....	63
1.2 Results and discussion.....	65
1.2.1 Design and structural optimization of ligands for efficient asymmetric catalysts.....	65
1.2.2 Ring-opening of epoxides with trivalent phosphorus nucleophiles.....	67
1.2.2.1 Ring-opening of unfunctionalized epoxides with phosphorus nucleophiles.....	73
1.2.3 <i>O</i> -Phosphorylation of phosphino alcohols with P(III) electrophiles.....	76
1.2.3.1 Immobilization of <i>P-OP</i> ligands onto solid support.....	83
1.2.4 Studies on the complexation of <i>P-O</i> and <i>P-OP</i> derivatives with Rhodium precursors.....	85
1.2.4.1 Complexation of hemilabile <i>P-O</i> ligands.....	85
1.2.4.2 Preparation and characterization of selected Rhodium(I) complexes with <i>P-OP</i> ligands.....	93
1.2.4.3 <sup>31</sup> P{ <sup>1</sup> H}-NMR titrations of enantiomerically pure <i>P-OP</i> ligands with Rhodium precursor.....	98
1.2.5 Catalytic studies of <i>P-OH</i> and <i>P-OP</i> ligands in Rhodium- catalyzed asymmetric hydrogenation.....	106

1.2.5.1 Evaluating the catalytic performance of Rhodium complexes of <i>P-OH</i> ligands in the asymmetric hydrogenation of functionalized alkenes.....	106
1.2.5.2 Evaluating the catalytic performance of Rhodium complexes of phosphine-phosphinite ligands in the asymmetric hydrogenation of functionalized alkenes.....	108
1.2.5.3 Evaluating the catalytic performance of Rhodium complexes of phosphine-phosphite ligands in the asymmetric hydrogenation of functionalized alkenes.....	116
1.2.6. Scope of phosphine-phosphite ligand <b>125k</b> in the Rhodium-catalyzed asymmetric hydrogenation of alkenes.....	134
1.2.6.1 Preparation of various structurally diverse functionalized alkenes.....	135
1.2.6.2 Substrate scope of phosphine-phosphite ligand <b>125k</b> in Rhodium-catalyzed asymmetric hydrogenations.....	141
1.2.7. Optimization of the reaction conditions for asymmetric hydrogenation of alkenes using the catalytic system derived from [Rh( <b>125k</b> )(nbd)]BF <sub>4</sub> .....	152
1.2.7.1 Studying the effects of hydrogen pressure with Z-MAC and MAA as substrates.....	152
1.2.7.2 Studying the catalytic activity of the system derived from the “lead” ligand using Z-MAC as substrate.....	153
1.2.8 Rationalization of the stereochemical outcome of hydrogenation reaction using “lead” <i>P-OP</i> ligand derived from ( <i>S</i> )-BINOL.....	156
EXPERIMENTAL PROCEDURE.....	167
1.3 Experimental Procedure.....	169
1.3.1 General remarks.....	169
1.3.2. General synthetic procedure of protected epoxides <b>113a-e</b> and <b>137</b> .....	170

1.3.2.1. Synthetic procedure of compounds <b>113a-d</b> .....	170
1.3.2.2. Synthetic procedure of (2 <i>S</i> ,3 <i>S</i> )-2-Phenyl-3-(trityloxymethyl)oxirane <b>113e</b> .....	171
1.3.2.3. Synthetic procedure of Trimethyl(3-(((2 <i>S</i> ,3 <i>S</i> )-3-phenyloxirane-2-yl)methoxy)prop-1-ynyl)silane <b>136</b> .....	171
1.3.3. General synthetic procedure of phosphine-borane adducts <b>118a-f</b> and <b>137</b> .....	172
1.3.3.1. Synthesis and general physical and spectroscopic data of phosphine-borane adducts <b>118a-e</b> and <b>137</b> .....	173
1.3.4. General synthetic procedure of phosphine-phosphinite ligands <b>124a-d</b> .....	179
1.3.4.1. Synthesis and general physical and spectroscopic data of phosphine-phosphinite ligands <b>124a-d</b> .....	179
1.3.5. General synthetic procedure of phosphine-phosphite ligands <b>125a-k</b> .....	183
1.3.5.1. Synthesis and general physical and spectroscopic data of phosphine-phosphite ligands <b>125a-k</b> .....	184
1.3.6. General synthetic procedure for the preparation of [Rh(P-OH)(nbd)]BF <sub>4</sub> complexes <b>138a</b> and <b>138e</b> .....	195
1.3.6.1. Synthesis and general physical and spectroscopic data of [Rh(P-OH)(nbd)]BF <sub>4</sub> complexes <b>138a</b> and <b>138e</b> .....	195
1.3.7. General synthetic procedure for the preparation of [Rh(P-OP)(nbd)]BF <sub>4</sub> complexes <b>141c</b> , <b>142a</b> , <b>142h</b> , <b>142k</b> and <b>143</b> .....	197
1.3.7.1 Synthesis and general physical and spectroscopic data of [Rh(P-OP)(nbd)]BF <sub>4</sub> complexes <b>141c</b> , <b>142a</b> , <b>142h</b> , <b>142k</b> and <b>143</b> .....	197
1.3.8. General synthetic procedure of substrates <b>32b</b> and <b>144c-y</b> ....	203
1.3.8.1. Synthesis and general spectroscopic data of substrate <b>32b</b> .....	203
1.3.8.2. Synthesis and general spectroscopic data of substrates <b>144c-g</b> .....	203

1.3.8.3. Synthesis and general spectroscopic data of substrates <b>144h-i</b> .....	206
1.3.8.4. Synthesis and general spectroscopic data of compound <b>151</b> .....	207
1.3.8.5. Synthesis and general spectroscopic data of substrates <b>144j-m</b> .....	208
1.3.8.6. Synthesis and general spectroscopic data of substrates <b>144n-o</b> .....	211
1.3.8.7. Synthesis and general spectroscopic data of substrate <b>144p</b> .....	212
1.3.8.8. Synthesis and general spectroscopic data of substrate <b>144s</b> .....	213
1.3.8.9. Synthesis and general spectroscopic data of substrate <b>144t</b> .....	214
1.3.8.10. Synthesis and general spectroscopic data of substrate <b>144u-w</b> .....	214
1.3.8.11. Synthesis and general spectroscopic data of substrate <b>144x</b> .....	216
1.3.8.12. Synthesis and general spectroscopic data of substrate <b>144y</b> .....	216
1.3.9 General procedure for the Rh-mediated asymmetric hydrogenation.....	217
1.3.9.1. Spectroscopic data and determination of enantiomeric excess of hydrogenated products.....	218
1.3.9.2. Determination of absolute configurations of hydrogenated products.....	224



<b>CHAPTER 2: PRELIMINARY INVESTIGATIONS INTO BIO-INSPIRED SUPRAMOLECULAR STRATEGIES FOR ASYMMETRIC CATALYSIS.....</b>	<b>227</b>
LITERATURE PRECEDENT.....	229
2.1 Literature Precedent.....	231
RESULTS AND DISCUSSION.....	243
2.2 Synthesis of crown ether diphosphine ligands with potential for allosteric modulation of catalytic activity.....	245
2.2.1. Synthesis of ( <i>rac</i> )-(6,6'-bis(methoxymethoxy)biphenyl-2,2'-diyl)bis(diphenylphosphine oxide) ( <b>191</b> ).....	246
2.2.2. Optical resolution of ( <i>rac</i> )-(6,6'-bis(methoxymethoxy)biphenyl-2,2'-diyl)bis(diphenylphosphine oxide) ( <b>191</b> ).....	250
2.2.3. Preparation of the crown ether-containing diphosphine ( <b>194</b> ).....	253
2.2.4. Future outlook.....	259
EXPERIMENTAL PROCEDURE.....	261
2.3 Experimental Procedure.....	263
2.3.1. General remarks.....	263
2.3.2. Experimental procedures and characterization.....	264
2.3.2.1. Synthesis and general physical and spectroscopic data of the intermediates in the synthesis of <i>rac</i> -(6,6'-bis(methoxymethoxy)biphenyl-2,2'-diyl)bis(diphenylphosphine oxide) ( <i>rac</i> )- <b>191</b> .....	264
2.3.2.2. Experimental procedure for the optical resolution of ( <i>rac</i> )-(6,6'-bis(methoxymethoxy)biphenyl-2,2'-diyl)bis(diphenylphosphine oxide) <b>191</b> .....	269
2.3.2.3. Synthesis and general physical and spectroscopic data of the intermediates in the synthesis of enantiomerically enriched biaryl diphosphine ligands <b>194</b> .....	270

<b>CONCLUSIONS</b> .....	275
<b>APPENDIX: SELECTION OF NMR SPECTRA AND X-RAY STRUCTURES</b> .....	279
I. Selected NMR spectra.....	281
II. X-Ray structure for <b>118e</b> .....	305
III. X-Ray structure for <b>118f</b> .....	313
IV. X-Ray structure for <b>142a</b> .....	318
V. X-Ray structure for <b>142h</b> .....	330
VI. X-Ray structure for the optical resolution of <b>191</b> .....	342
VII. X-Ray structure for ( <i>R</i> )- <b>191</b> .....	351
<b>ABBREVIATIONS</b>	

UNIVERSITAT ROVIRA I VIRGLI

TOWARDS HIGHLY EFFICIENT LIGANDS FOR ASYMMETRIC HYDROGENATIONS: A COVALENT MODULAR APPROACH AND  
INVESTIGATIONS INTO BIOINSPIRED SUPRAMOLECULAR STRATEGIES

Héctor Fernández Pérez

ISBN:978-84-693-3385-3 /DL:T.994-2010

## **INTRODUCTION**

UNIVERSITAT ROVIRA I VIRGLI

TOWARDS HIGHLY EFFICIENT LIGANDS FOR ASYMMETRIC HYDROGENATIONS: A COVALENT MODULAR APPROACH AND INVESTIGATIONS INTO BIOINSPIRED SUPRAMOLECULAR STRATEGIES

Héctor Fernández Pérez

ISBN:978-84-693-3385-3 /DL:T.994-2010

## INTRODUCTION

Only a few examples of enantioselective catalytic reactions were known in the literature up to 1968, apart from enzymatic processes. Industrial demand for enantiomerically pure compounds, chiefly, APIs (active pharmaceutical ingredients), as well as agrochemicals, flavours and fragrances, has led to massive research efforts in enantioselective synthesis.<sup>1</sup> Asymmetric catalysis is fundamental to enantioselective synthesis, since a chiral catalyst can be used to selectively promote the conversion of a prochiral substrate into the desired enantiomer<sup>2</sup> (Figure 1).

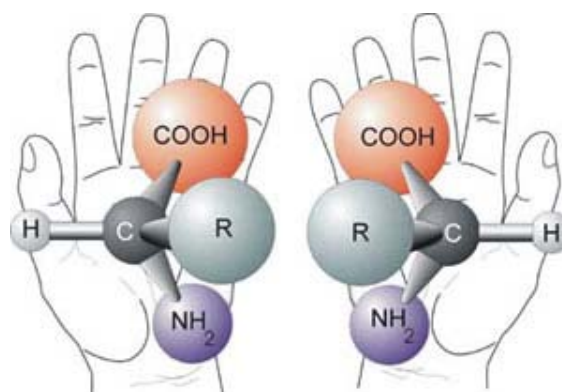


**Figure 1.** *L* and *D* enantiomers of an amino acid.<sup>3</sup>

Historically, enantiomerically pure compounds have been synthesized by four methods: the “chiral pool” approach;<sup>1</sup> the “chiral auxiliary” approach;<sup>1</sup> chiral separation of a racemic mixture;<sup>1</sup> and enzymatic methods.<sup>1</sup>

The “chiral pool” approach entails transformation of an inexpensive, readily available enantiomerically pure precursor, often derived from nature’s chiral pool, into a target molecule via well-established chemistry. Obviously, this strategy can only be applied if suitable starting materials are available.

<sup>1</sup> *Chirotechnology: Industrial Synthesis of Optically Active Compounds*; Sheldon, R. A., Ed.; Marcel Dekker: New York, 1993.

<sup>2</sup> Enantiomer: a stereoisomer that can not be superimposed on its mirror image.

<sup>3</sup> This image was borrowed from the website [www.catalysis-ed.org.uk](http://www.catalysis-ed.org.uk)

The “chiral auxiliary” approach is based on covalently bonding a chiral unit (auxiliary) to a substrate. The auxiliary, which is not contained in the final molecule, is responsible for stereodirecting the formation of one or more stereogenic centres in the product: its subsequent elimination gives the desired final product. The major drawback of using this approach in a synthesis is that it adds two<sup>4</sup> steps: introduction and removal of the chiral auxiliary.

Chiral separation of racemic mixtures is widely used. It is generally performed by one of the three following methods: direct preferential crystallization of one enantiomer, crystallization of diastereomeric derivatives, or kinetic resolution.

Conglomerates, racemates that comprise a mechanical mixture of two pure enantiomers, can be separated via preferential crystallization (*e.g.* by seeding with crystals of the desired enantiomer). Unfortunately, this technique is limited by the fact that less than 10% of all racemates are conglomerates. Most racemates are homogeneous solids comprising two enantiomers that coexist in the same unit cell. These enantiomers cannot be separated by preferential crystallization, and therefore, must be resolved by formation of diastereoisomers.

Racemic compounds can be derivatized with optically pure reagents to form pairs of diastereomers that can be separated by conventional techniques in organic chemistry (*e.g.* crystallization or chromatography). Given the simplicity of preparing diastereomeric salts using acids or bases, and the ease of cleaving them into the starting substrates, these salts are generally preferred to covalent diastereoisomers for resolving racemic mixtures.

Kinetic resolution is based on the fact that two enantiomers might react with the same enantiomerically pure reagent at different rates, and therefore, one of the components is more readily transformed than the other. Ideally, one enantiomer would be reactive, and the other one, inactive. In this case, the product formed by reaction of the reactive enantiomer can be separated from the

---

<sup>4</sup> In many cases the chiral auxiliary is degraded during cleavage, and consequently, must be chemically transformed before being reused.

remaining starting enantiomers by conventional techniques (*e.g.* crystallization or chromatography).

The highest theoretical yield for the desired enantiomer using any of these three techniques is only 50%. The remaining material must be either discarded or reconverted into the racemate, which is often not trivial.

Enzymatic methods for preparing chiral products exploit the natural activity of enzymes as asymmetric catalysts. Although enzymes offer relatively high enantioselectivities, they are currently limited to a narrow range of substrates and chemical transformations.<sup>1</sup>

Asymmetric (enantioselective) catalysis, in which each molecule of a chiral catalyst, by virtue of being continually regenerated, enables production of several molecules of a chiral target, is advantageous to the four methods described above. Apart from obviously offering higher economy for the chiral component, it does not require that this component be covalently attached to the substrate. Although asymmetric catalysts do not generally afford enantiomeric excesses as high as those obtained by enzymatic methods, synthetic catalysts have expanded this chemistry to encompass an ever-growing scope of substrates and chemical transformations. In fact, in the past 30 years, enantioselective catalysts have been developed for nearly every chemical transformation imaginable, enabling major breakthroughs in almost every one.<sup>5</sup>

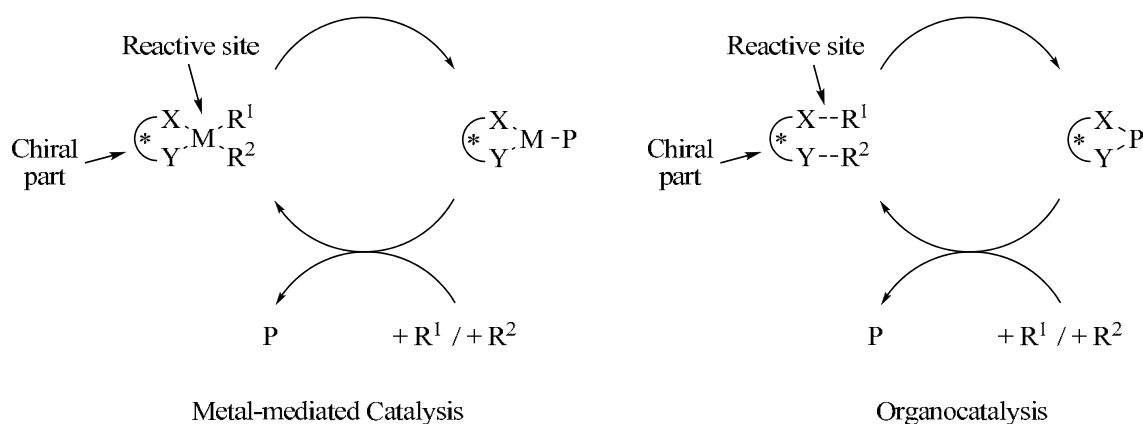
The key step in most catalytic asymmetric processes involves the assembly at the supramolecular level of the substrate and reagent(s), usually around a chiral organometallic complex (in ligand-accelerated catalysis)<sup>5</sup>, or around an enantiopure molecule (in organocatalysis)<sup>6</sup>. As in every supramolecular process, non-covalent interactions are responsible for the reversible assembly of the substrates and reagents around the chiral catalysts. In these catalytic systems, the chiral agent (organometallic complex or organic molecule) provides a low energy

---

<sup>5</sup> (a) *Asymmetric Catalysis in Organic Synthesis*; Noyori, R., Ed.; Wiley: New York, 1994. (b) *Comprehensive Asymmetric Catalysis*; Jacobsen, E. N., Pfaltz, A., Yamamoto, H. Eds.; Springer: Berlin, Germany, 1999; Vol 1-3. (c) *Catalytic Asymmetric Synthesis*; Ojima, I., Ed.; Wiley-VCH: New York, 2000.

<sup>6</sup> *Asymmetric Organocatalysis*; Berkessel, A., Gröger, H., Eds.; Wiley-VCH: Weinheim, 2005.

reaction pathway to the products. Furthermore, this agent is responsible for enantioselection, as it creates an asymmetric or disymmetric environment around the active site, ultimately enabling preferential recognition of an enantiotopic atom, group or face of the substrate. The nature and strength of the binding forces by which the reagents assemble around the catalyst are highly dependent on the nature of the catalyst (*i.e.* organometallic complex or chiral molecule), the chemical transformation and the mechanism of stereinduction. Metal-mediated and organocatalyzed asymmetric catalysis are illustrated in Scheme 1. Both cases encompass assembly of the reactant(s) around the chiral catalyst; the catalytic event with formation of the corresponding product(s); and finally, regeneration of the catalytic species, which then re-enter the catalytic cycle.



**Scheme 1.** Chiral catalysis via organometallic (left) and organic (right) chiral agents. X, Y: Binding groups; R<sup>1</sup>, R<sup>2</sup>: Reagents; P: Product.

Advances in asymmetric catalysts have led to the use of numerous chiral ligands—incorporating every conceivable type of molecular chirality—in almost every synthetic transformation amenable to catalysis. We believe that the remarkable progress in this field is down to two factors. First and foremost, the use of ligands derived from enantiopure non-natural starting materials has broadened the structural diversity of available catalysts. Secondly, the *modularity* of these ligands has facilitated their rapid and systematic optimization. Highly



efficient and enantioselective catalysis of asymmetric reactions demands fine-tuning of the catalyst to achieve a perfect match among ligand, metal ion (if present) and substrate(s): by using a modular catalyst design, the structural features responsible for improving asymmetric induction (the stereoelectronics of the molecular fragments) can be adjusted as needed.

The *Big Bang* of asymmetric catalysis occurred in 1968 with the development of the first asymmetric hydrogenations,<sup>7</sup> using enantiopure monophosphines. The field has grown considerably since then, and asymmetric hydrogenation is now standard issue in the synthetic chemist's toolbox. This transformation enables efficient catalytic reduction of prochiral alkenes, ketones and imines by dihydrogen, generating new CH-C, CH-O or CH-N stereogenic centres.<sup>5,8</sup> Its broad substrate scope, high reactivity and selectivity, and the minimal levels of by-products and waste resulting from its use, have rendered this transformation highly desirable for both academia and industry.

For all these reasons, it may be appropriate to begin with a brief historical overview. Asymmetric hydrogenation was made possible by Wilkinson, who discovered that a Rhodium(I) cationic complex  $[\text{Rh}(\text{PPh}_3)_3]\text{Cl}$  catalyzed the hydrogenation of olefins under homogeneous conditions.<sup>9</sup> Soon after, Knowles<sup>7a</sup> and Horner<sup>7b</sup> reported the first chiral versions of Wilkinson's catalytic cycle, which were based on the use of enantiopure monodentate phosphines with stereogenic phosphorus centres.

<sup>7</sup> (a) Knowles, W. S.; Sabacky, M. J. *Chem. Commun.* **1968**, 1445-6. (b) Horner, L.; Siegel, H.; Buethe, H. *Angew. Chem., Int. Ed. Engl.* **1968**, *7*, 942. (c) Knowles, W. S.; Sabacky, M. J.; Vineyard, B. D. *J. Chem. Soc., Chem. Commun.* **1972**, 10-11.

<sup>8</sup> (a) Rossen, K. *Angew. Chem., Int. Ed.* **2001**, *40*, 4611-4613. (b) Knowles, W. S. *Angew. Chem., Int. Ed.* **2002**, *41*, 1998-2007. (c) Noyori, R. *Angew. Chem., Int. Ed.* **2002**, *41*, 2008-2022. (d) Pfaltz, A.; Blankenstein, J.; Hilgraf, R.; Hormann, E.; McIntyre, S.; Menges, F.; Schonleber, M.; Smidt, S. P.; Wustenberg, B.; Zimmermann, N. *Adv. Synth. Catal.* **2003**, *345*, 33-44. (e) Tang, W.; Zhang, X. *Chem. Rev.* **2003**, *103*, 3029-3069. (f) Gridnev, I. D.; Imamoto, T. *Acc. Chem. Res.* **2004**, *37*, 633-644. (g) Cui, X.; Burgess, K. *Chem. Rev.* **2005**, *105*, 3272-3296. (h) Knowles, W. S.; Noyori, R. *Acc. Chem. Res.* **2007**, *40*, 1238-1239. (i) Minnaard, A. J.; Feringa, B. L.; Lefort, L.; de Vries, J. G. *Acc. Chem. Res.* **2007**, *40*, 1267-1277. (j) Zhang, W.; Chi, Y.; Zhang, X. *Acc. Chem. Res.* **2007**, *40*, 1278-1290.

<sup>9</sup> Osborn, J. A.; Jardine, F. H.; Young, J. F.; Wilkinson, G. *J. Chem. Soc., A* **1966**, 1711-32.

In the early 1970s, Kagan devised the  $C_2$ -symmetric chelating diphosphine DIOP (**1**)<sup>10</sup> and demonstrated that: firstly, chelating diphosphines with a chiral backbone catalyzed the Rh-mediated hydrogenation of C=C bonds with higher enantioselectivities than monodentate analogues; and secondly, enantiomerically enriched amino acids could be prepared by hydrogenation of the corresponding dehydroamino acids. Knowles combined the main topological features of DIOP (*i.e.*  $C_2$  symmetry and chelating coordination) with stereogenic phosphorus centres as stereogenic motifs to develop the ligand DIPAMP (**2**), a highly efficient catalyst for Rh-mediated asymmetric hydrogenation of functionalized C=C bonds.

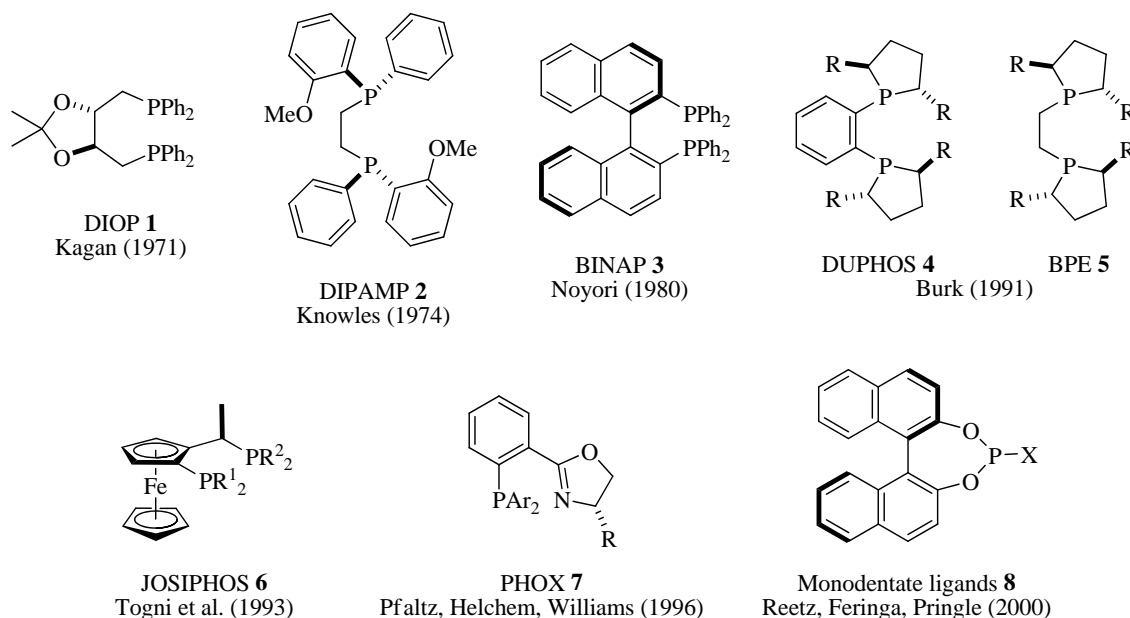


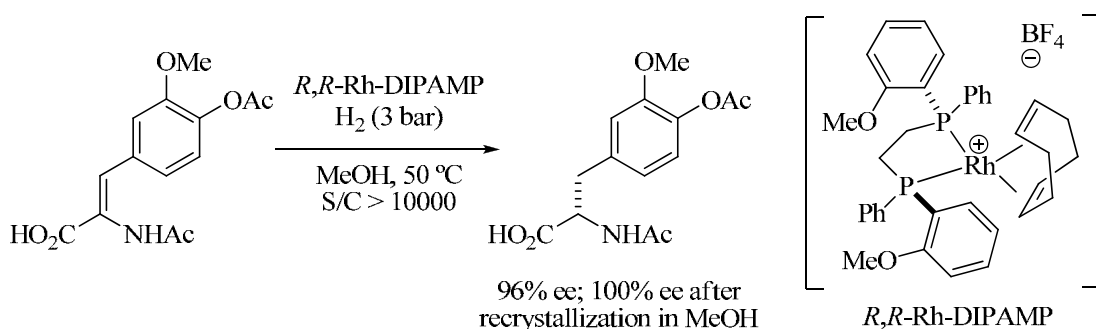
**Figure 2.** Historically important ligands for enantioselective hydrogenation.

The high conversions and enantioselectivities offered by [Rh(DIPAMP)(cod)]BF<sub>4</sub> as the pre-catalyst in the hydrogenation of functionalized C=C bonds, coupled with easy work-up and product separation, enabled Monsanto to produce the anti-Parkinson drug *L*-DOPA on an industrial scale using asymmetric hydrogenation (Scheme 2).<sup>11</sup> These exceptional results

<sup>10</sup> Kagan, H. B.; Dang Tuan, P. *J. Amer. Chem. Soc.* **1972**, *94*, 6429-33.

<sup>11</sup> (a) Vineyard, B. D.; Knowles, W. S.; Sabacky, M. J.; Bachman, G. L.; Weinkauff, D. J. *J. Am. Chem. Soc.* **1977**, *99*, 5946-52. (b) Knowles, W. S. *Acc. Chem. Res.* **1983**, *16*, 106-12.

paved the way to the development of a myriad of chelating diphosphine ligands in enantiomerically pure form. Chelating diphosphines with diverse backbones, leading to Rh-chelates of different sizes, were developed,<sup>12</sup> although it should be recalled at this point that they were almost exclusively limited to asymmetric hydrogenation of functionalized alkenes that can simultaneously coordinate to the Rh centre by the C=C bond and a suitably positioned carbonyl group (*i.e.* enamide precursors of  $\alpha$ -amino acids and itaconic acid derivatives).



**Scheme 2.** Asymmetric hydrogenation of a precursor of *L*-DOPA using *R,R*-DIPAMP as chiral ligand.

Noyori *et al.* achieved a major breakthrough in asymmetric hydrogenation in the early 1980's with their development of the C<sub>2</sub>-symmetric diphosphine ligand BINAP (**3**), which incorporates a stereogenic axis as chiral motif. They found that it facilitated Rh-mediated hydrogenation of C=C functionalized alkenes with very high enantioselectivities, but did not offer any advantages over other known ligands.<sup>13a</sup> However, when Rh(I) was replaced by Ru(II), the new catalytic system, operating through a novel metal-ligand bifunctional mechanism, greatly extended the substrate scope to other types of functionalized olefins (see Figure 3)<sup>13a,b</sup>; indeed, none of the previously known phosphines offered such broad

<sup>12</sup> *Phosphorus Ligands in Asymmetric Catalysis*; Börner, A., Ed.; Wiley-VCH: Weinheim, 2008; Vol 1-3.

<sup>13</sup> (a) Miyashita, A.; Yasuda, A.; Takaya, H.; Toriumi, K.; Ito, T.; Souchi, T.; Noyori, R. *J. Am. Chem. Soc.* **1980**, *102*, 7932-4. (b) Noyori, R.; Okhuma, T. *Angew. Chem., Int. Ed.* **2001**, *40*, 40-73.

applicability. Because of their contributions to this field, Noyori<sup>8c</sup> and Knowles<sup>8b</sup> were awarded the 2001 Nobel Prize in Chemistry for this and related work.<sup>14</sup>

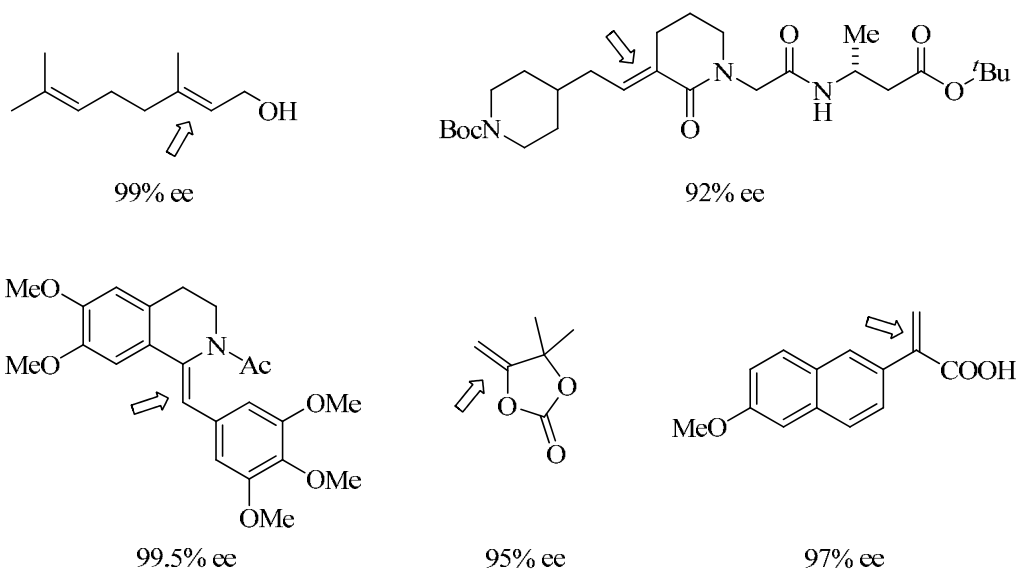


**Figure 3.** Representative substrates for asymmetric hydrogenation of olefins with Ru-BINAP complexes.

Many other enantiomerically pure phosphorus ligands for hydrogenation have since been developed; however, a complete summary of their catalytic activities is beyond the scope of this chapter.<sup>12,15</sup> Nonetheless, the ligands DUPHOS (**4**) and BPE (**5**), developed in 1990 by Burk *et al.*, warrant mention. These rigid, electron-donating bisphospholanes offer broad substrate applicability and unprecedented, consistently high enantioselectivities (> 99% ee).<sup>16</sup>

An important milestone in the initial “gold rush” for efficient chiral *P*-derivatives had already been set by Kagan in 1971 with DIOP: the combination of chelating coordination and  $C_2$ -symmetry. As previously explained, these elements were later combined in future ligands (DIPAMP, BINAP and

<sup>14</sup> They shared the Nobel Prize with Sharpless, who received it for his work on asymmetric epoxidations in industrial processes.

<sup>15</sup> *Handbook of Homogeneous Hydrogenation*; De Vries, J. G., Elsevier, C. J., Eds.; Wiley-VCH: Weinheim, 2007; Vol 1-3.

<sup>16</sup> (a) Burk, M. J. *J. Am. Chem. Soc.* **1991**, *113*, 8518-19. (b) Burk, M. J.; Feaster, J. E.; Nugent, W. A.; Harlow, R. L. *J. Am. Chem. Soc.* **1993**, *115*, 10125-38. (c) Burk, M. J. *Acc. Chem. Res.* **2000**, *33*, 363-372.

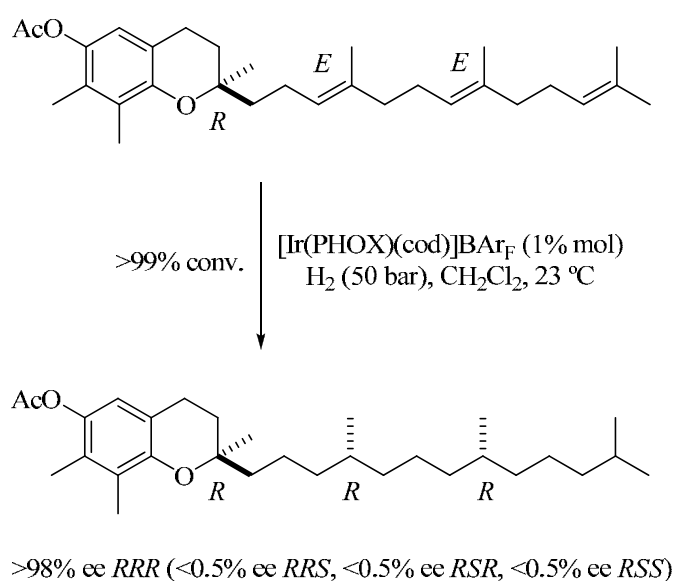
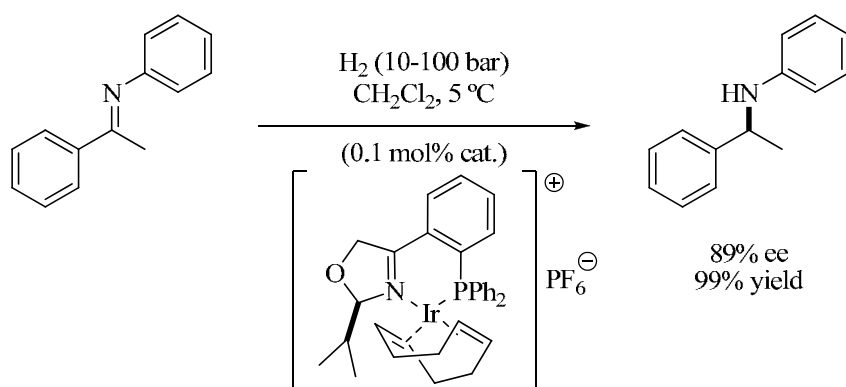
DUPHOS), all of which are highly efficient in asymmetric hydrogenation. Moreover, there are many other ligands, not been mentioned here, that exploit the main topological features of DIOP.  $C_2$ -symmetry is attractive because it halves the number of possible catalyst-substrate arrangements and, consequently, the number of competing reaction pathways. Apart from possibly enhancing enantioselectivity, this facilitates mechanistic studies and determination of the elements responsible for enantiocontrol. However, there is no fundamental reason for asymmetric/non- $C_2$ -symmetric ligands to be less efficient. Indeed, there are many examples of highly efficient  $C_1$ -symmetric ligands, including the chiral ferrocene-based JOSIPHOS<sup>17a</sup> (**6**) ligand family. By exploiting the fact that the two chelating phosphorus donor groups can be easily modified throughout the synthesis, Togni, Blaser and co-workers prepared an extensive library of ligands to meet the steric and electronic requirements of various catalytic reactions, with which they obtained excellent results.<sup>17b,c</sup> Pfaltz and others developed modular *P,N*-PHOX ligands (**7**) with two sterically and electronically non-equivalent donors,<sup>18</sup> achieving unprecedented enantioselectivities in the Ir-catalyzed asymmetric hydrogenation of imines and non-functionalized alkenes (Scheme 3).<sup>19</sup>

---

<sup>17</sup> (a) Togni, A.; Breutel, C.; Schnyder, A.; Spindler, F.; Landert, H.; Tijani, A. *J. Am. Chem. Soc.* **1994**, *116*, 4062-6. (b) Blaser, H.-U.; Brieden, W.; Pugin, B.; Spindler, F.; Studer, M.; Togni, A. *Top. Catal.* **2002**, *19*, 3-16. (c) Blaser, H.-U.; Pugin, B.; Spindler, F.; Thommen, M. *Acc. Chem. Res.* **2007**, *40*, 1240-1250.

<sup>18</sup> (a) Sprinz, J.; Helmchen, G. *Tetrahedron Lett.* **1993**, *34*, 1769-72. (b) von Matt, P.; Pfaltz, A. *Angewandte Chemie* **1993**, *105*, 614-15 (See also *Angew Chem*, Int Ed Engl, 1993, 32(4), 566-8). (c) Dawson, G. J.; Frost, C. G.; Williams, J. M. J.; Coote, S. J. *Tetrahedron Lett.* **1993**, *34*, 3149-50.

<sup>19</sup> (a) Helmchen, G.; Pfaltz, A. *Acc. Chem. Res.* **2000**, *33*, 336-345. (b) Pfaltz, A.; Drury, W. J., III *Proc. Natl. Acad. Sci. U. S. A.* **2004**, *101*, 5723-5726. (c) Bell, S.; Wuestenberg, B.; Kaiser, S.; Menges, F.; Netscher, T.; Pfaltz, A. *Science (Washington, DC, U. S.)* **2006**, *311*, 642-644.



**Scheme 3.** Enantioselective hydrogenations of *N*-arylimine (top) and a precursor of  $\gamma$ -tocopherol (bottom), a principal component of vitamin E, using Ir-PHOX catalysts.

A more recent conceptual breakthrough in asymmetric hydrogenation was the discovery of modular monodentate ligands (**8**), which showed that not only bidentate ligands, but monodentate ligands as well, could be ideal chiral agents.<sup>20</sup>

<sup>20</sup> (a) Gillon, A.; Heslop, K.; Hyett, D. J.; Martorell, A.; Orpen, A. G.; Pringle, P. G.; Claver, C.; Fernandez, E. *Chem. Commun. (Cambridge)* **2000**, 961-962. (b) Reetz, M. T.; Mehler, G. *Angew. Chem., Int. Ed.* **2000**, 39, 3889-3890. (c) van den Berg, M.; Minnaard, A. J.; Schudde, E. P.; van Esch, J.; de Vries, A. H. M.; de Vries, J. G.; Feringa, B. L. *J. Am. Chem. Soc.* **2000**, 122, 11539-11540.

Although asymmetric hydrogenation should be considered a remarkably advanced synthetic methodology, many groups are still actively pursuing new catalytic systems that offer higher activity and improved enantioselectivity for both challenging substrates and applications. Other researchers are endeavouring to develop chiral catalysts with an attractive industrial profile: compounds that offer high enantioselectivity, and are easily prepared and patentable. Other criteria that must be taken into account include catalytic efficiency (turnover number [TON] and turnover frequency [TOF]), application range, robustness, accessibility and functional group tolerance.

Albeit computational techniques are becoming increasingly important in the design of new chiral catalysts,<sup>21</sup> many approaches still chiefly rely on empirical methods. Not surprisingly, combinatorial and high-throughput synthetic strategies<sup>22</sup> have led to the development of some highly efficient monodentate and bidentate phosphorus ligands for asymmetric hydrogenation, utilizing either standard covalent chemistry<sup>23</sup> or supramolecular interactions.<sup>24</sup> In a complementary way, ligand tuning in asymmetric catalysis has enabled rapid

---

<sup>21</sup> (a) Vidal-Ferran, A.; Moyano, A.; Pericas, M. A.; Riera, A. *Tetrahedron Lett.* **1997**, *38*, 8773-8776. (b) Balcells, D.; Maseras, F.; Ujaque, G. *J. Am. Chem. Soc.* **2005**, *127*, 3624-3634. (c) Rudolph, J.; Bolm, C.; Norrby, P.-O. *J. Am. Chem. Soc.* **2005**, *127*, 1548-1552. (d) Zuidema, E.; Escorihuela, L.; Eichelsheim, T.; Carbo, J. J.; Bo, C.; Kamer, P. C. J.; van Leeuwen, P. W. N. *M. Chem. Eur. J.* **2008**, *14*, 1843-1853.

<sup>22</sup> (a) Dahmen, S.; Brase, S. *Synthesis* **2001**, 1431-1449. (b) Hagemeyer, A.; Jandeleit, B.; Liu, Y.; Poojary, D. M.; Turner, H. W.; Volpe, A. F.; Henry Weinberg, W. *Appl. Catal., A* **2001**, *221*, 23-43. (c) Reetz, M. T. *Angew. Chem., Int. Ed.* **2001**, *40*, 284-310. (d) de Vries, J. G.; de Vries, A. H. M. *Eur. J. Org. Chem.* **2003**, 799-811. (e) Gennari, C.; Piarulli, U. *Chem. Rev.* **2003**, *103*, 3071-3100. (f) Ding, K.; Du, H.; Yuan, Y.; Long, J. *Chem. Eur. J.* **2004**, *10*, 2872-2884.

<sup>23</sup> (a) Hoen, R.; Boogers, J. A. F.; Bernsmann, H.; Minnaard, A. J.; Meetsma, A.; Tiemersma-Wegman, T. D.; de Vries, A. H. M.; de Vries, J. G.; Feringa, B. L. *Angew. Chem., Int. Ed.* **2005**, *44*, 4209-4212. (b) Monti, C.; Gennari, C.; Piarulli, U.; de Vries, J. G.; de Vries, A. H. M.; Lefort, L. *Chem. Eur. J.* **2005**, *11*, 6701-6717. (c) Reetz, M. T.; Li, X. *Angew. Chem., Int. Ed.* **2005**, *44*, 2959-2962. (d) de Vries, J. G.; Lefort, L. *Chem. Eur. J.* **2006**, *12*, 4722-4734.

<sup>24</sup> (a) Breit, B. *Angew. Chem., Int. Ed.* **2005**, *44*, 6816-6825. (b) Weis, M.; Waloch, C.; Seiche, W.; Breit, B. *J. Am. Chem. Soc.* **2006**, *128*, 4188-9. (c) Jiang, X.-B.; Lefort, L.; Goudriaan, P. E.; de Vries, A. H. M.; van Leeuwen, P. W. N. M.; de Vries, J. G.; Reek, J. N. H. *Angew. Chem., Int. Ed.* **2006**, *45*, 1223-1227. (d) Sandee, A. J.; Van der Burg, A. M.; Reek, J. N. H. *Chem. Commun.* **2007**, 864-866. (e) Hattori, G.; Hori, T.; Miyake, Y.; Nishibayashi, Y. *J. Am. Chem. Soc.* **2007**, *129*, 12930-12931.

development of efficient catalytic systems. Our group<sup>21a,25</sup> and others<sup>26</sup> have fine-tuned the performance of modular ligands by modifying the stereoelectronics of their constituent modules.

The aforementioned work inspired us to design a new family of chiral *P-OP* (phosphine-phosphinite or phosphine-phosphite) ligands, readily available from enantiopure Sharpless<sup>27</sup> or Shi<sup>28</sup> epoxides, in which our research group has strong experience.<sup>29</sup> We envisaged that the chiral epoxides could be converted into the desired *P-OP* ligands in a two-step synthetic strategy (Scheme 4):

1.-Introduction of the phosphine functionality through epoxide ring opening with a nucleophilic trivalent phosphorus derivative.

---

<sup>25</sup> (a) Vidal-Ferran, A.; Moyano, A.; Pericas, M. A.; Riera, A. *J. Org. Chem.* **1997**, *62*, 4970-4982. (b) Vidal-Ferran, A.; Bamos, N.; Moyano, A.; Pericas, M. A.; Riera, A.; Sanders, J. K. M. *J. Org. Chem.* **1998**, *63*, 6309-6318. (c) Puigjaner, C.; Vidal-Ferran, A.; Moyano, A.; Pericas, M. A.; Riera, A. *J. Org. Chem.* **1999**, *64*, 7902-7911. (d) Pericas, M. A.; Puigjaner, C.; Riera, A.; Vidal-Ferran, A.; Gomez, M.; Jimenez, F.; Muller, G.; Rocamora, M. *Chem. Eur. J.* **2002**, *8*, 4164-4178. (e) Popa, D.; Puigjaner, C.; Gomez, M.; Benet-Buchholz, J.; Vidal-Ferran, A.; Pericas, M. A. *Adv. Synth. Catal.* **2007**, *349*, 2265-2278.

<sup>26</sup> See for example: (a) Trost, B. M.; Van Vranken, D. L.; Bingel, C. *J. Am. Chem. Soc.* **1992**, *114*, 9327-43. (b) Rajanbabu, T. V.; Casalnuovo, A. L.; Ayers, T. A. *Adv. Catal. Processes* **1997**, *2*, 1-41. (c) Kranich, R.; Eis, K.; Geis, O.; Muhle, S.; Bats, J. W.; Schmalz, H.-G. *Chem. Eur. J.* **2000**, *6*, 2874-2894. (d) Degrado, S. J.; Mizutani, H.; Hoveyda, A. H. *J. Am. Chem. Soc.* **2001**, *123*, 755-756. (e) Hamashima, Y.; Kanai, M.; Shibasaki, M. *Tetrahedron Lett.* **2001**, *42*, 691-694. (f) Pamies, O.; van Strijdonck, G. P. F.; Dieguez, M.; Deerenberg, S.; Net, G.; Ruiz, A.; Claver, C.; Kamer, P. C. J.; van Leeuwen, P. W. N. M. *J. Org. Chem.* **2001**, *66*, 8867-8871. (g) Dalko, P. I.; Moisan, L.; Cossy, J. *Angew. Chem., Int. Ed.* **2002**, *41*, 625-628. (h) Dieguez, M.; Ruiz, A.; Claver, C. *J. Org. Chem.* **2002**, *67*, 3796-3801. (i) Locatelli, M.; Cozzi, P. G. *Angew. Chem., Int. Ed.* **2003**, *42*, 4928-4930. (j) Jensen, J. F.; Sotofte, I.; Sorensen, H. O.; Johannsen, M. *J. Org. Chem.* **2003**, *68*, 1258-1265. (k) Jeulin, S.; De Paule, S. D.; Ratovelomanana-Vidal, V.; Genet, J.-P.; Champion, N.; Dellis, P. *Proc. Natl. Acad. Sci. U. S. A.* **2004**, *101*, 5799-5804. (l) Goldfuss, B.; Loeschmann, T.; Rominger, F. *Chem. Eur. J.* **2004**, *10*, 5422-5431. (m) Knoepfel, T. F.; Zarotti, P.; Ichikawa, T.; Carreira, E. M. *J. Am. Chem. Soc.* **2005**, *127*, 9682-9683. (n) Liu, Y.; Ding, K. *J. Am. Chem. Soc.* **2005**, *127*, 10488-10489. (o) Leroux, F. R.; Mettler, H. *Adv. Synth. Catal.* **2007**, *349*, 323-336. (p) Miller, J. J.; Sigman, M. S. *J. Am. Chem. Soc.* **2007**, *129*, 2752-2753.

<sup>27</sup> Gao, Y.; Klunder, J. M.; Hanson, R. M.; Masamune, H.; Ko, S. Y.; Sharpless, K. B. *J. Am. Chem. Soc.* **1987**, *109*, 5765-80.

<sup>28</sup> Wang, Z.-X.; Tu, Y.; Frohn, M.; Zhang, J.-R.; Shi, Y. *J. Am. Chem. Soc.* **1997**, *119*, 11224-11235. and references cited therein.

<sup>29</sup> (a) Nieto, N.; Molas, P.; Benet-Buchholz, J.; Vidal-Ferran, A. *J. Org. Chem.* **2005**, *70*, 10143-10146. (b) Nieto, N.; Munslow, I. J.; Barr, J.; Benet-Buchholz, J.; Vidal-Ferran, A. *Org. Biomol. Chem.* **2008**, *6*, 2276-2281. (c) Nieto, N.; Munslow, I. J.; Fernandez-Perez, H.; Vidal-Ferran, A. *Synlett* **2008**, 2856-2858.

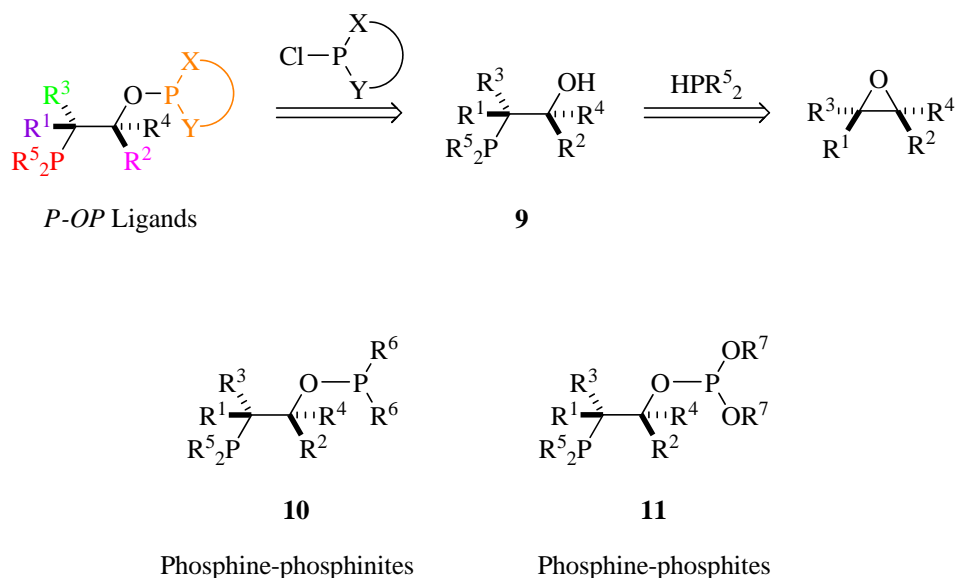


2.- The phosphinite or phosphite functionality could be introduced via phosphorylation of a phosphino-alcohol with a suitable electrophilic trivalent phosphorus reagent.

The combination of an enantiopure epoxide, a trivalent nucleophilic phosphorus reagent and a trivalent electrophilic phosphorus reagent should render our highly modular target *P-OP* ligands. Interestingly, preparation of the target *P-OP* ligands requires synthesis of the corresponding phosphino-alcohols (**9**), modular *P-OH* ligands whose catalytic properties in asymmetric transformations remain unexplored.

The modularity of our target *P-OP* ligands enables:

- incorporation of up to 6 molecular fragments.
- modification of the stereoelectronics of the phosphorus functionalities.
- control of the stereogenic centres between the phosphorus groups.



**Scheme 4.** Two-step retrosynthesis of *P-OP* ligands.

Phosphine-phosphites and phosphine-phosphinites have already found applications in many asymmetric transformations, providing excellent enantioselectivities in transformations such as asymmetric hydrogenation.<sup>30</sup>

Although the catalytic studies reported in this PhD Thesis concentrated on Rhodium-mediated asymmetric hydrogenation of functionalized alkenes, we think that our *P-OP* ligands have strong potential for a wide array of asymmetric transformations. Indeed, we believe it is important to design and prepare chiral catalysts with breadth of scope in mind.

---

<sup>30</sup> A summary of the applications of phosphine-phosphites and phosphine-phosphinites in asymmetric catalysis is provided in the following chapter.

Supramolecular catalysts have filled the gap between the two extreme cases of bidentate/monodentate catalytic action: that of two binding groups covalently linked through a carbon backbone (*e.g.* DIOP and DIPAMP) and that of simultaneous coordination of two monodentate ligands to a metal centre (*e.g.* Reetz's and Feringa's monodentate phosphorus ligands). Figure 4 illustrates a continuum of bidentate systems, from connected systems—in which the coordinating moieties ( $L^1$  and  $L^2$ ) are bound to each other with decreasing bonding strengths through covalent bonds, metal-ligand interactions,<sup>24c</sup> ion-dipole interactions<sup>24e</sup> or hydrogen bonding,<sup>24a-b</sup>—to unconnected monodentate ligands.<sup>20b-c</sup>

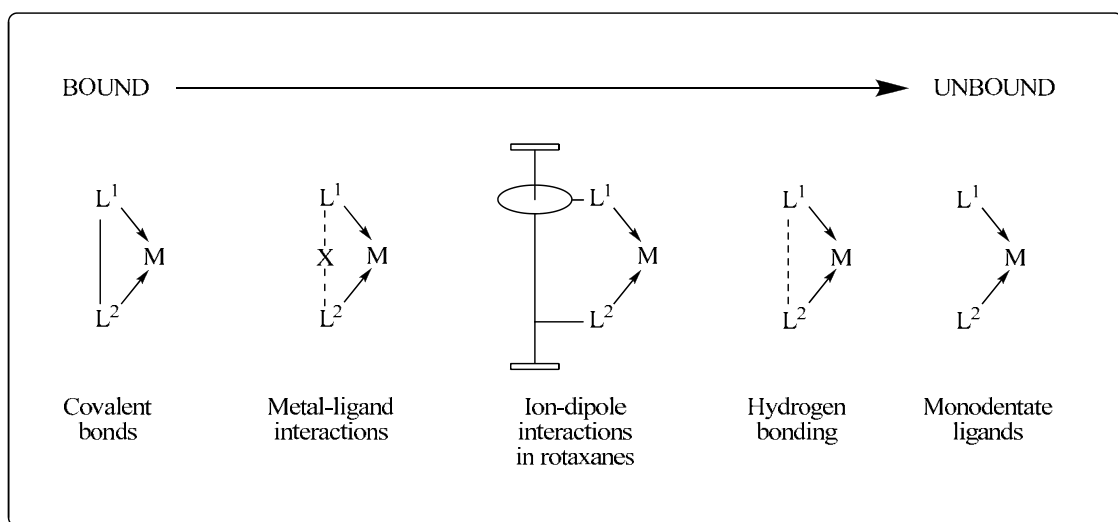
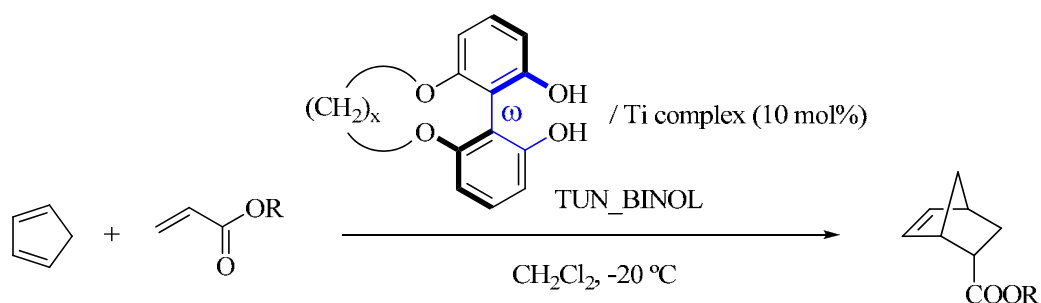


**Figure 4.** A range of bidentate ligand binding strength for the coordinating groups  $L^1$  and  $L^2$ : from strongly bound (left) to unbound (right).

We envisaged that supramolecular interactions could also be used to generate a broad range of geometries for the catalytic site. This had already been pursued by covalent chemistry:<sup>31</sup> for instance, Harada *et al.* demonstrated that modifying the ring size in TUN\_BINOL catalytic systems dramatically affects the reactivity

<sup>31</sup> (a) Harada, T.; Takeuchi, M.; Hatsuda, M.; Ueda, S.; Oku, A. *Tetrahedron: Asymmetry* **1996**, 7, 2479-2482. (b) Zhang, Z.; Qian, H.; Longmire, J.; Zhang, X. *J. Org. Chem.* **2000**, 65, 6223-6226.

and enantioselectivity of catalytic asymmetric Diels-Alder transformations (see Figure 5).



Catalyst	Yield	ee (endo)	Torsion angle ( $\omega$ )
( <i>R</i> )-BINOL	98%	69% ( <i>R</i> )	61.5°
( <i>S</i> )-TUN_BINOL: X=3	39%	29% ( <i>S</i> )	55.9°
( <i>S</i> )-TUN_BINOL: X=4	57%	65% ( <i>S</i> )	58.6°
( <i>S</i> )-TUN_BINOL: X=5	55%	70% ( <i>S</i> )	57.7°
( <i>S</i> )-TUN_BINOL: X=6	58%	77% ( <i>S</i> )	60.2°

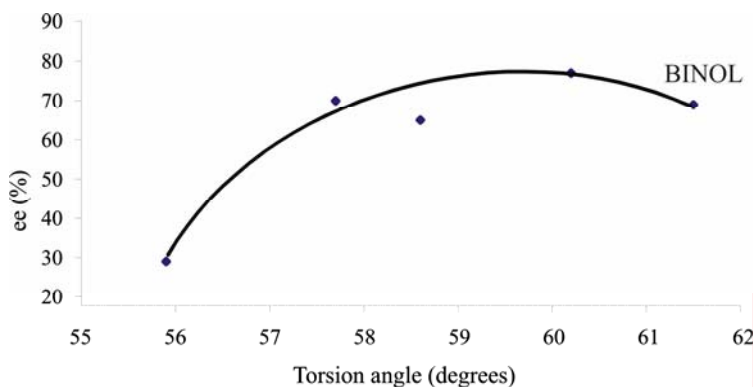


**Figure 5.** Effect of torsion angle on the enantioselectivity and reactivity of catalytic asymmetric Diels-Alder reactions.

We became interested in studying whether binding interactions in the supramolecular diphosphine catalysts shown in Figure 6 could have a more pronounced effect on the catalytic properties than the catalysts that we previously obtained via covalent tuning. These supramolecular structures are inspired by natural enzymes and biological macromolecules, in which conformational

changes induced by binding forces lead to *allosteric effects* and enable regulation of the catalytic activity.<sup>32</sup>

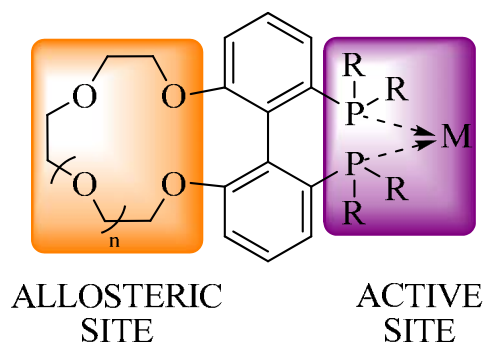


**Figure 6.** General structure of supramolecular catalysts inspired by natural enzymes and biological macromolecules.

As a minor project within the Thesis, we decided to develop a synthetic methodology for enantiomerically pure versions of these compounds.

<sup>32</sup> Koshland, D. E., Jr. *Enzymes*, 3rd Ed. **1970**, 1, 341-96.

In conclusion, our main objectives in the present research work were:

1. To develop a general synthesis for enantiomerically pure and highly modular phosphine-phosphinites and phosphine-phosphites (*P-OP* ligands) from epoxides.
2. To evaluate the catalytic activity of the *P-OP* ligands in Rhodium-mediated asymmetric hydrogenations of functionalized alkenes, and then optimize it by varying the modules.
3. To prepare biaryl diphosphine catalysts with an allosteric site (in the form of a crown ether) that might potentially generate changes in the active site geometry through non-covalent interactions.

**CHAPTER 1**  
***MODULAR COVALENT APPROACH***  
***TO ASYMMETRIC CATALYSIS***

UNIVERSITAT ROVIRA I VIRGLI

TOWARDS HIGHLY EFFICIENT LIGANDS FOR ASYMMETRIC HYDROGENATIONS: A COVALENT MODULAR APPROACH AND INVESTIGATIONS INTO BIOINSPIRED SUPRAMOLECULAR STRATEGIES

Héctor Fernández Pérez

ISBN:978-84-693-3385-3 /DL:T.994-2010



## **LITERATURE PRECEDENT**

UNIVERSITAT ROVIRA I VIRGLI

TOWARDS HIGHLY EFFICIENT LIGANDS FOR ASYMMETRIC HYDROGENATIONS: A COVALENT MODULAR APPROACH AND  
INVESTIGATIONS INTO BIOINSPIRED SUPRAMOLECULAR STRATEGIES

Héctor Fernández Pérez

ISBN:978-84-693-3385-3 /DL:T.994-2010

## 1.1. LITERATURE PRECEDENT

Preparing enantiomerically pure products generally remains challenging in modern organic synthesis. Chiral catalysts based on metal complexes are often employed, as they are relatively powerful and cost effective for use on both laboratory and industrial scales.<sup>1</sup> Owing to the special metal ligation properties of phosphorus derivatives, trivalent phosphorus compounds have played and still play an important role as ligands for metal catalysts in homogeneous catalysis. Since 1968, many phosphorus ligands have been synthesized and tested in various enantioselective transformations. Complexes of *soft* phosphorus ligands with *soft* metals (*e.g.* Rhodium, Ruthenium, Iridium and Palladium) are very stable and can catalyze pivotal organic transformations. Moreover, trivalent phosphorus derivatives are more amenable to steric and electronic modification than other binding groups (*e.g.* OH, NH<sub>2</sub> groups). Furthermore, a wide range of phosphorus ligands containing all possible stereogenic elements (centres, axes, planes and helices) has been developed.<sup>2</sup>

Despite the variety of phosphorus ligands now available, many transformations still lack effective chiral ligands. Furthermore, in many cases the enantioselectivities are substrate-dependent. Thus, there is a need for new, efficient chiral phosphorus ligands.

Trivalent phosphorus ligands can be based on different general structures according to stereoelectronic features and to coordination mode. In terms of electronic structure, the  $\pi$ -accepting properties of the phosphorus group can be strongly modified via replacement of the *P-C* bonds with *P-O* or *P-N* bonds (Figure 1). This leads to phosphinites, phosphonites and phosphites and their corresponding *P-N* analogues.

---

<sup>1</sup> (a) *Comprehensive Asymmetric Catalysis*; Jacobsen, E.N., Pfaltz, A., Yamamoto, H. Eds.; Springer: Berlin, Germany, 1999; Vol 1-3. (b) *Catalytic Asymmetric Synthesis*; Ojima, I., Ed.; Wiley-VCH: New York, 2000.

<sup>2</sup> *Phosphorus Ligands in Asymmetric Catalysis*; Börner, A., Ed.; Wiley-VCH: Weinheim, 2008; Vol 1-3.

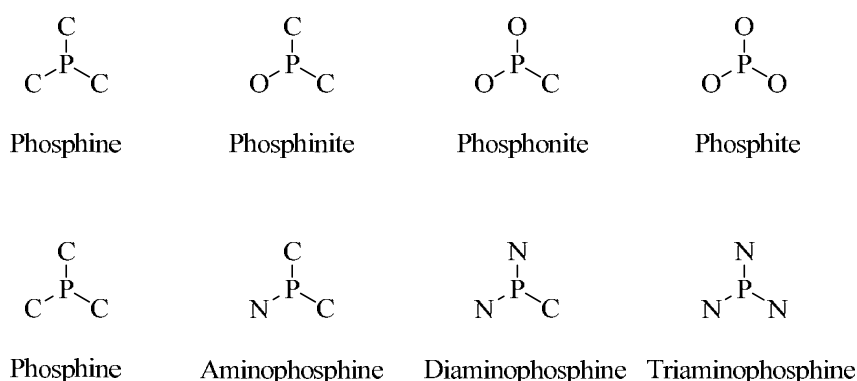


**Figure 1.** Various trivalent phosphorus ligand families that differ by electronic structure.

Alternatively, the coordination mode (*i.e.* monodentate, bidentate or polydentate) can be altered by changing the substituents on the phosphorus group (Figure 2). Furthermore, phosphorus can be combined with other ligating groups in mixed bidentate mode to form hybrid ligands, the majority of which contain *P-N*, *P-S*, *P-O* or *P-P'* (*e.g.* phosphine-phosphinites, phosphine-phosphites, or phosphine-phosphoramidites) binding groups.

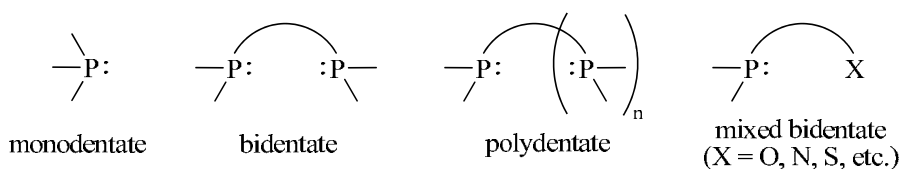
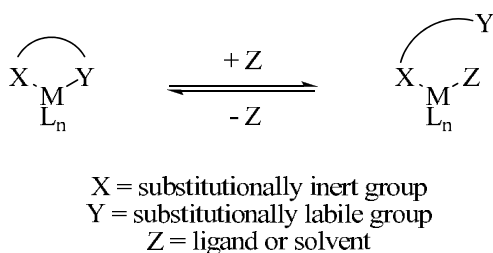


**Figure 2.** Trivalent phosphorus ligand types classified by coordination mode.

This section provides an overview of the literature precedent on chiral phosphino-alcohol, phosphine-phosphinite and phosphine-phosphite ligands and their respective applications in asymmetric catalysis.

### 1.1.1 PHOSPHINO-ALCOHOL LIGANDS

In the past 20 years, numerous strategies have been developed for the synthesis of chiral phosphino-alcohol derivatives,<sup>3</sup> and the chemistry of these compounds has received considerable attention.<sup>4</sup> Phosphino-alcohol ligands belong to a particular class of ligands, *hemilabile ligands*, which contain both substitutionally inert (phosphorus) and substitutionally labile (oxygen) binding groups. The basic components of these compounds are described in Scheme 1. Hemilabile ligands are polydentate chelates that contain at least two different types of ligating groups, denoted X and Y. X is strongly bound to the metal centre (M), whereas Y is only weakly bound, and therefore, easily displaceable by other molecules that could coordinate to M (*i.e.* other ligands, reagents, or solvent molecules). However, once displaced from M, Y remains available for recoordination, and therefore, this displacement reaction is reversible.



**Scheme 1.** Behaviour of a hemilabile ligand.

This behaviour has been exploited by several authors such as Hayashi, Ito and Kumada, who have shown that, if properly situated, Y can amplify the intrinsic stereodiscriminating ability of a metal catalyst.<sup>5</sup> This effect derives from attractive interactions between the functional group and either the substrate,<sup>5</sup> the metal centre (known as the *windscreen-wiper* effect),<sup>4</sup> or a suitable reagent (*e.g.* an incoming nucleophile).<sup>5</sup>

<sup>3</sup> Holz, J.; Quirmbach, M.; Borner, A. *Synthesis* **1997**, 983-1006.

<sup>4</sup> (a) Bader, A.; Lindner, E. *Coord. Chem. Rev.* **1991**, *108*, 27-110. (b) Slone, C. S.; Weinberger, D. A.; Mirkin, C. A. *Prog. Inorg. Chem.* **1999**, *48*, 233-350.

<sup>5</sup> Sawamura, M.; Ito, Y. *Chem. Rev.* **1992**, *92*, 857-71 and references cited therein.

*P,O*-ligands contain *hard* (oxygen) and *soft* (phosphine) coordination groups. In the reaction with transition metal complexes, both the phosphine and oxygen groups may act as ligating groups: chelates between *P,O*-ligands and either *soft* transition metals,<sup>6</sup> such as the Ni(II) *P,O*-chelate complex **12** (Figure 3), or *hard* transition metals,<sup>7</sup> such the Titanium complex **13** (Figure 3), which contains an *o*-phosphinephenol group,<sup>7b</sup> have been reported. In fact, the Ni-complex **12** has proven to be an effective catalyst for the oligomerization of ethane.<sup>6c</sup>

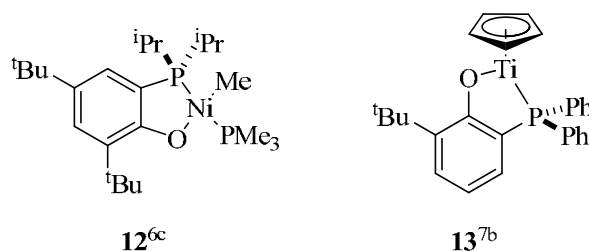


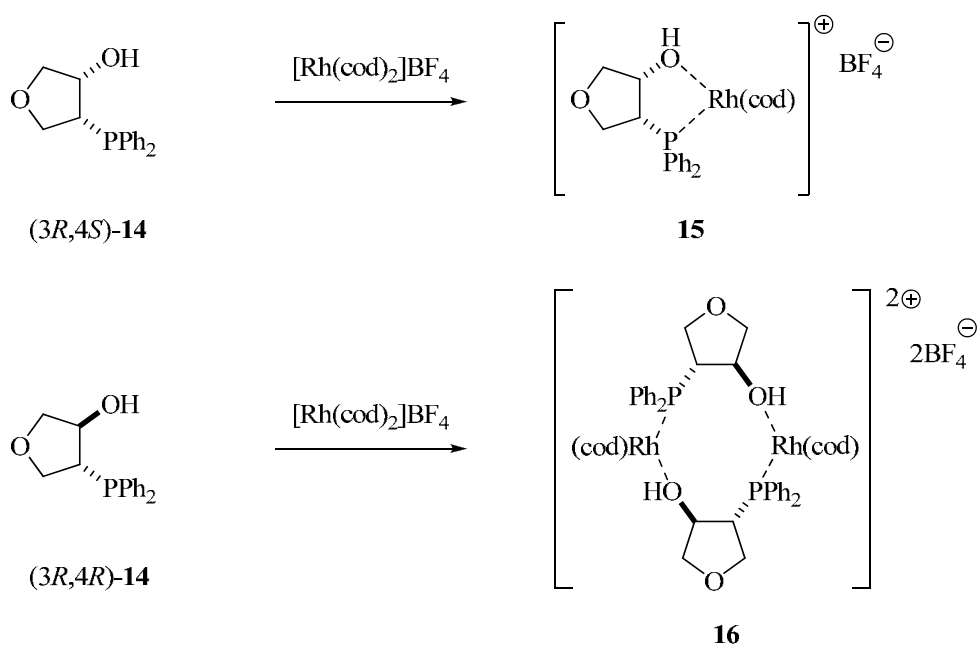
**Figure 3.** Examples of complexes in which a *P,O*-ligand is chelated to a metal centre.

Börner's group investigated the complexation of rigid *cis*- and *trans*-(diphenylphosphino)tetrahydrofuran-3-ols **14** with  $[\text{Rh}(\text{cod})_2]\text{BF}_4$  (Scheme 2).<sup>8</sup> With the *cis*-compound (3*R*,4*S*)-**14**, the 1:1 chelate **15** was readily isolated; whereas with the *trans*-compound (3*R*,4*R*)-**14**, the dimeric bridging *P,O*-complex **16** was formed, which was not isolated and which proved to be stable only in solution (as shown by NMR). The 2:2 coordination mode in the five-membered *P,O*-chelate with *trans* stereochemistry could be explained by unfavourable steric strain. Indeed, steric reasons are responsible for the generation of different complexes.

<sup>6</sup> (a) Sembiring, S. B.; Colbran, S. B.; Craig, D. C.; Scrudder, M. L. *J. Chem. Soc., Dalton Trans.* **1995**, 3731-41. (b) Heinicke, J.; Kadyrov, R.; Kindermann, M. K.; Kloss, M.; Fischer, A.; Jones, P. G. *Chem. Ber.* **1996**, *129*, 1061-1071. (c) Heinicke, J.; He, M.; Dal, A.; Klein, H.-F.; Hetsche, O.; Keim, W.; Florke, U.; Haupt, H.-J. *Eur. J. Inorg. Chem.* **2000**, 431-440.

<sup>7</sup> (a) van Doorn, J. A.; van der Heijden, H.; Orpen, A. G. *Organometallics* **1994**, *13*, 4271-7. (b) Willoughby, C. A.; Duff, R. R., Jr.; Davis, W. M.; Buchwald, S. L. *Organometallics* **1996**, *15*, 472-5.

<sup>8</sup> Boerner, A.; Kless, A.; Holz, J.; Baumann, W.; Tillack, A.; Kadyrov, R. *J. Organomet. Chem.* **1995**, *490*, 213-19.



**Scheme 2.** Complexation of *cis*- and *trans*-(diphenylphosphino)tetrahydrofuran-3-ol (**14**) with  $[\text{Rh}(\text{cod})_2]\text{BF}_4$  (Börner, *et al.*).

The aforementioned Rh complexes were inactive as catalysts in the Rh-mediated enantioselective hydrogenation of C=C bonds under atmospheric pressure.

The literature contains a few examples of phosphino-alcohols used as chiral ligands in metal-mediated asymmetric conjugate additions (see Figure 4). The ligands **17a**, **17b**<sup>9</sup> and **18a-e**<sup>10</sup> have stereogenic elements on the backbone. The former are prepared from (*S*)-(-)-ethyl lactate and (*S*)-(+)-ethyl mandelate, and the latter, from (*R*)-1,1'-binaphthol. The ligand **19**<sup>11</sup> contains a *P*-stereogenic centre and a rigid *o*-phenylene backbone.

<sup>9</sup> Christoffers, J.; Rossler, U. *Tetrahedron: Asymmetry* **1999**, *10*, 1207-1215.

<sup>10</sup> Ito, K.; Eno, S.; Saito, B.; Katsuki, T. *Tetrahedron Lett.* **2005**, *46*, 3981-3985.

<sup>11</sup> Takahashi, Y.; Yamamoto, Y.; Katagiri, K.; Danjo, H.; Yamaguchi, K.; Imamoto, T. *J. Org. Chem.* **2005**, *70*, 9009-9012.

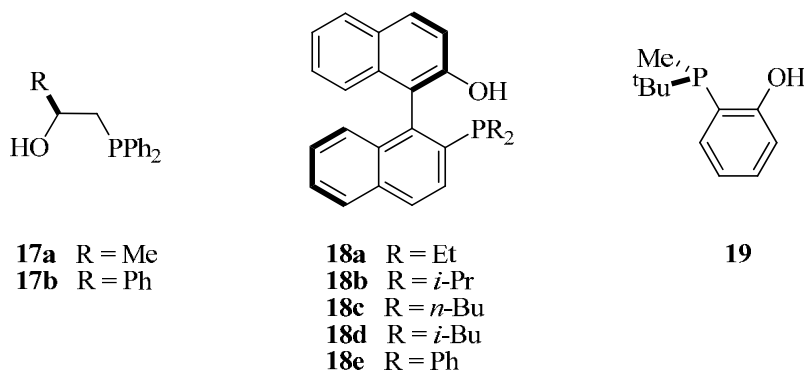
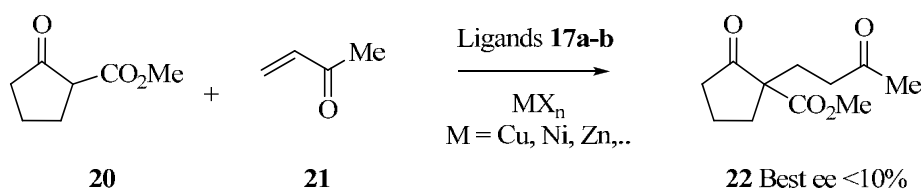


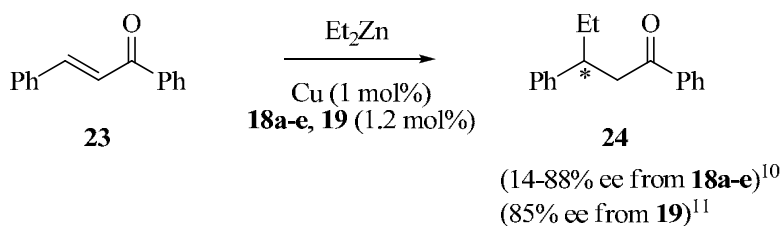
**Figure 4.** Enantioenriched phosphino alcohol ligands.

Metal complexes of phosphino alcohols **17a** and **17b** were tested as chiral ligands in the asymmetric Michael addition of methyl 2-oxocyclopentanecarboxylate (**20**) to methylacrylate (**21**) (Scheme 3). Unfortunately, low enantioselectivities (< 10% ee) were obtained in all cases.<sup>9</sup>



**Scheme 3.** Michael additions catalyzed by metal complexes ( $\text{MX}_n$ ) of ligands **17a** and **17b**.

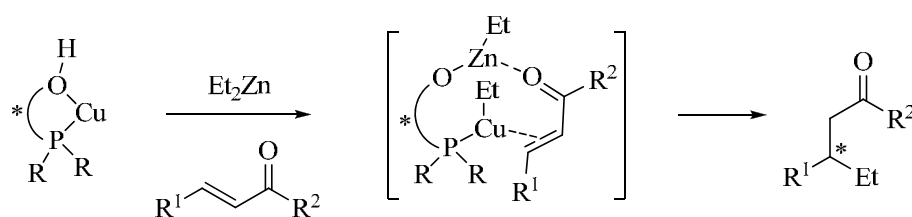
Despite their hemilability, phosphino alcohols **18a-e** and **19** are effective chiral ligands in the Cu-mediated asymmetric conjugate addition of dialkylzinc reagents to  $\alpha,\beta$ -unsaturated carbonyl compounds, as demonstrated in the Cu-catalyzed addition of diethylzinc to chalcone (**23**) (Scheme 4, up to 88% ee).



**Scheme 4.** Cu-catalyzed asymmetric conjugate addition of diethylzinc to chalcone using ligands **18a-e** and **19**.



Although the detailed mechanism has not yet been clarified, it has been proposed that the catalytic cycle involves a monoalkyl copper (I) species: complexing of the copper (I) centre to the C=C bond and coordination of its carbonyl oxygen to a Lewis acidic zinc species, are essential for alkyl transfer from the copper (I) centre to the enone (Scheme 5).<sup>10,12</sup>



**Scheme 5.** Suggested mechanism of the Cu-mediated asymmetric conjugate addition of diethylzinc to  $\alpha,\beta$ -unsaturated carbonyl compounds.

As previously explained, only a few phosphino alcohol ligands are known to be effective chiral ligands in enantioselective transformations. The ready derivatization of the hydroxyl group into other functional groups has made phosphino alcohols excellent precursors for myriad new chiral ligands ripe with potential for asymmetric catalysis.

<sup>12</sup> Feringa, B. L. *Acc. Chem. Res.* **2000**, 33, 346-353.

### 1.1.2 PHOSPHINE-PHOSPHINITE LIGANDS

Although  $C_2$ -symmetric diphosphines have played a prominent role in asymmetric catalysis, asymmetric bidentate phosphorus ligands have also found their niche in this field. Phosphine-phosphinites are one example. In these ligands, the phosphinite unit has two carbon constituents and one oxygen (see Figure 1, p. 26); this arrangement confers different electronic properties to the phosphinite compared to those of the phosphine. According to Achiwa,<sup>13</sup> two different donor sites can lead *a priori* to a better match in the intermediates and/or transition states that determine reactivity and selectivity in asymmetric hydrogenation: phosphinites can induce high enantioselectivity and often bring about increased stabilities.

Several phosphine-phosphinite ligands are known in the literature (see Figure 5). These ligands have typically been synthesized by multi-step routes. The phosphine functionality is normally introduced by nucleophilic displacement of a leaving group (*e.g.* tosylate) on a chiral backbone by a phosphanide nucleophile. In contrast, the phosphinite functionality is usually introduced by *O*-phosphorylation of an alcohol with the corresponding chlorophosphine in the presence of a base. Most of the known phosphine-phosphinite ligands derive from the “chiral pool”, which has provided diverse carbon backbones.

---

<sup>13</sup> Inoguchi, K.; Sakuraba, S.; Achiwa, K. *Synlett* **1992**, 169-78.

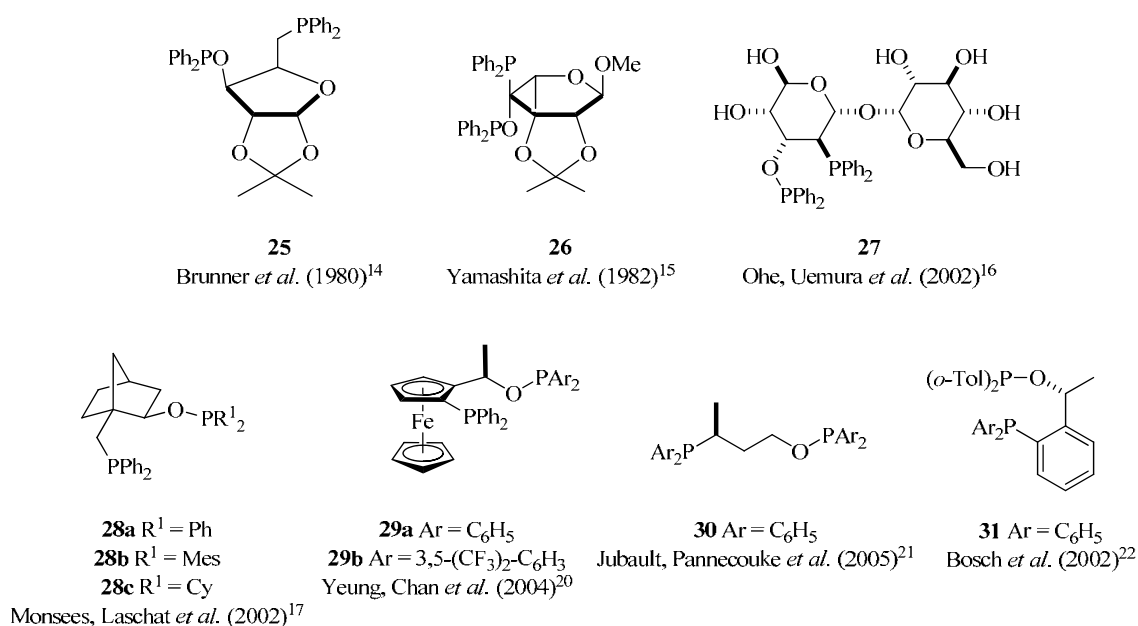


**Figure 5.** Known phosphine-phosphinite ligands.

The phosphine-phosphinite ligands **25**,<sup>14</sup> **26**<sup>15</sup> and **27**<sup>16</sup> derive from chiral pool carbohydrates. It should be recalled at this point that ligand **25** was the first phosphine-phosphinite reported in the literature (Brunner *et al.*, 1980).<sup>14</sup> Carbohydrates or sugar derivatives contain many hydroxy groups; therefore, the fundamental challenge in preparing these ligands comprised the selective transformation of a limited number of hydroxy groups into phosphine groups. The phosphine groups were usually introduced late in the synthesis, once the desired OH groups had been protected. These syntheses generally required very careful planning.

The rich chemistry of terpenes, and their availability from the chiral pool, has inspired researchers to use them as starting materials for chiral ligands. For example, the phosphine-phosphinites **28a-c** were obtained in six steps from (1*S*)-

<sup>14</sup> Brunner, H.; Pieronczyk, W. *J. Chem. Res., Synop.* **1980**, 76.

<sup>15</sup> Yamashita, M.; Hiramatsu, K.; Yamada, M.; Suzuki, N.; Inokawa, S. *Bull. Chem. Soc. Jpn.* **1982**, 55, 2917-21.

<sup>16</sup> Ohe, K.; Morioka, K.; Yonehara, K.; Uemura, S. *Tetrahedron: Asymmetry* **2002**, 13, 2155-2160.

(+)-camphorsulphonic acid.<sup>17</sup> The procedure enabled incorporation of different phosphinite moieties in the final ligands, facilitating the study of electronic and steric effects on asymmetric catalysis.

Chiral ligands containing ferrocene have proven invaluable in several transition metal-catalyzed asymmetric reactions.<sup>18</sup> Yeung & Chan *et al.* prepared a series of chiral phosphine-phosphinites (**29a** and **29b**) starting from enantiopure Ugi's<sup>19</sup>  $\alpha$ -dimethyl aminoethyl ferrocene.<sup>20</sup> Ligands **29a** and **29b** are very attractive for asymmetric catalysis, owing to their straightforward synthesis and their stability to air and moisture.

Finally, the ligands **30**<sup>21</sup> and **31**<sup>22</sup> were prepared from (*S*)-(+)-3-boronatodiphenylphosphonyl butanoic acid and enantioenriched haloaryl alcohol, respectively, using well-established procedures.

The catalytic activity of phosphine-phosphinite ligands **25-30** was tested in the Rh-catalyzed asymmetric hydrogenation of  $\alpha$ -dehydroamino acid derivatives **32a** and **32b**. The best conditions, with their corresponding results, are listed in Table 1.

---

<sup>17</sup> (a) Sell, T.; Laschat, S.; Dix, I.; Jones, P. G. *Eur. J. Org. Chem.* **2000**, 4119-4124. (b) Monsees, A.; Laschat, S. *Synlett* **2002**, 1011-1013.

<sup>18</sup> (a) Togni, A.; Halterman, R. L. in *Metallocenes*; Wiley-VCH: Weinheim, 1998; Vol. 2, p 685. (b) Richards, C. J.; Locke, A. J. *Tetrahedron: Asymmetry* **1998**, *9*, 2377-2407.

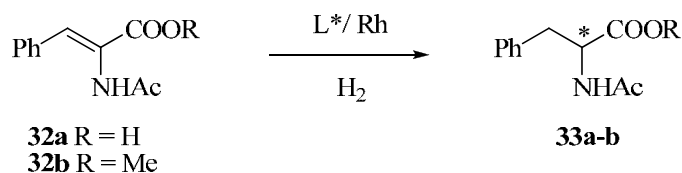
<sup>19</sup> Stueber, S.; Ugi, I. *Synthesis* **1973**, No. 5, 309.

<sup>20</sup> Jia, X.; Li, X.; Lam, W. S.; Kok, S. H. L.; Xu, L.; Lu, G.; Yeung, C.-H.; Chan, A. S. C. *Tetrahedron: Asymmetry* **2004**, *15*, 2273-2278.

<sup>21</sup> Boyer, N.; Leautey, M.; Jubault, P.; Pannecoucke, X.; Quirion, J.-C. *Tetrahedron: Asymmetry* **2005**, *16*, 2455-2458.

<sup>22</sup> Bosch, B. E.; Trauthwein, H.; Riermeier, T.; Dingerdissen, U.; Monsees, A. (Aventis Research & Technologies GmbH & Co Kg, Germany). Ger. Patent. DE 19918420, 2000.

**Table 1.** Asymmetric hydrogenation of dehydroaryl alanines **32** mediated by the complexes  $[\text{Rh}(\mathbf{25-30})]^+$ .<sup>a</sup>



Entry	Substrate	Ligand	Solvent	S/C ratio	H <sub>2</sub> (bar)	T (°C)	Conv. <sup>b</sup> (%)	ee <sup>c</sup> (%) (config.) <sup>d</sup>
1	<b>32a</b>	<b>25</b>	EtOH/benzene (1:1)	100	1.1	RT	> 99	35 ( <i>S</i> )
2	<b>32a</b>	<b>26</b>	EtOH/benzene (1:1)	100	50	RT	> 99	5 ( <i>R</i> )
3	<b>32b</b>	<b>27</b>	H <sub>2</sub> O/AcOEt (1:1)	50	50	RT	> 99 (> 99) <sup>e</sup>	73 (70) <sup>e</sup> ( <i>R</i> )
4	<b>32b</b>	<b>28b</b>	Toluene	200	5	RT	> 99	89 ( <i>S</i> )
5	<b>32b</b>	<b>29b</b>	Toluene/CH <sub>2</sub> Cl <sub>2</sub>	100	10	RT	> 99	90 ( <i>S</i> )
6	<b>32b</b>	<b>30</b>	CH <sub>2</sub> Cl <sub>2</sub>	200	1	RT	> 99	91 ( <i>S</i> )

<sup>a</sup> Depending on the case, the catalyst was either prepared “*in situ*” or previously synthesized.

<sup>b</sup> The conversion was quantified by <sup>1</sup>H-NMR or GC.

<sup>c</sup> The enantiomeric excesses were determined by HPLC or from reported values of optical rotation.

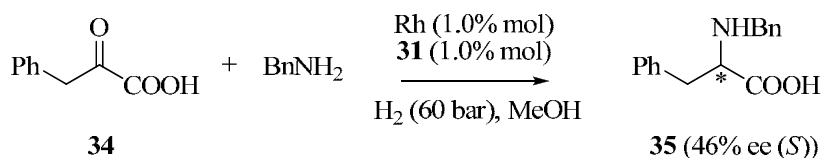
<sup>d</sup> The absolute configuration was assigned by comparison with published data.

<sup>e</sup> Results from the second catalytic cycle.

As observed in Table 1, phosphine-phosphinites **25-30** were very active, providing full conversion in all cases. Ligands **25-27** afforded poor enantioselectivities (5-73% ee, Entries 1-3), whereas **28-30** gave high enantioselectivities (89-91% ee, Entries 4-6).

Kadyrov, Börner *et al.* used high-throughput screening to identify highly enantioselective catalysts in the reductive amination of  $\alpha$ -ketoacids.<sup>23</sup> In this screening, phosphine-phosphinite ligand **31** was tested as a chiral catalyst in the Rh-mediated reductive amination of phenylpyruvic acid (**34**) with benzylamine, yielding moderate enantioselectivity (up to 46% ee, Scheme 6).

<sup>23</sup> Kadyrov, R.; Riermeier, T. H.; Dingerdissen, U.; Tararov, V.; Boerner, A. *J. Org. Chem.* **2003**, *68*, 4067-4070.



**Scheme 6.** Rh-catalyzed reductive amination of phenylpyruvic acid (**34**) with benzylamine using phosphine-phosphinite **31** as chiral ligand.

The most common trivalent phosphorus ligands contain stereogenic elements on the carbon backbone. There have been major advances in the synthesis of enantiopure phosphorus compounds containing stereogenic *P*-centres; these have primarily stemmed from using borane as protecting group.<sup>24</sup> This strategy has also been used to prepare ligands. Furthermore, enantiopure phosphorus derivatives with an *o*-hydroxyaryl group have recently gained attention as ligands in various asymmetric reactions<sup>25</sup> and as precursors to other phosphorus ligands. Figure 6 shows two representative ligands of this type: **38** and **41**, prepared from bromophenol derivatives **36** and **39**, respectively (Scheme 7).

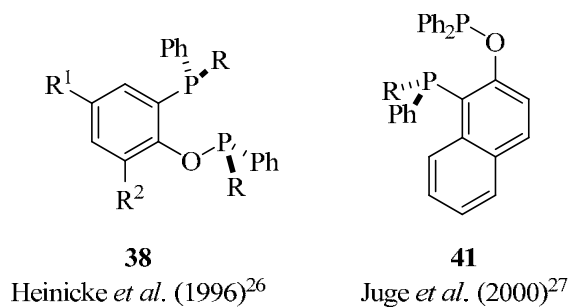
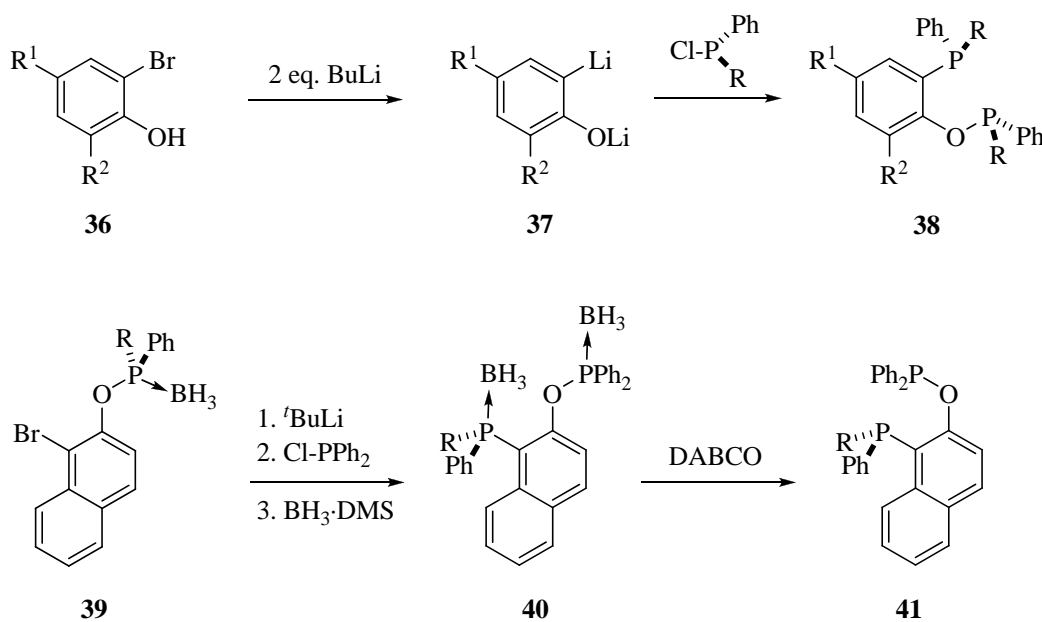


**Figure 6.** Phosphine-phosphinite ligands derived from *o*-hydroxyaryl derivatives.

<sup>24</sup> For a review see: Ohff, M.; Holz, J.; Quirnbach, M.; Boerner, A. *Synthesis* **1998**, 1391-1415.

<sup>25</sup> (a) Brunel, J.-M.; Constantieux, T.; Legrand, O.; Buono, G. *Tetrahedron Lett.* **1998**, *39*, 2961-2964. (b) Legrand, O.; Brunel, J.-M.; Buono, G. *Tetrahedron Lett.* **1998**, *39*, 9419-9422. (c) Buono, G.; Chiodi, O.; Wills, M. *Synlett* **1999**, 377-388. (d) Legrand, O.; Brunel, J.-M.; Buono, G. *Tetrahedron Lett.* **2000**, *41*, 2105-2109.

The ligands **38** were prepared by trapping the *C,O*-phenol dilithium reagents **37** (obtained from the corresponding bromophenols **36** by reaction with two equivalents of butyl lithium [Scheme 7]) with an appropriate chlorophosphine.<sup>6b,26</sup> Ligand **41** was synthesized rather elegantly (Scheme 7): firstly, the C-Br bond in **39** was lithiated, inducing an *ortho* Fries-like rearrangement, which leads to migration of the phosphorus group to the *ortho*-hydroxy carbon with retention of configuration; secondly, the rearranged product was trapped with chlorodiphenylphosphine and then protected with borane to give the intermediate **40**; and finally, the resulting borane complex was cleaved with DABCO.<sup>27</sup> However, to the best of our knowledge, there are no literature reports on using **38** or **41** as chiral ligands in asymmetric catalysis.

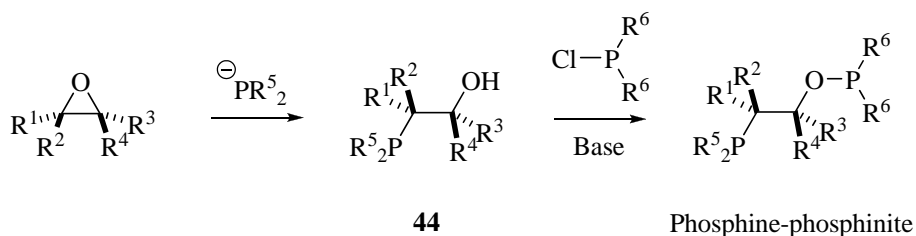


**Scheme 7.** Synthesis of phosphine-phosphinite ligands **38** and **41**.

<sup>26</sup> Heinicke, J.; Kadyrov, R.; Kindermann, M. K.; Koesling, M.; Jones, P. G. *Chem. Ber.* **1996**, *129*, 1547-1560.

<sup>27</sup> Moulin, D.; Bago, S.; Bauduin, C.; Darcel, C.; Juge, S. *Tetrahedron: Asymmetry* **2000**, *11*, 3939-3956.

Another convenient route to phosphine-phosphinite ligands is the ring-opening of epoxides followed by *O*-phosphorylation of the resulting products, which proceeds by an S<sub>N</sub>2 mechanism. Alkali metal (Li<sup>+</sup>, Na<sup>+</sup> or K<sup>+</sup>) phosphanides are normally employed as the phosphorus nucleophiles. The only drawback in this strategy is formation of the regioisomer in the ring-opening step. Further derivatization of the resulting phosphino alcohols **44** in the presence of base and the appropriate electrophilic trivalent phosphorus reagents leads to the desired phosphine-phosphinite ligands (see Scheme 8). Compounds **45** and **46** (Figure 7) were prepared by this route.



**Scheme 8.** General protocol for synthesizing phosphine-phosphinites via epoxide ring-opening.

Compound **45** represents a special class of ligands called “tripod ligands”, which contain at least three different binding groups capable of coordinating to metal centres (*e.g.* Rh).<sup>28</sup> Ligand **45**<sup>28</sup> was prepared from epichlorohydrin, whereas **46**<sup>29</sup> was synthesized from enantiomerically pure styrene oxide.

<sup>28</sup> (a) Scherer, J.; Huttner, G.; Buechner, M. *Chem. Ber.* **1996**, *129*, 697-713. (b) Scherer, J.; Huttner, G.; Buechner, M.; Bakos, J. *J. Organomet. Chem.* **1996**, *520*, 45-58. (c) Scherer, J.; Huttner, G.; Walter, O.; Janssen, B. C.; Zsolnai, L. *Chem. Ber.* **1996**, *129*, 1603-1615.

<sup>29</sup> Jiang, R.; He, W.; Wang, P.-a.; Li, X.-y.; Zhang, S.-y. *Fenzi Cuihua* **2006**, *20*, 207-210.



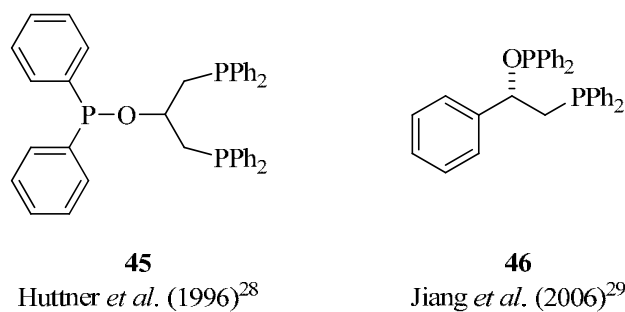
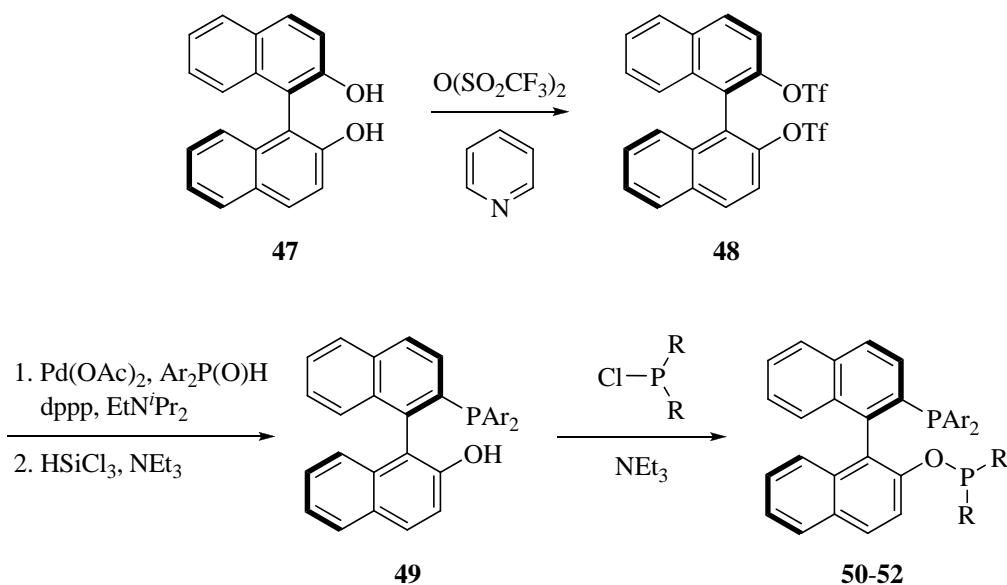


**Figure 7.** Phosphine-phosphinite ligands prepared via epoxide ring-opening.

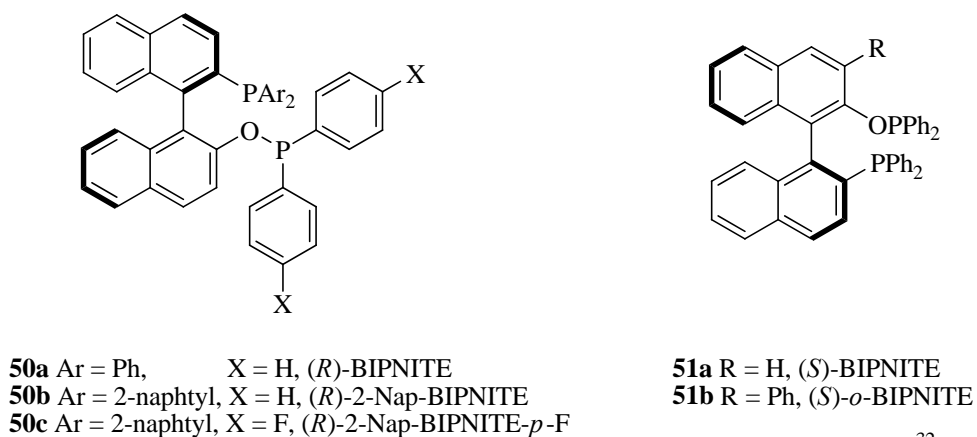
Rh(I)-complexes of **45** and **46** were studied as catalysts in the Rh-catalyzed enantioselective hydrogenation of functionalized alkenes such as dehydro  $\alpha$ -amino acids. The complexes based on **45** were catalytically rather inactive: both the conversion and enantioselectivity were rather low. The tridentate-coordination mode of **45** to the Rhodium centre appears to be detrimental to hydrogenation. In contrast, the complex based on **46** mediated the hydrogenation of methyl (*Z*)- $\alpha$ -acetamidocinnamate **32b** in 77% ee.

Ligands with a conformationally stable biaryl group, such as those with a binaphthyl backbone, have been widely used in asymmetric catalysis, providing excellent rates of conversion and enantioselectivities. Various binding groups have been attached to the binaphthyl backbone. In 1996 Takaya *et al.* developed phosphine-phosphinites **50a-c** (Figure 8), which contain a stereogenic axis.<sup>30</sup> Following Takaya's synthetic methodology, compounds **50-52** (Figure 8) were readily synthesized by reacting the phosphino alcohols **49** with the appropriate chlorophosphine, using triethylamine as base. Compounds **49** were prepared from enantiomerically pure BINOL (**47**), through generation of the ditriflate **48**, followed by Pd-catalyzed phosphorus-carbon bond formation, and finally, reduction of the resulting phosphine oxide with SiHCl<sub>3</sub>-NEt<sub>3</sub> (Scheme 9).

<sup>30</sup> Nozaki, K.; Kumobayashi, H.; Horiuchi, T.; Takaya, H.; Saito, T.; Yoshida, A.; Matsumura, K.; Kato, Y.; Imai, T.; Miura, T. *J. Org. Chem.* **1996**, *61*, 7658-7659.

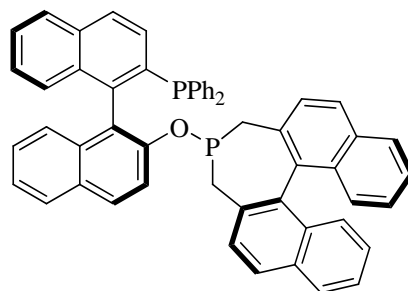


**Scheme 9.** General strategy for synthesizing the phosphine-phosphinites **50-52** from optically pure BINOL (**47**).



Zhang *et al.* (2004)<sup>32</sup>

Takaya, Nozaki *et al.* (1996)<sup>30</sup>

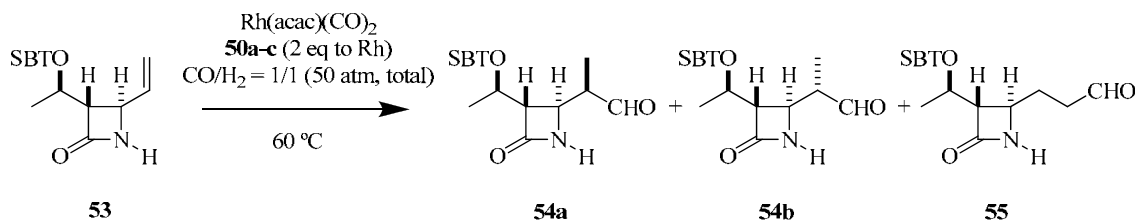


**52**

Beller *et al.* (2008)<sup>31</sup>

**Figure 8.** Phosphine-phosphinite ligands containing a stereogenic axis.

Phosphine-phosphinite ligands **50a-c** were investigated in the Rh-catalyzed asymmetric hydroformylation of 4-vinyl  $\beta$ -lactam (**53**), a precursor of  $\beta$ -methylcarbapenem antibiotics (Scheme 10).<sup>30</sup>



**Scheme 10.** Rh-catalyzed asymmetric hydroformylation of 4-vinyl  $\beta$ -lactam (**53**) using phosphine-phosphinite ligands **50a-c**.

For each of the ligands **50a-c**, the corresponding Rh complex provided the desired branched aldehyde **54a** with excellent enantioselectivity (90-92% ee); however, **50b** and **50c** offered higher regioselectivity (74/26 of **54/55**) than did **50a** (64/36 of **54/55**). Non-reproducible results were obtained for the Rh-catalyzed asymmetric hydroformylation of styrene using ligand **52**; this probably resulted from decomposition of the ligand during the reaction.<sup>31</sup>

The BIPNITE ligands **51a** and **51b** were tested in the Rh-mediated asymmetric hydrogenation of dehydroamino acid derivatives. The Rh-complex of ligand **51b** afforded excellent results (> 99% ee in almost all cases). This is probably due to the enhanced conformational rigidity of the phosphinite moiety caused by introduction of the *ortho* phenyl substituent.<sup>32</sup>

<sup>31</sup> Erre, G.; Enthaler, S.; Junge, K.; Gladiali, S.; Beller, M. *J. Mol. Catal. A: Chem.* **2008**, *280*, 148-155.

<sup>32</sup> Yan, Y.; Chi, Y.; Zhang, X. *Tetrahedron: Asymmetry* **2004**, *15*, 2173-2175.

### 1.1.3 PHOSPHINE-PHOSPHITE LIGANDS

Phosphine-phosphites have been widely studied in asymmetric catalysis. As in the case of phosphine-phosphinites, the two phosphorus groups are electronically distinct: when coordinated to a metal centre, the phosphine group behaves as a good  $\sigma$ -donor, whereas the phosphite moiety has a poorer  $\sigma$ -donor ability and an enhanced  $\pi$ -acceptor character (Figure 9).<sup>33</sup>

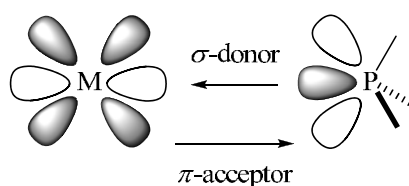


**Figure 9.**  $\sigma$ - and  $\pi$ -donation between a phosphorus ligand and a metal.

The synthetic strategies developed for phosphine-phosphites are quite similar to those described above for phosphine-phosphinite ligands (see Section 1.1.2): they primarily differ in that chlorophosphites, instead of chlorophosphines, are used as the electrophilic phosphorus reagents.

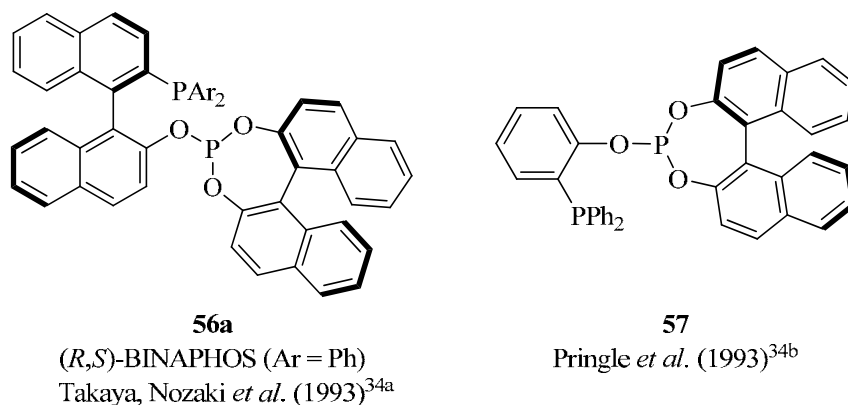


**Figure 10.** The first reported chiral phosphine-phosphites.

<sup>33</sup> *The Organometallic Chemistry of the Transition Metals*; Crabtree, R.H., Ed; John Wiley & Sons: New York, 1988.

The first examples of enantiopure phosphine-phosphites (Figure 10) were simultaneously reported in 1993 by the groups of Takaya and Pringle.<sup>34</sup> In these compounds, the two phosphorus groups are situated on structurally diverse carbon backbones. They both contain an axis as the stereogenic element that confers the stereodifferentiating properties to the ligand.

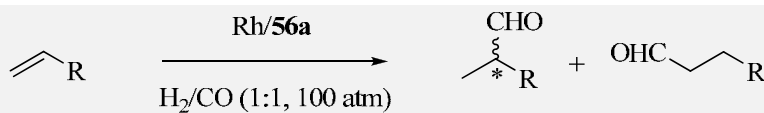
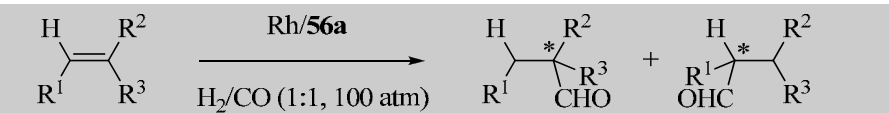
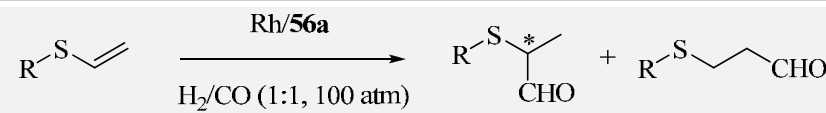
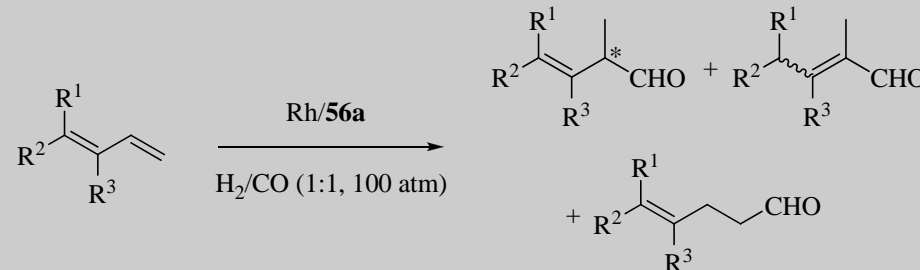
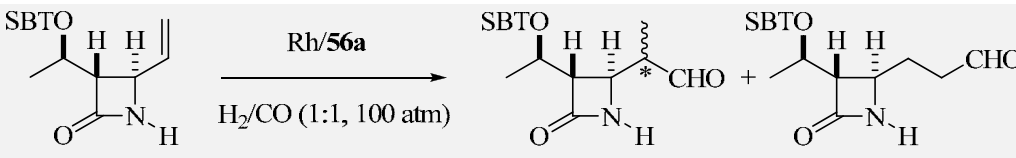
To the best of our knowledge, no catalytic applications have been described for the phosphine-phosphites reported by Pringle. Conversely, (*R,S*)-BINAPHOS (**56a**) is the most widely studied phosphine-phosphite in enantioselective catalysis and has afforded excellent enantioselectivities in various asymmetric transformations. As such, it should be regarded as a “*privileged structure*” in asymmetric catalysis.<sup>35</sup> (*R,S*)-BINAPHOS is prepared similarly to the phosphine-phosphinites **50-52** (Scheme 9), except that chlorophosphite is used instead of chlorodiarylphosphine. Application of (*R,S*)-BINAPHOS in catalytic asymmetric reactions is summarized in Table 2.

---

<sup>34</sup> (a) Sakai, N.; Mano, S.; Nozaki, K.; Takaya, H. *J. Am. Chem. Soc.* **1993**, *115*, 7033-4. (b) Baker, M. J.; Pringle, P. G. *J. Chem. Soc., Chem. Commun.* **1993**, 314-16.

<sup>35</sup> Yoon, T. P.; Jacobsen, E. N. *Science (Washington, DC, U. S.)* **2003**, *299*, 1691-1693. The term “*Privileged Chiral Ligand*” was coined by E. Jacobsen to indicate certain classes of enantioselective catalysts that are highly stereoselective over a wide range of mechanistically unrelated transformations. Noteworthy examples include chiral Salens, BINOL, BINAP, Duphos, metal complexes derived from Britzinger’s ligand, TADDOLates, bisoxazolines, and Cinchona alkaloids.

**Table 2.** Applications of (*R,S*)-BINAPHOS (**56a**) in asymmetric catalysis.

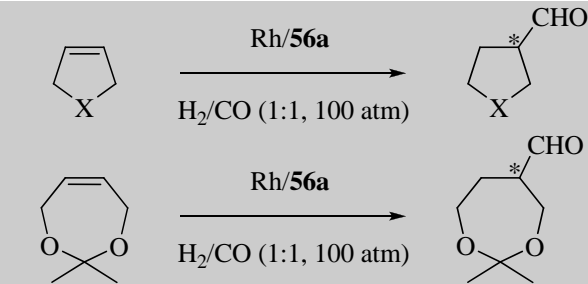
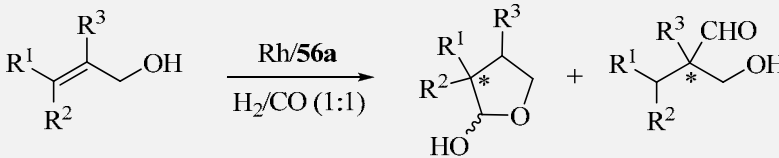
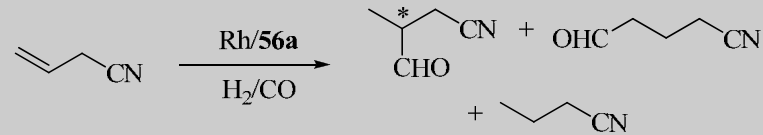
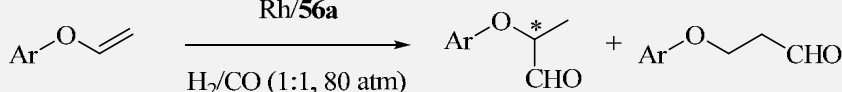
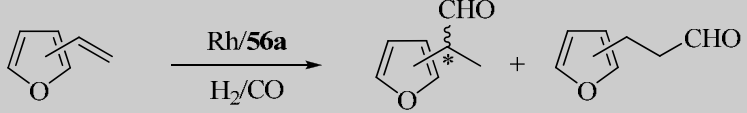
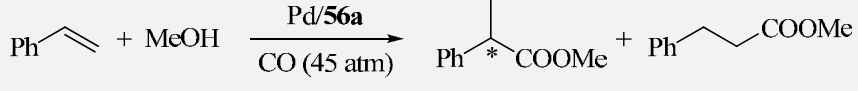
Entry	Metal-catalyzed enantioselective reactions
1	 <p style="text-align: center;">Rh-catalyzed asymmetric hydroformylation of olefins<sup>34a,36</sup></p>
2	 <p style="text-align: center;">Rh-catalyzed asymmetric hydroformylation of 1,2-disubstituted olefins<sup>37</sup></p>
3	 <p style="text-align: center;">Rh-catalyzed asymmetric hydroformylation of sulphur-containing olefins<sup>38</sup></p>
4	 <p style="text-align: center;">Rh-catalyzed asymmetric hydroformylation of conjugated dienes<sup>39</sup></p>
5	 <p style="text-align: center;">Rh-catalyzed asymmetric hydroformylation of vinyl <math>\beta</math>-lactams<sup>30</sup></p>

<sup>36</sup> Nozaki, K.; Sakai, N.; Nanno, T.; Higashijima, T.; Mano, S.; Horiuchi, T.; Takaya, H. *J. Am. Chem. Soc.* **1997**, *119*, 4413-4423.

<sup>37</sup> (a) Sakai, N.; Nozaki, K.; Takaya, H. *J. Chem. Soc., Chem. Commun.* **1994**, 395-6. (b) Nozaki, K.; Matsuo, T.; Shibahara, F.; Hiyama, T. *Adv. Synth. Catal.* **2001**, *343*, 61-63.

<sup>38</sup> Nanno, T.; Sakai, N.; Nozaki, K.; Takaya, H. *Tetrahedron: Asymmetry* **1995**, *6*, 2583-91.

<sup>39</sup> (a) Horiuchi, T.; Ohta, T.; Nozaki, K.; Takaya, H. *Chem. Comm.* **1996**, 155-56. (b) Horiuchi, T.; Ohta, T.; Shirakawa, E.; Nozaki, K.; Takaya, H. *Tetrahedron* **1997**, *53*, 7795-7804.

6	 <p>Rh-catalyzed asymmetric hydroformylation of heterocyclic olefins<sup>40</sup></p>
7	 <p>Rh-catalyzed asymmetric hydroformylation of allylic alcohols<sup>41</sup></p>
8	 <p>Rh-catalyzed asymmetric hydroformylation of allyl cyanides<sup>42</sup></p>
9	 <p>Rh-catalyzed asymmetric hydroformylation of aryl vinyl ethers<sup>43</sup></p>
10	 <p>Rh-catalyzed asymmetric hydroformylation of vinylfurans<sup>44</sup></p>
11	 <p>Rh-catalyzed asymmetric hydroesterification of styrene<sup>45</sup></p>

<sup>40</sup> Horiuchi, T.; Ohta, T.; Shirakawa, E.; Nozaki, K.; Takaya, H. *J. Org. Chem.* **1997**, *62*, 4285-4292.

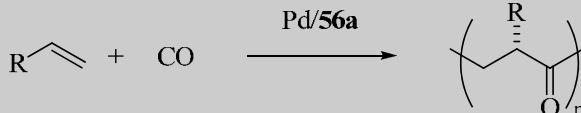
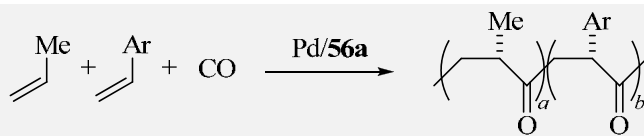
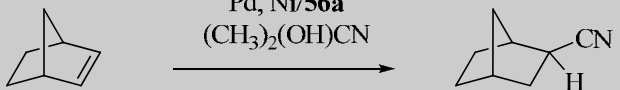
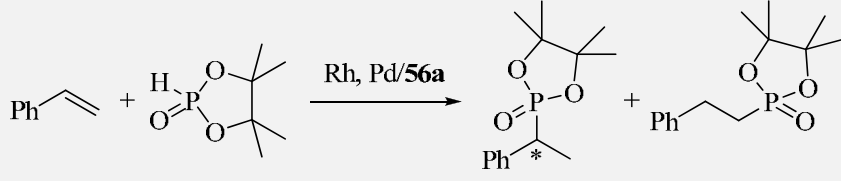
<sup>41</sup> Nozaki, K.; Li, W.-g.; Horiuchi, T.; Takaya, H. *Tetrahedron Lett.* **1997**, *38*, 4611-4614.

<sup>42</sup> (a) Lambers-Verstappen, M. M. H.; de Vries, J. G. *Adv. Synth. Catal.* **2003**, *345*, 478-482. (b) Cobley, C. J.; Gardner, K.; Klosin, J.; Praquin, C.; Hill, C.; Whiteker, G. T.; Zanotti-Gerosa, A.; Petersen, J. L.; Abboud, K. A. *J. Org. Chem.* **2004**, *69*, 4031-4040. (c) Cobley, C. J.; Klosin, J.; Qin, C.; Whiteker, G. T. *Org. Lett.* **2004**, *6*, 3277-3280.

<sup>43</sup> Solinas, M.; Gladiali, S.; Marchetti, M. *J. Mol. Catal. A: Chem.* **2005**, *226*, 141-147.

<sup>44</sup> (a) Nakano, K.; Tanaka, R.; Nozaki, K. *Helv. Chim. Acta* **2006**, *89*, 1681-1686. (b) Tanaka, R.; Nakano, K.; Nozaki, K. *J. Org. Chem.* **2007**, *72*, 8671-8676.

<sup>45</sup> Nozaki, K.; Lakshmi Kantam, M.; Horiuchi, T.; Takaya, H. *J. Mol. Catal. A: Chem.* **1997**, *118*, 247-253.

<b>12</b>	
	Pd-catalyzed alternating copolymerization of alkenes with carbon monoxide <sup>46</sup>
<b>13</b>	
	Pd-catalyzed asymmetric terpolymerization of aliphatic alkenes, vinylarenes with carbon monoxide <sup>47</sup>
<b>14</b>	
	Pd, Ni-catalyzed asymmetric hydrocyanation of norbornene <sup>48</sup>
<b>15</b>	
	Rh, Pd-catalyzed asymmetric hydrophosphorylation of vinylarenes <sup>49</sup>

As reflected in Table 2, metal complexes of (*R,S*)-BINAPHOS are invaluable for numerous enantioselective reactions, particularly in the Rh-catalyzed asymmetric hydroformylation of a broad variety of structurally diverse olefinic substrates (Table 2, Entries 1-10). The Rh-complex of (*R,S*)-BINAPHOS—usually generated *in situ*, by mixing [Rh(acac)(CO)<sub>2</sub>] with an excess of the ligand—has provided extremely high regio- and enantioselectivities in the hydroformylation of several terminal alkenes (see Table 3). Indeed, these results are among the best reported for hydroformylations.<sup>34a,36</sup>

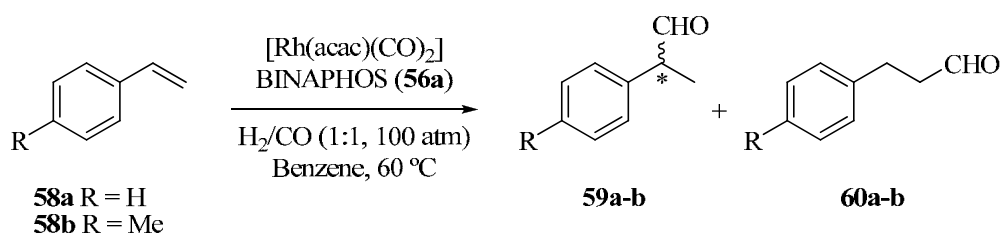
<sup>46</sup> (a) Nozaki, K.; Sato, N.; Takaya, H. *J. Am. Chem. Soc.* **1995**, *117*, 9911-12. (b) Nozaki, K.; Sato, N.; Tonomura, Y.; Yasutomi, M.; Takaya, H.; Hiyama, T.; Matsubara, T.; Koga, N. *J. Am. Chem. Soc.* **1997**, *119*, 12779-12795. (c) Nozaki, K.; Yasutomi, M.; Nakamoto, K.; Hiyama, T. *Polyhedron* **1998**, *17*, 1159-1164. (d) Nozaki, K.; Komaki, H.; Kawashima, Y.; Hiyama, T.; Matsubara, T. *J. Am. Chem. Soc.* **2001**, *123*, 534-544.

<sup>47</sup> (a) Nozaki, K.; Kawashima, Y.; Nakamoto, K.; Hiyama, T. *Macromolecules* **1999**, *32*, 5168-5170. (b) Kawashima, Y.; Nozaki, K.; Hiyama, T. *Inorg. Chim. Acta* **2003**, *350*, 577-582.

<sup>48</sup> Horiuchi, T.; Shirakawa, E.; Nozaki, K.; Takaya, H. *Tetrahedron: Asymmetry* **1997**, *8*, 57-63.

<sup>49</sup> Shulyupin, M. O.; Francio, G.; Beletskaya, I. P.; Leitner, W. *Adv. Synth. Catal.* **2005**, *347*, 667-672.



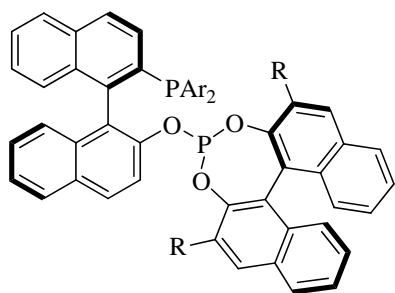
**Table 3.** Asymmetric hydroformylation of olefins catalyzed by the complex  $[\text{Rh}(\text{acac})(\text{CO})_2(\text{BINAPHOS})]$ .<sup>a</sup>

Entry	Substrate	Conv. (%)	Ratio of 59/60	% ee of 59
1	<b>58a</b>	>99	88/12	94
2	<b>58b</b>	>99	86/14	95

<sup>a</sup> The Rh-complex was prepared *in situ*.

The impact of BINAPHOS in the field of asymmetric catalysis has not only lied in its outstanding asymmetric properties, but also because it has served as inspiration for the preparation of the related phosphine-phosphite ligands **61-68** (Figure 11).<sup>34a</sup> These compounds have chiefly been employed as chiral ligands for hydroformylation (see Table 2). Rh-complexes of ligands **63** and **64**, which contain an atropisomerically stable biphenyl fragment, afforded high enantiomeric excesses in asymmetric hydroformylations of various alkenes.<sup>50</sup> Furthermore, in some asymmetric hydroformylations **65** and **66** gave higher regioselectivity than did BINAPHOS. However, they provided relatively low enantioselectivity, especially ligand **65**, whose phosphite moiety does not contain any stereogenic elements (Table 4, Entries 1 and 2).<sup>30,36</sup>

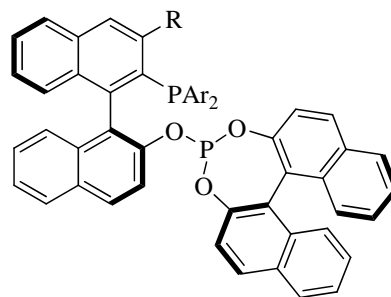
<sup>50</sup> Higashizima, T.; Sakai, N.; Nozaki, K.; Takaya, H. *Tetrahedron Lett.* **1994**, 35, 2023-6.



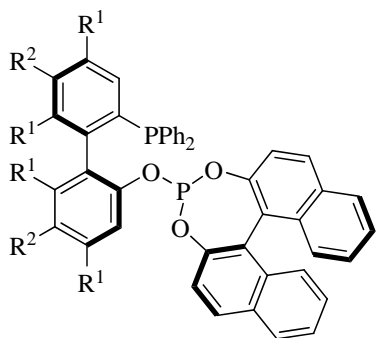
**61a-g** (Ar = Ph, 3,5-Me<sub>2</sub>-Ph, 3-MeO-Ph, 3-<sup>i</sup>PrO-Ph,  
 3,5-(MeO)<sub>2</sub>-Ph, 4-MeO-Ph, 3-Me-Ph;  
 R = H in all cases)

**61h-i** (Ar = Ph; R = H, Me)

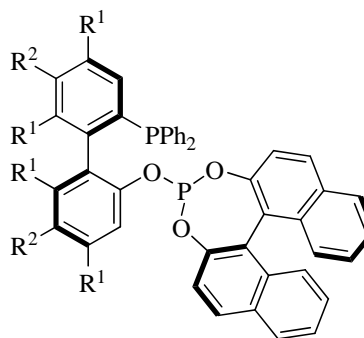
**61j** (Ar = ; R = H) (*R,S*)-3-H<sub>2</sub>F<sub>6</sub>-BINAPHOS



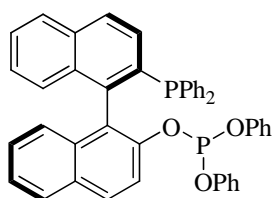
**62a** Ar = Ph; R = H (*S,R*)-BINAPHOS  
**62b** Ar = Ph; R = Ph (*S,R*)-*o*-BINAPHOS



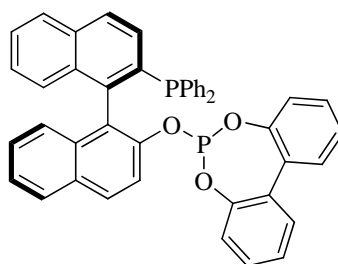
**63a** R<sup>1</sup> = Me; R<sup>2</sup> = Cl (*S,R*)-BIPHEMPHOS  
**63b** R<sup>1</sup> = R<sup>2</sup> = H



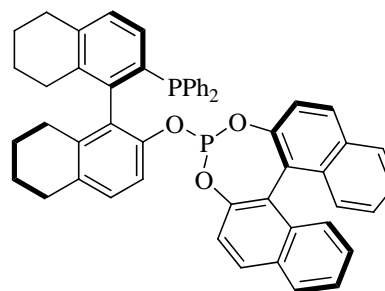
**64a** R<sup>1</sup> = Me; R<sup>2</sup> = Cl (*R,R*)-BIPHEMPHOS  
**64b** R<sup>1</sup> = R<sup>2</sup> = H



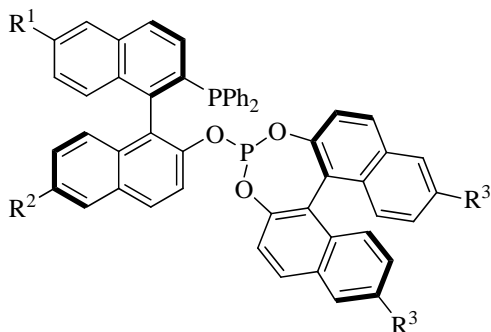
**65** (*R*)-BIPPHOS



**66**



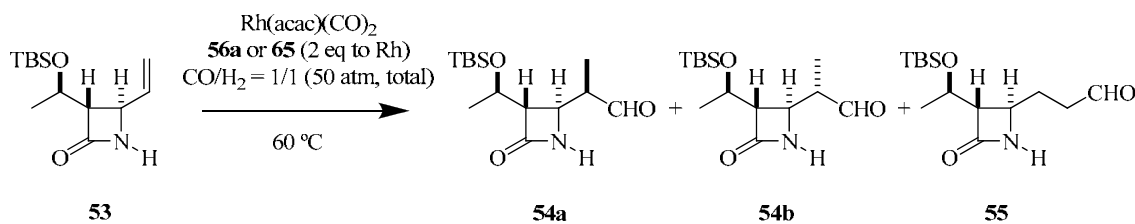
**67** (*R,S*)-H<sub>8</sub>-BINAPHOS



**68a** R<sup>1</sup> = R<sup>3</sup> = H, R<sup>2</sup> = CH=CH<sub>2</sub>  
**68b** R<sup>1</sup> = R<sup>2</sup> = H, R<sup>3</sup> = CH=CH<sub>2</sub>  
**68c** R<sup>1</sup> = H, R<sup>2</sup> = R<sup>3</sup> = CH=CH<sub>2</sub>  
**68d** R<sup>1</sup> = R<sup>2</sup> = R<sup>f</sup>(CH<sub>2</sub>)<sub>n</sub> (*R,S*)-[R<sup>f</sup>(CH<sub>2</sub>)<sub>n</sub>]<sub>m</sub>-BINAPHOS

**Figure 11.** BINAPHOS-related ligands.

**Table 4.** Asymmetric hydroformylation of 4-vinyl  $\beta$ -lactam (**53**) catalyzed by the Rh(I)-complex of either (*R,S*)-BINAPHOS (**56a**) or (*R*)-BIPPPOS (**65**).<sup>a</sup>



Entry	Ligand	Total CHO yield (%)	Ratio of 54/55	% ee of 54
1	<b>56a</b>	95	55/45	86
2	<b>65</b>	92	71/29	20

<sup>a</sup> The Rh-complex was prepared *in situ*.

Nozaki *et al.* revealed that the structure of ligand **67** is crucial in the Pd-catalyzed asymmetric alternating copolymerization of propene with carbon monoxide.<sup>46c</sup> Minor changes to the ligand structure (relative to BINAPHOS) produced completely isotactic copolymer in a highly enantioselective fashion.

In homogeneous catalysis there is a need for new developments in catalyst recycling and product separation. Ligands **68a-c** contain a vinyl group that enables incorporation of the chiral fragment into a polymer network, thereby making heterogeneous versions of BINAPHOS possible.<sup>51a</sup> Ligands **61j** and **68d** contain perfluoroalkyl-substituted groups in both the phosphine and phosphite moieties, which allows their use for asymmetric transformations in supercritical  $\text{CO}_2$  and which facilitates catalyst recovery.<sup>52a</sup> Catalytic systems composed of one of the ligands **61j** or **68a-d**, and either Rhodium or Palladium precursors,

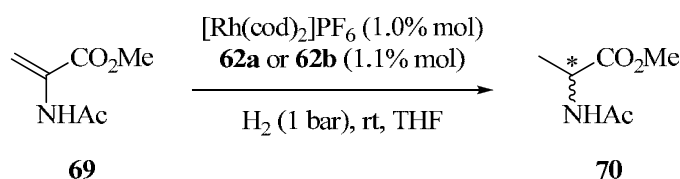
<sup>51</sup> (a) Nozaki, K.; Itoi, Y.; Shibahara, F.; Shirakawa, E.; Ohta, T.; Takaya, H.; Hiyama, T. *J. Am. Chem. Soc.* **1998**, *120*, 4051-4052. (b) Nozaki, K.; Shibahara, F.; Itoi, Y.; Shirakawa, E.; Ohta, T.; Takaya, H.; Hiyama, T. *Bull. Chem. Soc. Jpn.* **1999**, *72*, 1911-1918. (c) Nozaki, K.; Shibahara, F.; Hiyama, T. *Chem. Lett.* **2000**, 694-695. (d) Shibahara, F.; Nozaki, K.; Hiyama, T. *J. Am. Chem. Soc.* **2003**, *125*, 8555-8560. (e) Kinoshita, S.; Shibahara, F.; Nozaki, K. *Green Chem.* **2005**, *7*, 256-258.

<sup>52</sup> (a) Francio, G.; Leitner, W. *Chem. Comm.* **1999**, 1663-1664. (b) Bonafoux, D.; Hua, Z.; Wang, B.; Ojima, I. *J. Fluorine Chem.* **2001**, *112*, 101-108. (c) Francio, G.; Wittmann, K.; Leitner, W. *J. Organomet. Chem.* **2001**, *621*, 130-142. (d) Burgemeister, K.; Francio, G.; Hugl, H.; Leitner, W. *Chem. Comm.* **2005**, 6026-6028. (e) Burgemeister, K.; Francio, G.; Gego, V. H.; Greiner, L.; Hugl, H.; Leitner, W. *Chem.--Eur. J.* **2007**, *13*, 2798-2804.

have been used in hydroformylation, alternating copolymerization, and hydrogenation with excellent results.<sup>51,52</sup>

To the best of our knowledge, few examples of asymmetric hydrogenations using BINAPHOS or closely related analogues have been reported. Apart from perfluoroalkyl-substituted derivatives **61j** and **68d**,<sup>52</sup> Zhang *et al.* studied (*S,R*)-*o*-BINAPHOS (**62b**) in the Rh-mediated enantioselective hydrogenation of  $\alpha$ -dehydroamino acid derivatives. The Rh-complex of (*S,R*)-*o*-BINAPHOS (**62b**), prepared *in situ* from the ligand and suitable Rhodium precursors, afforded excellent enantioselectivities in the hydrogenations of methyl  $\alpha$ -acetamidoacrylate (**69**) and various related substrates (> 99% ee in almost all cases).<sup>32</sup> These results were slightly better than those obtained with the Rh-complex of (*S,R*)-BINAPHOS (**62a**) (Table 5, Entries 1 and 2).

**Table 5.** Rh-catalyzed asymmetric hydrogenation of methyl  $\alpha$ -acetamidoacrylate (**69**) using (*S,R*)-BINAPHOS (**62a**) or (*S,R*)-*o*-BINAPHOS (**62b**).<sup>a</sup>

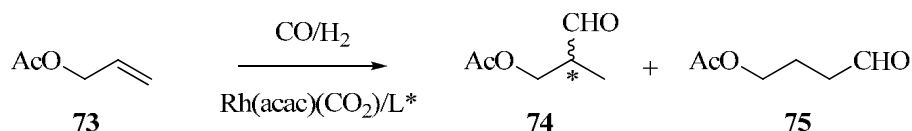


Entry	Ligand	Conv. (%)	ee (%) (conf)
1	<b>62a</b>	> 99	96 ( <i>S</i> )
2	<b>62b</b>	> 99	> 99 ( <i>S</i> )

<sup>a</sup> The Rh-complex was prepared *in situ*.

Several phosphine-phosphite ligands were later prepared in multistep reactions from “chiral pool” materials, thereby obviating the tedious step of optical resolution. The ligands **71** and **72** were prepared from enantiomerically pure *cis*- and *trans*-tetrahydrofuran derivatives, respectively, which are readily available from *L*- or *D*-ascorbic acid (Figure 12).<sup>53</sup>

Ligands **71** and **72** were evaluated in the Rh-mediated hydroformylation of allyl acetate **73** (Scheme 11), in which they provided enantioselectivities of up to 44% ee. The results depended on the bulk of the aromatic groups and the relative stereochemistry of the two phosphorus functionalities: thus, a *trans* arrangement of the substituents and an (*S*)-configuration for the binaphthyl unit, provided the highest ratio of branched isomer to linear isomer as well as the highest enantioselectivity.



**Scheme 11.** Rh-catalyzed asymmetric hydroformylation of allyl acetates.

Phosphine-phosphite ligands also can be synthesized via ring-opening of epoxides with phosphorus-containing nucleophilic reagents, followed by derivatization of the resulting phosphino alcohols with a chlorophosphite, analogously to the preparation of phosphine-phosphinite ligands (see Section 1.1.2, Scheme 8). This procedure has been used by different groups to prepare the enantiomerically pure phosphine-phosphite ligands **76-81** (Figure 12).

Huttner *et al.* prepared the tripod ligands **76-78** from epichlorohydrin.<sup>28</sup> They then isolated Rh-complexes of **76-78**, which they subsequently tested in Rh-mediated enantioselective hydrogenations of prochiral olefins, observing poor activity and low enantioselectivity.

<sup>53</sup> (a) Boerner, A.; Holz, J.; Ward, J.; Kagan, H. B. *J. Org. Chem.* **1993**, *58*, 6814-17. (b) Kless, A.; Holz, J.; Heller, D.; Kadyrov, R.; Selke, R.; Fischer, C.; Boerner, A. *Tetrahedron: Asymmetry* **1996**, *7*, 33-6.

Van Leeuwen *et al.* synthesized **79-81** from enantiomerically pure epoxides (propene oxide or styrene oxide) and a phosphorus-containing carbon nucleophiles or nucleophilic phosphorus reagents, which in some cases were enantiomerically pure.<sup>54</sup> Therefore, compounds **79-81** contained up to three stereogenic elements: a stereogenic carbon centre arising from the epoxide; an asymmetric phosphorus atom (provided that an enantiomerically pure phosphorus reagent was used in the ring-opening); and a configurationally stable biaryl unit (in compounds **81**). They systematically varied the stereogenic elements, and then studied the effects on enantioselectivity in several transformations. Van Leeuwen *et al.* evaluated **79-81** in several enantioselective transformations. Using **79e** as chiral ligand in Rh-catalyzed asymmetric hydrogenations of methyl (*N*)-acetylaminoacrylate (**69**) and methyl (*Z*)-(*N*)-acetylaminocinnamate (**32b**), they obtained excellent enantioselectivities (up to 99% ee).<sup>54d</sup> However, when using ligands **79-81** in Pd-catalyzed asymmetric allylic alkylations,<sup>54b</sup> Rh-catalyzed enantioselective hydroformylations,<sup>54a</sup> and Cu-mediated asymmetric 1,4-additions,<sup>54c</sup> they obtained only moderate to good enantioselectivities. In most of the transformations, the stereochemical outcome was dictated by the configurationally stable biaryl moiety.

---

<sup>54</sup> (a) Deerenberg, S.; Kamer, P. C. J.; Van Leeuwen, P. W. N. M. *Organometallics* **2000**, *19*, 2065-2072. (b) Deerenberg, S.; Schrekker, H. S.; Van Strijdonck, G. P. F.; Kamer, P. C. J.; Van Leeuwen, P. W. N. M.; Fraanje, J.; Goubitz, K. *J. Org. Chem.* **2000**, *65*, 4810-4817. (c) Dieguez, M.; Deerenberg, S.; Pamies, O.; Claver, C.; van Leeuwen, P. W. N. M.; Kamer, P. *Tetrahedron: Asymmetry* **2000**, *11*, 3161-3166. (d) Deerenberg, S.; Pamies, O.; Dieguez, M.; Claver, C.; Kamer, P. C. J.; van Leeuwen, P. W. N. M. *J. Org. Chem.* **2001**, *66*, 7626-7631.

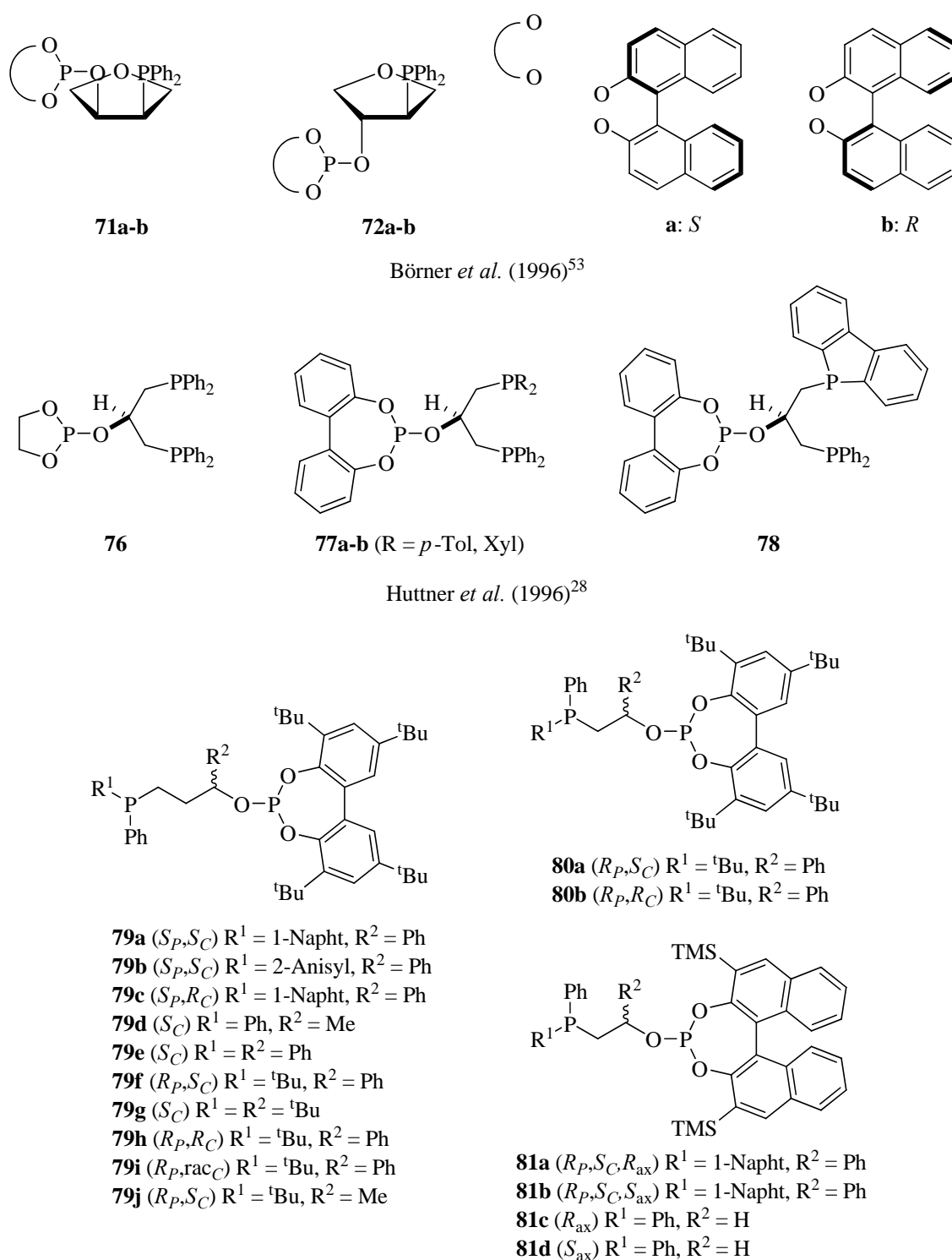


**Figure 12.** Examples of enantiomerically pure phosphine-phosphite ligands.

In 2000 Ruiz & Claver *et al.* synthesized the new family of phosphine-phosphite ligands **82a-d**, which contain a *D*-(+)-xylose derived carbohydrate backbone (Figure 13).<sup>55a</sup> To the best of our knowledge, this was the first report of phosphine-phosphite ligands applied to Rh-catalyzed enantioselective hydrogenation of  $\alpha$ -dehydroamino acid derivatives (**32b** and **69**). These ligands afforded excellent enantioselectivities (up to 99% ee in the case of ligand **82d**) and good activities (TOF > 1200 h<sup>-1</sup>) under mild reaction conditions.<sup>55</sup> The superb results obtained for the sugar derivative **82d** encouraged the authors to use it as chiral ligand in other enantioselective transformations. However, when using **82d** in Pd-catalyzed asymmetric allylic substitutions,<sup>56</sup> Cu-catalyzed asymmetric 1,4-additions,<sup>57</sup> and Rh-catalyzed asymmetric hydroformylations<sup>58</sup>, they only observed moderate selectivities.

---

<sup>55</sup> (a) Pamies, O.; Dieguez, M.; Net, G.; Ruiz, A.; Claver, C. *Chem. Comm.* **2000**, 2383-2384.

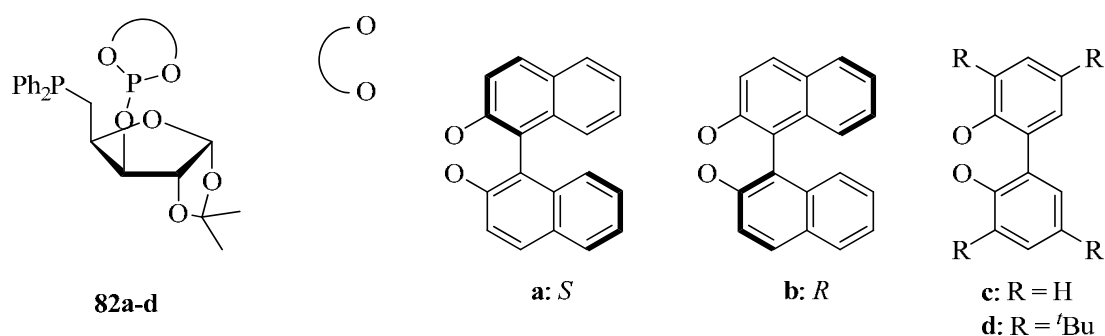
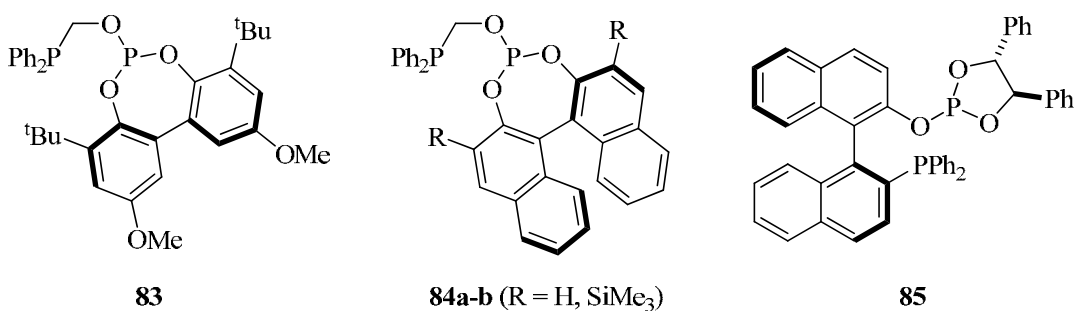
(b) Pamies, O.; Dieguez, M.; Net, G.; Ruiz, A.; Claver, C. *J. Org. Chem.* **2001**, *66*, 8364-8369.

<sup>56</sup> Pamies, O.; van Strijdonck, G. P. F.; Dieguez, M.; Deerenberg, S.; Net, G.; Ruiz, A.; Claver, C.; Kamer, P. C. J.; van Leeuwen, P. W. N. M. *J. Org. Chem.* **2001**, *66*, 8867-8871.

<sup>57</sup> Dieguez, M.; Pamies, O.; Net, G.; Ruiz, A.; Claver, C. *J. Mol. Catal. A: Chem.* **2002**, *185*, 11-16.

<sup>58</sup> Pamies, O.; Net, G.; Ruiz, A.; Claver, C. *Tetrahedron: Asymmetry* **2002**, *12*, 3441-3445.



Ruiz, Claver *et al.* (2000)<sup>55</sup>Faraone *et al.* (2000)<sup>59</sup>Matteoli *et al.* (2001)<sup>60</sup>

**Figure 13.** Chiral phosphine-phosphite ligands based on sugars (top) or derived from BINOL or TADDOL (bottom).

The phosphine-phosphite ligands **83-85** (Figure 13), derived from BINOL or TADDOL, are also interesting. These were prepared using well-known routes to phosphine-phosphites.<sup>59,60</sup> The Rh-complexes of ligands **83-85** were prepared and investigated in enantioselective hydroformylation of styrene, in which they yielded very high regioselectivity and moderate enantioselectivities (20 to 40% ee). Moreover, the corresponding Palladium complexes of **83** and **84a-b** afforded acceptable results (up to 71 % ee) in asymmetric allylic alkylations.

<sup>59</sup> (a) Arena, C. G.; Drommi, D.; Faraone, F. *Tetrahedron: Asymmetry* **2000**, *11*, 2765-2779. (b) Arena, C. G.; Faraone, F.; Graiff, C.; Tiripicchio, A. *Eur. J. Inorg. Chem.* **2002**, 711-716.

<sup>60</sup> Beghetto, V.; Scrivanti, A.; Matteoli, U. *Catal. Commun.* **2001**, *2*, 139-143.

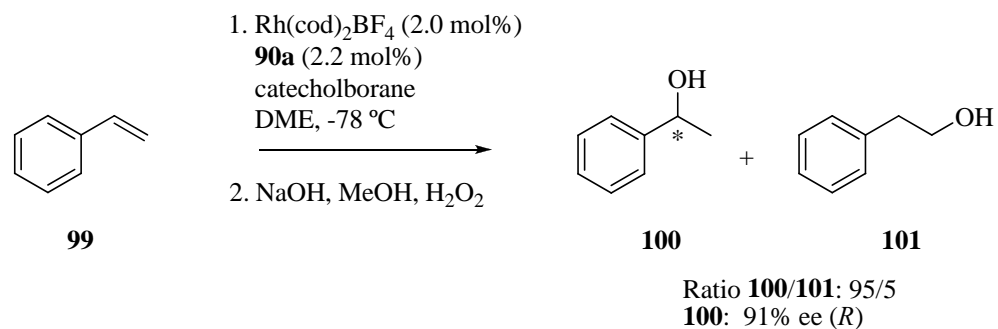
New ligand structures are typically rationally designed and then individually synthesized. This is rather time-consuming, especially considering that most of these ligands will never lead to an efficient catalyst. To accelerate catalyst discovery, Schmalz *et al.* developed a broad library of structurally diverse heterobidentate ligands derived from modular ligand architectures. Starting from hydroquinone and either phenol- or naphthol-derived backbones, and using a straightforward synthetic sequence, they separately introduced two donor moieties onto the starting material to generate the phosphine-phosphite ligands **86-98** (Figure 14).<sup>61</sup>

---

<sup>61</sup> (a) Kranich, R.; Eis, K.; Geis, O.; Muhle, S.; Bats, J. W.; Schmalz, H.-G. *Chem. Eur. J.* **2000**, *6*, 2874-2894. (b) Blume, F.; Zemelka, S.; Fey, T.; Kranich, R.; Schmalz, H.-G. *Adv. Synth. Catal.* **2002**, *344*, 868-883. (c) Velder, J.; Robert, T.; Weidner, I.; Neudoerfl, J.-M.; Lex, J.; Schmalz, H.-G. *Adv. Synth. Catal.* **2008**, *350*, 1309-1315.



unpredictable differences in the performance of the corresponding *in situ* generated Rh-complexes. They also employed this modular approach to identify and optimize ligands for other transition metal-catalyzed transformations (e.g. Cu-mediated enantioselective 1,4-additions).<sup>62</sup>

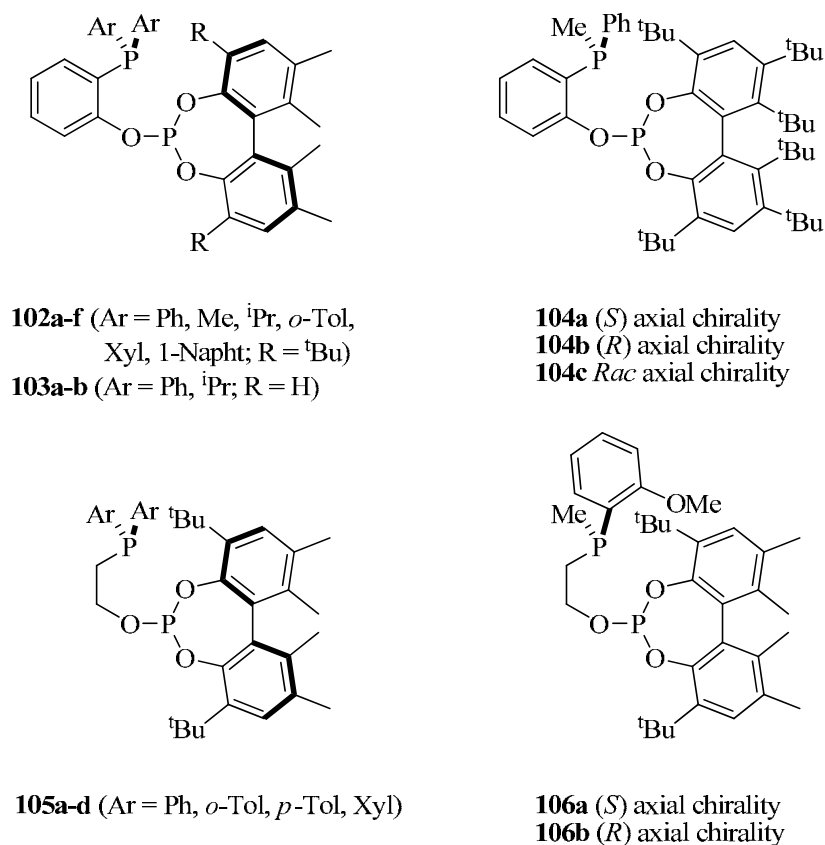


**Scheme 12.** Rh-mediated asymmetric hydroboration of styrene using **90a** as chiral ligand.

Meanwhile, Pizzano *et al.* have developed a versatile route to a new class of chiral phosphine-phosphite ligands, compounds **102-106** (Figure 15), starting from phosphino alcohols bridged by either an *o*-oxyphenylene fragment or the *o*-oxyethylene counterpart.<sup>63</sup> Their methodology is advantageous to that of Schmalz *et al.* in that it enables preparation of ligands from *P*-stereogenic phosphine fragments.

<sup>62</sup> (a) Werle, S.; Fey, T.; Neudoerfl, J. M.; Schmalz, H.-G. *Org. Lett.* **2007**, *9*, 3555-3558. (b) Robert, T.; Velder, J.; Schmalz, H.-G. *Angew. Chem., Int. Ed.* **2008**, *47*, 7718-7721.

<sup>63</sup> (a) Suarez, A.; Pizzano, A. *Tetrahedron: Asymmetry* **2001**, *12*, 2501-2504. (b) Suarez, A.; Mendez-Rojas, M. A.; Pizzano, A. *Organometallics* **2002**, *21*, 4611-4621. (c) Vargas, S.; Rubio, M.; Suarez, A.; Pizzano, A. *Tetrahedron Lett.* **2005**, *46*, 2049-2052. (d) Vargas, S.; Rubio, M.; Suarez, A.; Del Rio, D.; Alvarez, E.; Pizzano, A. *Organometallics* **2006**, *25*, 961-973.

Pizzano *et al.* (2001)<sup>63</sup>**Figure 15.** Phosphine-phosphite ligands synthesized by Pizzano *et al.*

Ligands **102a**, **103b** and **104b** have shown high enantioselectivity (> 99% ee) in Rh-mediated asymmetric hydrogenations of functionalized alkenes such as dimethyl itaconate,<sup>63a</sup>  $\alpha$ -dehydroamino acid<sup>63b</sup> and enol ester phosphonates.<sup>64</sup> Iridium complexes of these ligands, prepared *in situ* from [IrCl(cod)]<sub>2</sub>, afforded moderately high enantioselectivities (up to 85% ee for ligand **105a**) in hydrogenations of imines.<sup>63c-d</sup> In this last case, the degree of enantioselectivity was highly dependent on the flexibility of the ligand backbone: therefore, the oxyethylene moiety gave higher enantiomeric excesses than did its less flexible oxyphenylene counterpart. Finally, ligand **102f** afforded the best regioselectivity

<sup>64</sup> (a) Rubio, M.; Suarez, A.; Alvarez, E.; Pizzano, A. *Chem. Comm.* **2005**, 628-630. (b) Vargas, S.; Suarez, A.; Alvarez, E.; Pizzano, A. *Chem.--Eur. J.* **2008**, *14*, 9856-9859.

and enantioselectivity in Rh-mediated asymmetric hydroformylations of styrene.<sup>65</sup>

Figure 16 shows the latest phosphine-phosphite ligands to be reported in the literature: compounds **107-112**. Ligand **107** can be conveniently prepared from Ugi's amine,<sup>19</sup> similarly to **29a** and **29b**.<sup>20</sup> More recently, two novel types of phosphine-phosphite ligands, **108a-b** and **109-112**, derived from phosphabenzenes<sup>66</sup> and phosphabarrelenes,<sup>67</sup> respectively, were synthesized. These ligands are distinguished in that the phosphorus atom of the phosphine moiety is part of a heterocycle. This makes the phosphine fragment electronically different to that in other ligands, yielding phosphabenzenes and phosphabarrelenes that are interesting  $\pi$ -acceptor ligands for homogeneous catalysis, with electronic properties more akin to those of phosphites.

---

<sup>65</sup> Rubio, M.; Suarez, A.; Alvarez, E.; Bianchini, C.; Oberhauser, W.; Peruzzini, M.; Pizzano, A. *Organometallics* **2007**, *26*, 6428-6436.

<sup>66</sup> Mueller, C.; Lopez, L. G.; Kooijman, H.; Spek, A. L.; Vogt, D. *Tetrahedron Lett.* **2006**, *47*, 2017-2020.

<sup>67</sup> Breit, B.; Fuchs, E. *Synthesis* **2006**, 2121-2128.

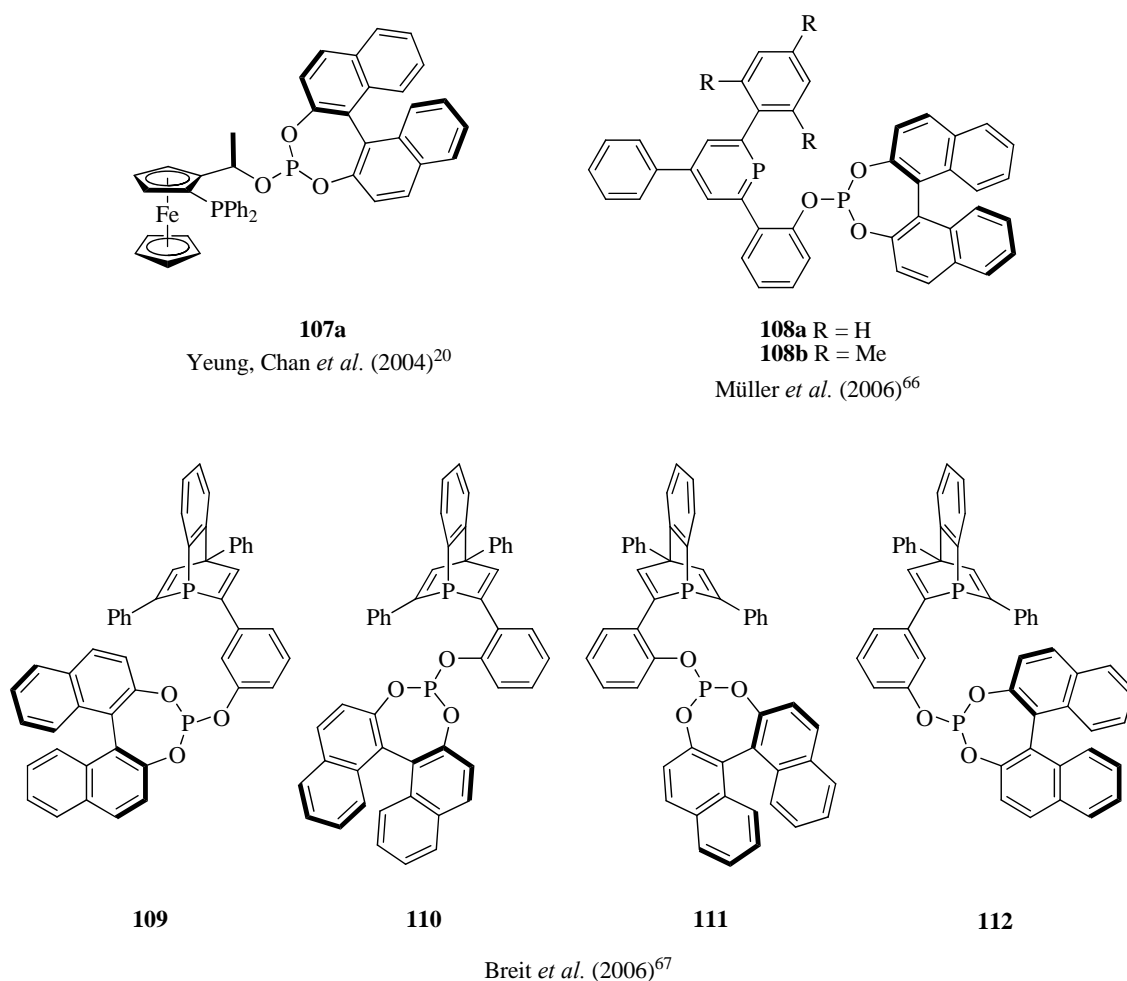


**Figure 16.** The most recently described phosphine-phosphite ligands in the literature. Note that the phosphorus atom of the phosphine moiety in **108-112** forms part of a heterocycle.

The selectivity of phosphine-phosphite ligands **107-112** was investigated in the Rh-mediated enantioselective hydrogenation of two benchmark  $\alpha$ -dehydroamino acid substrates: **32b** and **69**. The results are summarized in Table 6.





## **RESULTS AND DISCUSSION**

UNIVERSITAT ROVIRA I VIRGLI

TOWARDS HIGHLY EFFICIENT LIGANDS FOR ASYMMETRIC HYDROGENATIONS: A COVALENT MODULAR APPROACH AND  
INVESTIGATIONS INTO BIOINSPIRED SUPRAMOLECULAR STRATEGIES

Héctor Fernández Pérez

ISBN:978-84-693-3385-3 /DL:T.994-2010

## 1.2. RESULTS AND DISCUSSION

### 1.2.1 Design and structural optimization of ligands for efficient asymmetric catalysts

During the past few decades, transition metal-catalyzed reactions have become extremely powerful tools for asymmetric organic synthesis, and many classes of chiral ligands have been developed, providing highly efficient solutions for a growing number of asymmetric transformations.<sup>68</sup> However, catalyzing certain transformations remain a challenge, either because of the low activity for some substrates or because no asymmetric versions of these reactions have yet been developed. The efficiency of a given metal-catalyzed transformation depends on various factors, including a subtle interplay between the metal center and its coordinated ligands. Steric, geometric and electronic ligand effects are very important, but are not easy to predict, especially in asymmetric catalysis.

Since rational design is not always possible, the preparation of novel catalysts remains a rather empirical task. When developing or improving a catalytic process via catalyst tuning, it is crucial to start with a basic catalytic kit and to progressively move to a more efficient catalytic system according to mechanistic and molecular interaction principles. The versatility of the synthetic route should facilitate modification of the different *modules* (molecular fragments) of the ligands. If these modules are designed such that they can influence the catalytic site, then a more efficient catalytic system (in terms of conversion and enantioselectivity) should become accessible by changing their stereoelectronics. Indeed, the stereoelectronic properties of modules could be considered as the “input parameters” in the optimization process.

---

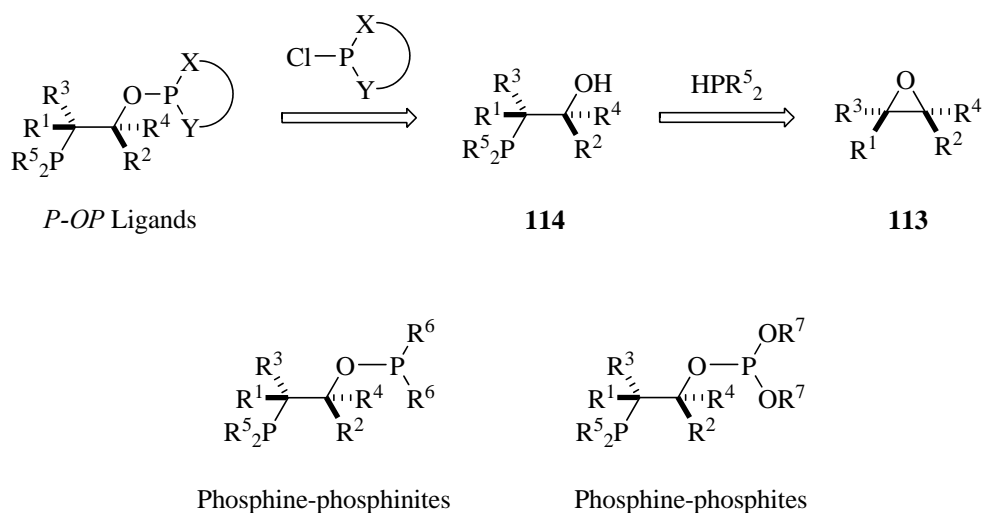
<sup>68</sup> (a) *Comprehensive Asymmetric Catalysis*; Jacobsen, E. N., Pfaltz, A., Yamamoto, H. Eds.; Springer: Berlin, Germany, 1999; Vol 1-3. (b) *Catalytic Asymmetric Synthesis*; Ojima, I., Ed.; Wiley-VCH: New York, 2000.

The following sections detail our efforts in the preparation of a new family of highly modular *P-OP* ligands, available from chiral epoxides.<sup>69</sup> We envisaged that these epoxides could be converted into the desired *P-OP* ligands in two-steps (Scheme 1):

1.- Ring-opening of the epoxide with a nucleophilic, trivalent phosphorus derivative would allow the introduction of the phosphine functionality.

2.- The phosphinite or phosphite functionality could be introduced by phosphorylation of a phosphino-alcohol with a suitable electrophilic, trivalent phosphorus reagent.

Interestingly, preparation of these *P-OP* ligands requires synthesis of the corresponding phosphino-alcohols **114** (modular *P-OH* ligands), whose catalytic properties in asymmetric transformations remain unexplored. The modular design of our target *P-OP* ligands provides several advantages: incorporation of up to six molecular fragments; modification of the stereoelectronics of the phosphorus functionalities; and control over the stereogenic centers between the phosphorus groups.

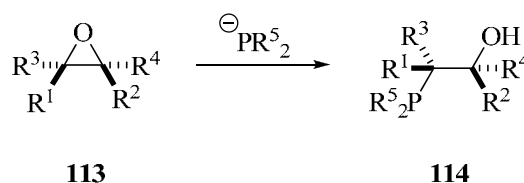


**Scheme 1**

<sup>69</sup> (a) Nieto, N.; Molas, P.; Benet-Buchholz, J.; Vidal-Ferran, A. *J. Org. Chem.* **2005**, *70*, 10143-10146. (b) Nieto, N.; Munslow, I. J.; Barr, J.; Benet-Buchholz, J.; Vidal-Ferran, A. *Org. Biomol. Chem.* **2008**, *6*, 2276-2281. (c) Nieto, N.; Munslow, I. J.; Fernandez-Perez, H.; Vidal-Ferran, A. *Synlett* **2008**, 2856-2858. (d) Fernandez-Perez, H.; Pericas, M. A.; Vidal-Ferran, A. *Adv. Synth. Catal.* **2008**, *350*, 1984-1990.

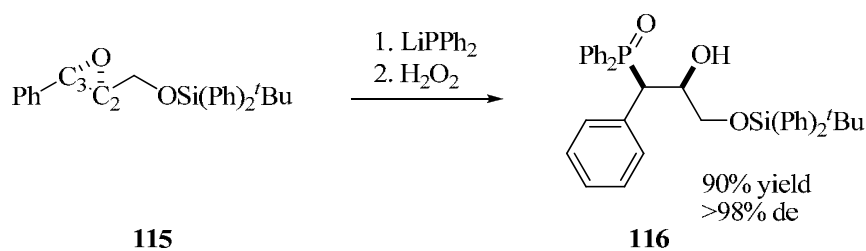
### 1.2.2 Ring-opening of epoxides with trivalent phosphorus nucleophiles

The first step in our synthetic strategy was the ring-opening of the enantiomerically pure epoxides **113** with nucleophilic, trivalent phosphorus derivatives, to incorporate the phosphine functionality into the chiral skeleton (Scheme 2).



**Scheme 2**

There is strong literature precedent for the ring-opening of epoxides using phosphorus nucleophiles.<sup>54,70</sup> Sharpless type epoxide ring-opening offers high regioselectivity and stereospecificity, as reported by Brunner<sup>70d</sup> and by Togni & Venanzi.<sup>70e</sup> Nucleophilic attack at the (2*S*,3*S*)-3-phenylglycidol derivative **115** has been reported at the benzylic position, with inversion of configuration (Scheme 3)<sup>70d,e</sup> at this position and retention at C<sub>2</sub>.



**Scheme 3.** Sharpless type epoxide ring-opening with phosphorus nucleophiles.

<sup>70</sup> (a) Issleib, K.; Rockstroh, K. *Chem. Ber.* **1963**, *96*, 407-10. (b) Connell, A. C.; Whitham, G. *H. J. Chem. Soc. Perkin Trans. 1* **1983**, 989-94. (c) Boeckh, D.; Huisgen, R.; Noeth, H. *J. Am. Chem. Soc.* **1987**, *109*, 1248-9. (d) Brunner, H.; Sicheneder, A. *Angew. Chem.* **1988**, *100*, 730-1. (e) Gorla, F.; Togni, A.; Venanzi, L. M.; Albinati, A.; Lianza, F. *Organometallics* **1994**, *13*, 1607-16.

Sharpless epoxy-ethers have provided excellent results in the development of nitrogen-containing ligands for various asymmetric transformations.<sup>71</sup> We considered that derivatives of Sharpless epoxides would be an ideal starting point for our target *P-OP* ligands. Furthermore, as detailed below, use of these epoxides allows introduction of an additional CH<sub>2</sub>OR group into the final chiral ligands. The steric environment at this position has proven fundamental to the catalytic activity of other chiral ligands derived from Sharpless epoxy alcohols in many enantioselective transformations.<sup>71a-d,71f-g</sup>

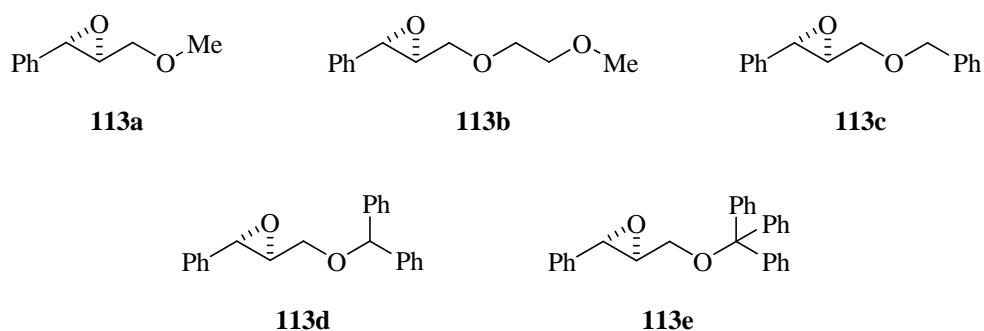


**Figure 1.** Sharpless type epoxy-ethers.

Ring-opening of epoxides **113a-e** (Figure 1, see Experimental Procedure for their preparation) with potassium diphenylphosphanide or lithium di-*tert*-butylphosphanide proceeded smoothly at -30 °C to room temperature: the reactions were clean, affording the desired phosphino alcohols as the major compounds. Unfortunately, the phosphino alcohols were rather prone to oxidation; consequently, standard aqueous work-up and subsequent silica-gel

<sup>71</sup> (a) Vidal-Ferran, A.; Moyano, A.; Pericas, M. A.; Riera, A. *J. Org. Chem.* **1997**, *62*, 4970-4982. (b) Vidal-Ferran, A.; Moyano, A.; Pericas, M. A.; Riera, A. *Tetrahedron Lett.* **1997**, *38*, 8773-8776. (c) Vidal-Ferran, A.; Bampos, N.; Moyano, A.; Pericas, M. A.; Riera, A.; Sanders, J. K. M. *J. Org. Chem.* **1998**, *63*, 6309-6318. (d) Puigjaner, C.; Vidal-Ferran, A.; Moyano, A.; Pericas, M. A.; Riera, A. *J. Org. Chem.* **1999**, *64*, 7902-7911. (e) Pericas, M. A.; Puigjaner, C.; Riera, A.; Vidal-Ferran, A.; Gomez, M.; Jimenez, F.; Muller, G.; Rocamora, M. *Chem. Eur. J.* **2002**, *8*, 4164-4178. (f) Jimeno, C.; Pasto, M.; Riera, A.; Pericas, M. A. *J. Org. Chem.* **2003**, *68*, 3130-3138. (g) Rodriguez, B.; Pasto, M.; Jimeno, C.; Pericas, M. A. *Tetrahedron: Asymmetry* **2006**, *17*, 151-160. (h) Jimeno, C.; Vidal-Ferran, A.; Pericas, M. A. *Org. Lett.* **2006**, *8*, 3895-3898. (i) Popa, D.; Puigjaner, C.; Gomez, M.; Benet-Buchholz, J.; Vidal-Ferran, A.; Pericas, M. A. *Adv. Synth. Catal.* **2007**, *349*, 2265-2278. (j) Alza, E.; Bastero, A.; Jansat, S.; Pericas, M. A. *Tetrahedron: Asymmetry* **2008**, *19*, 374-378.

chromatographic purification led to a mixture of the phosphino alcohols and their corresponding diphenylphosphoryl alcohols (see Figure 2, which corresponds to the  $^{31}\text{P}$ -NMR spectrum of the products obtained with **113d**).

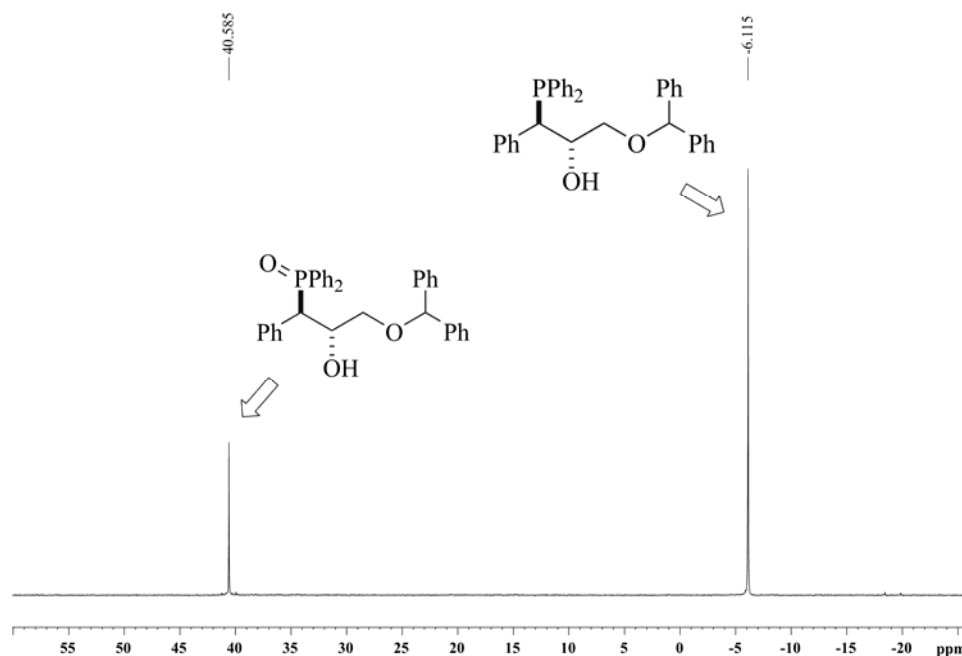
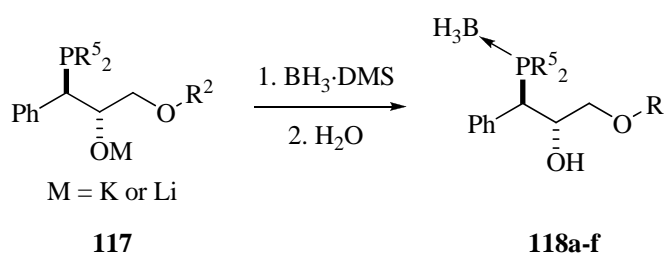


**Figure 2.**  $^{31}\text{P}\{^1\text{H}\}$ -NMR spectrum of the crude products obtained from ring-opening of epoxide **113d**.

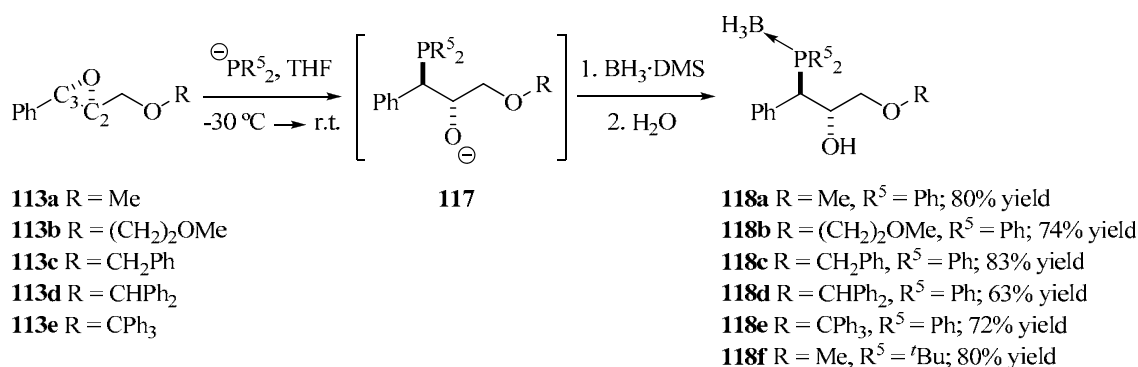
We then decided to protect the resulting phosphino alcohols as the corresponding borane adducts **118a-f**.<sup>72</sup> This was done *in situ* after the ring-opening using  $\text{BH}_3\cdot\text{DMS}$  at  $-10\text{ }^\circ\text{C}$  to room temperature (Scheme 4). The desired adducts were stable to oxidation and hydrolysis, which greatly facilitated aqueous work-up, column chromatography, and storage.

<sup>72</sup> (a) For a review see: Ohff, M.; Holz, J.; Quirnbach, M.; Boerner, A. *Synthesis* **1998**, 1391-1415. (b) Cacatian, S. T.; Fuchs, P. L. *Tetrahedron* **2003**, *59*, 7177-7187.



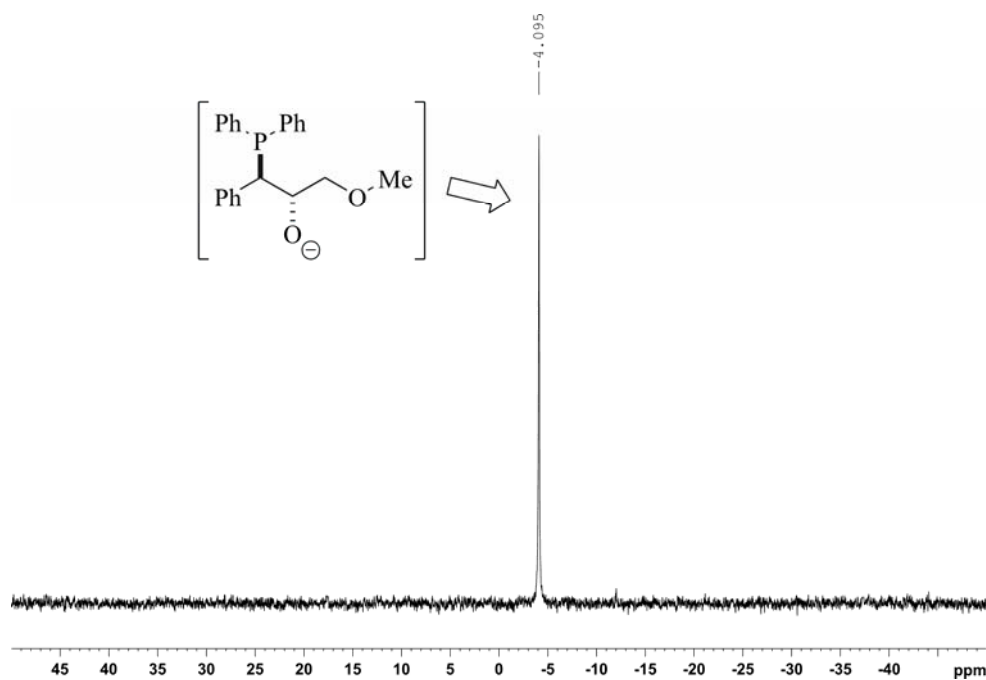
**Scheme 4.** Protection of the phosphine intermediates **117** as the corresponding borane adducts **118a-f**.

We were pleased that ring-opening of the Sharpless epoxides with trivalent phosphorus nucleophiles was indeed regioselective.<sup>70d,e</sup> This was confirmed by NMR, which showed only one signal in the  $^{31}\text{P}\{^1\text{H}\}$ -NMR spectrum of each crude mixture. For instance, the structure of the ring-opened product from chiral epoxide **113a** was assigned to the regioisomer arising from attack at the benzylic position by the nucleophile ( $\text{C}_3$  attack). The formation of the another regioisomer was not detected in the  $^{31}\text{P}\{^1\text{H}\}$ -NMR spectrum of the crude mixture (see Figure 3). The structures of **118a-f**, together with their corresponding yields, are shown in Scheme 5.



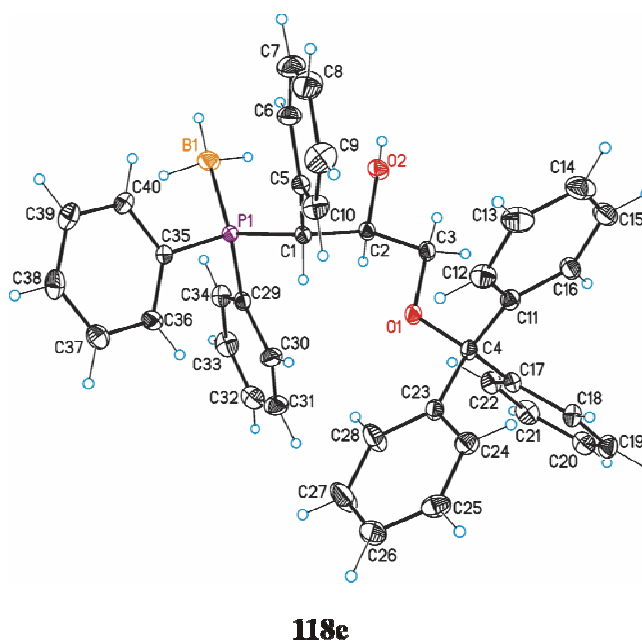
**Scheme 5.** Synthesis of the borane-protected phosphino-alcohols **118a-f** from the corresponding epoxides **113**.



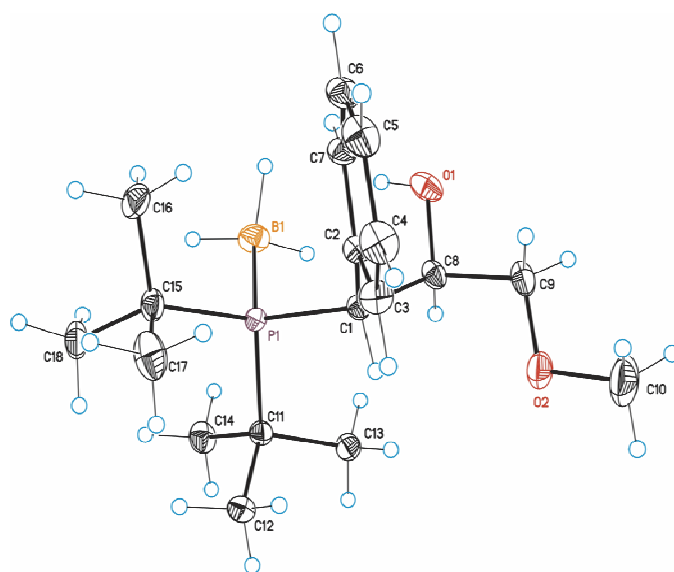


**Figure 3.**  $^{31}\text{P}\{^1\text{H}\}$ -NMR spectrum of the crude mixture obtained from ring-opening of epoxide **113a**.

These results were supported by X-ray analysis of borane adducts **118e** (Figure 4) and **118f** (Figure 5), which confirmed attack of the nucleophile at the  $\text{C}_3$  carbon. Selected distances and angles are summarized in Table 1.

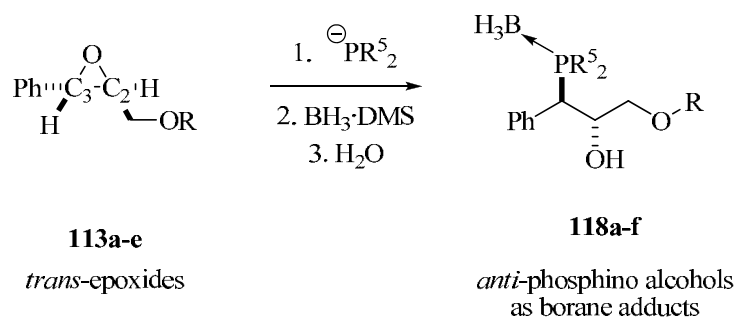


**Figure 4.** X-ray structure of the borane-protected phosphino alcohol **118e**.

**118f****Figure 5.** X-ray structure of the borane-protected phosphino alcohol **118f**.**Table 1.** Selected bond lengths (Å) and angles (deg) for the borane-protected phosphino alcohols **118e** and **118f**.

<b>118e</b>	P(1)-B(1)	1.9282(10)
	P(1)-C(1)	1.8430(9)
	P(1)-C(35)	1.8181(8)
	P(1)-C(29)	1.8209(8)
	C(1)-P(1)-B(1)	121.78(4)
	C(35)-P(1)-B(1)	111.50(5)
	C(29)-P(1)-B(1)	110.46(5)
<b>118f</b>	P(1)-B(1)	1.9349(9)
	P(1)-C(1)	1.8809(5)
	P(1)-C(15)	1.8854(7)
	P(1)-C(11)	1.8896(7)
	C(1)-P(1)-B(1)	111.31(3)
	C(15)-P(1)-B(1)	109.83(4)
	C(11)-P(1)-B(1)	109.57(3)

X-Ray analysis also confirmed that the ring-opening took place in a stereospecific fashion: inversion of configuration at the attacked carbon (ring-opening takes place via a  $S_N2$  mechanism onto  $C_3$ ) and retention of configuration at  $C_2$ . This ultimately means that *trans*-epoxides are converted into *anti*-phosphino alcohols (Scheme 6).

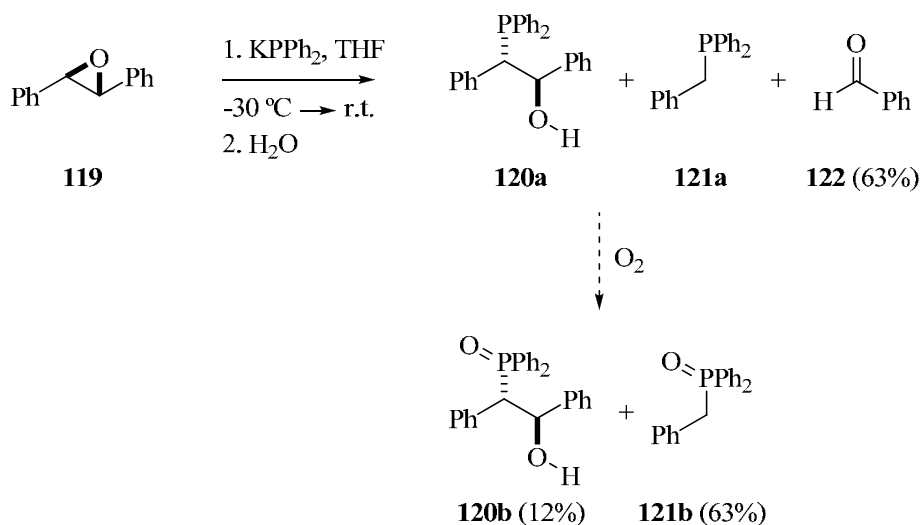


**Scheme 6**

### 1.2.2.1 Ring-opening of unfunctionalized epoxides with phosphorus nucleophiles

Unfunctionalized chiral epoxides<sup>69a-c</sup> are also good starting materials for chiral ligands prepared via our methodology. Particularly, we assayed the ring-opening of chiral *trans*-stilbene oxide (**119**) with potassium diphenylphosphanide as nucleophile in conditions similar to those we used for Sharpless epoxy-ethers **113a-e**. Cleavage at -30 °C to room temperature in THF provided the desired phosphino alkoxide as the only product, plus some unreacted starting material, as revealed by <sup>1</sup>H-NMR analysis. Surprisingly, upon aqueous work-up the phosphino alkoxide of **120a** partially evolved to the oxidized ring-opened compound **120b** (12% yield) along with the retroaldol like-products **121** and **122** (see Scheme 7).<sup>73</sup>

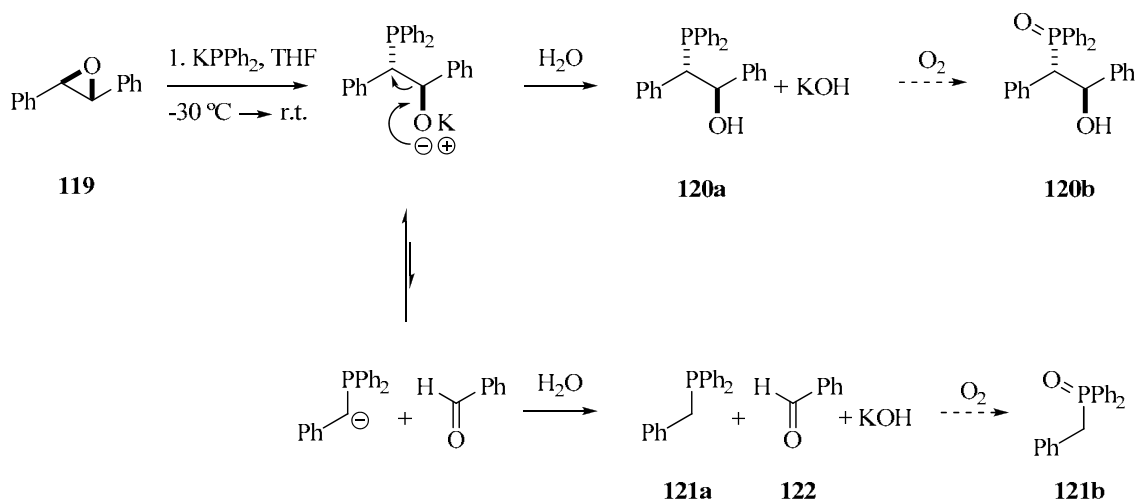
<sup>73</sup> The oxidized products must have arisen from incomplete oxygen exclusion during the work-up.



**Scheme 7.** Ring-opening of chiral *trans*-stilbene oxide (**119**), and subsequent evolution upon aqueous work-up.

Although cleavage of a phosphino<sup>74a</sup> or amino<sup>74b</sup> alcohol via a retroaldol-like process is known, we do not have a clear explanation for the fact that at room temperature, our phosphino alkoxide is stable in aprotic media but rapidly degrades in aqueous conditions. However, we have considered the possibility that aqueous work-up could stabilize the  $\text{Ph}_2\text{P-CH-Ph}$  anion by protonation, which would consequently drive the cleavage (see Scheme 8).

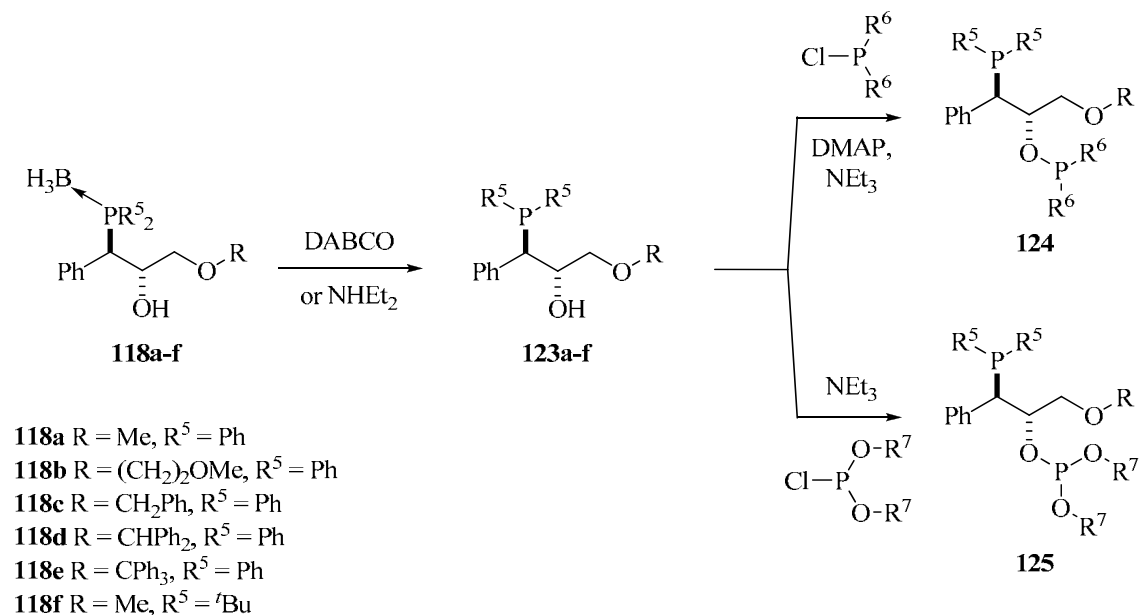
<sup>74</sup> (a) For the cleavage of related phosphorus derivatives, see: Kojima, S.; Kawaguchi, K.; Matsukawa, S.; Akiba, K.-y. *Tetrahedron* **2002**, *59*, 255-265. (b) For the cleavage of  $\beta$ -amino alcohols in basic media, see: (i) Subba Reddy, K.; Sola, L.; Moyano, A.; Pericas, M. A.; Riera, A. *Synthesis* **2000**, 165-176. (ii) Pericas, M. A.; Castellnou, D.; Rodriguez, I.; Riera, A.; Sola, L. *Adv. Synth. Catal.* **2003**, *345*, 1305-1313.



**Scheme 8.** Suggested rationalization for the outcome of the ring-opening of chiral *trans*-stilbene oxide (**119**).

### 1.2.3. *O*-Phosphorylation of phosphino alcohols with P(III) electrophiles

Once we obtained the borane-protected phosphino alcohols **118a-f**, we synthesized our target chiral phosphorus ligands such as the phosphino-alcohols **123**, the phosphine-phosphinites **124** and the phosphine-phosphites **125**, following the general protocol indicated in Scheme 9. Compounds **123** were prepared in quantitative yields from compounds **118a-e**, by cleaving the borane group with DABCO (60 °C, 2 hours).<sup>72a,75</sup> However, these conditions did not provide deprotection of the *tert*-butyl derivative **118f**; consequently, the free alcohol **123f** was obtained in quantitative yield by reacting **118f** in refluxing neat  $\text{NHET}_2$  for 4 hours.<sup>72a,76</sup> To prevent oxidation of the phosphorus centers during manipulation of the reaction mixtures, Schlenk techniques had to be used.

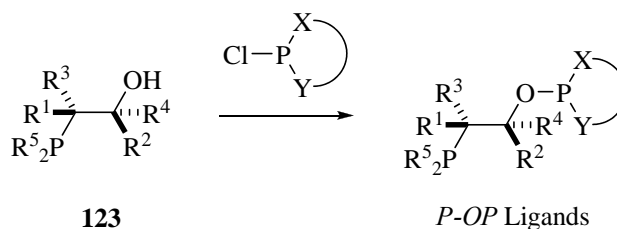


**Scheme 9.** Synthetic protocol for the preparation of *P-OP* ligands.

<sup>75</sup> Brisset, H.; Gourdel, Y.; Pellon, P.; Le Corre, M. *Tetrahedron Lett.* **1993**, *34*, 4523-6.

<sup>76</sup> Deerenberg, S.; Schrekker, H. S.; Van Strijdonck, G. P. F.; Kamer, P. C. J.; Van Leeuwen, P. W. N. M.; Fraanje, J.; Goubitz, K. *J. Org. Chem.* **2000**, *65*, 4810-4817.

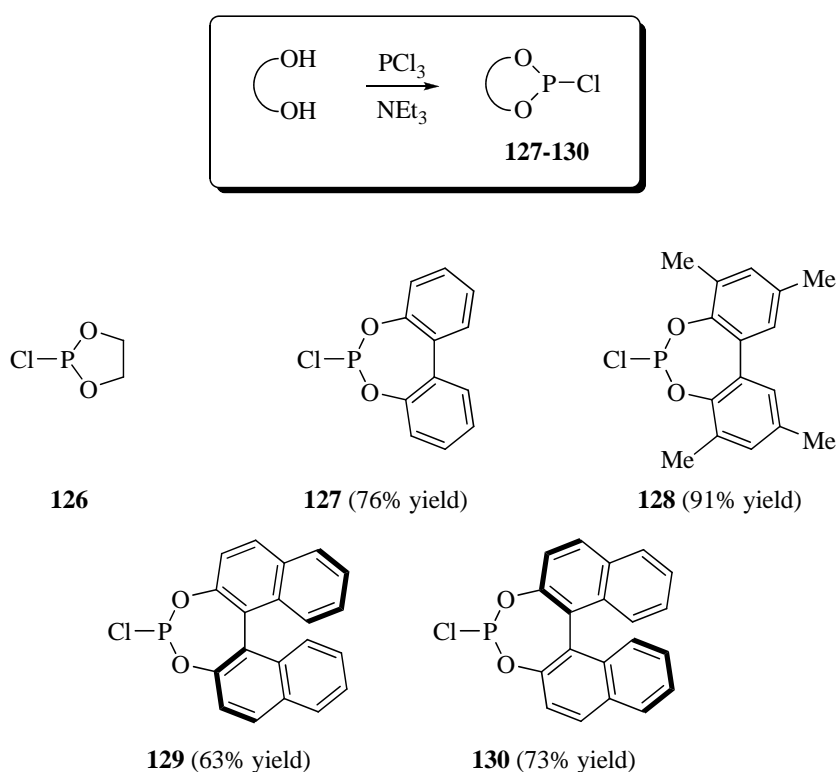
Having prepared **123a-f**, which are key intermediates in our modular approach, we turned our attention to the *O*-phosphorylation of these compounds to obtain our target *P-OP* ligands (Scheme 10).



**Scheme 10.** General procedure for the *O*-phosphorylation of phosphino alcohols **123**.

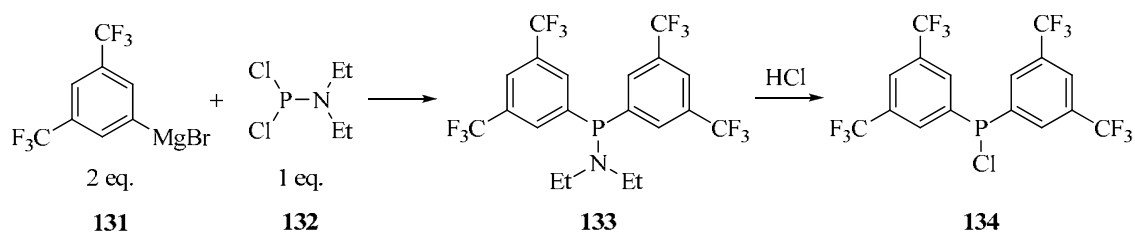
The required phosphorus electrophiles were either purchased (chlorodiphenylphosphine and 2-chloro-1,3,2-dioxaphospholane [**126**]) or readily prepared (**127-130**) by treating the corresponding diols with  $\text{PCl}_3$  under basic ( $\text{Et}_3\text{N}$ ) conditions (Scheme 11).<sup>77</sup>

<sup>77</sup> (a) Scherer, J.; Huttner, G.; Buechner, M.; Bakos, J. *J. Organomet. Chem.* **1996**, *520*, 45-58.  
(b) Lot, O.; Suisse, I.; Mortreux, A.; Agbossou, F. *J. Mol. Catal. A: Chem.* **2000**, *164*, 125-130.



**Scheme 11.** Synthesis of chlorophosphites **126-130** (preparation yields are indicated in brackets).

In contrast, bis[3,5-bis(trifluoromethyl)phenyl]chlorophosphine (**134**) was synthesized from [3,5-bis(trifluoromethyl)phenyl]magnesium bromide (**131**), which was slowly added to a solution of  $(\text{Et}_2\text{N})\text{PCl}_2$  in THF. Treatment of the resulting intermediate phosphoramidite **133** with anhydrous  $\text{HCl}/\text{EtO}_2$  provided **134** in 82% overall yield (Scheme 12).<sup>78</sup>

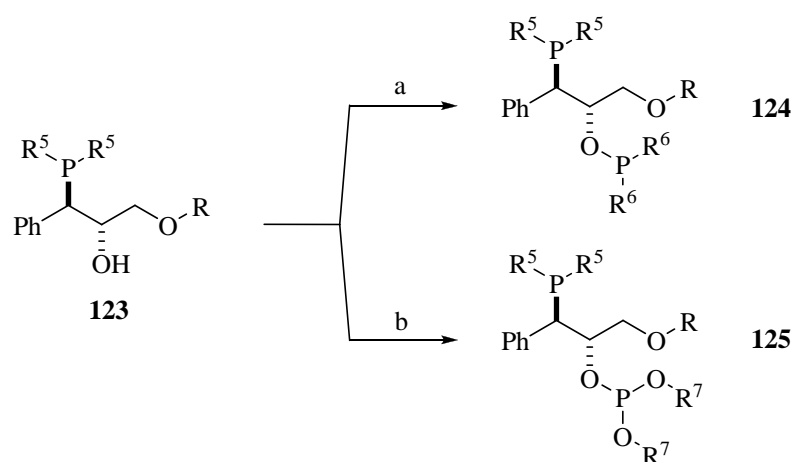


**Scheme 12.** Preparation of bis[3,5-bis(trifluoromethyl)phenyl]chlorophosphine (**134**).

<sup>78</sup> Casalnuovo, A. L.; RajanBabu, T. V.; Ayers, T. A.; Warren, T. H. *J. Am. Chem. Soc.* **1994**, *116*, 9869-82.



Phosphorylation of phosphino alcohols **123** with chlorodiarylyphosphines ( $[\text{R}^6]_2\text{PCl}$ ) or chlorophosphites ( $[\text{R}^7\text{O}]_2\text{PCl}$ ) in the presence of an auxiliary base afforded the target phosphine-phosphinites (**124**) or phosphine-phosphites (**125**).<sup>79,80</sup> These *P-OP* ligands were easily isolated by column chromatography; however, this required exclusion of oxygen and water to prevent oxidation of the phosphine fragment and hydrolysis of the phosphinite or phosphite moieties, respectively. The reaction conditions and yields for each case are summarized in Scheme 13 and Table 2.



**Scheme 13.** General synthesis of *P-OP* ligands **124** and **125**. Reaction conditions: (a)  $\text{Cl-P}(\text{R}^6)_2$  (1.1 eq.),  $\text{NEt}_3$  (1.1 eq.), DMAP (0.16 eq.), THF, 0 °C, 1 h; (b)  $\text{Cl-P}(\text{OR}^7)_2$  (1.1 eq.),  $\text{NEt}_3$  (2.0 eq.), Toluene, r.t., 16 h.

<sup>79</sup> For the *O*-phosphorylation of phosphino alcohols leading to phosphine-phosphinites see for example: (a) Yamashita, M.; Hiramatsu, K.; Yamada, M.; Suzuki, N.; Inokawa, S. *Bull. Chem. Soc. Jpn.* **1982**, *55*, 2917-21. (b) Monsees, A.; Laschat, S. *Synlett* **2002**, 1011-1013. (c) Ohe, K.; Morioka, K.; Yonehara, K.; Uemura, S. *Tetrahedron: Asymmetry* **2002**, *13*, 2155-2160. (d) Jia, X.; Li, X.; Lam, W. S.; Kok, S. H. L.; Xu, L.; Lu, G.; Yeung, C.-H.; Chan, A. S. C. *Tetrahedron: Asymmetry* **2004**, *15*, 2273-2278. (e) Boyer, N.; Leautey, M.; Jubault, P.; Pannecoucke, X.; Quirion, J.-C. *Tetrahedron: Asymmetry* **2005**, *16*, 2455-2458.

<sup>80</sup> For the *O*-phosphorylation of phosphino alcohols leading to phosphine-phosphites see for example references 76, 79d and: (a) Sakai, N.; Mano, S.; Nozaki, K.; Takaya, H. *J. Am. Chem. Soc.* **1993**, *115*, 7033-4. (b) Horiuchi, T.; Ohta, T.; Shirakawa, E.; Nozaki, K.; Takaya, H. *J. Org. Chem.* **1997**, *62*, 4285-4292. (c) Nozaki, K.; Sakai, N.; Nanno, T.; Higashijima, T.; Mano, S.; Horiuchi, T.; Takaya, H. *J. Am. Chem. Soc.* **1997**, *119*, 4413-4423. (d) Pamies, O.; Dieguez, M.; Net, G.; Ruiz, A.; Claver, C. *Chem. Comm.* **2000**, 2383-2384. (e) Suarez, A.; Pizzano, A. *Tetrahedron: Asymmetry* **2001**, *12*, 2501-2504. (f) Blume, F.; Zemolka, S.; Fey, T.; Kranich, R.; Schmalz, H.-G. *Adv. Synth. Catal.* **2002**, *344*, 868-883. (g) Suarez, A.; Mendez-Rojas, M. A.; Pizzano, A. *Organometallics* **2002**, *21*, 4611-4621. (h) Vargas, S.; Rubio, M.; Suarez, A.; Del Rio, D.; Alvarez, E.; Pizzano, A. *Organometallics* **2006**, *25*, 961-973. (i) Velder, J.; Robert, T.; Weidner, I.; Neudoerfl, J.-M.; Lex, J.; Schmalz, H.-G. *Adv. Synth. Catal.* **2008**, *350*, 1309-1315.

**Table 2.** Synthesis of ligands **124** and **125** according to Scheme 13.

Entry	R	R <sup>5</sup>	Electrophile	Final Ligand	Yield (%) <sup>a</sup>
1	Me	Ph	Cl-PPh <sub>2</sub>	<b>124a</b>	61
2	(CH <sub>2</sub> ) <sub>2</sub> OMe	Ph	Cl-PPh <sub>2</sub>	<b>124b</b>	84
3	CPh <sub>3</sub>	Ph	Cl-PPh <sub>2</sub>	<b>124c</b>	75
4	CPh <sub>3</sub>	Ph	<b>134</b>	<b>124d</b>	37
5	Me	Ph	<b>127</b>	<b>125a</b>	66
6	(CH <sub>2</sub> ) <sub>2</sub> OMe	Ph	<b>127</b>	<b>125b</b>	54
7	CH <sub>2</sub> Ph	Ph	<b>127</b>	<b>125c</b>	62
8	CHPh <sub>2</sub>	Ph	<b>127</b>	<b>125d</b>	61
9	CPh <sub>3</sub>	Ph	<b>127</b>	<b>125e</b>	64
10	Me	Ph	<b>128</b>	<b>125f</b>	48
11	CPh <sub>3</sub>	Ph	<b>128</b>	<b>125g</b>	50
12	Me	<i>tert</i> -Bu	<b>127</b>	<b>125h</b>	55
13	Me	Ph	<b>126</b>	<b>125i</b>	69
14	Me	Ph	<b>129</b>	<b>125j</b>	71
15	Me	Ph	<b>130</b>	<b>125k</b>	66

<sup>a</sup> Isolated yield

The structures of the various chiral phosphine-phosphinite and phosphine-phosphite ligands of type **124** and **125** synthesized over the course of this PhD Thesis are shown in Figures 6 and 7, respectively.

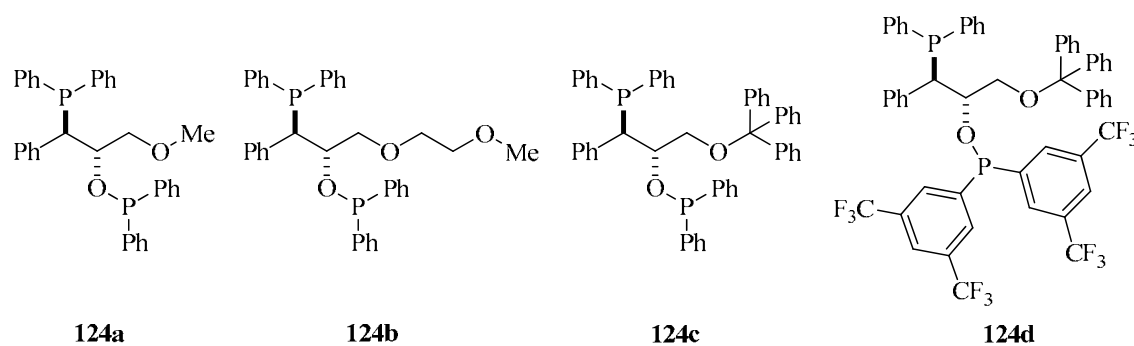


**Figure 6.** Library of chiral phosphine-phosphinite ligands synthesized for this thesis.

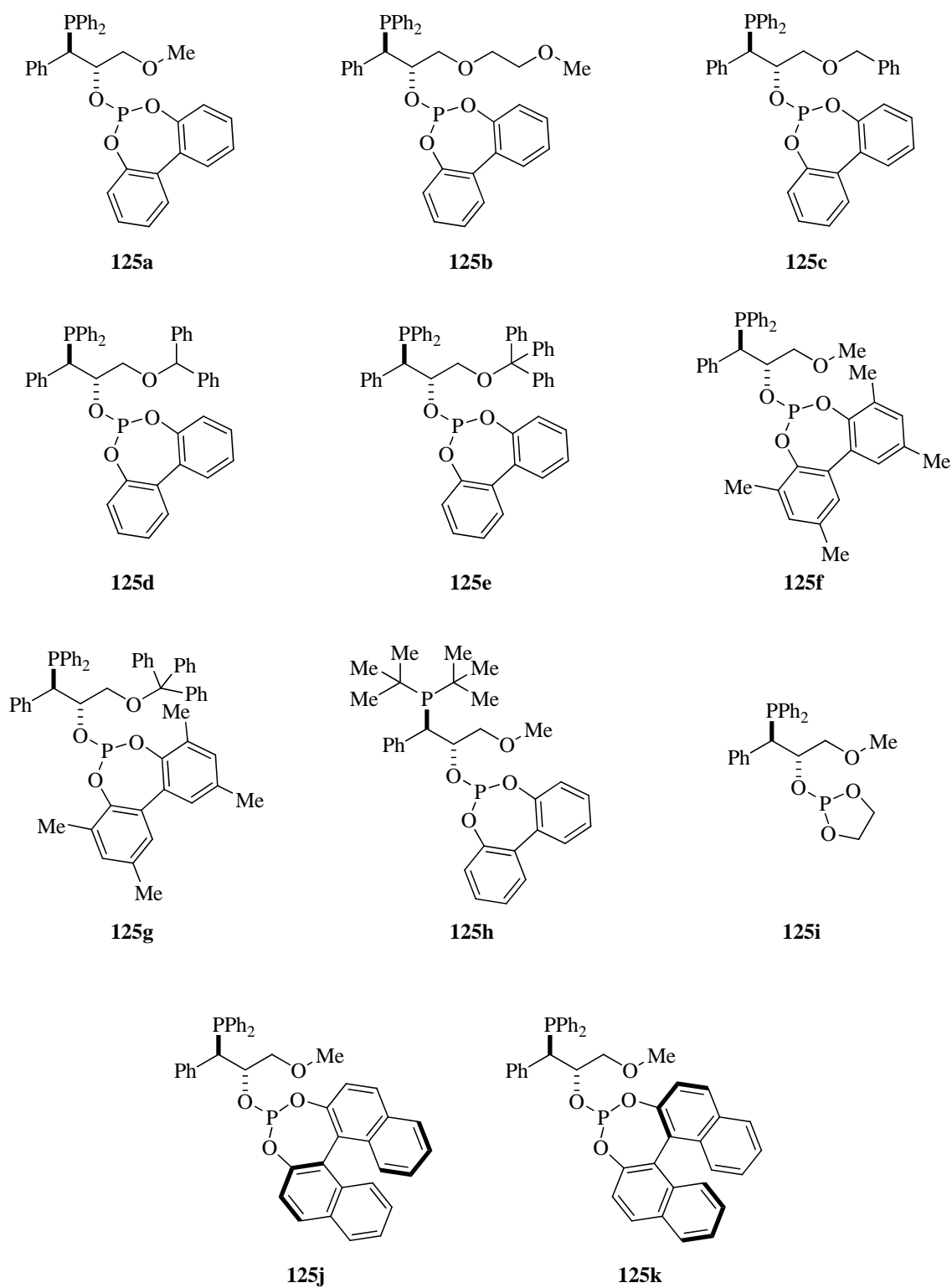


**Figure 7.** Library of chiral phosphine-phosphite ligands synthesized for this thesis.

These ligands differ according to the sterics of the group around the CH<sub>2</sub>OR chain, and by the nature of the phosphine fragment, the phosphinite moiety, or the phosphite moiety.

Phosphine-phosphites **125a-e** (Figure 7) span a wide range of steric bulk: encompassing methyl, methoxyethyl, benzyl, benzhydryl and trityl groups, respectively. Phosphine-phosphinites **124a** and **124c** (Figure 6), and phosphine-phosphites **125f** and **125g** (Figure 7), reflect the two steric extremes (methyl and trityl, respectively). Given that the electronic characteristics of the phosphorus functionalities in these three sets of ligands (**125a-e**, **124a-c** and **125f-g**) are equivalent, we were able to study the influence of sterics on their catalytic activity in Rhodium-mediated asymmetric hydrogenations.

Diphenylphosphino compound **125a** and di-*tert*-butylphosphino compound **125h** differ in the phosphine fragment (Figure 7).

Compounds **124c** and **124d** (Figure 6) differ in terms of the electron density of the phosphinite group: the two CF<sub>3</sub> groups in **124d**, at positions 3 and 5 of the phenyl ring, should make the phosphinite in this compound less basic than that of **124c**. Interestingly, different research groups have reported that 3,5-dialkylphenyl substituents on *P*-groups increase the rigidity of the catalytic system in related phosphorus ligands, leading to greater enantiomeric excesses.<sup>79d,81</sup>

Finally, ligands **125a-e** and **125f-g** (Figure 7) reflect differences in the phosphite fragment. We chose several biphenyl-2,2'-diol units whose corresponding conformers are capable of interconverting. We reasoned that interconversion should facilitate adjustment of the catalyst to the steric

---

<sup>81</sup> (a) RajanBabu, T. V.; Ayers, T. A.; Casalnuovo, A. L. *J. Am. Chem. Soc.* **1994**, *116*, 4101-2. (b) RajanBabu, T. V.; Ayers, T. A.; Halliday, G. A.; You, K. K.; Calabrese, J. C. *J. Org. Chem.* **1997**, *62*, 6012-6028. (c) Trabesinger, G.; Albinati, A.; Feiken, N.; Kunz, R. W.; Pregosin, P. S.; Tschoerner, M. *J. Am. Chem. Soc.* **1997**, *119*, 6315-6323. (d) Tschoerner, M.; Pregosin, P. S.; Albinati, A. *Organometallics* **1999**, *18*, 670-678. (e) Clyne, D. S.; Mermet-Bouvier, Y. C.; Nomura, N.; RajanBabu, T. V. *J. Org. Chem.* **1999**, *64*, 7601-7611. (f) RajanBabu, T. V.; Radetich, B.; You, K. K.; Ayers, T. A.; Casalnuovo, A. L.; Calabrese, J. C. *J. Org. Chem.* **1999**, *64*, 3429-3447. (g) Selvakumar, K.; Valentini, M.; Pregosin, P. S.; Albinati, A.; Eisentraeger, F. *Organometallics* **2000**, *19*, 1299-1307.

requirements of a given transformation. Ligands **125j** and **125k** were designed to incorporate an additional stereogenic element: their phosphite fragments are derived from (*R*)- or (*S*)-BINOL. Lastly, in ligand **125i**, which lacks biaryl groups, the two oxygen atoms are connected by an ethane bridge.

### 1.2.3.1 Immobilization of *P-OP* ligands onto solid support

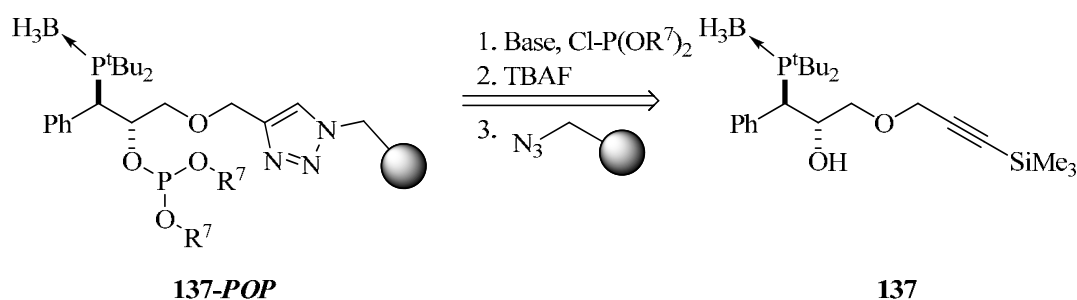
Immobilization of chiral catalysts onto solid supports (resins), is a well known strategy for preparing chiral ligands with greater efficiency, handling, and process control than other methods. Furthermore, compared to their homogeneous counterparts, immobilized catalysts can be more easily separated out from the reaction mixture and reused.<sup>82</sup> As part of an ongoing collaboration with the group of Prof. Pericàs,<sup>83</sup> we envisaged the phosphino alcohols **137**, subsequent *O*-phosphorylation should render the heterogeneized phosphine-phosphite **137-POP**, which contain anchoring groups for immobilization onto resins using click chemistry.<sup>84</sup> The proposed retrosynthetic strategy is depicted in Scheme 14. The key intermediate **137** was prepared as part of this PhD thesis, and will be further derivatized and immobilized onto resins in the near future by the Pericàs group (Scheme 14).

---

<sup>82</sup> *Chiral Catalyst Immobilization and Recycling*; D Vos, D. E.; Vankelecom, I. F. J., Jacobs, P. A. Eds; Wiley-VCH: Weinheim, 2000.

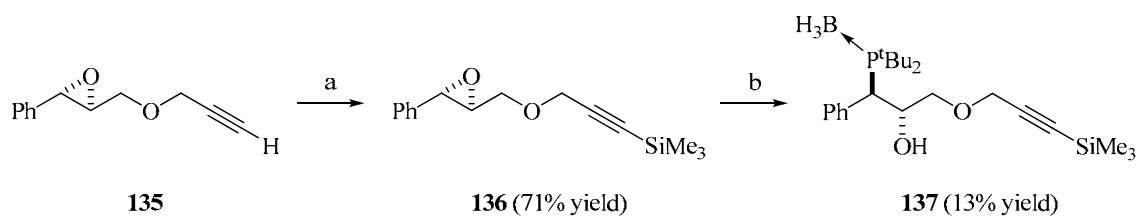
<sup>83</sup> Pericàs *et al.* have recently developed a strategy to anchor chiral ligands onto various polymer supports via click chemistry. See: (a) Font, D.; Jimeno, C.; Pericas, M. A. *Org. Lett.* **2006**, *8*, 653-4655; (b) Bastero, A.; Font, D.; Pericas, M. A. *J. Org. Chem.* **2007**, *72*, 2460-2468; Font, D.; Jimeno, C.; Pericas, M. A. *Org. Lett.* **2006**, *8*, 4653-4655; Font, D.; Bastero, A.; Sayalero, S.; Jimeno, C.; Pericas, M. A. *Org. Lett.* **2007**, *9*, 1943-1946; Alza, E.; Cambeiro, X. C.; Jimeno, C.; Pericas, M. A. *Org. Lett.* **2007**, *9*, 3717-3720; Font, D.; Sayalero, S.; Bastero, A.; Jimeno, C.; Pericas, M. A. *Org. Lett.* **2008**, *10*, 337-340.

<sup>84</sup> Kolb, H. C.; Finn, M. G.; Sharpless, K. B. *Angew. Chem., Int. Ed.* **2001**, *40*, 2004-2021.



**Scheme 14.** Retrosynthetic strategy for immobilization of the intermediate **137** onto a resin.

Ethynyl-substituted phosphine-borane **137** was prepared using a modified version of our standard procedure (Scheme 15). First, the terminal alkyne of the chiral epoxy-ether **135** was protected using *n*-BuLi and Cl-SiMe<sub>3</sub> at -78 °C to provide the TMS-protected epoxide **136**. Then, **136** was opened using lithium di-*tert*-butylphosphanide, and the resulting open-chain intermediate was subsequently protected at the phosphine fragment using BH<sub>3</sub>·DMS to afford the desired phosphino alcohol as the borane adduct **137**. Unfortunately, the reaction was not as clean as usual: the isolated yield of **137** was only 13%. Clearly, these transformations have yet to be optimized.



**Scheme 15.** Synthetic protocol for the preparation of phosphino alcohol **137**. Reaction conditions: (a) *n*-BuLi (1.1 eq.), Cl-SiMe<sub>3</sub> (1.1 eq.), THF, -78 °C to r.t., overnight; (b) Li-P<sup>*t*</sup>Bu<sub>2</sub> (1.2 eq.), THF, -30 °C to r.t., 1h, then BH<sub>3</sub>·DMS (3.0 eq.), -10 °C to r.t., 1h.

## 1.2.4. Studies on the complexation of *P-O* and *P-OP* derivatives with Rhodium precursors

### 1.2.4.1 Complexation of hemilabile *P-O* ligands

*Hemilabile ligands* contain both substitutionally inert and substitutionally labile binding groups. Phosphino alcohol ligands are hemilabile: the phosphorus is inert, and the oxygen, labile. The substitutionally inert coordinating groups are strongly bound to the metal center, whereas the other groups are only weakly bound, and therefore, easily displaced by potential coordinating groups such as other ligands, reagents, and solvent molecules. Once displaced from the metal center, the labile group can subsequently re-coordinate. Therefore, hemilabile ligands, especially *P-O* ligands, are very attractive for asymmetric catalysis (see Section 1.1.1, page 27).

Having obtained phosphino alcohols **123** (Figure 8), we decided to study their complexation to Rhodium precursors known to be catalytically active in reactions such as hydrogenation and hydroformylation.

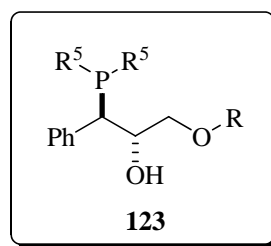
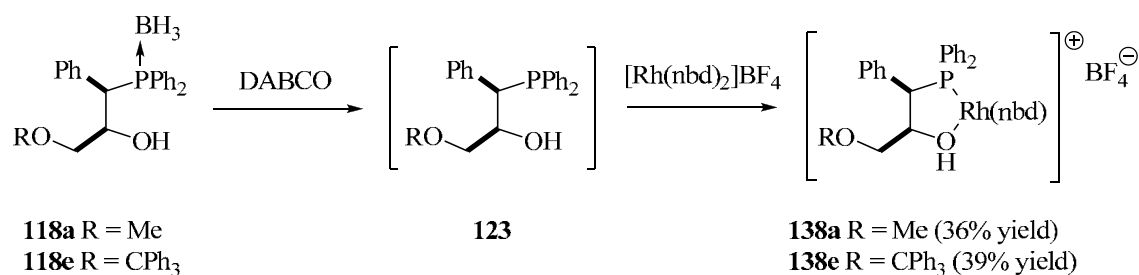


**Figure 8.** General structure of phosphino alcohols **123**.

We began by synthesizing two cationic phosphino Rhodium complexes. As starting materials for these, we chose the borane adducts **118a** and **118e**, since they represent minimum and maximum steric congestion in the CH<sub>2</sub>-OR group, respectively. We investigated the equimolar reaction between free phosphino

alcohol (obtained by deprotecting **118a** and **118e**, see Section 1.2.3, page 76) and  $[\text{Rh}(\text{nbd})_2]\text{BF}_4$  in THF at room temperature. After five hours of reaction, followed by precipitation with *n*-pentane, the corresponding cationic Rhodium complexes **138a** and **138e** were obtained in 36% and 39% yield, respectively (Scheme 16).



**Scheme 16.** Preparation of Rhodium complexes **138a** and **138e**.

The Rh(I)-complexes of phosphino-alcohols, **138a** and **138e**, were identified by mass spectroscopy, based on the corresponding  $[\text{M}-\text{BF}_4]^+$  peaks (Table 3).

**Table 3.** High-resolution mass spectroscopy data for Rhodium complexes **138a** and **138e**.

Rhodium complexes	Calculated mass $[\text{M}-\text{BF}_4]^+$	Found mass $[\text{M}-\text{BF}_4]^+$
<b>138a</b>	545.1117	545.1140
<b>138e</b>	773.2056	773.2086

The five-membered *O-Rh-P* chelate in each complex was basically confirmed by NMR. Hence, the NMR data for each complex agree with reported chemical shifts for the five-membered chelate in the Rhodium complex of *cis*-3-diphenylphosphanyl-4-hydroxytetrahydrofuran (**15**), which was synthesized and spectroscopically characterized in solution by Börner *et al.*<sup>85</sup> A doublet at  $\delta = 40.1$  ppm ( $^1J_{\text{P-Rh}} = 153$  Hz) indicates the formation of a five-membered chelate with a *cis* arrangement of the binding groups. However, use of *trans*-3-diphenylphosphanyl-4-hydroxytetrahydrofuran (**14**) led to formation of the

<sup>85</sup> Boerner, A.; Kless, A.; Holz, J.; Baumann, W.; Tillack, A.; Kadyrov, R. *J. Organomet. Chem.* **1995**, *490*, 213-19.



dimeric bridging *P,O*-complex **16** with more shielded signals in the  $^{31}\text{P}\{^1\text{H}\}$ -NMR spectrum ( $\delta = 26.7$  ppm) (Figure 9).

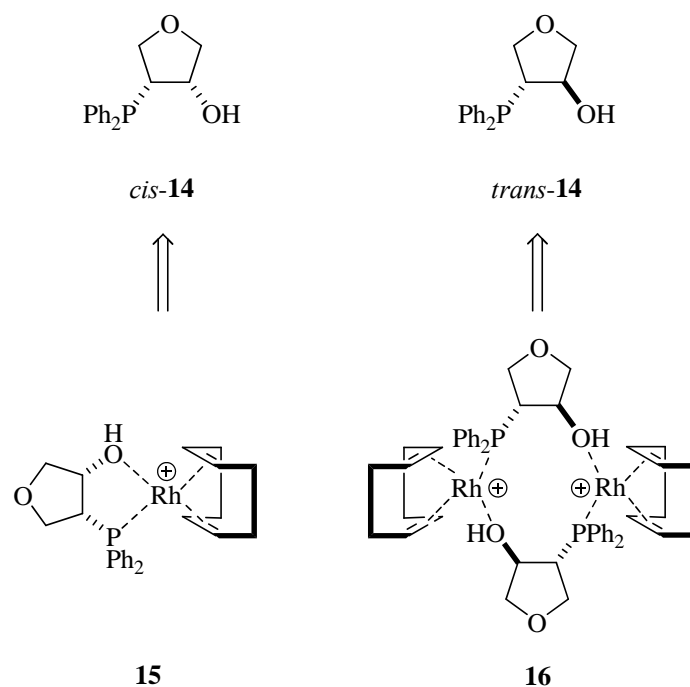


**Figure 9.** Rhodium complexes **15** and **16**.

**Table 4.**  $^{31}\text{P}\{^1\text{H}\}$ -NMR data for phosphino alcohols **123a** and **123e** and Rhodium complexes **15**, **16** and **138a** and **138e**.

Entry	Compounds	$^{31}\text{P}\{^1\text{H}\}$ -NMR	
		$\delta$ (ppm)	$J_{\text{Rh-P}}$ (Hz)
1	<i>cis</i> - <b>14</b>	-14.0	
2	<b>15</b>	40.1 (d)	153
3	<i>trans</i> - <b>14</b>	-11.8	
4	<b>16</b>	26.7 (d)	152
5	<b>123a</b>	-6.4	
6	<b>138a</b>	48.2 (d)	173
7	<b>123e</b>	-7.5	
8	<b>138e</b>	48.6 (d)	174

In all cases, the  $^{31}\text{P}\{^1\text{H}\}$ -NMR signals are observed as a doublet, which arises from coupling of the phosphorus to the Rhodium nuclei ( $^{103}\text{Rh}$  has 100% natural abundance and nuclear spin  $I = 1/2$ ; see Figure 10). The chemical shifts range from 48.2 to 48.6 ppm, and the coupling constants, from 173 to 174 Hz (see Table 4). As expected, based on Börner's observations,<sup>85</sup> the complexes **138** show a pronounced downfield shift in the phosphorus signals as compared to those in the unbound compounds **123** (compare Entries 5 and 6, and Entries 7 and 8, in Table 4). The chemical shifts are in agreement with those observed for a *cis*-five membered chelate (compare Entries 2 and 6, and Entries 2 and 8, in Table 4). The differences in sterics in the  $\text{CH}_2\text{OR}$  chains of **138a** (not-bulky) and **138e** (bulky) translate to only minor effects in the corresponding  $^{31}\text{P}$  chemical shifts at the phosphine moiety (compare entries 6 and 8, in Table 4). This suggests that the  $\text{CH}_2\text{OR}$  chain is extended outwards, away from the chelate ring.

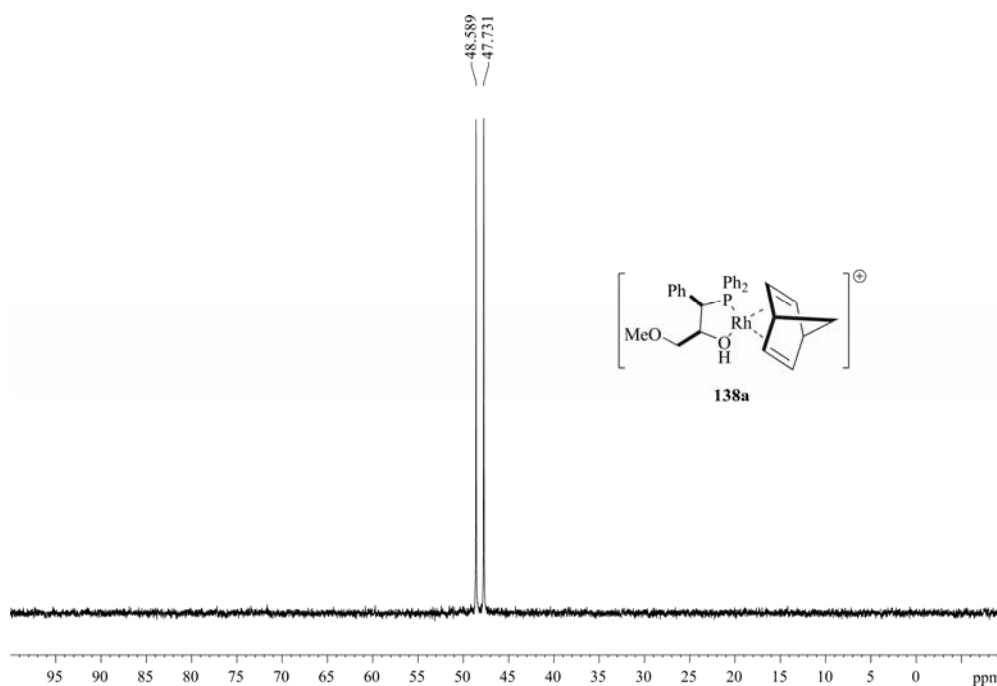


**Figure 10.**  $^{31}\text{P}\{^1\text{H}\}$ -NMR spectrum of Rhodium complex **138a**.

Signal assignment in the  $^1\text{H}$ -NMR spectrum of complex **138e** was not trivial: 2D-experiments were required. NOESY experiments in complex **138e** revealed an exchange process (interconversion) between two pairs of vinyl protons in the

norbornadiene unit (Figure 11). This behavior can be explained by a formal rotation of the diolefinic moiety, which would occur upon dissociation of one of the Rh-alkene bonds. Given that the phase sign of the cross-peaks arising from chemical exchange are opposite to those of NOE cross-peaks in small molecules,<sup>86</sup> we were able to identify these cross-peaks for **138e**. Thus, the signals at 3.88 and 4.10 ppm were assigned to the norbornadiene vinyl protons *trans* to the hydroxy group, and two broad signals observed at 5.65 and 5.88 ppm were assigned to the vinyl protons of the norbornadiene unit *trans* to the phosphine.

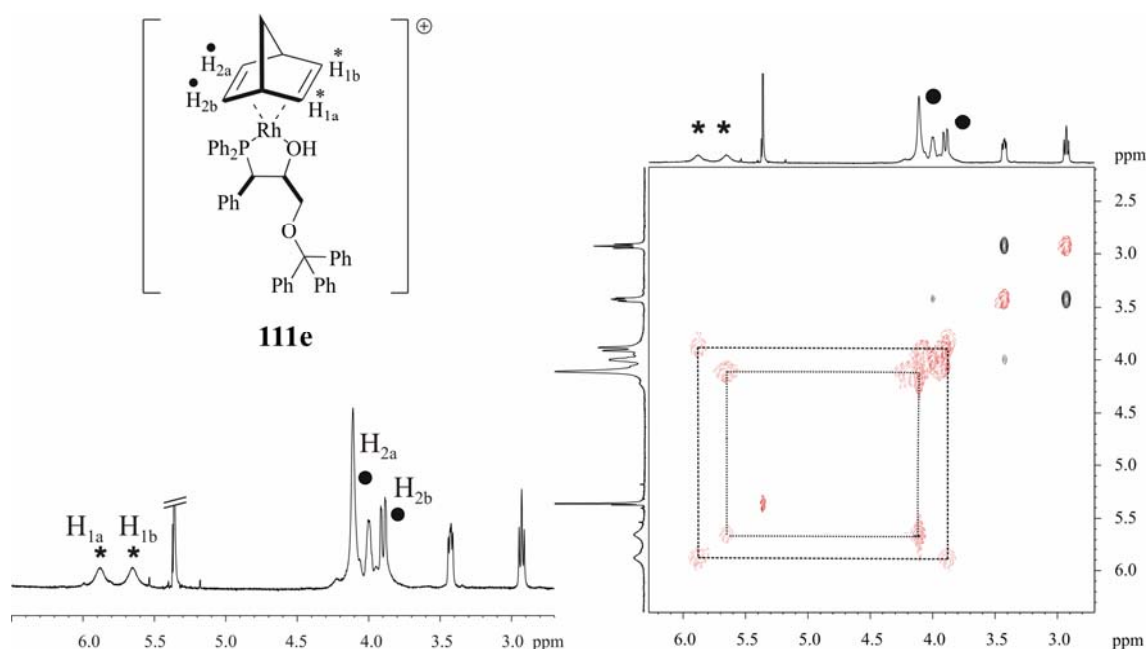


**Figure 11.**  $^1\text{H-NMR}$  and NOESY spectra of Rhodium complex **138e**.

The  $^1\text{H-NMR}$  chemical shifts observed for the olefinic protons in **138e** are listed in Table 5. We were pleased to find a remarkably high level of agreement between our results and those obtained by Börner *et al.* with complex **15** (see Table 5).

<sup>86</sup> NOE peaks in small molecules have an opposite sign to the one of the diagonal peaks for phase-sensitive NOESY experiments.

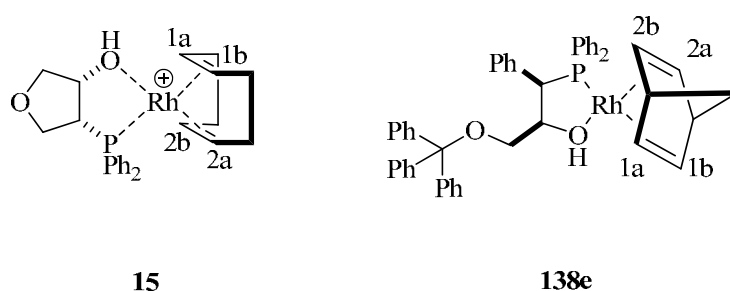


**Figure 12.** The vinyl protons in Rhodium complexes **15** and **138e**.

**Table 5.**  $^1\text{H-NMR}$  data for Rhodium complexes **15** and **138e**.<sup>a</sup>

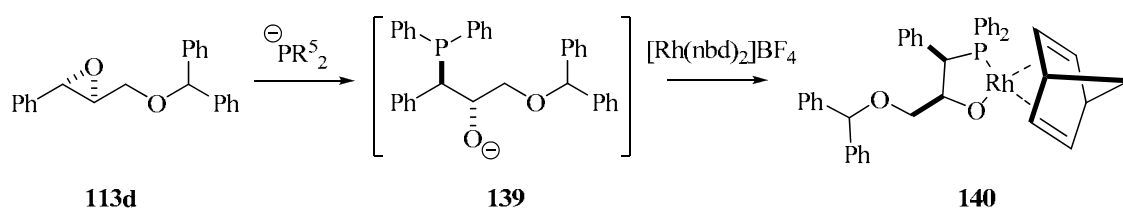
	COD or NBD			
	CH-1a	CH-1b	CH-2a	CH-2b
<b>15<sup>b</sup></b>	5.68	5.57	3.83	3.62
<b>138e<sup>c</sup></b>	5.88	5.65	4.10	3.88

<sup>a</sup> Chemical shift  $\delta$  in ppm

<sup>b</sup>  $^1\text{H-NMR}$  recorded in  $\text{CDCl}_3$

<sup>c</sup>  $^1\text{H-NMR}$  recorded in  $\text{CD}_2\text{Cl}_2$

We then sought to prepare neutral Rhodium complexes of enantiomerically pure *P-O* ligands by the strategy indicated in Scheme 17. We envisaged that the neutral Rhodium complexes could be synthesized in only two steps starting from our readily available chiral epoxides: ring-opening of the epoxide with a nucleophilic phosphorus reagent, followed by complexation of the resulting phosphino alkoxide with a Rhodium precursor (Scheme 17).



**Scheme 17.** Synthesis of neutral Rhodium complexes from chiral epoxides.

We started with chiral epoxide **113d** (see Scheme 17), which contains a benzhydryl group in the  $\text{CH}_2\text{OR}$  chain. After ring-opening of **113d** (1.0 mmol) with potassium diphenylphosphanide (0.98 mmol) under our standard conditions (see Section 1.2.2, page 70), the resulting intermediate was treated with  $[\text{Rh}(\text{nbd})_2]\text{BF}_4$  (1.0 mmol) at  $-10\text{ }^\circ\text{C}$ . The  $^{31}\text{P}\{^1\text{H}\}$ -NMR spectrum of the reaction mixture in  $\text{CD}_2\text{Cl}_2$  showed only one doublet at  $\delta = 54.9$  ppm with a large  $Rh$ - $P$  coupling value ( $^1J_{\text{P-Rh}} = 188$  Hz) (see Figure 13). The structure of this new Rh-complex **139** was established as a neutral five-membered chelate by comparing its  $^{31}\text{P}\{^1\text{H}\}$ - and  $^1\text{H}$ -NMR data with those of its cationic counterparts **138a** and **138e** (see Table 6), and based on mass spectroscopy, by confirming the corresponding  $\text{M-H}^+$  peak [found 697.20;  $\text{C}_{41}\text{H}_{39}\text{O}_2\text{PRh}$  requires 697.17].

**Table 6.**  $^{31}\text{P}\{^1\text{H}\}$ -NMR data for Rhodium complexes **138a**, **138e** and **139**.

Entry	Rhodium complexes	$^{31}\text{P}\{^1\text{H}\}$ -NMR	
		$\delta$ (ppm)	$J_{\text{P-Rh}}$ (Hz)
1	<b>138a</b>	48.2 (d)	173
2	<b>138e</b>	48.6 (d)	174
3	<b>140</b>	54.9 (d)	188

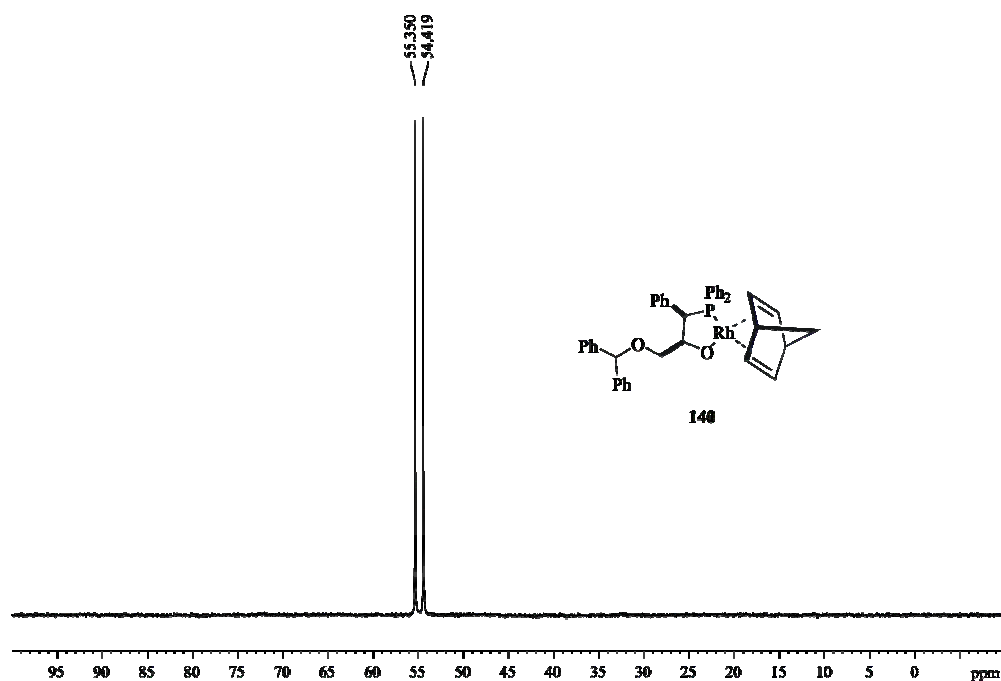


**Figure 13.**  $^{31}\text{P}\{^1\text{H}\}$ -NMR spectrum of neutral Rhodium complex **140**.

However, the biggest difference between **140** and its cationic counterparts **138a** and **138e** is that it is far more reactive. When the temperature was allowed to reach 25° C, the compound **140** evolves to an unknown complex. We have no sound data on the structure of this new species and, clearly, its one stands to be determined.

In summary, we have proven that the chiral phosphino-alcohol ligands **123** behave as bidentate ligands, reacting with Rhodium precursors to form the cationic Rhodium complexes **138a** and **138e** (Figure 14). These complexes are stable in solution and can be used as chiral catalysts for enantioselective transformations. In contrast, the corresponding neutral Rhodium complex **140** is only partially stable in solution, and therefore, warrants further study.

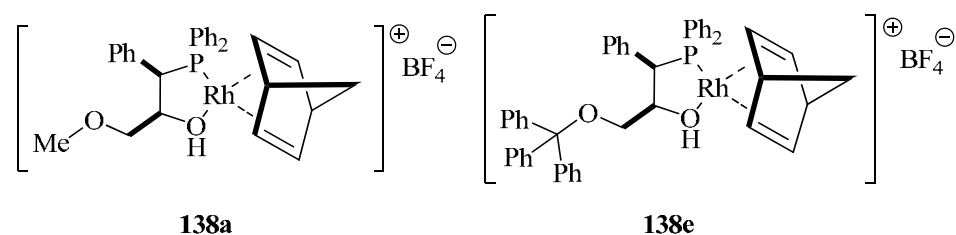
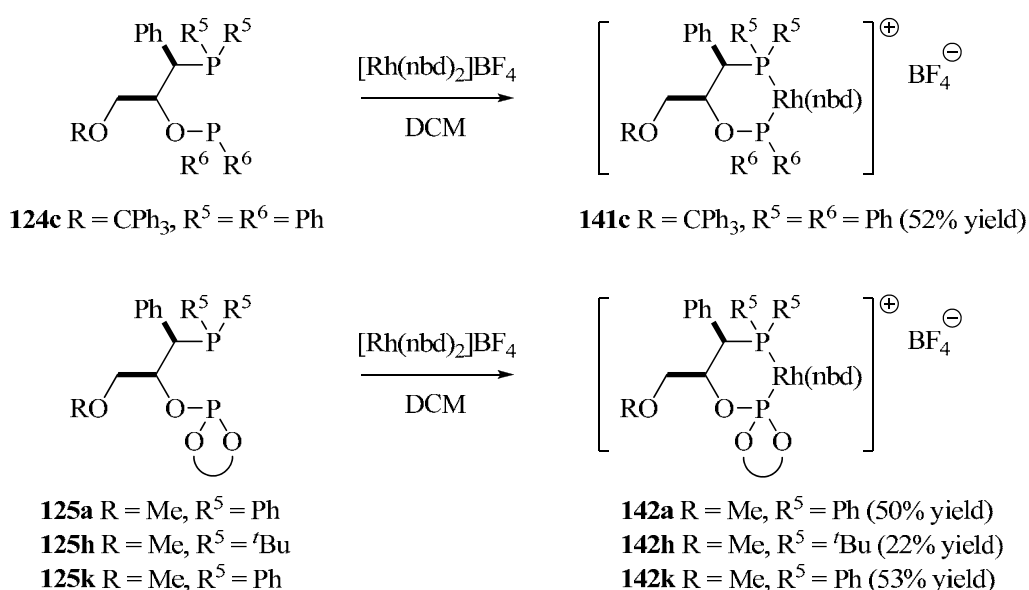


**Figure 14.** Cationic Rhodium complexes **138a** and **138e**, prepared from chiral phosphino-alcohol ligands.

#### 1.2.4.2 Preparation and characterization of selected Rhodium(I) complexes with *P-OP* ligands

To demonstrate the general ability of bidentate *P-OP* ligands **124** and **125** to form stable, well-defined complexes with transition metals, we converted several of these into olefinic cationic Rhodium(I) complexes following well established procedures.<sup>87</sup> Reaction of chiral *P-OP* ligands (**124c**, **125a**, **125h** and **125k**) with stoichiometric amounts of  $[\text{Rh}(\text{nbd})_2]\text{BF}_4$  in dichloromethane proceeded smoothly to provide the corresponding  $[\text{Rh}(\text{P-OP})(\text{nbd})]\text{BF}_4$  cationic complexes **141c**, **142a**, **142h** and **142k** (Scheme 18) in yields ranging from 22% to 53% after isolation.

<sup>87</sup> Deerenberg, S.; Pamies, O.; Dieguez, M.; Claver, C.; Kamer, P. C. J.; van Leeuwen, P. W. N. *M. J. Org. Chem.* **2001**, *66*, 7626-7631.



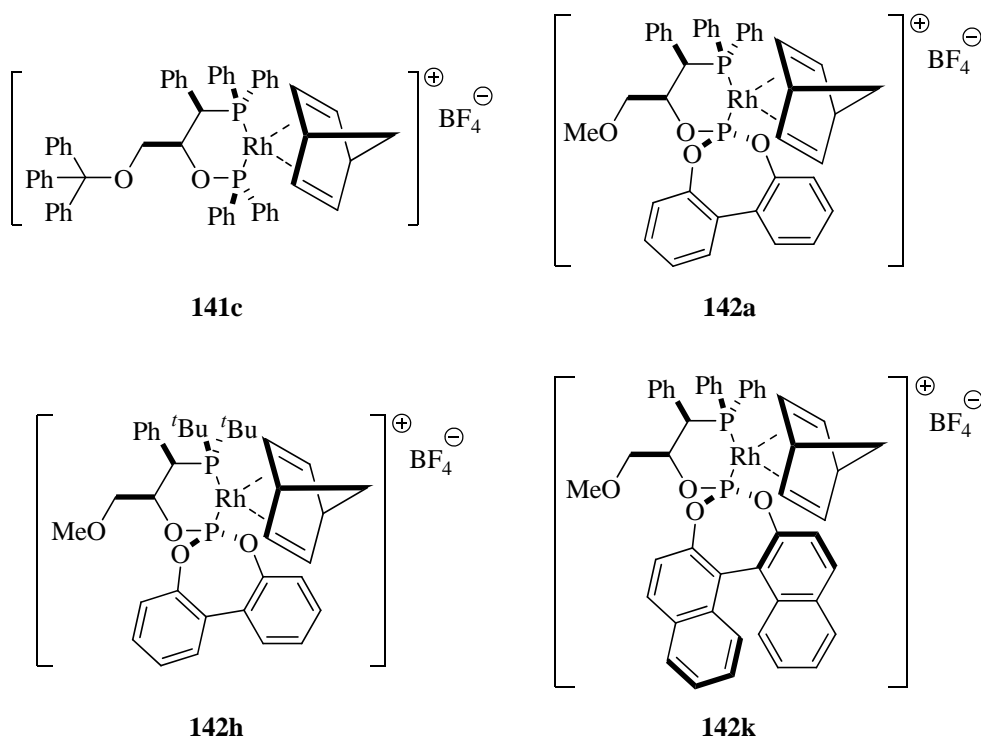
**Scheme 18.** Synthesis of cationic Rhodium(I) complexes with *P-OP* ligands.

Complexes **141c**, **142a**, **142h** and **142k** (Figure 14) crystallized out as orange, air-stable solids upon addition of diethyl ether to their dichloromethane solutions. Their high-resolution ESI mass spectra were in agreement with the cationic mononuclear species. The <sup>1</sup>H-NMR data revealed an unsymmetrical coordination pattern between the ligand backbone and the norbornadiene unit. Finally, the <sup>31</sup>P{<sup>1</sup>H}-NMR spectra for **141c**, **142a**, **142h** and **142k** showed two sharp doublets of doublets, from the <sup>31</sup>P-<sup>103</sup>Rh and <sup>31</sup>P-<sup>31</sup>P couplings (Table 7). All of these results are consistent with the presence of a six-membered chelate ring in these complexes (Figure 15).



**Table 7.**  $^{31}\text{P}\{^1\text{H}\}$ -NMR data for complexes  $[\text{Rh}(\text{P-OP})(\text{nbd})]\text{BF}_4$  **141c**, **142a**, **142h**, and **142k**.<sup>a</sup>

Complex	<i>P-O</i> (phosphinite or phosphite moieties)			<i>P-C</i> (phosphine moiety)		
	$\delta$ (ppm)	$J_{\text{P-Rh}}$ (Hz)	$J_{\text{P-P}}$ (Hz)	$\delta$ (ppm)	$J_{\text{P-Rh}}$ (Hz)	$J_{\text{P-P}}$ (Hz)
<b>141c</b>	128.80	174	48	25.96	152	48
<b>142a</b>	135.74	266	66	30.20	146	66
<b>142h</b>	138.61	277	54	65.14	139	54
<b>142k</b>	138.92	268	65	35.23	144	65

<sup>a</sup> The spectra were recorded at room temperature.**Figure 15.** Rhodium(I) complexes prepared according to Scheme 18.

Furthermore, we characterized **142a** and **142h** by X-ray crystallography to confirm the coordination mode of our bidentate *P-OP* ligands. An ORTEP view of the molecular structure of **142a** and of **142h** is shown in Figures 16 and 17, respectively, and the values of selected bond lengths and angles in these compounds are summarized in Tables 8 and 9, respectively.

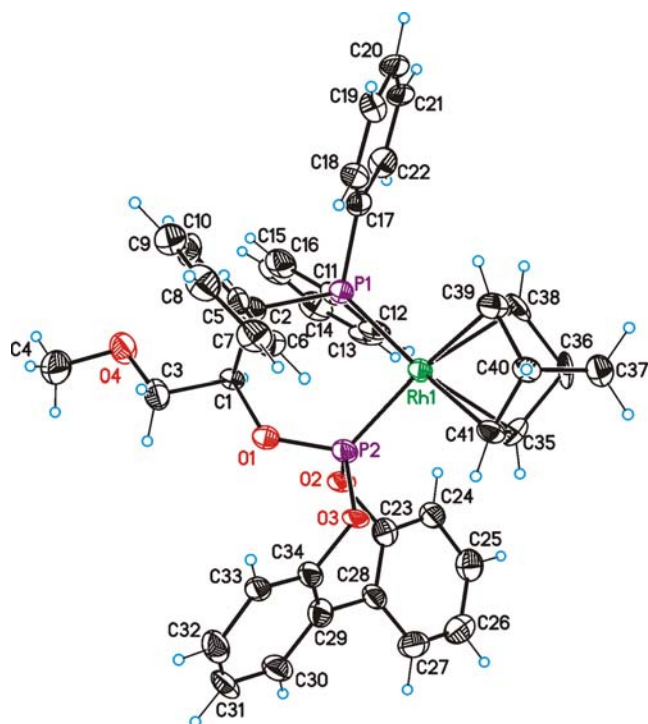


**Figure 16.** ORTEP drawing of cationic Rhodium complex **142a** with the atom-labeling scheme. The hydrogen atoms and  $\text{BF}_4$  have been omitted for clarity.

**Table 8.** Selected bond lengths (Å) and angles (deg) for complex **142a**.

Rh(1)-P(1)	2.298(2)
Rh(1)-P(2)	2.208(2)
Rh(1)-C(38)	2.275(8)
Rh(1)-C(39)	2.249(8)
Rh(1)-C(35)	2.207(7)
Rh(1)-C(41)	2.201(9)
C(38)-C(39)	1.353(14)
C(35)-C(41)	1.364(12)
P(2)-Rh(1)-P(1)	89.37(9)

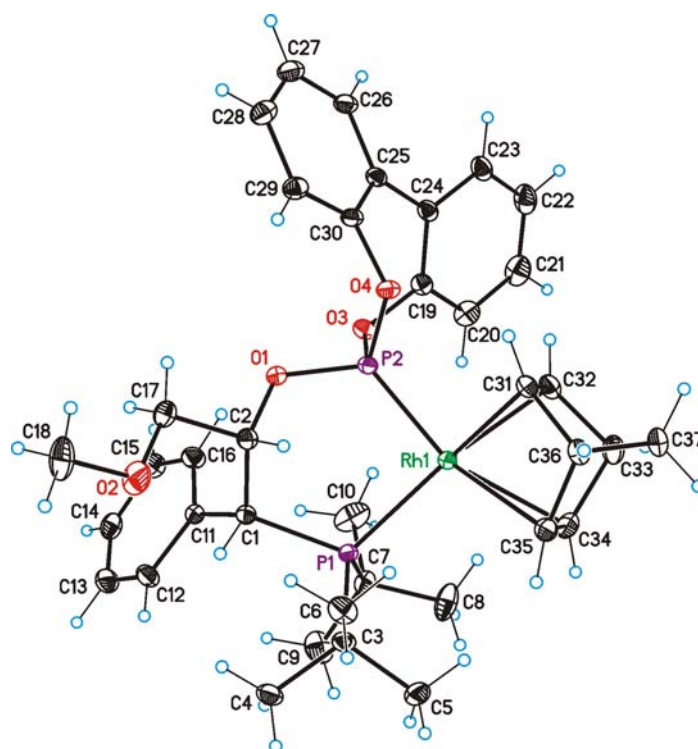


**Figure 17.** ORTEP drawing of cationic Rhodium complex **142h** with the atom-labeling scheme. The hydrogen atoms and  $\text{BF}_4$  have been omitted for clarity.

**Table 9.** Selected bond lengths (Å) and angles (deg) for complex **142h**.

Rh(1)-P(1)	2.4105(3)
Rh(1)-P(2)	2.1882(3)
Rh(1)-C(34)	2.3450(11)
Rh(1)-C(35)	2.3541(12)
Rh(1)-C(31)	2.1759(11)
Rh(1)-C(32)	2.1783(10)
C(34)-C(35)	1.3644(18)
C(31)-C(32)	1.3925(17)
P(2)-Rh(1)-P(1)	91.330(10)

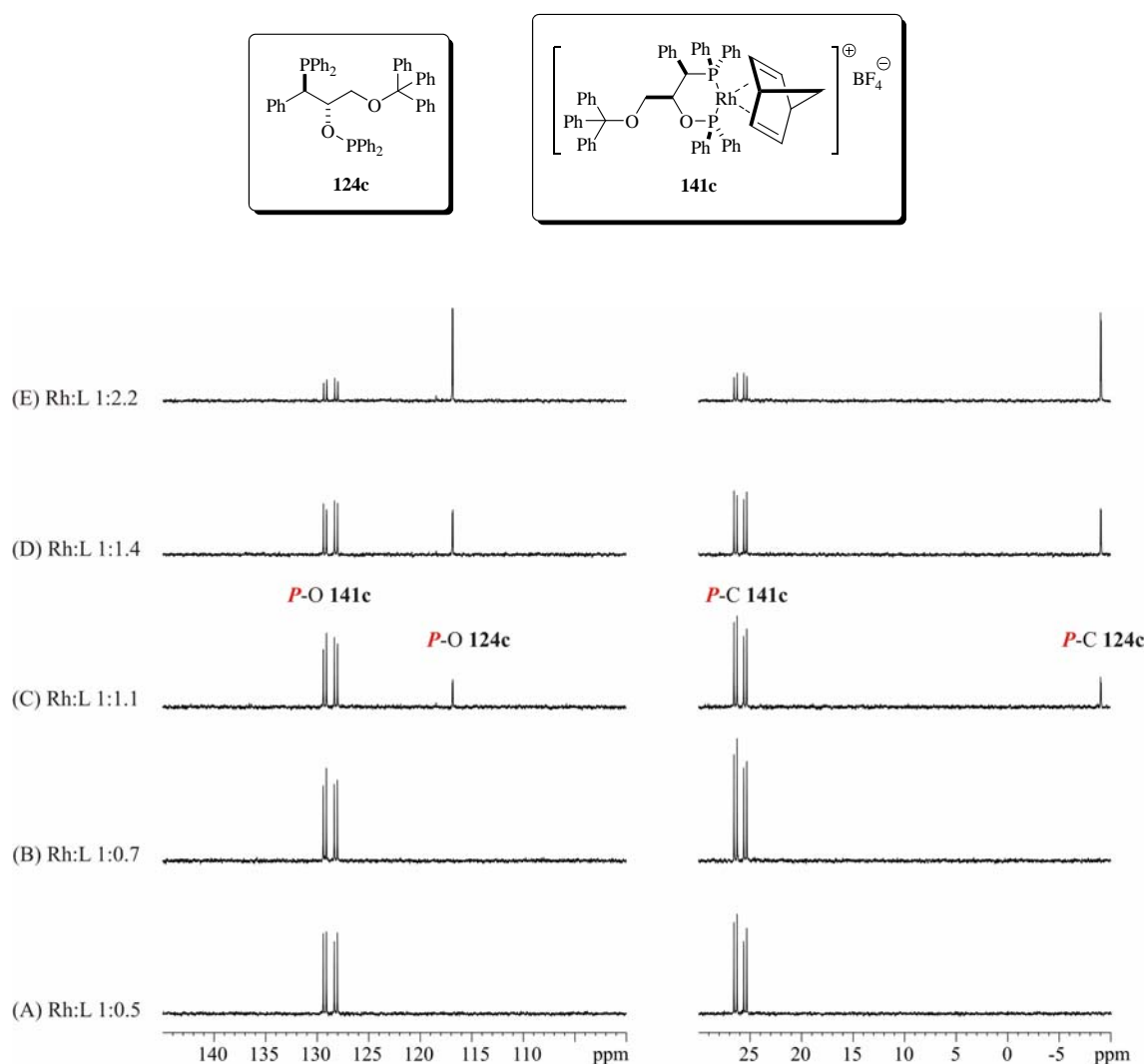
### 1.2.4.3 $^{31}\text{P}\{^1\text{H}\}$ -NMR titrations of enantiomerically pure *P-OP* ligands with Rhodium precursors

To study the formation of complexes in solution between our *P-OP* ligands and  $[\text{Rh}(\text{nbd})_2]\text{BF}_4$ , we prepared numerous solutions containing different relative molar amounts of ligand and Rhodium compound.

To study the complexation of phosphine-phosphinite compounds with  $[\text{Rh}(\text{nbd})_2]\text{BF}_4$ , we used **124c** as representative compound. Solutions containing molar ratios (Rhodium precursor/ligand) from 1:0.5 to *ca.* 1:2 were prepared by adding a solution of **124c** to the required amounts of  $[\text{Rh}(\text{nbd})_2]\text{BF}_4$ , such that the overall ligand concentration remained roughly constant.  $^{31}\text{P}\{^1\text{H}\}$ -NMR analysis of the different solutions (see Figure 18) clearly illustrated the complexation phenomena at different relative ratios of the reagents.

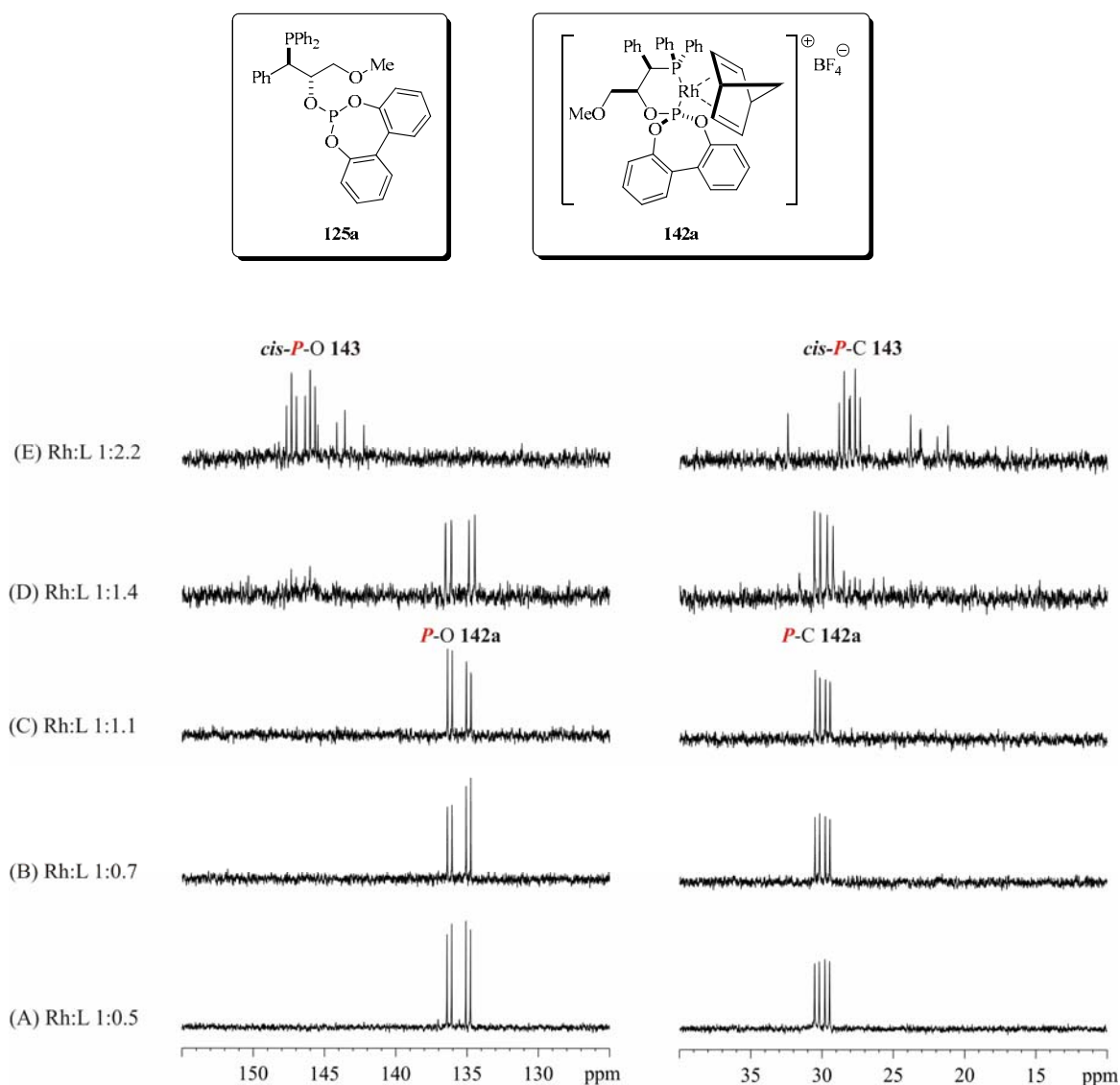
When an excess of Rhodium precursor was present in the solution (see A and B in Figure 18), two sharp doublets of doublets were observed and indicated the formation of the cationic Rhodium complex **141c** as the dominant species in solution. When an excess of ligand was added ( $[\text{Rh}(\text{nbd})_2]\text{BF}_4/[\text{124c}] < 1.0$ ; see C, D and E in Figure 18), the resulting  $^{31}\text{P}\{^1\text{H}\}$ -NMR spectrum followed the same trend, except that the intensity of the signals corresponding to unbound ligand **124c** increased with increasing ligand.

The main conclusion that can be drawn from these experiments is that the 1:1 chelate between  $[\text{Rh}(\text{nbd})_2]\text{BF}_4$  and **124c** is the only Rhodium complex formed in the concentration range (mM scale) and molar ratios ( $0.5 < [\text{Rh}(\text{nbd})_2]\text{BF}_4/[\text{124c}] < \text{ca. } 2$ ) studied.



**Figure 18.**  $^{31}\text{P}\{^1\text{H}\}$ -NMR titration (400MHz, dichloromethane- $d_2$ ) of chiral *P-OP* **124c** with  $[\text{Rh}(\text{nbd})_2]\text{BF}_4$  at different ratios.

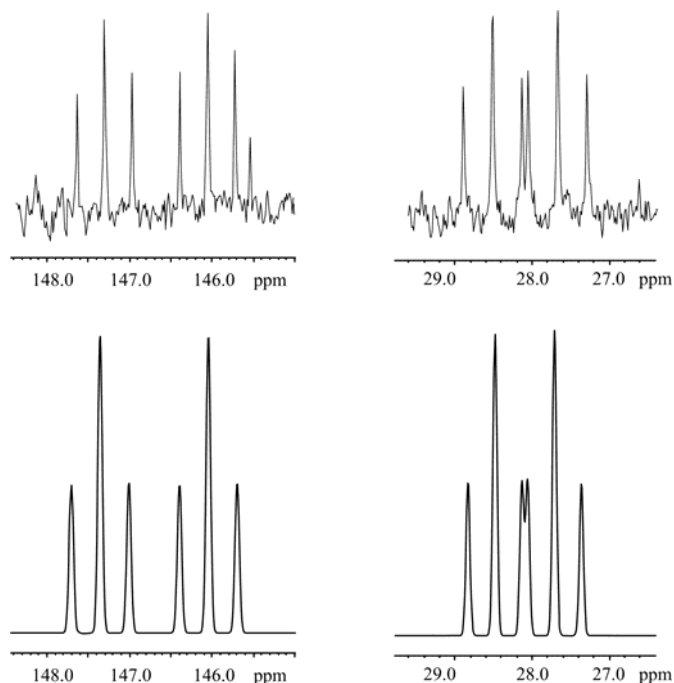
We then studied the complexation behavior of our phosphine-phosphites **125** with  $[\text{Rh}(\text{nbd})_2]\text{BF}_4$  in a similar experiment, using **125a** as representative compound for our phosphine-phosphites. We assessed solutions at molar ratios  $[\text{Rh}(\text{nbd})_2]\text{BF}_4/[\mathbf{125a}]$  ranging from 1:0.5 to *ca.* 1:2, prepared analogously to those described above for **124a**. The overall ligand concentration also remained roughly constant throughout this study.



**Figure 19.** Changes in the  $^{31}\text{P}\{^1\text{H}\}$ -NMR (400 MHz, dichloromethane- $d_2$ ) spectra acquired at 298 K during the titration of **125a** with  $[\text{Rh}(\text{nbd})_2]\text{BF}_4$ .

With an excess of  $[\text{Rh}(\text{nbd})_2]\text{BF}_4$  (see A and B in Figure 19),  $^{31}\text{P}\{^1\text{H}\}$ -NMR analysis showed that the target complex **142a** was the major species in solution. Interestingly, new Rhodium-containing species were formed when an excess of phosphine-phosphite was used (see D and E in Figure 19). Thus, when the Rhodium precursor to ligand ratio was *ca.* 1:2, the  $^{31}\text{P}\{^1\text{H}\}$ -NMR spectrum showed two sharp doublets of triplets corresponding to the new compound **143**, as major product, plus other, non-assigned peaks (see E in Figure 19). The  $^{31}\text{P}\{^1\text{H}\}$  data for **143** is in agreement with an  $\text{A}_2\text{X}_2$  spin system (Figure 20)

consisting of one doublet of triplets in the characteristic phosphine region and the same signal multiplicity in the phosphite region.

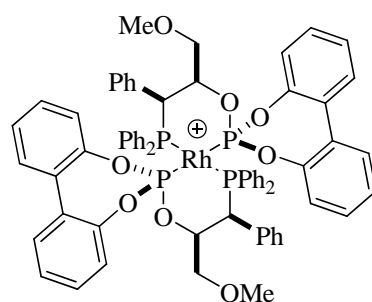


**Figure 20.** Experimentally measured (top) and calculated (bottom)  $^{31}\text{P}\{^1\text{H}\}$ -NMR spectra for complex **143**. Coupling constants used for the simulated spectrum:  $^{88}J_{\text{P-C,Rh}} = 125$  Hz;  $J_{\text{P-O,Rh}} = 212$  Hz; and  $J_{\text{P-C,P-O}} = 56$  Hz.

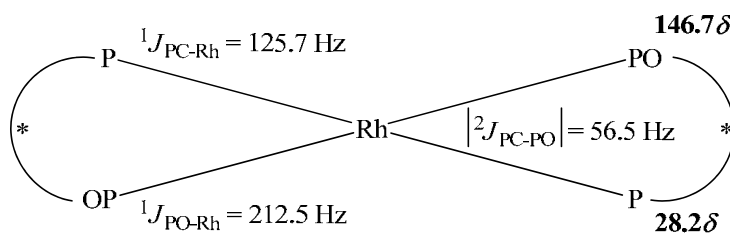
The simplicity of the signals suggested a highly symmetric molecule, such as a 2:1 chelate between **125a** and the Rhodium precursor with a *cis* arrangement of the phosphine and the phosphite groups (*cis*-**143**, Figure 21). In this complex, the two phosphine and the two phosphite nuclei are magnetically equivalent, and the signals corresponding to each kind of phosphorus functionality are observed as a doublet of triplets by virtue of their coupling to one Rhodium nucleus and to the two other phosphorus nuclei. This type of structure has been reported by Pizzano *et al.* for work on related chiral phosphine-phosphite ligands.<sup>89</sup>

<sup>88</sup>  $^{31}\text{P}\{^1\text{H}\}$ -NMR simulated spectrum by g-NMR v 5.0.

<sup>89</sup> Rubio, M.; Vargas, S.; Suarez, A.; Alvarez, E.; Pizzano, A. *Chem. Eur. J.* **2007**, *13*, 1821-1833.

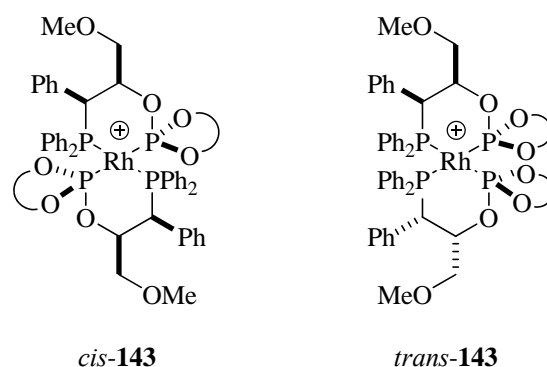
*cis*-**143****Figure 21.** Hypothetical structure for the complex *cis*-**143**.

The  $^{31}\text{P}\{^1\text{H}\}$  chemical shifts, and  $^1J_{\text{P-Rh}}$ , and  $^2J_{\text{PC-PO}}$  coupling constants, were directly extracted from the spectra by first order analysis. The  $^{31}\text{P}\{^1\text{H}\}$ -NMR spectral parameters are illustrated in Figure 22.

**Figure 22.**  $^{31}\text{P}\{^1\text{H}\}$ -NMR spectra data for the complex *cis*-**143**.

Complex **143** was prepared by reacting 1.0 equivalent of  $[\text{Rh}(\text{nbd})_2]\text{BF}_4$  with 2.2 equivalents of **125a** in dichloromethane at room temperature. After 5 hours of stirring, the desired  $[\text{Rh}(\text{125a})_2]\text{BF}_4$  complex **143** was isolated upon precipitation with diethyl ether (48% yield). Its structure was confirmed by high-resolution ESI mass spectroscopy (found: 1231.2296;  $\text{C}_{68}\text{H}_{60}\text{O}_8\text{P}_4\text{Rh} (\text{M-BF}_4)^+$  requires: 1231.2294). Moreover, the  $^{31}\text{P}\{^1\text{H}\}$ -NMR and  $^1\text{H}$ -NMR data revealed that the isolated Rhodium complex comprised a mixture of *cis* and *trans* isomers in the ratio 1.3:1 (see Figures 23 and 24).





Ratio *cis/trans*-**143**: 1.3/1

**Figure 23.** Complex **143** as a mixture of *cis* and *trans* isomers.

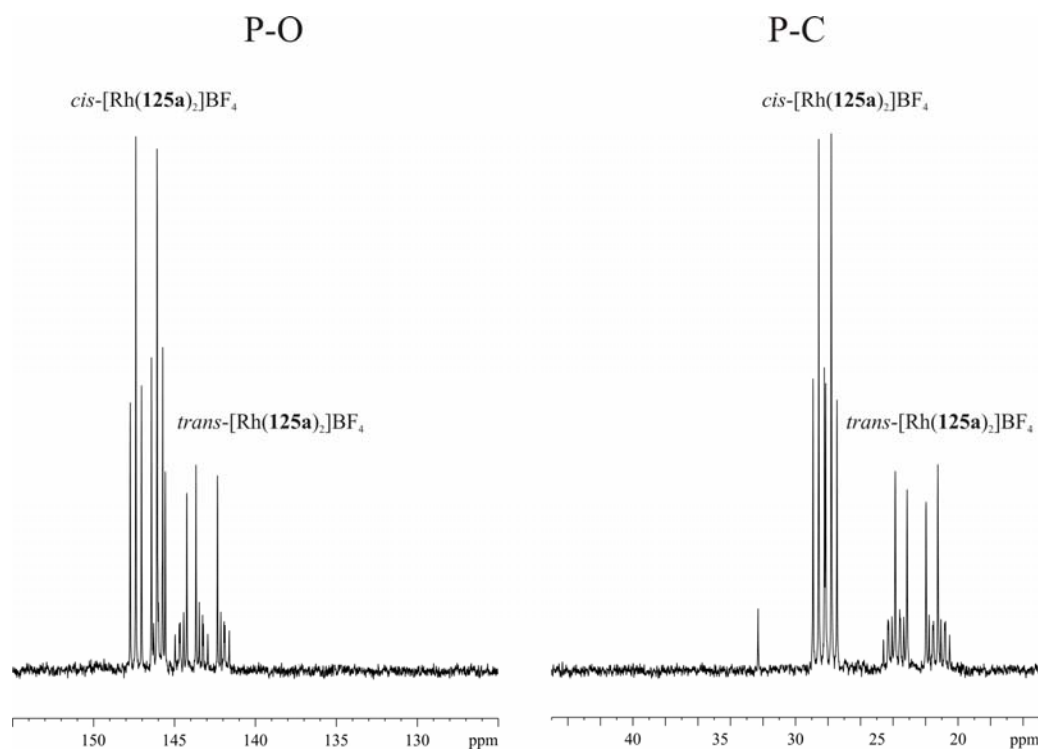


**Figure 24.**  $^{31}\text{P}\{^1\text{H}\}$ -NMR spectrum of complex **143**.

These data were in good agreement with the NMR titration experiment under the same Rhodium to chiral ligand ratio (see E in Figure 19) and allowed us to assign the other unknown signals in the  $^{31}\text{P}\{^1\text{H}\}$ -NMR spectrum to complex *trans*-**143** (Figure 25).

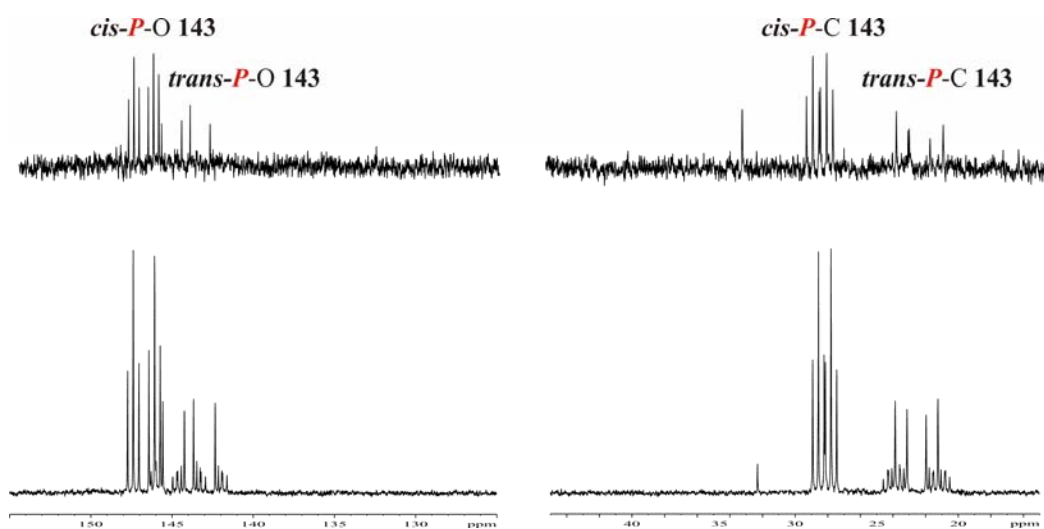


**Figure 25.**  $^{31}\text{P}\{^1\text{H}\}$ -NMR spectra comparison for the NMR titration (top) and Rhodium complex **143** (bottom).

The signal multiplicity for the phosphorus nuclei in complex *trans*-**143** is in agreement with an AA'XX' spin system. In this case, the two phosphorus nuclei corresponding to the phosphine groups (or to the phosphite phosphorus nuclei) are magnetically inequivalent. As such, a second order  $^{31}\text{P}\{^1\text{H}\}$ -NMR spectrum is observed. Simulation programs are required to extract the spectral parameters from an AA'XX' spin system. The simulated and experimental  $^{31}\text{P}\{^1\text{H}\}$ -NMR spectra for complex *trans*-**143**, along with the  $^{31}\text{P}\{^1\text{H}\}$  chemical shifts and coupling constants ( $^1J_{\text{P-Rh}}$  and  $^2J_{\text{P-P}}$ ), are summarized in Figure 26.<sup>88</sup>

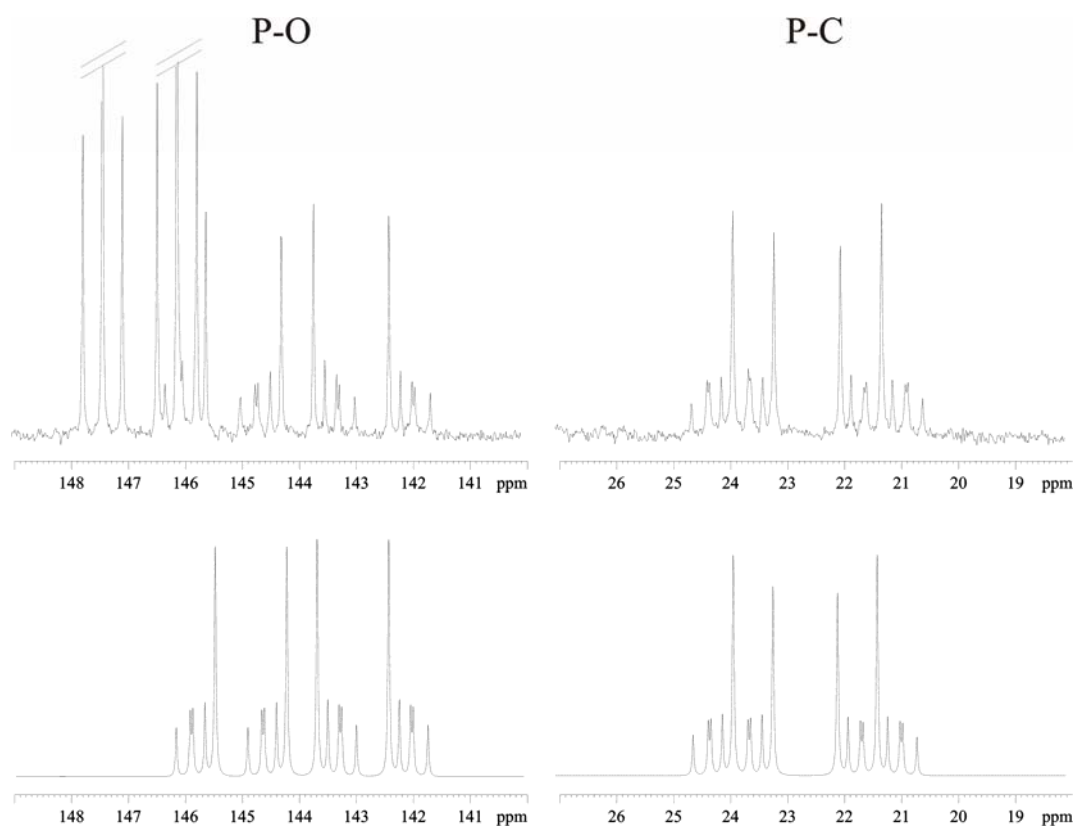
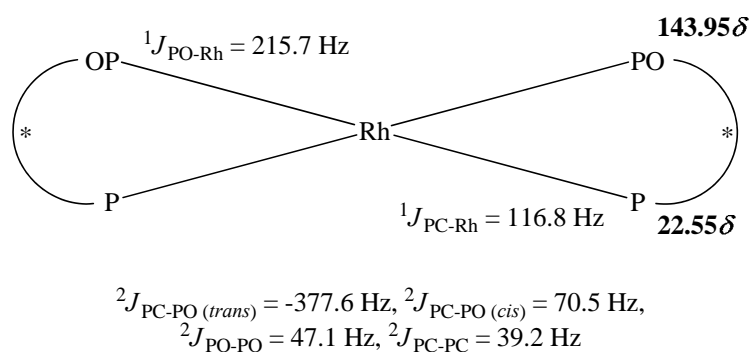


**Figure 26.** Experimentally measured (top) and calculated (bottom)  ${}^{31}\text{P}\{^1\text{H}\}$ -NMR spectra for complex **143**. Coupling constants used for the simulated spectrum:<sup>88</sup>  $J_{\text{P-C,Rh}} = 117 \text{ Hz}$ ,  $J_{\text{P-O,Rh}} = 215 \text{ Hz}$ ,  ${}^2J_{\text{PC-PO (trans)}} = -378 \text{ Hz}$ ,  ${}^2J_{\text{PC-PO (cis)}} = 70 \text{ Hz}$ ,  ${}^2J_{\text{PO-PO}} = 47 \text{ Hz}$ ,  ${}^2J_{\text{PC-PC}} = 39 \text{ Hz}$ .

In conclusion, an excess of our chiral phosphine-phosphite ligands with respect to the Rhodium precursor favors the formation of 2:1 chelates. Thus, the differences in complexation behavior between the phosphine-phosphite ligands and the phosphine-phosphinite ligands should be noted.

## 1.2.5. Catalytic studies of *P-OH* and *P-OP* ligands in Rhodium-catalyzed asymmetric hydrogenation

### 1.2.5.1 Evaluating the catalytic performance of Rhodium complexes of *P-OH* ligands in the asymmetric hydrogenation of functionalized alkenes

We have shown our progress in the design, preparation and optimization of new, highly modular phosphino alcohol (*P-OH*), and phosphino-phosphinite and phosphino-phosphite (*P-OP*), ligands featuring original structural motifs (Figure 27), whereby  $R^1$ - $R^4$  can be modified by changing the starting epoxide. The *P-OP* ligands comprise a set of ligands with different substituents on the phosphino group ( $R^5$  = Ph or alkyl) and on the phosphinite or phosphite group ( $R^6$ ,  $R^7$  = Ph, 2,2'-biaryl compounds, or alkyl). All these ligands are highly modular in terms of the stereoelectronic characteristics of their molecular fragments. Once we prepared these ligands, we assessed their performance in Rhodium-catalyzed asymmetric hydrogenation.

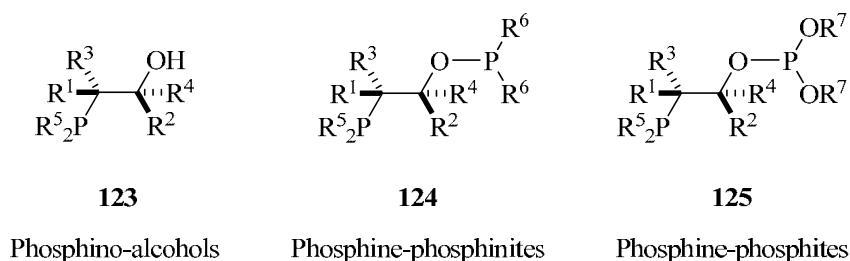
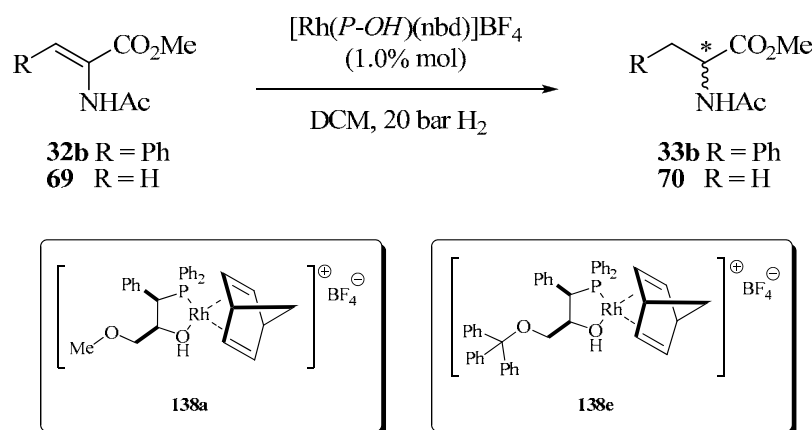


**Figure 27**

As mentioned in the previous section (see p. 68), *P-OH* ligands have been underexplored in metal-catalyzed asymmetric transformations. Therefore, we were interested in testing the activity of our *P-OH* ligands in Rhodium-catalyzed asymmetric transformations of functionalized alkenes. We evaluated the performance of  $[Rh(P-OH)(nbd)]BF_4$  complexes **138a** and **138e** in asymmetric

hydrogenations of methyl (*Z*)-(*N*)-acetylaminoacrylate (*Z*-MAC) (**32b**) and methyl-(*N*)-acetylaminoacrylate (MAA) (**69**). The results are shown in Table 10.

**Table 10.** Asymmetric hydrogenation of functionalized substrates methyl (*Z*)-(*N*)-acetylaminoacrylate (**32b**) and methyl-(*N*)-acetylaminoacrylate (**69**) catalyzed by [Rh(*P*-*OH*)(nbd)]BF<sub>4</sub> complexes.



Entry	Substrate	[Rh] complex	T (°C)	Conv. (%) <sup>a</sup>	ee (%) <sup>b</sup> (config) <sup>c</sup>
1	<b>32b</b>	<b>138a</b>	RT	14	Racemic
2	<b>32b</b>	<b>138e</b>	RT	16	Racemic
3	<b>32b</b>	<b>138a</b>	-40	0	nd <sup>d</sup>
4	<b>32b</b>	<b>138e</b>	-40	0	nd <sup>d</sup>
5	<b>69</b>	<b>138a</b>	RT	92	Racemic
6	<b>69</b>	<b>138e</b>	RT	80	43 ( <i>S</i> )
7	<b>69</b>	<b>138a</b>	-40	0	nd <sup>d</sup>
8	<b>69</b>	<b>138e</b>	-40	0	nd <sup>d</sup>

<sup>a</sup> Conversion was determined by <sup>1</sup>H-NMR spectroscopy.

<sup>b</sup> Enantiomeric excess was determined by HPLC or GC.

<sup>c</sup> The absolute configuration of the hydrogenated compounds was assigned by comparing optical rotation values or elution orders with reported values (see experimental section for details).

<sup>d</sup> nd: not determined.

As observed in Table 10, the catalytic activity of both cationic Rhodium complexes **138a** and **138e** was highly influenced by the substrate. Thus, at room temperature, low conversions were obtained for *Z*-MAC (Entries 1 and 2),

whereas high conversions were achieved for MAA (Entries 5 and 6). Furthermore, when the reactions were carried out at lower temperature (-40 °C), no conversion was observed for either substrate. Regarding enantioselectivity, Rhodium complex **138e** provided moderate enantioselectivity in the hydrogenation of MAA (up to 43% ee, Entry 6). However, in all other cases a racemic mixture was observed. The low conversions and enantioselectivities of these Rhodium complexes is probably due to the hemilabile character of phosphino alcohol ligands, as observed by Börner *et al.* in their work on related Rhodium complexes.<sup>85</sup> The enantioselectivity of Rhodium complex **138e**, which contains the bulkiest group (CPh<sub>3</sub>) around the CH<sub>2</sub>OR chain in the ligand backbone, remains to be understood.

To the best of our knowledge, this is the first report of chiral phosphino alcohols that can induce chirality in the Rhodium-catalyzed hydrogenation of functionalized alkenes.

#### *1.2.5.2 Evaluating the catalytic performance of Rhodium complexes of phosphine-phosphinite ligands in the asymmetric hydrogenation of functionalized alkenes*

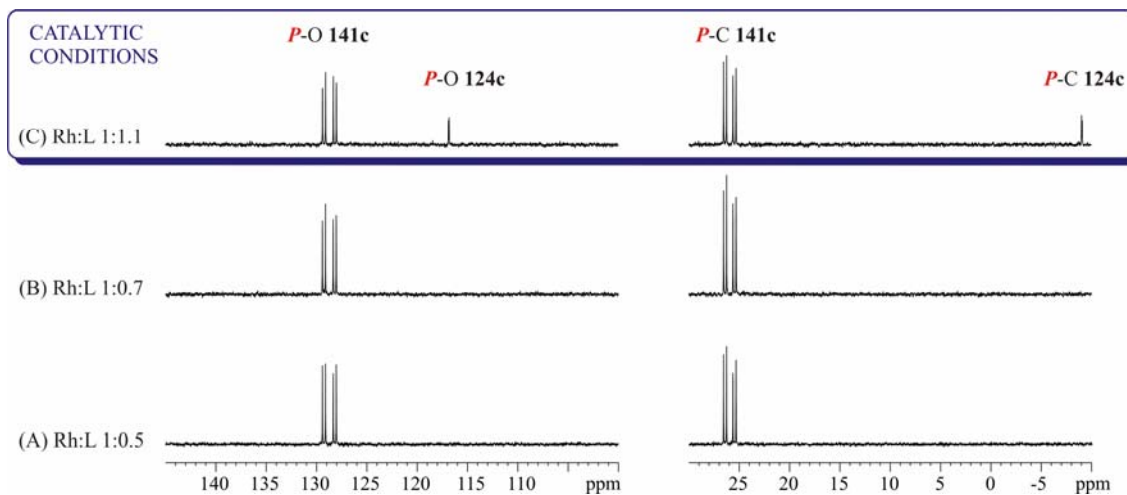
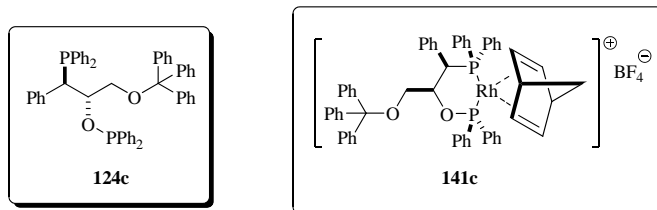
We then tested phosphine-phosphinite ligands **124a-d** in the same chemistry as above. Using an established protocol,<sup>79d</sup> the pre-catalysts for hydrogenation ([Rh(**124a-d**)(nbd)]BF<sub>4</sub>) were prepared *in situ* by adding a 10% molar excess of the corresponding phosphine-phosphinite to the Rhodium precursor [Rh(nbd)<sub>2</sub>]BF<sub>4</sub>. The results are summarized in Tables 11 and 12.

The effects of the solvent, catalyst preparation method, and pressure were investigated for the catalytic precursors containing ligands **124a** and **124c** on Z-MAC as substrate. Enantioselectivity was found to be influenced by the solvent (Table 11, Entries 1-4 and 6-9). Interestingly, despite the fact that Rhodium-catalyzed asymmetric hydrogenations are commonly performed in methanol, we

observed the lowest enantioselectivity when using this solvent (Table 11, Entries 1 and 7); similar results were observed for THF (Table 11, Entry 8). In contrast, the best results were obtained with DCM (Table 11, Entries 4 and 10).

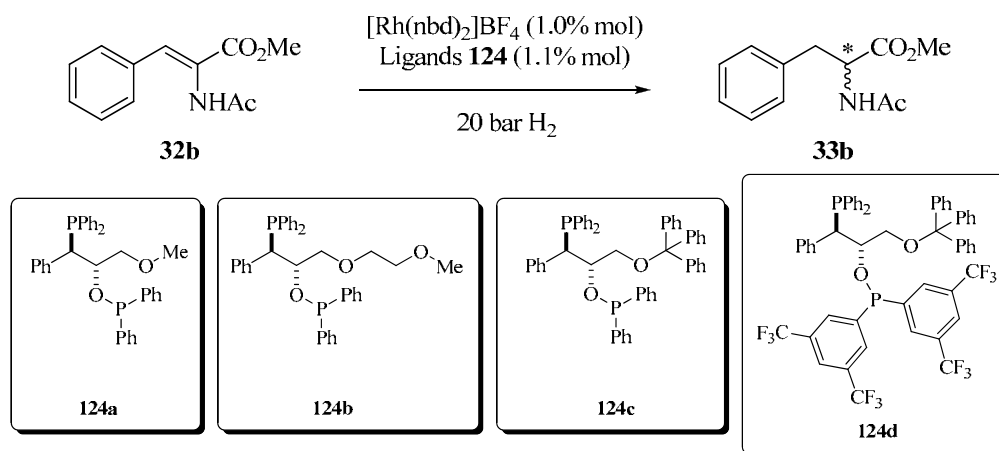
Although we used a pressure of 20 bars in our standard conditions, we were able to achieve high conversion at only 10 bar (Table 11, Entry 12).

The way by which the pre-catalyst was formed did not affect either conversion or enantioselectivity: the same results were obtained when the catalyst precursor was generated *in situ* (using  $[\text{Rh}(\text{nbd})_2]\text{BF}_4$  and **124c**) as when it was pre-formed (using  $[\text{Rh}(\text{124c})(\text{nbd})]\text{BF}_4$  **141c**) (Table 11, Entries 10 and 11, respectively). This result is in good agreement with the  $^{31}\text{P}\{^1\text{H}\}$ -NMR titration data for chiral phosphine-phosphinite ligands (see Section 1.2.4.3, p. 98). As observed in Figure 28, under the catalytic hydrogenation conditions (a 1:1.1 Rhodium to ligand ratio), the  $^{31}\text{P}\{^1\text{H}\}$ -NMR spectrum showed only two sets of signals, which is consistent with pre-catalyst **141c** being the only Rhodium-containing species.



**Figure 28.** <sup>31</sup>P{<sup>1</sup>H}-NMR titration (400 MHz, dichloromethane-*d*<sub>2</sub>) of chiral *P-OP* 124c with [Rh(nbd)<sub>2</sub>]BF<sub>4</sub> at different ratios.



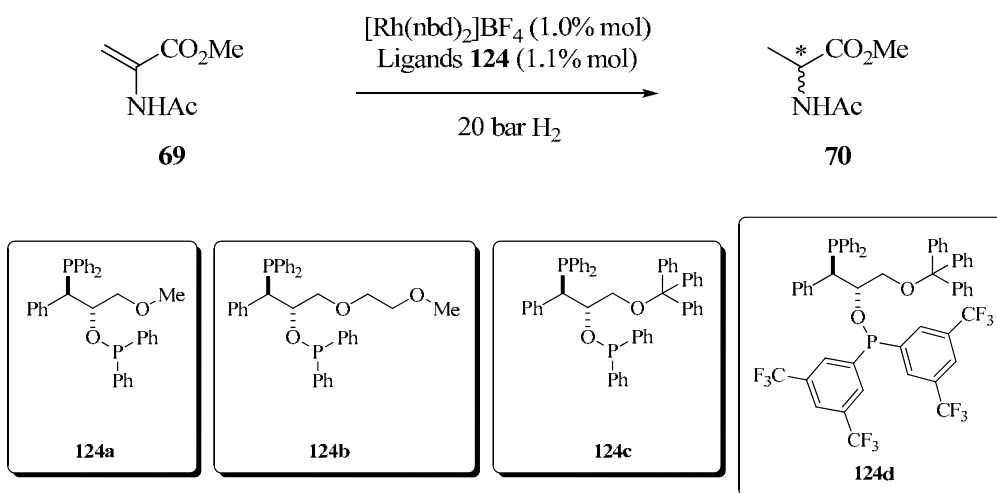
**Table 11.** Asymmetric hydrogenation of methyl (Z)-(*N*)-acetylaminoacinnamate (**32b**) catalyzed by [Rh(**124a-d**)(nbd)]BF<sub>4</sub>.<sup>a</sup>

Entry	Ligand	Solvent	Conv. (%) <sup>b</sup>	ee (%) <sup>c</sup> (config) <sup>d</sup>
1	<b>124a</b>	MeOH	>99	17 ( <i>S</i> )
2	<b>124a</b>	Toluene	>99	17 ( <i>S</i> )
3	<b>124a</b>	DCM/Toluene	>99	24 ( <i>S</i> )
4	<b>124a</b>	DCM	>99	26 ( <i>S</i> )
5	<b>124b</b>	Toluene	>99	15 ( <i>S</i> )
6	<b>124b</b>	DCM	>99	24 ( <i>S</i> )
7	<b>124c</b>	MeOH	>99	37 ( <i>S</i> )
8	<b>124c</b>	THF	>99	39 ( <i>S</i> )
9	<b>124c</b>	DCM/Toluene	>99	44 ( <i>S</i> )
10	<b>124c</b>	DCM	>99	52 ( <i>S</i> )
11 <sup>e</sup>	<b>124c</b>	DCM	>99	52 ( <i>S</i> )
12 <sup>f</sup>	<b>124c</b>	DCM	>99	52 ( <i>S</i> )
13 <sup>g</sup>	<b>124c</b>	DCM	>99	37 ( <i>S</i> )
14 <sup>h</sup>	<b>124c</b>	DCM	0	nd
15	<b>124d</b>	DCM	>99	54 ( <i>R</i> )

<sup>a</sup> All hydrogenations were run at room temperature under 20 bar of H<sub>2</sub>, except for Entry 12.<sup>b</sup> Conversion was determined by <sup>1</sup>H-NMR spectroscopy.<sup>c</sup> Enantiomeric excess was determined by HPLC.<sup>d</sup> The absolute configuration of the hydrogenated compounds was assigned by comparing optical rotation values or elution orders with reported values (see experimental section for details).<sup>e</sup> Using pre-formed catalyst (**141c**).<sup>f</sup> The hydrogenation reaction was run under 10 bar of H<sub>2</sub>.<sup>g,h</sup> PPh<sub>3</sub> and dppp (1.1% mol) were respectively used as additives in the hydrogenation.

The complexes ( $[\text{Rh}(\mathbf{124a-d})(\text{nbd})]\text{BF}_4$ ) were also evaluated in the hydrogenation of MAA under standard conditions (*i.e.* a ligand to Rhodium ratio of 1.1:1, DCM, and 20 bar of  $\text{H}_2$ ) (Table 12). Each complex provided complete conversion within 12 hours at room temperature.

**Table 12.** Asymmetric hydrogenation of methyl (*N*)-acetylaminoacrylate (**69**) catalyzed by  $[\text{Rh}(\mathbf{124a-d})(\text{nbd})]\text{BF}_4$ .<sup>a</sup>



Entry	Ligand	Solvent	Conv. (%) <sup>b</sup>	ee (%) <sup>c</sup> (config) <sup>d</sup>
1	<b>124a</b>	DCM	>99	40 ( <i>S</i> )
2	<b>124b</b>	DCM	>99	40 ( <i>S</i> )
3	<b>124c</b>	DCM	>99	64 ( <i>S</i> )
4 <sup>e</sup>	<b>124c</b>	DCM	>99	13 ( <i>S</i> )
5 <sup>f</sup>	<b>124c</b>	DCM	0	nd <sup>g</sup>
6	<b>124d</b>	DCM	>99	32 ( <i>R</i> )

<sup>a</sup> All hydrogenations were run at room temperature under 20 bar of  $\text{H}_2$ .

<sup>b</sup> Conversion was determined by  $^1\text{H-NMR}$  spectroscopy.

<sup>c</sup> Enantiomeric excess was determined by GC.

<sup>d</sup> The absolute configuration of the hydrogenated compounds was assigned by comparing optical rotation values or elution orders with reported values (see experimental section for details).

<sup>e</sup>  $\text{PPh}_3$  (1.1% mol) was added as additive in the hydrogenation.

<sup>f</sup>  $\text{dppp}$  (1.1% mol) was added as additive in the hydrogenation.

<sup>g</sup> not determined.

The complexes provided poor to moderate enantioselectivities (26-64% ee) in the hydrogenation of *Z*-MAC and MAA, indicating that the stereoelectronics around their respective Rhodium centers were not optimal. However, steric congestion at the CH<sub>2</sub>OR chain was found to favor enantioselectivity for both substrates: the triphenylmethyl-substituted ligand **124c** provided greater enantioselectivity than did the methyl-substituted ligand **124a** (in Table 11, compare Entries 4 and 10; and in Table 12, compare Entries 1 and 3).

As expected, no differences in either conversion or and enantioselectivity in the hydrogenation of *Z*-MAC were observed when the pre-formed catalyst was used (Table 11, Entry 11). In terms of hydrogen pressure, the same trend was obtained when 10 bar of H<sub>2</sub> were used (Table 11, Entry 12).

Feringa *et al.* recently reported<sup>90</sup> that the use of achiral additives (triaryl- and trialkyl-phosphines) in Rhodium-catalyzed asymmetric hydrogenations mediated by chiral monodentate phosphoramidites might enhance enantioselectivity. Upon addition of these additives, they observed remarkable improvements in the selectivity and activity of their asymmetric catalyst, which they attributed to the formation of mixed complexes comprising one phosphoramidite and one achiral additive, both of which coordinate to the Rhodium center.

Inspired by the findings of Feringa *et al.*, yet keeping in mind that the aforementioned activation mechanism might not be apply to our bidentate ligands, we investigated the hydrogenation of substrates *Z*-MAC and MAA by the Rhodium complex of **124c** (1.1 mol%) using PPh<sub>3</sub> (1.1 mol%) or dppp (1.1 mol%) as additives. PPh<sub>3</sub> led to a sharp decrease in enantioselectivity (in Table 11, compare Entries 10 with 13; and in Table 12, compare Entries 3 with 4). The presence of different Rhodium complexes incorporating both **124c** and the achiral PPh<sub>3</sub> ligand probably leads to a less stereodiscriminating reaction pathway. When dppp was added, no conversion was observed (Table 11, Entry

<sup>90</sup> (a) Hoen, R.; Boogers, J. A. F.; Bernsmann, H.; Minnaard, A. J.; Meetsma, A.; Tiemersma-Wegman, T. D.; de Vries, A. H. M.; de Vries, J. G.; Feringa, B. L. *Angew. Chem., Int. Ed.* **2005**, *44*, 4209-4212. (b) Panella, L.; Aleixandre, A. M.; Kruidhof, G. J.; Robertus, J.; Feringa, B. L.; De Vries, J. G.; Minnaard, A. J. *J. Org. Chem.* **2006**, *71*, 2026-2036.

14; and Table 12, Entry 5). Use of this additive probably leads to formation of complexes such as  $[\text{Rh}(\mathbf{124c})(\text{dppp})]\text{BF}_4$ , which would deactivate the Rhodium center of the catalyst in the hydrogenation of alkenes.

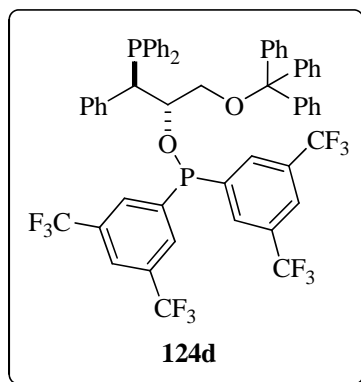


**Figure 29.** Phosphine-phosphinite ligand **124d**, featuring  $\text{CF}_3$  groups at the phosphinite moiety.

The two  $\text{CF}_3$  groups (at positions 3 and 5) on the phenyl ring in the phosphinite moiety of **124d**, which contains a trityl group at the  $\text{CH}_2\text{OR}$  chain (Figure 29), did not favor enantioselectivity. In fact, compared to the diphenyl-substituted **124c**, **124d** provided similar enantioselectivities for *Z*-MAC (in Table 11, compare Entries 10 and 15), and worse enantioselectivities for MAA (in Table 12, compare Entries 3 and 6).

Interestingly, **124c** and **124d** provided opposite enantioselectivities for the hydrogenated derivatives of *Z*-MAC and MAA (**33b** and **70**, respectively): **124c** led to the corresponding (*S*)-enantiomers, whereas **124d** led to the corresponding (*R*)-enantiomers. A similar reversal of configuration was observed by the groups of Pizzano<sup>80e</sup> and Monsees<sup>79b</sup> in related bidentate ligands upon modification of the coordination properties of the phosphorus groups (by changing from aromatic to alkyl substituents). We suggest that the different stereoelectronic properties of ligands **124c** and **124d** control the coordination mode of the functionalized alkene, thereby inducing preferred formation of different diastereomeric Rh(III)-

dihydride complexes, and consequently, yielding opposite enantiomers of the corresponding hydrogenated products.<sup>91,92</sup>

The design and optimization of ligands for catalysis is increasingly based on analysis of the diastereomeric transition states in the corresponding processes. This work has been facilitated by recent advances in computational chemistry—namely, the availability of tools for studying molecular systems of the size and nature of those involved in enantioselective catalysis. Thereby, the group of Prof. Maseras (ICIQ) is currently performing computational studies on our phosphine-phosphinite ligands. By examining the theoretical results from several examples of the same reaction, they aim to reach several fundamental conclusions. First, they are assessing how the structure of the ligands (in our case, the CH<sub>2</sub>OR group, and the substituents on the phosphine and phosphinite groups) affects the rate and enantioselectivity of the reaction. Specifically, they are trying to determine how the sterics and electronics of the ligand affect the reaction. Second, they are aiming to identify those substrates that should lead to higher conversion and enantioselectivity. We will then design and synthesize new potential ligands for asymmetric hydrogenations, based on their computational findings.

In summary, the Rhodium complexes of phosphine-phosphinite ligands **124a-d** are moderate catalysts (in terms of enantioselectivity) for asymmetric hydrogenation of functionalized olefins. This may be due to their conformational flexibility as well as to the fact that the phosphinite group is quite far away from the stereogenic centers.

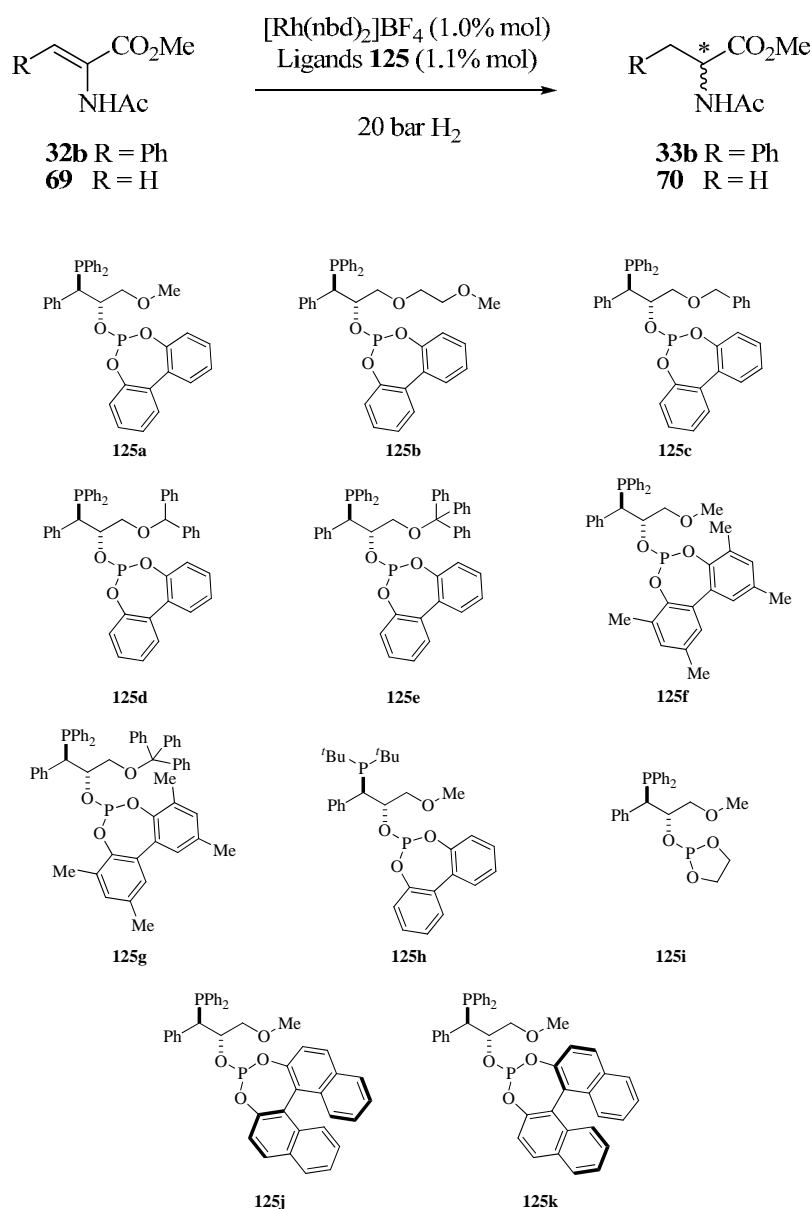
---

<sup>91</sup> (a) Pamies, O.; Dieguez, M.; Net, G.; Ruiz, A.; Claver, C. *J. Org. Chem.* **2001**, *66*, 8364-8369. (b) Deerenberg, S.; Pamies, O.; Dieguez, M.; Claver, C.; Kamer, P. C. J.; van Leeuwen, P. W. N. M. *J. Org. Chem.* **2001**, *66*, 7626-7631.

<sup>92</sup> (a) Landis, C. R.; Halpern, J. *J. Am. Chem. Soc.* **1987**, *109*, 1746-54. (b) Feldgus, S.; Landis, C. R. *J. Am. Chem. Soc.* **2000**, *122*, 12714-12727. (c) Landis, C. R.; Feldgus, S. *Angew. Chem., Int. Ed.* **2000**, *39*, 2863-2866.

### 1.2.5.3 Evaluating the catalytic performance of Rhodium complexes of phosphine-phosphite ligands in the asymmetric hydrogenation of functionalized alkenes

Finally, we tested phosphine-phosphite ligands **125a-k** in the same chemistry used to screen the other ligands (Scheme 19).



**Scheme 19.** Screening of phosphine-phosphites **125** in Rhodium-catalyzed asymmetric hydrogenation.

Following the same procedure described in the previous section, the complexes  $[\text{Rh}(\mathbf{125a-k})(\text{nbd})]\text{BF}_4$  were prepared *in situ* by mixing the corresponding Rhodium precursor with 1.1 molar equivalents of the ligands **125** under inert atmosphere in a suitable solvent. Hydrogenation was performed at different temperatures and under 20 bar of  $\text{H}_2$  in the presence of the pre-catalyst (1 mol%). In a first round of experiments, we sought to optimize the reaction conditions (*i.e.* solvent, Rhodium precursor, and temperature) using the catalytic precursor of ligands **125a** or **125e**, and Z-MAC as substrate. It should be recalled that phosphine-phosphites **125a** and **125e** represent the two extreme scenarios of steric bulk around the metal center (least bulky and bulkiest, respectively).

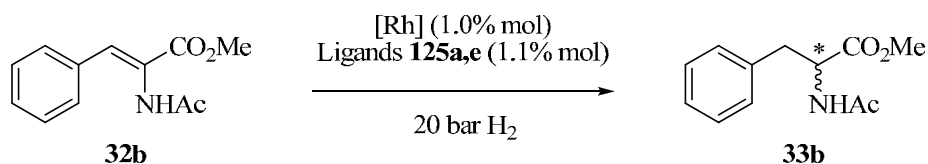
The solvent was observed to be critical to reaction outcome (Table 13). Although Rhodium-catalyzed asymmetric hydrogenations are usually performed in methanol, we decided to omit this solvent, since phosphite ligands are known to decompose in protic solvents under certain conditions.<sup>93</sup> The best enantioselectivities were obtained with THF (92% ee), and were slightly higher than those obtained with DCM (86% ee) for the catalysts containing ligand **125a** (in Table 13, compare Entries 1 and 2) and the same trend is observed for **125e** (in Table 13, compare Entries 3 and 4).

The enantioselectivities were slightly lower for the trityl-substituted ligand **125e** than for its methyl-substituted analog **125a** (in Table 13, compare Entries 1 and 3, or 2 and 4). These initial results reflected a trend that held constant throughout our subsequent studies: steric congestion around the metal center is detrimental to stereoselection.

---

<sup>93</sup> (a) Baker, M. J.; Harrison, K. N.; Orpen, A. G.; Pringle, P. G.; Shaw, G. *J. Chem. Soc., Chem. Commun.* **1991**, 803-4. (b) Nirchio, P. C.; Wink, D. J. *Organometallics* **1991**, *10*, 336-40.

**Table 13.** Solvent effects in the asymmetric hydrogenation of methyl (*Z*)-(*N*)-acetylaminoacinnamate (**32b**) with phosphine-phosphite ligands **125a** and **125e**.<sup>a</sup>



Entry	Ligand	Rh precursor	Solvent	T (°C)	Conv. (%) <sup>b</sup>	ee (%) <sup>c</sup> (config) <sup>d</sup>
1	<b>125a</b>	[Rh(nbd) <sub>2</sub> ]BF <sub>4</sub>	DCM	RT	>99	86 ( <i>R</i> )
2	<b>125a</b>	[Rh(nbd) <sub>2</sub> ]BF <sub>4</sub>	THF	RT	>99	92 ( <i>R</i> )
3	<b>125e</b>	[Rh(nbd) <sub>2</sub> ]BF <sub>4</sub>	DCM	RT	>99	79 ( <i>R</i> )
4	<b>125e</b>	[Rh(nbd) <sub>2</sub> ]BF <sub>4</sub>	THF	RT	>99	86 ( <i>R</i> )

<sup>a</sup> All hydrogenations were run at room temperature under 20 bar of H<sub>2</sub>.

<sup>b</sup> Conversion was determined by <sup>1</sup>H-NMR spectroscopy.

<sup>c</sup> Enantiomeric excess was determined by HPLC.

<sup>d</sup> The absolute configuration of the hydrogenated compounds was assigned by comparing optical rotation values or elution orders with reported values (see experimental section for details).

We also studied the influence of the Rhodium precursor on the stereochemical outcome of the reaction. The two commercially available precursors ([Rh(nbd)<sub>2</sub>]BF<sub>4</sub> and [Rh(cod)<sub>2</sub>]BF<sub>4</sub>) provided very similar conversions and enantioselectivities (in Table 14, compare Entries 1 and 2). These results are in agreement with literature reports. For example,<sup>94</sup> although the presence of norbornadiene (nbd) or cyclooctadiene (cod) in the initial Rhodium precursor is known to strongly influence the transformation of the precatalytic species into the catalytic species,<sup>95</sup> it normally has a much less pronounced effect on stereoselectivity. Compared to the tetrafluoroborate counteranion, the bulkier hexafluoroantimoniate (SbF<sub>6</sub><sup>-</sup>)<sup>96</sup> leads to slightly worse enantioselectivities for

<sup>94</sup> Drexler, H.-J.; Baumann, W.; Spannenberg, A.; Fischer, C.; Heller, D. *J. Organomet. Chem.* **2001**, *621*, 89-102.

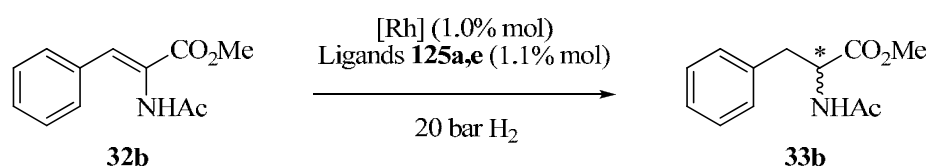
<sup>95</sup> No comparative measurements of the conversion at low reaction times were made at this stage.

<sup>96</sup> Adatia, T.; Curtis, H.; Johnson, B. F. G.; Lewis, J.; McPartlin, M.; Morris, J. *J. Chem. Soc., Dalton Trans.* **1994**, 3069-74.



both **125a** and **125e** (in Table 14, compare Entries 3 and 4, or 5 and 6, respectively). This observation further confirms our finding that steric congestion around the metal center is detrimental to enantioselectivity. In DCM, the counteranion would be positioned closely to the metal center, in order to compensate for the charge of the cationic Rhodium center. Thus, the larger the counteranion, the greater the congestion around the metal center.

**Table 14.** Effect of the Rhodium precursor on the asymmetric hydrogenation of methyl (*Z*)-(*N*)-acetylaminoacinnamate (**32b**) with phosphine-phosphite ligands **125a** and **125e**.<sup>a</sup>



Entry	Ligand	Rh precursor	Solvent	T (°C)	Conv. (%) <sup>b</sup>	ee (%) <sup>c</sup> (config) <sup>d</sup>
1	<b>125a</b>	[Rh(nbd) <sub>2</sub> ]BF <sub>4</sub>	THF	RT	>99	92 ( <i>R</i> )
2	<b>125a</b>	[Rh(cod) <sub>2</sub> ]BF <sub>4</sub>	THF	RT	>99	91 ( <i>R</i> )
3	<b>125a</b>	[Rh(nbd) <sub>2</sub> ]BF <sub>4</sub>	DCM	RT	>99	86 ( <i>R</i> )
4	<b>125a</b>	[Rh(cod) <sub>2</sub> ]SbF <sub>6</sub>	DCM	RT	>99	79 ( <i>R</i> )
5	<b>125e</b>	[Rh(nbd) <sub>2</sub> ]BF <sub>4</sub>	DCM	RT	>99	79 ( <i>R</i> )
6	<b>125e</b>	[Rh(cod) <sub>2</sub> ]SbF <sub>6</sub>	DCM	RT	>99	70 ( <i>R</i> )

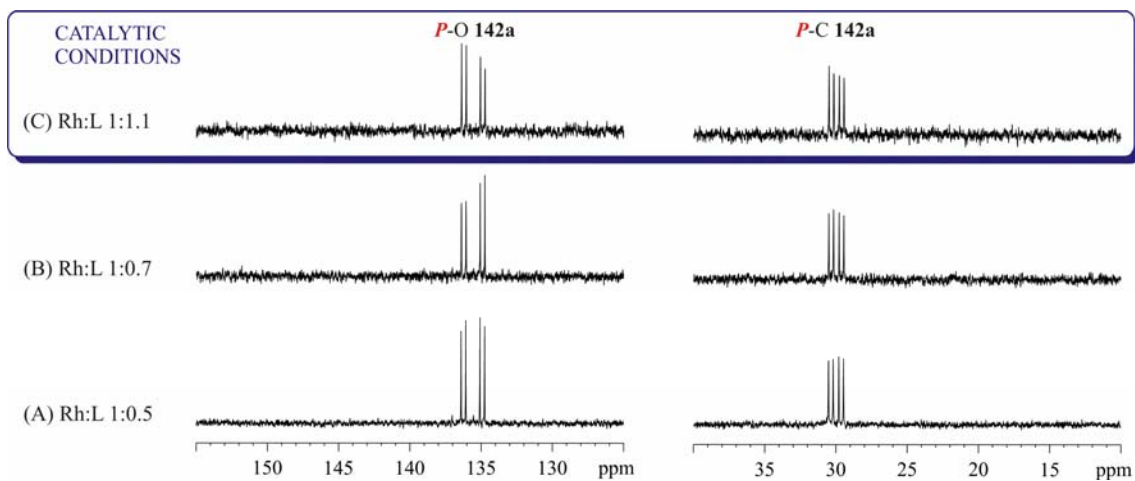
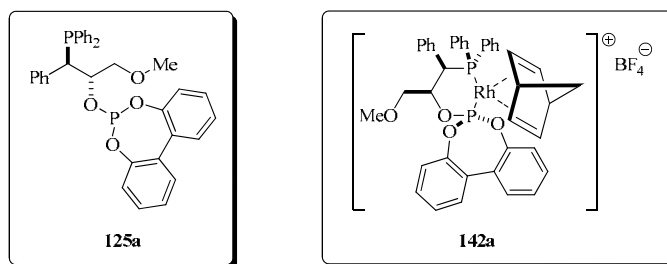
<sup>a</sup> All hydrogenations were run at room temperature under 20 bar of H<sub>2</sub>.

<sup>b</sup> Conversion was determined by <sup>1</sup>H-NMR spectroscopy.

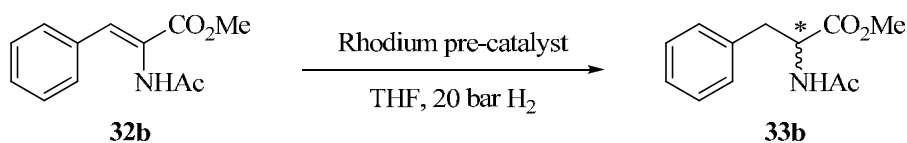
<sup>c</sup> Enantiomeric excess was determined by HPLC.

<sup>d</sup> The absolute configuration of the hydrogenated compounds was assigned by comparing optical rotation values or elution orders with reported values (see experimental section for details).

We also assessed how the stage at which the pre-catalyst [Rh(**125a**)(nbd)]BF<sub>4</sub> is prepared (*i.e.* pre-formed vs. *in situ* preparation) affects the reaction (Table 15). As mentioned in section 1.2.4.3 (page 102), mixture of [Rh(nbd)<sub>2</sub>]BF<sub>4</sub> with a 10% molar excess of phosphine-phosphite affords the desired 1:1 chelate [Rh(**125a**)(nbd)]BF<sub>4</sub> as the major Rhodium-containing species (see Figure 30).



**Figure 30.** <sup>31</sup>P{<sup>1</sup>H}-NMR titration (400 MHz, dichloromethane-*d*<sub>2</sub>) of chiral *P-OP* **125a** with [Rh(nbd)<sub>2</sub>]BF<sub>4</sub> at different molar ratios.

**Table 15.** Effects of the catalyst preparation method in asymmetric hydrogenation of methyl (*Z*)-(*N*)-acetylaminoacinnamate (**32b**) catalyzed by [Rh(**125a**)(nbd)]BF<sub>4</sub>.<sup>a</sup>

Entry	Catalyst preparation	T (°C)	Conv. (%) <sup>b</sup>	ee (%) <sup>c</sup> (config) <sup>d</sup>
1	<i>in situ</i> formation <sup>e</sup>	RT	>99	92 ( <i>R</i> )
2	pre-formation	RT	>99	92 ( <i>R</i> )

<sup>a</sup> All hydrogenations were run at room temperature under 20 bar of H<sub>2</sub>.

<sup>b</sup> Conversion was determined by <sup>1</sup>H-NMR spectroscopy.

<sup>c</sup> Enantiomeric excess was determined by HPLC.

<sup>d</sup> The absolute configuration of the hydrogenated compounds was assigned by comparing optical rotation values or elution orders with reported values (see experimental section for details).

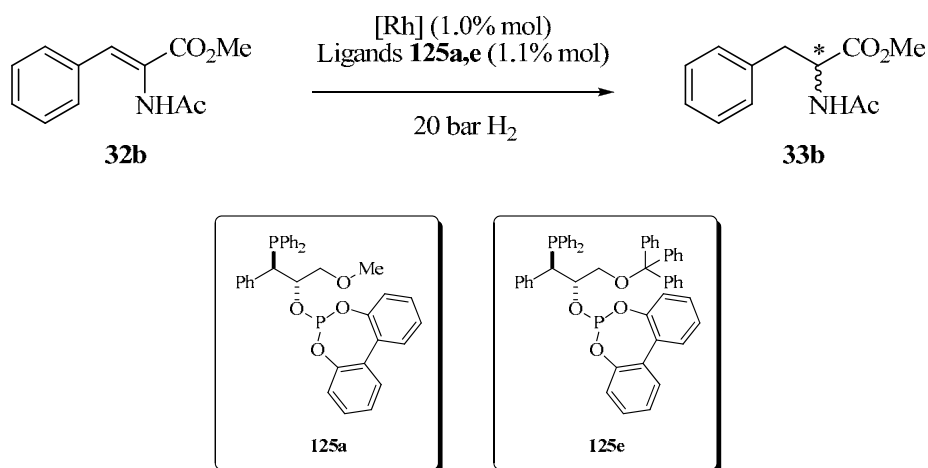
<sup>e</sup> See Section 1.2.4.3 for the details of the *in situ* preparation of [Rh(**125a**)(nbd)]BF<sub>4</sub>.

As reflected in Table 15, no differences in catalytic performance were observed between the two methods. However, it should be recalled that an excess of phosphine-phosphite ligand in the *in situ* preparation of the pre-catalyst [Rh(**125a**)(nbd)]BF<sub>4</sub> can be detrimental to catalytic activity. As described earlier (see Section 1.2.4.3, p. 102), a molar excess of ligand **125** with respect to the Rhodium centers provides the 2:1 chelate [Rh(**125a**)<sub>2</sub>]BF<sub>4</sub>. Since these 2:1 complexes are undesired in asymmetric hydrogenations,<sup>89</sup> *in situ* formation of the pre-catalyst demands careful control over the relative stoichiometry of [Rh(nbd)<sub>2</sub>]BF<sub>4</sub>.

We were able to enhance the enantioselectivities by running the hydrogenations at lower temperature (down to -40 °C): for ligand **125a**, the enantioselectivity improved from 92%, at room temperature, to 98% ee, at -40 °C (in Table 16, compare Entries 1 and 4, respectively). Similar improvements were observed for the trityl-substituted ligand **125e**, although the general trend that greater steric

bulk leads to worse enantioselectivity held true: all the enantioselectivities for this ligand were lower than the corresponding values for **125a**.

**Table 16.** Effects of temperature on the asymmetric hydrogenation of methyl (*Z*)-(*N*)-acetylaminoacinnamate (**32b**) with phosphine-phosphite ligands **125a** and **125e**.<sup>a</sup>



Entry	Ligand	Rh precursor	Solvent	T (°C)	Conv. (%) <sup>b</sup>	ee (%) <sup>c</sup> (config) <sup>d</sup>
1	<b>125a</b>	[Rh(nbd) <sub>2</sub> ] <sub>2</sub> BF <sub>4</sub>	THF	RT	>99	92 ( <i>R</i> )
2	<b>125a</b>	[Rh(nbd) <sub>2</sub> ] <sub>2</sub> BF <sub>4</sub>	THF	0	>99	93 ( <i>R</i> )
3	<b>125a</b>	[Rh(nbd) <sub>2</sub> ] <sub>2</sub> BF <sub>4</sub>	THF	-20	>99	95 ( <i>R</i> )
4	<b>125a</b>	[Rh(nbd) <sub>2</sub> ] <sub>2</sub> BF <sub>4</sub>	THF	-40	>99	98 ( <i>R</i> )
5	<b>125e</b>	[Rh(nbd) <sub>2</sub> ] <sub>2</sub> BF <sub>4</sub>	THF	RT	>99	86 ( <i>R</i> )
6	<b>125e</b>	[Rh(nbd) <sub>2</sub> ] <sub>2</sub> BF <sub>4</sub>	THF	0	>99	86 ( <i>R</i> )
7	<b>125e</b>	[Rh(nbd) <sub>2</sub> ] <sub>2</sub> BF <sub>4</sub>	THF	-40	>99	92 ( <i>R</i> )

<sup>a</sup> The hydrogenations were run at different temperatures under 20 bar of H<sub>2</sub>.

<sup>b</sup> Conversion was determined by <sup>1</sup>H-NMR spectroscopy.

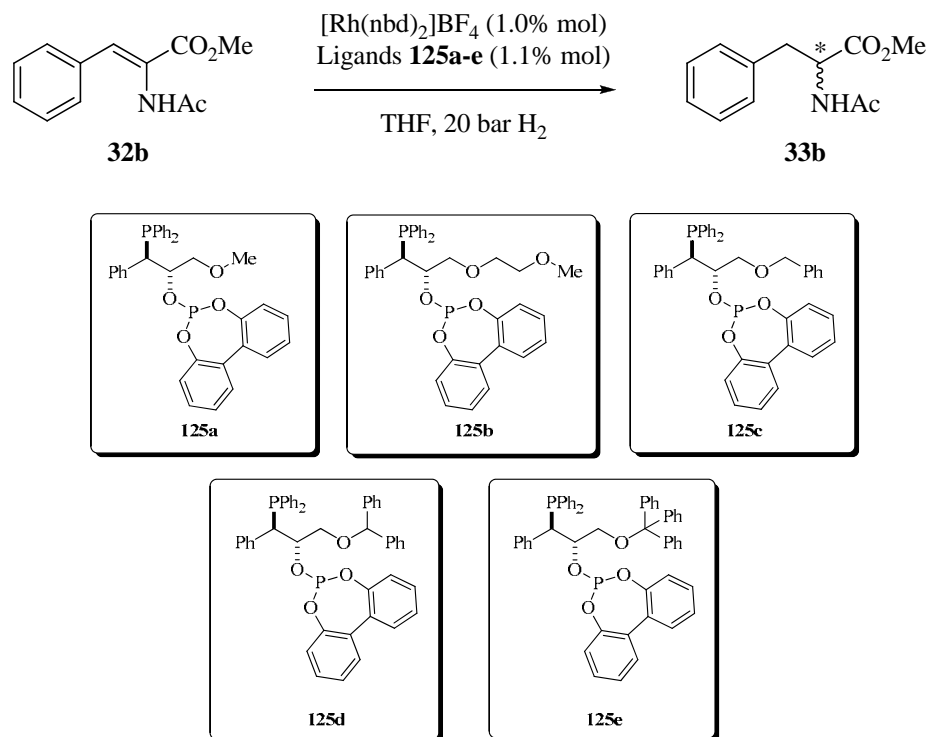
<sup>c</sup> Enantiomeric excess was determined by HPLC.

<sup>d</sup> The absolute configuration of the hydrogenated compounds was assigned by comparing optical rotation values or elution orders with reported values (see experimental section for details).

The influence of steric congestion around the metal center was studied by analyzing the activity of catalysts incorporating phosphine-phosphites that contain increasingly larger R-substituents in the CH<sub>2</sub>OR group (R = Me,

CH<sub>2</sub>CH<sub>2</sub>OMe, Bn, Bzh and Tr). As expected, the smaller the size of R, the higher the enantioselectivity (see Table 17).

**Table 17.** Effect of the size of the CH<sub>2</sub>OR group on the asymmetric hydrogenation of methyl (*Z*)-(*N*)-acetylcinnamate (**32b**) with phosphine-phosphite ligands **125a-e**.<sup>a</sup>



Entry	Ligand	T (°C)	Conv. (%) <sup>b</sup>	ee (%) <sup>c</sup> (config) <sup>d</sup>
1	<b>125a</b>	-40	>99	98 ( <i>R</i> )
2	<b>125b</b>	-40	>99	98 ( <i>R</i> )
3	<b>125c</b>	-40	>99	97 ( <i>R</i> )
4	<b>125d</b>	-40	94	95 ( <i>R</i> )
5	<b>125e</b>	-40	>99	92 ( <i>R</i> )

<sup>a</sup> All reactions were run at -40 °C under 20 bar of H<sub>2</sub>.

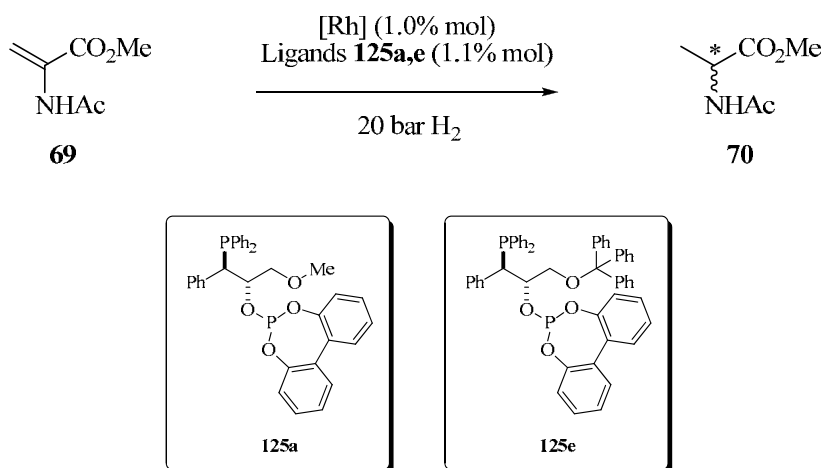
<sup>b</sup> Conversion was determined by <sup>1</sup>H-NMR spectroscopy.

<sup>c</sup> Enantiomeric excess was determined by HPLC.

<sup>d</sup> The absolute configuration of the hydrogenated compounds was assigned by comparing optical rotation values or elution orders with reported values (see experimental section for details).

To verify that this trend would extend to other substrates, we then performed the same chemistry using MAA instead of Z-MAC. The results are summarized in Table 18.

**Table 18.** Asymmetric hydrogenation of methyl (*N*)-acetylaminoacrylate (**69**) with phosphine-phosphite ligands **125a** and **125e**.<sup>a</sup>



Entry	Ligand	Rh precursor	Solvent	T (°C)	Conv. (%) <sup>b</sup>	ee (%) <sup>c</sup> (config) <sup>d</sup>
1	<b>125a</b>	[Rh(nbd) <sub>2</sub> ]BF <sub>4</sub>	DCM	RT	>99	84 ( <i>R</i> )
2	<b>125a</b>	[Rh(nbd) <sub>2</sub> ]BF <sub>4</sub>	THF	RT	>99	90 ( <i>R</i> )
3	<b>125a</b>	[Rh(cod) <sub>2</sub> ]BF <sub>4</sub>	THF	RT	>99	84 ( <i>R</i> )
4	<b>125a</b>	[Rh(nbd) <sub>2</sub> ]BF <sub>4</sub>	THF	-20	>99	94 ( <i>R</i> )
5	<b>125a</b>	[Rh(nbd) <sub>2</sub> ]BF <sub>4</sub>	THF	-40	>99	96 ( <i>R</i> )
6	<b>125e</b>	[Rh(nbd) <sub>2</sub> ]BF <sub>4</sub>	DCM	RT	>99	82 ( <i>R</i> )
7	<b>125e</b>	[Rh(nbd) <sub>2</sub> ]BF <sub>4</sub>	THF	RT	>99	82 ( <i>R</i> )
8	<b>125e</b>	[Rh(nbd) <sub>2</sub> ]BF <sub>4</sub>	THF	-40	>99	86 ( <i>R</i> )

<sup>a</sup> All hydrogenations were run under 20 bar of H<sub>2</sub>.

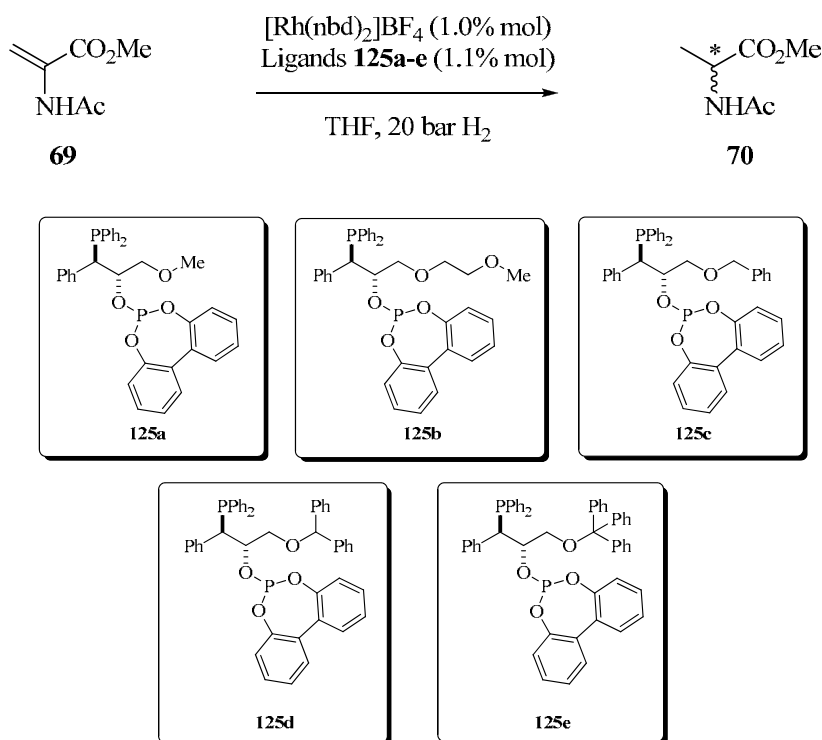
<sup>b</sup> Conversion was determined by <sup>1</sup>H-NMR spectroscopy.

<sup>c</sup> Enantiomeric excess was determined by GC.

<sup>d</sup> The absolute configuration of the hydrogenated compounds was assigned by comparing optical rotation values or elution orders with reported values (see experimental section for details).

As expected, the results for MAA (Table 18) were analogous to those for *Z*-MAC (Tables 13-17):

- i. Hydrogenation of MAA proceeded with slightly lower enantioselectivities than in the case of *Z*-MAC (96% ee vs. 98% ee, respectively).
- ii. Products **33b** (from *Z*-MAC) and **70** (from MAA) have the same configuration, thus indicating that hydrogen transfer occurs at the same enantiotopic face of each alkene.
- iii. THF was again found to provide the best enantioselectivity, based on the results obtained with ligand **125a** (in Table 18 compare Entries 1 and 2).
- iv. For both assayed ligands the best enantioselectivities were obtained at the lowest temperatures (in Table 18 compare Entries 2 and 5, for **125a**; and Entries 7 and 8, for **125e**).
- v. Steric congestion around the Rhodium center was again found to be detrimental to stereoiduction, as reflected in the results at -40 °C for the trityl-substituted phosphino-phosphite **125e** (86% ee) compared to those for the methyl-substituted analog **125a** (96% ee). Table 19 clearly illustrates this trend for all the R-substituents tested (Me, CH<sub>2</sub>CH<sub>2</sub>OMe, Bn, Bzh and Tr) for the CH<sub>2</sub>OR group.

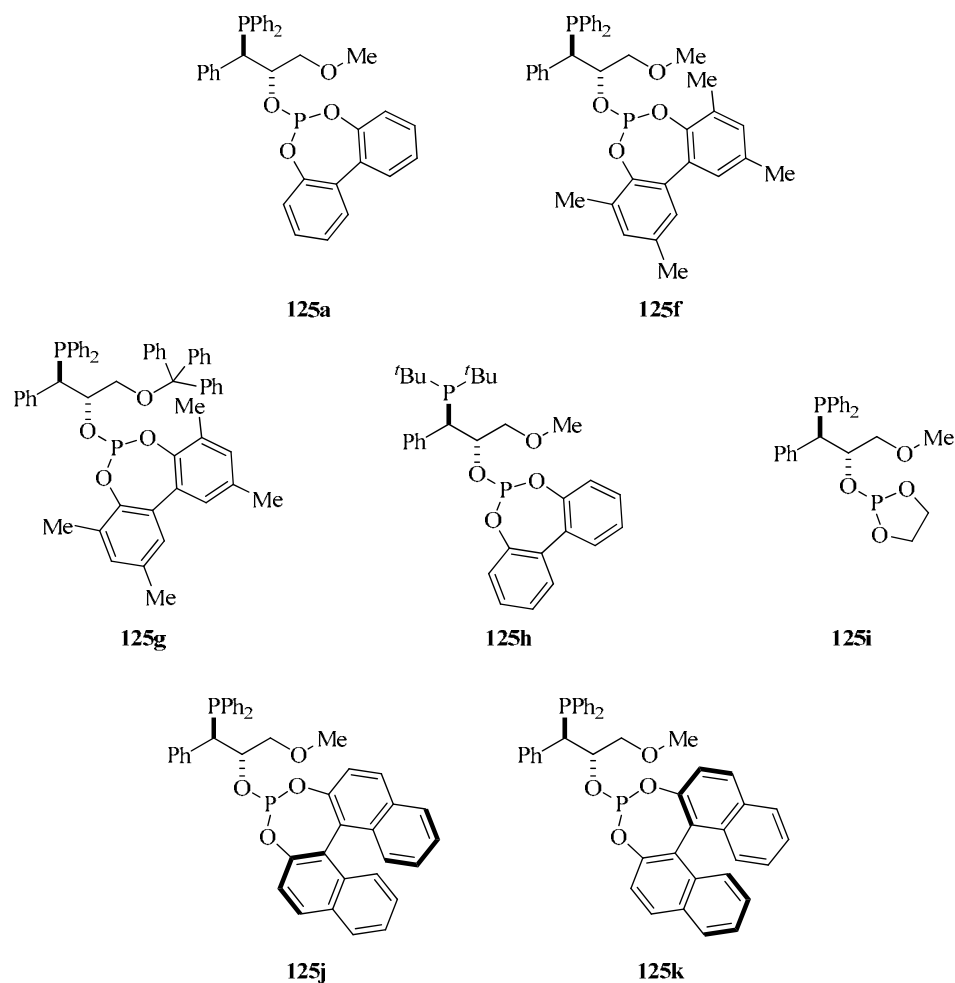
**Table 19.** Effect of the sterics of the CH<sub>2</sub>OR group in the asymmetric hydrogenation of methyl (*N*-acetylaminoacrylate (**69**) with phosphine-phosphite ligands **125a-e**.<sup>a</sup>

Entry	Ligand	T (°C)	Conv. (%) <sup>b</sup>	ee (%) <sup>c</sup> (config) <sup>d</sup>
1	<b>125a</b>	-40	>99	96 ( <i>R</i> )
2	<b>125b</b>	-40	>99	96 ( <i>R</i> )
3	<b>125c</b>	-40	>99	95 ( <i>R</i> )
4	<b>125d</b>	-40	>99	89 ( <i>R</i> )
5	<b>125e</b>	-40	>99	86 ( <i>R</i> )

<sup>a</sup> All hydrogenations were run at -40 °C under 20 bar of H<sub>2</sub>.<sup>b</sup> Conversion was determined by <sup>1</sup>H-NMR spectroscopy.<sup>c</sup> Enantiomeric excess was determined by GC.<sup>d</sup> The absolute configuration of the hydrogenated compounds was assigned by comparing optical rotation values or elution orders with reported values (see experimental section for details).

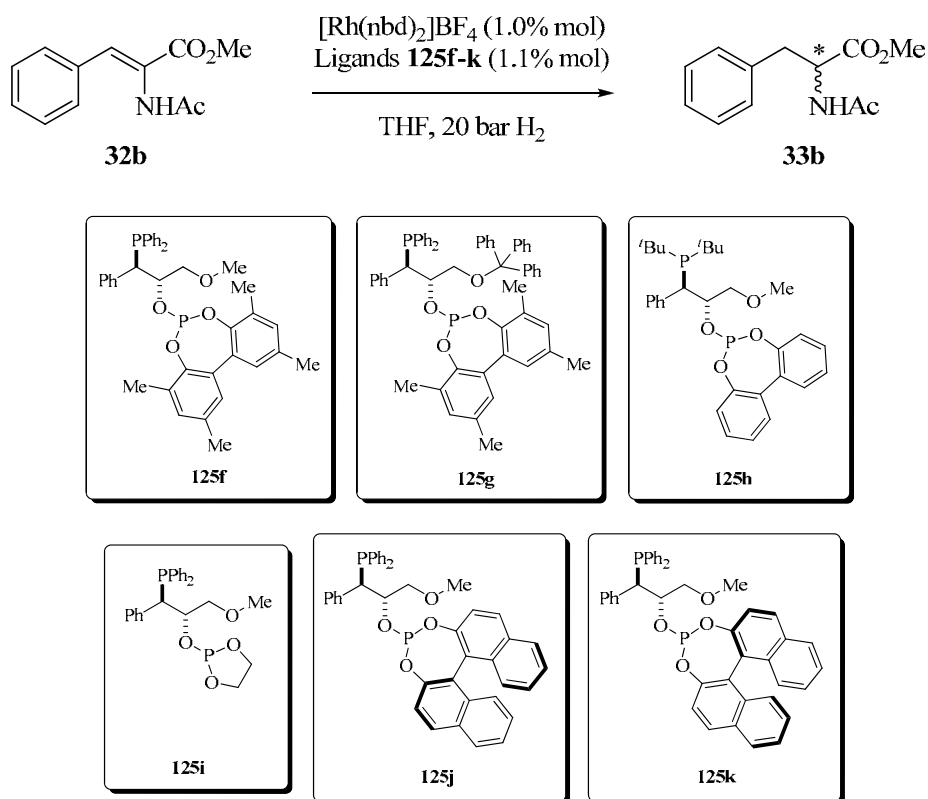


To complete our study on the correlation of the stereoelectronics at phosphine and phosphite moieties with the enantioselectivity, we then tested ligands **125f-k** (Figure 31) in the asymmetric hydrogenation of Z-MAC and MAA under the optimized reaction conditions (*i.e.* a ligand to Rhodium ratio of 1.1:1, THF, 20 bar of H<sub>2</sub>). The results are shown in Tables 20 and 21.



**Figure 31.** Phosphine-phosphite ligands **125a** and **125f-k**.

The results of this study are shown in Tables 20 and 21.

**Table 20.** Asymmetric hydrogenation of methyl (*Z*)-(*N*)-acetylaminoacinnamate (**32b**) with ligands **125f-k**.<sup>a</sup>

Entry	Ligand	T (°C)	Conv. (%) <sup>b</sup>	ee (%) <sup>c</sup> (config) <sup>d</sup>
<b>1<sup>e</sup></b>	<b>125f</b>	RT	>99	47 ( <i>R</i> )
<b>2<sup>e</sup></b>	<b>125g</b>	RT	>99	60 ( <i>R</i> )
<b>3</b>	<b>125h</b>	RT	>99	85 ( <i>R</i> )
<b>4</b>	<b>125i</b>	RT	>99	78 ( <i>R</i> )
<b>5</b>	<b>125j</b>	RT	>99	84 ( <i>S</i> )
<b>6</b>	<b>125k</b>	RT	>99	99 ( <i>R</i> )
<b>7<sup>f</sup></b>	<b>125a</b>	RT	>99	92 ( <i>R</i> )
<b>8<sup>f</sup></b>	<b>125e</b>	RT	>99	86 ( <i>R</i> )

<sup>a</sup> All hydrogenations were run at room temperature under 20 bar of H<sub>2</sub>.<sup>b</sup> Conversion was determined by <sup>1</sup>H-NMR spectroscopy.<sup>c</sup> Enantiomeric excess was determined by HPLC.<sup>d</sup> The absolute configuration of the hydrogenated compounds was assigned by comparing optical rotation values or elution orders with reported values (see experimental section for details).<sup>e</sup> Hydrogenations were run in DCM.<sup>f</sup> Results included for the sake of comparison (Entries 7 and 8 in this table coincide with Entries 2 and 4, respectively, in Table 13).

The first modification to the phosphite moiety was incorporation of substituents  $\alpha$  to the hydroxyl groups in the biaryl-2,2'-dioxy ring, while retaining interconversion between the corresponding conformers. We readily prepared phosphine-phosphites **125f** and **125g** using our synthetic strategy. We were very disappointed to find that the methyl groups in the *ortho*-positions of the biphenyl moiety were detrimental to enantioselectivity: the catalysts incorporating **125f** and **125g** provided ee's of only 47% and 60%, respectively (see Table 20, Entries 1 and 2); in contrast, the catalysts containing either **125a** or **125e**, both of which contain a BIPOL unit, gave 92% and 86%, respectively (see Table 20, Entries 7 and 8). Although the trend that steric congestion around the metal center due is detrimental to stereoinduction held true in terms of the groups on the bisaryl unit, the opposite case was observed for the R group on the CH<sub>2</sub>OR chain: the ligand **125f** (R = methyl) performed worse than the more bulky **125g** (R = trityl).

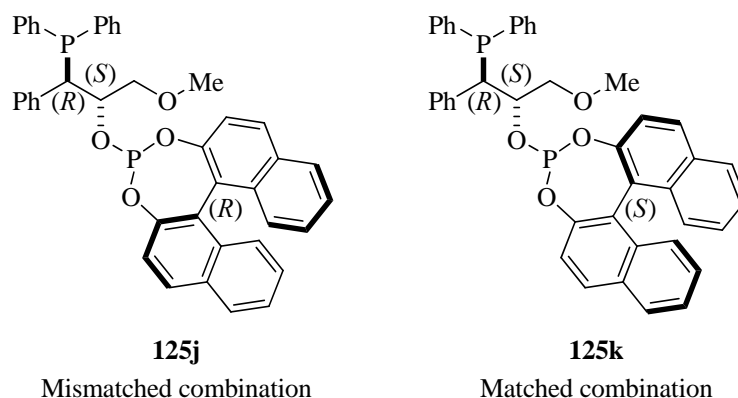
Ligand **125h** (R<sup>5</sup> = di[*tert*-butyl]), which contains a bulkier phosphine moiety, gave an ee of 85% (see Table 20, Entry 3), compared to the ligand **125a** (R<sup>5</sup> = diphenyl, respectively), which gave an ee of 92% under the same conditions (see Table 20, Entry 7). Thus, we observed that the diphenylphosphine moiety better meets the stereoelectronic requirements of the Rhodium catalytic center than does its di(*tert*-butyl)phosphino congener, and consequently, achieves better enantioselective hydride transfer onto one enantiotopic face of the alkene.

To test the influence of the biphenyl unit at the phosphite moiety, we synthesized ligand **125i**, which contains a dioxaphospholane fragment instead of the BIPOL unit found in the other ligands. Ligand **125i** afforded the *R*-enantiomer in a lower enantioselectivity (78% ee, see Table 20, Entry 4).

Although the enantioselectivities achieved with **125a** were reasonably high, the low temperatures required of this chemistry limit its applicability. Therefore, we sought to develop a ligand with similar performance, but that would be more amenable to mild reaction conditions. We thought that this could be achieved by introducing a new element of diversity in the phosphite moiety: a stereogenic

axis. Our obvious candidates of choice were ligands **125j** and **125k**, which differ from **125a-i**, by incorporating an (*R*)- or (*S*)-BINOL unit in their backbone, respectively. These two ligands were readily prepared using our modular synthetic strategy (see Section 1.2.1, p. 66). Both ligands afforded high enantioselectivity in the Rhodium catalyzed asymmetric hydrogenation of Z-MAC (see Table 20, Entries 5 and 6). Whereas **125j**, which incorporates the (*R*)-BINOL group, did not match the performance of **125a** (84% ee for the *S*-enantiomer), we were pleased to discover that **125k**, which incorporates the (*S*)-BINOL fragment, performed better in this chemistry than any other ligand that we had developed up to that point (99% ee for the *R*-product). Consequently, **125k** should be regarded as the *matched* combination of the stereogenic centers in the carbon backbone between the two phosphorus functionalities and the stereogenic axis in the phosphite group. Analogously, **125j** should be regarded as the *mismatched* combination.

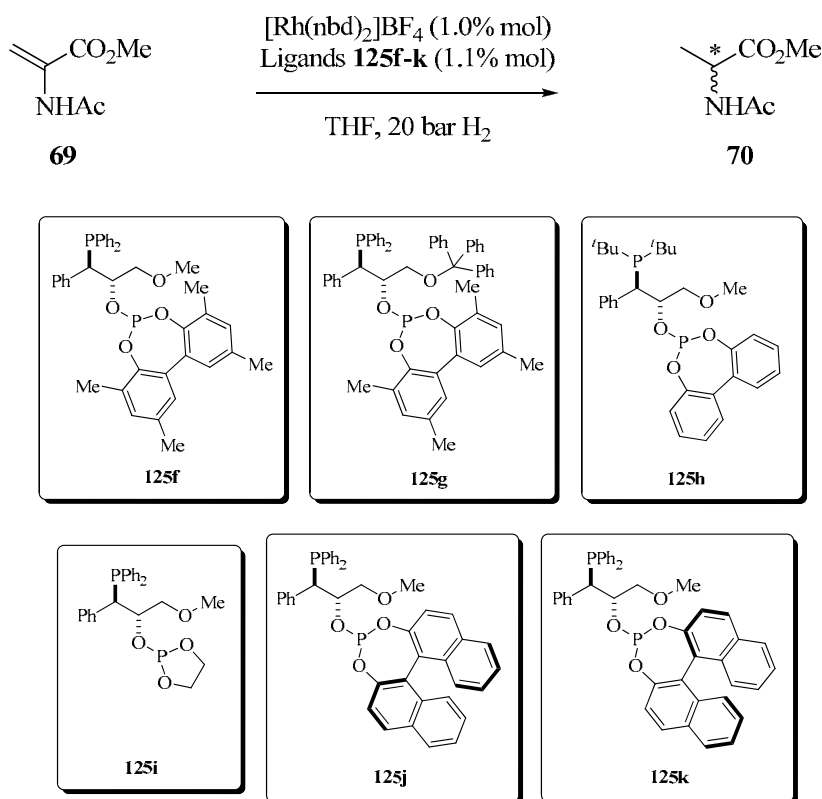
Interestingly, **125j** and **125k** led to opposite stereochemical outcomes: **125j** provided the (*S*)-enantiomer, whereas **125k** gave the (*R*)-enantiomer. This indicates that the direction of stereodiscrimination was predominantly controlled by the binaphthyl group (Figure 32).



**Figure 32.** Phosphine-phosphite ligands derived from (*R*)- and (*S*)-BINOL.

Table 21 shows the results of the Rhodium-catalyzed hydrogenation of MAA using ligands **125f-k**. In general, the same trends observed for Z-MAC were also

observed for MAA. The catalyst containing ligand **125k** gave the highest enantiomeric excess (99% ee, *R*-product) for this series (Table 21, Entry 6). The final products from the two substrates had the same configuration, thus indicating that hydrogenation occurs via hydride transfer onto the same enantiotopic face of the alkene.

**Table 21.** Asymmetric hydrogenation of methyl (*N*-acetylaminoacrylate (**69**) with phosphine-phosphite ligands **125f-k**.<sup>a</sup>

Entry	Ligand	T (°C)	Conv. (%) <sup>b</sup>	ee (%) <sup>c</sup> (config) <sup>d</sup>
1 <sup>e</sup>	<b>125f</b>	RT	>99	22 ( <i>R</i> )
2 <sup>e</sup>	<b>125g</b>	RT	>99	42 ( <i>R</i> )
3	<b>125h</b>	RT	>99	81 ( <i>R</i> )
4	<b>125i</b>	RT	>99	72 ( <i>R</i> )
5	<b>125j</b>	RT	>99	88 ( <i>S</i> )
6	<b>125k</b>	RT	>99	99 ( <i>R</i> )

<sup>a</sup> All hydrogenations were run at room temperature under 20 bar of H<sub>2</sub>.

<sup>b</sup> Conversion was determined by <sup>1</sup>H-NMR spectroscopy.

<sup>c</sup> Enantiomeric excess was determined by GC.

<sup>d</sup> The absolute configuration of the hydrogenated compounds was assigned by comparing optical rotation values or elution orders with reported values (see experimental section for details).

<sup>e</sup> Hydrogenations were run in DCM.

In summary, we have been able to demonstrate that the highly modular nature of our synthetic strategy was extremely useful for the development of efficient catalytic systems. We screened our *P-OH* (phosphino alcohols **123**) and *P-OP* (phosphine-phosphinites **124** and phosphine-phosphites **125**) ligands in Rhodium-catalyzed hydrogenations of *Z*-MAC and MAA. Phosphine-phosphite **125k** (Figure 33) consistently showed the best conversion and enantioselectivity, and therefore, was chosen for further development.

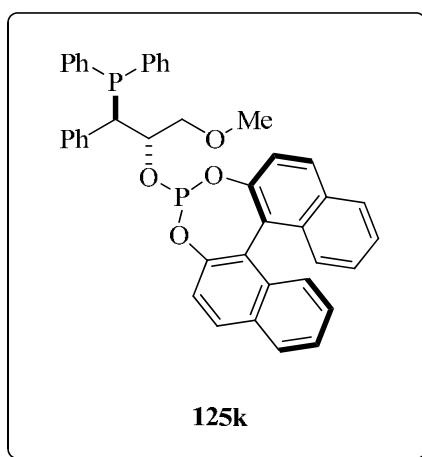


**Figure 33.** Phosphine-phosphite **125k**, the highest-performing ligand.

### 1.2.6. Scope of phosphine-phosphite ligand **125k** in the Rhodium-catalyzed asymmetric hydrogenation of alkenes

To investigate the scope of our highest performing ligand, **125k**, we decided to screen it in Rhodium-catalyzed enantioselective hydrogenations of a broader variety of substrates, the alkenes **144a-y** (Figure 34).

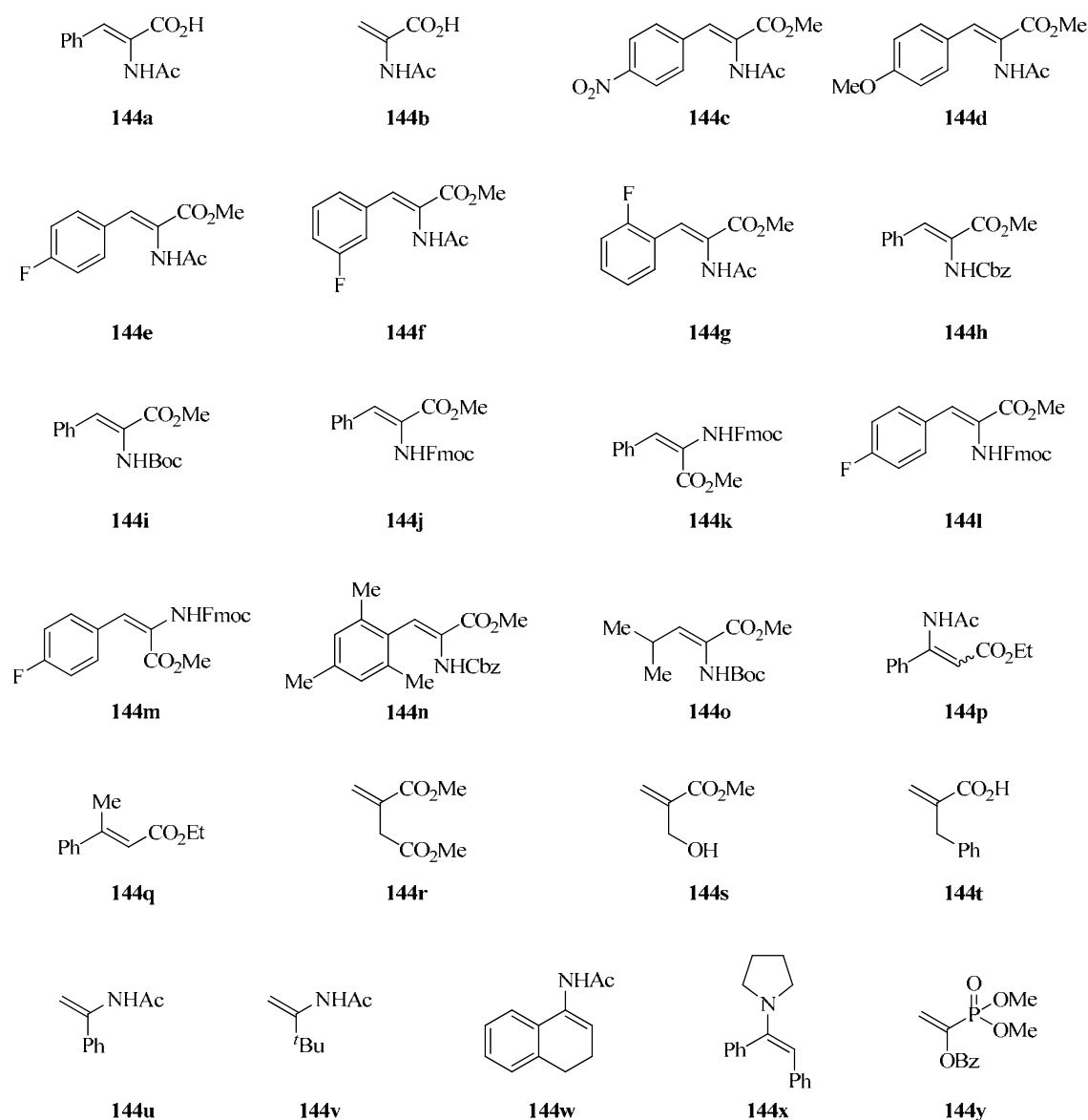
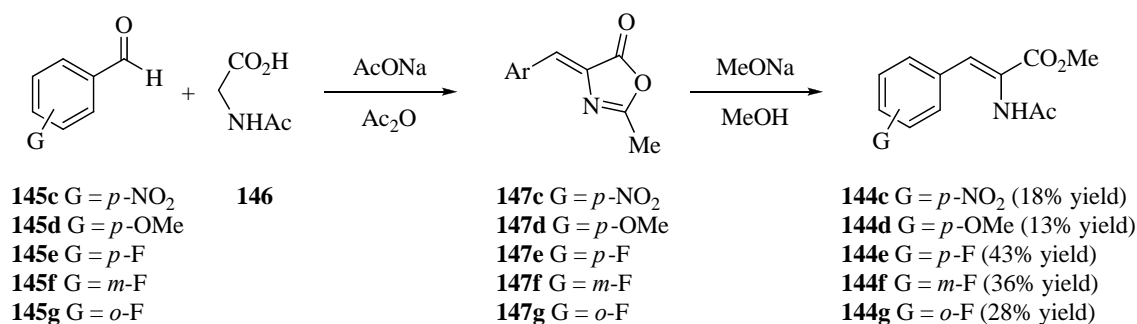


**Figure 34.** Alkene substrates used to test the scope of ligand **125k** in Rhodium-catalyzed asymmetric hydrogenations.



### 1.2.6.1- Preparation of various structurally diverse functionalized alkenes

We had to synthesize most of the alkenes required for our study, as only **144a**, **144b**, **144q** and **144r** are commercially available. Alkenes **144c-g** were prepared in two steps starting from the corresponding aldehydes **145** (Scheme 20): condensation of the aldehydes with acetyl glycine (**146**) in acetic anhydride in the presence of sodium acetate yielded the corresponding 2-methyloxazol-5(4*H*)-ones **147c-g**,<sup>97</sup> subsequent methanolysis of **147c-g** under basic conditions gave the desired corresponding  $\alpha$ -amino cinnamates in yields ranging from 13 to 43%.<sup>98</sup> This method affords the most thermodynamically stable isomers: the *Z*-isomers. Functionalization in the substrates encompassed electron-withdrawing groups (**144c**), electron-donating groups (**144d**), and a fluorine substituent at the *ortho* (**144g**), *meta* (**144f**) or *para* (**144e**) positions.



**Scheme 20.** Synthetic route to  $\alpha$ -amino cinnamates **144c-g**.

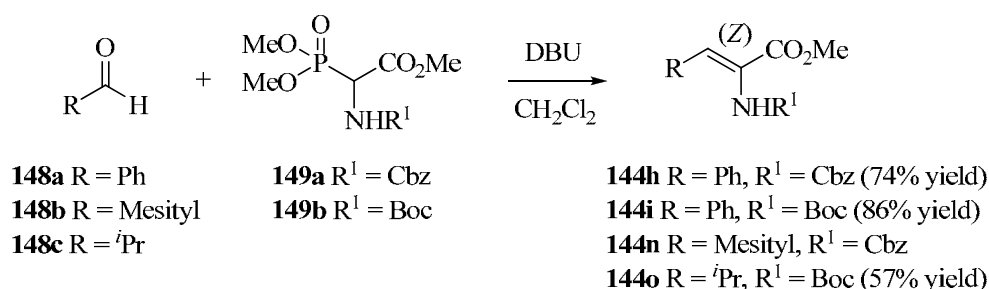
*N*-Cbz- or *N*-Boc-protected (*Z*)- $\alpha$ -dehydroamino acid esters **144h**, **144i**, **144n**<sup>99</sup> and **144o** were readily synthesized via a Horner-Wadsworth-Emmons reaction.<sup>100</sup> Condensation of dimethoxyphosphorylglycine esters **149** with aldehydes in DCM with DBU as a base furnished the corresponding products in excellent yields and with high purity (Scheme 21).

<sup>97</sup> Herbst, R. M.; Shemin, D. *Org. Synth.* **1939**, *19*, No pp given.

<sup>98</sup> Suh, J.; Lee, E.; Myoung, Y. C.; Kim, M.; Kim, S. *J. Org. Chem.* **1985**, *50*, 977-80.

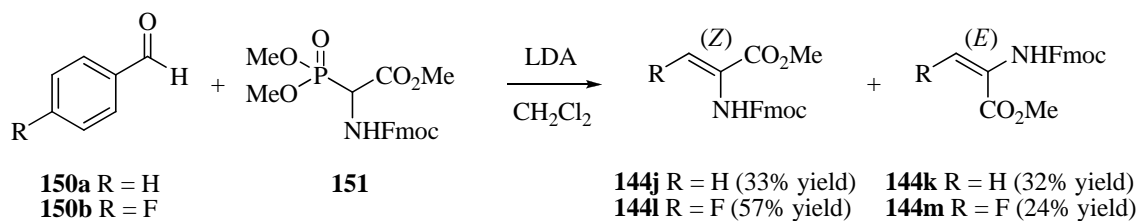
<sup>99</sup> The alkene **144n** was synthesized in Riera's research group from the University of Barcelona.

<sup>100</sup> Schmidt, U.; Griesser, H.; Leitenberger, V.; Lieberknecht, A.; Mangold, R.; Meyer, R.; Riedl, B. *Synthesis* **1992**, 487-90.



**Scheme 21.** Diastereoselective formation of  $\alpha$ -dehydroamino acid esters **144h**, **144i**, **144n** and **144o**.

We were unable to form the *N*-Fmoc-protected substrates **144j** and **144l** using the aforementioned conditions, because the Fmoc group is cleaved in the presence of DBU. Therefore, we switched to LDA as base, which enabled us to synthesize **144j** and **144l**. However, unlike the case of the *N*-Boc- or *N*-Cbz-protected compounds **144h-i** and **144n-o**, the condensation was not stereoselective for Fmoc-substituted dimethoxyphosphorylglycine (**151**), leading to a 1.4:1 mixture of the *Z* and *E* isomers which had to be separated by column chromatography (Scheme 22).



**Scheme 22.** Preparation of *N*-Fmoc-protected derivatives **144j-m**.

The geometry of the carbon-carbon double bond in **144j** and in **144k** was established by analysis of their 2D-NOESY spectra. The spectrum for **144j** featured an intense NOE cross-peak between the aromatic proton at the *ortho* position of the phenyl group and the amide proton (Figure 35), thereby strongly supporting characterization of this compound as the *Z*-isomer.

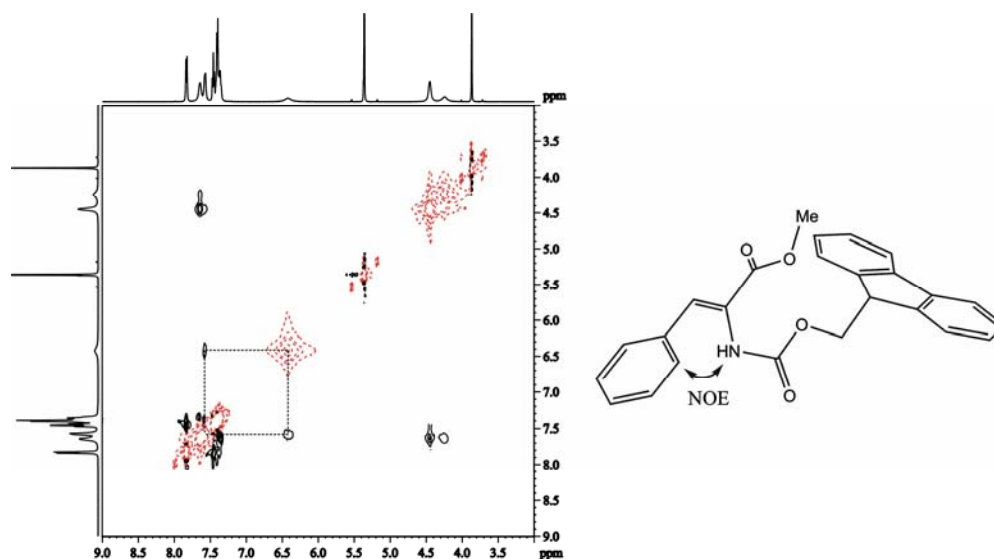


**Figure 35.** 2D-NOESY spectrum of Fmoc-protected substrate **144j**.

Analogously, the spectrum of compound **144k** showed an intense NOE cross-peak between the aromatic proton at the *ortho* position of the phenyl group and the methyl ester protons (Figure 36), thus strongly corroborating identification of this compound as the *E*-isomer.

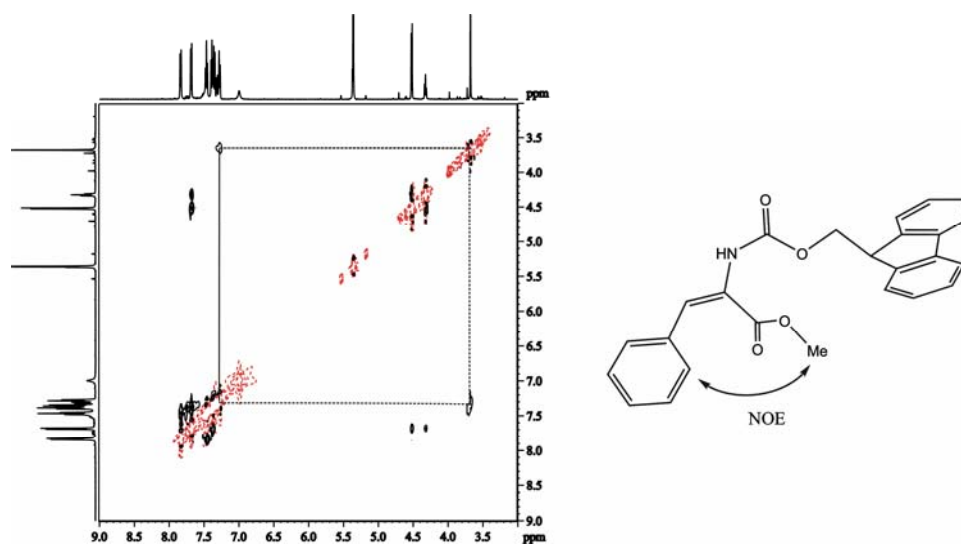
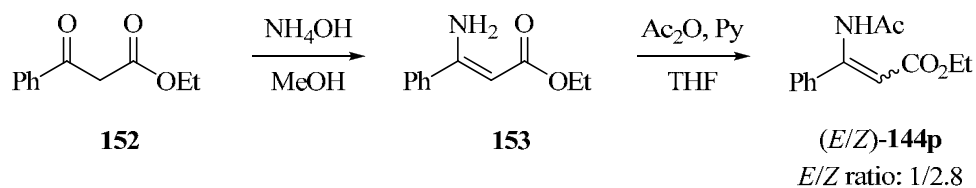


**Figure 36.** 2D-NOESY spectrum of Fmoc-protected substrate **144k**.

The fluorine derivatives corresponding to **144j** and **144k** had analogous geometries: **144l** (*Z*) and **144m** (*E*), respectively.

Catalytic asymmetric hydrogenation of  $\beta$ -dehydroamino acid derivatives is a highly convenient route to optically pure  $\beta$ -amino acids, which are crucial components of numerous biologically active natural products.<sup>101</sup> For this reason, we prepared  $\beta$ -dehydroamino acid **144p** in two steps starting from the corresponding ethyl  $\beta$ -keto alkananoate **152** (Scheme 23):<sup>102</sup> C=N bond formation followed by acetylation of the resulting 3-amino-3-phenylacrylate **153**. In this case, the resulting *E*- and *Z*-isomers could not be separated by chromatography; therefore, the mixture (*E/Z* ratio = 1:2.8) was directly subjected to asymmetric hydrogenation.



**Scheme 23.** Two-step synthesis of  $\beta$ -dehydroamino acid **144p**.

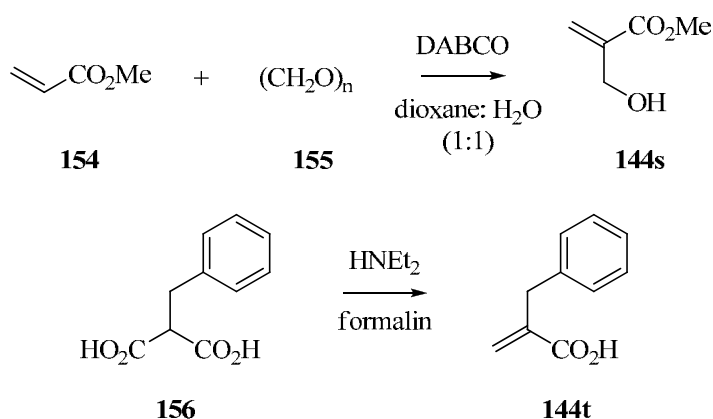
Roche's ester (**144s**)<sup>103</sup> and 2-benzylacrylic acid (**144t**)<sup>104</sup> were readily prepared in one step according to literature procedures (Scheme 24): the former, by Morita-Baylis-Hillman reaction of methyl acrylate **154** and paraformaldehyde **155**, and the latter, via Mannich reaction of benzylmalonic acid **156**.

<sup>101</sup> *Enantioselective Synthesis of Amino Acids*, Juaristi, E., Ed.; Wiley-VCH: New York, 1997.

<sup>102</sup> Lee, S.-g.; Zhang Yong, J. *Org Lett* **2002**, *4*, 2429-31.

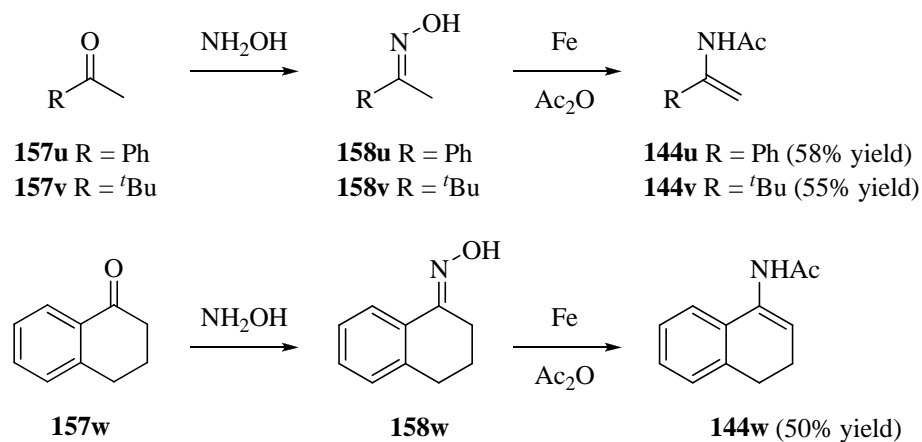
<sup>103</sup> Sawamura, K.; Yoshida, K.; Suzuki, A.; Motozaki, T.; Kozawa, I.; Hayamizu, T.; Munakata, R.; Takao, K.-i.; Tadano, K.-i. *The Journal of organic chemistry* **2007**, *72*, 6143-8.

<sup>104</sup> Liu, X.; Hu, X. E.; Tian, X.; Mazur, A.; Ebetino, F. H. *J. Organomet. Chem.* **2002**, *646*, 212-222.



**Scheme 24.** One-step syntheses of Roche's ester (**144s**) and 2-benzylacrylic acid (**144t**).

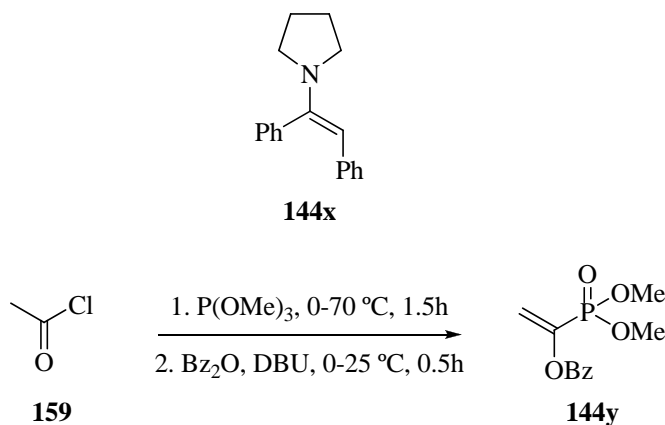
Acetylated enamides **144u-w** were prepared in two-steps from the corresponding ketones **157u-w**:<sup>105</sup> transformation of the ketones into the corresponding oximes (**158u-w**), followed by reduction with iron metal in the presence of acetic anhydride (Scheme 25).



**Scheme 25.** Two-step syntheses of enamide substrates **144u-w**.

<sup>105</sup> Burk, M. J.; Casy, G.; Johnson, N. B. *J. Org. Chem.* **1998**, *63*, 6084-6085.

*N,N*-dialkylenamine **144x**<sup>106</sup> (Scheme 26) was readily obtained by condensation of 1,2-diphenylethanone and pyrrolidine under acidic catalysis. 1-(Dimethoxyphosphoryl)vinyl benzoate **144y** was prepared using the method of Burk *et al.* (Scheme 26).<sup>107</sup>



**Scheme 26.** *N,N*-dialkylenamine **144x** and preparation of enol ester phosphonate **144y**.

<sup>106</sup> Hou, G.-H.; Xie, J.-H.; Wang, L.-X.; Zhou, Q.-L. *J. Am. Chem. Soc.* **2006**, *128*, 11774-11775.

<sup>107</sup> Burk, M. J.; Stammers, T. A.; Straub, J. A. *Org. Lett.* **1999**, *1*, 387-390.

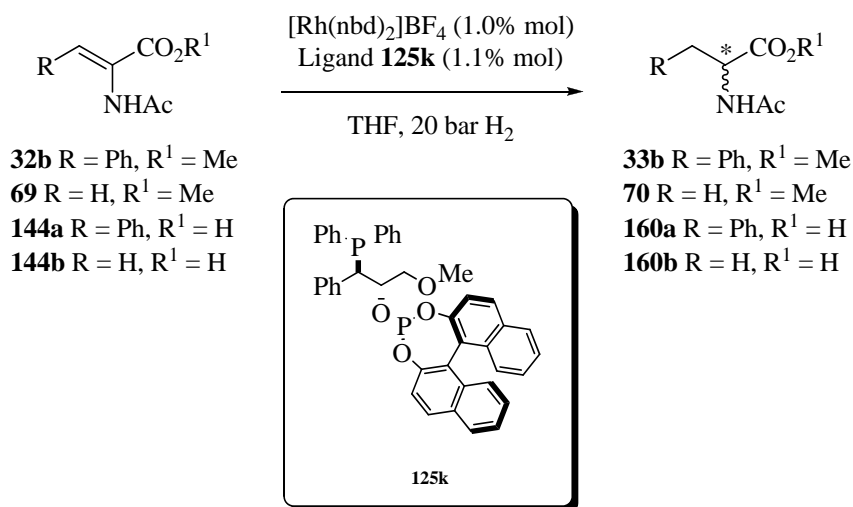
### 1.2.6.2 Substrate scope of phosphine-phosphite ligand **125k** in Rhodium-catalyzed asymmetric hydrogenations

We evaluated the substrate scope of our best ligand, **125k**, in asymmetric hydrogenations of different substrates under the conditions optimized for *Z*-MAC and MAA during the preliminary catalytic studies: *in situ* generation of the pre-catalyst (1 mol%, [Rh(**125k**)(nbd)]BF<sub>4</sub>), 0.2 M substrate in organic solvent (normally, THF), room temperature, and 20 bar of hydrogen. The hydrogenations were run in an autoclave that enables parallel reactions (up to 24). Lastly, all reaction mixtures were magnetically stirred at 300 rpm.<sup>108</sup>

The catalyst based on **125k** provided excellent conversion and very high enantioselectivities in the hydrogenation of *Z*-MAC and MAA (Table 22, Entries 1 and 2, respectively), as well as their corresponding acid derivatives (Table 22, Entries 3 and 4, respectively). It is noteworthy to observe that ligand **125k** mediated very efficiently the hydrogenation both for carboxylic acid or their methyl esters in a non protic solvent (THF).

---

<sup>108</sup> Hydrogenations were run in a stainless steel reactor (CAT 24, HEL, London, England) equipped with manifold, pressure relief (100 bar g), Fike rupture disc (110 bar g +/- 5%), 100-bar gauge, and inlet and outlet valves.

**Table 22.** Asymmetric hydrogenations of Z-MAC, MAA and their corresponding acid derivatives catalyzed by [Rh(**125k**)(nbd)]BF<sub>4</sub>.<sup>a</sup>

Entry	Substrate	Pressure (bar)	Solvent	Conv. (%) <sup>b</sup>	ee (%) <sup>c</sup> (config) <sup>d</sup>
1	<b>32b</b>	20	THF	>99	99 ( <i>R</i> )
2	<b>69</b>	20	THF	>99	99 ( <i>R</i> )
3	<b>144a</b>	20	THF	>99	99 ( <i>R</i> )
4	<b>144b</b>	20	THF	>99	98 ( <i>R</i> )

<sup>a</sup> All hydrogenations were run at room temperature under 20 bar of H<sub>2</sub>.

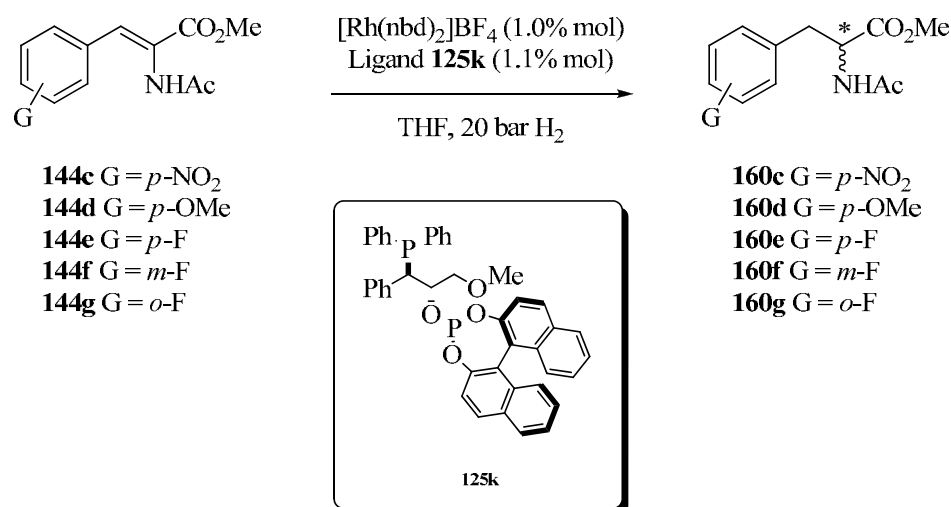
<sup>b</sup> Conversion was determined by <sup>1</sup>H-NMR spectroscopy.

<sup>c</sup> Enantiomeric excess was determined by HPLC.

<sup>d</sup> The absolute configuration of the hydrogenated compounds was assigned by comparing optical rotation values or elution orders with reported values (see experimental section for details).

We then studied aryl cinnamates as substrates, for which ligand **125k** gave excellent conversions and enantiomeric excesses of up to 99% (see Table 23). Very high levels of stereoselection (99% ee) were observed for electron-withdrawing (**144c**; Table 23, Entry 1) and electron-donating (**144d**; Table 23, Entry 2) groups, and for *ortho*- (**144g**; Table 23, Entry 5), *meta*- (**144f**; Table 23, Entry 4) or *para*- (**144e**; Table 23, Entry 3) fluorophenyl compounds. In all cases, the corresponding (*R*)-methyl 2-acetamido-3-arylpropanoates (**160c-g**) were obtained. These results indicate that the substituents on the aryl group do not alter the direction of stereoselection.



**Table 23.** Asymmetric hydrogenation of aryl-substituted cinnamates **144c-g** catalyzed by  $[\text{Rh}(\mathbf{125k})(\text{nbd})]\text{BF}_4$ .<sup>a</sup>

Entry	Substrate	Pressure (bar)	Solvent	Conv. (%) <sup>b</sup>	ee (%) <sup>c</sup> (config) <sup>d</sup>
1	<b>144c</b>	20	THF	>99	99 ( <i>R</i> )
2	<b>144d</b>	20	THF	>99	99 ( <i>R</i> )
3	<b>144e</b>	20	THF	>99	99 ( <i>R</i> )
4	<b>144f</b>	20	THF	>99	99 ( <i>R</i> )
5	<b>144g</b>	20	THF	>99	99 ( <i>R</i> )

<sup>a</sup> All hydrogenations were run at room temperature under 20 bar of H<sub>2</sub>.

<sup>b</sup> Conversion was determined by <sup>1</sup>H-NMR spectroscopy.

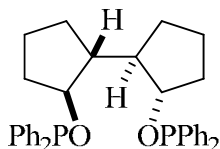
<sup>c</sup> Enantiomeric excess was determined by HPLC.

<sup>d</sup> The absolute configuration of the hydrogenated compounds was assigned by comparing optical rotation values or elution orders with reported values (see experimental section for details).

Excellent enantioselectivities (96-99% ee) were also observed with the *N*-protected (Ac, Cbz, Boc or Fmoc) aryl-substituted cinnamates **32b**, **144h-j** and **144l** (Table 24, Entries 1-5). In fact, to the best of our knowledge, compounds **144j** and **144l** are the first reported examples of Fmoc-protected, enantiopure non-natural aryl alanines acids prepared by catalytic enantioselective hydrogenation.

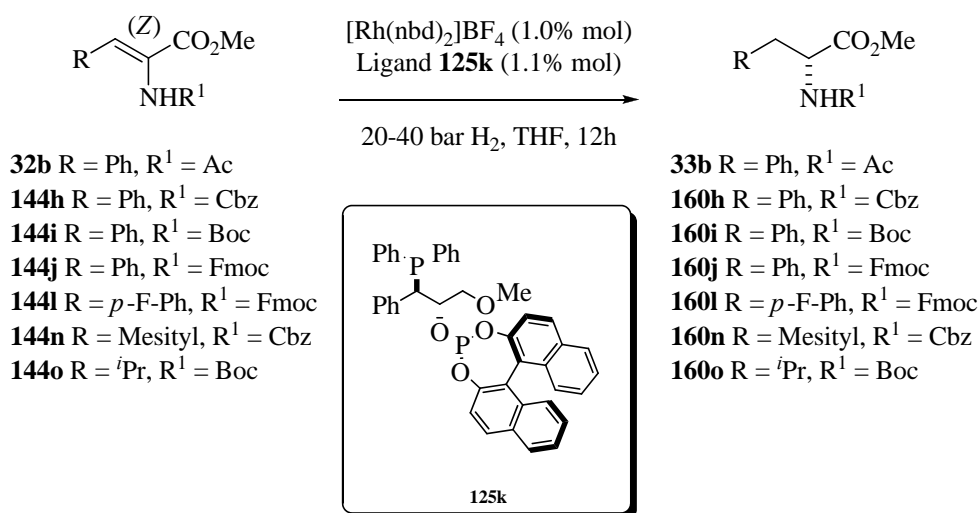
Unfortunately, the catalyst based on ligand **125k** was inactive for the  $\alpha$ -dehydroamino acid substrate **144n**, even at 40 bar of hydrogen (Table 24, Entry 6). This may be due to the steric bulk of the mesityl group in this compound.

Certain ligands, such as diphosphinite ligand (1*R*,1*R'*,2*S*,2*S'*)-BICPO (Figure 37), that afford high enantioselectivities for some aromatic amino acids but not for the corresponding alkyl-substituted analogs.<sup>109</sup> However, we were pleased to discover that our catalytic system derived from [Rh(**125k**)(nbd)]BF<sub>4</sub>, in addition to performing extremely well for enantioenriched aryl amino acids, also afforded high enantioselectivity for the *N*-Boc-alkylamino acid substrate **144o** (Table 24, Entry 7), which is the isopropyl analog of the phenyl compound **144i**.



**Figure 37.** Structure of (1*R*,1*R'*,2*S*,2*S'*)-BICPO ligand.

<sup>109</sup> (a) Zhu, G.; Cao, P.; Jiang, Q.; Zhang, X. *J. Am. Chem. Soc.* **1997**, *119*, 1799-1800. (b) Zhu, G.; Zhang, X. *J. Org. Chem.* **1998**, *63*, 3133-3136.

**Table 24.** Asymmetric hydrogenation of *N*-protected aryl-substituted cinnamates catalyzed by [Rh(**125k**)(nbd)]BF<sub>4</sub>.<sup>a</sup>

Entry	Substrate	<i>N</i> -Substituent	Pressure (bar)	Solvent	Conv. (%) <sup>b</sup>	ee (%) <sup>c</sup> (config) <sup>d</sup>
1	<b>32b</b>	Ac	20	THF	>99	99 ( <i>R</i> )
2	<b>144h</b>	Cbz	20	THF	>99	98 ( <i>R</i> )
3	<b>144i</b>	Boc	20	THF	>99	96 ( <i>R</i> )
4	<b>144j</b>	Fmoc	40	THF	>99	98 ( <i>R</i> )
5	<b>144l</b>	Fmoc	40	THF	94	97 ( <i>R</i> )
6	<b>144n</b>	Cbz	40	THF	0	nd <sup>e</sup>
7	<b>144o</b>	Boc	40	THF	70	92 ( <i>R</i> )

<sup>a</sup> All hydrogenations were run at room temperature under different hydrogen pressures.

<sup>b</sup> Conversion was determined by <sup>1</sup>H-NMR spectroscopy.

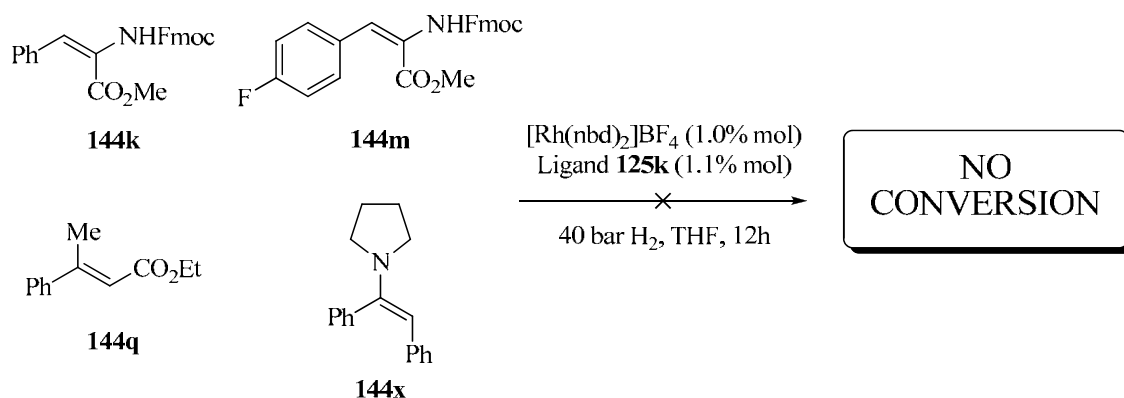
<sup>c</sup> Enantiomeric excess was determined by HPLC.

<sup>d</sup> The absolute configuration of the hydrogenated compounds was assigned by comparing optical rotation values or elution orders with reported values (see experimental section for details).

<sup>e</sup> not determined.

We were surprised to observe a total lack of catalytic activity with the *E*-isomers of the Fmoc-protected dehydroalanines **144k** and **144m** as substrates, even at 40 bar pressure. Likewise, no activity was observed for alkenes **144q** or **144x** (Scheme 27). Interestingly, these four substrates share a structural feature:

the binding group in the molecule, through which the alkene should bind to the Rhodium centre, has a substituent on the alkene placed in the *trans*-position. Conversely, all the substrates that have been hydrogenated in excellent enantioselectivities with the mediation of ligand **125k** have a *cis*-substituent with respect to the NH-CO group (binding group to Rhodium, see Introduction, page 9).

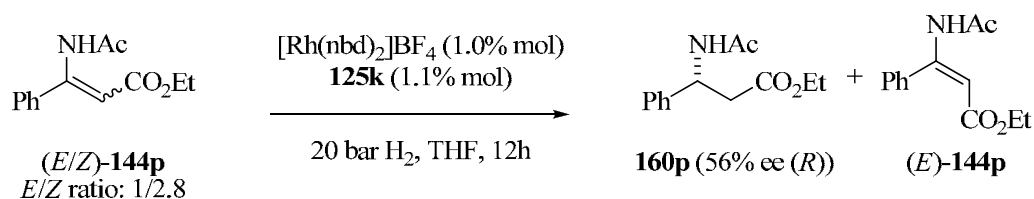


**Scheme 27.** Attempted asymmetric hydrogenation of *E*-Fmoc-protected dehydroalanines **144k** and **144m**, and *E*-alkenes **144q** and **144x**, using [Rh(**125k**)(nbd)]BF<sub>4</sub> as catalyst.

It should be recalled that for  $\beta$ -dehydroamino acid **144p**, which contains a mixture of *E/Z* isomers, [Rh(**125k**)(nbd)]BF<sub>4</sub> only provides moderate enantioselectivity for the *Z*-isomer (56% ee; see Scheme 28), and is inactive for the *E*-isomer, which is a shortcoming for our ligand.<sup>110</sup> However, these results are consistent with those obtained for the *trans*-substituted alkenes **144k**, **144m**, **144q** and **144x**. Therefore, we deduced that hydrogenations catalyzed by [Rh(**125k**)(nbd)]BF<sub>4</sub> seem to require a relative configuration of *Z* between the  $\beta$ -substituent on the olefin and the group that contains the donor atom responsible for binding to the Rhodium center. This prerequisite has been observed with several other ligands.<sup>111</sup>

<sup>110</sup> DUPHOS can catalyze the hydrogenation of both isomers of  $\beta$ -dehydroamino acids with excellent enantioselectivities: Burk, M. J. *Acc. Chem. Res.* **2000**, *33*, 363-372.

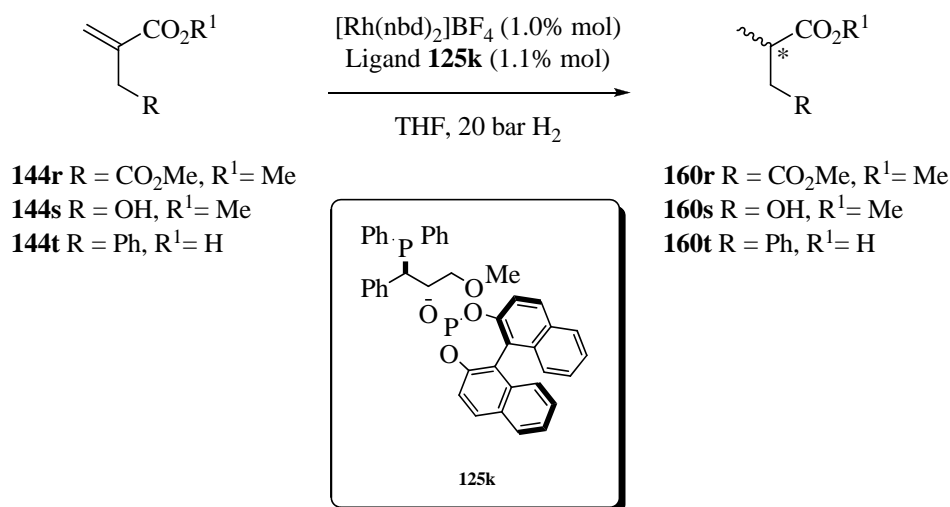
<sup>111</sup> Reference 1b, pp 11-12.



**Scheme 28.** Rh-mediated asymmetric hydrogenation of  $\beta$ -dehydroamino acids **144p**.

Itaconate derivatives are another class of compounds that yield interesting enantiopure derivatives upon asymmetric hydrogenation. We tested our catalytic system derived from  $[\text{Rh}(\mathbf{125k})(\text{nbd})]\text{BF}_4$  in the hydrogenation of dimethyl itaconate (**144r**) and the related compounds Roche's ester<sup>103</sup> (**144s**) and **144t**. Excellent enantioselectivities were obtained for **144r** (99% ee; Table 25, Entry 1) and Roche's ester **144s** (90% ee; Table 25, Entry 2). Not surprisingly, enantioselectivity in the hydrogenation of substrate **144t**, which lacks a donor atom for allowing a stable chelate with the Rhodium center, was poor (15% ee; Table 25, Entry 3).

**Table 25.** Asymmetric hydrogenation of itaconic acid (**144r**) and related compounds (Roche's ester [**144s**] and **144t**) catalyzed by [Rh(**125k**)(nbd)]BF<sub>4</sub>.<sup>a</sup>



Entry	Substrate	Pressure (bar)	Solvent	Conv. (%) <sup>b</sup>	ee (%) <sup>c</sup> (config) <sup>d</sup>
1	<b>144r</b>	20	CH <sub>2</sub> Cl <sub>2</sub>	>99	99 ( <i>R</i> )
2	<b>144s</b>	20	THF	>99	90 ( <i>S</i> )
3	<b>144t</b>	20	THF	>99	15 ( <i>S</i> )

<sup>a</sup> All hydrogenations were run at room temperature under 20 bar of H<sub>2</sub>.

<sup>b</sup> Conversion was determined by <sup>1</sup>H-NMR spectroscopy.

<sup>c</sup> Enantiomeric excess was determined by GC.

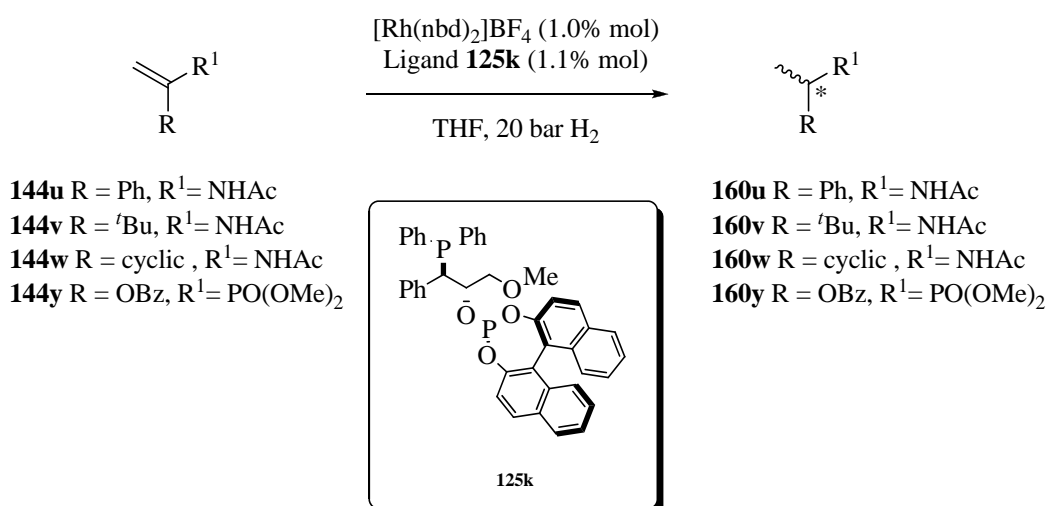
<sup>d</sup> The absolute configuration of the hydrogenated compounds was assigned by comparing optical rotation values or elution orders with reported values (see experimental section for details).

We then evaluated the catalytic performance of [Rh(**125k**)(nbd)]BF<sub>4</sub> using enamides **144u-w** and enol ester phosphonate **144y** as substrates. The results are summarized in Table 26. High enantioselectivity was obtained for the  $\alpha$ -aryl enamide **144u** (98% ee; Entry 1), whereas only moderate selectivity was observed for the  $\alpha$ -tetralone-derived enamide **144w** (58% ee; Entry 3), and poor enantioselectivity was observed for the  $\alpha$ -alkyl enamide counterpart **144v** (23% ee; Entry 2), whose product showed opposite configuration (*S*-enantiomer). The intriguing inversion of configuration that occurred with **144v** has been reported by other authors.<sup>107</sup> Stereoinduction during the hydrogenation of enamides is very

sensitive to the functionalization of the substrate, as demonstrated by the fact that the respective products obtained from hydrogenation of **144u**, which has a phenyl group, and **144v**, which has a *tert*-butyl group, have opposite configurations. Landis<sup>92c</sup> *et al.* anticipated that modulation of the stereoelectronic features of the  $\alpha$ -substituent would strongly influence both the orientation of the enamide (relative to the coordination plane in the square planar catalyst-substrate adducts) and the relative stabilities of the reaction intermediates.

Finally, high enantioselectivity was also obtained for the enol ester phosphonate **144y** (92% ee; Table 26, Entry 4).

**Table 26.** Asymmetric hydrogenation of enamides **144u-w** and enol ester phosphonate **144y** catalyzed by  $[\text{Rh}(\mathbf{125k})(\text{nbd})]\text{BF}_4$ .<sup>a</sup>



Entry	Substrate	Pressure (bar)	Solvent	Conv. (%) <sup>b</sup>	ee (%) <sup>c</sup> (config) <sup>d</sup>
1	<b>144u</b>	20	THF	>99	98 ( <i>R</i> )
2	<b>144v</b>	20	THF	>99	23 ( <i>S</i> )
3	<b>144w</b>	20	THF	>99	58 ( <i>R</i> )
4	<b>144y</b>	20	CH <sub>2</sub> Cl <sub>2</sub>	>99	92 ( <i>S</i> )

<sup>a</sup> All hydrogenations were run at room temperature under 20 bar of H<sub>2</sub>.

<sup>b</sup> Conversion was determined by <sup>1</sup>H-NMR spectroscopy.

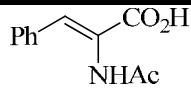
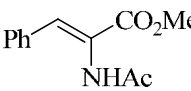
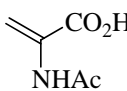
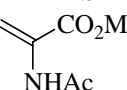
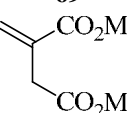
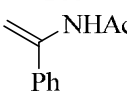
<sup>c</sup> Enantiomeric excess was determined by HPLC.

<sup>d</sup> The absolute configuration of the hydrogenated compounds was assigned by comparing optical rotation values or elution orders with reported values (see experimental section for details).

Having screened our ligand **125k** in Rhodium-catalyzed asymmetric hydrogenations of structurally diverse alkenes (*e.g.*  $\alpha$ -dehydroamino acids, itaconates, enamides and enol derivatives), we decided to compare its performance to that of so-called *milestone* ligands such as DUPHOS, JOSIPHOS and BINAP (see Table 27). As observed in the Table, the Rhodium complex of **125k** provided similar or better levels of enantioselectivity to those reported for Rhodium complexes of the aforementioned ligands.



**Table 27.** Comparison of the enantioselectivities obtained with our ligand **125k** to those obtained with standard ligands in Rhodium-catalyzed asymmetric hydrogenations of various alkenes.

S \ L	(R,R)- DIOP	(R,R)- DIPAMP	(S)- BINAP	(S,S)-Me- DUPHOS	(R)-(S)- JOSIPHOS	125k
	72 (R) <sup>112</sup>	94 (S) <sup>113</sup>	96 (R) <sup>114</sup>	-	84 (S) <sup>115</sup>	99 (R)
<b>144a</b>						
	68 (R) <sup>116</sup>	96 (S) <sup>113</sup>	93 (R) <sup>114</sup>	98 (S) <sup>117</sup>	96 (S) <sup>115</sup>	99 (R)
<b>32b</b>						
	73 (R) <sup>112</sup>	-	98 (R) <sup>114</sup>	-	-	99 (R)
<b>144b</b>						
	-	-	21 (R) <sup>118</sup>	99 (S) <sup>117</sup>	88 (S) <sup>115</sup>	99 (R)
<b>69</b>						
	25 (R) <sup>119</sup>	88 (R) <sup>120</sup>	94 (S) <sup>121</sup>	97 (R) <sup>122</sup>	98 (S) <sup>115</sup>	99 (R)
<b>144r</b>						
	53 (S) <sup>123</sup>	-	11 (R) <sup>118</sup>	95 (R) <sup>124</sup>	-	98 (R)
<b>144u</b>						

S = Substrate; L = Ligand.

<sup>112</sup> Kagan, H. B.; Dang Tuan, P. *J. Amer. Chem. Soc.* **1972**, *94*, 6429-33.<sup>113</sup> Vineyard, B. D.; Knowles, W. S.; Sabacky, M. J.; Bachman, G. L.; Weinkauff, D. J. *J. Am. Chem. Soc.* **1977**, *99*, 5946-52.<sup>114</sup> Miyashita, A.; Yasuda, A.; Takaya, H.; Toriumi, K.; Ito, T.; Souchi, T.; Noyori, R. *J. Am. Chem. Soc.* **1980**, *102*, 7932-4.<sup>115</sup> Togni, A.; Breutel, C.; Schnyder, A.; Spindler, F.; Landert, H.; Tijani, A. *J. Am. Chem. Soc.* **1994**, *116*, 4062-6.<sup>116</sup> Kreuzfeld, H. J.; Doebler, C.; Krause, H. W.; Facklam, C. *Tetrahedron: Asymmetry* **1993**, *4*, 2047-51.<sup>117</sup> Burk, M. J. *J. Am. Chem. Soc.* **1991**, *113*, 8518-19.<sup>118</sup> Hopkins, J. M.; Dalrymple, S. A.; Parvez, M.; Keay, B. A. *Org. Lett.* **2005**, *7*, 3765-3768.<sup>119</sup> Sento, T.; Shimazu, S.; Ichikuni, N.; Uematsu, T. *J. Mol. Catal. A: Chem.* **1999**, *137*, 263-267.<sup>120</sup> Christophel, W. C.; Vineyard, B. D. *J. Am. Chem. Soc.* **1979**, *101*, 4406-8.<sup>121</sup> Donate, P. M.; Frederico, D.; da Silva, R.; Constantino, M. G.; Del Ponte, G.; Bonatto, P. S. *Tetrahedron: Asymmetry* **2003**, *14*, 3253-3256.<sup>122</sup> Burk, M. J.; Bienewald, F.; Harris, M.; Zanotti-Gerosa, A. *Angew. Chem., Int. Ed.* **1998**, *37*, 1931-1933.<sup>123</sup> Yan, Y.-Y.; RajanBabu, T. V. *Org. Lett.* **2000**, *2*, 4137-4140.<sup>124</sup> Burk, M. J.; Wang, Y. M.; Lee, J. R. *J. Am. Chem. Soc.* **1996**, *118*, 5142-5143.

## 1.2.7. Optimization of the reaction conditions for asymmetric hydrogenation of alkenes using the catalytic system derived from $[\text{Rh}(\mathbf{125k})(\text{nbd})]\text{BF}_4$

### 1.2.7.1 Studying the effects of hydrogen pressure with Z-MAC and MAA as substrates

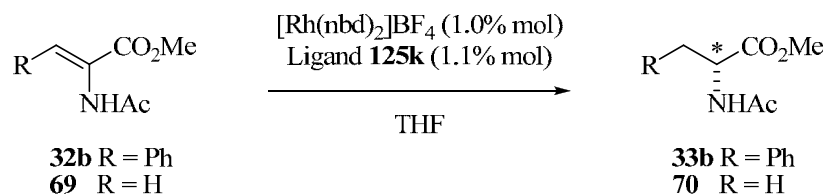
In many known catalytic asymmetric hydrogenations, the amount of hydrogen pressure can strongly influence the conversion and enantioselectivity.<sup>125</sup> Therefore, we assessed the effects of hydrogen pressure on the performance of our precatalyst  $[\text{Rh}(\mathbf{125k})(\text{nbd})]\text{BF}_4$  in the hydrogenation of methyl (Z)-(N)-acetylaminoacrylate (Z-MAC, **32b**) and methyl (N)-acetylaminoacrylate (MAA, **69**) to alanine derivatives **33b** and **70**, respectively (Table 28). Interestingly, the conversions and enantioselectivities obtained were relatively unaffected by changes in the hydrogen pressure. Almost no variation in the enantiomeric excess (99% ee) was observed over the pressure range of 1 to 20 bar  $\text{H}_2$  (Table 28; Entries 1-4 and 6-8). However, at 80 bar, a slight decrease in enantioselectivity was observed (98% ee; Table 28, Entries 5 and 8).

Most remarkably,  $[\text{Rh}(\mathbf{125k})(\text{nbd})]\text{BF}_4$  catalyzed the hydrogenation of Z-MAC and MAA at atmospheric pressure in very high yields (up to > 99%, Table 28, Entry 6) within 12 hours, which is testament to the high performance of our catalyst.

---

<sup>125</sup> Brown, J. M. in *Comprehensive Asymmetric Catalysis*; Jacobsen, E. N., Pfaltz, A., Yamamoto, H. Eds.; Springer: Berlin, Germany, 1999; Vol 1, pp 121-182 and references cited therein.

**Table 28.** The effects of different levels of hydrogen pressure in the asymmetric hydrogenation of methyl (Z)-(N)-acetylaminoacrylate (**32b**) and methyl (N)-acetylaminoacrylate (**69**) catalyzed by [Rh(**125k**)(nbd)]BF<sub>4</sub>.<sup>a</sup>



Entry	Substrate	H <sub>2</sub> pressure (bar)	Conv. (%) <sup>b</sup>	ee (%) <sup>c</sup> (config) <sup>d</sup>
1	<b>32b</b>	1	90	99 ( <i>R</i> )
2	<b>32b</b>	3	>99	99 ( <i>R</i> )
3	<b>32b</b>	10	>99	99 ( <i>R</i> )
4	<b>32b</b>	20	>99	99 ( <i>R</i> )
5	<b>32b</b>	80	>99	98 ( <i>R</i> )
6	<b>69</b>	1	>99	99 ( <i>R</i> )
7	<b>69</b>	10	>99	99 ( <i>R</i> )
8	<b>69</b>	20	>99	99 ( <i>R</i> )
9	<b>69</b>	80	>99	98 ( <i>R</i> )

<sup>a</sup> All hydrogenations were run at room temperature for 12 hours with magnetic stirring (300 rpm), but under different levels of H<sub>2</sub> pressure.

<sup>b</sup> Conversion was determined by <sup>1</sup>H-NMR spectroscopy.

<sup>c</sup> Enantiomeric excess was determined by HPLC or GC.

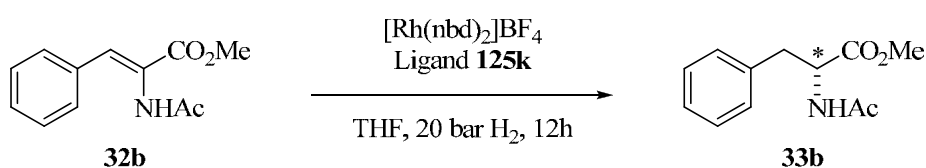
<sup>d</sup> The absolute configuration of the hydrogenated compounds was assigned by comparing optical rotation values or elution orders with reported values (see experimental section for details).

### 1.2.7.2 Studying the catalytic activity of the system derived from the “lead” ligand using Z-MAC as substrate

There is a need in asymmetric catalysis to combine high enantioselectivity and high catalytic activity (TOF and TON). Transfer to industrial processes should be facilitated in those cases in which enantioselectivity and catalytic activity are properly balanced. For this reason, in addition to the high

enantioselectivity, substrate scope, accessibility and functional group tolerance that our “lead” asymmetric catalyst has proven to have, we decided to study its catalytic activity in the hydrogenation of methyl (*Z*)-(*N*)-acetylaminoacinnamate **32b**. We explored the effects of different substrate to catalyst ratios in the asymmetric reaction of *Z*-MAC using our optimized conditions. The results are summarized in Table 29.

**Table 29.** The effects of different substrate to catalyst ratios in the asymmetric hydrogenation of methyl (*Z*)-(*N*)-acetylaminoacinnamate (**32b**) catalyzed by [Rh(**125k**)(nbd)]BF<sub>4</sub>.<sup>a</sup>



Entry	S/C ratio <sup>b</sup>	Conv. (%) <sup>c</sup>	ee (%) <sup>d</sup> (config) <sup>e</sup>
1	100	>99	99 ( <i>R</i> )
2	200	>99	99 ( <i>R</i> )
3	500	>99	99 ( <i>R</i> )
4	1000	>99	99 ( <i>R</i> )
5	2000	>99	99 ( <i>R</i> )
6	2500	>99	99 ( <i>R</i> )
7	5000	18	nd <sup>f</sup>

<sup>a</sup> All hydrogenations were run at room temperature under 20 bar H<sub>2</sub> for 12h with magnetic stirring (300 rpm).

<sup>b</sup> S = substrate, C = catalyst

<sup>c</sup> Conversion was determined by <sup>1</sup>H-NMR spectroscopy.

<sup>d</sup> Enantiomeric excess was determined by HPLC.

<sup>e</sup> The absolute configuration of the hydrogenated compounds was assigned by comparing optical rotation values or elution orders with reported values (see experimental section for details).

<sup>f</sup> not determined.

We were pleased to find that [Rh(**125k**)(nbd)]BF<sub>4</sub> performed well even at low catalyst loadings (substrate to catalyst ratios up to 2500; Table 29, Entry 6) with excellent enantioselectivities (up to 99% ee). Furthermore, it also showed

convenient reaction rates: at a substrate to catalyst ratio of 100, full conversion (> 99%) was observed after only 10 minutes. The turnover frequency for [Rh(**125k**)(nbd)]BF<sub>4</sub> was determined for *Z*-MAC as substrate **32b**, and then compared to those of Rhodium complexes of other ligands (Table 30). A turnover frequency higher than 1600 h<sup>-1</sup> (at 80% conversion) was measured using a catalyst loading of 0.1% mol (Entry 4, Table 30).<sup>126</sup>

**Table 30.** Catalyst activity comparison for the enantioselective hydrogenation of methyl (*Z*)-(*N*)-acetylamino-cinnamate (**32b**).

Entry	Ligand	S/C ratio <sup>a</sup>	TOF (h <sup>-1</sup> )	ee (%)
1	DIPAMP	1000	440 <sup>127</sup>	92
2	Me-DUPHOS	10000	4800 <sup>127</sup>	97
3	JOSIPHOS	600	>600 <sup>128</sup>	99
4	<b>125k</b>	1000	>1600	99

<sup>a</sup> S = substrate, C = catalyst

As reflected by the results in Table 30, our catalytic system derived from [Rh(**125k**)nbd]BF<sub>4</sub> has a very attractive catalytic profile in terms of both conversion and enantioselectivity. Although a comparative study of our ligand **125k** to all known ligands for Rhodium-catalyzed asymmetric hydrogenations would clearly lie beyond the scope of this PhD thesis, we have shown that it performs comparably to certain *milestone* ligands such as JOSIPHOS or DIPAMP.

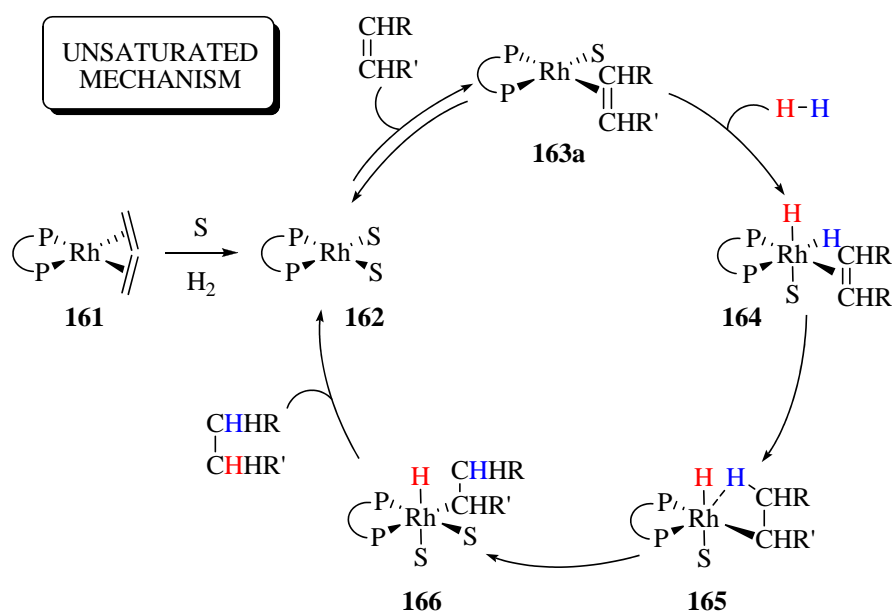
<sup>126</sup> TOF expressed in mol product x mol Rh<sup>-1</sup> x h<sup>-1</sup>, as measured by <sup>1</sup>H-NMR after 30 minutes reaction time.

<sup>127</sup> Boaz, N. W.; Mackenzie, E. B.; Debenham, S. D.; Large, S. E.; Ponasik, J. A., Jr. *J. Org. Chem.* **2005**, *70*, 1872-1880.

<sup>128</sup> *Handbook of Homogeneous Hydrogenation*; De Vries, J. G., Elsevier, C. J., Eds.; Wiley-VCH: Weinheim, Germany, 2007; Vol 1-3.

### 1.2.8. Rationalization of the stereochemical outcome of hydrogenation reaction using “lead” *P-OP* ligand derived from (*S*)-BINOL

The mechanism of enantioselective hydrogenation catalyzed by cationic Rhodium(I) complexes has been extensively studied by Halpern<sup>92a,129</sup> and Brown.<sup>125,130</sup> Most catalysts operate via the so-called “unsaturated” mechanism shown in Scheme 29.



**Scheme 29.** “Unsaturated” Rh-mediated hydrogenation mechanism.

The catalytic Rh(I) precursor **161** is first hydrogenated yielding the corresponding solvate complex **162**, which is considered the first species in the catalytic cycle. Initial reversible formation of a bidentate catalyst-substrate complex **163a** is followed by oxidative addition of dihydrogen affording Rhodium(III) dihydride species **164**. Migratory insertion to form an alkyl hydride complex **165** is finally followed by reductive elimination to regenerate the unsaturated Rhodium(I) complex **162**. The stereochemistry of the product is

<sup>129</sup> (a) Halpern, J.; Riley, D. P.; Chan, A. S. C.; Pluth, J. J. *J. Am. Chem. Soc.* **1977**, *99*, 8055-7.

(b) Halpern, J. *Science (Washington, DC, United States)* **1982**, *217*, 401-7.

<sup>130</sup> (a) Brown, J. M.; Chaloner, P. A. *J. Chem. Soc., Chem. Commun.* **1980**, 344-6.

determined at the first irreversible step (**163a**  $\rightarrow$  **164**; oxidative addition) where the hydride groups are delivered to the olefin from the metal side. However, it should be recalled at this point that recent theoretical investigations suggest the possibility that the process from **163a** to **164** is reversible and the step **164**  $\rightarrow$  **166** (migratory insertion) constitutes the turnover-limiting step.<sup>131</sup>

The BINAP-Rh-catalyzed hydrogenation of enamides is proposed to proceed with the Halpern-Brown mechanism.<sup>114,132</sup> In this mechanism (Scheme 29), the observed enantioselectivity of the hydrogenated product is a result of the reactivity and stability of the diastereomeric adducts **163a** toward dihydrogen. Thus, there are two possibilities:

- i. An anti “*lock-and-key*” mechanism, in which the major enantiomer arises from hydrogenation of the prochiral face of the C=C bond that binds less favorably to the catalyst. In several systems it has been found that the hydrogenation reaction proceeds via an anti “*lock-and-key*” mechanism.<sup>92a,130a,133</sup>
- ii. A “*lock-and-key*” mechanism, in which the major catalyst-substrate isomer complex possesses the C=C double bond coordinated according to the observed sense of stereoiduction.<sup>134</sup>

However, further observations by Gridnev, Imamoto *et al.* have shown that using electron rich *P*-stereogenic ligands, the Rh-catalyzed hydrogenation proceeds via a different mechanism.<sup>135</sup> The main difference in this hydrogenation

<sup>131</sup> Landis, C. R.; Hilfenhaus, P.; Feldgus, S. *J. Am. Chem. Soc.* **1999**, *121*, 8741-8754.

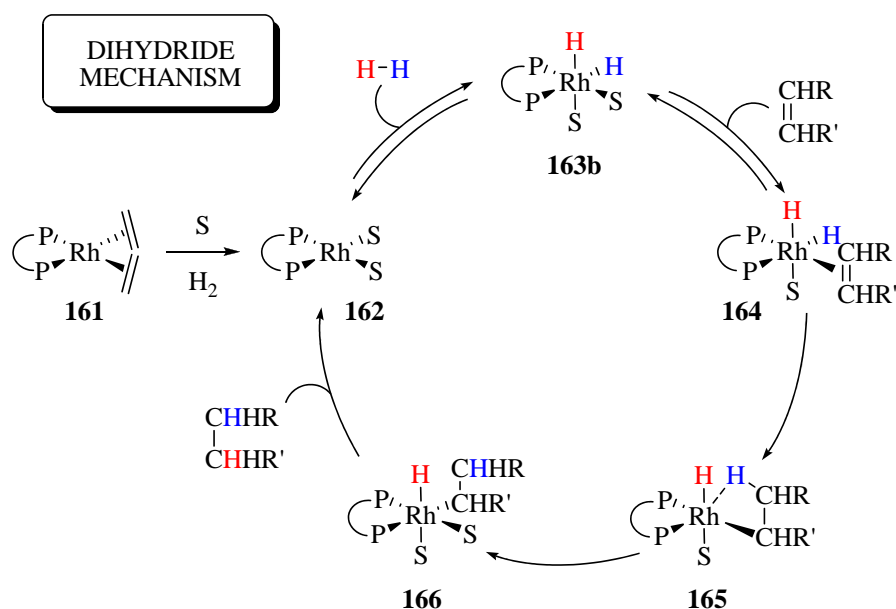
<sup>132</sup> Noyori, R.; Kitamura, M.; Ohkuma, T. *Proc. Natl. Acad. Sci. U. S. A.* **2004**, *101*, 5356-5362.

<sup>133</sup> (a) Brown, J. M.; Chaloner, P. A.; Morris, G. A. *J. Chem. Soc., Perkin Trans. 2* **1987**, 1583-8. (b) McCulloch, B.; Halpern, J.; Thompson, M. R.; Landis, C. R. *Organometallics* **1990**, *9*, 1392-5. (c) Landis, C. R.; Feldgus, S. *Angew. Chem., Int. Ed.* **2000**, *39*, 2863-2866. (d) Feldgus, S.; Landis, C. R. *J. Am. Chem. Soc.* **2000**, *122*, 12714-12727.

<sup>134</sup> (a) Evans, D. A.; Michael, F. E.; Tedrow, J. S.; Campos, K. R. *J. Am. Chem. Soc.* **2003**, *125*, 3534-3543. (d) Drexler, H.-J.; Bauman, W.; Schmidt, T.; Zhang, S.; Sun, A.; Spannenberg, A.; Fischer, C.; Buschmann, H.; Heller, D. *Angew. Chem., Int. Ed.* **2005**, *44*, 1184-1188. (c) Schmidt, T.; Baumann, W.; Drexler, H.-J.; Arrieta, A.; Heller, D.; Buschmann, H. *Organometallics* **2005**, *24*, 3842-3848.

<sup>135</sup> (a) Gridnev, I. D.; Higashi, N.; Asakura, K.; Imamoto, T. *J. Am. Chem. Soc.* **2000**, *122*, 7183-7194. (b) Gridnev, I. D.; Higashi, N.; Imamoto, T. *Organometallics* **2001**, *20*, 4542-4553.

cycle is that dihydrogen is activated prior to substrate coordination (Scheme 30) giving the so-called “*dihydride*” mechanism. Here, the rate-determining step is believed to be the migratory insertion.



Scheme 30

This mechanism is also suggested by Brown *et al.*<sup>136</sup> in their work on the detection of agostic intermediates in the asymmetric hydrogenation of dehydroamino acids using Rh-PANEPHOS complex.

Hence, it is now accepted that the mechanism of enantioselection is dependent on the exact combination of the ligand, the substrate and the reaction conditions.

Thus, to better understand the ongoing stereinduction processes we first studied the coordination mode of *Z*-MAC **32b** in [Rh(**125k**)(**32b**)]<sup>+</sup> complexes. To prepare these complexes/adducts, we followed the methodology described by

(c) Gridnev, I. D.; Imamoto, T. *Acc. Chem. Res.* **2004**, *37*, 633-644. (d) Gridnev et al *J. Am. Chem. Soc.* **2008**, 2560.

<sup>136</sup> (a) Giernoth, R.; Heinrich, H.; Adams, N. J.; Deeth, R. J.; Bargon, J.; Brown, J. M. *J. Am. Chem. Soc.* **2000**, *122*, 12381-12382. (b) Heinrich, H.; Bargon, J.; Giernoth, R.; Brown, J. M. *Chem. Commun. (Cambridge, U. K.)* **2001**, 1296-1297.





face of the alkene to the Rhodium centre (pro-*R* and pro-*S* enantiotopic faces of the alkene).

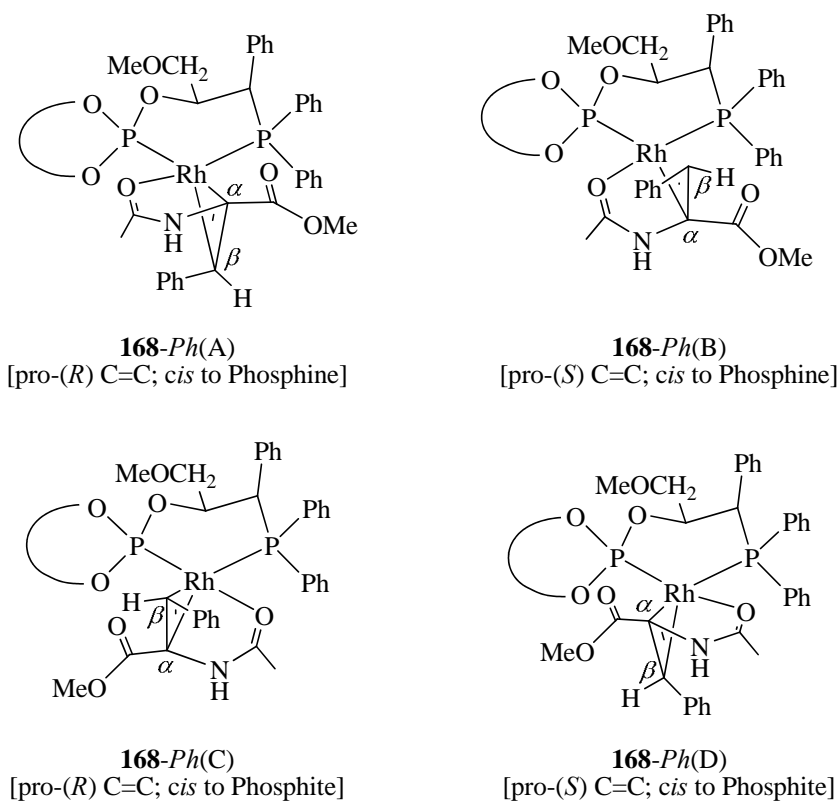


**Figure 38.** Diastereomers of  $[\text{Rh}(\text{P-OP})(\text{Z-MAC})]^+$  complexes (**168-Ph**).

We investigated the coordination of the enamide by analyzing the structure of complex **168-Ph** by NMR experiments. Thus, the 2D  $^{31}\text{P}$ - $^1\text{H}$  correlation experiment showed a cross-peak between the olefinic proton (assigned in turn by a 2D  $^{13}\text{C}$ - $^1\text{H}$  correlation experiment) and the phosphorus atom of the phosphite moiety, but not with the phosphine (Figures 39 and 40). This observation is in agreement with the conclusions obtained with related phosphine-phosphite ligands, studied by Pizzano *et al.*,<sup>80g</sup> and diphosphine compounds, studied by Gridnev and Imamoto.<sup>135a</sup> In these cases, the corresponding olefinic proton couples only with the phosphorus nucleus *cis* to the alkene fragment. Therefore, these literature data support structures **168-Ph(C)** [pro-*R*) C=C; *cis* to Phosphite] and **168-Ph(D)** [pro-*S*) C=C; *cis* to Phosphite] in Figure 38, which possess the

olefin group coordinated *cis* with respect to the phosphite unit. However, it was not possible by NMR studies to discriminate between structures **168-Ph(C)** [pro-(*R*) C=C; *cis* to Phosphite] and **168-Ph(D)** [pro-(*S*) C=C; *cis* to Phosphite], which only differ in the coordinated face of the alkene.

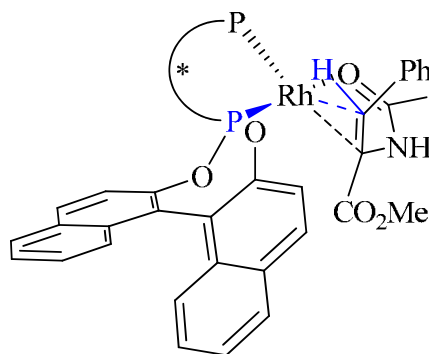


**Figure 39.** One of the two preferential coordination modes in  $[\text{Rh}(\mathbf{125k})(\mathbf{32b})]^+$  complexes ([pro-(*R*) C=C; *cis* Phosphite]; blue colour indicates the atoms and bonds that are coupled through three bonds).

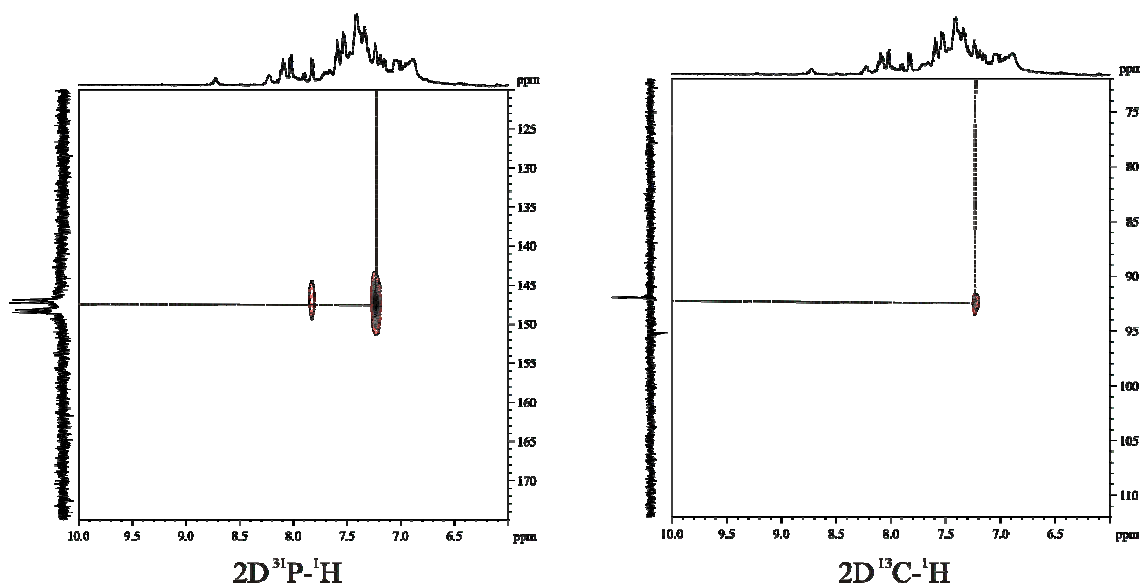


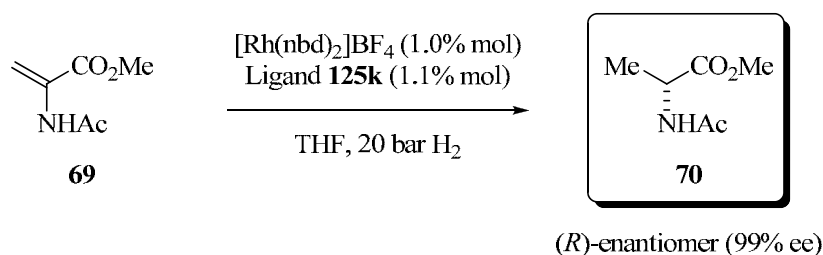
**Figure 40.** 2D NMR correlation experiments of complex **168-Ph**.

Computational studies carried out in Dr. Maseras' group<sup>137</sup> on the  $[\text{Rh}(\mathbf{125k})(\mathbf{69})]^+$  complexes **168-H** containing the acrylate instead of the cinnamate group also supported the preferential coordination of the C=C bond *trans* to the phosphine. Ligands with stronger *trans*-influence prefer to be coordinated opposite those with weaker *trans*-influence.<sup>134a</sup> In our substrate, the olefin has the stronger *trans*-influence of the substrate donors,<sup>134a</sup> so it prefers to be *trans* to the phosphine. Furthermore, these computational studies revealed a preferential coordination mode of the pro-(*S*) alkene face to the Rhodium centre. The relative energies of the four diastereomeric Rhodium complexes containing ligand **125k** and the acrylate **69** have been depicted in Figure 41. Calculations predict a 1.42 kcal/mol energy gap between the *cis*-phosphite diastereoisomers differing in the coordinated alkene face.

The preferential **168-H(C)** [pro-(*R*) C=C; *cis* Phosphite] coordination mode of the acrylate **69** to the Rhodium centre would suggest that an anti “*lock-and-key*” process operates, as our major experimentally observed hydrogenated product from these system is of opposite configuration to the favoured computed  $[\text{Rh}(\mathbf{125k})(\mathbf{69})]^+$  complex **168-H(D)** ([pro-(*S*) C=C; *cis* Phosphite], see Scheme 32 and Figure 41). The ongoing detailed computational analysis of the intermediates and transition states for all possible hydrogenation manifolds from each diastereomeric  $[\text{Rh}(\mathbf{125k})(\mathbf{69})]^+$  complex will hopefully lead to a deeper understanding of the stereinduction processes in the asymmetric hydrogenation mediated by our “lead” catalyst.

---

<sup>137</sup> Computational calculations were performed by Dr. Steven Donald in Dr. Maseras' research group using the B3LYP functional, as implemented in Gaussian 03. Stuttgart ECP's and basis functions for the Rhodium and phosphorus atoms (with added f or d polarisation functions respectively) were used. 6-31G\* basis set was used for the six membered Rh-chelate. 6-31G was used on all phenyl substituents and the ether group on the backbone. Corrections for solvation are being considered. Detailed computational data will be reported elsewhere.



**Scheme 32.** *In situ* Rh-catalyzed asymmetric hydrogenation of MAA using chiral *P-OP* ligand **125k**.

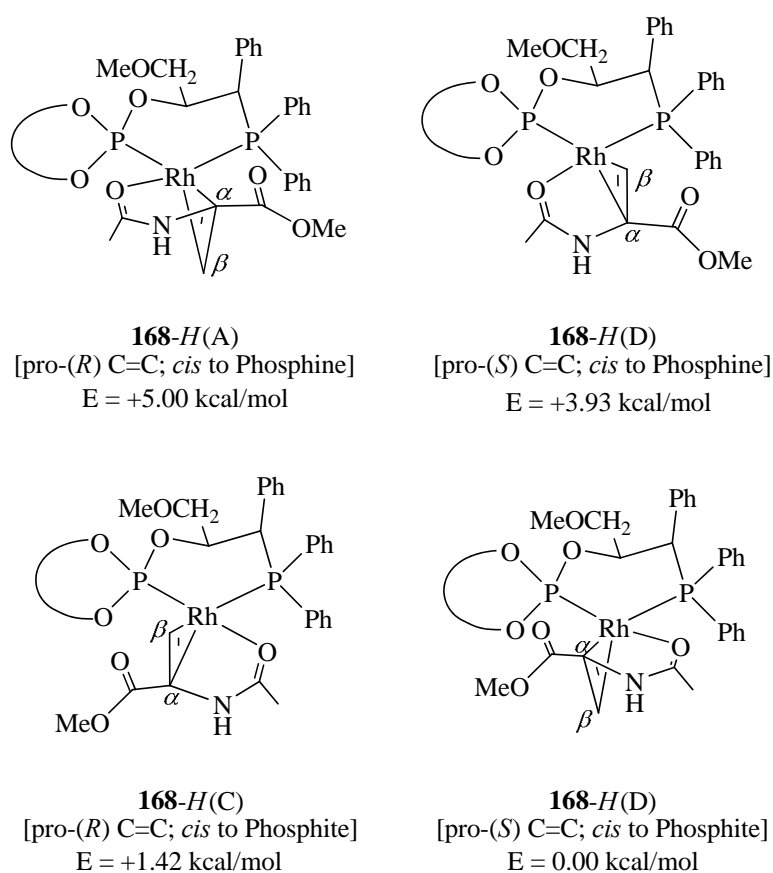


**Figure 41.** Diastereomers of  $[\text{Rh}(\mathbf{125k})(\mathbf{69})]^+$  complexes.

Meanwhile, a preliminary rough rationalization of the stereochemical outcome of the asymmetric hydrogenation mediated by the catalytic system derived from ligand **125k** can be done using Knowles quadrant diagram analysis.<sup>138</sup> Thus, the *S*-BINOL fragment in **125k** would be expected to exert a

<sup>138</sup> Knowles, W. S. *Acc. Chem. Res.* **1983**, *16*, 106-12.

high steric hindrance in the upper left quadrant (Figure 42) and the phosphine substituents a less pronounced effect on the upper right quadrant. This observation is in agreement with our hydrogenation experiments, as they show that the binaphthyl fragment has the strongest effect on enantioselectivity and that the configuration of the BINOL derivative predominantly controls the enantiomer produced. Thus, ligand **125k** with *S* configuration at the phosphite produced the *R* enantiomer of the product (99% ee, see Section 1.2.5.3, page 130), while **125j** with *R* configuration produced the opposite *S* enantiomer, though with slightly lower enantioselectivity (88% ee, see Section 1.2.5.3, page 130). Furthermore, the preferential coordination of the double bond in a *trans* fashion to the phosphine moiety implies that the right-hand quadrants are electronically blocked, since the alkene binds preferentially *trans* to the phosphine group. Hence, the bottom-left quadrant is the most favoured one for C=C binding to the metal center.

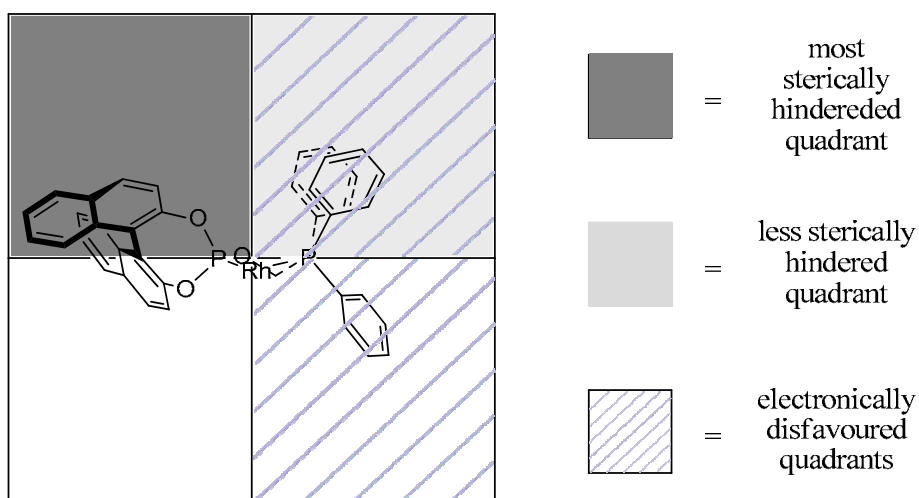


**Figure 42.** Knowles quadrant analysis for the catalytic system incorporating ligand **125k**.

Assuming that our system follows the classical Halpern-Brown mechanism (Scheme 29), the observed sense of induction would suggest that hydrogen activation would mainly take place on **168-H(C)** (Figure 43).

168-H(C)

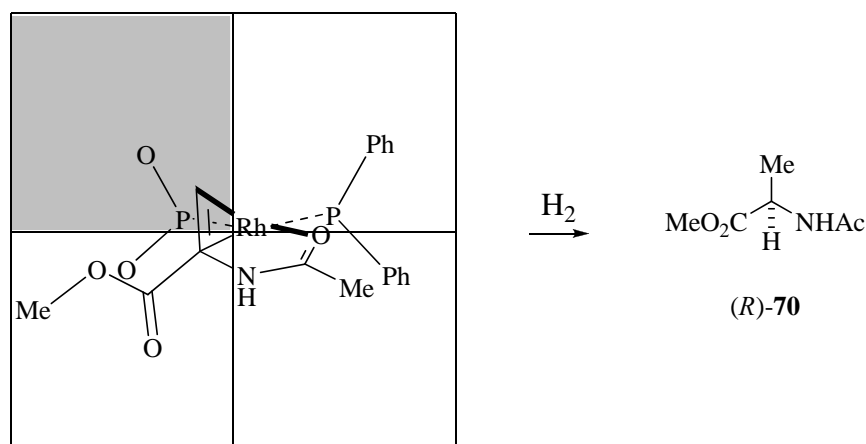


**Figure 43.** Rationalization of the stereochemical outcome using the simple quadrant model.

In conclusion, the stereochemical outcome of the hydrogenation can be roughly rationalised by the following statements: the upper left quadrant containing the largest steric hindrance, the right side being electronically disfavoured, C=C binding to the metal centre in the left bottom quadrant and delivery of the hydrogen from the side of the metal. Ongoing detailed computational studies on our system will hopefully unequivocally establish the step in the hydrogenation which controls the stereoiduction.

It should finally be emphasized that in the case of our “lead” ligand, although excellent enantioselectivities can be achieved with the (*S*)-binaphthyl group in the phosphite fragment, the chiral ligand backbone also plays an important role: an opposite *R* configuration of the binaphthyl group in the phosphite moiety afforded the opposite enantiomer of the product with lower selectivity. Hence, we suggest that the high selectivity is the result of a combined action between the chiral phosphite moiety and ligand backbone chirality.





## **EXPERIMENTAL PROCEDURE**

UNIVERSITAT ROVIRA I VIRGLI

TOWARDS HIGHLY EFFICIENT LIGANDS FOR ASYMMETRIC HYDROGENATIONS: A COVALENT MODULAR APPROACH AND  
INVESTIGATIONS INTO BIOINSPIRED SUPRAMOLECULAR STRATEGIES

Héctor Fernández Pérez

ISBN:978-84-693-3385-3 /DL:T.994-2010

## 1.3. EXPERIMENTAL PROCEDURE

### 1.3.1. General remarks

All manipulations and reactions were performed under argon, either in a Braun glovebox or with standard Schlenk-type techniques. Glassware was dried before use with a hot gun. Dimethylformamide, dichloromethane, tetrahydrofuran, toluene and diethyl ether were dried and deoxygenated by using a Solvent Purification System (SPS). Triethylamine was distilled from CaH<sub>2</sub>. Silica gel 60 (230-400 mesh) and neutral alumina, previously dried under vacuo (oil pump), were used for column chromatography. NMR spectra were recorded on Bruker Avance 400 and 500 Ultrashield spectrometers in CDCl<sub>3</sub> unless otherwise cited. <sup>1</sup>H-NMR and <sup>13</sup>C-NMR chemical shifts are quoted in ppm relative to residual solvent peaks whereas <sup>31</sup>P{<sup>1</sup>H}-NMR chemical shifts are quoted in ppm relative to 85% phosphoric acid in water. <sup>11</sup>B-NMR chemical shifts are quoted in ppm relative to BF<sub>3</sub>·EtOEt in CDCl<sub>3</sub>. <sup>19</sup>F{<sup>1</sup>H}-NMR chemical shifts are quoted in ppm relative to CFCl<sub>3</sub> in CDCl<sub>3</sub>. IR spectra were recorded on a Bruker Tensor 27 spectrometer in Fourier transform mode. ESI mass spectra were obtained on a Waters LCT Premier mass spectrometer. Optical rotations were measured on a Jasco P-1030 polarimeter. Melting points were determined in open capillaries on a Büchi B-540 instrument and are uncorrected for phosphine-phosphinite **124a-d** and phosphine-phosphite **125a-k**. Enantiomeric excesses were determined by HPLC on Agilent 1100 Series chromatograph with a UV detector and by GC on a Agilent Technologies 6890N gas chromatograph with a FID detector.

Crystal structure determination was carried out using a Bruker-Nonius diffractometer equipped with APPEX 2 4K CCD area detector, a FR591 rotating anode with MoK<sub>α</sub> radiation, Montel mirrors as monochromator and a Kryoflex low temperature device (T = 100K). Fullsphere data was collected using omega and phi scans. Apex2 V. 1.0-22 (Bruker-Nonius 2004) for the data reduction and

SADABS V. 2.10 (2003) for the absorption correction. Crystal structure was achieved using direct methods as implemented in SHELXTL Version 6.10 (Sheldrick, Universität Göttingen (Germany), 2000). Least-squares refinement on F<sup>2</sup> using all measured intensities was carried out using the program SHELXTL Version 6.10 (Sheldrick, Universität Göttingen (Germany), 2000). All non hydrogen atoms were refined including anisotropic displacement parameters.

### 1.3.2. General synthetic procedure of protected epoxides **113a-e** and **137**

#### 1.3.2.1. Synthetic procedure of compounds **113a-d**

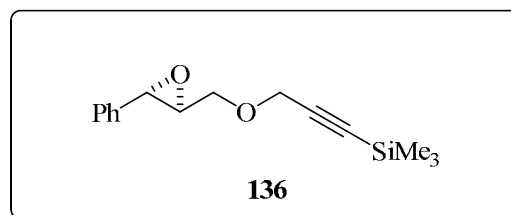
A solution of Sharpless epoxide (1.0 g, 6.66 mmol) in DMF (7.0 mL) was added via cannula to a suspension of sodium hydride (231 mg, ca. 7.7 mmol) in DMF (8.0 mL) at -20 °C. The mixture was stirred for 20 min at this temperature, then the corresponding electrophile (8.66 mmol of MeI **113a**, MeO(CH<sub>2</sub>)<sub>2</sub>-I **113b**, PhCH<sub>2</sub>Br **113c** or Ph<sub>2</sub>CHBr **113d**) was syringed in and stirring continued for 4h. The solution was allowed to reach either room temperature (for compounds **113a** and **113c**) or 0° C (for compounds **113b** and **113d**) and further stirred (1h for **113a** and **113c** and 22h for **113b** and **113d**). MeOH (25.0 mL) and brine (25.0 mL) were added. The aqueous solution was extracted with CH<sub>2</sub>Cl<sub>2</sub> (3 x 50.0 mL). The combined organic extracts were dried over MgSO<sub>4</sub> and concentrated *in vacuo*. The residual oil was chromatographed on silica gel using hexane:AcOEt as eluents to give **113a-d**.

### 1.3.2.2. Synthetic procedure of (2*S*,3*S*)-2-Phenyl-3-(trityloxymethyl)oxirane **113e**

Sharpless epoxide (1.00 g, 6.66 mmol), chlorotriphenylmethane (2.084 g, 7.32 mmol), DMAP (24.4 mg, 0.20 mmol) and Et<sub>3</sub>N (2.8 mL, 20.0 mmol) in CH<sub>2</sub>Cl<sub>2</sub> (25.0 mL) were refluxed for 2 h. The mixture was then washed with HCl 10% (3 x 30.0 mL) and H<sub>2</sub>O (2 x 25.0 mL). The solvent was removed *in vacuo*, and the residual oil was chromatographed on silica gel using hexane:AcOEt (100:0/70:30) as eluent to give 1.90 g (72% yield) of **113e** as a white solid.

### 1.3.2.3. Synthetic procedure of Trimethyl(3-(((2*S*,3*S*)-3-phenyloxirane-2-yl)methoxy)prop-1-ynyl)silane **136**

A solution of Sharpless epoxide (1.00 g, 6.66 mmol) in DMF (10.0 mL) was added via cannula to a suspension of sodium hydride (0.319 g, 7.99 mmol) in DMF (10.0 mL) at -20 °C. This mixture



was stirred for 20 minutes at this temperature. Propargyl bromide (1.1 mL, 9.99 mmol) was syringed dropwise to this mixture and stirred at -20°C for 1 h. The reaction was allowed to reach room temperature and stirred overnight. MeOH (25.0 mL) and brine (25.0 mL) were added. The aqueous solution was extracted with Et<sub>2</sub>O (3 x 50.0 mL). The combined organic extracts were washed with NaCl solution (2 x 25.0 mL), dried over MgSO<sub>4</sub> and concentrated *in vacuo*. The residual oil was chromatographed through SiO<sub>2</sub> using hexanes/AcOEt (100:0/80:20) to give **135** as colorless oil (0.922 g; 74% yield). To a THF solution of the intermediate epoxide **135** (0.484 g, 2.57 mmol) was added dropwise *n*-BuLi (1.2 mL, 2.5 M, 2.83 mmol) at -78°C. The mixture was stirred at this temperature for 45 minutes and then Me<sub>3</sub>SiCl (0.37 mL, 2.83 mmol) was added. The reaction was allowed to reach room temperature and stirred

overnight. The reaction mixture was quenched with saturated solution of  $\text{NH}_4\text{Cl}$  (15.0 mL) and extracted with  $\text{AcOEt}$  (3 x 25.0 mL), dried over  $\text{MgSO}_4$  and concentrated under reduced pressure. The residue was purified by flash chromatography through  $\text{SiO}_2$  using hexane/ $\text{AcOEt}$  (100:0/90:10) to obtain **136** (0.479 g, 71% yield) as colorless oil.  $^1\text{H-NMR}$  (400 MHz,  $\text{CDCl}_3$ )  $\delta$  7.37-7.27 (m, 5H,  $H_{\text{arom}}$ ), 4.38 (d,  $^2J_{\text{H-H}} = 16.0$  Hz, 1H,  $\text{CHH-C}\equiv\text{C-SiMe}_3$ ), 4.23 (d,  $^2J_{\text{H-H}} = 16.0$  Hz, 1H,  $\text{CHH-C}\equiv\text{C-SiMe}_3$ ), 3.89 (dd,  $^2J_{\text{H-H}} = 11.6$  Hz,  $^3J_{\text{H-H}} = 3.2$  Hz, 1H,  $\text{CHH-O-CH}_2\text{-C}\equiv\text{C-SiMe}_3$ ), 3.82 (d,  $^3J_{\text{H-H}} = 2.0$  Hz, 1H,  $\text{Ph-CH-O}$ ), 3.69 (dd,  $^2J_{\text{H-H}} = 11.6$  Hz,  $^3J_{\text{H-H}} = 5.2$  Hz, 1H,  $\text{CHH-O-CH}_2\text{-C}\equiv\text{C-SiMe}_3$ ), 3.24 (m, 1H,  $\text{O-CH-CH}_2\text{-O}$ ), 0.19 (s, 9H,  $\text{SiMe}_3$ );  $^{13}\text{C}\{^1\text{H}\}\text{-NMR}$  (100 MHz,  $\text{CDCl}_3$ )  $\delta$  136.9 ( $\text{C}_{\text{q arom}}$ ), 128.6 ( $\text{CH}_{\text{m arom}}$ ), 128.4 ( $\text{CH}_{\text{p arom}}$ ), 125.8 ( $\text{CH}_{\text{o arom}}$ ), 101.0 ( $\text{C}\equiv\text{C-SiMe}_3$ ), 92.1 ( $\text{C}\equiv\text{C-SiMe}_3$ ), 69.5 ( $\text{CH}_2\text{-O-CH}_2\text{-C}\equiv\text{C-SiMe}_3$ ), 60.8 ( $\text{O-CH-CH}_2\text{-O}$ ), 59.5 ( $\text{CH}_2\text{-C}\equiv\text{C-SiMe}_3$ ), 56.1 ( $\text{Ph-CH-O}$ ), -0.1 (3Me,  $\text{SiMe}_3$ ); IR (neat,  $\text{cm}^{-1}$ )  $\nu$  2174 ( $\text{C}\equiv\text{C}_{\text{st}}$ ); MS HR-ESI [found 283.1127;  $\text{C}_{15}\text{H}_{20}\text{O}_2\text{SiNa}$  ( $\text{M}+\text{Na}$ ) $^+$  requires 283.1127];  $[\alpha]_{\text{D}}^{25} = -44.9$  ( $c = 1.05$  g/100 mL,  $\text{CHCl}_3$ ).

### 1.3.3. General synthetic procedure of phosphine-borane adducts **118a-f** and **137**

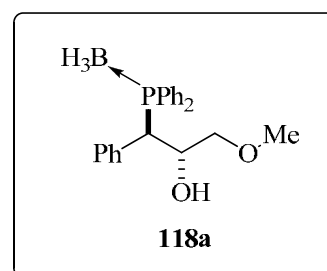
A solution of the phosphorus nucleophile in THF (0.98 mmol) was syringed into a cooled solution ( $-30$  °C) of the corresponding epoxy ether (1.00 mmol) in dry THF (8.0 mL). The mixture was stirred for 1h at this temperature and then was slowly allowed to reach room temperature and further stirred for 1h. Then, the mixture was cooled at  $-10$  °C and  $\text{BH}_3\cdot\text{DMS}$  (2.94 mmol) was added dropwise. The mixture was stirred for 1h at this temperature and then allowed to warm to room temperature and further stirred for 1h. The reaction mixture was quenched with water (8.0 mL), and the two phases were separated. The aqueous phase was extracted with  $\text{AcOEt}$  (3 x 15.0 ml). The combined organic phases were washed with brine (2 x 15.0 mL), dried over  $\text{MgSO}_4$  and concentrated

under reduced pressure. The resulting residue was purified by flash chromatography through SiO<sub>2</sub> using hexane/AcOEt as eluent to give the corresponding phosphino-alcohols as borane complexes.

### 1.3.3.1. Synthesis and general physical and spectroscopic data of phosphine-borane adducts **118a-e** and **137**

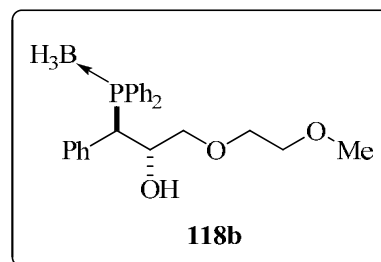
#### (1*R*,2*S*)-1-(diphenylphosphino borane)-3-methoxy-1-phenylpropan-2-ol (**118a**).

Phosphine-borane complex **118a** was obtained following the general procedure from epoxy ether **113a** (0.309 g, 1.88 mmol), KPPH<sub>2</sub> (3.7 mL, 1.84 mmol) and BH<sub>3</sub>·DMS complex (0.53 mL, 5.65 mmol) after column chromatography through SiO<sub>2</sub> (hexanes/AcOEt 100:0/80:20) as a white solid (0.552 g, 80% yield). <sup>1</sup>H-NMR (400 MHz, CDCl<sub>3</sub>) δ 8.01-7.96 (m, 2H, *H*<sub>arom</sub>), 7.57 -7.12 (m, 13H, *H*<sub>arom</sub>), 4.48 (m, 1H, CH-OH), 4.15 (dd, <sup>2</sup>*J*<sub>H-P</sub> = 17.2 Hz, <sup>3</sup>*J*<sub>H-H</sub> = 3.6 Hz, 1H, CH-PPh<sub>2</sub>·BH<sub>3</sub>), 3.21 (ddd, <sup>2</sup>*J*<sub>H-H</sub> = 9.6 Hz, <sup>3</sup>*J*<sub>H-H</sub> = 5.2 Hz, <sup>4</sup>*J*<sub>H-P</sub> = 1.6 Hz, 1H, CHH-OMe), 3.13 (s, 3H, *Me*), 3.12 (dd, <sup>2</sup>*J*<sub>H-H</sub> = 9.6 Hz, <sup>3</sup>*J*<sub>H-H</sub> = 6.8 Hz, 1H, CHH-OMe), 3.01 (d, <sup>3</sup>*J*<sub>H-H</sub> = 4.0 Hz, 1H, OH), 1.81-0.77 (bs, 3H, BH<sub>3</sub>); <sup>13</sup>C{<sup>1</sup>H}-NMR (100 MHz, CDCl<sub>3</sub>) δ 133.0 (d, *J*<sub>C-P</sub> = 8.6 Hz, CH<sub>arom</sub>), 132.9 (d, *J*<sub>C-P</sub> = 8.4 Hz, CH<sub>arom</sub>), 131.7 (d, *J*<sub>C-P</sub> = 2.2 Hz, CH<sub>arom</sub>), 131.4 (d, *J*<sub>C-P</sub> = 4.9 Hz, CH<sub>arom</sub>), 131.0 (d, *J*<sub>C-P</sub> = 2.1 Hz, CH<sub>arom</sub>), 129.1 (d, *J*<sub>C-P</sub> = 9.7 Hz, CH<sub>arom</sub>), 128.6 (C<sub>q</sub> arom), 128.2 (CH<sub>arom</sub>), 128.2 (C<sub>q</sub> arom), 128.1 (CH<sub>arom</sub>), 128.1 (C<sub>q</sub> arom), 127.6 (C<sub>q</sub> arom), 127.5 (d, *J*<sub>C-P</sub> = 2.1 Hz, CH<sub>arom</sub>), 73.2 (d, <sup>3</sup>*J*<sub>C-P</sub> = 8.1 Hz, CH<sub>2</sub>-OMe), 69.1 (d, <sup>2</sup>*J*<sub>C-P</sub> = 5.9 Hz, CH-OH), 58.8 (*Me*), 45.0 (d, <sup>1</sup>*J*<sub>C-P</sub> = 31.9 Hz, CH-PPh<sub>2</sub>·BH<sub>3</sub>); <sup>31</sup>P{<sup>1</sup>H}-NMR (162 MHz, CDCl<sub>3</sub>) δ 20.6 (bs, PPh<sub>2</sub>·BH<sub>3</sub>); <sup>11</sup>B-NMR (128 MHz, CDCl<sub>3</sub>) δ -39.0 (bs, BH<sub>3</sub>); IR (neat, cm<sup>-1</sup>) ν 3449 (O-H<sub>st</sub>), 2389 (B-H<sub>st</sub>); MS HR-ESI [found 387.1658; C<sub>22</sub>H<sub>26</sub>O<sub>2</sub>PBNa (M+Na)<sup>+</sup> requires 387.1661]; [α]<sub>D</sub><sup>25</sup> = -154.2 (c = 1.00 g/100 mL, CHCl<sub>3</sub>); M.p. 117.1-117.6 °C.



**(1*R*,2*S*)-1-(diphenylphosphino borane)-3-(2-methoxyethoxy)-1-phenylpropan-2-ol (118b).**

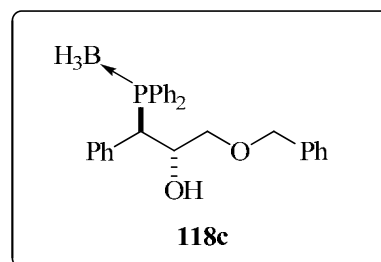
Phosphine-borane complex **118b** was obtained following the general procedure from epoxy ether **113b** (0.599 g, 2.88 mmol),  $KPPh_2$  (5.6 mL, 2.82



mmol) and  $BH_3 \cdot DMS$  complex (0.7 mL, 8.46 mmol) after column chromatography through  $SiO_2$  (hexanes/ $AcOEt$  100:0/70:30) as a white solid (0.875 g, 74% yield).  $^1H$ -NMR (400 MHz,  $CDCl_3$ )  $\delta$  8.00-7.95 (m, 2H,  $H_{arom}$ ), 7.56-7.12 (m, 13H,  $H_{arom}$ ), 4.50 (m, 1H,  $CH-OH$ ), 4.15 (dd,  $^2J_{H-P} = 17.2$  Hz,  $^3J_{H-H} = 3.2$  Hz, 1H,  $CH-PPh_2 \cdot BH_3$ ), 3.48-3.40 (m, 4H,  $CH_2-CH_2-OMe$ ), 3.36 (s, 3H,  $Me$ ), 3.29 (ddd,  $^2J_{H-H} = 9.7$  Hz,  $^3J_{H-H} = 5.6$  Hz,  $^2J_{H-P} = 1.6$  Hz, 1H,  $CHH-O(CH_2)_2-OMe$ ), 3.22 (dd,  $^2J_{H-H} = 9.7$  Hz,  $^3J_{H-H} = 7.0$  Hz, 1H,  $CHH-O-(CH_2)_2-OMe$ ), 1.81-0.77 (bs, 3H,  $BH_3$ );  $^{13}C\{^1H\}$ -NMR (100 MHz,  $CDCl_3$ )  $\delta$  133.0 (d,  $J_{C-P} = 8.2$  Hz,  $CH_{arom}$ ), 133.0 (d,  $J_{C-P} = 8.8$  Hz,  $CH_{arom}$ ), 131.7 (d,  $J_{C-P} = 2.2$  Hz,  $CH_{arom}$ ), 131.5 (d,  $J_{C-P} = 5.0$  Hz,  $CH_{arom}$ ), 131.0 (d,  $J_{C-P} = 2.4$  Hz,  $CH_{arom}$ ), 129.1 (d,  $J_{C-P} = 9.9$  Hz,  $CH_{arom}$ ), 128.7 ( $C_q$   $arom$ ), 128.2 (d,  $J_{C-P} = 10.1$  Hz,  $CH_{arom}$ ), 128.1 (d,  $J_{C-P} = 1.1$  Hz,  $CH_{arom}$ ), 127.7 ( $C_q$   $arom$ ), 127.4 (d,  $J_{C-P} = 2.0$  Hz,  $CH_{arom}$ ), 72.1 (d,  $^3J_{C-P} = 8.8$  Hz,  $CH_2-O-(CH_2)_2-OMe$ ), 71.8 ( $CH_2-CH_2-OMe$ ), 70.4 ( $CH_2-CH_2-OMe$ ), 69.2 (d,  $^2J_{C-P} = 5.6$  Hz,  $CH-OH$ ), 59.1 ( $Me$ ), 45.0 (d,  $^1J_{C-P} = 32.1$  Hz,  $CH-PPh_2 \cdot BH_3$ );  $^{31}P\{^1H\}$ -NMR (162 MHz,  $CDCl_3$ )  $\delta$  21.1 (bs,  $PPh_2 \cdot BH_3$ );  $^{11}B$ -NMR (128 MHz,  $CDCl_3$ )  $\delta$  -38.8 (bs,  $BH_3$ ); IR (neat,  $cm^{-1}$ )  $\nu$  3464 ( $O-H_{st}$ ), 2391 ( $B-H_{st}$ ); MS HR-ESI [found 431.1908;  $C_{24}H_{30}O_3PNa$  ( $M+Na$ ) $^+$  requires 431.1923];  $[\alpha]_D^{25} = -131.1$  ( $c = 1.00$  g/100 mL,  $CHCl_3$ ); M.p. 110.4-111.6  $^{\circ}C$ .

**(1*R*,2*S*)-3-(benzyloxy)-1-(diphenylphosphino borane)-1-phenylpropan-2-ol (118c).**

Phosphine-borane complex **118c** was obtained following the general procedure from epoxy ether **113c** (0.231 g, 0.96 mmol),  $KPPh_2$  (1.9 mL, 0.94



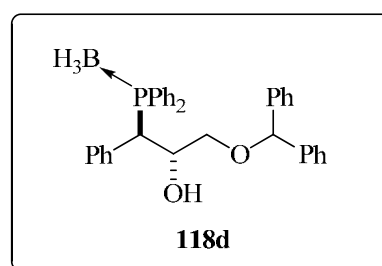
mmol) and  $BH_3 \cdot DMS$  complex (0.27 mL, 2.88 mmol) after column



chromatography through SiO<sub>2</sub> (hexanes/AcOEt 100:0/80:20) as a white solid (0.351 g, 83% yield). <sup>1</sup>H-NMR (400 MHz, CDCl<sub>3</sub>) δ 7.99-7.94 (m, 2H, *H*<sub>arom</sub>), 7.56-7.09 (m, 18H, *H*<sub>arom</sub>), 4.52 (m, 1H, *CH*-OH), 4.34 (d, <sup>2</sup>*J*<sub>H-H</sub> = 11.6 Hz, 1H, *CHH*-Ph), 4.30 (d, <sup>2</sup>*J*<sub>H-H</sub> = 11.6 Hz, 1H, *CHH*-Ph), 4.20 (dd, <sup>2</sup>*J*<sub>H-P</sub> = 17.2 Hz, <sup>3</sup>*J*<sub>H-H</sub> = 3.2 Hz, *CH*-PPh<sub>2</sub>·BH<sub>3</sub>), 3.33 (ddd, <sup>2</sup>*J*<sub>H-H</sub> = 9.4 Hz, <sup>3</sup>*J*<sub>H-H</sub> = 5.3 Hz, <sup>4</sup>*J*<sub>H-P</sub> = 1.9 Hz, 1H, *CHH*-O-CH<sub>2</sub>Ph), 3.22 (dd, <sup>2</sup>*J*<sub>H-H</sub> = 9.4 Hz, <sup>3</sup>*J*<sub>H-H</sub> = 7.6 Hz, 1H, *CHH*-O-CH<sub>2</sub>Ph), 1.80-0.78 (bs, 3H, BH<sub>3</sub>); <sup>13</sup>C{<sup>1</sup>H}-NMR (100 MHz, CDCl<sub>3</sub>) δ 138.1 (*C*<sub>q</sub> arom), 133.0 (d, *J*<sub>C-P</sub> = 8.7 Hz, *CH*<sub>arom</sub>), 133.0 (d, *J*<sub>C-P</sub> = 8.3 Hz, *CH*<sub>arom</sub>), 132.8 (*C*<sub>q</sub> arom), 131.7 (d, *J*<sub>C-P</sub> = 2.4 Hz, *CH*<sub>arom</sub>), 131.5 (d, *J*<sub>C-P</sub> = 4.9 Hz, *CH*<sub>arom</sub>), 131.0 (d, *J*<sub>C-P</sub> = 2.4 Hz, *CH*<sub>arom</sub>), 129.1 (d, *J*<sub>C-P</sub> = 9.8 Hz, *CH*<sub>arom</sub>), 128.7 (*C*<sub>q</sub> arom), 128.5 (*CH*<sub>arom</sub>), 128.2 (d, *J*<sub>C-P</sub> = 10.2 Hz, *CH*<sub>arom</sub>), 128.2 (*C*<sub>q</sub> arom), 128.1 (d, *J*<sub>C-P</sub> = 1.0 Hz, *CH*<sub>arom</sub>), 127.8 (*CH*<sub>arom</sub>), 127.7 (*CH*<sub>arom</sub>), 127.6 (*C*<sub>q</sub> arom), 127.5 (d, *J*<sub>C-P</sub> = 2.0 Hz, *CH*<sub>arom</sub>), 73.2 (*CH*<sub>2</sub>-Ph), 71.0 (d, <sup>3</sup>*J*<sub>C-P</sub> = 8.8 Hz, *CH*<sub>2</sub>-OCH<sub>2</sub>Ph), 69.2 (d, <sup>2</sup>*J*<sub>C-P</sub> = 5.4 Hz, *CH*-OH), 45.0 (d, <sup>1</sup>*J*<sub>C-P</sub> = 32.4 Hz, *CH*-PPh<sub>2</sub>·BH<sub>3</sub>); <sup>31</sup>P{<sup>1</sup>H}-NMR (162 MHz, CDCl<sub>3</sub>) δ 20.8 (bs, PPh<sub>2</sub>·BH<sub>3</sub>); <sup>11</sup>B-NMR (128 MHz, CDCl<sub>3</sub>) δ -39.0 (bs, BH<sub>3</sub>); IR (neat, cm<sup>-1</sup>) ν 3528 (O-H<sub>st</sub>), 2386 (B-H<sub>st</sub>); MS HR-ESI [found 463.1979; C<sub>28</sub>H<sub>30</sub>O<sub>2</sub>PBNa (M+Na)<sup>+</sup> requires 463.1974]; [α]<sub>D</sub><sup>25</sup> = -118 (c = 1.00 g/100 mL, CHCl<sub>3</sub>); M.p. 99.4-100.4 °C.

**(1*R*,2*S*)-3-(benzhydryloxy)-1-(diphenylphosphino borane)-1-phenylpropan-**

**2-ol (118d).** Phosphine-borane complex **118d** was obtained following the general procedure from epoxy ether **113d** (1.100 g, 3.48 mmol), KPPH<sub>2</sub>

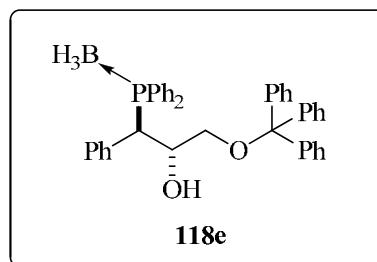


(6.8 mL, 3.41 mmol) and BH<sub>3</sub>·DMS complex (1.0 mL, 10.22 mmol) after column chromatography through SiO<sub>2</sub> (hexanes/AcOEt 100:0/80:20) as a white solid (1.120 g, 63% yield). <sup>1</sup>H-NMR (400 MHz, CDCl<sub>3</sub>) δ 7.98-7.94 (m, 2H, *H*<sub>arom</sub>), 7.56-7.06 (m, 23H, *H*<sub>arom</sub>), 5.17 (s, 1H, *CH*-Ph<sub>2</sub>), 4.54 (m, 1H, *CH*-OH), 4.28 (dd, <sup>2</sup>*J*<sub>H-P</sub> = 17.2 Hz, <sup>3</sup>*J*<sub>H-H</sub> = 1.6 Hz, 1H, *CH*-PPh<sub>2</sub>·BH<sub>3</sub>), 3.30 (ddd, <sup>2</sup>*J*<sub>H-H</sub> = 8.8 Hz, <sup>3</sup>*J*<sub>H-H</sub> = 5.2 Hz, <sup>4</sup>*J*<sub>H-P</sub> = 2.0 Hz, 1H, *CHH*-O-CHPh<sub>2</sub>), 3.16 (dd, <sup>2</sup>*J*<sub>H-H</sub> = <sup>3</sup>*J*<sub>H-H</sub> = 8.8 Hz,

$^1\text{H}$ ,  $\text{CHH-O-CHPh}_2$ ), 1.80-0.80 (bs, 3H,  $\text{BH}_3$ );  $^{13}\text{C}\{^1\text{H}\}$ -NMR (100 MHz,  $\text{CDCl}_3$ )  $\delta$  142.0 ( $\text{C}_q$  arom), 141.9 ( $\text{C}_q$  arom), 133.0 (d,  $J_{\text{C-P}} = 8.7$  Hz,  $\text{CH}_{\text{arom}}$ ), 133.0 (d,  $J_{\text{C-P}} = 8.5$  Hz,  $\text{CH}_{\text{arom}}$ ), 132.6 ( $\text{C}_q$  arom), 131.7 (d,  $J_{\text{C-P}} = 5.2$  Hz,  $\text{CH}_{\text{arom}}$ ), 131.6 (d,  $J_{\text{C-P}} = 3.0$  Hz,  $\text{CH}_{\text{arom}}$ ), 129.1 (d,  $J_{\text{C-P}} = 9.7$  Hz,  $\text{CH}_{\text{arom}}$ ), 128.9 ( $\text{C}_q$  arom), 128.5 (d,  $J_{\text{C-P}} = 6.1$  Hz,  $\text{CH}_{\text{arom}}$ ), 128.4 ( $\text{C}_q$  arom), 128.2 (d,  $J_{\text{C-P}} = 10.1$  Hz,  $\text{CH}_{\text{arom}}$ ), 128.0 ( $\text{CH}_{\text{arom}}$ ), 127.7 ( $\text{CH}_{\text{arom}}$ ), 127.6 ( $\text{CH}_{\text{arom}}$ ), 127.4 (d,  $J_{\text{C-P}} = 1.7$  Hz,  $\text{CH}_{\text{arom}}$ ), 127.2 ( $\text{CH}_{\text{arom}}$ ), 126.8 ( $\text{CH}_{\text{arom}}$ ), 84.0 ( $\text{CH-Ph}_2$ ), 69.4 (d,  $^3J_{\text{C-P}} = 9.2$  Hz,  $\text{CH}_2\text{-OCHPh}_2$ ), 69.2 (d,  $^2J_{\text{C-P}} = 5.4$  Hz,  $\text{CH-OH}$ ), 44.9 (d,  $^1J_{\text{C-P}} = 33.0$  Hz,  $\text{CH-PPh}_2\cdot\text{BH}_3$ );  $^{31}\text{P}\{^1\text{H}\}$ -NMR (162 MHz,  $\text{CDCl}_3$ )  $\delta$  20.9 (bs,  $\text{PPh}_2\cdot\text{BH}_3$ );  $^{11}\text{B}$ -NMR (128 MHz,  $\text{CDCl}_3$ )  $\delta$  -38.9 (bs,  $\text{BH}_3$ ); IR (neat,  $\text{cm}^{-1}$ )  $\nu$  3499 ( $\text{O-H}_{\text{st}}$ ), 2385 ( $\text{B-H}_{\text{st}}$ ); MS HR-ESI [found 539.2283;  $\text{C}_{34}\text{H}_{34}\text{O}_2\text{PBNa}$  ( $\text{M}+\text{Na}$ ) $^+$  requires 539.2287];  $[\alpha]_{\text{D}}^{25} = -87.8$  ( $c = 1.00$  g/100 mL,  $\text{CHCl}_3$ ); M.p. 53.6-54.8 °C.

**(1R,2S)-1-(diphenylphosphino borane)-1-phenyl-3-(trityloxy)propan-2-ol (118e).**

Phosphine-borane complex **118e** was obtained following the general procedure from epoxy ether **113e** (0.901 g, 2.30 mmol),  $\text{KPPh}_2$  (4.50 mL, 2.25

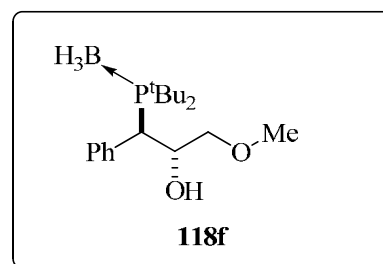


mmol) and  $\text{BH}_3\cdot\text{DMS}$  complex (0.65 mL, 6.89 mmol) after column chromatography through  $\text{SiO}_2$  (hexanes/ $\text{AcOEt}$  100:0/80:20) as a white solid (0.976 g, 72% yield).  $^1\text{H}$ -NMR (400 MHz,  $\text{CDCl}_3$ )  $\delta$  8.04-7.99 (m, 2H,  $H_{\text{arom}}$ ), 7.59-6.98 (m, 28H,  $H_{\text{arom}}$ ), 4.49 (m, 1H,  $\text{CH-OH}$ ), 4.33 (dd,  $^2J_{\text{H-P}} = 17.6$  Hz,  $^3J_{\text{H-H}} = 2.0$  Hz, 1H,  $\text{CH-PPh}_2\cdot\text{BH}_3$ ), 3.13 (ddd,  $^2J_{\text{H-H}} = 8.9$  Hz,  $^3J_{\text{H-H}} = 5.0$  Hz,  $^4J_{\text{H-P}} = 2.4$  Hz, 1H,  $\text{CHH-O-CPh}_3$ ), 2.74 (dd,  $^2J_{\text{H-H}} = 8.9$  Hz,  $^3J_{\text{H-H}} = 8.6$  Hz, 1H,  $\text{CHH-O-CPh}_3$ ), 1.80-0.81 (bs, 3H,  $\text{BH}_3$ );  $^{13}\text{C}\{^1\text{H}\}$ -NMR (100 MHz,  $\text{CDCl}_3$ )  $\delta$  143.8 ( $\text{C}_q$  arom), 133.1 (d,  $J_{\text{C-P}} = 8.7$  Hz,  $\text{CH}_{\text{arom}}$ ), 133.0 (d,  $J_{\text{C-P}} = 8.2$  Hz,  $\text{CH}_{\text{arom}}$ ), 132.4 ( $\text{C}_q$  arom), 131.7 (d,  $J_{\text{C-P}} = 3.4$  Hz,  $\text{CH}_{\text{arom}}$ ), 131.6 (d,  $J_{\text{C-P}} = 5.3$  Hz,  $\text{CH}_{\text{arom}}$ ), 131.0 (d,  $J_{\text{C-P}} = 1.7$  Hz,  $\text{CH}_{\text{arom}}$ ), 129.3 ( $\text{C}_q$  arom), 129.2 (d,  $J_{\text{C-P}} = 9.5$  Hz,  $\text{CH}_{\text{arom}}$ ), 128.7 ( $\text{CH}_{\text{arom}}$ ), 128.3 (d,  $J_{\text{C-P}} = 10.1$  Hz,  $\text{CH}_{\text{arom}}$ ), 128.1 ( $\text{C}_q$  arom), 128.0 ( $\text{CH}_{\text{arom}}$ ), 127.9 ( $\text{CH}_{\text{arom}}$ ), 127.3 (d,  $J_{\text{C-P}} = 2.4$  Hz,  $\text{CH}_{\text{arom}}$ ), 127.2 ( $\text{CH}_{\text{arom}}$ ), 87.1 ( $\text{C-Ph}_3$ ), 69.4 (d,

$^2J_{C-P} = 5.2$  Hz, CH-OH), 64.0 (d,  $^3J_{C-P} = 9.5$  Hz, CH<sub>2</sub>-O-CPh<sub>3</sub>), 45.2 (d,  $^1J_{C-P} = 33.2$  Hz, CH-PPh<sub>2</sub>·BH<sub>3</sub>);  $^{31}P\{^1H\}$ -NMR (162 MHz, CDCl<sub>3</sub>)  $\delta$  20.3 (bs, PPh<sub>2</sub>·BH<sub>3</sub>);  $^{11}B$ -NMR (128 MHz, CDCl<sub>3</sub>)  $\delta$  -38.8 (bs, BH<sub>3</sub>); IR (neat, cm<sup>-1</sup>)  $\nu$  3505 (O-H<sub>st</sub>), 2378 (B-H<sub>st</sub>); MS HR-ESI [found 615.2624; C<sub>40</sub>H<sub>38</sub>O<sub>2</sub>PBNa (M+Na)<sup>+</sup> requires 615.2600];  $[\alpha]_D^{25} = -83.7$  (c = 1.00 g/100 mL, CHCl<sub>3</sub>); M.p. 144.7-146.6 °C.

**(1R,2S)-1-(di-tert-butylphosphino borane)-3-methoxy-1-phenylpropan-2-ol (118f).**

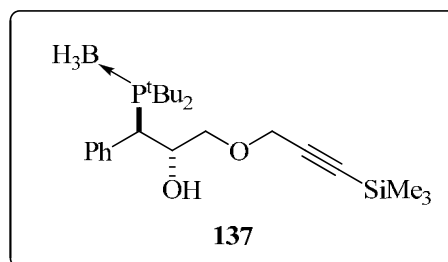
Phosphine-borane complex **118f** was obtained following the general procedure from epoxy ether **113a** (0.350 g, 2.13 mmol), LiP<sup>t</sup>Bu<sub>2</sub> prepared from HP<sup>t</sup>Bu<sub>2</sub> (0.38



g, 2.56 mmol) and *n*-BuLi (1.0 mL, 2.6M, 2.56 mmol), and BH<sub>3</sub>·DMS complex (0.65 mL, 6.39 mmol) after column chromatography through SiO<sub>2</sub> (hexanes/AcOEt 100:0/85:15) as a white solid (0.510 g, 74% yield).  $^1H$ -NMR (400 MHz, CDCl<sub>3</sub>)  $\delta$  7.28 (bs, 5H, *H*<sub>arom</sub>), 4.67 (m, 1H, CH-OH), 3.75 (bd,  $^2J_{H-P} = 15.6$  Hz, 1H, CH-<sup>t</sup>Bu<sub>2</sub>·BH<sub>3</sub>), 3.68 (d,  $^3J_{H-H} = 2.8$  Hz, 1H, OH), 3.21 (s, 3H, Me), 3.18 (m, 1H, CHH-OMe), 2.78 (dd,  $^2J_{H-H} = ^3J_{H-H} = 8.8$  Hz, 1H, CHH-OMe), 1.44 (d,  $^3J_{H-P} = 12.6$  Hz, 9H, <sup>t</sup>Bu<sub>2</sub>·BH<sub>3</sub>), 1.07 (d,  $^2J_{H-P} = 12.6$  Hz, 9H, <sup>t</sup>Bu<sub>2</sub>·BH<sub>3</sub>), 1.61-0.47 (bs, 3H, BH<sub>3</sub>);  $^{13}C\{^1H\}$ -NMR (100 MHz, CDCl<sub>3</sub>)  $\delta$  134.8 (d,  $J_{C-P} = 3.0$  Hz, C<sub>q</sub> arom), 132.7 (d,  $^3J_{C-P} = 3.7$  Hz, CH<sub>o</sub> arom), 127.9 (CH<sub>m</sub> arom), 127.7 (d,  $^3J_{C-P} = 1.2$  Hz, CH<sub>p</sub> arom), 73.2 (d,  $^3J_{C-P} = 9.0$  Hz, CH<sub>2</sub>-OMe), 70.9 (CH-OH), 59.1 (Me), 41.8 (d,  $^1J_{C-P} = 20.8$  Hz, CH-P<sup>t</sup>Bu<sub>2</sub>·BH<sub>3</sub>), 35.2 (d,  $^1J_{C-P} = 24.1$  Hz, C<sub>q</sub>, <sup>t</sup>Bu<sub>2</sub>·BH<sub>3</sub>), 35.1 (d,  $^1J_{C-P} = 22.9$  Hz, C<sub>q</sub>, <sup>t</sup>Bu<sub>2</sub>·BH<sub>3</sub>), 29.6 (3Me, <sup>t</sup>Bu<sub>2</sub>·BH<sub>3</sub>), 29.4 (3Me, <sup>t</sup>Bu<sub>2</sub>·BH<sub>3</sub>);  $^{31}P\{^1H\}$ -NMR (162 MHz, CDCl<sub>3</sub>)  $\delta$  51.6 (bs, P<sup>t</sup>Bu<sub>2</sub>·BH<sub>3</sub>);  $^{11}B$ -NMR (128 MHz, CDCl<sub>3</sub>)  $\delta$  -40.5 (bs, BH<sub>3</sub>); IR (neat, cm<sup>-1</sup>)  $\nu$  3480 (O-H<sub>st</sub>), 2390 (B-H<sub>st</sub>); MS HR-ESI [found 347.2295; C<sub>18</sub>H<sub>34</sub>O<sub>2</sub>PBNa (M+Na)<sup>+</sup> requires 347.2287];  $[\alpha]_D^{25} = -39.6$  (c = 1.02 g/100 mL, CHCl<sub>3</sub>); M.p. 103.2-106.0 °C.

**(1*R*,2*S*)-1-(di-*tert*-butylphosphino borane)-  
1-phenyl-3-(3-trimethylsilyl)prop-2-**

**nyloxy)propan-2-ol (137).** Phosphine-  
borane complex **137** was obtained following  
the general procedure from epoxy ether **136**



(0.434 g, 1.66 mmol),  $\text{LiP}^t\text{Bu}_2$  prepared from  $\text{HP}^t\text{Bu}_2$  (0.298 g, 2.00 mmol) and *n*-BuLi (0.8 mL, 2.6 M, 2.00 mmol), and  $\text{BH}_3\cdot\text{DMS}$  complex (0.46 mL, 4.88 mmol) after column chromatography through  $\text{SiO}_2$  (hexanes/AcOEt 100:0/85:15) as a colorless oil (0.103 g, 13% yield).  $^1\text{H-NMR}$  (400 MHz,  $\text{CDCl}_3$ )  $\delta$  7.29-7.26 (m, 5H,  $H_{\text{arom}}$ ), 4.70 (m, 1H,  $\text{CH-OH}$ ), 4.05 (d,  $^2J_{\text{H-H}} = 16.0$  Hz, 1H,  $\text{CHH-C}\equiv\text{C-SiMe}_3$ ), 3.98 (d,  $^2J_{\text{H-H}} = 16.0$  Hz, 1H,  $\text{CHH-C}\equiv\text{C-SiMe}_3$ ), 3.75 (bdd,  $^2J_{\text{H-P}} = 15.2$  Hz,  $^3J_{\text{H-H}} = 1.2$  Hz, 1H,  $\text{CH-P}^t\text{Bu}\cdot\text{BH}_3$ ), 3.70 (d,  $^3J_{\text{H-H}} = 3.2$  Hz, 1H,  $\text{OH}$ ), 3.35 (ddd,  $^2J_{\text{H-H}} = 8.9$  Hz,  $^3J_{\text{H-H}} = 4.9$  Hz,  $^4J_{\text{H-P}} = 2.1$  Hz, 1H,  $\text{CHH-O-CH}_2\text{-C}\equiv\text{C-SiMe}_3$ ), 2.91 (dd,  $^2J_{\text{H-H}} = ^3J_{\text{H-H}} = 8.9$  Hz, 1H,  $\text{CHH-O-CH}_2\text{-C}\equiv\text{C-SiMe}_3$ ), 1.44 (d,  $^3J_{\text{H-P}} = 12.4$  Hz, 9H,  ${}^t\text{Bu}_2\cdot\text{BH}_3$ ), 1.07 (d,  $^3J_{\text{H-P}} = 12.4$  Hz, 9H,  ${}^t\text{Bu}_2\cdot\text{BH}_3$ ), 1.54-0.42 (bs, 3H,  $\text{BH}_3$ ), 0.13 (s, 3H,  $\text{SiMe}_3$ ).  $^{13}\text{C}\{^1\text{H}\}\text{-NMR}$  (100 MHz,  $\text{CDCl}_3$ )  $\delta$  134.6 (d,  $J_{\text{C-P}} = 3.0$  Hz,  $\text{C}_q$  arom), 132.7 (d,  $^3J_{\text{C-P}} = 3.6$  Hz,  $\text{CH}_o$  arom), 127.9 ( $\text{CH}_m$  arom), 127.7 (d,  $^3J_{\text{C-P}} = 1.2$  Hz,  $\text{CH}_p$  arom), 101.2 ( $\text{C}_q$ ,  $\text{C}\equiv\text{C-SiMe}_3$ ), 91.7 ( $\text{C}_q$ ,  $\text{C}\equiv\text{C-SiMe}_3$ ), 70.9 (d,  $^2J_{\text{C-P}} = 1.1$  Hz,  $\text{CH-OH}$ ), 70.3 (d,  $^3J_{\text{C-P}} = 9.2$  Hz,  $\text{CH}_2\text{-O-CH}_2\text{-C}\equiv\text{C-SiMe}_3$ ), 59.3 ( $\text{CH}_2\text{-C}\equiv\text{C-SiMe}_3$ ), 41.8 (d,  $^1J_{\text{C-P}} = 20.8$  Hz,  $\text{CH-P}^t\text{Bu}_2\cdot\text{BH}_3$ ), 35.2 (d,  $^1J_{\text{C-P}} = 23.6$  Hz,  $\text{C}_q$ ,  ${}^t\text{Bu}_2\cdot\text{BH}_3$ ), 35.1 (d,  $^1J_{\text{C-P}} = 23.6$  Hz,  $\text{C}_q$ ,  ${}^t\text{Bu}_2\cdot\text{BH}_3$ ), 29.6 (3Me,  ${}^t\text{Bu}_2\cdot\text{BH}_3$ ), 29.4 (3Me,  ${}^t\text{Bu}_2\cdot\text{BH}_3$ ), -0.1 (3Me,  $\text{SiMe}_3$ );  $^{31}\text{P}\{^1\text{H}\}\text{-NMR}$  (162 MHz,  $\text{CDCl}_3$ )  $\delta$  51.7 (bs,  $\text{P}^t\text{Bu}_2\cdot\text{BH}_3$ );  $^{11}\text{B-NMR}$  (128 MHz,  $\text{CDCl}_3$ )  $\delta$  -40.5 (bs,  $\text{BH}_3$ ); IR (neat,  $\text{cm}^{-1}$ )  $\nu$  3484 ( $\text{O-H}_{\text{st}}$ ), 2382 ( $\text{B-H}_{\text{st}}$ ); MS HR-ESI [found 443.2687;  $\text{C}_{23}\text{H}_{42}\text{O}_2\text{PBSiNa}$  ( $\text{M}+\text{Na}$ ) $^+$  requires 443.2682];  $[\alpha]_{\text{D}}^{25} = -29.6$  ( $c = 0.54$  g/100 mL,  $\text{CHCl}_3$ ).

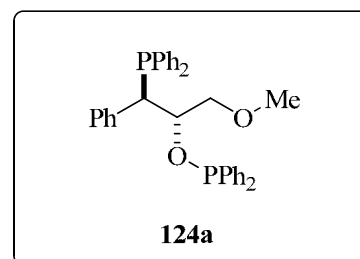
### 1.3.4. General synthetic procedure of phosphine-phosphinite ligands **124a-d**

The phosphine-borane complexes (**118**, 1.00 mmol) and diazabicyclo[2.2.2]octane (2.20 mmol) were charged in a flame-dried schlenk flask. Toluene (5.0 mL) was added. The reaction mixture was heated at 60 °C for 2h. After cooling down to room temperature, the solution was passed through a short SiO<sub>2</sub> pad (3.0 g) and further eluted with toluene (6.0 mL). Toluene was removed *in vacuo* to give the corresponding phosphino-alcohol as white solid. DMAP (0.16 mmol) and THF (12.0 mL) were added under Ar to the phosphino-alcohol and the solution was cooled at 0°C. NEt<sub>3</sub> (1.10 mmol) and chlorodiphenylphosphine (1.10 mmol) were added dropwise to the phosphino alcohol-containing solution. The mixture was stirred at 0°C for 1h. The solvent was removed *in vacuo*. The resulting residue was dissolved in diethyl ether (10.0 mL) and passed through a short pad of alumina (3.0 g) which was further eluted with diethyl ether (20.0 mL). Solvent evaporation yielded the corresponding phosphine phosphinite ligands.

#### 1.3.4.1. Synthesis and general physical and spectroscopic data of phosphine-phosphinite ligands **124a-d**

##### ((**1R,2S**)-1-(diphenylphosphino)-3-methoxy-1-phenylpropan-2-yl)oxy)diphenylphosphine (**124a**).

Phosphine-phosphinite **124a** was obtained following the general procedure, starting from **118a** (0.125 g, 0.34 mmol), DABCO (0.084 g, 0.75 mmol), DMAP



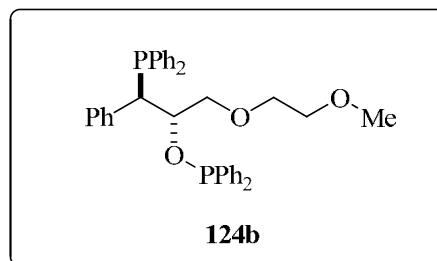
(7 mg, 0.05 mmol), NEt<sub>3</sub> (52 μL, 0.37 mmol) and ClPPh<sub>2</sub> (68 μL, 0.37 mmol) as a white solid (0.110 g, 61% yield). <sup>1</sup>H-NMR (500 MHz, CDCl<sub>3</sub>) δ 7.66-7.09 (m, 25H, *H*<sub>arom</sub>), 4.25 (m, 1H, CH-OPPh<sub>2</sub>), 3.95 (bdd, <sup>2</sup>*J*<sub>H-P</sub> = <sup>3</sup>*J*<sub>H-H</sub> = 4.0 Hz, 1H, CH-PPh<sub>2</sub>), 3.14 (dd, <sup>2</sup>*J*<sub>H-H</sub> = 9.5 Hz, <sup>3</sup>*J*<sub>H-H</sub> = 6.5 Hz, 1H, CHH-OMe), 3.08 (dd, <sup>2</sup>*J*<sub>H-H</sub> = 9.5 Hz, <sup>3</sup>*J*<sub>H-H</sub> = 6.0 Hz, 1H, CHH-OMe), 2.93 (s, 3H, Me); <sup>13</sup>C{<sup>1</sup>H}-NMR (125

MHz, CDCl<sub>3</sub>)  $\delta$  143.9 (d,  $J_{C-P}$  = 19.5 Hz,  $C_{q\text{ arom}}$ ), 142.8 (d,  $J_{C-P}$  = 14.5 Hz,  $C_{q\text{ arom}}$ ), 137.6 (d,  $J_{C-P}$  = 10.9 Hz,  $C_{q\text{ arom}}$ ), 137.5 (d,  $J_{C-P}$  = 15.8 Hz,  $C_{q\text{ arom}}$ ), 133.1 (d,  $J_{C-P}$  = 18.6 Hz,  $CH_{\text{arom}}$ ), 131.2 (d,  $J_{C-P}$  = 8.4 Hz,  $CH_{\text{arom}}$ ), 130.7 (d,  $J_{C-P}$  = 3.1 Hz,  $CH_{\text{arom}}$ ), 130.5 (d,  $J_{C-P}$  = 3.4 Hz,  $CH_{\text{arom}}$ ), 130.0 (d,  $J_{C-P}$  = 22.4 Hz,  $CH_{\text{arom}}$ ), 129.4 ( $CH_{\text{arom}}$ ), 128.9 (d,  $J_{C-P}$  = 17.5 Hz,  $CH_{\text{arom}}$ ), 128.6 (d,  $J_{C-P}$  = 7.6 Hz,  $CH_{\text{arom}}$ ), 128.2 ( $CH_{\text{arom}}$ ), 128.1 ( $CH_{\text{arom}}$ ), 128.0 (d,  $J_{C-P}$  = 2.6 Hz,  $CH_{\text{arom}}$ ), 127.9 ( $CH_{\text{arom}}$ ), 127.8 (d,  $J_{C-P}$  = 6.4 Hz,  $CH_{\text{arom}}$ ), 126.6 ( $CH_{\text{arom}}$ ), 78.7 (dd,  $^2J_{C-P}$  = 18.4 Hz,  $^2J_{C-P}$  = 12.8 Hz  $CH-OPPh_2$ ), 73.9 (dd,  $^3J_{C-P}$  =  $^3J_{C-P}$  = 3.6 Hz,  $CH_2-OMe$ ), 58.3 (*Me*), 48.6 (dd,  $^1J_{C-P}$  = 14.5 Hz,  $^3J_{C-P}$  = 7.4 Hz,  $CH-PPh_2$ );  $^{31}P\{^1H\}$ -NMR (202 MHz, CDCl<sub>3</sub>)  $\delta$  116.5 (bs, *P-O*), -5.9 (bs, *P-C*). MS HR-ESI [found 535.1930; C<sub>34</sub>H<sub>33</sub>O<sub>2</sub>P<sub>2</sub> (M+H)<sup>+</sup> requires 535.1936];  $[\alpha]_D^{26}$  = -127.4 (c = 1.02 g/100 mL, THF); M.p. 89.7-92.2 °C.

**(S)-3-((R)-**

**(diphenylphosphino)(phenyl)methyl)-1,1-diphenyl-2,5,8-trioxa-1-phosphanone**

**(124b)**. Phosphine-phosphinite **124b** was obtained following the general procedure,

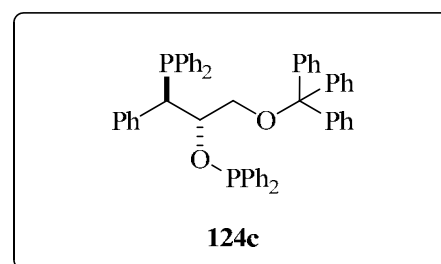


starting from **118b** (0.159 g, 0.39 mmol), DABCO (0.096 g, 0.86 mmol), DMAP (8 mg, 0.06 mmol), NEt<sub>3</sub> (61  $\mu$ L, 0.43 mmol) and ClPPh<sub>2</sub> (79  $\mu$ L, 0.43 mmol) as a colorless oil (0.191 g, 84% yield).  $^1H$ -NMR (500 MHz, CDCl<sub>3</sub>)  $\delta$  7.68-7.09 (m, 25H,  $H_{\text{arom}}$ ), 4.31 (m, 1H,  $CH-OPPh_2$ ), 3.96 (dd,  $^2J_{H-P}$  =  $^3J_{H-H}$  = 4.0 Hz, 1H,  $CH-PPh_2$ ), 3.30 (s, 3H, *Me*), 3.27-3.18 (m, 5H,  $CHH-O-(CH_2)_2-OMe$  and  $CH_2-CH_2-OMe$ ), 3.08 (m, 1H,  $CHH-O-(CH_2)_2-OMe$ );  $^{13}C\{^1H\}$ -NMR (125 MHz, CDCl<sub>3</sub>)  $\delta$  144.0 (d,  $J_{C-P}$  = 19.8 Hz,  $C_{q\text{ arom}}$ ), 142.9 (d,  $J_{C-P}$  = 14.6 Hz,  $C_{q\text{ arom}}$ ), 137.6 (d,  $J_{C-P}$  = 11.0 Hz,  $C_{q\text{ arom}}$ ), 137.6 (d,  $J_{C-P}$  = 16.1 Hz,  $C_{q\text{ arom}}$ ), 136.2 (d,  $J_{C-P}$  = 17.2 Hz,  $C_{q\text{ arom}}$ ), 134.7 (d,  $J_{C-P}$  = 21.2 Hz,  $CH_{\text{arom}}$ ), 133.1 (d,  $J_{C-P}$  = 18.6 Hz,  $CH_{\text{arom}}$ ), 131.3 (d,  $J_{C-P}$  = 8.4 Hz,  $CH_{\text{arom}}$ ), 130.7 (d,  $J_{C-P}$  = 3.1 Hz,  $CH_{\text{arom}}$ ), 130.6 (d,  $J_{C-P}$  = 3.0 Hz,  $CH_{\text{arom}}$ ), 129.9 (d,  $J_{C-P}$  = 22.1 Hz,  $CH_{\text{arom}}$ ), 129.4 ( $CH_{\text{arom}}$ ), 128.9 (d,  $J_{C-P}$  = 24.8 Hz,  $CH_{\text{arom}}$ ), 128.6 (d,  $J_{C-P}$  = 7.5 Hz,  $CH_{\text{arom}}$ ), 128.1 ( $CH_{\text{arom}}$ ), 128.0 ( $CH_{\text{arom}}$ ), 127.9 (d,  $J_{C-P}$  = 16.9 Hz,  $CH_{\text{arom}}$ ), 127.7 (d,  $J_{C-P}$  = 6.4 Hz,  $CH_{\text{arom}}$ ), 126.6 (d,  $J_{C-P}$  =

2.1 Hz,  $\text{CH}_{\text{arom}}$ ), 78.7 (dd,  $^2J_{\text{C-P}} = 18.8$  Hz,  $^2J_{\text{C-P}} = 12.2$  Hz  $\text{CH-OPPh}_2$ ), 72.7 (dd,  $^3J_{\text{C-P}} = ^3J_{\text{C-P}} = 3.6$  Hz,  $\text{CH}_2\text{-OCH}_2\text{CH}_2\text{Me}$ ), 71.5 ( $\text{CH}_2\text{-CH}_2\text{-Me}$ ), 70.1 ( $\text{CH}_2\text{-CH}_2\text{-Me}$ ), 58.9 (*Me*), 48.6 (dd,  $^1J_{\text{C-P}} = 14.6$  Hz,  $^3J_{\text{C-P}} = 7.3$  Hz,  $\text{CH-PPh}_2$ );  $^{31}\text{P}\{^1\text{H}\}$ -NMR (202 MHz,  $\text{CDCl}_3$ )  $\delta$  116.1 (d,  $^4J_{\text{P-P}} = 4.8$  Hz, *P-O*), -6.0 (d,  $^4J_{\text{P-P}} = 4.8$  Hz, *P-C*); MS HR-ESI [found 579.2201;  $\text{C}_{36}\text{H}_{37}\text{O}_3\text{P}_2$  ( $\text{M}+\text{H}$ ) $^+$  requires 579.2218];  $[\alpha]_{\text{D}}^{25} = -130.7$  ( $c = 0.99$  g/100 mL, THF).

**((1*R*,2*S*)-1-(diphenylphosphino)-1-phenyl-3-(trityloxy)propan-2-**

**oxy)diphenylphosphine (124c).** Phosphine-phosphinite **124c** was obtained following the general procedure, starting from **118e** (0.284 g,



0.48 mmol), DABCO (0.118 g, 1.06 mmol), DMAP (9 mg, 0.08 mmol),  $\text{NEt}_3$  (74  $\mu\text{L}$ , 0.53 mmol) and  $\text{ClPPh}_2$  (97  $\mu\text{L}$ , 0.53 mmol) as a white solid (0.276 g, 75% yield).  $^1\text{H}$ -NMR (500 MHz,  $\text{CDCl}_3$ )  $\delta$  7.65-7.10 (m, 40H,  $H_{\text{arom}}$ ), 4.39 (m, 1H,  $\text{CH-OPPh}_2$ ), 4.11 (dd,  $^2J_{\text{H-P}} = ^3J_{\text{H-H}} = 3.8$  Hz, 1H,  $\text{CH-PPh}_2$ ), 3.06 (bdd,  $^2J_{\text{H-H}} = 9.2$  Hz,  $^3J_{\text{H-H}} = 5.8$  Hz, 1H,  $\text{CHH-OCPh}_3$ ), 2.86 (dd,  $^2J_{\text{H-H}} = 9.2$  Hz,  $^3J_{\text{H-H}} = 7.8$  Hz, 1H,  $\text{CHH-OCPh}_3$ );  $^{13}\text{C}\{^1\text{H}\}$ -NMR (125 MHz,  $\text{CDCl}_3$ )  $\delta$  143.91 ( $C_{\text{q arom}}$ ), 143.38 (d,  $J_{\text{C-P}} = 19.8$  Hz,  $C_{\text{q arom}}$ ), 142.50 (d,  $J_{\text{C-P}} = 15.4$  Hz,  $C_{\text{q arom}}$ ), 137.74 (d,  $J_{\text{C-P}} = 15.8$  Hz,  $C_{\text{q arom}}$ ), 137.15 (d,  $J_{\text{C-P}} = 10.0$  Hz,  $C_{\text{q arom}}$ ), 137.07 (d,  $J_{\text{C-P}} = 16.5$  Hz,  $C_{\text{q arom}}$ ), 134.86 (d,  $J_{\text{C-P}} = 21.2$  Hz,  $\text{CH}_{\text{arom}}$ ), 133.23 (d,  $J_{\text{C-P}} = 18.5$  Hz,  $\text{CH}_{\text{arom}}$ ), 131.38 (d,  $J_{\text{C-P}} = 8.5$  Hz,  $\text{CH}_{\text{arom}}$ ), 131.15 (d,  $J_{\text{C-P}} = 2.0$  Hz,  $\text{CH}_{\text{arom}}$ ), 130.98 (d,  $J_{\text{C-P}} = 1.9$  Hz,  $\text{CH}_{\text{arom}}$ ), 130.43 (d,  $J_{\text{C-P}} = 22.1$  Hz,  $\text{CH}_{\text{arom}}$ ), 129.50 ( $\text{CH}_{\text{arom}}$ ), 129.11 ( $\text{CH}_{\text{arom}}$ ), 128.87 ( $\text{CH}_{\text{arom}}$ ), 128.74 ( $\text{CH}_{\text{arom}}$ ), 128.70 ( $\text{CH}_{\text{arom}}$ ), 128.14 ( $\text{CH}_{\text{arom}}$ ), 128.09 ( $\text{CH}_{\text{arom}}$ ), 128.05 ( $\text{CH}_{\text{arom}}$ ), 128.04 ( $\text{CH}_{\text{arom}}$ ), 127.98 ( $\text{CH}_{\text{arom}}$ ), 127.89 ( $\text{CH}_{\text{arom}}$ ), 127.84 ( $\text{CH}_{\text{arom}}$ ), 127.79 ( $\text{CH}_{\text{arom}}$ ), 127.76 ( $\text{CH}_{\text{arom}}$ ), 126.94 ( $\text{CH}_{\text{arom}}$ ), 126.48 ( $\text{CH}_{\text{arom}}$ ), 87.18 ( $\text{C-Ph}_3$ ), 79.52 (dd,  $^2J_{\text{C-P}} = 19.1$  Hz,  $^2J_{\text{C-P}} = 14.9$  Hz  $\text{CH-OPPh}_2$ ), 64.74 (dd,  $^3J_{\text{C-P}} = ^3J_{\text{C-P}} = 5.1$  Hz,  $\text{CH}_2\text{-OCPh}_3$ ), 48.68 (dd,  $^1J_{\text{C-P}} = 14.4$  Hz,  $^3J_{\text{C-P}} = 6.3$  Hz,  $\text{CH-PPh}_2$ );  $^{31}\text{P}\{^1\text{H}\}$ -NMR (202 MHz,  $\text{CDCl}_3$ )  $\delta$  117.37 (d,  $^4J_{\text{P-P}} = 9.6$  Hz, *P-O*), -7.74 (d,  $^4J_{\text{P-P}} = 9.6$  Hz, *P-C*); MS HR-ESI [found 763.2894;  $\text{C}_{52}\text{H}_{44}\text{O}_2\text{P}_2$

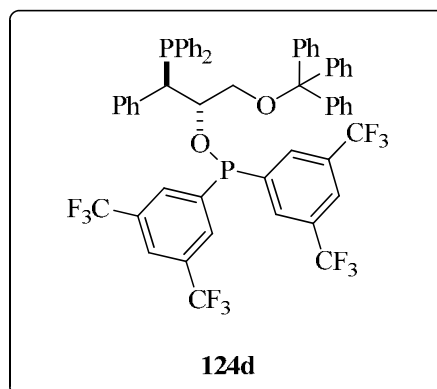
(M+H)<sup>+</sup> requires 763.2895];  $[\alpha]_D^{25} = -90.6$  (c= 0.53 g/100 mL, THF); M.p. 88.3-94.3 °C.

**((1R,2S)-2-**

**bis(frufuoromethyl)phenyl)phosphinoxy)-  
1-phenyl-3-**

**(trytyloxy)propyl)diphenylphosphine**

**(124d)**. Phosphine-phosphinite **124d** was obtained following the general procedure, starting from **118e** (0.160 g, 0.27 mmol), DABCO (0.066 g, 0.59 mmol), DMAP (5 mg,



0.04 mmol), NEt<sub>3</sub> (42 μL, 0.30 mmol) and chlorophosphine ClPAr<sub>2</sub> **134** (0.328 g,

0.30 mmol) as a white solid (0.106 g, 37% yield). <sup>1</sup>H-NMR (400 MHz, CDCl<sub>3</sub>) δ 7.85-7.67 (m, 5H, H<sub>arom</sub>), 7.46-6.89 (m, 31H, H<sub>arom</sub>), 4.65 (m, 1H, CH-OPAr<sub>2</sub>), 3.84 (dd, <sup>2</sup>J<sub>H-P</sub>= <sup>3</sup>J<sub>H-H</sub>= 5.0 Hz, 1H, CH-PPh<sub>2</sub>), 3.16 (dd, <sup>2</sup>J<sub>H-H</sub>= 9.9 Hz, <sup>3</sup>J<sub>H-H</sub>= 4.0 Hz, 1H, CHH-OCPh<sub>3</sub>), 2.74 (dd, <sup>2</sup>J<sub>H-H</sub>= 9.9 Hz, <sup>3</sup>J<sub>H-H</sub>= 8.4 Hz, 1H, CHH-OCPh<sub>3</sub>); <sup>13</sup>C{<sup>1</sup>H}-NMR (100 MHz, CDCl<sub>3</sub>) δ 146.1 (d, J<sub>C-P</sub>= 19.4 Hz, CH<sub>arom</sub>), 145.2 (d, J<sub>C-P</sub>= 17.9 Hz, C<sub>q</sub> arom), 143.4 (C<sub>q</sub> arom), 136.6 (d, J<sub>C-P</sub>= 6.0 Hz, C<sub>q</sub> arom), 136.3 (d, J<sub>C-P</sub>= 12.0 Hz, C<sub>q</sub> arom), 136.0 (d, J<sub>C-P</sub>= 10.8 Hz, C<sub>q</sub> arom), 134.2 (d, J<sub>C-P</sub>= 17.3 Hz, CH<sub>arom</sub>), 133.5 (d, J<sub>C-P</sub>= 15.5 Hz, CH<sub>arom</sub>), 131.7 (d, <sup>2</sup>J<sub>C-F</sub>= 26.3 Hz, C<sub>q</sub> arom), 131.6 (d, <sup>2</sup>J<sub>C-F</sub>= 26.5 Hz, C<sub>q</sub> arom), 131.6 (d, <sup>2</sup>J<sub>C-F</sub>= 26.3 Hz, C<sub>q</sub> arom), 131.5 (d, <sup>2</sup>J<sub>C-F</sub>= 26.1 Hz, C<sub>q</sub> arom), 130.2 (CH<sub>arom</sub>), 130.1 (CH<sub>arom</sub>), 130.0 (CH<sub>arom</sub>), 129.9 (CH<sub>arom</sub>), 129.8 (CH<sub>arom</sub>), 129.1 (CH<sub>arom</sub>), 129.0 (CH<sub>arom</sub>), 128.9 (d, J<sub>C-P</sub>= 6.4 Hz, CH<sub>arom</sub>), 128.5 (CH<sub>arom</sub>), 128.4 (CH<sub>arom</sub>), 128.2 (CH<sub>arom</sub>), 127.9 (d, J<sub>C-P</sub>= 5.8 Hz, CH<sub>arom</sub>), 127.8 (CH<sub>arom</sub>), 127.1 (CH<sub>arom</sub>), 126.9 (CH<sub>arom</sub>), 123.5 (CH<sub>arom</sub>), 123.4 (CH<sub>arom</sub>), 123.3 (d, <sup>1</sup>J<sub>C-F</sub>= 217.0 Hz, 2C<sub>q</sub> arom, CF<sub>3</sub>), 123.1 (d, <sup>1</sup>J<sub>C-F</sub>= 217.0 Hz, 2C<sub>q</sub> arom, CF<sub>3</sub>), 87.8 (C-Ph<sub>3</sub>), 83.7 (dd, <sup>2</sup>J<sub>C-P</sub>= 18.4 Hz, <sup>2</sup>J<sub>C-P</sub>= 15.8 Hz CH-OPAr<sub>2</sub>), 66.8 (CH<sub>2</sub>-OCPh<sub>3</sub>), 48.8 (dd, <sup>1</sup>J<sub>C-P</sub>= 13.0 Hz, <sup>3</sup>J<sub>C-P</sub>= 4.4 Hz, CH-PPh<sub>2</sub>); <sup>31</sup>P{<sup>1</sup>H}-NMR (162 MHz, CDCl<sub>3</sub>) δ 107.0 (d, <sup>4</sup>J<sub>P-P</sub>= 3.6 Hz, P-O), -7.1 (bs, P-C); MS HR-ESI



[found 1035.2404;  $C_{56}H_{41}O_2P_2F_{12}$  (M+H)<sup>+</sup> requires 1035.2390];  $[\alpha]_D^{25} = -81.4$  (c = 0.49 g/100 mL, THF); M.p 119.7-124.0 °C.

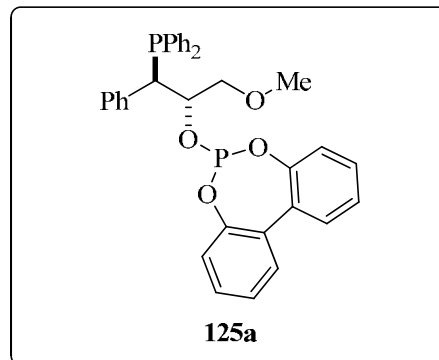
### 1.3.5. General synthetic procedure of phosphine-phosphite ligands 125a-k

The phosphine-borane complexes (**118**, 1.00 mmol) and diazabicyclo[2.2.2]octane (2.2 mmol) were charged in a flame-dried schlenk flask. Toluene (5.0 mL) was added. The reaction mixture was heated at 60 °C for 2 h. After cooling down to room temperature, the solution was passed through a short SiO<sub>2</sub> pad (3.0 g) and further eluted with toluene (6.0 mL). The corresponding phosphino-alcohol solution was immediately used in the following step. This solution was added dropwise via cannula to a solution of the appropriate chlorophosphite (1.10 mmol) and NEt<sub>3</sub> (2.00 mmol) in toluene (17.0 mL). The mixture was stirred for 16 h at room temperature. The reaction mixture was filtered through celite and the filtrate was evaporated *in vacuo*. The resulting residue was dissolved in diethyl ether (20.0 mL) and passed through a short pad of alumina (3.0 g). Solvent evaporation yielded the corresponding phosphine-phosphite ligands.

### 1.3.5.1. Synthesis and general physical and spectroscopic data of phosphine-phosphite ligands **125a-k**

#### 6-((1*R*,2*S*)-1-(diphenylphosphino)-3-methoxy-1-phenylpropen-2-yloxy)dibenzo[*d,f*][1,3,2]dioxaphosphepine (**125a**).

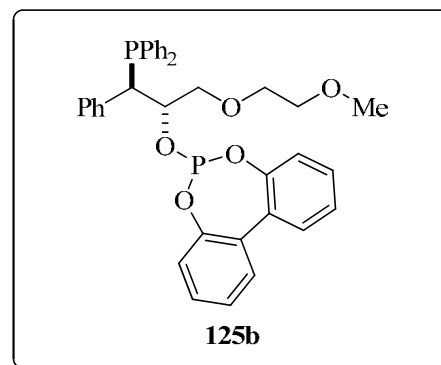
Phosphine-phosphite **125a** was obtained following the general procedure, starting from **118a** (0.499 g, 1.37 mmol), DABCO (0.338 g, 3.01 mmol), NEt<sub>3</sub> (0.4 mL,



2.76 mmol) and the chlorophosphite derived from biphenyl-2,2'-diol **127** (0.378 g, 1.51 mmol) as a white solid (0.514 g, 66% yield). <sup>1</sup>H-NMR (500 MHz, CDCl<sub>3</sub>) δ 7.81-7.77 (m, 2H, *H*<sub>arom</sub>), 7.54-7.09 (m, 20H, *H*<sub>arom</sub>), 7.00-6.98 (m, 1H, *H*<sub>arom</sub>), 4.50 (m, 1H, CH-OPO<sub>2</sub>), 3.80 (dd, <sup>2</sup>*J*<sub>H-P</sub> = 4.5 Hz, <sup>3</sup>*J*<sub>H-H</sub> = 3.5 Hz, 1H, CH-PPh<sub>2</sub>), 3.25 (dd, <sup>2</sup>*J*<sub>H-H</sub> = 9.6 Hz, <sup>3</sup>*J*<sub>H-H</sub> = 5.2 Hz, 1H, CHH-OMe), 3.22 (s, 3H, *Me*), 3.07 (dd, <sup>2</sup>*J*<sub>H-H</sub> = 9.6 Hz, <sup>3</sup>*J*<sub>H-H</sub> = 7.0 Hz, 1H, CHH-OMe); <sup>13</sup>C{<sup>1</sup>H}-NMR (125 MHz, CDCl<sub>3</sub>) δ 150.1 (d, *J*<sub>C-P</sub> = 5.5 Hz, *C*<sub>q</sub> arom), 149.6 (d, *J*<sub>C-P</sub> = 4.8 Hz, *C*<sub>q</sub> arom), 137.0 (d, *J*<sub>C-P</sub> = 15.8 Hz, *C*<sub>q</sub> arom), 136.9 (d, *J*<sub>C-P</sub> = 11.2 Hz, *C*<sub>q</sub> arom), 136.0 (d, *J*<sub>C-P</sub> = 17.4 Hz, *C*<sub>q</sub> arom), 135.0 (d, *J*<sub>C-P</sub> = 21.6 Hz, CH<sub>arom</sub>), 133.2 (d, *J*<sub>C-P</sub> = 18.6 Hz, CH<sub>arom</sub>), 131.8 (d, *J*<sub>C-P</sub> = 2.9 Hz, *C*<sub>q</sub> arom), 131.4 (d, *J*<sub>C-P</sub> = 2.9 Hz, *C*<sub>q</sub> arom), 131.1 (d, *J*<sub>C-P</sub> = 8.1 Hz, CH<sub>arom</sub>), 129.9 (d, *J*<sub>C-P</sub> = 17.0 Hz, CH<sub>arom</sub>), 129.8 (CH<sub>arom</sub>), 129.0 (CH<sub>arom</sub>), 128.9 (d, *J*<sub>C-P</sub> = 10.1 Hz, CH<sub>arom</sub>), 128.3 (CH<sub>arom</sub>), 128.1 (CH<sub>arom</sub>), 128.0 (d, *J*<sub>C-P</sub> = 10.1 Hz, CH<sub>arom</sub>), 126.9 (CH<sub>arom</sub>), 125.0 (CH<sub>arom</sub>), 122.9 (d, *J*<sub>C-P</sub> = 3.6 Hz, CH<sub>arom</sub>), 122.3 (CH<sub>arom</sub>), 74.5 (bs, CH<sub>2</sub>-OMe), 74.4 (dd, <sup>2</sup>*J*<sub>C-P</sub> = 16.6 Hz, <sup>2</sup>*J*<sub>C-P</sub> = 12.3 Hz, CH-OPO<sub>2</sub>), 58.9 (*Me*), 48.1 (dd, <sup>1</sup>*J*<sub>C-P</sub> = 14.8 Hz, <sup>3</sup>*J*<sub>C-P</sub> = 6.1 Hz, CH-PPh<sub>2</sub>); <sup>31</sup>P{<sup>1</sup>H}-NMR (202 MHz, CDCl<sub>3</sub>) δ 155.2 (d, <sup>4</sup>*J*<sub>P-P</sub> = 7.5 Hz, P-O), -5.2 (d, <sup>4</sup>*J*<sub>P-P</sub> = 7.5 Hz, P-C); MS HR-ESI [found 587.1533; C<sub>34</sub>H<sub>30</sub>O<sub>4</sub>P<sub>2</sub>Na (M+Na)<sup>+</sup> requires 587.1517]; [*α*]<sub>D</sub><sup>25</sup> = -135.2 (c = 1.00 g/100 mL, THF); M.p. 138.0-143.3 °C.

**6-((1*R*,2*S*)-1-(diphenylphosphino)-3-(2-methoxyethoxy)-1-phenylpropen-2-yloxy)dibenzo[*d,f*][1,3,2]dioxaphosphepine**

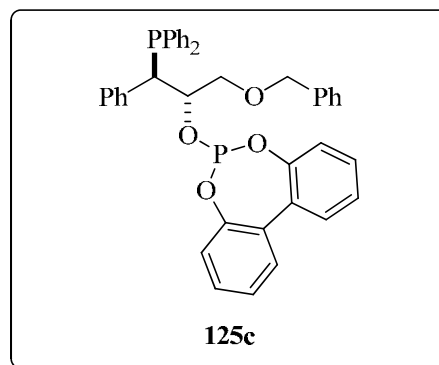
**(125b).** Phosphine-phosphite **125b** was obtained following the general procedure, starting from **118b** (0.122 g, 0.30 mmol), DABCO (0.074 g, 0.66 mmol), NEt<sub>3</sub> (84 μL,



0.60 mmol) and the chlorophosphite derived from biphenyl-2,2'-diol **127** (0.083 g, 0.33 mmol) as a colorless oil (0.099 g, 54% yield). <sup>1</sup>H-NMR (500 MHz, CDCl<sub>3</sub>) δ 7.80-7.76 (m, 2H, *H*<sub>arom</sub>), 7.58-7.56 (m, 1H, *H*<sub>arom</sub>), 7.49-7.08 (m, 19H, *H*<sub>arom</sub>), 7.00-6.98 (m, 1H, *H*<sub>arom</sub>), 4.55 (m, 1H, CH-OPO<sub>2</sub>), 3.78 (dd, <sup>2</sup>*J*<sub>H-P</sub> = 5.0 Hz, <sup>3</sup>*J*<sub>H-H</sub> = 3.5 Hz, 1H, CH-PPh<sub>2</sub>), 3.55-3.42 (m, 4H, O-CH<sub>2</sub>CH<sub>2</sub>-OMe), 3.38 (dd, <sup>2</sup>*J*<sub>H-H</sub> = 9.9 Hz, <sup>3</sup>*J*<sub>H-H</sub> = 5.0 Hz, 1H, CHH-O(CH<sub>2</sub>)<sub>2</sub>-OMe), 3.35 (s, 3H, *Me*), 3.11 (dd, <sup>2</sup>*J*<sub>H-H</sub> = 9.9 Hz, <sup>3</sup>*J*<sub>H-H</sub> = 7.8 Hz, 1H, CHH-O(CH<sub>2</sub>)<sub>2</sub>-OMe); <sup>13</sup>C{<sup>1</sup>H}-NMR (125 MHz, CDCl<sub>3</sub>) δ 150.1 (d, *J*<sub>C-P</sub> = 5.2 Hz, *C*<sub>q</sub> arom), 149.7 (d, *J*<sub>C-P</sub> = 4.6 Hz, *C*<sub>q</sub> arom), 137.1 (d, *J*<sub>C-P</sub> = 15.4 Hz, *C*<sub>q</sub> arom), 137.0 (d, *J*<sub>C-P</sub> = 11.0 Hz, *C*<sub>q</sub> arom), 136.0 (d, *J*<sub>C-P</sub> = 17.6 Hz, *C*<sub>q</sub> arom), 135.1 (d, *J*<sub>C-P</sub> = 21.8 Hz, CH<sub>arom</sub>), 133.2 (d, *J*<sub>C-P</sub> = 18.5 Hz, CH<sub>arom</sub>), 131.9 (d, *J*<sub>C-P</sub> = 3.5 Hz, *C*<sub>q</sub> arom), 131.4 (d, *J*<sub>C-P</sub> = 2.8 Hz, *C*<sub>q</sub> arom), 131.1 (d, *J*<sub>C-P</sub> = 8.0 Hz, CH<sub>arom</sub>), 129.9 (d, *J*<sub>C-P</sub> = 13.1 Hz, CH<sub>arom</sub>), 129.8 (CH<sub>arom</sub>), 129.0 (CH<sub>arom</sub>), 128.9 (d, *J*<sub>C-P</sub> = 3.8 Hz, CH<sub>arom</sub>), 128.3 (CH<sub>arom</sub>), 128.1 (CH<sub>arom</sub>), 128.0 (d, *J*<sub>C-P</sub> = 6.4 Hz, CH<sub>arom</sub>), 126.9 (d, *J*<sub>C-P</sub> = 1.2 Hz, CH<sub>arom</sub>), 125.0 (CH<sub>arom</sub>), 123.0 (d, *J*<sub>C-P</sub> = 4.2 Hz, CH<sub>arom</sub>), 122.2 (CH<sub>arom</sub>), 74.6 (dd, <sup>2</sup>*J*<sub>C-P</sub> = 16.6 Hz, <sup>2</sup>*J*<sub>C-P</sub> = 12.1 Hz, CH-OPO<sub>2</sub>), 73.5 (d, <sup>2</sup>*J*<sub>C-P</sub> = 2.6 Hz, CH<sub>2</sub>-O(CH<sub>2</sub>)<sub>2</sub>OMe), 71.9 (O-CH<sub>2</sub>CH<sub>2</sub>-OMe), 70.7 (O-CH<sub>2</sub>CH<sub>2</sub>-OMe), 59.2 (*Me*), 48.2 (dd, <sup>1</sup>*J*<sub>C-P</sub> = 14.9 Hz, <sup>3</sup>*J*<sub>C-P</sub> = 6.1 Hz, CH-PPh<sub>2</sub>); <sup>31</sup>P{<sup>1</sup>H}-NMR (202 MHz, CDCl<sub>3</sub>) δ 155.7 (d, <sup>4</sup>*J*<sub>P-P</sub> = 6.0 Hz, *P*-O), -5.1 (d, <sup>4</sup>*J*<sub>P-P</sub> = 6.0 Hz, *P*-C); MS HR-ESI [found 631.1786; C<sub>36</sub>H<sub>34</sub>O<sub>5</sub>P<sub>2</sub>Na (M+Na)<sup>+</sup> requires 631.1779]; [*α*]<sub>D</sub><sup>25</sup> = -130.7 (c = 0.50 g/100 mL, THF).

**6-((1*R*,2*S*)-1-(diphenylphosphino)-3-(benzyloxy)-1-phenylpropen-2-yloxy)dibenzo[*d,f*][1,3,2]dioxaphosphepine (125c).**

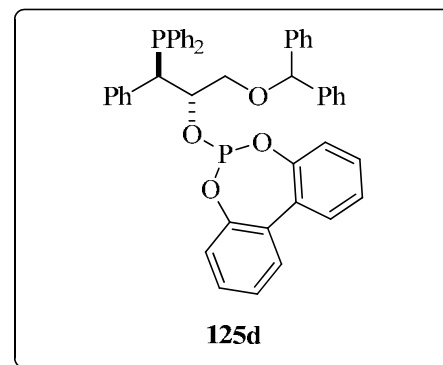
Phosphine-phosphite **125c** was obtained following the general procedure, starting from **118c** (0.176 g, 0.40 mmol), DABCO (0.099 g, 0.88 mmol), NEt<sub>3</sub> (111 μL,



0.79 mmol) and the chlorophosphite derived from biphenyl-2,2'-diol **127** (0.109 g, 0.44 mmol) as a white solid (0.158 g, 62% yield). <sup>1</sup>H-NMR (500 MHz, CDCl<sub>3</sub>) δ 7.81-7.77 (m, 2H, *H*<sub>arom</sub>), 7.54-7.08 (m, 25H, *H*<sub>arom</sub>), 6.84-6.82 (m, 1H, *H*<sub>arom</sub>), 4.61 (m, 1H, CH-OPO<sub>2</sub>), 4.43 (d, <sup>2</sup>*J*<sub>H-H</sub> = 11.5 Hz, 1H, CHH-Ph), 4.32 (d, <sup>2</sup>*J*<sub>H-H</sub> = 11.5 Hz, CHH-Ph), 3.82 (dd, <sup>2</sup>*J*<sub>H-P</sub> = 4.8 Hz, <sup>3</sup>*J*<sub>H-H</sub> = 3.8 Hz, 1H, CH-PPh<sub>2</sub>), 3.39 (dd, <sup>2</sup>*J*<sub>H-H</sub> = 9.8 Hz, <sup>3</sup>*J*<sub>H-H</sub> = 4.8 Hz, 1H, CHH-OCH<sub>2</sub>Ph), 3.20 (dd, <sup>2</sup>*J*<sub>H-H</sub> = 9.8 Hz, <sup>3</sup>*J*<sub>H-H</sub> = 7.2 Hz, 1H, CHH-OCH<sub>2</sub>Ph); <sup>13</sup>C{<sup>1</sup>H}-NMR (125 MHz, CDCl<sub>3</sub>) δ 150.1 (d, *J*<sub>C-P</sub> = 5.5 Hz, *C*<sub>q</sub> arom), 149.5 (d, *J*<sub>C-P</sub> = 4.6 Hz, *C*<sub>q</sub> arom), 138.1 (*C*<sub>q</sub> arom), 137.0 (d, *J*<sub>C-P</sub> = 15.5 Hz, *C*<sub>q</sub> arom), 136.9 (d, *J*<sub>C-P</sub> = 11.0 Hz, *C*<sub>q</sub> arom), 135.9 (d, *J*<sub>C-P</sub> = 17.5 Hz, *C*<sub>q</sub> arom), 135.0 (d, *J*<sub>C-P</sub> = 21.8 Hz, CH<sub>arom</sub>), 133.2 (d, *J*<sub>C-P</sub> = 18.5 Hz, CH<sub>arom</sub>), 131.8 (d, *J*<sub>C-P</sub> = 3.5 Hz, *C*<sub>q</sub> arom), 131.3 (d, *J*<sub>C-P</sub> = 2.8 Hz, *C*<sub>q</sub> arom), 131.1 (d, *J*<sub>C-P</sub> = 7.8 Hz, CH<sub>arom</sub>), 129.9 (d, *J*<sub>C-P</sub> = 19.9 Hz, CH<sub>arom</sub>), 129.8 (CH<sub>arom</sub>), 129.0 (d, *J*<sub>C-P</sub> = 7.4 Hz, CH<sub>arom</sub>), 128.9 (d, *J*<sub>C-P</sub> = 2.4 Hz, CH<sub>arom</sub>), 128.5 (CH<sub>arom</sub>), 128.3 (CH<sub>arom</sub>), 128.2 (CH<sub>arom</sub>), 128.0 (d, *J*<sub>C-P</sub> = 6.5 Hz, CH<sub>arom</sub>), 127.7 (CH<sub>arom</sub>), 126.9 (d, *J*<sub>C-P</sub> = 1.4 Hz, CH<sub>arom</sub>), 125.0 (CH<sub>arom</sub>), 123.0 (d, *J*<sub>C-P</sub> = 4.4 Hz, CH<sub>arom</sub>), 122.3 (CH<sub>arom</sub>), 74.7 (dd, <sup>2</sup>*J*<sub>C-P</sub> = 17.1 Hz, <sup>2</sup>*J*<sub>C-P</sub> = 12.8 Hz, CH-OPO<sub>2</sub>), 73.3 (CH<sub>2</sub>-Ph), 72.7 (bd, <sup>3</sup>*J*<sub>C-P</sub> = 3.0 Hz, CH<sub>2</sub>-OCH<sub>2</sub>Ph), 48.3 (dd, <sup>1</sup>*J*<sub>C-P</sub> = 15.1 Hz, <sup>3</sup>*J*<sub>C-P</sub> = 5.9 Hz, CH-PPh<sub>2</sub>); <sup>31</sup>P{<sup>1</sup>H}-NMR (202 MHz, CDCl<sub>3</sub>) δ 155.5 (d, <sup>4</sup>*J*<sub>P-P</sub> = 7.2 Hz, P-O), -5.1 (d, <sup>4</sup>*J*<sub>P-P</sub> = 7.2 Hz, P-C); MS HR-ESI [found 663.1860; C<sub>40</sub>H<sub>34</sub>O<sub>4</sub>P<sub>2</sub>Na (M+Na)<sup>+</sup> requires 663.1830]; [α]<sub>D</sub><sup>25</sup> = -137.4 (c = 0.50 g/100 mL, THF); M.p. 84.1-89.3 °C.

**6-((1*R*,2*S*)-1-(diphenylphosphino)-1-phenyl-3-(benzhydryloxy)-propan-2-yloxy)dibenzo[*d,f*][1,3,2]dioxaphosphepine**

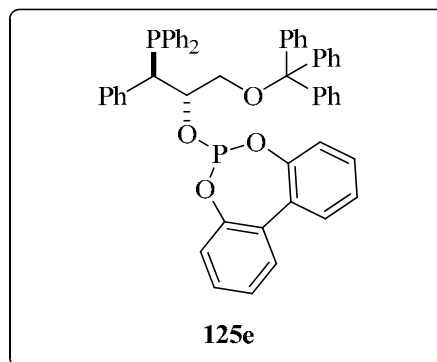
**(125d).** Phosphine-phosphite **125d** was obtained following the general procedure, starting from **118d** (0.429 g, 0.83 mmol), DABCO (0.205 g, 1.83 mmol), NEt<sub>3</sub> (0.2 mL,



1.66 mmol) and the chlorophosphite derived from biphenyl-2,2'-diol **127** (0.229 g, 0.91 mmol) as a white solid (0.363 g, 61% yield). <sup>1</sup>H-NMR (500 MHz, CDCl<sub>3</sub>) δ 7.78-7.74 (m, 2H, *H*<sub>arom</sub>), 7.45-7.05 (m, 30H, *H*<sub>arom</sub>), 6.48 (d, <sup>3</sup>*J*<sub>H-H</sub> = 8.0 Hz, 1H, *H*<sub>arom</sub>), 5.19 (s, 1H, CH-Ph<sub>2</sub>), 4.69 (m, 1H, CH-OPO<sub>2</sub>), 3.81 (dd, <sup>2</sup>*J*<sub>H-P</sub> = <sup>3</sup>*J*<sub>H-H</sub> = 4.0 Hz, 1H, CH-PPh<sub>2</sub>), 3.29 (dd, <sup>2</sup>*J*<sub>H-H</sub> = 9.9 Hz, <sup>3</sup>*J*<sub>H-H</sub> = 5.0 Hz, 1H, CHH-O-CH<sub>2</sub>Ph), 3.18 (dd, <sup>2</sup>*J*<sub>H-H</sub> = 9.9 Hz, <sup>3</sup>*J*<sub>H-H</sub> = 7.2 Hz, 1H, CHH-O-CH<sub>2</sub>Ph); <sup>13</sup>C{<sup>1</sup>H}-NMR (125 MHz, CDCl<sub>3</sub>) δ 150.1 (d, *J*<sub>C-P</sub> = 5.9 Hz, *C*<sub>q</sub> arom), 149.4 (d, *J*<sub>C-P</sub> = 4.2 Hz, *C*<sub>q</sub> arom), 142.3 (*C*<sub>q</sub> arom), 142.0 (*C*<sub>q</sub> arom), 136.9 (d, *J*<sub>C-P</sub> = 16.4 Hz, *C*<sub>q</sub> arom), 136.8 (d, *J*<sub>C-P</sub> = 10.4 Hz, *C*<sub>q</sub> arom), 136.0 (d, *J*<sub>C-P</sub> = 22.8 Hz, *C*<sub>q</sub> arom), 135.0 (d, *J*<sub>C-P</sub> = 21.4 Hz, CH<sub>arom</sub>), 133.3 (d, *J*<sub>C-P</sub> = 18.8 Hz, CH<sub>arom</sub>), 131.8 (d, *J*<sub>C-P</sub> = 3.2 Hz, *C*<sub>q</sub> arom), 131.2 (d, *J*<sub>C-P</sub> = 2.5 Hz, *C*<sub>q</sub> arom), 131.1 (d, *J*<sub>C-P</sub> = 7.5 Hz, CH<sub>arom</sub>), 129.9 (d, *J*<sub>C-P</sub> = 13.6 Hz, CH<sub>arom</sub>), 129.6 (CH<sub>arom</sub>), 129.0 (CH<sub>arom</sub>), 128.9 (CH<sub>arom</sub>), 128.5 (CH<sub>arom</sub>), 128.4 (CH<sub>arom</sub>), 128.3 (CH<sub>arom</sub>), 128.1 (CH<sub>arom</sub>), 128.0 (d, *J*<sub>C-P</sub> = 6.5 Hz, CH<sub>arom</sub>), 127.7 (CH<sub>arom</sub>), 127.4 (CH<sub>arom</sub>), 127.3 (CH<sub>arom</sub>), 126.9 (CH<sub>arom</sub>), 126.8 (CH<sub>arom</sub>), 124.9 (d, *J*<sub>C-P</sub> = 4.8 Hz, CH<sub>arom</sub>), 123.0 (d, *J*<sub>C-P</sub> = 4.5 Hz, CH<sub>arom</sub>), 122.3 (CH<sub>arom</sub>), 84.2 (CH-Ph<sub>2</sub>), 74.8 (dd, <sup>2</sup>*J*<sub>C-P</sub> = 17.0 Hz, <sup>2</sup>*J*<sub>C-P</sub> = 14.8 Hz, CH-OPO<sub>2</sub>), 71.0 (bd, <sup>3</sup>*J*<sub>C-P</sub> = 4.0 Hz, CH<sub>2</sub>-OCHPh<sub>2</sub>), 48.2 (dd, <sup>1</sup>*J*<sub>C-P</sub> = 15.2 Hz, <sup>3</sup>*J*<sub>C-P</sub> = 5.5 Hz, CH-PPh<sub>2</sub>); <sup>31</sup>P{<sup>1</sup>H}-NMR (202 MHz, CDCl<sub>3</sub>) δ 155.1 (d, <sup>4</sup>*J*<sub>P-P</sub> = 9.1 Hz, P-O), -5.2 (d, <sup>4</sup>*J*<sub>P-P</sub> = 9.1 Hz, P-C); MS HR-ESI [found 739.2112; C<sub>46</sub>H<sub>38</sub>O<sub>4</sub>P<sub>2</sub>Na (M+Na)<sup>+</sup> required 739.2143]; [α]<sub>D</sub><sup>25</sup> = -117.4 (c = 1.00 g/100 mL, THF); M.p. 96.3-101.0 °C.

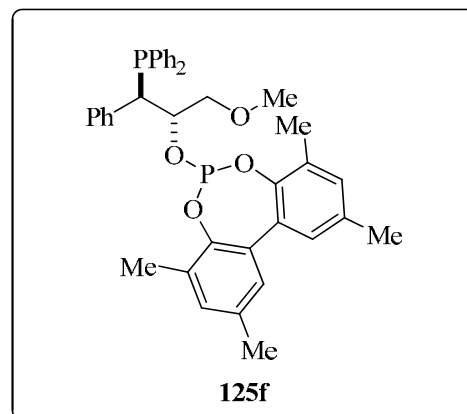
**6-((1*R*,2*S*)-1-(diphenylphosphino)-1-phenyl-3-(trityloxy)propan-2-yloxy)dibenzo[*d,f*][1,3,2]dioxaphosphepine (125e).**

Phosphine-phosphite **125e** was obtained following the general procedure, starting from **118e** (0.219 g, 0.37 mmol), DABCO (0.091 g, 0.81 mmol), NEt<sub>3</sub> (0.1 mL,



0.74 mmol) and the chlorophosphite derived from biphenyl-2,2'-diol **127** (0.102 g, 0.41 mmol) as a white solid (0.188 g, 64% yield). <sup>1</sup>H-NMR (500 MHz, CDCl<sub>3</sub>) δ 7.69-7.66 (m, 2H, *H*<sub>arom</sub>), 7.46-7.03 (m, 35H, *H*<sub>arom</sub>), 6.71 (d, <sup>3</sup>*J*<sub>H-H</sub> = 8.0 Hz, 1H, *H*<sub>arom</sub>), 4.75 (m, 1H, *CH*-OPO<sub>2</sub>), 3.82 (dd, <sup>2</sup>*J*<sub>H-P</sub> = <sup>3</sup>*J*<sub>H-H</sub> = 4.8 Hz, 1H, *CH*-PPh<sub>2</sub>), 3.06 (dd, <sup>2</sup>*J*<sub>H-H</sub> = 9.6 Hz, <sup>3</sup>*J*<sub>H-H</sub> = 5.5 Hz, 1H, *CHH*-OCPh<sub>3</sub>), 3.00 (dd, <sup>2</sup>*J*<sub>H-H</sub> = 9.6 Hz, <sup>3</sup>*J*<sub>H-H</sub> = 7.8 Hz, 1H, *CHH*-OPh<sub>3</sub>); <sup>13</sup>C{<sup>1</sup>H}-NMR (125 MHz, CDCl<sub>3</sub>) δ 149.9 (d, *J*<sub>C-P</sub> = 5.5 Hz, *C*<sub>q</sub> arom), 149.5 (d, *J*<sub>C-P</sub> = 4.4 Hz, *C*<sub>q</sub> arom), 143.9 (*C*<sub>q</sub> arom), 136.8 (d, *J*<sub>C-P</sub> = 8.4 Hz, *C*<sub>q</sub> arom), 136.7 (d, *J*<sub>C-P</sub> = 14.6 Hz, *C*<sub>q</sub> arom), 136.2 (d, *J*<sub>C-P</sub> = 16.4 Hz, *C*<sub>q</sub> arom), 134.7 (d, *J*<sub>C-P</sub> = 21.4 Hz, *CH*<sub>arom</sub>), 133.5 (d, *J*<sub>C-P</sub> = 19.1 Hz, *CH*<sub>arom</sub>), 131.6 (d, *J*<sub>C-P</sub> = 3.0 Hz, *C*<sub>q</sub> arom), 131.2 (d, *J*<sub>C-P</sub> = 2.6 Hz, *C*<sub>q</sub> arom), 130.8 (d, *J*<sub>C-P</sub> = 7.2 Hz, *CH*<sub>arom</sub>), 129.8 (*CH*<sub>arom</sub>), 129.7 (d, *J*<sub>C-P</sub> = 8.4 Hz, *CH*<sub>arom</sub>), 128.9 (*CH*<sub>arom</sub>), 128.8 (d, *J*<sub>C-P</sub> = 4.6 Hz, *CH*<sub>arom</sub>), 128.4 (*CH*<sub>arom</sub>), 128.3 (*CH*<sub>arom</sub>), 128.0 (*CH*<sub>arom</sub>), 127.9 (*CH*<sub>arom</sub>), 127.9 (d, *J*<sub>C-P</sub> = 7.1 Hz, *CH*<sub>arom</sub>), 127.1 (*CH*<sub>arom</sub>), 126.6 (bs, *CH*<sub>arom</sub>), 124.9 (d, *J*<sub>C-P</sub> = 2.0 Hz, *CH*<sub>arom</sub>), 122.8 (d, *J*<sub>C-P</sub> = 2.6 Hz, *CH*<sub>arom</sub>), 122.3 (*CH*<sub>arom</sub>), 87.5 (OCPh<sub>3</sub>), 75.9 (dd, <sup>2</sup>*J*<sub>C-P</sub> = <sup>2</sup>*J*<sub>C-P</sub> = 19.0 Hz, *CH*-OPO<sub>2</sub>), 66.0 (bd, <sup>3</sup>*J*<sub>C-P</sub> = 4.4 Hz, *CH*<sub>2</sub>-OCPh<sub>3</sub>), 48.4 (dd, <sup>1</sup>*J*<sub>C-P</sub> = 15.8 Hz, <sup>3</sup>*J*<sub>C-P</sub> = 4.8 Hz, *CH*-PPh<sub>2</sub>); <sup>31</sup>P{<sup>1</sup>H}-NMR (202 MHz, CDCl<sub>3</sub>) δ 155.4 (d, <sup>4</sup>*J*<sub>P-P</sub> = 11.9 Hz, *P*-O), -6.0 (d, <sup>4</sup>*J*<sub>P-P</sub> = 11.9 Hz, *P*-C); MS HR-ESI [found 793.2599; C<sub>52</sub>H<sub>43</sub>O<sub>4</sub>P<sub>2</sub> (M+H)<sup>+</sup> requires 793.2637]; [ $\alpha$ ]<sub>D</sub><sup>25</sup> = -125.64 (c = 0.50 g/100 mL, THF); M.p. 97.3-102.7 °C.

**6-((1*R*,2*S*)-1-(diphenylphosphino)-3-methoxy-1-phenylpropen-2-yloxy)-2,4,8,10-tetramethyldibenzo[*d,f*][1,3,2]dioxaphosphine (**125f**).** Phosphine-phosphite **125f** was obtained following the general procedure, starting from **118a** (0.256 g, 0.70 mmol), DABCO (0.173 g, 1.54 mmol), NEt<sub>3</sub>



(0.2 mL, 1.40 mmol) and the chlorophosphite derived from 3,3',5,5'-tetramethylbiphenyl-2,2'-diol **128** (0.236 g, 0.77 mmol) as a white solid (0.206 g, 48% yield). <sup>1</sup>H-NMR (400 MHz, CDCl<sub>3</sub>) δ 7.74-7.70 (m, 2H, *H*<sub>arom</sub>), 7.40-6.97 (m, 17H, *H*<sub>arom</sub>), 4.56 (m, 1H, CH-OPO<sub>2</sub>), 3.85 (dd, <sup>2</sup>*J*<sub>H-P</sub> = <sup>3</sup>*J*<sub>H-H</sub> = 4.8 Hz, 1H, CH-PPh<sub>2</sub>), 3.17-3.15 (m, 5H, OMe and CH<sub>2</sub>-OMe), 2.44 (bs, 3H, Me), 2.35 (bs, 6H, Me), 2.08 (bs, 3H, Me); <sup>13</sup>C{<sup>1</sup>H}-NMR (100 MHz, CDCl<sub>3</sub>) δ 146.0 (d, *J*<sub>C-P</sub> = 6.4 Hz, C<sub>q</sub> arom), 145.9 (d, *J*<sub>C-P</sub> = 5.3 Hz, C<sub>q</sub> arom), 137.0 (C<sub>q</sub> arom), 136.8 (C<sub>q</sub> arom), 136.8 (d, *J*<sub>C-P</sub> = 10.5 Hz, C<sub>q</sub> arom), 136.4 (d, *J*<sub>C-P</sub> = 17.5 Hz, C<sub>q</sub> arom), 134.7 (d, *J*<sub>C-P</sub> = 21.4 Hz, CH<sub>arom</sub>), 133.7 (d, *J*<sub>C-P</sub> = 18.4 Hz, C<sub>q</sub> arom), 133.4 (d, *J*<sub>C-P</sub> = 19.1 Hz, CH<sub>arom</sub>), 131.6 (d, *J*<sub>C-P</sub> = 3.5 Hz, C<sub>q</sub> arom), 131.3 (d, *J*<sub>C-P</sub> = 2.9 Hz, C<sub>q</sub> arom), 131.2 (d, *J*<sub>C-P</sub> = 8.1 Hz, CH<sub>arom</sub>), 131.0 (d, *J*<sub>C-P</sub> = 10.0 Hz, CH<sub>arom</sub>), 130.5 (d, *J*<sub>C-P</sub> = 1.1 Hz, C<sub>q</sub> arom), 130.1 (C<sub>q</sub> arom), 129.7 (CH<sub>arom</sub>), 128.8 (d, *J*<sub>C-P</sub> = 7.7 Hz, CH<sub>arom</sub>), 128.3 (CH<sub>arom</sub>), 128.1 (CH<sub>arom</sub>), 128.0 (d, *J*<sub>C-P</sub> = 10.3 Hz, CH<sub>arom</sub>), 127.9 (d, *J*<sub>C-P</sub> = 6.8 Hz, CH<sub>arom</sub>), 126.8 (CH<sub>arom</sub>), 74.0 (dd, <sup>3</sup>*J*<sub>C-P</sub> = <sup>3</sup>*J*<sub>C-P</sub> = 3.2 Hz, CH<sub>2</sub>-OMe), 73.5 (dd, <sup>2</sup>*J*<sub>C-P</sub> = <sup>2</sup>*J*<sub>C-P</sub> = 13.2 Hz, CH-OPO<sub>2</sub>), 58.7 (O-Me), 47.8 (dd, <sup>1</sup>*J*<sub>C-P</sub> = 14.6 Hz, <sup>3</sup>*J*<sub>C-P</sub> = 5.0 Hz, CH-PPh<sub>2</sub>), 21.0 (bs, 2 Me), 17.4 (d, <sup>4</sup>*J*<sub>C-P</sub> = 4.3 Hz, Me), 16.7 (Me); <sup>31</sup>P{<sup>1</sup>H}-NMR (162 MHz, CDCl<sub>3</sub>) δ 151.1 (d, <sup>4</sup>*J*<sub>P-P</sub> = 17.6 Hz, P-O), -7.3 (d, <sup>4</sup>*J*<sub>P-P</sub> = 17.6 Hz, P-C); MS HR-ESI [found 621.2299; C<sub>38</sub>H<sub>39</sub>O<sub>4</sub>P<sub>2</sub> (M+H)<sup>+</sup> requires 621.2324]; [α]<sub>D</sub><sup>25</sup> = -96.0 (c = 1.00 g/100 mL, THF); M.p. 70.7-74.6 °C.

**6-((1*R*,2*S*)-1-(diphenylphosphino)-3-trityloxy-1-phenylpropen-2-yloxy)-2,4,8,10-tetramethyldibenzo[*d,f*][1,3,2]dioxaphosph**

**epine (125g).** Phosphine-phosphite **125g** was

obtained following the general procedure, starting from **118e** (0.172 g, 0.29 mmol),

DABCO (0.072 g, 0.64 mmol),  $\text{NEt}_3$  (81  $\mu\text{L}$ ,

0.58 mmol) and the chlorophosphite derived from 3,3',5,5'-tetramethylbiphenyl-

2,2'-diol **128** (0.097 g, 0.32 mmol) as a white solid (0.123 g, 50% yield).  $^1\text{H}$ -

NMR (500 MHz,  $\text{CDCl}_3$ )  $\delta$  7.80-6.87 (m, 34H,  $H_{\text{arom}}$ ), 4.55 (m, 1H,  $\text{CH-OPO}_2$ ),

4.04 (bdd,  $^2J_{\text{H-P}} = 5.0$  Hz,  $^3J_{\text{H-H}} = 2.0$  Hz, 1H,  $\text{CH-PPh}_2$ ), 2.98 (m, 1H,  $\text{CHH-}$

$\text{OCPh}_3$ ), 2.73 (dd,  $^2J_{\text{H-H}} = ^3J_{\text{H-H}} = 8.8$  Hz, 1H,  $\text{CHH-OCPh}_3$ ), 2.32 (s, 3H, *Me*), 2.28

(bs, 6H, 2 *Me*), 1.83 (s, 3H, *Me*);  $^{13}\text{C}\{^1\text{H}\}$ -NMR (125 MHz,  $\text{CDCl}_3$ )  $\delta$  145.8 (d,

$J_{\text{C-P}} = 5.0$  Hz,  $C_{\text{q arom}}$ ), 145.8 (d,  $J_{\text{C-P}} = 6.2$  Hz,  $C_{\text{q arom}}$ ), 143.8 ( $C_{\text{q arom}}$ ), 137.4 (d,  $J_{\text{C-}}$

$\text{P} = 15.5$  Hz,  $C_{\text{q arom}}$ ), 137.0 (d,  $J_{\text{C-P}} = 16.8$  Hz,  $C_{\text{q arom}}$ ), 136.2 (d,  $J_{\text{C-P}} = 10.2$  Hz,

$\text{CH}_{\text{arom}}$ ), 134.9 (d,  $J_{\text{C-P}} = 21.4$  Hz,  $\text{CH}_{\text{arom}}$ ), 133.6 (d,  $J_{\text{C-P}} = 7.2$  Hz,  $C_{\text{q arom}}$ ), 133.2

(d,  $J_{\text{C-P}} = 18.8$  Hz,  $\text{CH}_{\text{arom}}$ ), 131.4 (d,  $J_{\text{C-P}} = 8.6$  Hz,  $\text{CH}_{\text{arom}}$ ), 131.3 ( $C_{\text{q arom}}$ ), 130.9

(d,  $J_{\text{C-P}} = 4.6$  Hz,  $\text{CH}_{\text{arom}}$ ), 130.5 ( $C_{\text{q arom}}$ ), 130.1 ( $C_{\text{q arom}}$ ), 129.7 ( $\text{CH}_{\text{arom}}$ ), 128.9 (d,

$J_{\text{C-P}} = 7.8$  Hz,  $\text{CH}_{\text{arom}}$ ), 128.7 ( $\text{CH}_{\text{arom}}$ ), 128.2 ( $\text{CH}_{\text{arom}}$ ), 128.0 ( $\text{CH}_{\text{arom}}$ ), 127.9

( $\text{CH}_{\text{arom}}$ ), 127.8 ( $\text{CH}_{\text{arom}}$ ), 127.7 ( $\text{CH}_{\text{arom}}$ ), 127.1 ( $\text{CH}_{\text{arom}}$ ), 87.2 ( $\text{C-Ph}_3$ ), 73.6 (dd,

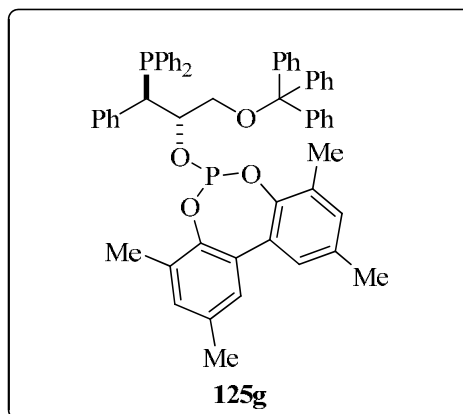
$^2J_{\text{C-P}} = ^2J_{\text{C-P}} = 12.2$  Hz,  $\text{CH-OPO}_2$ ), 64.1 (bs,  $\text{CH}_2\text{-OCPh}_3$ ), 47.6 (dd,  $^1J_{\text{C-P}} = 13.1$

Hz,  $^3J_{\text{C-P}} = 4.1$  Hz,  $\text{CH-PPh}_2$ ), 21.0 (bs, 2 *Me*), 17.1 (d,  $^4J_{\text{C-P}} = 3.0$  Hz, *Me*), 16.8

(*Me*);  $^{31}\text{P}\{^1\text{H}\}$ -NMR (202 MHz,  $\text{CDCl}_3$ )  $\delta$  150.5 (d,  $^4J_{\text{P-P}} = 25.4$  Hz,  $\text{P-O}$ ), -8.6 (d,

$^4J_{\text{P-P}} = 25.4$  Hz,  $\text{P-C}$ ); MS HR-ESI [found 849.3243;  $\text{C}_{56}\text{H}_{51}\text{O}_4\text{P}_2$  ( $\text{M}+\text{H}$ ) $^+$  requires

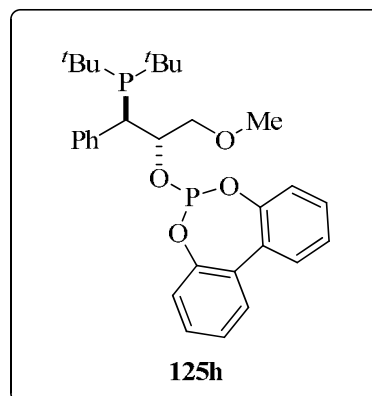
849.3263];  $[\alpha]_{\text{D}}^{25} = -58.9$  ( $c = 0.49$  mg/100 mL, THF); M.p. 91.5-95.9  $^\circ\text{C}$ .





**6-((1*R*,2*S*)-1-(di-*tert*-butylphosphino)-3-methoxy-1-phenylpropan-2-yloxy)dibenzo[*d,f*][1,3,2]dioxaphosphepine**

**(125h)**. Phosphine-phosphite **125h** was obtained following the general procedure with minor changes: Phosphino alcohol as borane adduct **118f** (0.250 g, 0.77 mmol) was dissolved in HNEt<sub>2</sub> (16.0 mL, 154.20 mmol) and stirred for 4h at 50 °C. The



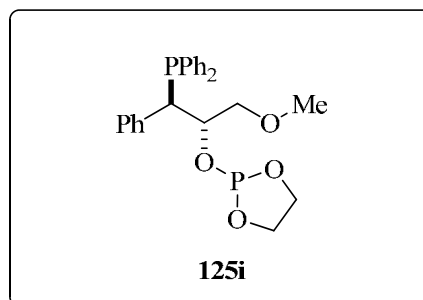
reaction mixture was concentrated *in vacuo*. The resulting phosphino alcohol was

dissolved in toluene (10.0 mL). This solution was added dropwise via cannula to a solution of the chlorophosphite **127** (0.213 g, 0.85 mmol) and NEt<sub>3</sub> (214 μL, 1.54 mmol) in toluene (17.0 mL). The mixture was stirred for 16 h at room temperature. The reaction mixture was filtered through celite and the filtrate was evaporated *in vacuo*. The resulting residue was dissolved in diethyl ether (20.0 mL) and passed through a short pad of alumina (3.0 g). Solvent evaporation yielded the corresponding phosphine-phosphite ligands **125h** (0.277 g, 80% purity, 55% yield). Application of the general procedure described for phosphine-phosphite ligands (see Section 1.3.5, page 181) yielded slightly impure compound **125h**. Further purification attempts led to product decomposition, but these impurities do not interfere in the preparation of complex **142h** [Rh(nbd)(**125h**)]BF<sub>4</sub>. <sup>1</sup>H-NMR (400 MHz, CDCl<sub>3</sub>) δ 7.45-7.16 (m, 11H, *H*<sub>arom</sub>), 7.02 (bd, <sup>3</sup>*J*<sub>H-H</sub> = 7.6 Hz, 1H, *H*<sub>arom</sub>), 6.89 (bd, <sup>3</sup>*J*<sub>H-H</sub> = 7.6 Hz, 1H, *H*<sub>arom</sub>), 4.99 (m, 1H, CH-OPO<sub>2</sub>), 3.70 (dd, <sup>2</sup>*J*<sub>H-H</sub> = 9.9 Hz, <sup>3</sup>*J*<sub>H-H</sub> = 4.4 Hz, 1H, CHH-OMe), 3.56 (dd, <sup>2</sup>*J*<sub>H-P</sub> = 5.4 Hz, <sup>3</sup>*J*<sub>H-H</sub> = 3.0 Hz, 1H, CH-P<sup>*t*</sup>Bu<sub>2</sub>), 3.36 (s, 3H, OMe), 3.33 (dd, <sup>2</sup>*J*<sub>H-H</sub> = 9.9 Hz, <sup>3</sup>*J*<sub>H-H</sub> = 7.8 Hz, 1H, CHH-OMe), 1.35 (d, <sup>3</sup>*J*<sub>H-P</sub> = 10.8 Hz, 9H, 3Me, <sup>*t*</sup>Bu<sub>2</sub>P), 0.93 (d, <sup>3</sup>*J*<sub>H-P</sub> = 10.8 Hz, 9H, 3Me, <sup>*t*</sup>Bu<sub>2</sub>P); <sup>31</sup>P{<sup>1</sup>H}-NMR (162 MHz, CDCl<sub>3</sub>) δ 155.4 (d, <sup>4</sup>*J*<sub>P-O</sub> = 12.7 Hz, P-O), 47.8 (d, <sup>4</sup>*J*<sub>P-P</sub> = 12.7 Hz, P-C); MS HR-ESI [found 525.2326; C<sub>30</sub>H<sub>39</sub>O<sub>4</sub>P<sub>2</sub> (M+H)<sup>+</sup> requires 525.2324].

**2-((1*R*,2*S*)-1-(diphenylphosphino)-3-methoxy-1-phenylpropen-2-yloxy)-1,3,2-**

**dioxaphospholane (125i).** Phosphine-phosphite

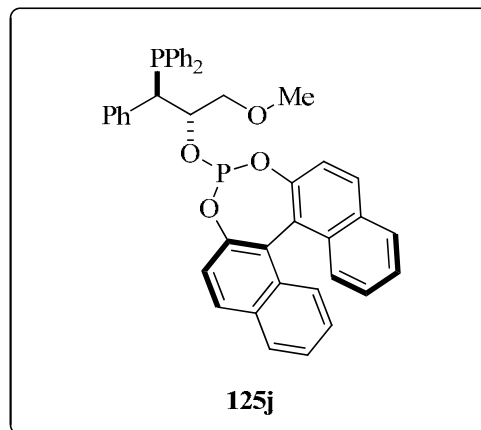
**125i** was obtained following the general procedure, starting from **118a** (0.200 g, 0.55 mmol), DABCO (0.137 g, 1.21 mmol), NEt<sub>3</sub>



and the chlorophosphite **126** (56  $\mu$ L, 0.60 mmol) as a colorless oil (0.166 g, 69% yield). <sup>1</sup>H-NMR (400 MHz, CDCl<sub>3</sub>)  $\delta$  7.76-7.72 (m, 2H, *H*<sub>arom</sub>), 7.45-7.33 (m, 5H, *H*<sub>arom</sub>), 7.22-7.06 (m, 8H, *H*<sub>arom</sub>), 4.31-4.22 (m, 2H, *CH*-OPO<sub>2</sub> and -O*CHH*-CH<sub>2</sub>-O-), 4.08-3.88 (m, 3H, -O*CHH*-CH<sub>2</sub>-O-), 3.79 (dd, <sup>2</sup>*J*<sub>H-P</sub> = 5.2 Hz, <sup>3</sup>*J*<sub>H-H</sub> = 2.8 Hz, 1H, *CH*-PPh<sub>2</sub>), 3.18 (s, 3H, *Me*), 3.10 (dd, <sup>2</sup>*J*<sub>H-H</sub> = 9.6 Hz, <sup>3</sup>*J*<sub>H-H</sub> = 6.4 Hz, 1H, *CHH*-OMe), 3.03 (dd, <sup>2</sup>*J*<sub>H-H</sub> = 9.6 Hz, <sup>3</sup>*J*<sub>H-H</sub> = 6.8 Hz, 1H, *CHH*-OMe); <sup>13</sup>C{<sup>1</sup>H}-NMR (100 MHz, CDCl<sub>3</sub>)  $\delta$  137.1 (d, *J*<sub>C-P</sub> = 10.6 Hz, *C*<sub>q</sub> arom), 137.0 (d, *J*<sub>C-P</sub> = 13.7 Hz, *C*<sub>q</sub> arom), 136.4 (d, *J*<sub>C-P</sub> = 16.6 Hz, *C*<sub>q</sub> arom), 134.9 (d, *J*<sub>C-P</sub> = 21.4 Hz, *CH*<sub>arom</sub>), 133.2 (d, *J*<sub>C-P</sub> = 18.6 Hz, *CH*<sub>arom</sub>), 131.1 (d, *J*<sub>C-P</sub> = 8.6 Hz, *CH*<sub>arom</sub>), 129.8 (*CH*<sub>arom</sub>), 128.9 (d, *J*<sub>C-P</sub> = 7.8 Hz, *CH*<sub>arom</sub>), 128.3 (*CH*<sub>arom</sub>), 128.0 (*CH*<sub>arom</sub>), 127.9 (d, *J*<sub>C-P</sub> = 6.8 Hz, *CH*<sub>arom</sub>), 126.8 (d, *J*<sub>C-P</sub> = 1.4 Hz, *CH*<sub>arom</sub>), 74.2 (dd, <sup>3</sup>*J*<sub>C-P</sub> = 4.2 Hz, <sup>3</sup>*J*<sub>C-P</sub> = 2.2 Hz, *CH*<sub>2</sub>-OMe), 71.7 (dd, <sup>2</sup>*J*<sub>C-P</sub> = <sup>2</sup>*J*<sub>C-P</sub> = 13.2 Hz, *CH*-OPO<sub>2</sub>), 64.0 (d, <sup>2</sup>*J*<sub>C-P</sub> = 8.3 Hz, -O*CH*<sub>2</sub>CH<sub>2</sub>O-), 63.8 (d, <sup>2</sup>*J*<sub>C-P</sub> = 8.6 Hz, -O*CH*<sub>2</sub>CH<sub>2</sub>O-), 58.9 (s, *Me*), 47.6 (dd, <sup>1</sup>*J*<sub>C-P</sub> = 13.2 Hz, <sup>3</sup>*J*<sub>C-P</sub> = 4.4 Hz, *CH*-PPh<sub>2</sub>); <sup>31</sup>P{<sup>1</sup>H}-NMR (162 MHz, CDCl<sub>3</sub>)  $\delta$  138.8 (d, <sup>4</sup>*J*<sub>P-P</sub> = 12.0 Hz, *P*-O), -7.0 (d, <sup>4</sup>*J*<sub>P-P</sub> = 12.0 Hz, *P*-C); MS HR-ESI [found 441.1396; C<sub>24</sub>H<sub>27</sub>O<sub>4</sub>P<sub>2</sub> (M+H)<sup>+</sup> requires 441.1385]; [ $\alpha$ ]<sub>D</sub><sup>25</sup> = -146.1 (c = 0.99 mg/100 mL, THF).

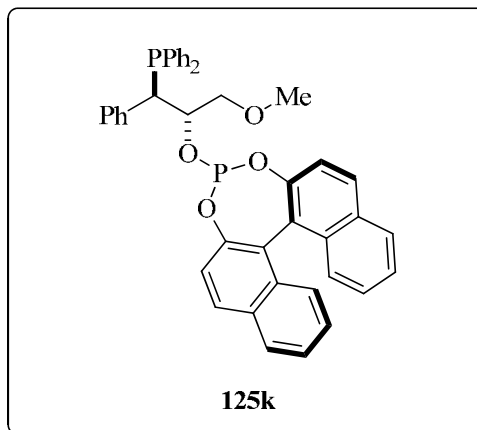
**(11bR)-4-((1R,2S)-1-(diphenylphosphino)-3-methoxy-1-phenylpropan-2-yloxy)dinaphtho[2,1-d:1',2'-f][1,3,2]dioxaphosphepine (125j).**

Phosphine-phosphite **125j** was obtained following the general procedure, starting from **118a** (0.215 g, 0.59 mmol), DABCO (0.146 g, 1.30 mmol),  $\text{NEt}_3$  (0.16 mL, 1.19



mmol) and the chlorophosphite derived from (*R*)-BINOL **129** (0.236 g, 0.65 mmol) as a white solid (0.281 g, 71% yield).  $^1\text{H-NMR}$  (500 MHz,  $\text{CDCl}_3$ )  $\delta$  8.09-8.05 (m, 2H,  $H_{\text{arom}}$ ), 7.99- 7.98 (m, 1H,  $H_{\text{arom}}$ ), 7.92-7.90 (m, 2H,  $H_{\text{arom}}$ ), 7.84-7.81 (m, 2H,  $H_{\text{arom}}$ ), 7.46-7.00 (m, 20H,  $H_{\text{arom}}$ ), 4.44 (m, 1H,  $\text{CH-OPO}_2$ ), 3.75 (dd,  $^2J_{\text{H-P}} = 4.5$  Hz,  $^3J_{\text{H-H}} = 3.5$  Hz, 1H,  $\text{CH-PPh}_2$ ), 3.22 (dd,  $^2J_{\text{H-H}} = 9.8$  Hz,  $^3J_{\text{H-H}} = 4.5$  Hz, 1H,  $\text{CHH-OMe}$ ), 3.21 (s, 3H, *Me*), 2.91 (dd,  $^2J_{\text{H-H}} = 9.8$  Hz,  $^3J_{\text{H-H}} = 7.8$  Hz, 1H,  $\text{CHH-OMe}$ );  $^{13}\text{C}\{^1\text{H}\}$ -NMR (125 MHz,  $\text{CDCl}_3$ )  $\delta$  148.8 (d,  $J_{\text{C-P}} = 4.4$  Hz,  $C_{\text{q arom}}$ ), 147.9 (d,  $J_{\text{C-P}} = 2.5$  Hz,  $C_{\text{q arom}}$ ), 137.2 (d,  $J_{\text{C-P}} = 15.6$  Hz,  $C_{\text{q arom}}$ ), 136.9 (d,  $J_{\text{C-P}} = 11.2$  Hz,  $C_{\text{q arom}}$ ), 136.0 (d,  $J_{\text{C-P}} = 17.5$  Hz,  $C_{\text{q arom}}$ ), 135.1 (d,  $J_{\text{C-P}} = 21.8$  Hz,  $\text{CH}_{\text{arom}}$ ), 133.1 (d,  $J_{\text{C-P}} = 18.4$  Hz,  $\text{CH}_{\text{arom}}$ ), 132.9 (d,  $J_{\text{C-P}} = 36.5$  Hz,  $C_{\text{q arom}}$ ), 131.5 (d,  $J_{\text{C-P}} = 16.6$  Hz,  $C_{\text{q arom}}$ ), 130.9 (d,  $J_{\text{C-P}} = 8.1$  Hz,  $\text{CH}_{\text{arom}}$ ), 130.1 (d,  $J_{\text{C-P}} = 6.9$  Hz,  $\text{CH}_{\text{arom}}$ ), 129.6 ( $\text{CH}_{\text{arom}}$ ), 129.0 (d,  $J_{\text{C-P}} = 7.6$  Hz,  $\text{CH}_{\text{arom}}$ ), 128.4 ( $\text{CH}_{\text{arom}}$ ), 128.3 ( $\text{CH}_{\text{arom}}$ ), 128.2 ( $\text{CH}_{\text{arom}}$ ), 128.1 (d,  $J_{\text{C-P}} = 6.2$  Hz,  $\text{CH}_{\text{arom}}$ ), 127.2 (d,  $J_{\text{C-P}} = 7.5$  Hz,  $\text{CH}_{\text{arom}}$ ), 126.9 ( $\text{CH}_{\text{arom}}$ ), 126.2 (d,  $J_{\text{C-P}} = 33.0$  Hz,  $\text{CH}_{\text{arom}}$ ), 124.9 (d,  $J_{\text{C-P}} = 25.5$  Hz,  $\text{CH}_{\text{arom}}$ ), 124.6 (d,  $J_{\text{C-P}} = 5.1$  Hz,  $C_{\text{q arom}}$ ), 123.4 (d,  $J_{\text{C-P}} = 7.6$  Hz,  $\text{CH}_{\text{arom}}$ ), 123.1 (d,  $J_{\text{C-P}} = 1.9$  Hz,  $C_{\text{q arom}}$ ), 122.1 ( $\text{CH}_{\text{arom}}$ ), 75.0 (dd,  $^2J_{\text{C-P}} = 17.3$  Hz,  $^3J_{\text{C-P}} = 12.3$  Hz,  $\text{CH-OPO}_2$ ), 74.7 (bd,  $^3J_{\text{C-P}} = 3.0$  Hz,  $\text{CH}_2\text{-OMe}$ ), 58.9 (*Me*), 48.2 (dd,  $^1J_{\text{C-P}} = 15.1$  Hz,  $^3J_{\text{C-P}} = 6.6$  Hz,  $\text{CH-PPh}_2$ );  $^{31}\text{P}\{^1\text{H}\}$ -NMR (202 MHz,  $\text{CDCl}_3$ )  $\delta$  156.6 (bs, *P-O*), -4.5 (bs, *P-C*); MS HR-ESI [found 665.2028;  $\text{C}_{42}\text{H}_{35}\text{O}_4\text{P}_2$  ( $\text{M}+\text{H}$ ) $^+$  requires 665.2011];  $[\alpha]_{\text{D}}^{25} = 395.2$  ( $c = 0.60$  mg/100 mL, THF); M.p. 147.6-151.1  $^\circ\text{C}$ .

**(11bS)-4-((1R,2S)-1-(diphenylphosphino)-  
3-methoxy-1-phenylpropan-2-  
yloxy)dinaphtho[2,1-d:1',2'-  
f][1,3,2]dioxaphosphepine (125k).**



Phosphine-phosphite **125k** was obtained following the general procedure, starting from **118a** (0.233 g, 0.64 mmol), DABCO (0.158 g, 1.41 mmol),  $\text{NEt}_3$  (0.18 mL, 1.27 mmol) and the chlorophosphite derived from (*S*)-BINOL **130** (0.264 g, 0.70 mmol) as a white solid (0.279 g, 66% yield).  $^1\text{H-NMR}$  (500 MHz,  $\text{CDCl}_3$ )  $\delta$  7.99-7.92 (m, 3H,  $H_{\text{arom}}$ ), 7.82-7.75 (m, 3H,  $H_{\text{arom}}$ ), 7.54-7.41 (m, 8H,  $H_{\text{arom}}$ ), 7.30-7.04 (m, 13H,  $H_{\text{arom}}$ ), 4.52 (m, 1H,  $\text{CH-OPO}_2$ ), 3.78 (dd,  $^2J_{\text{H-P}} = ^3J_{\text{H-H}} = 4.2$  Hz, 1H,  $\text{CH-PPh}_2$ ), 3.30 (dd,  $^2J_{\text{H-H}} = 10.0$  Hz,  $^3J_{\text{H-H}} = 5.0$  Hz, 1H,  $\text{CHH-OMe}$ ), 3.28 (s, 3H, *Me*), 3.23 (dd,  $^2J_{\text{H-H}} = 10.0$  Hz,  $^3J_{\text{H-H}} = 7.2$  Hz, 1H,  $\text{CHH-OMe}$ );  $^{13}\text{C}\{^1\text{H}\}$ -NMR (125 MHz,  $\text{CDCl}_3$ )  $\delta$  148.2 (d,  $J_{\text{C-P}} = 4.5$  Hz,  $C_{\text{q arom}}$ ), 148.0 (d,  $J_{\text{C-P}} = 1.6$  Hz,  $C_{\text{q arom}}$ ), 136.8 (d,  $J_{\text{C-P}} = 11.1$  Hz,  $C_{\text{q arom}}$ ), 136.7 (d,  $J_{\text{C-P}} = 15.4$  Hz,  $C_{\text{q arom}}$ ), 136.0 (d,  $J_{\text{C-P}} = 17.5$  Hz,  $C_{\text{q arom}}$ ), 134.9 (d,  $J_{\text{C-P}} = 21.6$  Hz,  $\text{CH}_{\text{arom}}$ ), 133.3 (d,  $J_{\text{C-P}} = 19.1$  Hz,  $\text{CH}_{\text{arom}}$ ), 132.9 (d,  $J_{\text{C-P}} = 29.6$  Hz,  $C_{\text{q arom}}$ ), 131.4 (d,  $J_{\text{C-P}} = 46.1$  Hz,  $C_{\text{q arom}}$ ), 130.1 (d,  $J_{\text{C-P}} = 31.8$  Hz,  $\text{CH}_{\text{arom}}$ ), 129.5 ( $\text{CH}_{\text{arom}}$ ), 128.9 (d,  $J_{\text{C-P}} = 7.8$  Hz,  $\text{CH}_{\text{arom}}$ ), 128.5 ( $\text{CH}_{\text{arom}}$ ), 128.3 (d,  $J_{\text{C-P}} = 6.6$  Hz,  $\text{CH}_{\text{arom}}$ ), 128.1 ( $\text{CH}_{\text{arom}}$ ), 127.9 (d,  $J_{\text{C-P}} = 6.9$  Hz,  $\text{CH}_{\text{arom}}$ ), 127.2 (d,  $J_{\text{C-P}} = 19.1$  Hz,  $\text{CH}_{\text{arom}}$ ), 124.9 (d,  $J_{\text{C-P}} = 20.1$  Hz,  $\text{CH}_{\text{arom}}$ ), 124.7 (d,  $J_{\text{C-P}} = 5.2$  Hz,  $C_{\text{q arom}}$ ), 123.3 (d,  $J_{\text{C-P}} = 1.8$  Hz,  $C_{\text{q arom}}$ ), 122.4 ( $\text{CH}_{\text{arom}}$ ), 122.3 ( $\text{CH}_{\text{arom}}$ ), 74.8-74.7 (m,  $\text{CH}_2\text{-OMe}$  and  $\text{CH-OPO}_2$ ), 58.9 (*Me*), 48.0 (dd,  $^1J_{\text{C-P}} = 14.8$  Hz,  $^3J_{\text{C-P}} = 5.9$  Hz,  $\text{CH-PPh}_2$ );  $^{31}\text{P}\{^1\text{H}\}$ -NMR (202 MHz,  $\text{CDCl}_3$ )  $\delta$  156.2 (d,  $^4J_{\text{P-P}} = 11.4$  Hz, *P-O*), -5.5 (d,  $^4J_{\text{P-P}} = 11.4$  Hz, *P-C*); MS HR-ESI [found 665.2020;  $\text{C}_{42}\text{H}_{35}\text{O}_4\text{P}_2$  ( $\text{M}+\text{H}$ ) $^+$  requires 665.2020];  $[\alpha]_{\text{D}}^{25} = 161.9$  ( $c = 0.50$  mg/100 mL, THF); M.p. 103.4-108.7  $^\circ\text{C}$ .

### 1.3.6. General synthetic procedure for the preparation of [Rh(*P-OH*)(*nbd*)]BF<sub>4</sub> complexes **138a** and **138e**

The phosphine-borane complexes (**118**, 1.00 mmol) and diazabicyclo[2.2.2]octane (2.20 mmol) were charged in a flame-dried schlenk flask. Toluene (5.0 mL) was added. The reaction mixture was heated at 60 °C for 2h. After cooling down to room temperature, the solution was passed through a short SiO<sub>2</sub> pad (3.0 g) and further eluted with toluene (6.0 mL). Toluene was removed *in vacuo* to give the corresponding phosphino-alcohol as a white solid. Then, [Rh(*nbd*)<sub>2</sub>]BF<sub>4</sub> (0.98 mmol) and dry THF (8.0 mL) were added under argon into the schlenk flask. The reaction mixture was stirred at room temperature for 5h and THF was evaporated until 2 mL of the solvent were left. After the addition of *n*-pentane (8.0 mL) a precipitate was formed which was filtered off and washed with a small quantity of *n*-pentane (2 x 4.0 mL) to give the desired Rhodium complexes as a yellow-orange powder.

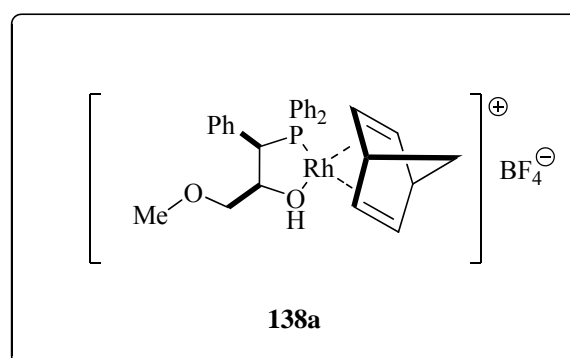
#### 1.3.6.1. Synthesis and general physical and spectroscopic data of [Rh(*P-OH*)(*nbd*)]BF<sub>4</sub> complexes **138a** and **138e**

##### [Rh(*P-OH*)(*nbd*)]BF<sub>4</sub> complex

(**138a**).<sup>138</sup> Rhodium complex **138a**

was obtained following the general procedure, starting from **118a** (0.164 g, 0.45 mmol), DABCO (0.111 g, 0.99 mmol) and [Rh(*nbd*)<sub>2</sub>]BF<sub>4</sub> (0.164 g, 0.44 mmol) as a yellow-

orange powder (0.101 g, 36% yield). <sup>1</sup>H-NMR (500 MHz, CD<sub>2</sub>Cl<sub>2</sub>) δ 8.04-8.01 (m, 2H, *H*<sub>arom</sub>), 7.76-7.63 (m, 5H, *H*<sub>arom</sub>), 7.41-7.18 (m, 5H, *H*<sub>arom</sub>), 6.91-6.88 (m,

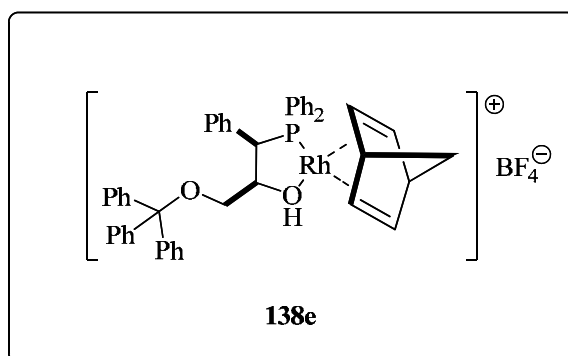


<sup>138</sup> The signals corresponding to the vinyl protons were not observed in the <sup>1</sup>H-NMR and <sup>13</sup>C{<sup>1</sup>H}-NMR spectra. Possibly, this indicates a fast exchange between them in the NMR time scale.

3H,  $H_{\text{arom}}$ ), 4.14 (bs, 2H, allylic CH, NBD), 4.12 (m, 1H, CH-OH-Rh), 3.79 (bd,  $^2J_{\text{H-P}} = 14.5$  Hz, 1H, CH-PPh<sub>2</sub>-Rh), 3.32 (dd,  $^2J_{\text{H-P}} = 9.0$  Hz,  $^3J_{\text{H-H}} = 6.5$  Hz, 1H, CHH-OMe), 3.18 (bs, 4H, CHH-OMe and Me) 1.61 (bs, 2H, CH<sub>2</sub>, NBD);  $^{13}\text{C}\{^1\text{H}\}$ -NMR (125 MHz, CD<sub>2</sub>Cl<sub>2</sub>)  $\delta$  133.9 (d,  $J_{\text{C-P}} = 13.1$  Hz, CH<sub>arom</sub>), 133.0 (d,  $J_{\text{C-P}} = 10.8$  Hz, CH<sub>arom</sub>), 132.7 ( $C_{\text{q}}$  arom), 132.0 (CH<sub>arom</sub>), 131.0 (CH<sub>arom</sub>), 130.9 (d,  $J_{\text{C-P}} = 6.2$  Hz, CH<sub>arom</sub>), 129.6 (d,  $J_{\text{C-P}} = 10.4$  Hz, CH<sub>arom</sub>), 129.3 ( $C_{\text{q}}$  arom), 128.9 (CH<sub>arom</sub>), 128.6 (d,  $J_{\text{C-P}} = 10.2$  Hz, CH<sub>arom</sub>), 128.0 (CH<sub>arom</sub>), 78.6 (d,  $^2J_{\text{C-P}} = 6.5$  Hz, CH-OH-Rh), 71.1 (d,  $^3J_{\text{C-P}} = 9.6$  Hz, CH<sub>2</sub>-O-Me), 64.8 (CH<sub>2</sub>, NBD), 58.9 (Me), 52.9 (allylic CH, NBD), 49.4 (d,  $^1J_{\text{C-P}} = 21.5$  Hz, CH-PPh<sub>2</sub>-Rh);  $^{31}\text{P}\{^1\text{H}\}$ -NMR (202 MHz, CD<sub>2</sub>Cl<sub>2</sub>)  $\delta$  48.2 (d,  $^1J_{\text{P-Rh}} = 173.1$  Hz, PPh<sub>2</sub>-Rh); MS HR-ESI [found 545.1140; C<sub>29</sub>H<sub>31</sub>O<sub>2</sub>PRh (M-BF<sub>4</sub>)<sup>+</sup> requires 545.1117].

### [Rh(P-OH)(nbd)]BF<sub>4</sub> complex

(**138e**). Rhodium complex **138e** was obtained following the general procedure, starting from **118e** (0.207 g, 0.35 mmol), DABCO (0.086 g, 0.77 mmol) and [Rh(nbd)<sub>2</sub>]BF<sub>4</sub> (0.129 g, 0.34 mmol) as a yellow-



orange powder (0.119 g, 39% yield).  $^1\text{H}$ -NMR (500 MHz, CD<sub>2</sub>Cl<sub>2</sub>)  $\delta$  8.02-7.99 (m, 2H,  $H_{\text{arom}}$ ), 7.72-7.57 (m, 3H,  $H_{\text{arom}}$ ), 7.35-6.82 (m, 25H,  $H_{\text{arom}}$ ), 5.88 (bs, 1H, CH=, NBD), 5.65 (bs, 1H, CH=, NBD), 4.11 (bs, 2H, allylic CH, NBD), 4.05 (bs, 1H, CH=, NBD), 4.00 (m, 1H, CH-OH-Rh), 3.90 (dd,  $^2J_{\text{H-P}} = 14.5$  Hz,  $^3J_{\text{H-H}} = 3.0$  Hz, 1H, CH-PPh<sub>2</sub>-Rh), 3.87 (bs, 1H, CH=, NBD), 3.43 (dd,  $^2J_{\text{H-H}} = 8.9$  Hz,  $^3J_{\text{H-H}} = 5.8$  Hz, 1H, CHH-OCPh<sub>3</sub>), 2.93 (dd,  $^2J_{\text{H-H}} = 8.9$  Hz,  $^3J_{\text{H-H}} = 8.8$  Hz, 1H, CHH-OCPh<sub>3</sub>), 1.58 (bs, 2H, CH<sub>2</sub>, NBD);  $^{13}\text{C}\{^1\text{H}\}$ -NMR (125 MHz, CD<sub>2</sub>Cl<sub>2</sub>)  $\delta$  143.4 ( $C_{\text{q}}$  arom), 133.8 (d,  $J_{\text{C-P}} = 12.8$  Hz, CH<sub>arom</sub>), 133.1 (d,  $J_{\text{C-P}} = 10.8$  Hz, CH<sub>arom</sub>), 132.5 ( $C_{\text{q}}$  arom), 132.0 (CH<sub>arom</sub>), 131.0 (d,  $J_{\text{C-P}} = 5.6$  Hz, CH<sub>arom</sub>), 130.9 (CH<sub>arom</sub>), 129.7 (d,  $J_{\text{C-P}} = 10.2$  Hz, CH<sub>arom</sub>), 128.7 (CH<sub>arom</sub>), 128.4 (d,  $J_{\text{C-P}} = 10.4$  Hz, CH<sub>arom</sub>), 128.3 (CH<sub>arom</sub>), 127.8 (CH<sub>arom</sub>), 127.1 (CH<sub>arom</sub>), 91.2 (bs, CH=, NBD),

88.9 (bs, CH=, NBD), 87.4 (O-CPh<sub>3</sub>), 79.0 (d, <sup>2</sup>J<sub>C-P</sub> = 7.9 Hz, CH-OH-Rh) 64.9 (CH<sub>2</sub>, NBD), 62.4 (d, <sup>3</sup>J<sub>C-P</sub> = 8.6 Hz, CH<sub>2</sub>-O-CPh<sub>3</sub>), 55.2 (bs, CH=, NBD), 52.9 (allylic CH, NBD), 51.7 (bs, CH=, NBD), 49.8 (d, <sup>1</sup>J<sub>C-P</sub> = 20.8 Hz, CH-PPh<sub>2</sub>-Rh); <sup>31</sup>P{<sup>1</sup>H}-NMR (202 MHz, CD<sub>2</sub>Cl<sub>2</sub>) δ 48.6 (d, <sup>1</sup>J<sub>P-Rh</sub> = 173.8 Hz, PPh<sub>2</sub>-Rh); MS HR-ESI [found 773.2086; C<sub>47</sub>H<sub>43</sub>O<sub>2</sub>PRh (M-BF<sub>4</sub>)<sup>+</sup> requires 773.2056].

### 1.3.7. General synthetic procedure for the preparation of [Rh(*P-OP*)(nbd)]BF<sub>4</sub> complexes **141c**, **142a**, **142h**, **142k** and **143**

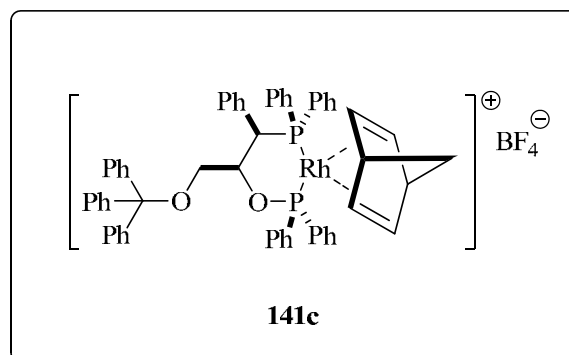
The chiral *P-OP* ligand (**124c**, **125a**, **125h** and **125k**, 1.00 mmol) and [Rh(nbd)<sub>2</sub>]BF<sub>4</sub> (0.98 mmol) were charged in a flame-dried schlenk flask. Dichloromethane (6.0 mL) was added. The reaction mixture was stirred at room temperature for 4h after which dichloromethane was evaporated to the fourth of the volume. After the addition of diethyl ether (15.0 mL) a precipitate was formed which was filtered off and washed with a small quantity of diethyl ether (2 x 5.0 mL) to give the desired Rhodium complexes as an orange powder.

#### 1.3.7.1. Synthesis and general physical and spectroscopic data of [Rh(*P-OP*)(nbd)]BF<sub>4</sub> complexes **141c**, **142a**, **142h**, **142k** and **143**

##### [Rh(*P-OP*)(nbd)]BF<sub>4</sub> (**141c**).

Rhodium complex **141c** was obtained following the general procedure, starting from **124c** (0.267 g, 0.35 mmol) and [Rh(nbd)<sub>2</sub>]BF<sub>4</sub> (0.129 g, 0.34 mmol) as an orange powder (0.189 g, 52% yield). <sup>1</sup>H-NMR (400

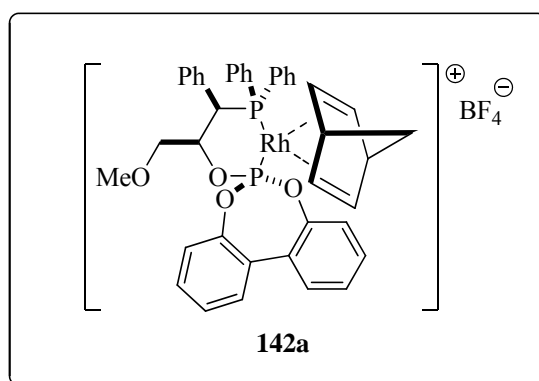
MHz, CD<sub>2</sub>Cl<sub>2</sub>) δ 8.10-8.05 (m, 2H, *H*<sub>arom</sub>), 7.84-7.08 (m, 2H, *H*<sub>arom</sub>), 7.71-7.08 (m, 34H, *H*<sub>arom</sub>), 6.65-6.61 (m, 2H, *H*<sub>arom</sub>), 5.53 (bs, 2H, CH=, NBD), 4.69 (bs,



1H, CH=, NBD), 4.49 (bs, 1H, CH=, NBD), 4.43 (bs, 1H, allylic CH, NBD), 4.32 (bd,  $^1J_{C-P}$  = 15.6 Hz, 1H, CH-PPh<sub>2</sub>), 4.01 (bs, 1H, allylic CH, NBD), 3.95 (m, 1H, CH-OPPh<sub>2</sub>-Rh), 3.16 (ddd,  $^2J_{H-H}$  = 9.2 Hz,  $^3J_{H-H}$  = 4.8 Hz,  $^4J_{H-P}$  = 2.3 Hz, 1H, CHH-OCPh<sub>3</sub>), 2.94 (dd,  $^2J_{H-H}$  =  $^3J_{H-H}$  = 9.2 Hz, 1H, CHH-OCPh<sub>3</sub>), 1.82 (d,  $^2J_{H-H}$  = 7.8 Hz, 1H, CHH, NBD), 1.75 (d,  $^2J_{H-H}$  = 7.8 Hz, 1H, CHH, NBD);  $^{13}C\{^1H\}$ -NMR (100 MHz, CD<sub>2</sub>Cl<sub>2</sub>)  $\delta$  143.2 (C<sub>q</sub> arom), 135.6 (d,  $J_{C-P}$  = 13.1 Hz, CH<sub>arom</sub>), 133.2 (CH<sub>arom</sub>), 132.9 (d,  $J_{C-P}$  = 15.7 Hz, CH<sub>arom</sub>), 132.8 (CH<sub>arom</sub>), 132.5 (C<sub>q</sub> arom), 132.2 (C<sub>q</sub> arom), 132.1 (d,  $J_{C-P}$  = 2.2 Hz, C<sub>q</sub> arom), 131.8 (d,  $J_{C-P}$  = 9.1 Hz, CH<sub>arom</sub>), 131.3 (CH<sub>arom</sub>), 130.7 (CH<sub>arom</sub>), 129.7 (d,  $J_{C-P}$  = 10.6 Hz, CH<sub>arom</sub>), 129.5 (d,  $J_{C-P}$  = 11.2 Hz, CH<sub>arom</sub>), 129.2 (CH<sub>arom</sub>), 129.1 (CH<sub>arom</sub>), 129.0 (CH<sub>arom</sub>), 128.9 (CH<sub>arom</sub>), 128.7 (d,  $J_{C-P}$  = 9.8 Hz, CH<sub>arom</sub>), 128.2 (CH<sub>arom</sub>), 127.9 (CH<sub>arom</sub>), 127.3 (CH<sub>arom</sub>), 93.6 (bs, CH=, NBD), 93.5 (bs, CH=, NBD), 90.8 (bs, CH=, NBD), 87.7 (O-CPh<sub>3</sub>), 85.8 (bs, CH=, NBD), 74.9 (allylic CH, NBD), 74.4 (bs, CH<sub>2</sub>OPPh<sub>2</sub>), 71.3 (CH<sub>2</sub>, NBD), 63.0 (dd,  $^3J_{C-P}$  =  $^3J_{C-P}$  = 7.8 Hz, CH<sub>2</sub>-O-CPh<sub>3</sub>), 55.4 (allylic CH, NBD), 41.7 (d,  $^1J_{C-P}$  = 29.8 Hz, CH-PPh<sub>2</sub>-Rh);  $^{31}P\{^1H\}$ -NMR (162 MHz, CD<sub>2</sub>Cl<sub>2</sub>)  $\delta$  128.8 (dd,  $^1J_{P-Rh}$  = 174.2 Hz,  $^2J_{P-P}$  = 47.8 Hz, P-O), 26.0 (dd,  $^1J_{P-Rh}$  = 152.4 Hz,  $^2J_{P-P}$  = 47.8 Hz, P-C); MS HR-ESI [found 957.2525; C<sub>59</sub>H<sub>52</sub>O<sub>2</sub>P<sub>2</sub>Rh (M-BF<sub>4</sub>)<sup>+</sup> requires 957.2498].

#### [Rh(P-OP)(nbd)]BF<sub>4</sub> (142a).

Rhodium complex **142a** was obtained following the general procedure, starting from **125a** (0.056 g, 0.10 mmol) and [Rh(nbd)<sub>2</sub>]<sup>+</sup>BF<sub>4</sub><sup>-</sup> (0.037 g, 0.098 mmol) as an orange powder (0.042 g, 50% yield).  $^1H$ -



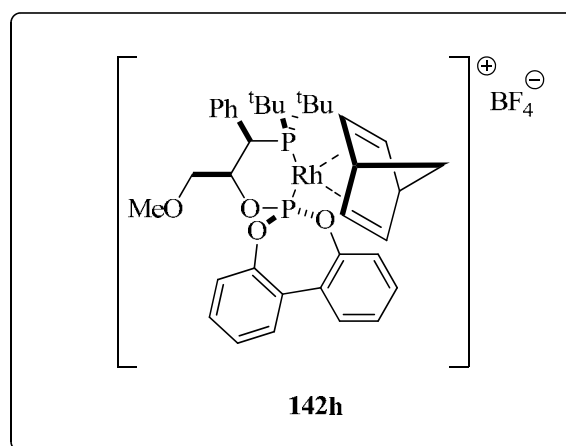
NMR (500 MHz, CD<sub>2</sub>Cl<sub>2</sub>)  $\delta$  8.04-8.00 (m, 2H, H<sub>arom</sub>), 7.81-7.79 (m, 3H, H<sub>arom</sub>), 7.65-7.35 (m, 14H, H<sub>arom</sub>), 7.29-7.25 (m, 2H, H<sub>arom</sub>), 6.92-6.88 (m, 3H, H<sub>arom</sub>), 5.72 (bs, 1H, CH=, NBD), 5.36-5.27 (bs, 3H, CH=, NBD), 4.80 (m, 1H, CH-OPO<sub>2</sub>-Rh), 4.22 (d,  $^1J_{H-P}$  = 15.5 Hz, 1H, CH-PPh<sub>2</sub>-Rh), 4.20 (bs, 1H, allylic CH,



NBD), 4.15 (bs, 1H, allylic CH, NBD), 3.21 (dd,  $^2J_{\text{H-H}} = 9.8$  Hz,  $^3J_{\text{H-H}} = 8.0$  Hz, 1H, CHH-OMe), 3.19 (s, 3H, Me), 3.16 (dd,  $^2J_{\text{H-H}} = 9.8$  Hz,  $^3J_{\text{H-H}} = 6.2$  Hz, 1H, CHH-OMe), 1.80 (bs, 1H, CHH, NBD), 1.73 (bs, 1H, CHH, NBD);  $^{13}\text{C}\{^1\text{H}\}$ -NMR (125 MHz,  $\text{CD}_2\text{Cl}_2$ )  $\delta$  148.3 (d,  $J_{\text{C-P}} = 10.4$  Hz,  $\text{C}_{\text{q arom}}$ ), 147.7 (d,  $J_{\text{C-P}} = 10.0$  Hz,  $\text{C}_{\text{q arom}}$ ), 134.1 (d,  $J_{\text{C-P}} = 12.1$  Hz,  $\text{CH}_{\text{arom}}$ ), 133.4 (d,  $J_{\text{C-P}} = 10.8$  Hz,  $\text{CH}_{\text{arom}}$ ), 132.8 (d,  $J_{\text{C-P}} = 1.9$  Hz,  $\text{CH}_{\text{arom}}$ ), 131.8 ( $\text{C}_{\text{q arom}}$ ), 131.5 (d,  $J_{\text{C-P}} = 2.4$  Hz,  $\text{CH}_{\text{arom}}$ ), 131.5 (d,  $J_{\text{C-P}} = 2.4$  Hz,  $\text{CH}_{\text{arom}}$ ), 130.6 ( $\text{CH}_{\text{arom}}$ ), 130.3 ( $\text{CH}_{\text{arom}}$ ), 130.1 ( $\text{CH}_{\text{arom}}$ ), 130.1 (d,  $J_{\text{C-P}} = 10.0$  Hz,  $\text{CH}_{\text{arom}}$ ), 129.5 ( $\text{C}_{\text{q arom}}$ ), 129.2 (d,  $J_{\text{C-P}} = 1.6$  Hz,  $\text{C}_{\text{q arom}}$ ), 129.1 (d,  $J_{\text{C-P}} = 3.1$  Hz,  $\text{C}_{\text{q arom}}$ ), 129.0 ( $\text{CH}_{\text{arom}}$ ), 128.9 ( $\text{CH}_{\text{arom}}$ ), 128.8 ( $\text{CH}_{\text{arom}}$ ), 128.7 (d,  $J_{\text{C-P}} = 2.2$  Hz,  $\text{CH}_{\text{arom}}$ ), 127.0 (d,  $J_{\text{C-P}} = 16.6$  Hz,  $\text{CH}_{\text{arom}}$ ), 121.7 (d,  $J_{\text{C-P}} = 2.8$  Hz,  $\text{CH}_{\text{arom}}$ ), 121.6 (d,  $J_{\text{C-P}} = 2.2$  Hz,  $\text{CH}_{\text{arom}}$ ), 101.8 ( $\text{CH} =$ , NBD), 100.9 ( $\text{CH} =$ , NBD), 89.8 ( $\text{CH} =$ , NBD), 89.2 ( $\text{CH} =$ , NBD), 76.7 (d,  $^2J_{\text{C-P}} = 7.2$  Hz,  $\text{CH-OPO}_2\text{-Rh}$ ), 72.2 ( $\text{CH}_2$ , NBD), 71.6 (dd,  $^3J_{\text{C-P}} = ^3J_{\text{C-P}} = 8.7$  Hz,  $\text{CH}_2\text{-OMe}$ ), 58.9 (Me), 55.6 (allylic CH, NBD), 55.4 (allylic CH, NBD), 43.5 (d,  $^1J_{\text{C-P}} = 28.1$  Hz,  $\text{CH-PPH}_2\text{-Rh}$ );  $^{31}\text{P}\{^1\text{H}\}$ -NMR (202 MHz,  $\text{CD}_2\text{Cl}_2$ )  $\delta$  135.7 (dd,  $^1J_{\text{P-Rh}} = 266.5$  Hz,  $^2J_{\text{P-P}} = 66.5$  Hz, P-O), 30.2 (dd,  $^1J_{\text{P-Rh}} = 145.5$  Hz,  $^2J_{\text{P-P}} = 66.5$  Hz, P-C); MS HR-ESI [found 759.1276;  $\text{C}_{41}\text{H}_{38}\text{O}_4\text{P}_2\text{Rh}$  ( $\text{M-BF}_4$ ) $^+$  requires 759.1300].

**[Rh(P-OP)(nbd)]BF<sub>4</sub> (142h).**

Rhodium complex **142h** was obtained following the general procedure, starting from **125h** (0.330 g, 80% purity, 0.50 mmol) and  $[\text{Rh}(\text{nbd})_2]\text{BF}_4$  (0.183 g, 0.49 mmol) as an orange powder (0.100 g, 22% yield).  $^1\text{H}$ -NMR (500 MHz,

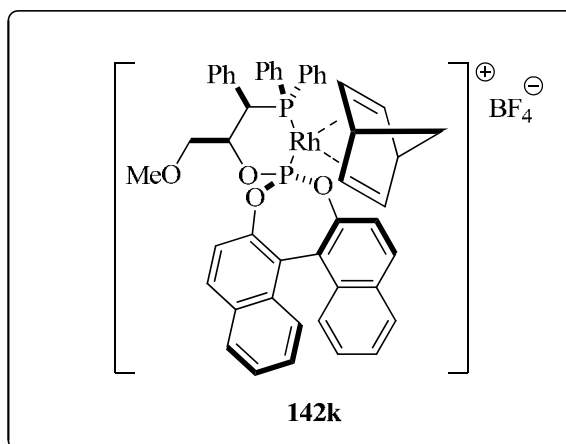


$\text{CD}_2\text{Cl}_2$ )  $\delta$  7.91 (d,  $^3J_{\text{H-H}} = 8.0$  Hz, 1H,  $H_{\text{arom}}$ ), 7.65-7.31 (m, 12H,  $H_{\text{arom}}$ ), 6.49 (bs, 2H,  $\text{CH} =$ , NBD), 5.34 (bs, 1H,  $\text{CH} =$ , NBD), 5.05 (m, 1H,  $\text{CH-OPO}_2\text{-Rh}$ ), 4.76 (bs, 1H,  $\text{CH} =$ , NBD), 4.16 (bs, 1H, allylic CH, NBD), 4.09 (bs, 1H, allylic CH, NBD), 3.83 (d,  $^2J_{\text{H-P}} = 13.0$  Hz, 1H,  $\text{CH-P}^t\text{Bu}_2\text{-Rh}$ ), 3.36 (ddd,  $^2J_{\text{H-H}} = 9.5$  Hz,  $^3J_{\text{H-}}$

$^1\text{H}$  = 6.2 Hz,  $^4J_{\text{H-P}} = 2.0$  Hz, 1H, CHH-OMe), 3.28 (s, 3H, Me), 3.18 (dd,  $^2J_{\text{H-H}} = ^3J_{\text{H-H}} = 9.5$  Hz, 1H, CHH-OMe), 1.90 (d,  $^2J_{\text{H-H}} = 9.2$  Hz, 1H, CHH, NBD), 1.82 (d,  $^2J_{\text{H-H}} = 9.2$  Hz, 1H, CHH, NBD), 1.62 (d,  $^3J_{\text{H-P}} = 13.8$  Hz, 9H, 3Me,  $^t\text{Bu}_2\text{P}$ ), 1.28 (d,  $^3J_{\text{H-P}} = 13.8$  Hz, 9H, 3Me,  $^t\text{Bu}_2\text{P}$ );  $^{13}\text{C}\{^1\text{H}\}$ -NMR (125 MHz,  $\text{CD}_2\text{Cl}_2$ )  $\delta$  148.4 (d,  $^2J_{\text{C-P}} = 12.5$  Hz,  $C_{\text{q arom}}$ ), 148.2 (d,  $^2J_{\text{C-P}} = 7.6$  Hz,  $C_{\text{q arom}}$ ), 132.5 (d,  $^2J_{\text{C-P}} = 3.4$  Hz,  $C_{\text{q arom}}$ ), 132.4 (d,  $^3J_{\text{C-P}} = 4.1$  Hz,  $\text{CH}_{\text{arom}}$ ), 131.7 ( $\text{CH}_{\text{arom}}$ ), 130.7 ( $\text{CH}_{\text{arom}}$ ), 130.6 ( $\text{CH}_{\text{arom}}$ ), 130.2 ( $\text{CH}_{\text{arom}}$ ), 130.0 ( $\text{CH}_{\text{arom}}$ ), 129.4 ( $C_{\text{q arom}}$ ), 129.1 (d,  $^3J_{\text{C-P}} = 1.4$  Hz,  $C_{\text{q arom}}$ ), 128.7 ( $\text{CH}_{\text{arom}}$ ), 128.6 ( $\text{CH}_{\text{arom}}$ ), 128.4 ( $\text{CH}_{\text{arom}}$ ), 127.1 ( $\text{CH}_{\text{arom}}$ ), 126.8 ( $\text{CH}_{\text{arom}}$ ), 121.8 ( $\text{CH}_{\text{arom}}$ ), 121.8 ( $\text{CH}_{\text{arom}}$ ), 121.6 ( $\text{CH}_{\text{arom}}$ ), 121.5 ( $\text{CH}_{\text{arom}}$ ), 105.1 (dd,  $^1J_{\text{C-Rh}} = 12.1$  Hz,  $^2J_{\text{C-P}} = 3.6$  Hz,  $\text{CH}=\text{, NBD}$ ), 103.9 (dd,  $^1J_{\text{C-Rh}} = 12.9$  Hz,  $^2J_{\text{C-P}} = 3.6$  Hz,  $\text{CH}=\text{, NBD}$ ), 81.5 (ddd,  $^1J_{\text{C-Rh}} = ^2J_{\text{C-P}} = 7.6$  Hz,  $^2J_{\text{C-P}} = 2.2$  Hz,  $\text{CH}=\text{, NBD}$ ), 80.6 (dd,  $^2J_{\text{C-P}} = ^2J_{\text{C-P}} = 9.1$  Hz,  $\text{CH-O-PO}_2\text{-Rh}$ ), 79.4 (ddd,  $^1J_{\text{C-Rh}} = ^2J_{\text{C-P}} = 7.5$  Hz,  $^2J_{\text{C-P}} = 1.8$  Hz,  $\text{CH}=\text{, NBD}$ ), 73.1 (bs,  $\text{CH}_2\text{, NBD}$ ), 71.7 (dd,  $^3J_{\text{C-P}} = ^3J_{\text{C-P}} = 9.1$  Hz,  $\text{CH}_2\text{-OMe}$ ), 59.0 (Me), 54.7 (allylic CH, NBD), 54.0 (allylic CH, NBD), 40.8 (d,  $^1J_{\text{C-P}} = 9.9$  Hz,  $C_{\text{q, } ^t\text{BuP-Rh}}$ ), 40.4 (d,  $^1J_{\text{C-P}} = 11.6$  Hz,  $\text{CH- } ^t\text{BuP-Rh}$ ), 40.2 (d,  $^1J_{\text{C-P}} = 9.9$  Hz,  $C_{\text{q, } ^t\text{BuP-Rh}}$ ), 31.8 (d,  $^2J_{\text{C-P}} = 4.4$  Hz, 3Me,  $^t\text{Bu}_2\text{P}$ ), 30.9 (d,  $^2J_{\text{C-P}} = 4.4$  Hz, 3Me,  $^t\text{Bu}_2\text{P}$ );  $^{31}\text{P}\{^1\text{H}\}$ -NMR (202 MHz,  $\text{CD}_2\text{Cl}_2$ )  $\delta$  138.6 (dd,  $^1J_{\text{P-Rh}} = 276.7$  Hz,  $^2J_{\text{P-P}} = 54.6$  Hz,  $\text{P-O}$ ), 65.1 (dd,  $^1J_{\text{P-Rh}} = 138.9$  Hz,  $^2J_{\text{P-P}} = 54.6$  Hz,  $\text{P-C}$ ); MS HR-ESI [found 719.1895;  $\text{C}_{37}\text{H}_{46}\text{O}_4\text{P}_2\text{Rh}$  ( $\text{M-BF}_4$ ) $^+$  requires 719.1926].

### [Rh(*P-OP*)(nbd)]BF<sub>4</sub> (142k).

Rhodium complex **142k** was obtained following the general procedure, starting from **125k** (0.213 g, 0.32 mmol) and [Rh(nbd)<sub>2</sub>]**BF**<sub>4</sub> (0.117 g, 0.31 mmol) as an orange powder (0.160 g, 53% yield).  $^1\text{H}$ -NMR (500 MHz,  $\text{CD}_2\text{Cl}_2$ )  $\delta$  8.39 (d,



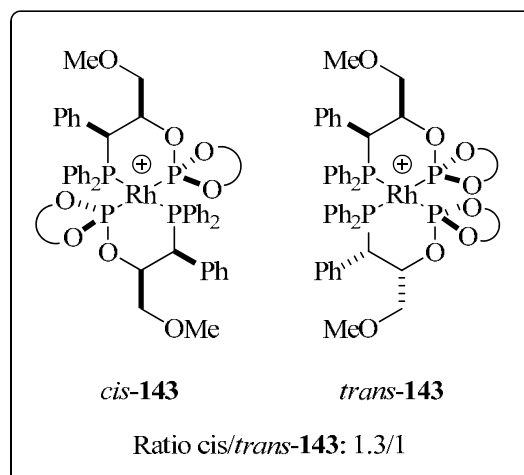
$^3J_{\text{H-H}} = 8.5$  Hz, 1H,  $H_{\text{arom}}$ ), 8.17 (d,  $^3J_{\text{H-H}} = 8.5$  Hz, 1H,  $H_{\text{arom}}$ ), 8.06-7.98 (m, 3H,

$H_{\text{arom}}$ ), 7.68-7.11 (m, 22H,  $H_{\text{arom}}$ ), 5.72 (bs, 1H, CH=, NBD), 5.52 (bs, 1H, CH=, NBD), 5.37 (m, 1H, CH-OPO<sub>2</sub>-Rh), 5.05 (bs, 1H, CH=, NBD), 4.80 (bs, 1H, CH=, NBD), 4.25 (d,  $^1J_{\text{H-P}} = 14.0$  Hz, 1H, CH-PPh<sub>2</sub>-Rh), 4.15 (bs, 1H, allylic CH, NBD), 4.04 (bs, 1H, allylic CH, NBD), 3.35 (s, 3H, Me), 3.29 (m, 2H, CH<sub>2</sub>-OMe), 1.69 (bs, 2H, CH<sub>2</sub>, NBD);  $^{13}\text{C}\{^1\text{H}\}$ -NMR (125 MHz, CD<sub>2</sub>Cl<sub>2</sub>)  $\delta$  146.5 (d,  $J_{\text{C-P}} = 12.2$  Hz,  $C_{\text{q arom}}$ ), 146.1 (d,  $J_{\text{C-P}} = 5.4$  Hz,  $C_{\text{q arom}}$ ), 135.7 (d,  $J_{\text{C-P}} = 13.0$  Hz, CH<sub>arom</sub>), 132.6 ( $C_{\text{q arom}}$ ), 132.3 ( $C_{\text{q arom}}$ ), 132.2 (CH<sub>arom</sub>), 132.0 ( $C_{\text{q arom}}$ ), 131.9 (d,  $J_{\text{C-P}} = 9.9$  Hz, CH<sub>arom</sub>), 131.8 ( $C_{\text{q arom}}$ ), 131.7 (CH<sub>arom</sub>), 131.0 (CH<sub>arom</sub>), 130.9 (CH<sub>arom</sub>), 130.4 ( $C_{\text{q arom}}$ ), 130.1 ( $C_{\text{q arom}}$ ), 129.9 (d,  $J_{\text{C-P}} = 10.1$  Hz, CH<sub>arom</sub>), 128.9 (CH<sub>arom</sub>), 128.8 (CH<sub>arom</sub>), 128.5 (CH<sub>arom</sub>), 128.0 (CH<sub>arom</sub>), 127.6 ( $C_{\text{q arom}}$ ), 127.2 (d,  $J_{\text{C-P}} = 22.4$  Hz, CH<sub>arom</sub>), 126.9 (CH<sub>arom</sub>), 126.6 (CH<sub>arom</sub>), 126.3 (CH<sub>arom</sub>), 126.0 (CH<sub>arom</sub>), 123.0 ( $C_{\text{q arom}}$ ), 122.0 ( $C_{\text{q arom}}$ ), 120.7 (CH<sub>arom</sub>), 120.5 (CH<sub>arom</sub>), 104.4 (CH=, NBD), 100.5 (CH=, NBD), 91.0 (CH=, NBD), 88.4 (CH=, NBD), 79.4 (dd,  $^2J_{\text{C-P}} = ^2J_{\text{C-P}} = 8.6$  Hz, CH-OPO<sub>2</sub>-Rh), 72.3 (CH<sub>2</sub>, NBD), 72.2 (dd,  $^3J_{\text{C-P}} = ^3J_{\text{C-P}} = 10.1$  Hz, CH<sub>2</sub>-OMe), 58.9 (Me), 55.9 (allylic CH, NBD), 55.3 (allylic CH, NBD), 45.1 (d,  $^1J_{\text{C-P}} = 26.5$  Hz, CH-PPh<sub>2</sub>-Rh);  $^{31}\text{P}\{^1\text{H}\}$ -NMR (202 MHz, CD<sub>2</sub>Cl<sub>2</sub>)  $\delta$  138.9 (dd,  $^1J_{\text{P-Rh}} = 268.0$  Hz,  $^2J_{\text{P-P}} = 65.4$  Hz, P-O), 35.3 (dd,  $^1J_{\text{P-Rh}} = 144.1$  Hz,  $^2J_{\text{P-P}} = 65.4$  Hz, P-C); MS HR-ESI [found 859.1589; C<sub>49</sub>H<sub>42</sub>O<sub>4</sub>P<sub>2</sub>Rh (M-BF<sub>4</sub>)<sup>+</sup> requires 859.1613].

***cis/trans*-[Rh(P-OP)<sub>2</sub>]BF<sub>4</sub> (143).**

Rhodium complex **143**, as a *cis/trans* isomers mixture (1.3/1), was obtained following the general procedure, starting from **125a** (0.050 g, 0.09 mmol) and [Rh(nbd)<sub>2</sub>]BF<sub>4</sub> (0.016 g, 0.04 mmol) as a yellow powder (0.026 g, 48% yield).  $^1\text{H}$ -NMR (400 MHz, CD<sub>2</sub>Cl<sub>2</sub>); *cis*-**143**  $\delta$  8.39-8.35 (m, 2H,  $H_{\text{arom}}$ ), 7.89-6.86 (m,

38H,  $H_{\text{arom}}$ ), 6.38-6.32 (m, 3H,  $H_{\text{arom}}$ ), 6.01-5.93 (m, 3H,  $H_{\text{arom}}$ ), 4.77 (m, 2H, 2 x



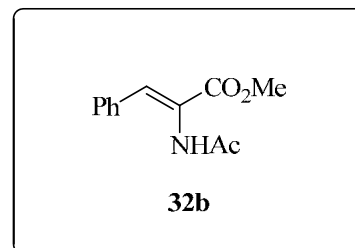
*CH*-OPO<sub>2</sub>-Rh), 4.09 (bs, 2H, 2 x *CH*-PPh<sub>2</sub>-Rh), 3.02 (dd, <sup>2</sup>*J*<sub>H-H</sub> = 10.0 Hz, <sup>3</sup>*J*<sub>H-H</sub> = 7.2 Hz, 2H, 2 x *CHH*-OMe), 2.92 (s, 6H, 2 x *Me*), 2.88 (dd, <sup>2</sup>*J*<sub>H-H</sub> = 10.0 Hz, <sup>3</sup>*J*<sub>H-H</sub> = 7.2 Hz, 2H, 2 x *CHH*-OMe); *trans*-**143** δ 8.39-8.35 (m, 2H, *H*<sub>arom</sub>), 7.89-6.86 (m, 38H, *H*<sub>arom</sub>), 6.38-6.32 (m, 3H, *H*<sub>arom</sub>), 6.01-5.93 (m, 3H, *H*<sub>arom</sub>), 4.26 (m, 2H, 2 x *CH*-OPO<sub>2</sub>-Rh), 3.57 (bd, <sup>2</sup>*J*<sub>H-P</sub> = 18.0 Hz, 2H, 2 x *CH*-PPh<sub>2</sub>-Rh), 2.90 (s, 6H, 2 x *Me*), 2.88 (dd, <sup>2</sup>*J*<sub>H-H</sub> = 8.4 Hz, <sup>3</sup>*J*<sub>H-H</sub> = 5.8 Hz, 2H, 2 x *CHH*-OMe), 2.80 (dd, <sup>2</sup>*J*<sub>H-H</sub> = 8.4 Hz, <sup>3</sup>*J*<sub>H-H</sub> = 5.8 Hz, 2H, 2 x *CHH*-OMe); <sup>13</sup>C{<sup>1</sup>H}-NMR (100 MHz, CD<sub>2</sub>Cl<sub>2</sub>); *cis*-**143** δ 149.1-120.7 (m, *C*<sub>q</sub> *arom* and *CH*<sub>arom</sub>), 75.6 (bs, 2 x *CH*-OPO<sub>2</sub>-Rh), 72.2 (bs, 2 x *CH*<sub>2</sub>-OMe), 58.7 (2 x *Me*), 43.3 (d, <sup>1</sup>*J*<sub>C-P</sub> = 13.8 Hz, 1 x *CH*-PPh<sub>2</sub>-Rh), 43.1 (d, <sup>1</sup>*J*<sub>C-P</sub> = 13.8 Hz, 1 x *CH*-PPh<sub>2</sub>-Rh); *trans*-**143** δ 149.1-120.7 (m, *C*<sub>q</sub> *arom* and *CH*<sub>arom</sub>), 73.8 (bs, 2 x *CH*-OPO<sub>2</sub>-Rh), 72.1 (bs, 2 x *CH*<sub>2</sub>-OMe), 58.7 (2 x *Me*), 44.4 (d, <sup>1</sup>*J*<sub>C-P</sub> = 27.0 Hz, 2 x *CH*-PPh<sub>2</sub>-Rh); <sup>31</sup>P{<sup>1</sup>H}-NMR (162 MHz, CD<sub>2</sub>Cl<sub>2</sub>) *cis*-**143** δ 146.7 (dt, <sup>1</sup>*J*<sub>P-Rh</sub> = 212.5 Hz, <sup>2</sup>*J*<sub>P-P</sub> = 56.5 Hz, *P*-O), 28.1 (dt, <sup>1</sup>*J*<sub>P-Rh</sub> = 125.7 Hz, <sup>2</sup>*J*<sub>P-P</sub> = 56.5 Hz, *P*-C); *trans*-**143** δ 143.9 (m, <sup>1</sup>*J*<sub>P-Rh</sub> = 215.7 Hz, <sup>2</sup>*J*<sub>P-P</sub> = 377.6, 70.5, 47.1, 39.2 Hz, *P*-O), 22.5 (m, <sup>1</sup>*J*<sub>P-Rh</sub> = 116.8 Hz, *J*<sub>P-P</sub> = 377.6, 70.5, 47.1, 39.2 Hz, *P*-C); MS HR-ESI [found 1231.2296; C<sub>60</sub>H<sub>68</sub>O<sub>8</sub>P<sub>4</sub>Rh (M-BF<sub>4</sub>)<sup>+</sup> requires 1231.2294].

### 1.3.8. General synthetic procedure of substrates **32b** and **144c-y**

#### 1.3.8.1. Synthesis and general spectroscopic data of substrate **32b**

##### (*Z*)-methyl 2-acetamido-3-phenylacrylate (**32b**).

To a three-necked 250 mL flask, equipped with a reflux condenser and an addition funnel, was dissolved  $\alpha$ -acetoamidocinnamic acid (2.932 g, 14.0 mmol) in 40.0 mL of THF. Diazomethane was added



dropwise over the stirred reaction mixture at room temperature. The reaction was monitorized by TLC. When all the starting material was consumed, the excess of diazomethane was eliminated bubling nitrogen through the reaction mixture. After this, the solution was concentrated *in vacuo* and purified by flash chromatography on SiO<sub>2</sub> using hexane: AcOEt as eluent (100:0-30:70) to give **32b** (2.625 g, 85% yield) as a white solid. <sup>1</sup>H-NMR (400 MHz, CDCl<sub>3</sub>)  $\delta$  7.45-7.18 (m, 7H,  $H_{\text{arom}}$ , CH= and NHAc), 3.83 (s, 3H, CO<sub>2</sub>Me), 2.10 (s, 3H, Me, NHAc).

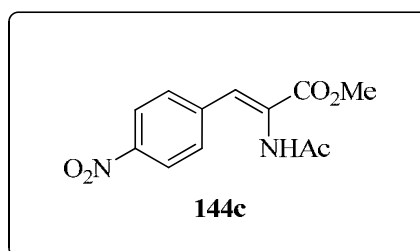
#### 1.3.8.2. Synthesis and general spectroscopic data of substrates **144c-g**

A mixture of *N*-acetyl glycine (8.45 mmol), anhydrous sodium acetate (6.34 mmol), the substituted benzaldehyde (12.68 mmol) and acetic anhydride (21.13 mmol) were placed in a flame-dried bottom-flask. The flask was warmed with occasional stirring until solution is complete. The resulting solution was refluxed for 1h, cooled and placed in a refrigerator overnight. The resulting slurry was treated with cold water (30.0 mL) to yield the corresponding methyl derivatives of (*Z*)-4-benzylideneoxolin-5-one (**147c-g**) as a brown solid. The solid was filtered and washed thoroughly with cold water and dried in a vacuum desiccator over phosphorus pentoxide and KOH. To a solution of **147c-g** (8.45 mmol) in toluene (9.0 mL) was cannulated a solution of NaOMe (8.45 mmol) in 5.0 mL of

MeOH. The reaction mixture was kept at 0-5 °C during the addition and was then allowed to warm to room temperature. Acidification with 4.0 mL of 1N hydrochloric acid yielded to a solid identified as **144c-g** which was recrystallized from hexane:AcOEt (50:50).

**(Z)-methyl 2-acetamido-3-(4-nitrophenyl)acrylate (144c).**

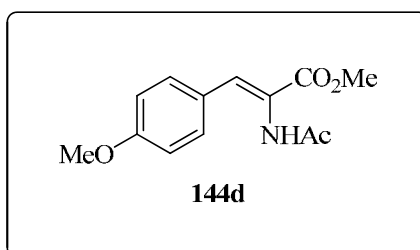
Substrate **144c** was obtained following the general procedure, starting from *N*-acetyl glycine (1.000 g, 8.45 mmol), anhydrous sodium acetate (0.525 g,



6.34 mmol), 4-nitrobenzaldehyde (1.936 g, 12.68 mmol), acetic anhydride (2.0 mL, 21.13 mmol) and then with NaOMe (0.481 g, 8.45 mmol) as a white solid (0.400 g, 18 % yield). <sup>1</sup>H-NMR (400 MHz, CDCl<sub>3</sub>) δ 8.20 (d, sist. AB, <sup>3</sup>J<sub>H-H</sub>= 8.6 Hz, 2H, *H*<sub>arom</sub>), 7.54 (d, sist. AB, <sup>3</sup>J<sub>H-H</sub>= 8.6 Hz, 2H, *H*<sub>arom</sub>), 7.40 (s, 1H, CH=), 7.34 (bs, 1H, NHAc), 3.90 (s, 3H, CO<sub>2</sub>Me), 2.14 (s, 3H, Me, NHAc).

**(Z)-methyl 2-acetamido-3-(4-methoxyphenyl)acrylate (144d).**

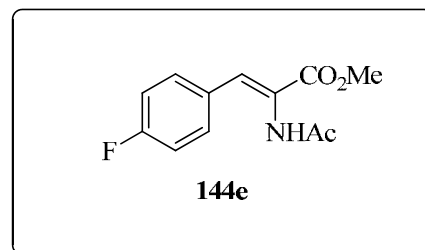
Substrate **144d** was obtained following the general procedure, starting from *N*-acetyl glycine (5.000 g, 42.27 mmol), anhydrous sodium



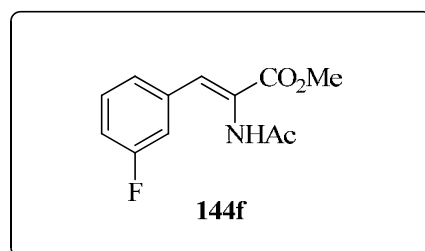
acetate (2.627 g, 31.70 mmol), 4-methoxybenzaldehyde (7.9 mL, 63.41 mmol), acetic anhydride (10.0 mL, 105.68 mmol) and then with NaOMe (2.404 g, 42.27 mmol) as a white solid (1.349 g, 13% yield). <sup>1</sup>H-NMR (400 MHz, CDCl<sub>3</sub>) δ 7.44 (d, sist. AB, <sup>3</sup>J<sub>H-H</sub>= 8.4 Hz, 2H, *H*<sub>arom</sub>), 7.39 (s, 1H, CH=), 7.08 (bs, 1H, NHAc), 6.87 (d, sist. AB, <sup>3</sup>J<sub>H-H</sub>= 8.2 Hz, 2H, *H*<sub>arom</sub>), 3.81 (s, 6H, MeO-Ph and CO<sub>2</sub>Me), 2.14 (s, 3H, Me, NHAc).

**(Z)-methyl 2-acetamido-3-(4-****fluorophenyl)acrylate (144e).**

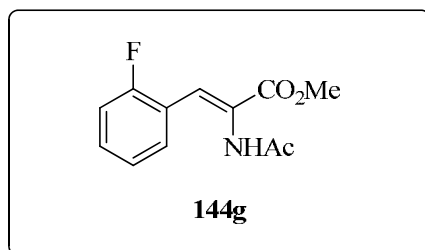
Substrate **144e** was obtained following the general procedure, starting from *N*-acetyl glycine (2.000 g, 16.91 mmol), anhydrous sodium acetate (1.051 g, 12.68 mmol), 4-fluorobenzaldehyde (2.8 mL, 25.36 mmol), acetic anhydride (4.0 mL, 42.27 mmol) and then with NaOMe (0.961 g, 16.91 mmol) as a white solid (1.710 g, 43% yield).  $^1\text{H-NMR}$  (400 MHz,  $\text{CDCl}_3$ )  $\delta$  7.44 (bs, sist. AB, 2H,  $H_{\text{arom}}$ ), 7.37 (s, 1H,  $\text{CH=}$ ), 7.16 (bs, 1H,  $\text{NHAc}$ ), 7.04 (dd, sist. AB,  $^3J_{\text{H-H}} = ^3J_{\text{H-H}} = 8.2$  Hz, 2H,  $H_{\text{arom}}$ ), 3.83 (s, 3H,  $\text{CO}_2\text{Me}$ ), 2.13 (s, 3H,  $\text{Me}$ ,  $\text{NHAc}$ ).  $^{19}\text{F}\{^1\text{H}\}$ -NMR (376 MHz,  $\text{CDCl}_3$ )  $\delta$  -115.7.

**(Z)-methyl 2-acetamido-3-(3-****fluorophenyl)acrylate (144f).**

Substrate **144f** was obtained following the general procedure, starting from *N*-acetyl glycine (1.300 g, 10.99 mmol), anhydrous sodium acetate (0.683 g, 8.24 mmol), 3-fluorobenzaldehyde (1.8 mL, 16.49 mmol), acetic anhydride (2.6 mL, 27.48 mmol) and then with NaOMe (0.625 g, 10.99 mmol) as a white solid (0.941 g, 36% yield).  $^1\text{H-NMR}$  (400 MHz,  $\text{CDCl}_3$ )  $\delta$  7.34-7.03 (m, 6H,  $H_{\text{arom}}$ ,  $\text{CH=}$  and  $\text{NHAc}$ ), 3.86 (s, 3H,  $\text{CO}_2\text{Me}$ ), 2.14 (s, 3H,  $\text{Me}$ ,  $\text{NHAc}$ ).  $^{19}\text{F}\{^1\text{H}\}$ -NMR (376 MHz,  $\text{CDCl}_3$ )  $\delta$  -112.8.

**(Z)-methyl 2-acetamido-3-(2-****fluorophenyl)acrylate (144g).**

Substrate **144g** was obtained following the general procedure, starting from *N*-acetyl glycine (2.000 g, 16.91 mmol), anhydrous sodium acetate (1.051 g, 12.68 mmol), 2-fluorobenzaldehyde (2.8 mL, 25.36 mmol), acetic anhydride (4.0 mL, 42.27 mmol) and then with NaOMe (0.961 g, 16.91 mmol) as a white solid

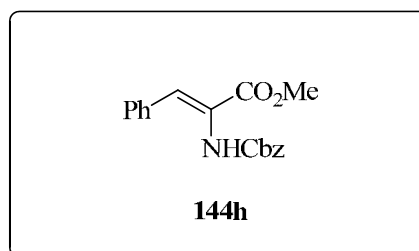


(1.100 g, 28% yield).  $^1\text{H-NMR}$  (400 MHz,  $\text{CDCl}_3$ )  $\delta$  7.43-7.06 (m, 6H,  $H_{\text{arom}}$ ,  $\text{CH=}$  and  $\text{NHAc}$ ), 3.87 (s, 3H,  $\text{CO}_2\text{Me}$ ), 2.11 (s, 3H,  $\text{Me}$ ,  $\text{NHAc}$ ).  $^{19}\text{F}\{^1\text{H}\}$ -NMR (376 MHz,  $\text{CDCl}_3$ )  $\delta$  -111.9.

### 1.3.8.3. Synthesis and general spectroscopic data of substrates **144h-i**

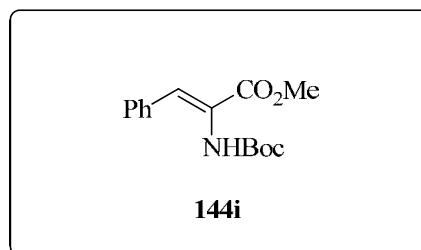
To a solution of *N*-protected- $\alpha$ -phosphonoglycine trimethyl ester (1.40 mmol) in  $\text{CH}_2\text{Cl}_2$  (3.0 mL) was syringed dropwise DBU (1.28 mmol) at room temperature. The reaction mixture was further stirred for 15 min. A solution of freshly distilled benzaldehyde (1.2 mmol) in  $\text{CH}_2\text{Cl}_2$  (3.0 mL) was cannulated to the reaction mixture and stirred at room temperature for 4h. The reaction mixture was evaporated and the crude purified by flash chromatography on  $\text{SiO}_2$  using as eluent hexane:AcOEt (100:0-80:20) to give **144h-i**.

**(Z)-methyl 2-(benzyloxycarbonylamino)-3-phenylacrylate (144h)**. Substrate **144h** was obtained following the general procedure, starting from *N*-Cbz- $\alpha$ -phosphonoglycine trimethyl ester (0.478 g, 1.40 mmol), DBU (0.2



mL, 1.28 mmol) and benzaldehyde (120  $\mu\text{L}$ , 1.17 mmol) as colorless oil (0.267 g, 74% yield).  $^1\text{H-NMR}$  (400 MHz,  $\text{CDCl}_3$ )  $\delta$  7.51-7.33 (m, 11H,  $H_{\text{arom}}$  and  $\text{CH=}$ ), 6.33 (bs, 1H,  $\text{NHCbz}$ ), 5.12 (s, 2H,  $\text{OCH}_2\text{-Ph}$ ), 3.82 (s, 3H,  $\text{CO}_2\text{Me}$ ).

**(Z)-methyl 2-(tertbutoxycarbonylamino)-3-phenylacrylate (144i)**. Substrate **144i** was obtained following the general procedure, starting from *N*-Boc- $\alpha$ -phosphonoglycine trimethyl ester (0.429 g, 1.40 mmol), DBU (0.2



mL, 1.28 mmol) and benzaldehyde (120  $\mu\text{L}$ , 1.17 mmol) as colorless oil (0.278 g, 86% yield).  $^1\text{H-NMR}$  (400 MHz,  $\text{CDCl}_3$ )  $\delta$  7.53 (d,  $^3J_{\text{H-H}} = 7.6$  Hz, 2H,  $H_{\text{arom}}$ ),

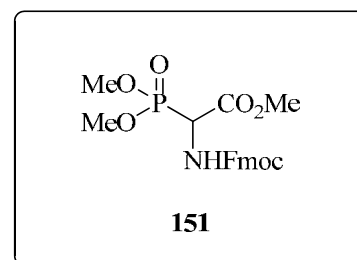


7.38-7.25 (m, 5H,  $H_{\text{arom}}$ , CH= and NHBoc), 3.86 (s, 3H, CO<sub>2</sub>Me), 1.40 (s, 9H, 3Me, O-<sup>t</sup>Bu).

#### 1.3.8.4. Synthesis and general spectroscopic data of compound **151**

##### ***N***-(Fmoc)- $\alpha$ -phosphoglycine trimethyl ester (**151**).

A suspension of *N*-(Cbz)- $\alpha$ -phosphoglycine trimethyl ester (1.000 g, 2.93 mmol) and 5% Pd/C (0.156 g, 0.15 mmol) in MeOH (25.0 mL) was hydrogenated at 1 atm for 1h. The resulting



methanolic solution was filtered through celite and concentrated *in vacuo*. The residue was dissolved in dichloromethane (20.0 mL) and 2,6-Lutidine (0.5 mL, 1.10 mmol) was added. Then, a solution of 9-fluorenylmethyl chloroformate (0.928 g, 3.51 mmol) in dichloromethane (10.0 mL) was syringed in. The reaction mixture was stirred at room temperature for 24h. The solvent was removed and the resulting residue was purified by flash chromatography through SiO<sub>2</sub> using hexanes/AcOEt (100:0/15:85) as the eluent to give the desired product **151** as a white solid (1.154 g, 94% yield). <sup>1</sup>H-NMR (400 MHz, CDCl<sub>3</sub>)  $\delta$  7.77 (d, <sup>3</sup>J<sub>H-H</sub> = 7.6 Hz, 2H,  $H_{\text{arom}}$ , Fmoc), 7.60 (bd, <sup>3</sup>J<sub>H-H</sub> = 5.2 Hz, 2H,  $H_{\text{arom}}$ , Fmoc), 7.41 (dd, <sup>3</sup>J<sub>H-H</sub> = <sup>3</sup>J<sub>H-H</sub> = 7.4 Hz, 2H,  $H_{\text{arom}}$ , Fmoc), 7.32 (dd, <sup>3</sup>J<sub>H-H</sub> = <sup>3</sup>J<sub>H-H</sub> = 7.4 Hz, 2H,  $H_{\text{arom}}$ , Fmoc), 5.61 (d, <sup>3</sup>J<sub>H-H</sub> = 8.7 Hz, 1H, NHFmoc), 4.94 (dd, <sup>2</sup>J<sub>H-P</sub> = 22.2 Hz, <sup>3</sup>J<sub>H-H</sub> = 8.7 Hz, 1H, CH-P(O)(OMe)<sub>2</sub>), 4.46 (bs, 2H, O-CH<sub>2</sub>-CH, Fmoc), 4.24 (dd, <sup>3</sup>J<sub>H-H</sub> = 6.8 Hz, 1H, O-CH<sub>2</sub>-CH, Fmoc), 3.85 (s, 3H, CO<sub>2</sub>Me), 3.84 (d, <sup>3</sup>J<sub>H-P</sub> = 11.2 Hz, 3H, OMe, P(O)(OMe)<sub>2</sub>), 3.81 (d, <sup>3</sup>J<sub>H-P</sub> = 11.2 Hz, 3H, OMe, P(O)(OMe)<sub>2</sub>); <sup>13</sup>C{<sup>1</sup>H}-NMR (100 MHz, CDCl<sub>3</sub>)  $\delta$  167.2 (C<sub>q</sub>, CO<sub>2</sub>Me), 155.7 (C<sub>q</sub>, NHCO, Fmoc), 143.6 (C<sub>q</sub> arom, Fmoc), 143.6 (C<sub>q</sub> arom, Fmoc), 141.3 (C<sub>q</sub> arom, Fmoc), 127.8 (CH<sub>arom</sub>, Fmoc), 127.1 (CH<sub>arom</sub>, Fmoc), 125.1 (CH<sub>arom</sub>, Fmoc), 120.1 (CH<sub>arom</sub>, Fmoc), 67.7 (CH<sub>2</sub>, Fmoc), 54.2 (d, <sup>2</sup>J<sub>C-P</sub> = 6.4 Hz, OCH<sub>3</sub>, P(O)(OMe)<sub>2</sub>), 54.2 (d, <sup>2</sup>J<sub>C-P</sub> = 6.4 Hz, OCH<sub>3</sub>, P(O)(OMe)<sub>2</sub>), 53.4 (CH<sub>3</sub>, CO<sub>2</sub>Me), 52.1 (d, <sup>1</sup>J<sub>C-P</sub> = 73.8 Hz, CH-P(O)(OMe)<sub>2</sub>), 47.0 (CH, Fmoc); <sup>31</sup>P{<sup>1</sup>H}-NMR (162

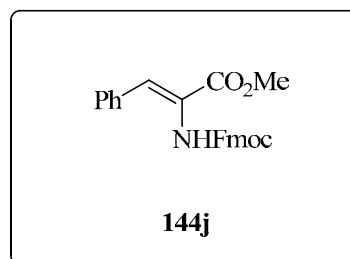
MHz, CDCl<sub>3</sub>)  $\delta$  21.5 (s, P(O)(OMe)<sub>2</sub>); IR (neat, cm<sup>-1</sup>)  $\nu$  3254 (N-H<sub>st</sub>), 1734 (C=O<sub>st</sub>, amide I), 1716 (C=O<sub>st</sub>, ester), 1525 (C=O<sub>st</sub>, amide II), 1240 (P=O<sub>st</sub>); MS HR-ESI [found 442.1036; C<sub>20</sub>H<sub>22</sub>NO<sub>7</sub>PNa (M+Na)<sup>+</sup> requires 442.1032].

### 1.3.8.5. Synthesis and general spectroscopic data of substrates **144j-m**

A solution of *N*-(Fmoc)- $\alpha$ -phosphoglycine trimethyl ester **151** (1.2 mmol) in dichloromethane (6.0 mL) was slowly added at -20 °C under nitrogen to a solution of freshly prepared LDA (diisopropylamine 1.1 mmol and *n*-BuLi 1.1 mmol). The reaction mixture was further stirred for 15 min at this temperature. Then, a solution of the aldehyde (1.0 mmol) in dichloromethane (6.0 mL) was added via cannula into to the reaction mixture. The mixture was stirred for 12 h at -20°C, after which, it was allowed to reach room temperature. The solvent was removed *in vacuo* and the resulting residue was dissolved in AcOEt (40.0 mL) and washed with 10% NH<sub>4</sub>Cl solution (40.0 mL). The aqueous solution was extracted with AcOEt (3 x 40 mL) and the combined organic extracts were washed with 10% NaCl solution (2 x 60.0 mL), dried over MgSO<sub>4</sub>, filtered and concentrated *in vacuo*. Finally, the reaction residue was purified by flash chromatography through SiO<sub>2</sub> using hexane/AcOEt as eluent to give **144j-m**.

#### (*Z*)-methyl 2-(((9*H*-fluoren-9-yl)methoxy)carbonylamino)-3-phenylacrylate

(**144j**). Substrate **144j** was obtained following the general procedure, starting from lithium diisopropylamine (iPr<sub>2</sub>NH (36  $\mu$ L, 0.26 mmol) and

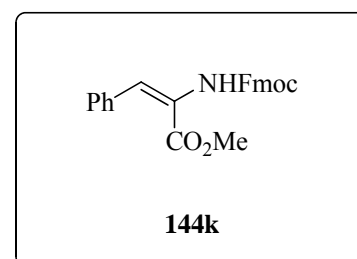


*n*-BuLi (0.1 mL, 2.5 M in hexanes, 0.26 mmol), compound **151** (0.117 g, 0.28 mmol) and benzaldehyde (24  $\mu$ L, 0.23 mmol) as a white solid (0.031 g, 33% yield). <sup>1</sup>H-NMR (500 MHz, CD<sub>2</sub>Cl<sub>2</sub>)  $\delta$  7.83 (d, <sup>3</sup>J<sub>H-H</sub> = 7.5 Hz, 2H, H<sub>arom</sub>), 7.64 (bs, 2H, H<sub>arom</sub>), 7.57 (bs, 2H, H<sub>arom</sub>), 7.46 (dd, <sup>3</sup>J<sub>H-H</sub> = <sup>3</sup>J<sub>H-H</sub> = 7.5 Hz, 2H, H<sub>arom</sub>), 7.41-7.36 (m, 6H, H<sub>arom</sub> and CH=), 6.42 (bs, 1H, NHFmoc), 4.45 (bs, 2H, O-

$CH_2-CH$ , Fmoc), 4.24 (bs, 1H,  $O-CH_2-CH$ , Fmoc), 3.87 (s, 3H,  $CO_2Me$ );  $^{13}C\{^1H\}$ -NMR (125 MHz,  $CD_2Cl_2$ )  $\delta$  165.7 ( $C_q$ ,  $CO_2Me$ ), 153.9 ( $C_q$ ,  $NHCO$ , Fmoc), 143.8 ( $C_{q\text{ arom}}$ , Fmoc), 141.3 ( $C_{q\text{ arom}}$ , Fmoc), 133.7 ( $C_{q\text{ arom}}$ , Ph), 131.7 ( $CH_p\text{ arom}$ , Ph), 129.9 ( $CH_o\text{ arom}$ , Ph), 129.5 ( $CH=$ ), 128.7 ( $CH_m\text{ arom}$ , Ph), 127.7 ( $CH_{\text{arom}}$ , Fmoc), 127.1 ( $CH_{\text{arom}}$ , Fmoc), 125.1 ( $CH_{\text{arom}}$ , Fmoc), 124.5 ( $C_q$ , Ph- $CH=C$ ), 120.0 ( $CH_{\text{arom}}$ , Fmoc), 67.4 ( $CH_2$ , Fmoc), 52.6 ( $CH_3$ ), 47.1 ( $CH$ , Fmoc); IR (neat,  $cm^{-1}$ )  $\nu$  3257 ( $N-H_{st}$ ), 1732 ( $C=O_{st}$ , amide I), 1700 ( $C=O_{st}$ , ester), 1644 ( $C=C_{st}$ ), 1511 ( $C=O_{st}$ , amide II); MS HR-ESI [found 422.1373;  $C_{25}H_{21}NO_4Na$  ( $M+Na$ ) $^+$  requires 422.1368]; M.p.: 161.8-162.5 °C.

**(E)-methyl 2-(((9H-fluoren-9-yl)methoxy)carbonylamino)-3-phenylacrylate**

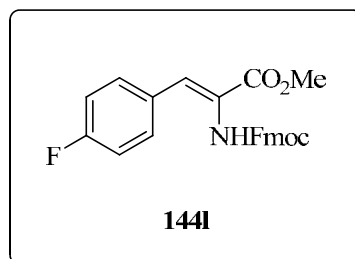
**(144k)**. Substrate **144k** was obtained following the general procedure, starting from lithium diisopropylamine ( $iPr_2NH$  (36  $\mu$ L, 0.26 mmol) and



*n*-BuLi (0.1 mL, 2.5 M in hexanes, 0.26 mmol), compound **151** (0.117 g, 0.28 mmol) and benzaldehyde (24  $\mu$ L, 0.23 mmol) as a white solid (0.030 g, 32% yield).  $^1H$ -NMR (500 MHz,  $CD_2Cl_2$ )  $\delta$  7.84 (d,  $^3J_{H-H}$  = 7.5 Hz, 2H,  $H_{\text{arom}}$ ), 7.68 (d,  $^3J_{H-H}$  = 7.5 Hz, 2H,  $H_{\text{arom}}$ ), 7.47 (dd,  $^3J_{H-H}$  =  $^3J_{H-H}$  = 7.5 Hz, 2H,  $H_{\text{arom}}$ ), 7.40-7.27 (m, 8H,  $H_{\text{arom}}$  and  $CH=$ ), 7.00 (bs, 1H,  $NHFmoc$ ), 4.52 (d,  $^3J_{H-H}$  = 6.8 Hz, 2H,  $O-CH_2-CH$ , Fmoc), 4.32 (bt,  $^3J_{H-H}$  = 6.8 Hz, 1H,  $O-CH_2-CH$ , Fmoc), 3.68 (s, 3H,  $CO_2Me$ );  $^{13}C\{^1H\}$ -NMR (125 MHz,  $CD_2Cl_2$ )  $\delta$  164.9 ( $C_q$ ,  $CO_2Me$ ), 153.5 ( $C_q$ ,  $NHCO$ , Fmoc), 143.8 ( $C_{q\text{ arom}}$ , Fmoc), 141.3 ( $C_{q\text{ arom}}$ , Fmoc), 135.2 ( $C_{q\text{ arom}}$ , Ph), 128.7 ( $CH_o\text{ arom}$ , Ph), 127.9 ( $CH_{\text{arom}}$ , Fmoc and  $CH_p\text{ arom}$ , Ph), 127.8 ( $CH_m\text{ arom}$ , Ph), 127.6 ( $CH=$ ), 127.1 ( $CH_{\text{arom}}$ , Fmoc), 126.1 ( $C_q$ , Ph- $CH=C$ ), 125.0 ( $CH_{\text{arom}}$ , Fmoc), 120.0 ( $CH_{\text{arom}}$ , Fmoc), 67.2 ( $CH_2$ , Fmoc), 52.2 ( $CH_3$ ), 47.1 ( $CH$ , Fmoc); IR (neat,  $cm^{-1}$ )  $\nu$  3306 ( $N-H_{st}$ ), 1701 (bs,  $C=O_{st}$ , amide I and ester), 1637 ( $C=C_{st}$ ), 1514 ( $C=O_{st}$ , amide II); MS HR-ESI [found 422.1361;  $C_{25}H_{21}NO_4Na$  ( $M+Na$ ) $^+$  requires 422.1368]; M.p.: 160.9-162.4 °C.

**(Z)-methyl 2-(((9H-fluoren-9-yl)methoxy)carbonylamino)-3-(4-**

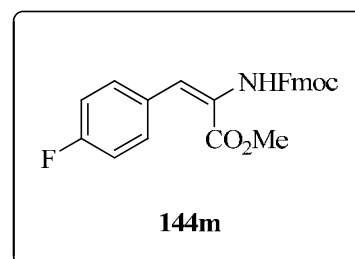
**fluorophenylacrylate (144l).** Substrate **144l** was obtained following the general procedure, starting from lithium diisopropylamine ( $i\text{Pr}_2\text{NH}$  (120  $\mu\text{L}$ ,



0.87 mmol) and *n*-BuLi (0.6 mL, 2.5 M in hexanes, 0.87 mmol), compound **151** (0.397 g, 0.95 mmol) and 4-fluorobenzaldehyde (86  $\mu\text{L}$ , 0.79 mmol) as a white solid (0.187 g, 57% yield).  $^1\text{H-NMR}$  (400 MHz,  $\text{CDCl}_3$ )  $\delta$  7.77 (d,  $^3J_{\text{H-H}} = 7.6$  Hz, 2H,  $H_{\text{arom}}$ ), 7.57-7.29 (m, 9H,  $H_{\text{arom}}$  and  $\text{CH}=\text{C}$ ), 7.03 (dd,  $^3J_{\text{H-F}} = ^3J_{\text{H-H}} = 8.8$  Hz, 2H,  $H_{\text{arom}}$ ), 6.31 (bs, 1H,  $\text{NHFmoc}$ ), 4.44 (bs, 2H,  $\text{O-CH}_2\text{-CH}$ , Fmoc), 4.19 (bs, 1H,  $\text{O-CH}_2\text{-CH}$ , Fmoc), 3.85 (s, 3H,  $\text{CO}_2\text{Me}$ );  $^{13}\text{C}\{^1\text{H}\}\text{-NMR}$  (100 MHz,  $\text{CDCl}_3$ )  $\delta$  165.8 ( $C_{\text{q}}$ ,  $\text{CO}_2\text{Me}$ ), 163.2 (d,  $^1J_{\text{C-F}} = 248.6$  Hz,  $C_{\text{q}}$  arom, Ph), 154.0 ( $C_{\text{q}}$ ,  $\text{NHCO}$ , Fmoc), 143.7 ( $C_{\text{q}}$  arom, Fmoc), 141.5 ( $C_{\text{q}}$  arom, Fmoc), 132.0 (d,  $^3J_{\text{C-F}} = 8.4$  Hz,  $\text{CH}_o$  arom, Ph), 131.9 ( $\text{CH}=\text{C}$ ), 129.9 ( $C_{\text{q}}$  arom, Ph), 127.9 ( $\text{CH}_{\text{arom}}$ , Fmoc), 127.2 ( $\text{CH}_{\text{arom}}$ , Fmoc), 125.1 ( $\text{CH}_{\text{arom}}$ , Fmoc), 123.8 ( $C_{\text{q}}$ ,  $\text{Ph-CH}=\text{C}$ ), 120.2 ( $\text{CH}_{\text{arom}}$ , Fmoc), 115.9 (d,  $^2J_{\text{C-F}} = 21.5$  Hz,  $\text{CH}_m$  arom, Ph), 67.6 ( $\text{CH}_2$ , Fmoc), 52.9 ( $\text{CH}_3$ ), 47.2 ( $\text{CH}$ , Fmoc);  $^{19}\text{F}\{^1\text{H}\}\text{-NMR}$  (376 MHz,  $\text{CDCl}_3$ )  $\delta$  -109.8; IR (neat,  $\text{cm}^{-1}$ )  $\nu$  3258 ( $\text{N-H}_{\text{st}}$ ), 1721 ( $\text{C}=\text{O}_{\text{st}}$ , amide I), 1697 ( $\text{C}=\text{O}_{\text{st}}$ , ester), 1644 ( $\text{C}=\text{C}_{\text{st}}$ ), 1519 ( $\text{C}=\text{O}_{\text{st}}$ , amide II); MS HR-ESI [found 440.1273;  $\text{C}_{25}\text{H}_{20}\text{FNO}_4\text{Na}$  ( $\text{M}+\text{Na}$ ) $^+$  requires 440.1274]; M.p.: 180.9-182.6  $^\circ\text{C}$ .

**(E)-methyl 2-(((9H-fluoren-9-yl)methoxy)carbonylamino)-3-(4-**

**fluorophenylacrylate (144m).** Substrate **144m** was obtained following the general procedure, starting from lithium diisopropylamine ( $i\text{Pr}_2\text{NH}$  (120  $\mu\text{L}$ ,



0.87 mmol) and *n*-BuLi (0.6 mL, 2.5 M in hexanes, 0.87 mmol), compound **151** (0.397 g, 0.95 mmol) and 4-fluorobenzaldehyde (86  $\mu\text{L}$ , 0.79 mmol) as a white solid (0.080 g, 24% yield).  $^1\text{H-NMR}$  (400 MHz,  $\text{CDCl}_3$ )  $\delta$  7.77 (d,  $^3J_{\text{H-H}} = 7.2$  Hz, 2H,  $H_{\text{arom}}$ ), 7.62 (d,  $^3J_{\text{H-H}} = 7.2$  Hz, 2H,  $H_{\text{arom}}$ ), 7.61 (s, 1H,  $\text{CH}=\text{C}$ ), 7.42 (dd,  $^3J_{\text{H-H}} =$

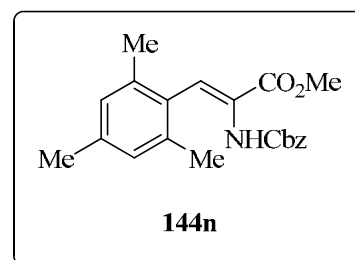
$^3J_{\text{H-H}} = 7.5$  Hz, 2H,  $H_{\text{arom}}$ ), 7.22 (dd,  $^3J_{\text{H-H}} = 8.4$  Hz,  $^4J_{\text{H-F}} = 5.6$  Hz, 2H,  $H_{\text{arom}}$ ), 7.00 (dd,  $^3J_{\text{H-H}} = ^3J_{\text{H-F}} = 8.8$  Hz, 2H,  $H_{\text{arom}}$ ), 7.00 (bs, 1H, NHFmoc), 4.49 (d,  $^3J_{\text{H-H}} = 6.8$  Hz, 2H, O-CH<sub>2</sub>-CH, Fmoc), 4.27 (t,  $^3J_{\text{H-H}} = 6.8$  Hz, 1H, O-CH<sub>2</sub>-CH, Fmoc), 3.66 (s, 3H, CO<sub>2</sub>Me);  $^{13}\text{C}\{^1\text{H}\}$ -NMR (100 MHz, CDCl<sub>3</sub>)  $\delta$  164.8 ( $C_{\text{q}}$ , CO<sub>2</sub>Me), 162.3 (d,  $^1J_{\text{C-F}} = 245.8$  Hz,  $C_{\text{q}}$  arom, Ph), 153.7 ( $C_{\text{q}}$ , NHCO, Fmoc), 143.7 ( $C_{\text{q}}$  arom, Fmoc), 141.4 ( $C_{\text{q}}$  arom, Fmoc), 131.4 ( $C_{\text{q}}$  arom, Ph), 130.6 (d,  $^3J_{\text{C-F}} = 8.0$  Hz, CH<sub>o</sub> arom, Ph), 127.9 (CH<sub>arom</sub>, Fmoc), 127.3 (CH<sub>arom</sub>, Fmoc), 125.7 ( $C_{\text{q}}$ , Ph-CH=C), 125.1 (CH<sub>arom</sub>, Fmoc), 124.0 (CH=), 120.2 (CH<sub>arom</sub>, Fmoc), 114.9 (d,  $^2J_{\text{C-F}} = 21.4$  Hz, CH<sub>m</sub> arom, Ph), 67.4 (CH<sub>2</sub>, Fmoc), 52.49 (CH<sub>3</sub>), 47.13 (CH, Fmoc);  $^{19}\text{F}\{^1\text{H}\}$ -NMR (376 MHz, CDCl<sub>3</sub>)  $\delta$  -114.2; IR (neat, cm<sup>-1</sup>)  $\nu$  3286 (N-H<sub>st</sub>), 1725 (C=O<sub>st</sub>, amide I), 1687 (C=O<sub>st</sub>, ester), 1642 (C=C<sub>st</sub>), 1499 (C=O<sub>st</sub>, amide II); MS HR-ESI [found 440.1283; C<sub>25</sub>H<sub>20</sub>FNO<sub>4</sub>Na (M+Na)<sup>+</sup> requires 440.1274]; M.p.: 89.2-91.7 °C.

#### 1.3.8.6. Synthesis and general spectroscopic data of substrates **144n-o**

To a solution of *N*-protected- $\alpha$ -phosphonoglycine trimethyl ester (1.40 mmol) in dichloromethane (3.0 mL) was syringed dropwise DBU (1.28 mmol) at room temperature. The reaction mixture was further stirred for 15 min. Then, a solution of freshly distilled aldehyde (1.17 mmol) in dichloromethane (3.0 mL) was cannulated into the reaction mixture and stirred at room temperature for 4h. The reaction mixture was evaporated in rotary-evaporator and purified by flask chromatography on SiO<sub>2</sub> using as eluent Hexane:AcOEt (100:0-80:20) to give **144n-o**.

**(Z)-methyl 2-(benzyloxycarbonylamino)-3-mesitylacrylate (144n)**. Substrate **144n** was obtained following the general procedure and synthesized in Riera's research group as colorless oil.

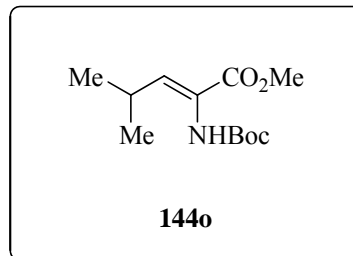
$^1\text{H}$ -NMR (400 MHz, CDCl<sub>3</sub>)  $\delta$  7.33-7.25 (m, 5H,  $H_{\text{arom}}$ , Ph, Cbz), 7.10 (s, 1H, CH=), 6.86 (s, 2H,  $H_{\text{arom}}$ , Mes), 6.00 (bs, 1H,



NHCbz), 5.03 (s, 2H, OCH<sub>2</sub>-Ph), 3.83 (s, 3H, CO<sub>2</sub>Me), 2.27 (s, 3H, Me, Mes), 2.14 (s, 6H, 2Me, Mes).

**(Z)-methyl 2-(tertbutoxycarbonylamino)-4-methylpent-2-enoate (144o).**

Substrate **144o** was obtained following the general procedure, starting from *N*-Boc- $\alpha$ -phosphonoglycine trimethyl ester (0.357 g, 1.20 mmol), DBU (161  $\mu$ L, 1.08 mmol)



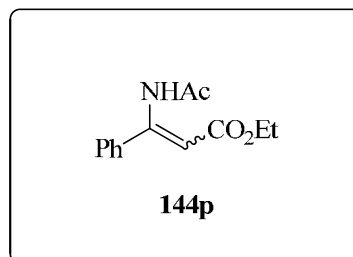
and isobutiraldehyde (91  $\mu$ L, 1.00 mmol) as a colorless oil (0.139 g, 57% yield).

<sup>1</sup>H-NMR (400 MHz, CDCl<sub>3</sub>)  $\delta$  6.36 (d, <sup>3</sup>J<sub>H-H</sub> = 10.0 Hz, 1H, <sup>i</sup>Pr-CH=), 5.89 (bs, 1H, NHBoc), 3.74 (s, 3H, CO<sub>2</sub>Me), 2.69 (m, 1H, Me<sub>2</sub>-CH), 1.44 (s, 9H, 3Me, O-<sup>t</sup>Bu), 1.03 (d, <sup>3</sup>J<sub>H-H</sub> = 6.4 Hz, 6H, Me<sub>2</sub>-CH). <sup>13</sup>C{<sup>1</sup>H}-NMR (100 MHz, CDCl<sub>3</sub>)  $\delta$  165.8 (C<sub>q</sub>, CO<sub>2</sub>Me), 153.9 (C<sub>q</sub>, NHCO, Boc), 144.1 (<sup>i</sup>Pr-CH=), 124.1 (C<sub>q</sub>, <sup>i</sup>Pr-CH=C), 80.51 (C<sub>q</sub>, O-<sup>t</sup>Bu), 52.3 (Me, CO<sub>2</sub>Me), 28.3 (3Me, O-<sup>t</sup>Bu), 27.6 (Me<sub>2</sub>-CH), 21.8 (2Me, Me<sub>2</sub>-CH). IR (neat, cm<sup>-1</sup>)  $\nu$  3336 (N-H<sub>st</sub>), 1704 (bs, C=O<sub>st</sub>, amide I and ester), 1656 (C=C<sub>st</sub>). MS HR-ESI [found 266.1359; C<sub>12</sub>H<sub>21</sub>NO<sub>4</sub>Na (M+Na)<sup>+</sup> requires 266.1368].

*1.3.8.7. Synthesis and general spectroscopic data of substrate 144p*

**(E/Z)-methyl 3-acetamido-3-phenylacrylate (144p).**

A solution of ethyl-3-oxo-3-phenylpropanoate (2.20 mL, 11.71 mmol) and NH<sub>4</sub>OAc (4.51 g, 58.53 mmol) in MeOH (15.0 mL) was stirred at room temperature for 48 h. After the

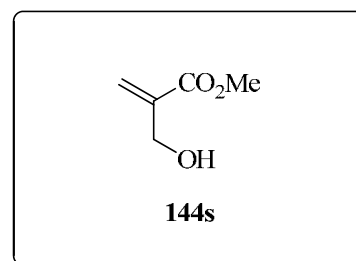


solvent was evaporated under reduced pressure, the residue was diluted with CHCl<sub>3</sub>. The resulting solid was filtered off and washed with CHCl<sub>3</sub>. The combined filtrate was washed with water and brine, and dried over sodium sulfate. Evaporation of the solvent gave ethyl 3-amino-3-phenylacrylate, which was used for the next step without purification. To a solution of ethyl 3-amino-3-

phenylacrylate in THF (12.0 mL) were added pyridine (2.0 mL, 24.00 mmol) and excess amounts of acetic anhydride (6.0 mL, 63.61 mmol). The reaction mixture was then heated under reflux for 24 h. After the mixture was cool to room temperature, the volatile was evaporated. The residue was dissolved in EtOAc (20.0 mL), and the solution was washed with water (1 x 10.0 mL), 1N HCl (1 x 10.0 mL), 1M KH<sub>2</sub>PO<sub>4</sub> (1 x 10.0 mL), saturated aqueous NaHCO<sub>3</sub> (1 x 10.0 mL), and brine (2 x 10.0 mL). After the solution was dried over sodium sulfate, the solvent was evaporated under reduced pressure. Chromatography of the residue on SiO<sub>2</sub> using hexane:AcOEt (100:0-80:20) to give (*E/Z*)-**144p** (*E/Z*= 1/2.8) as a colorless oil (1.468 g, 54% yield). <sup>1</sup>H-NMR (400 MHz, CDCl<sub>3</sub>) (*E*)-**144p**: δ 7.53-7.34 (m, 5H, *H*<sub>arom</sub>), 6.64 (s, 1H, CH=), 4.21 (q, <sup>3</sup>*J*<sub>H-H</sub>= 7.2 Hz, 2H, OCH<sub>2</sub>CH<sub>3</sub>), 2.37 (s, 3H, C(O)CH<sub>3</sub>), 1.27 (t, *J*<sub>H-H</sub>= 7.2 Hz, 3H, OCH<sub>2</sub>CH<sub>3</sub>); (*Z*)-**144p**: δ 10.64 (bs, 1H, NH), 7.53-7.34 (m, 5H, *H*<sub>arom</sub>), 5.28 (s, 1H, CH=), 4.22 (q, <sup>3</sup>*J*<sub>H-H</sub>= 7.2 Hz, 2H, OCH<sub>2</sub>CH<sub>3</sub>), 2.16 (s, 3H, C(O)CH<sub>3</sub>), 1.29 (t, <sup>3</sup>*J*<sub>H-H</sub>= 7.2 Hz, 3H, OCH<sub>2</sub>CH<sub>3</sub>).

#### 1.3.8.8. Synthesis and general spectroscopic data of substrate **144s**

**Methyl 2-(hydroxymethyl)acrylate (144s).** *para*-Formaldehyde (3.500 g, 117.00 mmol) was dissolved in a mixture of 1,4-dioxane and H<sub>2</sub>O (1:1, 16.0 mL) and the solution was stirred for 20 min. To this solution were added methyl acrylate (21.0 mL, 23.00

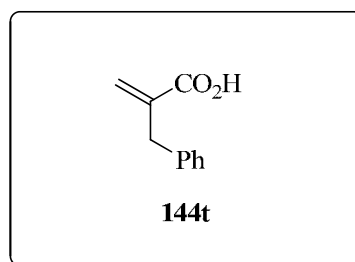


mmol) and 1,4-diazabicyclo[2.2.2]octane (13.100 g, 117.00 mmol). The mixture was stirred for 14 h and then it was diluted with a saturated aqueous solution of NaCl (200.0 mL). The reaction mixture was extracted with Et<sub>2</sub>O (3 x 50.0 mL). The combined organic layers were dried over MgSO<sub>4</sub> and concentrated in vacuo. The residue was purified by chromatography on SiO<sub>2</sub> using hexane:AcOEt (80:20 to 50:50) as eluent to give **117s** as a colorless oil (7.664 g, 56% yield). <sup>1</sup>H-

NMR (400 MHz, CDCl<sub>3</sub>)  $\delta$  6.27 (s, 1H, CH=), 5.87 (s, 1H, CH=), 4.34 (d,  $^3J_{\text{H-H}} = 6.20$  Hz, 2H, CH<sub>2</sub>-OH), 3.80 (s, 3H, OCH<sub>3</sub>), 2.37 (t,  $^3J_{\text{H-H}} = 6.20$  Hz, 1H, OH).

#### 1.3.8.9. Synthesis and general spectroscopic data of substrate **144t**

**2-benzylacrylic acid (144t)**. To a stirred solution of benzylmalonic acid (10.000 g, 51.50 mmol) and 37% formalin (22.0 mL, 268.70 mmol) was added NHEt<sub>2</sub> (5.3 mL, 51.50 mmol) at room temperature. The solution was stirred at room temperature for 3 h and



then was refluxed for additional 2 h. The reaction mixture was cooled down to room temperature, diluted with CHCl<sub>3</sub> (100.0 mL) and extracted with saturated aqueous NaHCO<sub>3</sub> (3 x 50.0 mL). The basic aqueous layer was acidified with 2M HCl to pH < 1 and was extracted with CHCl<sub>3</sub> (3 x 50.0 mL). The organic layers were combined, dried over anhydrous Na<sub>2</sub>SO<sub>4</sub> and evaporated under reduced pressure to give **144t** as a white solid (6.527 g, 78% yield). <sup>1</sup>H-NMR (400 MHz, CDCl<sub>3</sub>)  $\delta$  7.33-7.20 (m, 5H, *H*<sub>arom</sub>), 6.39 (s, 1H, CH=), 5.87 (bs, 1H, CH=), 6.34 (bs, 2H, CH<sub>2</sub>-Ph).

#### 1.3.8.10. Synthesis and general spectroscopic data of substrate **144u-w**

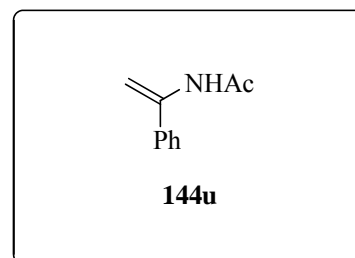
Sodium acetate (33 mmol) was added to a suspension of hydroxylamine hydrochloride (33 mmol), in MeOH (15.0 mL). After stirring for 30 minutes, ketone (30.0 mmol) was added dropwise over 1.5 h. The mixture was then stirred for 2-8 h. Water (15.0 mL) was added dropwise and then the resulting suspension was stirred for a further 1 h, filtered and the solid precipitate was washed with water and dried under vacuum to afford the ketoxime in yields over 90%. Acetic anhydride (81 mmol) was added, in portions, to a solution of oxime (27 mmol) in toluene (40.0 mL) under argon atmosphere. Acetic acid (81 mmol) was then added, followed by Fe powder (54 mmol). The mixture was then heated to 70°C



overnight. The reaction was then cooled to room temperature, filtered over celite and washed with toluene (2 x 10.0 mL). The combined filtrates were cooled in an ice bath and washed with 2M NaOH (2 x 30.0 mL). The organic phase was separated, dried over anhydrous MgSO<sub>4</sub> and evaporated to afford the enamides **144u-w**.

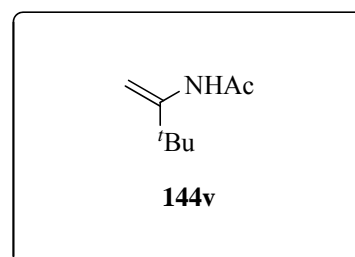
***N*-(1-phenylvinyl)acetamide (144u)**. Substrate **144u**

was obtained following the general procedure, starting from sodium acetate (2.707 g, 33.00 mmol), hydroxylamine hydrochloride (2.294 g, 33.00 mmol), acetophenone (3.5 mL, 30.00 mmol), acetic anhydride (7.7 mL, 81.00 mmol), acetic acid (4.6 mL, 81.00 mmol) and Fe powder (2.848 g, 54.00 mmol) as a colorless solid (2.805 g, 58% yield). <sup>1</sup>H-NMR (400 MHz, CDCl<sub>3</sub>) δ 7.42-7.35 (m, 5H, *H*<sub>arom</sub>), 6.76 (s, 1H, NHAc), 5.89 (s, 1H, CHH=), 5.09 (s, 1H, CHH=), 2.14 (s, 3H, *Me*, NHAc).



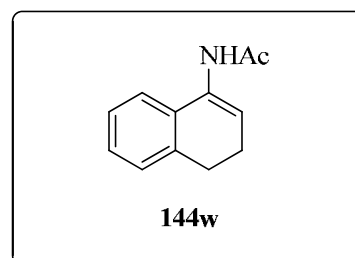
***N*-(1-tertbutylvinyl)acetamide (144v)**. Substrate **144v**

was obtained following the general procedure, starting from sodium acetate (2.707 g, 33.00 mmol), hydroxylamine hydrochloride (2.294 g, 33.00 mmol), tertbutylmethylketone (3.7 mL, 30.00 mmol), acetic anhydride (7.7 mL, 81.00 mmol), acetic acid (4.6 mL, 81.00 mmol) and Fe powder (2.848 g, 54.00 mmol) as a colorless solid (2.330 g, 55% yield). <sup>1</sup>H-NMR (400 MHz, CDCl<sub>3</sub>) δ 6.48 (s, 1H, NH), 5.63 (s, 1H, CH=), 4.80 (s, 1H, CH=), 2.10 (s, 3H, C(O)CH<sub>3</sub>), 1.13 (s, 9H, <sup>*t*</sup>Bu).



***N*-(3,4-dihydronaphthalen-1-yl)acetamide (144w)**.

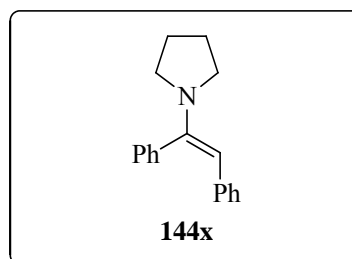
Substrate **144w** was obtained following the general procedure, starting from sodium acetate (2.707 g, 33.00 mmol), hydroxylamine hydrochloride (2.294 g,



33.00 mmol), 3,4-dihydronaphthalen-1-one (4.0 mL, 30.00 mmol), acetic anhydride (7.7 mL, 81.00 mmol), acetic acid (4.6 mL, 81.00 mmol) and Fe powder (2.848 g, 54.00 mmol) as a colorless solid (2.809, 50% yield).  $^1\text{H-NMR}$  (400 MHz,  $\text{CDCl}_3$ )  $\delta$  (3:1 mixture of rotamers) 7.30-7.05 (m, 4H,  $H_{\text{arom}}$ ), 6.84 (bs, 0.75 H, NH), 6.70 (bs, 0.25 H, NH), 6.44 (bt, 0.75 H, CH=), 5.98 (bt, 0.25 H, CH=), 2.88-2.68 (m, 2H, C- $\text{CH}_2$ - $\text{CH}_2$ ), 2.28-2.24 (m, 2H, C- $\text{CH}_2$ - $\text{CH}_2$ ), 2.18 (s, 2.25 H, C(O) $\text{CH}_3$ ), 1.96 (s, 0.75 H, C(O) $\text{CH}_3$ ).

#### 1.3.8.11. Synthesis and general spectroscopic data of substrate **144x**

**(E)-1-(pyrrolidinyl)-1,2-diphenylethene (144x)**. A mixture of deoxybenzoin (5.90 g, 29.16 mmol), pyrrolidine (9.8 mL, 116.65 mmol), and boron trifluoride etherate (0.4 mL, 2.92 mmol) in toluene (150.0 mL) was refluxed over 4 Å molecule sieves

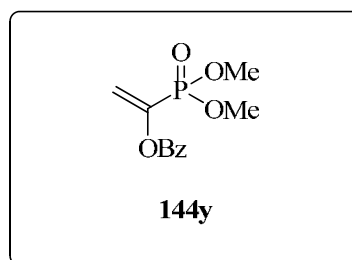


for 43 h under nitrogen. The mixture was concentrated in vacuum, and the residue was distilled at 160 °C /  $2.1 \times 10^{-1}$  mbar to give **(E)-144x** as a yellow oil, (3.00 g, 92% yield).  $^1\text{H-NMR}$  (400 MHz,  $\text{CDCl}_3$ )  $\delta$  7.35-7.27 (m, 5H,  $H_{\text{arom}}$ ), 6.97-6.93 (m, 2H,  $H_{\text{arom}}$ ), 6.83-6.79 (m, 1H,  $H_{\text{arom}}$ ), 6.65 (d,  $J_{\text{H-H}} = 7.6$  Hz, 2H,  $H_{\text{arom}}$ ), 5.33 (s, 1H, C=CH), 3.09-3.06 (m, 4H,  $\text{CH}_2\text{CH}_2$ ), 1.91-1.87 (m, 4H,  $\text{CH}_2\text{CH}_2$ ).

#### 1.3.8.12. Synthesis and general spectroscopic data of substrate **144y**

##### **1-Benzoyloxy-1-dimethylphosphonylethene**

**(144y)**. Acetyl chloride (5.0 mL, 69.61 mmol) was chilled to 0 °C in an oven-dried flask fitted with an addition funnel. Trimethylphosphite (8.5 mL, 69.61 mmol) was added dropwise under nitrogen. A



balloon was used to compensate for the released methylchloride. When the

addition was complete the reaction was warmed to 70 °C and stirred for 15 minutes. Vacuum distillation was used to isolate 6.67 g (44.51 mmol) of dimethyl acetyl phosphonate as a colorless oil. Benzoic anhydride (16.83 g, 66.83 mmol) was combined with the  $\alpha$ -keto phosphonate (6.67 g, 44.51 mmol) and chilled to 0 °C. DBU (6.7 mL, 44.55 mmol) was added slowly and the reaction was stirred for 15 minutes, warming to room temperature. The reaction mixture was diluted with EtOAc (150.0 mL), washed with sat. NaHCO<sub>3</sub> (3 x 30.0 mL) and brine (1 x 30.0 mL), and then dried with MgSO<sub>4</sub>. Solvent was removed *in vacuo* to give a colorless oil. Purification using SiO<sub>2</sub> chromatography (hexane:AcOEt 80:20) to give **144y** (5.68 g, 32%) as a waxy white solid. <sup>1</sup>H-NMR (400 MHz, CDCl<sub>3</sub>)  $\delta$  8.10 (d,  $J_{\text{H-H}} = 7.8$  Hz, 2H,  $H_{\text{arom}}$ ), 7.63 (t,  $J_{\text{H-H}} = 7.6$  Hz, 1H,  $H_{\text{arom}}$ ), 7.49 (t,  $J_{\text{H-H}} = 7.9$  Hz, 2H,  $H_{\text{arom}}$ ), 6.20 (dd,  $J_{\text{P-H}} = 11.1$  Hz,  $^2J_{\text{H-H}} = 2.0$  Hz, 1H, CH=), 5.94 (dd, 1H,  $J_{\text{P-H}} = 35.2$  Hz,  $^2J_{\text{H-H}} = 2.0$  Hz, 1H), 3.84 (d,  $J_{\text{P-H}} = 11.3$  Hz, 6H, OMe).

### 1.3.9. General procedure for the Rh-mediated asymmetric hydrogenation

A solution of the chiral ligand (0.011 mmol), bis(norbornadiene)rhodium tetrafluoroborate (0.01 mmol) and the substrate (1 mmol) in the corresponding dry and deoxygenated solvent (0.6 mL) was charged into an autoclave under N<sub>2</sub> atmosphere. The autoclave was purged three times with hydrogen gas (10 bar). Finally, the autoclave was pressurized with hydrogen to the desired pressure. The reaction mixture was stirred at the desired temperature for the stated reaction time. The autoclave was subsequently depressurized and the conversion was determined by <sup>1</sup>H-NMR. The ee's were determined by chiral chromatography, and the configurations of the hydrogenated products were established by comparison with either reported retention times or optical rotations.

### 1.3.9.1. Spectroscopic data and determination of enantiomeric excess of hydrogenated products

**Hydrogenation product of 32b.** <sup>139</sup> <sup>1</sup>H-NMR (400 MHz, CDCl<sub>3</sub>) δ 7.33-7.24 (m, 3H, *H*<sub>arom</sub>), 7.12-7.10 (m, 2H, *H*<sub>arom</sub>), 5.96 (bd, <sup>3</sup>*J*<sub>H-H</sub> = 7.5 Hz, 1H, *NHAc*), 4.90 (ddd, <sup>3</sup>*J*<sub>H-H</sub> = 7.5 Hz, <sup>3</sup>*J*<sub>H-H</sub> = <sup>3</sup>*J*<sub>H-H</sub> = 5.8 Hz, 1H, *CH-NHAc*), 3.74 (s, 3H, *CO<sub>2</sub>Me*), 3.17 (dd, <sup>2</sup>*J*<sub>H-H</sub> = 13.9 Hz, <sup>3</sup>*J*<sub>H-H</sub> = 5.8 Hz, 1H, *Ph-CHH*), 3.10 (dd, <sup>2</sup>*J*<sub>H-H</sub> = 13.9 Hz, <sup>3</sup>*J*<sub>H-H</sub> = 5.8 Hz, 1H, *Ph-CHH*), 2.00 (s, 3H, *Me*, *NHAc*). HPLC (Chiracel OJ-H [Chiral Technologies], 25 x 0.46 cm, 93:7 hexane:isopropanol, 1 mL/min, λ = 216 nm): *t<sub>R</sub>*(*R*) 18.3 min, *t<sub>R</sub>*(*S*) 29.4 min.

**Hydrogenation product of 69.** <sup>1</sup>H-NMR (400 MHz, CDCl<sub>3</sub>) δ 6.03 (bs, 1H, *NHAc*), 4.60 (dt, <sup>3</sup>*J*<sub>H-H</sub> = <sup>3</sup>*J*<sub>H-H</sub> = 7.2 Hz, 1H, *CH-NHAc*), 3.76 (s, 3H, *CO<sub>2</sub>Me*), 2.02 (s, 3H, *Me*, *NHAc*), 1.40 (d, <sup>3</sup>*J*<sub>H-H</sub> = 7.2 Hz, 1H, *CH<sub>3</sub>-CH*). GC (BETA DEX 125 [Supelco], 30 m x 0.25 mm, film thickness 0.25 mm, 90 °C, isothermal, 15 psi He): *t<sub>R</sub>*(*S*) 63.2 min, *t<sub>R</sub>*(*R*) 65.1 min.

**Hydrogenation product of 144a.** <sup>1</sup>H-NMR (400 MHz, DMSO-*d*<sub>6</sub>) δ 12.64 (bs, 1H, *CO<sub>2</sub>H*), 8.16 (d, <sup>3</sup>*J*<sub>H-H</sub> = 8.0 Hz, 1H, *NHAc*), 7.29-7.18 (m, 5H, *H*<sub>arom</sub>), 4.40 (ddd, <sup>3</sup>*J*<sub>H-H</sub> = 9.6 Hz, <sup>3</sup>*J*<sub>H-H</sub> = 8.0 Hz, <sup>3</sup>*J*<sub>H-H</sub> = 5.0 Hz, 1H, *CH-NHAc*), 3.03 (dd, <sup>3</sup>*J*<sub>H-H</sub> = 13.7 Hz, <sup>3</sup>*J*<sub>H-H</sub> = 5.0 Hz, 1H, *Ph-CHH*), 2.83 (dd, <sup>3</sup>*J*<sub>H-H</sub> = 13.7 Hz, <sup>3</sup>*J*<sub>H-H</sub> = 9.6 Hz, 1H, *Ph-CHH*), 1.77 (s, 3H, *Me*, *NHAc*). For the determination of the enantiomeric purity and the configuration, a sample was treated with diazomethane to prepare the methyl ester.

**Hydrogenation product of 144b.** <sup>1</sup>H-NMR (400 MHz, DMSO-*d*<sub>6</sub>) δ 12.43 (bs, 1H, *CO<sub>2</sub>H*), 8.13 (d, <sup>3</sup>*J*<sub>H-H</sub> = 7.3 Hz, 1H, *NHAc*), 4.16 (dt, <sup>3</sup>*J*<sub>H-H</sub> = <sup>3</sup>*J*<sub>H-H</sub> = 7.3 Hz, 1H, *CH-NHAc*), 1.82 (s, 3H, *Me*, *NHAc*), 1.24 (d, <sup>3</sup>*J*<sub>H-H</sub> = 7.3 Hz, 3H, *CH<sub>3</sub>-CH*).

<sup>139</sup> Evans, D. A.; Michael, F. E.; Tedrow, J. S.; Campos, K. R. *J. Am. Chem. Soc.* **2003**, *125*, 3534-3543.

For the determination of the enantiomeric purity and the configuration, a sample was treated with diazomethane to prepare the methyl ester.

**Hydrogenation product of 144c.**  $^1\text{H-NMR}$  (400 MHz,  $\text{CDCl}_3$ )  $\delta$  8.16 (d, sist. AB,  $^3J_{\text{H-H}} = 8.6$  Hz, 2H,  $H_{\text{arom}}$ ), 7.28 (d, sist. AB,  $^3J_{\text{H-H}} = 8.6$  Hz, 2H,  $H_{\text{arom}}$ ), 5.97 (d,  $^3J_{\text{H-H}} = 7.3$  Hz, 1H, *NHAc*), 4.93 (ddd,  $^3J_{\text{H-H}} = 7.3$  Hz,  $^3J_{\text{H-H}} = ^3J_{\text{H-H}} = 5.8$  Hz, 1H, *CH-NHAc*), 3.75 (s, 3H,  $\text{CO}_2\text{Me}$ ), 3.30 (dd,  $^2J_{\text{H-H}} = 13.8$  Hz,  $^3J_{\text{H-H}} = 5.8$  Hz, 1H, *para-NO}\_2\text{-Ph-CHH}), 3.19 (dd,  $^2J_{\text{H-H}} = 13.8$  Hz,  $^3J_{\text{H-H}} = 5.8$  Hz, 1H, *para-NO}\_2\text{-Ph-CHH}), 2.01 (s, 3H, *Me*, *NHAc*). HPLC (Chiracel OD-H [Chiral Technologies], 25 x 0.46 cm, 85:15 hexane:isopropanol, 1 mL/min,  $\lambda = 216$  nm):  $t_{\text{R}}(\text{R})$  16.7 min,  $t_{\text{R}}(\text{S})$  19.0 min.**

**Hydrogenation product of 144d.**  $^1\text{H-NMR}$  (400 MHz,  $\text{CDCl}_3$ )  $\delta$  7.00 (d, sist. AB,  $^3J_{\text{H-H}} = 8.4$  Hz, 2H,  $H_{\text{arom}}$ ), 6.82 (d, sist. AB,  $^3J_{\text{H-H}} = 8.4$  Hz, 2H,  $H_{\text{arom}}$ ), 5.88 (d,  $^3J_{\text{H-H}} = 7.8$  Hz, 1H, *NHAc*), 4.85 (ddd,  $^3J_{\text{H-H}} = 7.8$  Hz,  $^3J_{\text{H-H}} = ^3J_{\text{H-H}} = 5.7$  Hz, 1H, *CH-NHAc*), 3.79 (s, 3H, *para-MeO-Ph*), 3.75 (s, 3H,  $\text{CO}_2\text{Me}$ ), 3.09 (dd,  $^2J_{\text{H-H}} = 14.2$  Hz,  $^3J_{\text{H-H}} = 5.7$  Hz, 1H, *para-MeO-Ph-CHH*), 3.04 (dd,  $^2J_{\text{H-H}} = 14.2$  Hz,  $^3J_{\text{H-H}} = 5.7$  Hz, 1H, *para-MeO-Ph-CHH*), 1.99 (s, 3H, *Me*, *NHAc*). HPLC (Chiracel OJ-H [Chiral Technologies], 25 x 0.46 cm, 85:15 hexane:isopropanol, 1 mL/min,  $\lambda = 216$  nm):  $t_{\text{R}}(\text{R})$  13.2 min,  $t_{\text{R}}(\text{S})$  27.0 min.

**Hydrogenation product of 144e.**  $^1\text{H-NMR}$  (400 MHz,  $\text{CDCl}_3$ )  $\delta$  7.05 (d,  $^3J_{\text{H-H}} = 8.8$  Hz,  $^4J_{\text{H-F}} = 5.6$  Hz, 2H,  $H_{\text{arom}}$ ), 6.98 (d,  $^3J_{\text{H-H}} = ^3J_{\text{H-F}} = 8.8$  Hz, 2H,  $H_{\text{arom}}$ ), 5.92 (d,  $^3J_{\text{H-H}} = 7.4$  Hz, 1H, *NHAc*), 4.86 (ddd,  $^3J_{\text{H-H}} = 7.4$  Hz,  $^3J_{\text{H-H}} = ^3J_{\text{H-H}} = 5.8$  Hz, 1H, *CH-NHAc*), 3.73 (s, 3H,  $\text{CO}_2\text{Me}$ ), 3.13 (dd,  $^2J_{\text{H-H}} = 14.0$  Hz,  $^3J_{\text{H-H}} = 5.8$  Hz, 1H, *para-F-Ph-CHH*), 3.06 (dd,  $^2J_{\text{H-H}} = 14.0$  Hz,  $^3J_{\text{H-H}} = 5.8$  Hz, 1H, *para-F-Ph-CHH*), 1.99 (s, 3H, *Me*, *NHAc*). HPLC (Chiracel OJ-H [Chiral Technologies], 25 x 0.46 cm, 93:7 hexane:isopropanol, 1 mL/min,  $\lambda = 216$  nm):  $t_{\text{R}}(\text{R})$  19.4 min,  $t_{\text{R}}(\text{S})$  27.8 min.

**Hydrogenation product of 144f.**  $^1\text{H-NMR}$  (400 MHz,  $\text{CDCl}_3$ )  $\delta$  7.28-7.22 (m, 1H,  $H_{\text{arom}}$ ), 6.97-6.78 (m, 3H,  $H_{\text{arom}}$ ), 5.92 (d,  $^3J_{\text{H-H}} = 7.2$  Hz, 1H,  $\text{NHAc}$ ), 4.88 (ddd,  $^3J_{\text{H-H}} = 7.2$  Hz,  $^3J_{\text{H-H}} = ^3J_{\text{H-H}} = 5.6$  Hz, 1H,  $\text{CH-NHAc}$ ), 3.74 (s, 3H,  $\text{CO}_2\text{Me}$ ), 3.16 (dd,  $^2J_{\text{H-H}} = 13.8$  Hz,  $^3J_{\text{H-H}} = 5.6$  Hz, 1H, *meta*-F-Ph-CHH), 3.09 (dd,  $^2J_{\text{H-H}} = 13.8$  Hz,  $^3J_{\text{H-H}} = 5.6$  Hz, 1H, *meta*-F-Ph-CHH), 2.00 (s, 3H, *Me*,  $\text{NHAc}$ ). HPLC (Chiracel OJ-H [Chiral Technologies], 25 x 0.46 cm, 90:10 hexane:isopropanol, 1 mL/min,  $\lambda = 216$  nm):  $t_{\text{R}}(\text{R})$  13.0 min,  $t_{\text{R}}(\text{S})$  16.1 min.

**Hydrogenation product of 144g.**  $^1\text{H-NMR}$  (400 MHz,  $\text{CDCl}_3$ )  $\delta$  7.26-6.98 (m, 4H,  $H_{\text{arom}}$ ), 5.97 (d,  $^3J_{\text{H-H}} = 7.3$  Hz, 1H,  $\text{NHAc}$ ), 4.87 (ddd,  $^3J_{\text{H-H}} = 7.3$  Hz,  $^3J_{\text{H-H}} = ^3J_{\text{H-H}} = 5.9$  Hz, 1H,  $\text{CH-NHAc}$ ), 3.74 (s, 3H,  $\text{CO}_2\text{Me}$ ), 3.22 (dd,  $^2J_{\text{H-H}} = 14.1$  Hz,  $^3J_{\text{H-H}} = 5.9$  Hz, 1H, *ortho*-F-Ph-CHH), 3.13 (dd,  $^2J_{\text{H-H}} = 14.1$  Hz,  $^3J_{\text{H-H}} = 5.9$  Hz, 1H, *ortho*-F-Ph-CHH), 1.97 (s, 3H, *Me*,  $\text{NHAc}$ ). HPLC (Chiracel OJ-H [Chiral Technologies], 25 x 0.46 cm, 90:10 hexane:isopropanol, 1 mL/min,  $\lambda = 216$  nm):  $t_{\text{R}}(\text{R})$  12.4 min,  $t_{\text{R}}(\text{S})$  19.2 min.

**Hydrogenation product of 144h.**  $^1\text{H-NMR}$  (400 MHz,  $\text{CDCl}_3$ )  $\delta$  7.38-7.22 (m, 3H,  $H_{\text{arom}}$ ), 7.10-7.08 (m, 2H,  $H_{\text{arom}}$ ), 5.20 (d,  $^3J_{\text{H-H}} = 7.8$  Hz, 1H,  $\text{NHCbz}$ ), 5.12 (d, sist. AB,  $^2J_{\text{H-H}} = 12.4$  Hz, 1H, O-CHH-Ph), 5.08 (d, sist. AB,  $^2J_{\text{H-H}} = 12.4$  Hz, 1H, O-CHH-Ph), 4.67 (bdd,  $^3J_{\text{H-H}} = 7.8$  Hz,  $^3J_{\text{H-H}} = 5.8$  Hz, 1H,  $\text{CH-NHCbz}$ ), 3.72 (s, 3H,  $\text{CO}_2\text{Me}$ ), 3.14 (dd,  $^2J_{\text{H-H}} = 14.0$  Hz,  $^3J_{\text{H-H}} = 5.9$  Hz, 1H, Ph-CHH), 3.08 (dd,  $^2J_{\text{H-H}} = 14.0$  Hz,  $^3J_{\text{H-H}} = 5.9$  Hz, 1H, Ph-CHH). HPLC (Chiracel OJ-H [Chiral Technologies], 25 x 0.46 cm, 80:20 hexane:isopropanol, 0.9 mL/min,  $\lambda = 216$  nm):  $t_{\text{R}}(\text{S})$  21.0 min,  $t_{\text{R}}(\text{R})$  29.3 min.

**Hydrogenation product of 144i.**  $^1\text{H-NMR}$  (400 MHz,  $\text{CDCl}_3$ )  $\delta$  7.32-7.22 (m, 3H,  $H_{\text{arom}}$ ), 7.13-7.12 (d,  $^3J_{\text{H-H}} = 6.8$  Hz, 2H,  $H_{\text{arom}}$ ), 4.96 (d,  $^3J_{\text{H-H}} = 6.8$  Hz, 1H,  $\text{NHBoc}$ ), 4.59 (bdd,  $^3J_{\text{H-H}} = 6.8$  Hz,  $^3J_{\text{H-H}} = 5.8$  Hz, 1H,  $\text{CH-NHBoc}$ ), 3.71 (s, 3H,  $\text{CO}_2\text{Me}$ ), 3.12 (bdd,  $^2J_{\text{H-H}} = 13.8$  Hz,  $^3J_{\text{H-H}} = 5.8$  Hz, 1H, Ph-CHH), 3.04 (bdd,  $^2J_{\text{H-H}} = 13.8$  Hz,  $^3J_{\text{H-H}} = 5.8$  Hz, 1H, Ph-CHH), 1.42 (s, 9H, 3*Me*, O-*t*Bu). HPLC

(Chiracel OJ-H [Chiral Technologies], 25 x 0.46 cm, 95:5 hexane:isopropanol, 0.6 mL/min,  $\lambda = 216$  nm):  $t_R(R)$  12.7 min,  $t_R(S)$  14.3 min.

**Hydrogenation product of 144j.**  $^1\text{H-NMR}$  (400 MHz,  $\text{CDCl}_3$ )  $\delta$  7.78 (d,  $^3J_{\text{H-H}} = 7.6$  Hz, 2H,  $H_{\text{arom}}$ ), 7.57 (dd,  $^3J_{\text{H-H}} = ^3J_{\text{H-H}} = 6.4$  Hz, 2H,  $H_{\text{arom}}$ ), 7.41 (dd,  $^3J_{\text{H-H}} = ^3J_{\text{H-H}} = 7.6$  Hz, 2H,  $H_{\text{arom}}$ ), 7.33-7.27 (m, 5H,  $H_{\text{arom}}$ ), 7.10 (d,  $^3J_{\text{H-H}} = 6.8$  Hz, 2H,  $H_{\text{arom}}$ ), 5.26 (d,  $^3J_{\text{H-H}} = 7.8$  Hz, 1H,  $\text{NHFmoc}$ ), 4.68 (bdd,  $^3J_{\text{H-H}} = 7.8$  Hz,  $^3J_{\text{H-H}} = 6.0$  Hz, 1H,  $\text{CH-NHFmoc}$ ), 4.45 (dd,  $^2J_{\text{H-H}} = 10.5$  Hz,  $^3J_{\text{H-H}} = 6.9$  Hz, 1H,  $\text{O-CHH-CH}$ , Fmoc), 4.35 (dd,  $^2J_{\text{H-H}} = 10.5$  Hz,  $^3J_{\text{H-H}} = 6.9$  Hz, 1H,  $\text{O-CHH-CH}$ , Fmoc), 4.21 (dd,  $^3J_{\text{H-H}} = ^3J_{\text{H-H}} = 6.9$  Hz, 1H,  $\text{O-CH}_2\text{-CH}$ , Fmoc), 3.74 (s, 3H,  $\text{CO}_2\text{Me}$ ), 3.16 (dd,  $^2J_{\text{H-H}} = 14.0$  Hz,  $^3J_{\text{H-H}} = 5.8$  Hz, 1H,  $\text{Ph-CHH}$ ), 3.10 (dd,  $^2J_{\text{H-H}} = 14.0$  Hz,  $^3J_{\text{H-H}} = 5.8$  Hz, 1H,  $\text{Ph-CHH}$ );  $^{13}\text{C}\{^1\text{H}\}$ -NMR (100 MHz,  $\text{CDCl}_3$ )  $\delta$  172.1 ( $\text{C}_q$ ,  $\text{CO}_2\text{Me}$ ), 155.7 ( $\text{C}_q$ ,  $\text{NHCO}$ , Fmoc), 144.0 ( $\text{C}_q$   $_{\text{arom}}$ , Fmoc), 143.9 ( $\text{C}_q$   $_{\text{arom}}$ , Fmoc), 141.5 ( $\text{C}_q$   $_{\text{arom}}$ , Fmoc), 135.8 ( $\text{C}_q$   $_{\text{arom}}$ , Ph), 129.4 ( $\text{CH}_o$   $_{\text{arom}}$ , Ph), 128.8 ( $\text{CH}_m$   $_{\text{arom}}$ , Ph), 127.9 ( $\text{CH}_{\text{arom}}$ , Fmoc), 127.3 ( $\text{CH}_p$   $_{\text{arom}}$ , Ph), 125.3 ( $\text{CH}_{\text{arom}}$ , Fmoc), 125.2 ( $\text{CH}_{\text{arom}}$ , Fmoc), 120.1 ( $\text{CH}_{\text{arom}}$ , Fmoc), 67.1 ( $\text{CH}_2$ , Fmoc), 54.9 ( $\text{CH-NHFmoc}$ ), 52.5 ( $\text{CH}_3$ ), 47.3 ( $\text{CH}$ , Fmoc), 38.4 ( $\text{Ph-CH}_2$ );  $[\alpha]_D^{26} = -34.1^\circ$  ( $c = 0.91$  g/ 100 mL,  $\text{CHCl}_3$ ); IR (neat,  $\text{cm}^{-1}$ )  $\nu$  3316 ( $\text{N-H}_{\text{st}}$ ), 1739 ( $\text{C=O}_{\text{st}}$ , amide I), 1691 ( $\text{C=O}_{\text{st}}$ , ester), 1543 ( $\text{C=O}_{\text{st}}$ , amide II); MS HR-ESI [found 424.1537;  $\text{C}_{25}\text{H}_{23}\text{NO}_4\text{Na}$  ( $\text{M}+\text{Na}$ ) $^+$  requires 424.1525]. HPLC (Chiracel OJ-H [Chiral Technologies], 25 x 0.46 cm, 80:20 hexane:isopropanol, 0.9 mL/min,  $\lambda = 216$  nm):  $t_R(S)$  24.8 min,  $t_R(R)$  30.3 min.

**Hydrogenation product of 144l.**  $^1\text{H-NMR}$  (400 MHz,  $\text{CDCl}_3$ )  $\delta$  7.78 (d,  $^3J_{\text{H-H}} = 7.6$  Hz, 2H,  $H_{\text{arom}}$ ), 7.57 (m, 2H,  $H_{\text{arom}}$ ), 7.41 (dd,  $^3J_{\text{H-H}} = ^3J_{\text{H-H}} = 7.4$  Hz, 2H,  $H_{\text{arom}}$ ), 7.32 (dd,  $^3J_{\text{H-H}} = ^3J_{\text{H-H}} = 7.6$  Hz, 2H,  $H_{\text{arom}}$ ), 7.03 (dd,  $^3J_{\text{H-H}} = 8.4$  Hz,  $^4J_{\text{H-F}} = 5.2$  Hz, 2H,  $H_{\text{arom}}$ ), 6.97 (dd,  $^3J_{\text{H-H}} = ^3J_{\text{H-F}} = 8.4$  Hz, 2H,  $H_{\text{arom}}$ ), 5.24 (d,  $^3J_{\text{H-H}} = 7.6$  Hz, 1H,  $\text{NHFmoc}$ ), 4.64 (bdd,  $^3J_{\text{H-H}} = 7.6$  Hz,  $^3J_{\text{H-H}} = 6.1$  Hz, 1H,  $\text{CH-NHFmoc}$ ), 4.48 (dd,  $^2J_{\text{H-H}} = 10.7$  Hz,  $^3J_{\text{H-H}} = 6.8$  Hz, 1H,  $\text{O-CHH-CH}$ , Fmoc), 4.38 (dd,  $^2J_{\text{H-H}} = 10.7$  Hz,  $^3J_{\text{H-H}} = 6.8$  Hz, 1H,  $\text{O-CHH-CH}$ , Fmoc), 4.21 (dd,  $^3J_{\text{H-H}} = ^3J_{\text{H-H}} = 6.8$

Hz, 1H, O-CH<sub>2</sub>-CH, Fmoc), 3.73 (s, 3H, CO<sub>2</sub>Me), 3.12 (dd, <sup>2</sup>J<sub>H-H</sub> = 13.8 Hz, <sup>3</sup>J<sub>H-H</sub> = 6.1 Hz, 1H, *para*-F-Ph-CHH), 3.05 (dd, <sup>2</sup>J<sub>H-H</sub> = 13.8 Hz, <sup>3</sup>J<sub>H-H</sub> = 6.1 Hz, 1H, *para*-F-Ph-CHH); <sup>13</sup>C{<sup>1</sup>H}-NMR (100 MHz, CDCl<sub>3</sub>) δ 171.9 (C<sub>q</sub>, CO<sub>2</sub>Me), 162.2 (d, <sup>1</sup>J<sub>C-F</sub> = 244.2 Hz, C<sub>q</sub> arom, *para*-F-Ph), 155.6 (C<sub>q</sub>, NHCO, Fmoc), 144.0 (C<sub>q</sub> arom, Fmoc), 143.8 (C<sub>q</sub> arom, Fmoc), 141.5 (C<sub>q</sub> arom, Fmoc), 131.6 (C<sub>q</sub> arom, *para*-F-Ph), 130.9 (d, <sup>3</sup>J<sub>C-F</sub> = 7.8 Hz, CH<sub>o</sub> arom, *para*-F-Ph), 127.9 (CH<sub>arom</sub>, Fmoc), 127.2 (CH<sub>arom</sub>, Fmoc), 125.2 (CH<sub>arom</sub>, Fmoc), 125.1 (CH<sub>arom</sub>, Fmoc), 120.2 (CH<sub>arom</sub>, Fmoc), 120.1 (CH<sub>arom</sub>, Fmoc), 115.6 (d, <sup>3</sup>J<sub>C-F</sub> = 21.2 Hz, CH<sub>m</sub> arom, *para*-F-Ph), 67.0 (CH<sub>2</sub>, Fmoc), 54.9 (CH-NHFmoc), 52.6 (CH<sub>3</sub>), 47.3 (CH, Fmoc), 37.6 (*para*-F-Ph-CH<sub>2</sub>); <sup>19</sup>F{<sup>1</sup>H}-NMR (376 MHz, CDCl<sub>3</sub>) δ -115.6; M.p.: 156.5-159.1 °C; [α]<sub>D</sub><sup>26</sup> = -31.2° (c = 1.13 g/100 mL, CHCl<sub>3</sub>); IR (neat, cm<sup>-1</sup>) ν 3301 (N-H<sub>st</sub>), 1739 (C=O<sub>st</sub>, amide I), 1688 (C=O<sub>st</sub>, ester), 1546 (C=O<sub>st</sub>, amide II); MS HR-ESI [found 442.1430; C<sub>25</sub>H<sub>22</sub>FNO<sub>4</sub>Na (M+Na)<sup>+</sup> requires 442.1431]. HPLC (Chiracel OJ-H [Chiral Technologies], 25 x 0.46 cm, 80:20 hexane:isopropanol, 0.9 mL/min, λ = 216 nm): t<sub>R</sub>(S) 23.4 min, t<sub>R</sub>(R) 30.6 min.

**Hydrogenation product of 144o.** <sup>1</sup>H-NMR (400 MHz, CDCl<sub>3</sub>) δ 4.87 (bd, <sup>3</sup>J<sub>H-H</sub> = 6.0 Hz, 1H, NHBoc), 4.31 (bd, <sup>3</sup>J<sub>H-H</sub> = 6.0 Hz, 1H, CH-NHBoc), 3.73 (s, 3H, CO<sub>2</sub>Me), 1.75-1.44 (m, 12H, Me<sub>2</sub>CH, <sup>i</sup>Pr-CH<sub>2</sub> and 3Me, O-<sup>t</sup>Bu), 0.95 (d, <sup>3</sup>J<sub>H-H</sub> = 6.6 Hz, 3H, MeMe-CH), 0.94 (d, <sup>3</sup>J<sub>H-H</sub> = 6.6 Hz, 3H, MeMe-CH). GC (BETA DEX 125 [Supelco], 30 m x 0.25 mm, film thickness 0.25 mm, 140 °C, isothermal, 15 psi He): t<sub>R</sub>(S) 23.1 min, t<sub>R</sub>(R) 23.7 min.

**Hydrogenation product of 144p.** <sup>1</sup>H-NMR (400 MHz, CDCl<sub>3</sub>) δ 7.37-7.24 (m, 5H, H<sub>arom</sub>), 6.55 (d, <sup>3</sup>J<sub>H-H</sub> = 7.9 Hz, 1H, NHAc), 5.43 (ddd, <sup>3</sup>J<sub>H-H</sub> = 7.9 Hz, <sup>3</sup>J<sub>H-H</sub> = <sup>3</sup>J<sub>H-H</sub> = 5.9 Hz, 1H, CH-NHAc), 4.07 (q, <sup>3</sup>J<sub>H-H</sub> = 7.1 Hz, 2H, O-CH<sub>2</sub>-CH<sub>3</sub>), 2.92 (dd, <sup>2</sup>J<sub>H-H</sub> = 15.6 Hz, <sup>3</sup>J<sub>H-H</sub> = 5.9 Hz, 1H, CHH-CO<sub>2</sub>Et), 2.82 (dd, <sup>2</sup>J<sub>H-H</sub> = 15.6 Hz, <sup>3</sup>J<sub>H-H</sub> = 5.9 Hz, 1H, CHH-CO<sub>2</sub>Et), 2.03 (s, 3H, Me, NHAc), 1.16 (t, <sup>3</sup>J<sub>H-H</sub> = 7.1 Hz, 2H, O-CH<sub>2</sub>-CH<sub>3</sub>). HPLC (Chiracel OD-H [Chiral Technologies], 25 x 0.46 cm, 98:2 hexane:EtOH, 1.3 mL/min, λ = 216 nm): t<sub>R</sub>(R) 20.6 min, t<sub>R</sub>(S) 26.0 min.



**Hydrogenation product of 144r.**  $^1\text{H-NMR}$  (400 MHz,  $\text{CDCl}_3$ )  $\delta$  3.69 (s, 3H,  $\text{CO}_2\text{Me}$ ), 3.68 (s, 3H,  $\text{CO}_2\text{Me}$ ), 2.92 (m, 1H,  $\text{CH-CO}_2\text{Me}$ ), 2.74 (dd,  $^2J_{\text{H-H}} = 16.5$  Hz,  $^3J_{\text{H-H}} = 8.0$  Hz, 1H,  $\text{CHH-CO}_2\text{Me}$ ), 2.41 (dd,  $^2J_{\text{H-H}} = 16.5$  Hz,  $^3J_{\text{H-H}} = 8.0$  Hz, 1H,  $\text{CHH-CO}_2\text{Me}$ ), 1.22 (d,  $^3J_{\text{H-H}} = 7.2$  Hz, 3H,  $\text{Me-CH}$ ). GC (BETA DEX 225 [Supelco], 30 m x 0.25 mm, film thickness 0.25 mm, 70 °C, isothermal, 15 psi He):  $t_{\text{R}}(\text{R})$  44.6 min,  $t_{\text{R}}(\text{S})$  50.8 min.

**Hydrogenation product of 144s.**  $^1\text{H-NMR}$  (400 MHz,  $\text{CDCl}_3$ )  $\delta$  3.76-3.68 (m, 5H,  $\text{CH}_2\text{-OH}$  and  $\text{CO}_2\text{Me}$ ), 2.68 (m, 1H,  $\text{CH-CO}_2\text{Me}$ ), 1.18 (d,  $^3J_{\text{H-H}} = 7.2$  Hz, 3H,  $\text{Me-CH}$ ). GC (BETA DEX 225 [Supelco], 30 m x 0.25 mm, film thickness 0.25 mm, 100 °C, isothermal, 15 psi He):  $t_{\text{R}}(\text{S})$  9.6 min,  $t_{\text{R}}(\text{R})$  10.5 min.

**Hydrogenation product of 144t.**  $^1\text{H-NMR}$  (400 MHz,  $\text{CDCl}_3$ )  $\delta$  7.32-7.18 (m, 5H,  $H_{\text{arom}}$ ), 3.09 (dd,  $^2J_{\text{H-H}} = 13.5$  Hz,  $^3J_{\text{H-H}} = 6.2$  Hz, 1H,  $\text{Ph-CHH}$ ), 2.78 (m, 1H,  $\text{CH-CO}_2\text{H}$ ), 2.68 (dd,  $^2J_{\text{H-H}} = 13.5$  Hz,  $^3J_{\text{H-H}} = 8.0$  Hz, 1H,  $\text{Ph-CHH}$ ), 1.19 (d,  $^3J_{\text{H-H}} = 7.2$  Hz, 3H,  $\text{Me-CH}$ ). GC (BETA DEX 225 [Supelco], 30 m x 0.25 mm, film thickness 0.25 mm, 105 °C, isothermal, 15 psi He):  $t_{\text{R}}(\text{R})$  148.2 min,  $t_{\text{R}}(\text{S})$  150.8 min.

**Hydrogenation product of 144u.**  $^1\text{H-NMR}$  (400 MHz,  $\text{CDCl}_3$ )  $\delta$  7.37-7.25 (m, 5H,  $H_{\text{arom}}$ ), 5.63 (bs, 1H,  $\text{NHAc}$ ), 5.14 (dt,  $^3J_{\text{H-H}} = ^3J_{\text{H-H}} = 7.2$  Hz, 1H,  $\text{CH-NHAc}$ ), 1.99 (s, 3H,  $\text{Me}$ ,  $\text{NHAc}$ ), 1.50 (d,  $^3J_{\text{H-H}} = 7.2$  Hz, 3H,  $\text{Me-CH}$ ). HPLC (Chiracel AD-H [Chiral Technologies], 25 x 0.46 cm, 95:5 hexane:isopropanol, 1 mL/min,  $\lambda = 216$  nm):  $t_{\text{R}}(\text{R})$  10.5 min,  $t_{\text{R}}(\text{S})$  13.6 min.

**Hydrogenation product of 144v.**  $^1\text{H-NMR}$  (400 MHz,  $\text{CDCl}_3$ )  $\delta$  5.32 (bs, 1H,  $\text{NHAc}$ ), 3.87 (dq,  $^3J_{\text{H-H}} = 10.0$  Hz,  $^3J_{\text{H-H}} = 6.9$  Hz, 1H,  $\text{CH-NHAc}$ ), 1.98 (s, 3H,  $\text{Me}$ ,  $\text{NHAc}$ ), 1.04 (d,  $^3J_{\text{H-H}} = 6.9$  Hz, 3H,  $\text{Me-CH}$ ), 0.89 (s, 9H, 3Me,  $^t\text{Bu}$ ). GC

(BETA DEX 125 [Supelco], 30 m x 0.25 mm, film thickness 0.25 mm, 105 °C, isothermal, 15 psi He):  $t_R(S)$  16.9 min,  $t_R(R)$  17.4 min.

**Hydrogenation product of 144w.**  $^1\text{H-NMR}$  (400 MHz,  $\text{CDCl}_3$ )  $\delta$  7.28-7.26 (m, 1H,  $H_{\text{arom}}$ ), 7.18-7.16 (m, 2H,  $H_{\text{arom}}$ ), 7.10-7.08 (m, 1H,  $H_{\text{arom}}$ ), 5.72 (bs, 1H,  $\text{NHAc}$ ), 5.18 (bdd,  $^3J_{\text{H-H}} = 7.2$  Hz,  $^3J_{\text{H-H}} = 5.6$  Hz, 1H,  $\text{CH-NHAc}$ ), 2.85-2.71 (m, 2H,  $=\text{C-CH}_2\text{-CH}_2$ ), 2.07-2.01 (m, 4H,  $\text{CHH-CH}_2\text{-CH}$  and  $\text{Me}$ ,  $\text{NHAc}$ ), 1.86-1.79 (m, 3H,  $\text{CHH-CH}_2\text{-CH}$ ). HPLC (Chiracel OJ-H [Chiral Technologies], 25 x 0.46 cm, 90:10 hexane:isopropanol, 0.75 mL/min,  $\lambda = 216$  nm):  $t_R(S)$  13.3 min,  $t_R(R)$  16.9 min.

**Hydrogenation product of 144y.**  $^{140}$   $^1\text{H-NMR}$  (400 MHz,  $\text{CDCl}_3$ )  $\delta$  8.09-8.06 (m, 2H,  $H_{\text{arom}}$ ), 7.61-7.57 (m, 1H,  $H_{\text{arom}}$ ), 7.48-7.44 (m, 2H,  $H_{\text{arom}}$ ), 5.56 (dq,  $^2J_{\text{H-P}} = 8.4$  Hz,  $^3J_{\text{H-H}} = 7.2$  Hz, 1H,  $\text{CH-P(O)(OMe)}_2$ ), 3.83 (d,  $^3J_{\text{P-H}} = 10.6$  Hz, 3H,  $\text{OMe}$ ), 3.82 (d,  $^3J_{\text{P-H}} = 10.6$  Hz, 3H,  $\text{OMe}$ ), 1.60 (dd,  $^3J_{\text{H-P}} = 16.8$  Hz,  $^3J_{\text{H-H}} = 7.2$  Hz, 3H,  $\text{Me-CH}$ ). HPLC (Chiracel OJ-H [Chiral Technologies], 25 x 0.46 cm, 98.5:1.5 hexane:isopropanol, 1 mL/min,  $\lambda = 216$  nm):  $t_R(S)$  29.6 min,  $t_R(R)$  32.6 min.

### 1.3.9.2. Determination of absolute configurations of hydrogenated products

The absolute configurations were established by comparison of the sign of the optical rotation of our reaction products with the ones reported in the literature: Hydrogenation products of **32b** and **144a** ((*R*)-(-)-Methyl 2-acetamido-3-phenylpropanoate),<sup>141</sup> hydrogenation products of **69** and **144b** ((*S*)-(-)-Methyl 2-acetamidopropanoate),<sup>142</sup> hydrogenation product of **144c** ((*S*)-(+)-Methyl 2-

<sup>140</sup> Rubio, M.; Vargas, S.; Suarez, A.; Alvarez, E.; Pizzano, A. *Chem. Eur. J.* **2007**, *13*, 1821-1833.

<sup>141</sup> Burk, M. J.; Feaster, J. E.; Nugent, W. A.; Harlow, R. L. *J. Am. Chem. Soc.* **1993**, *115*, 10125-38.

<sup>142</sup> Wolf, J. P., III; Niemann, C. *Biochemistry* **1963**, *2*, 493-7.

acetamido-3-(4-nitrophenyl)propanoate),<sup>143</sup> hydrogenation product of **144d** ((*S*)-(+)-Methyl 2-acetamido-3-(4-methoxyphenyl)propanoate),<sup>144</sup> hydrogenation product of **144e** ((*R*)-(-)-Methyl 2-acetamido-3-(4-fluorophenyl)propanoate),<sup>141</sup> hydrogenation product of **144f** ((*S*)-(+)-Methyl 2-acetamido-3-(3-fluorophenyl)propanoate),<sup>141</sup> hydrogenation product of **144g** ((*S*)-(+)-Methyl 2-acetamido-3-(2-fluorophenyl)propanoate),<sup>141</sup> hydrogenation product of **144h** ((*S*)-(-)-Methyl 2-(benzyloxycarbonylamino)-3-phenylpropanoate),<sup>145</sup> hydrogenation product of **144i** ((*S*)-(-)-Methyl 2-(tertbutoxycarbonylamino)-3-phenylpropanoate),<sup>146</sup> hydrogenation product of **144j** ((*R*)-(-)-Methyl 2-(((9*H*-fluoren-9-yl)methoxy)carbonylamino)-3-phenylpropanoate),<sup>147</sup> hydrogenation product of **144o** ((*S*)-(-)-Methyl 2-(benzyloxycarbonyl)-4-methylpentanoate),<sup>148</sup> hydrogenation product of **144p** ((*S*)-(-)-Ethyl 3-acetamido-3-phenylpropanoate),<sup>149</sup> hydrogenation product of **144r** (Dimethyl (*R*)-(+)-2-methylsuccinate),<sup>150</sup> hydrogenation product of **144s** ((*S*)-(+)-Methyl 3-hydroxy-2-methylpropanoate),<sup>151</sup> hydrogenation product of **144t** ((*S*)-2-Methyl-3-phenylpropanoic acid),<sup>152</sup> hydrogenation product of **144u** ((*R*)-(+)-*N*-(1-phenylvinyl)acetamide),<sup>153</sup> hydrogenation product of **144v** ((*R*)-(-)-*N*-(3,3-dimethylbutan-2-yl)acetamide),<sup>154</sup> hydrogenation product of **144w** ((*R*)-(+)-*N*-(1,2,3,4-tetrahydronaphthalen-1-yl)acetamide)<sup>153</sup> and hydrogenation product of **144y** ((*S*)-(-)-1-(Dimethoxyphosphoryl)ethyl benzoate).<sup>155</sup>

<sup>143</sup> Staszewska, A.; Stefanowicz, P.; Szweczek, Z. *Tetrahedron Lett.* **2005**, *46*, 5525-5528.

<sup>144</sup> Hebel, D.; Lerman, O.; Rozen, S. *Bull. Soc. Chim. Fr.* **1986**, 861-3.

<sup>145</sup> Ohfuné, Y.; Sakaitani, M. EP217243 A2 (**1987**).

<sup>146</sup> Chankeshwara, S. V.; Chakraborti, A. K. *Org. Lett.* **2006**, *8*, 3259-3262.

<sup>147</sup> Hang, J.; Tian, S.-K.; Tang, L.; Deng, L. *J. Am. Chem. Soc.* **2001**, *123*, 12696-12697.

<sup>148</sup> Burk, M. J.; Allen, J. G. *J. Org. Chem.* **1997**, *62*, 7054-7057.

<sup>149</sup> Wu, H.-P.; Hoge, G. *Org. Lett.* **2004**, *6*, 3645-3647.

<sup>150</sup> Serrano, I.; Rodriguez, M.; Romero, I.; Llobet, A.; Parella, T.; Campelo, J. M.; Luna, D.; Marinas, J. M.; Benet-Buchholz, J. *Inorg. Chem.* **2006**, *45*, 2644-2651.

<sup>151</sup> Wassenaar, J.; Kuil, M.; Reek, J. N. H. *Adv. Synth. Catal.* **2008**, *350*, 1610-1614.

<sup>152</sup> Le, T. N.; Nguyen, Q. P. B.; Kim, J. N.; Kim, T. H. *Tetrahedron Lett.* **2007**, *48*, 7834-7837.

<sup>153</sup> Kim, M.-J.; Kim, W.-H.; Han, K.; Choi, Y. K.; Park, J. *Org. Lett.* **2007**, *9*, 1157-1159.

<sup>154</sup> Burk, M. J.; Casy, G.; Johnson, N. B. *J. Org. Chem.* **1998**, *63*, 6084-6085.

<sup>155</sup> Wang, D.-Y.; Huang, J.-D.; Hu, X.-P.; Deng, J.; Yu, S.-B.; Duan, Z.-C.; Zheng, Z. *J. Org. Chem.* **2008**, *73*, 2011-2014.



**CHAPTER 2**  
***PRELIMINARY INVESTIGATIONS INTO BIO-  
INSPIRED SUPRAMOLECULAR STRATEGIES  
FOR ASYMMETRIC CATALYSIS***

UNIVERSITAT ROVIRA I VIRGLI

TOWARDS HIGHLY EFFICIENT LIGANDS FOR ASYMMETRIC HYDROGENATIONS: A COVALENT MODULAR APPROACH AND  
INVESTIGATIONS INTO BIOINSPIRED SUPRAMOLECULAR STRATEGIES

Héctor Fernández Pérez

ISBN:978-84-693-3385-3 /DL:T.994-2010

## **LITERATURE PRECEDENT**

UNIVERSITAT ROVIRA I VIRGLI

TOWARDS HIGHLY EFFICIENT LIGANDS FOR ASYMMETRIC HYDROGENATIONS: A COVALENT MODULAR APPROACH AND  
INVESTIGATIONS INTO BIOINSPIRED SUPRAMOLECULAR STRATEGIES

Héctor Fernández Pérez

ISBN:978-84-693-3385-3 /DL:T.994-2010



## 2.1. LITERATURE PRECEDENT

Cooperative interactions are ubiquitous in biological systems. Chemists may be able to exploit similar interactions in synthetic systems to harness new and otherwise inaccessible chemistry. One example is allosteric regulation, in which a signaling molecule modulates an enzyme's catalytic activity by binding to it at a site distinct from its catalytic center. Albeit this regulatory mechanism is found throughout nature,<sup>1</sup> artificial allosteric catalytic systems remain underexplored.<sup>2</sup>

Recent advances in supramolecular chemistry have enabled the design, construction and study of complex, multicomponent assemblies with exquisite detail. Researchers endeavoring to bridge the gap between synthetic and natural allosteric systems have devised numerous artificial assemblies that closely resemble their natural counterparts. In fact, the first efforts towards the development of artificial allosteric catalysts have recently been described.<sup>3,4</sup>

To date, there have been two distinct approaches to mimicking the biological regulation of catalysis via allosteric modulation. First, Mirkin *et al.* used the Weak-Link Approach (WLA)<sup>3</sup> with supramolecular coordination chemistry to build the large, multimetallic macrocyclic complexes **169** and **170**, which can be

<sup>1</sup> Traut, T. in *Handbook of Proteins: Structure, Formation and Methods*, Cox, M. M.; Philips, G. N., Jr. Eds., Wiley-VCH: Weinheim, 2007, Vol. I, p. 470.

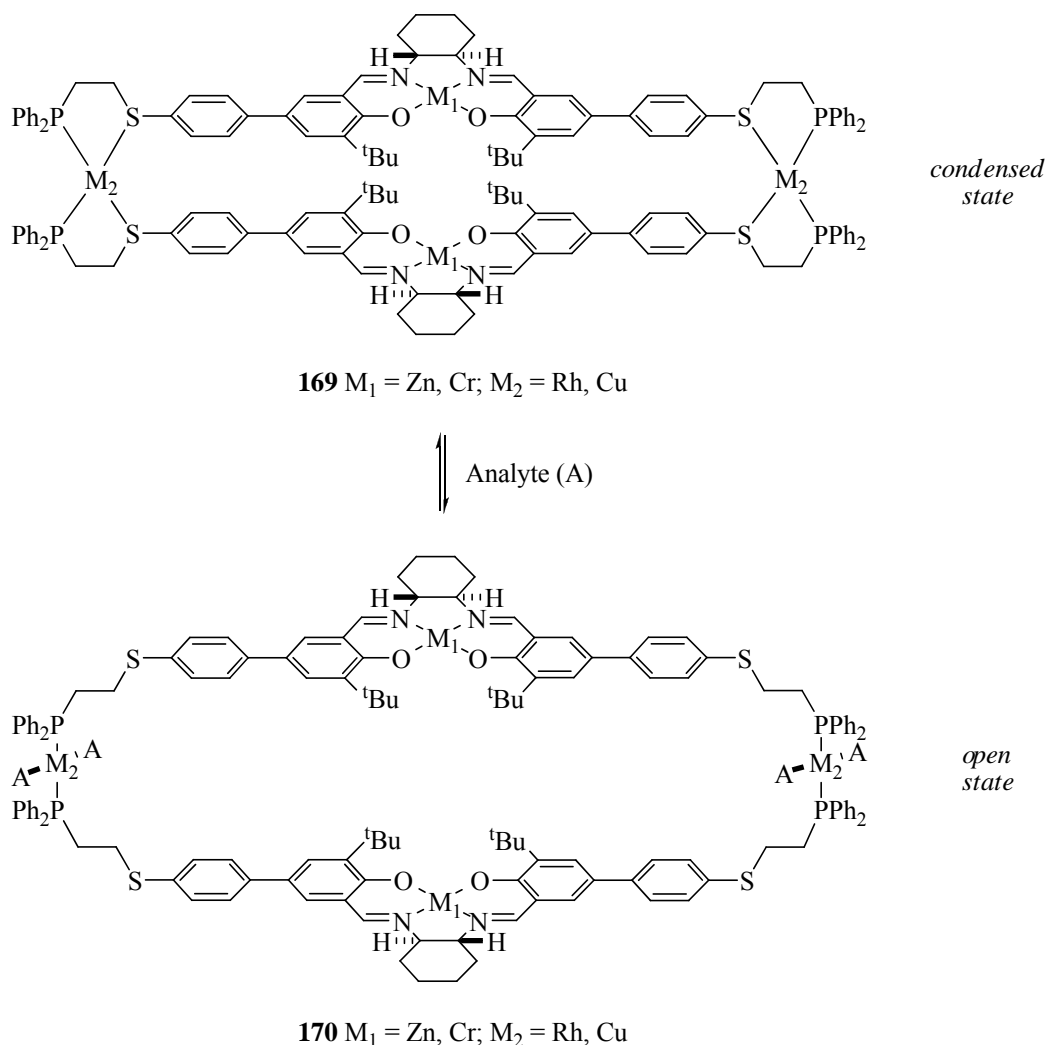
<sup>2</sup> Kovbasyuk, L.; Kraemer, R. *Chem. Rev. (Washington, DC, U. S.)* **2004**, *104*, 3161-3187.

<sup>3</sup> (a) Masar, M. S., III; Gianneschi, N. C.; Oliveri, C. G.; Stern, C. L.; Nguyen, S. T.; Mirkin, C. A. *J. Am. Chem. Soc.* **2007**, *129*, 10149-10158. (b) Oliveri, C. G.; Gianneschi, N. C.; Nguyen, S. T.; Mirkin, C. A.; Stern, C. L.; Wawrzak, Z.; Pink, M. *J. Am. Chem. Soc.* **2006**, *128*, 16286-16296. (c) Gianneschi, N. C.; Nguyen, S. T.; Mirkin, C. A. *J. Am. Chem. Soc.* **2005**, *127*, 1644-1645. (d) Gianneschi, N. C.; Masar, M. S., III; Mirkin, C. A. *Acc. Chem. Res.* **2005**, *38*, 825-837. (e) Gianneschi, N. C.; Cho, S.-H.; Nguyen, S. B. T.; Mirkin, C. A. *Angew. Chem., Int. Ed.* **2004**, *43*, 5503-5507. (f) Gianneschi, N. C.; Bertin, P. A.; Nguyen, S. T.; Mirkin, C. A.; Zakharov, L. N.; Rheingold, A. L. *J. Am. Chem. Soc.* **2003**, *125*, 10508-10509.

<sup>4</sup> (a) Kovbasyuk, L.; Pritzkow, H.; Kraemer, R.; Fritsky, I. O. *Chem. Commun. (Cambridge, U. K.)* **2004**, 880-881. (b) Takebayashi, S.; Ikeda, M.; Takeuchi, M.; Shinkai, S. *Chem. Commun. (Cambridge, U. K.)* **2004**, 420-421. (c) Saghatelian, A.; Guckian, K. M.; Thayer, D. A.; Ghadiri, M. R. *J. Am. Chem. Soc.* **2003**, *125*, 344-345. (d) Scarso, A.; Scheffer, U.; Gobel, M.; Broxterman, Q. B.; Kaptein, B.; Formaggio, F.; Toniolo, C.; Scrimin, P. *Proc. Natl. Acad. Sci. U. S. A.* **2002**, *99*, 5144-5149. (e) Tozawa, T.; Tokita, S.; Kubo, Y. *Tetrahedron Lett.* **2002**, *43*, 3455-3457. (f) Fritsky, I. O.; Ott, R.; Pritzkow, H.; Kramer, R. *Chem.--Eur. J.* **2001**, *7*, 1221-1231. (g) Fritsky, I. O.; Ott, R.; Kramer, R. *Angew. Chem., Int. Ed.* **2000**, *39*, 3255-3258.

*Preliminary Investigations into Bio-inspired Supramolecular Strategies for Asymmetric Catalysis: Literature Precedent*

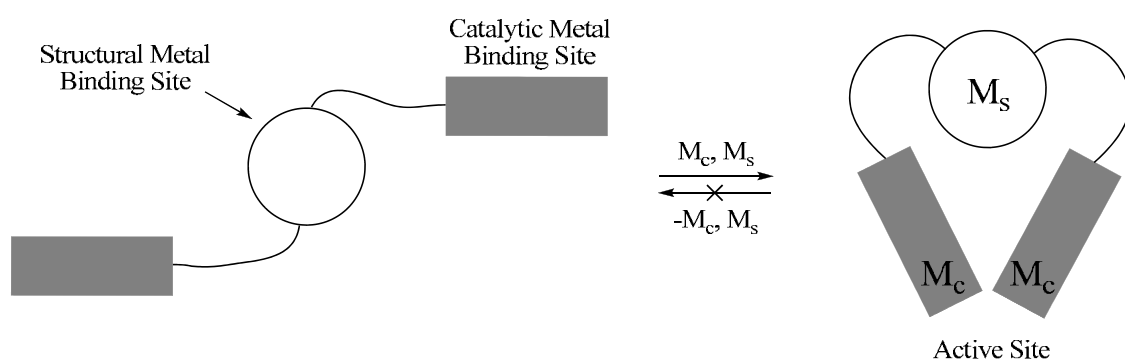
chemically interconverted *in situ* between their *condensed* and *open* states using small molecules (analytes). With this strategy, the authors designed a series of allosteric catalysts that differ in the shape of their structural center, and consequently, in their catalytic activity (Scheme 1).



**Scheme 1.** General structure of the supramolecular allosteric catalysts designed by Mirkin *et al.*, shown in the condensed and open states.

They then employed these catalysts in the ring-opening of cyclohexene oxide by  $\text{TMSN}_3^{3e-f}$  and in the acyl transfer reaction between 1-acetylimidazole and 4-pyridylcarbinol<sup>3a-c</sup>. In summary, the artificial allosteric catalysts developed by Mirkin *et al.* enable control over catalytic activity and selectivity and can be

reversibly interconverted between their states *in situ*. In the second approach, an organic ligand binds to structural metal ions to form an intermediate, which then binds to catalytic metal ions to form a catalytically active complex (Scheme 2 and Figure 1).<sup>4,5</sup> The order of the binding events is crucial to formation of the catalyst: the structural metal ions act as the allosteric modulator of the ligand, preparing it for binding to the catalytic metal ions.



**Scheme 2.** A ligand binds to one or more structural metal ions ( $M_s$ ), and the resulting intermediate, having adopted the appropriate configuration, then binds to one or more catalytic metal ions ( $M_c$ ) to form a catalytically active complex. Depending on the system,  $M_s$  and  $M_c$  may be different or equivalent.

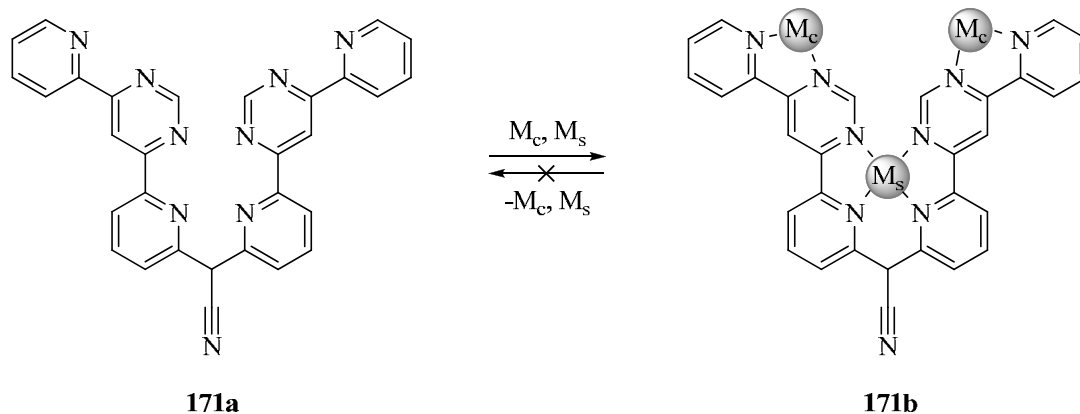


**Figure 1.** Ligand **171a** binds to structural metal ions ( $M_s$ ), and then to catalytic metal ions ( $M_c$ ), to form the supramolecular allosteric catalyst **171b** (see Scheme 2).  $M_s = \text{Cu, Ni or Pd}$ .  $M_c = \text{Cu}$ .<sup>4f-g</sup>

<sup>5</sup> (a) Hua, J.; Lin, W. *Org. Lett.* **2004**, *6*, 861-864. (b) Lee, S. J.; Hu, A.; Lin, W. *J. Am. Chem. Soc.* **2002**, *124*, 12948-12949. (c) Merlau, M. L.; Del Pilar Mejia, M.; Nguyen, S. T.; Hupp, J. T. *Angew. Chem., Int. Ed.* **2001**, *40*, 4239-4242. (d) Nakash, M.; Clyde-Watson, Z.; Feeder, N.; Davies, J. E.; Teat, S. J.; Sanders, J. K. M. *J. Am. Chem. Soc.* **2000**, *122*, 5286-5293.

*Preliminary Investigations into Bio-inspired Supramolecular Strategies for  
Asymmetric Catalysis: Literature Precedent*

---

However, in a biological context, this strategy is more reminiscent of the way that structural metals define the tertiary structure of certain enzymes statically rather than dynamically and reversibly.

Researchers have sought to extrapolate principles of allosteric modulation into much smaller and synthetically accessible organic ligands. Work in this area has led to studies correlating binding forces to catalytic activity.<sup>6</sup> Artificial allosteric systems require an active (catalytic) site, a remote (allosteric modulation) site, and finally, a mechanical mechanism linking these sites.

We envisaged using predictable, structurally well-defined binding interactions to assemble supramolecular catalysts based on biological allosteric systems. Herein, we describe our system **172**, a chiral biaryl derivative containing crown ether groups of different chain lengths (Figure 2). It incorporates a bidentate catalytic site, and a remote site capable of conformational changes upon binding to cationic species via ion-dipole interactions.<sup>7</sup> The mechanism for allosteric modulation is based on changes in the biaryl dihedral angle.

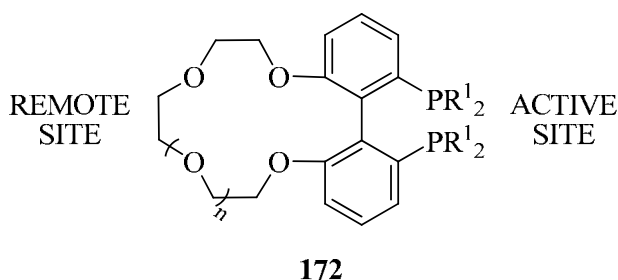


**Figure 2.** General structure of the bio-inspired supramolecular catalyst **172**, which has potential for allosteric modulation.

---

<sup>6</sup> Rebek, J., Jr. *Acc. Chem. Res.* **1984**, *17*, 258-64 and references therein.

<sup>7</sup> (a) *Supramolecular Chemistry: A Concise Introduction*, Steed, J. W.; Atwood, J. L., Eds.; Wiley: New York, 2000. (b) *Cation Binding by Macrocycles: Complexation of Cationic Species by Crown Ethers*, Inoue, Y.; Gokel, G. W., Eds.; Marcel Dekker: New York, 1990.

The fundamental structural requirement for chiral biaryl ligands used in asymmetric catalysis is restricted rotation around the single C-C bond at room temperature (see Figure 3). Extensive studies on the inversion rates between the two atropisomers of numerous biaryl derivatives<sup>8</sup> have shown that most tetra-*ortho*-substituted biphenyls are configurationally stable at room (or higher) temperatures,<sup>9</sup> and consequently, the corresponding enantiomers can be isolated, and then used independently as chiral asymmetric ligands.

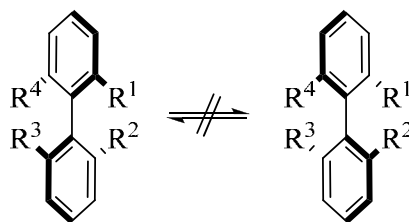


**Figure 3.** Atropisomers derived from tetra-*ortho*-substituted biphenyls.

In the nearly three decades following the first report of its synthesis and catalytic applications by Noyori and Takaya,<sup>10</sup> BINAP (Figure 4) has been used in a myriad of asymmetric transformations, becoming the ligand of choice for many of them. The fragment that confers BINAP with high levels of stereodiscrimination is a chiral biaryl backbone.

<sup>8</sup> Eliel, E. L.; Wilen, S.H.; Mander, L. N. *Stereochemistry of Organic Compounds*; Wiley: New York, 1994.

<sup>9</sup> Atropisomers are stereoisomers resulting from hindered rotation about single bonds in which the steric strain barrier to rotation is high enough to allow for the isolation of the conformers. Oki defined atropisomers as conformers that interconvert with a half-life ( $t_{1/2}$ ) longer than 1000 s (16.7 min) at 300 K, which corresponds to a rotational barrier of 22 kcal/mol (Oki, M. *Top. Stereochem.* **1983**, *14*, 1-81.)

<sup>10</sup> (a) Miyashita, A.; Yasuda, A.; Takaya, H.; Toriumi, K.; Ito, T.; Souchi, T.; Noyori, R. *J. Am. Chem. Soc.* **1980**, *102*, 7932-4. (b) Miyashita, A.; Takaya, H.; Souchi, T.; Noyori, R. *Tetrahedron* **1984**, *40*, 1245-53.

*Preliminary Investigations into Bio-inspired Supramolecular Strategies for  
Asymmetric Catalysis: Literature Precedent*

---

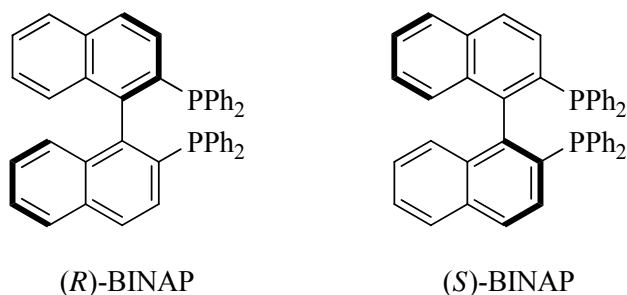


**Figure 4.** (R)- and (S)-BINAP.

BINAP analogs containing several biaryl units have been synthesized in order to achieve higher activities and enantioselectivities.<sup>11</sup> Modification of the electronic properties of the phosphorus functionalities<sup>12</sup> and modification of the sterics in the catalytic site<sup>13</sup> have spawned various BINAP analogs (Figure 5).

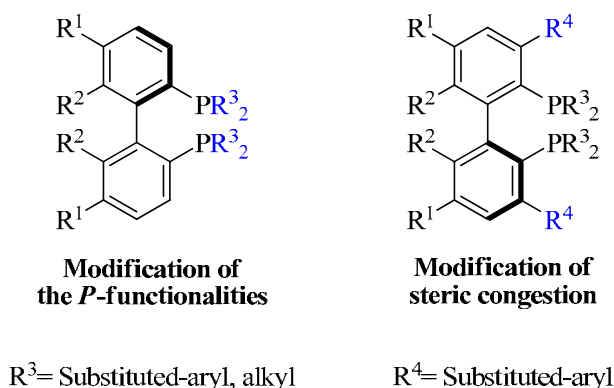


**Figure 5.** General structure of BINAP analogs.

<sup>11</sup> (a) Shimizu, H.; Nagasaki, I.; Saito, T. *Tetrahedron* **2005**, *61*, 5405-5432. (b) Andersen, N. G.; McDonald, R.; Keay, B. A. *Tetrahedron: Asymmetry* **2001**, *12*, 263-269. (c) Inoue, S.; Osada, M.; Koyano, K.; Takaya, H.; Noyori, R. *Chem. Lett.* **1985**, 1007-8.

<sup>12</sup> (a) Henschke, J. P.; Zanutti-Gerosa, A.; Moran, P.; Harrison, P.; Mullen, B.; Casy, G.; Lennon, I. C. *Tetrahedron Lett.* **2003**, *44*, 4379-4383. (b) Chiba, T.; Miyashita, A.; Nohira, H. *Tetrahedron Lett.* **1993**, *34*, 2351-4. (c) Chiba, T.; Miyashita, A.; Nohira, H.; Takaya, H. *Tetrahedron Lett.* **1991**, *32*, 4745-8.

<sup>13</sup> (a) Wu, S.; He, M.; Zhang, X. *Tetrahedron: Asymmetry* **2004**, *15*, 2177-2180. (b) Tang, W.; Chi, Y.; Zhang, X. *Org. Lett.* **2002**, *4*, 1695-1698.

Another strategy for modulating the catalytic activity of BINAP is modification of the dihedral angle ( $\theta$ ), which ultimately causes a change in the bite angle ( $\beta$ ) of the phosphorus groups coordinated to the metal center (Figure 6). The potential for allosteric modulation of the catalytic activity of **172** lies in this strategy. Numerous studies have revealed that optimal dihedral or bite angles in catalytic systems derived from axially-chiral diphosphines are essential for high enantioselectivities in asymmetric catalysis.<sup>14</sup>

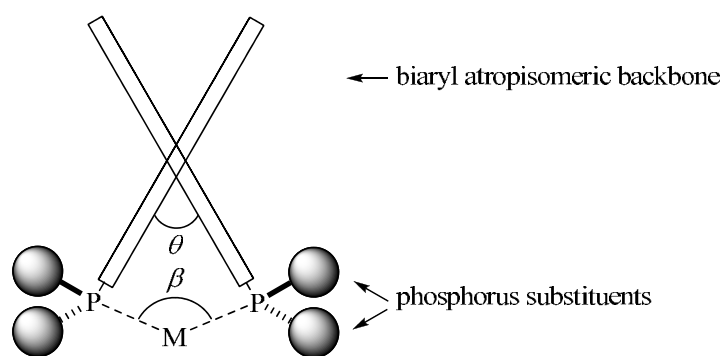


**Figure 6.** Tunable BINAP analogs. M = transition metal center;  $\beta$  = bite angle; and  $\theta$  = dihedral angle.

<sup>14</sup> (a) Birkholz, M.-N.; Freixa, Z.; van Leeuwen, P. W. N. M. *Chem. Soc. Rev.* **2009**, *38*, 1099-1118. (b) Rivillo, D.; Gulyas, H.; Benet-Buchholz, J.; Escudero-Adan, E. C.; Freixa, Z.; van Leeuwen, P. W. N. M. *Angew. Chem., Int. Ed.* **2007**, *46*, 7247-7250. (c) Jeulin, S.; Duprat de Paule, S.; Ratovelomanana-Vidal, V.; Genet, J.-P.; Champion, N.; Dellis, P. *Angew. Chem., Int. Ed.* **2004**, *43*, 320-325. (d) Duprat de Paule, S.; Jeulin, S.; Ratovelomanana-Vidal, V.; Genet, J.-P.; Champion, N.; Dellis, P. *Eur. J. Org. Chem.* **2003**, 1931-1941. (e) Duprat de Paule, S.; Jeulin, S.; Ratovelomanana-Vidal, V.; Genet, J.-P.; Champion, N.; Dellis, P. *Tetrahedron Lett.* **2003**, *44*, 823-826. (f) Saito, T.; Yokozawa, T.; Ishizaki, T.; Moroi, T.; Sayo, N.; Miura, T.; Kumobayashi, H. *Adv. Synth. Catal.* **2001**, *343*, 264-267. (g) Dierkes, P.; van Leeuwen, P. W. N. M. *J. Chem. Soc., Dalton Trans.* **1999**, 1519-1530. (h) Davies, I. W.; Deeth, R. J.; Larsen, R. D.; Reider, P. J. *Tetrahedron Lett.* **1999**, *40*, 1233-1236. (i) Van der Veen, L. A.; Boele, M. D. K.; Bregman, F. R.; Kamer, P. C. J.; Van Leeuwen, P. W. N. M.; Goubitz, K.; Fraanje, J.; Schenk, H.; Bo, C. *J. Am. Chem. Soc.* **1998**, *120*, 11616-11626. (j) Meessen, P.; Vogt, D.; Keim, W. *J. Organomet. Chem.* **1998**, *551*, 165-170. (k) Sakaki, S.; Takeuchi, K.; Sugimoto, M.; Kurosawa, H. *Organometallics* **1997**, *16*, 2995-3003. (l) Harada, T.; Takeuchi, M.; Hatsuda, M.; Ueda, S.; Oku, A. *Tetrahedron: Asymmetry* **1996**, *7*, 2479-2482. (m) Kranenburg, M.; van der Burgt, Y. E. M.; Kamer, P. C. J.; van Leeuwen, P. W. N. M.; Goubitz, K.; Fraanje, J. *Organometallics* **1995**, *14*, 3081-9.

A complete summary of all known biaryl derivatives, and how the dimensions and shape of the biaryl group influence the dihedral angle, would be beyond the scope of this section. However, we can briefly review the work of Saito *et al.*, who studied the relationship between dihedral angle and catalytic activity in Ruthenium-catalyzed asymmetric hydrogenations of 1-hydroxypropan-2-one (see Table 1). They obtained the highest enantioselectivities with the ligands having the narrowest dihedral angle (MeO-BIPHEP and related ligands) (Figure 7).

**Table 1.** Correlation between dihedral angle and catalytic activity for chiral diphosphine ligands in Ruthenium-catalyzed asymmetric hydrogenation.

Ligand	BINAP	BIPHEMP	MeO-BIPHEP
Dihedral angle $\theta$ (deg) <sup>a</sup>	73.5	72.1	68.6
ee (%)	89	93	96

<sup>a</sup> As estimated by CAChe MM2 calculations.

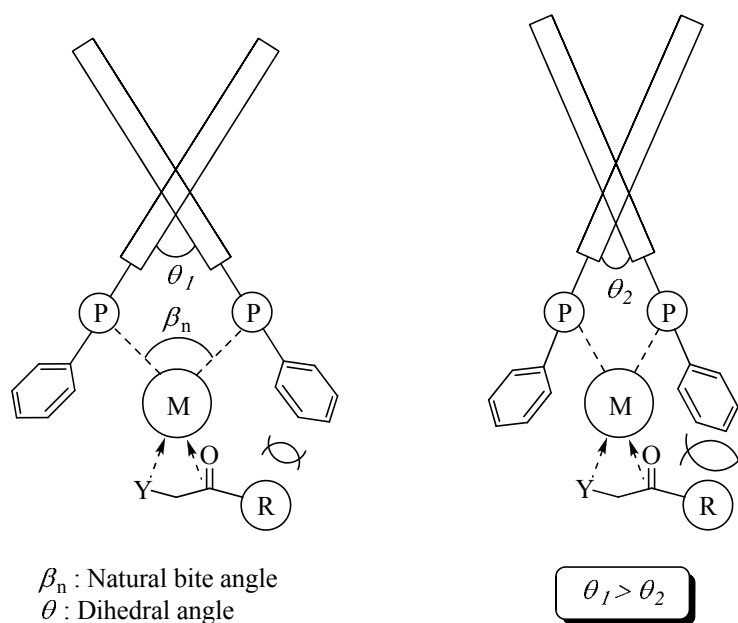
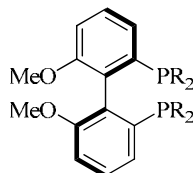


**Figure 7.** BINAP analogs: modifying the dihedral angle ( $\theta$ ) in the biaryl backbone alters the sterics of the phosphine groups.

Strategies to modify the dihedral angle in biaryl derivatives without altering the biaryl group itself are more relevant to our possible allosteric modulation of



the catalytic activity of **172**. Therefore, we have provided a brief overview of these strategies here. All known examples of this category entail the use of MeO-BIPHEP (**173a**)—developed by Schmid *et al.*<sup>15</sup> and later used in various transformations—or related ligands (Figure 8).<sup>16</sup>



- 173a** R = Ph, MeO-BIPHEP  
**173b** R = 3,5-Me<sub>2</sub>-Ph  
**173c** R = 3,5-(<sup>t</sup>Bu)<sub>2</sub>-Ph  
**173d** R = Cy  
**173e** R = 2-thienyl

**Figure 8.** MeO-BIPHEP and related ligands.

Zhang *et al.* suggested that BINAP and MeO-BIPHEP, due to their lack of rigidity, were occasionally not efficient ligands for the asymmetric hydrogenation of substrates such as  $\beta$ -aryl- $\beta$ -ketoesters<sup>17</sup> and  $\beta$ -trifluoromethyl- $\beta$ -ketoesters<sup>14c-e</sup>. Thus, they prepared a series of bridged ligands of different ring sizes, which they called C<sub>n</sub>-TunaPHOS ligands (**174-180**), whereby *n* represents the number of methylene units in the bridging chain.<sup>17</sup> C<sub>n</sub>-TunaPHOS ligands are more rigid than MeO-BIPHEP and have different dihedral angles (Figure 9). The authors demonstrated the importance of the dihedral angle to enantioselectivity in asymmetric hydrogenations,<sup>17,18</sup> observing that the best ligand (in terms of enantiomeric excess) depended on the substrate: C<sub>4</sub>-TunaPHOS for  $\beta$ -ketoesters<sup>17</sup>

<sup>15</sup> Schmid, R.; Foricher, J.; Cereghetti, M.; Schoenholzer, P. *Helv. Chim. Acta* **1991**, *74*, 370-89.

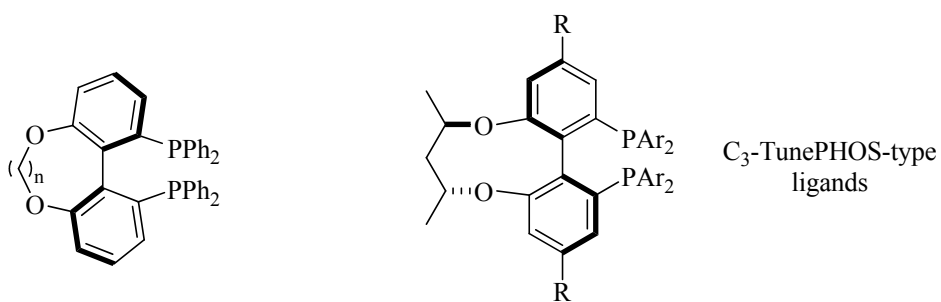
<sup>16</sup> (a) Chapuis, C.; Barthe, M.; De Saint Laumer, J.-Y. *Helv. Chim. Acta* **2001**, *84*, 230-242. (b) Schmid, R.; Broger, E. A.; Cereghetti, M.; Cramer, Y.; Foricher, J.; Lalonde, M.; Muller, R. K.; Scalone, M.; Schoettl, G.; Zutter, U. *Pure Appl. Chem.* **1996**, *68*, 131-8.

<sup>17</sup> Zhang, Z.; Qian, H.; Longmire, J.; Zhang, X. *J. Org. Chem.* **2000**, *65*, 6223-6226.

<sup>18</sup> (a) Wang, C.-J.; Sun, X.; Zhang, X. *Synlett* **2006**, 1169-1172. (b) Wang, C.-J.; Sun, X.; Zhang, X. *Angew. Chem., Int. Ed.* **2005**, *44*, 4933-4935. (c) Lei, A.; Wu, S.; He, M.; Zhang, X. *J. Am. Chem. Soc.* **2004**, *126*, 1626-1627. (d) Tang, W.; Wu, S.; Zhang, X. *J. Am. Chem. Soc.* **2003**, *125*, 9570-9571.

*Preliminary Investigations into Bio-inspired Supramolecular Strategies for Asymmetric Catalysis: Literature Precedent*

and  $\alpha$ -ketoesters,<sup>18a</sup> C<sub>3</sub>-TunaPHOS for allylphthalimides<sup>18b</sup> and  $\alpha$ -phthalimideketones,<sup>18c</sup> and C<sub>2</sub>-C<sub>5</sub>-TunaPHOS for  $\beta$ -acylaminoacrylates.<sup>18d</sup> They later observed the same trend in Palladium-catalyzed allylic alkylations, concluding that the ligand bite angle dramatically influenced the enantioselectivities.<sup>19</sup>



**174** n = 1, C<sub>1</sub>-TunaPHOS  
**175** n = 2, C<sub>2</sub>-TunaPHOS  
**176** n = 3, C<sub>3</sub>-TunaPHOS  
**177** n = 4, C<sub>4</sub>-TunaPHOS  
**178** n = 5, C<sub>5</sub>-TunaPHOS  
**179** n = 6, C<sub>6</sub>-TunaPHOS

**180a** R = H, Ar = Ph  
**180b** R = H, Ar = 4-Me-Ph  
**180c** R = H, Ar = 3,5-Me<sub>2</sub>-Ph  
**180d** R = H, Ar = 3,5-<sup>t</sup>Bu<sub>2</sub>-Ph  
**180e** R = H, Ar = 4-MeO-3,5-<sup>t</sup>Bu<sub>2</sub>-Ph  
**180f** R = <sup>t</sup>Bu, Ar = Ph

Ligand	174	175	176	177	178	179	173a
Calc. Dihedral angle (deg)	60	74	77	88	94	106	87

**Figure 9.** C<sub>n</sub>-TunaPHOS and C<sub>3</sub>-TunePHOS chiral ligands (Zhang *et al.*).

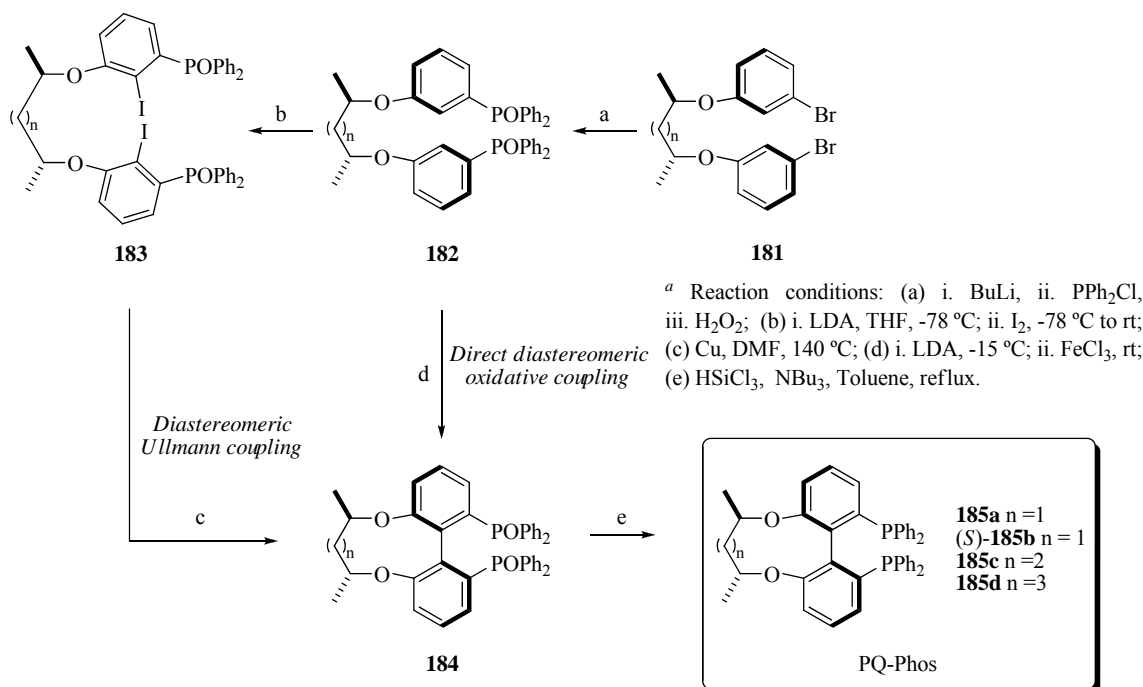
Zhang *et al.*<sup>20</sup> prepared, following a known strategy,<sup>21</sup> a series of modular, fine-tunable, chiral-bridge atropisomeric diphosphine ligands (**180a-f**). This new method is advantageous in that it obviates the tedious optical resolution required by other methods: the authors achieved this by exploiting the concept of central-to-axial chirality transfer, which had been designed by Chan *et al.* to make the

<sup>19</sup> Raghunath, M.; Zhang, X. *Tetrahedron Lett.* **2005**, *46*, 8213-8216.

<sup>20</sup> (a) Wang, C.-J.; Wang, C.-B.; Chen, D.; Yang, G.; Wu, Z.; Zhang, X. *Tetrahedron Lett.* **2009**, *50*, 1038-1040. (b) Sun, X.; Zhou, L.; Li, W.; Zhang, X. *J. Org. Chem.* **2008**, *73*, 1143-1146.

<sup>21</sup> (a) Qiu, L.; Kwong, F. Y.; Wu, J.; Lam, W. H.; Chan, S.; Yu, W.-Y.; Li, Y.-M.; Guo, R.; Zhou, Z.; Chan, A. S. C. *J. Am. Chem. Soc.* **2006**, *128*, 5955-5965. (b) Qiu, L.; Wu, J.; Chan, S.; Au-Yeung, T. T. L.; Ji, J.-X.; Guo, R.; Pai, C.-C.; Zhou, Z.; Li, X.; Fan, Q.-H.; Chan, A. S. C. *Proc. Natl. Acad. Sci. U. S. A.* **2004**, *101*, 5815-5820.

diphosphine ligands **185**, so-called PQ-Phos ligands.<sup>21</sup> Chan's strategy is depicted in Scheme 3.



**Scheme 3.** Pathways for synthesizing PQ-Phos ligands **185**, featuring intramolecular diastereoselective couplings (Chan *et al.*).<sup>a</sup>

The arylphosphine oxides **182** were synthesized from **181**, which contains two stereogenic centers in its backbone, by halogen/lithium exchange, followed by capture of the dilithium derivative with chlorodiphenylphosphine, and finally, oxidation of the phosphino groups (Scheme 3, Step *a*). The diiododerivatives **183** were easily prepared by direct *ortho*-lithiation of **182** and subsequent quenching with iodine (Scheme 3, Step *b*). Finally, diastereomerically pure biaryl derivatives **184** were obtained by intramolecular Ullmann coupling of **183** (Scheme 3, Step *c*). Alternatively, phosphine oxide **184** was also directly prepared by an asymmetric ring-closure reaction, via oxidative intramolecular coupling of **182** (Scheme 3, Step *d*). It should be noted that the stereogenic centers in the bridging chain of **182** provided very high diastereoselectivity in both routes (d.e. > 99%), as reflected in the fact that the other possible

*Preliminary Investigations into Bio-inspired Supramolecular Strategies for  
Asymmetric Catalysis: Literature Precedent*

---

diastereomer was not detected in either case. Finally, the tunable phosphines **185** were readily synthesized by reduction of the P=O bonds using well-established synthetic procedures (Scheme 3, Step *e*).

The bridging chain enables fine-tuning of the dihedral angle of the biaryl group. This feature was exploited by the authors to obtain excellent asymmetric performance from the corresponding Ruthenium and Iridium complexes with PQ-Phos ligands **185** in hydrogenations of ketones, imines and alkenes.<sup>21</sup>

## **RESULTS AND DISCUSSION**

UNIVERSITAT ROVIRA I VIRGLI

TOWARDS HIGHLY EFFICIENT LIGANDS FOR ASYMMETRIC HYDROGENATIONS: A COVALENT MODULAR APPROACH AND  
INVESTIGATIONS INTO BIOINSPIRED SUPRAMOLECULAR STRATEGIES

Héctor Fernández Pérez

ISBN:978-84-693-3385-3 /DL:T.994-2010

## 2.2. SYNTHESIS OF CROWN ETHER DIPHOSPHINE LIGANDS WITH POTENTIAL FOR ALLOSTERIC MODULATION OF CATALYTIC ACTIVITY

As explained in the introduction, this thesis includes as a minor project the synthesis of catalytic ligands with potential for allosteric modulation: the biaryl diphosphine ligands **172** (Figure 10), which contain a crown ether as the allosteric site. The premise behind the allosteric mechanism is that changes in the allosteric site (crown ether) at **172**, via binding forces, would alter the active site geometry, thereby modulating the catalytic activity.

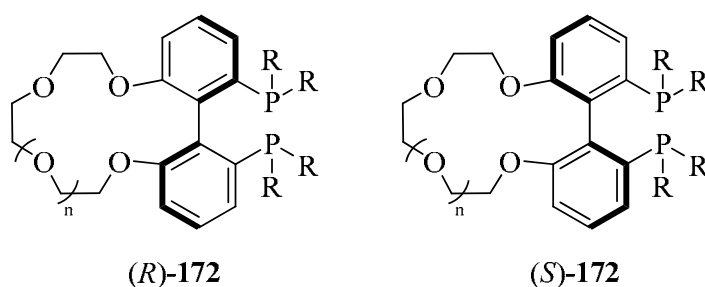
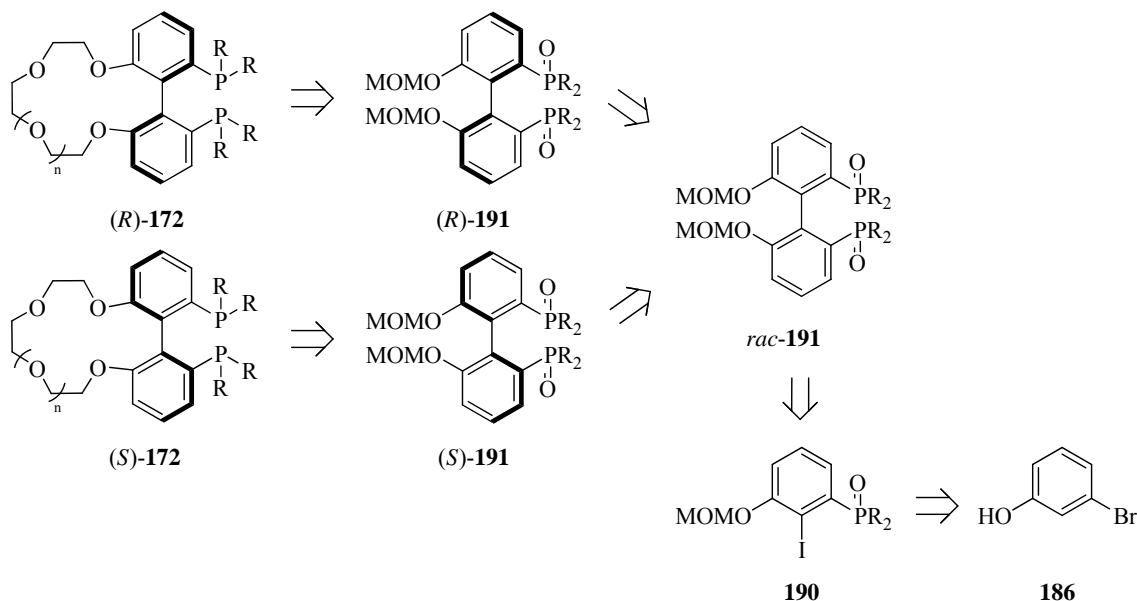


**Figure 10.** Atropisomerically pure biaryl diphosphine ligands designed for allosteric modulation.

The key step in synthesizing ligands **172** was to prepare the corresponding atropisomeric biaryl compounds (*rac*)-**191** as phosphine oxides, according to the retrosynthetic strategy shown in Scheme 4.

Preliminary Investigations into Bio-inspired Supramolecular Strategies for  
Asymmetric Catalysis: Results and Discussion



**Scheme 4.** Retrosynthetic strategy for the synthesis of chiral ligands **172**.

The route comprised the following key steps: reaction of 3-bromophenol (**186**) to form (2-iodo-3-(methoxymethoxy)phenyl)diphenylphosphine oxide (**190**); Ullmann homocoupling of **189** to form **191** in its racemic form; subsequent chemical resolution of (*R*)- and (*S*)-**191**; formation of the crown ether; and lastly, reduction of the phosphine oxide (P=O), to afford (*R*)- and (*S*)-**172**.

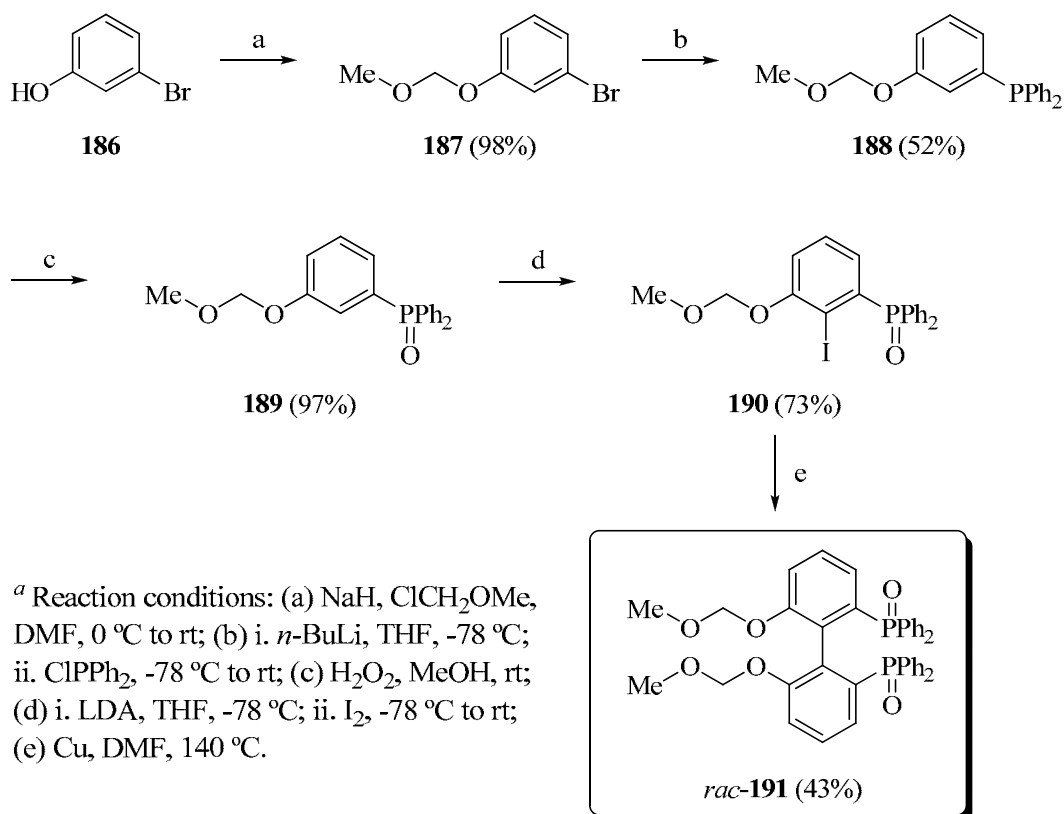
### 2.2.1. Synthesis of (*rac*)-(6,6'-bis(methoxymethoxy)biphenyl-2,2'-diyl)bis(diphenylphosphine oxide) (**191**)

Treatment of 3-bromophenol (**186**) with chloro(methoxy)methane and base afforded the MOM-protected bromoaryl derivative **187** in practically quantitative yield (98%)<sup>22</sup> (Scheme 5, Step *a*). Compound **187** was then lithiated, and reacted with chlorodiphenylphosphine to provide the corresponding arylphosphine **188** in

<sup>22</sup> Kaiser, F.; Schwink, L.; Velder, J.; Schmalz, H.-G. *J. Org. Chem.* **2002**, *67*, 9248-9256.



52% yield (Scheme 5, Step *b*). Oxidation of the phosphine moiety was required for the subsequent steps: this entailed using 30% H<sub>2</sub>O<sub>2</sub> in MeOH as solvent and provided excellent yield (97%) (Scheme 5, Step *c*).



**Scheme 5.** Synthesis of the atropisomeric biaryl-diphosphine racemate (*rac*)-**191**.<sup>a</sup>

Directed *ortho*-lithiation at C<sub>2</sub> of the *m*-MOM-aryl ether **189** with LDA at -78 °C followed by quenching with iodine provided the iodo derivative **190** in 73% overall yield. As expected, the directed lithiation proceeded smoothly. We had reasoned that it would be facilitated by the donor oxygen groups at the *ortho* positions (the MOM-oxy and diphenylphosphoryl groups; see Figure 11).

*Preliminary Investigations into Bio-inspired Supramolecular Strategies for  
Asymmetric Catalysis: Results and Discussion*

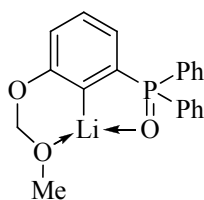


**Figure 11.** *Ortho*-lithiation of compound **189**.

The temperature and the order of addition were critical to the success of the lithiation. At  $-78\text{ }^{\circ}\text{C}$ , the lithium species precipitated as a solid, providing high yields of **190**; contrariwise, at higher temperatures, lower yields were observed.<sup>15</sup> During process development, we found that addition of lithiated **189** in THF to the iodine solution at  $-78\text{ }^{\circ}\text{C}$  gave better yields than did the reverse order of addition (73% vs. 40%, respectively). Thus, under the optimized reaction conditions, treatment of **189** with 1.1 equiv. of LDA in THF at  $-78\text{ }^{\circ}\text{C}$ , followed by quenching the reaction with 1.1 equiv. of I<sub>2</sub>, provided **190** in 73% isolated yield. Furthermore, we were able to recover *ca.* 9% of the starting material (**189**) (see Figure 12, the <sup>31</sup>P{<sup>1</sup>H}-NMR spectrum of the reaction mixture).

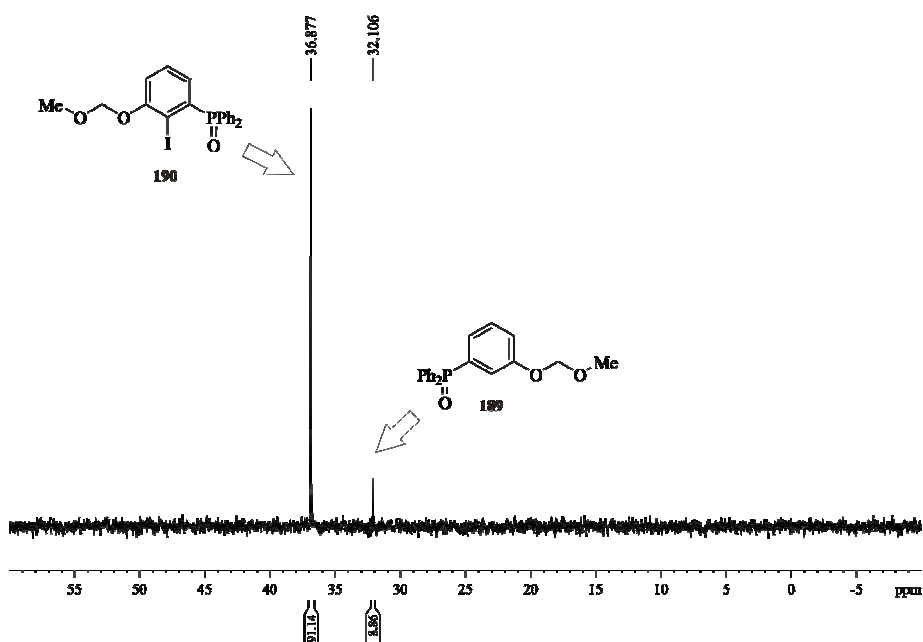


**Figure 12.** <sup>31</sup>P{<sup>1</sup>H}-NMR spectrum of *ortho*-lithiation/iodination reaction.

Finally, the racemate (*rac*)-**191** was prepared via Ullmann homocoupling<sup>23</sup> of **190**, using activated copper powder in DMF solution. After 3 hours at 140 °C, no starting material was detected, and compound **191** was obtained along with the deiodinated byproduct **189** (deiodination is a known side reaction in Ullman couplings)<sup>23</sup> in a 70:30 ratio (**191**:**189**), as calculated by <sup>31</sup>P{<sup>1</sup>H}-NMR (Figure 13). The optimal temperature for the coupling was 140 °C: lower temperatures (120 °C) did not lead to full conversion, whereas higher temperatures (150 °C) led to a greater proportion of **189**. Compound (*rac*)-**191** was easily purified by precipitation and was obtained in 43% yield.

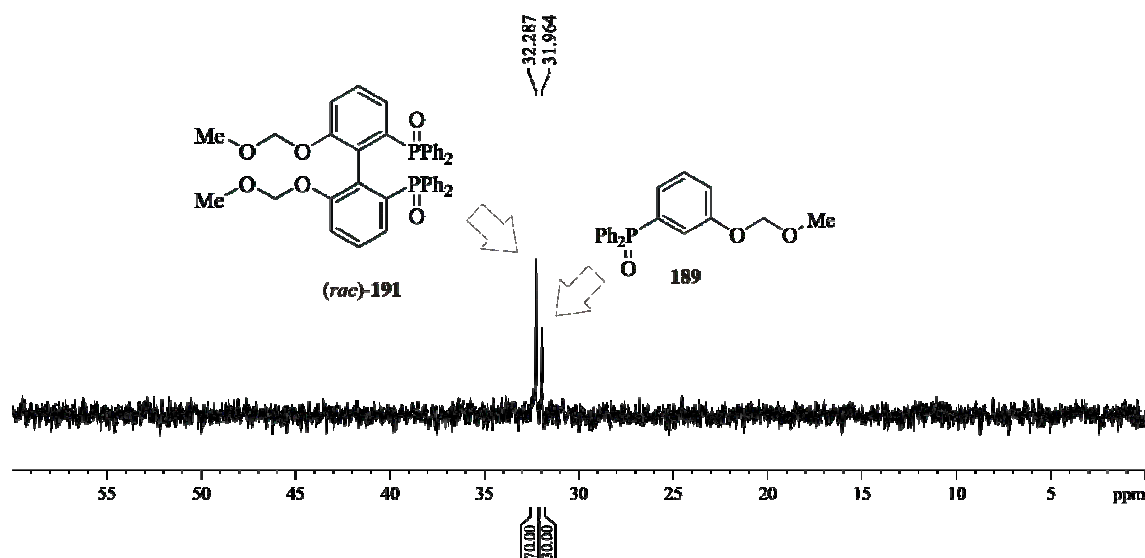
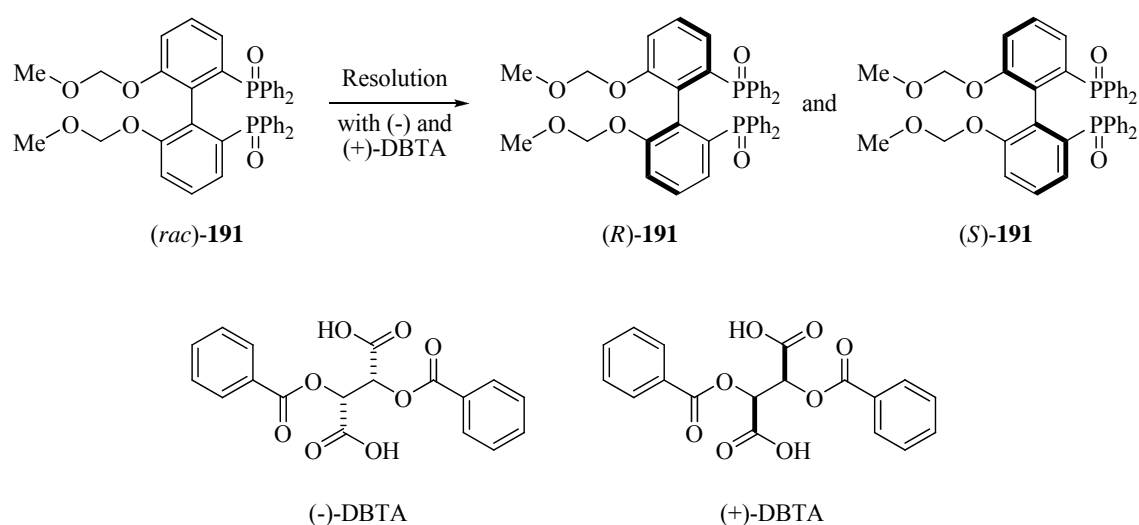


Figure 13. <sup>31</sup>P{<sup>1</sup>H}-NMR spectrum of the Ullmann homocoupling of **190** to form (*rac*)-**191**.

<sup>23</sup> Nelson, T. D.; Crouch, R. D. in *Organic Reactions*, Overmann, L. E. Ed.; John Wiley & Sons, 2004, Vol. 63, p. 265.

### 2.2.2. Optical resolution of (*rac*)-(6,6'-bis(methoxymethoxy)biphenyl-2,2'-diyl)bis(diphenylphosphine oxide) (**191**)

With (*rac*)-**191** in hand, we turned to optical resolution of the corresponding enantiomers. We chose (–) and (+) 2,3-*O,O*-dibenzoyl tartaric acid (DBTA) as resolving agents (Scheme 6),<sup>24</sup> since they had been successfully used in the resolution of the methyl substituted analog of **191**.<sup>15</sup>



**Scheme 6.** Optical resolution of (*rac*)-**191** using (–) and (+) 2,3-*O,O*-dibenzoyl tartaric acid (DBTA) as resolving agents.

Thus, (*rac*)-**191** was first resolved with (–)-DBTA, by fractional crystallization. A solution of (*rac*)-**191** in refluxing dichloromethane was mixed with a hot (50 °C) solution of (–)-DBTA in ethyl acetate (1:1.3 ratio of CH<sub>2</sub>Cl<sub>2</sub>/EtOAc). The mixture was allowed to cool slowly with stirring, and was then placed in the refrigerator (approximately 5 °C) overnight. Crystals that had formed at that temperature were filtered, washed with a cold mixture of CH<sub>2</sub>Cl<sub>2</sub>/EtOAc (1:1.3), and dried. Fortunately, these crystals were suitable for X-

<sup>24</sup> Brunner, H.; Pieronczyk, W.; Schoenhammer, B.; Streng, K.; Bernal, I.; Korp, J. *Chem. Ber.* **1981**, *114*, 1137-49.

ray analysis, which revealed a 1:1 complex between (–)-DBTA and (*R*)-**191** (see Figure 14).

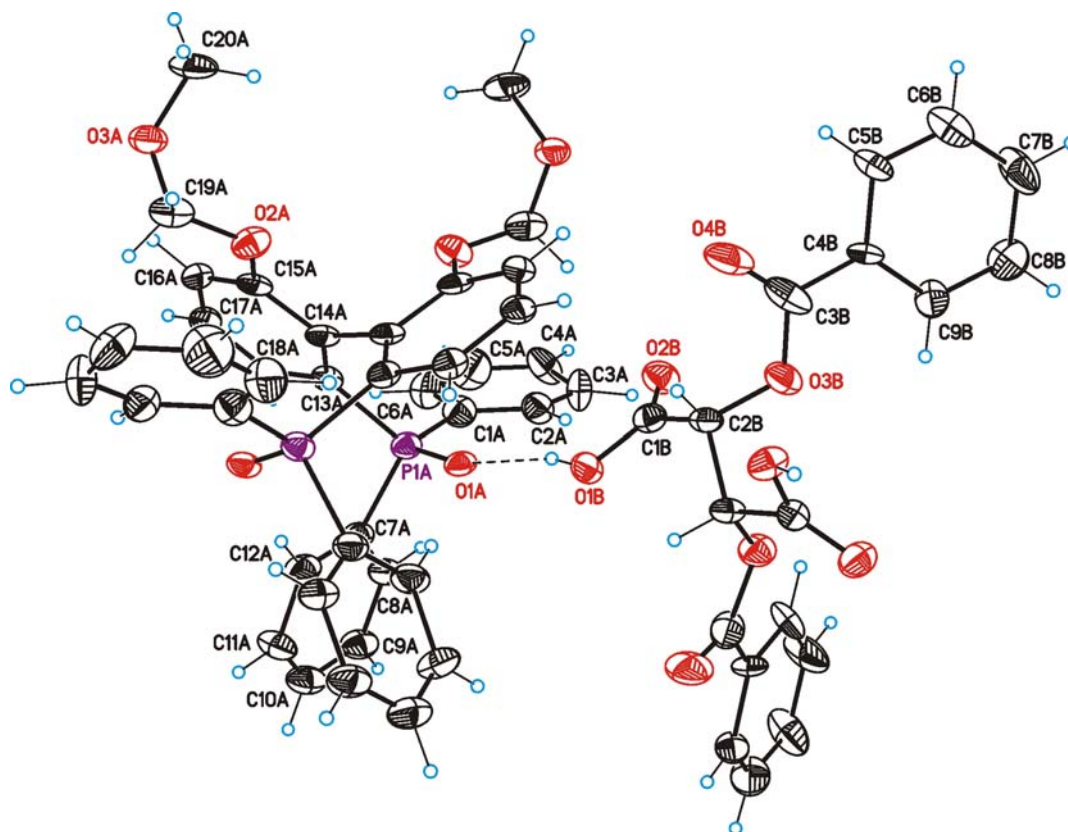


**Figure 14.** X-ray structure of the 1:1 complex between (*R*)-**191** and (–)-DBTA.

Treatment of the tartrate complex with an aqueous basic solution (2M NaOH) provided enantiomerically enriched (*R*)-**191** (ee = 94%, according to HPLC analysis, Chiracel IA column), as shown in Figure 15.<sup>25</sup> The absolute configuration of (*R*)-**191** was again confirmed by X-ray analysis. Crystals of compound **191** suitable for X-ray anomalous dispersion<sup>26</sup> were grown, and then evaluated by this technique, which confirmed the absolute configuration of (*R*)-**191** (Figure 16).

<sup>25</sup> A similar procedure, employed for the solid obtained upon removing the solvent from the mother liquors of the resolution, led to enantiomerically enriched (*S*)-**191** (ee = 70%, according to HPLC analysis, Chiracel IA column).

<sup>26</sup> Soejima, Y.; Kuwajima, S. *Trans. Mater. Res. Soc. Jpn.* **1999**, *24*, 687-690.

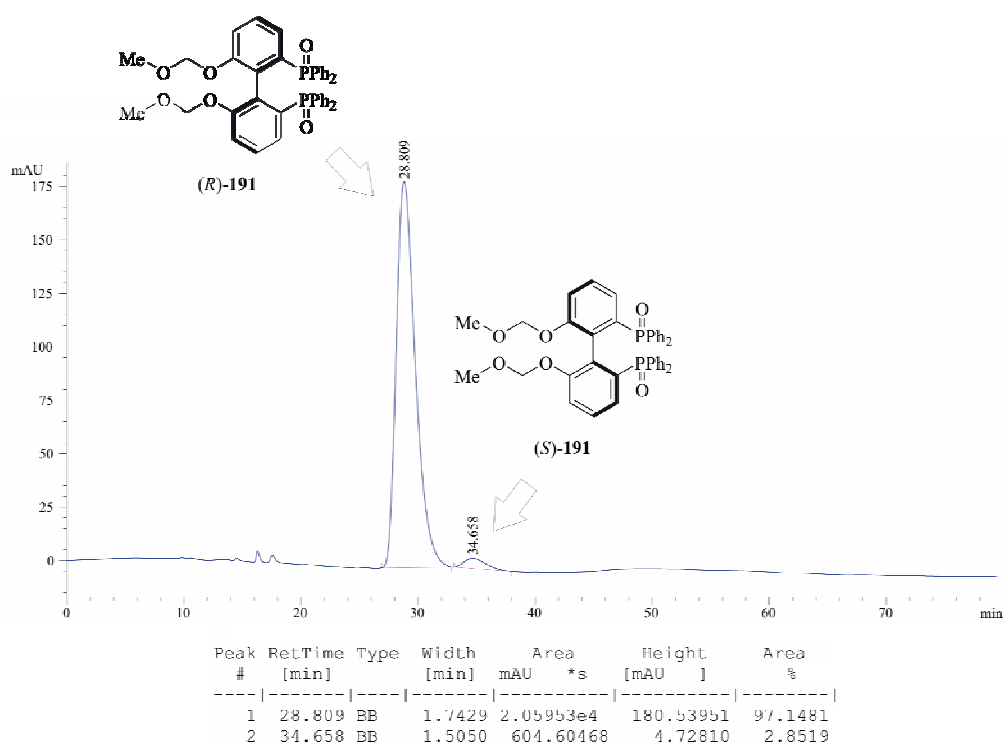


**Figure 15.** HPLC analysis to determine the optical purity of (R)-191.

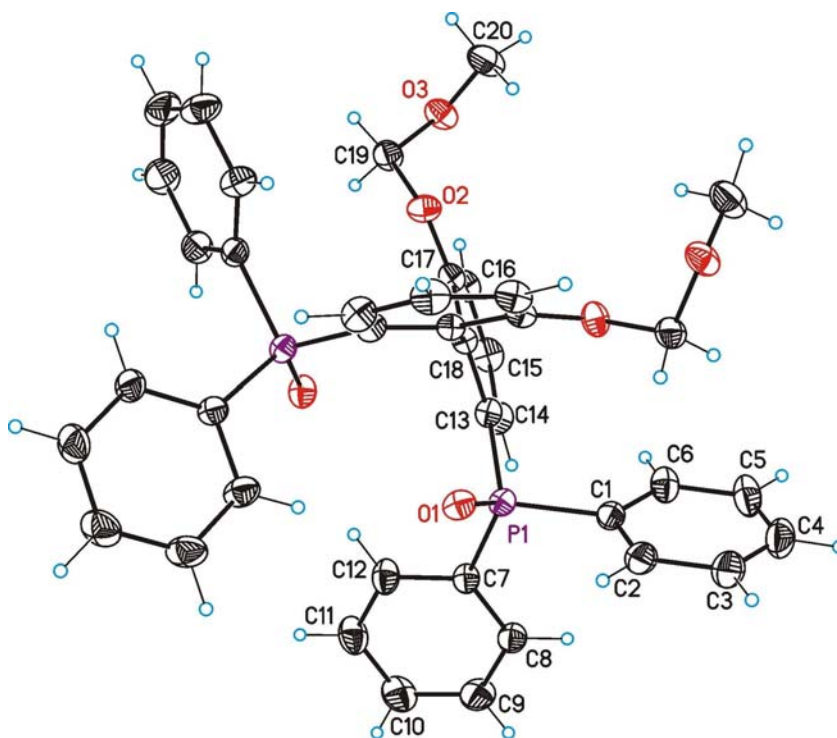
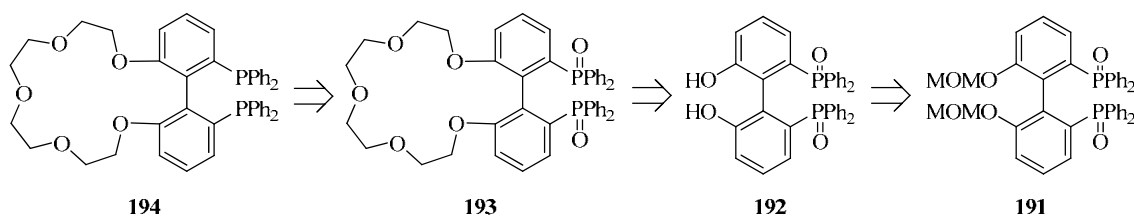


**Figure 16.** Anomalous X-ray dispersion analysis of (R)-191.

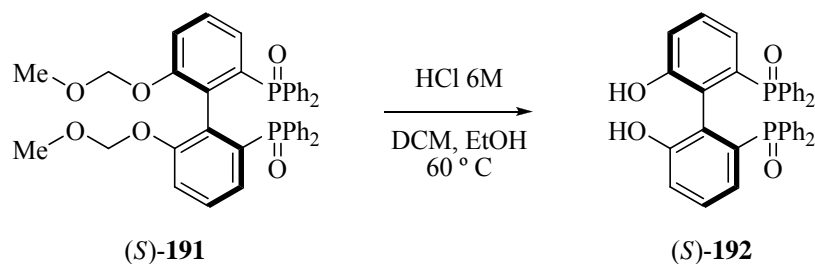
### 2.2.3. Preparation of the crown ether-containing diphosphine (**194**)

The crown ether diphosphine **194** was prepared from **191** according to the strategy indicated in Scheme 7: cleavage of the MOM protecting groups; formation of the crown ether via cyclization; and finally, reduction of the P=O groups.



**Scheme 7.** Final retrosynthetic strategy for the preparation of crown ether diphosphine **194**.

Enantiomerically enriched (*S*)-**191** (70% ee) (see footnote 25 on page 251) was used as the starting material to study the feasibility of our synthetic strategy towards the target compound **194**. The MOM protecting groups from (*S*)-**191** were easily cleaved using concentrated HCl in ethanol at 60 °C, affording compound (*S*)-**192** in good yield (83%) after purification (Scheme 8).<sup>27</sup>

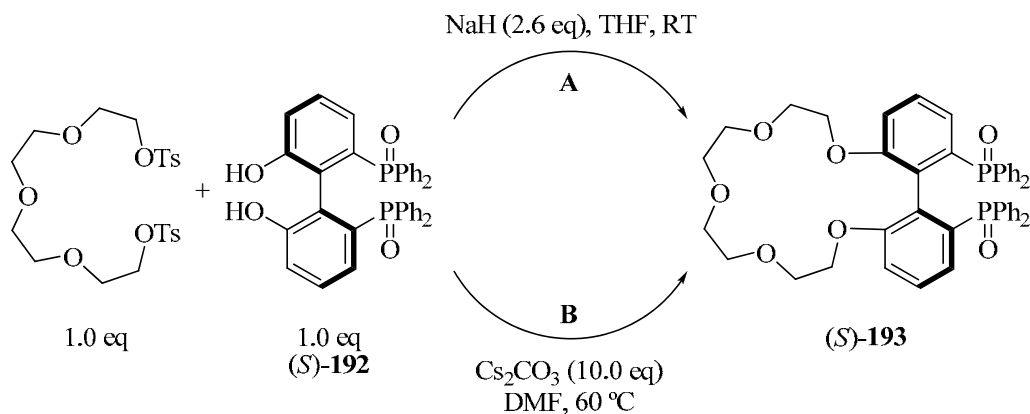


**Scheme 8.** Deprotection of the methoxy-methyl groups in (*S*)-**191** under acidic conditions.

For the cyclization reaction between the biaryl derivative **192** and tetraethylene glycol ditosylate, we explored two different sets of conditions for

<sup>27</sup> Hu, T.; Li, Y.-G.; Liu, J.-Y.; Li, Y.-S. *Organometallics* **2007**, *26*, 2609-2615.

deprotonating the biphenol unit (Scheme 9): NaH in THF (Path A), and Cs<sub>2</sub>CO<sub>3</sub> in DMF (Path B). The cyclization reactions were performed under high-dilution conditions by slow addition of a solution of the ditosylate to the deprotonated biaryl derivative in order to minimize formation of any polymer byproducts.



**Scheme 9.** Reaction conditions evaluated for the cyclization leading to the crown ether derivative (S)-193.

When NaH was used as base, and THF as solvent, only tiny amounts of the desired product (S)-193 were obtained, together with polymeric material derived from tetraethylene glycol ditosylate that was difficult to separate out. In contrast, when Cs<sub>2</sub>CO<sub>3</sub> was used as base, and DMF as solvent, (S)-193 was obtained in better yield. Moreover, the amount of side-products was markedly lower than in the other case and the target compound was easily separated from the reaction mixture by column chromatography (40% isolated yield). Optically enriched (S)-193 was fully characterized by NMR spectroscopy and high-resolution mass spectroscopy (see Experimental Procedure). We did not attempt to rationalize the notably different levels of reactivity and selectivity found under the two sets of conditions. However, one possibility is that the Cs<sup>+</sup> cation, due to its larger size, might act as a better template than Na<sup>+</sup> for the formation of the target crown



ether. This effect has been well studied in the templated synthesis of crown ethers.<sup>28</sup>

(*S*)-**193** was obtained from (*S*)-**191** with an enantiomeric excess of 70% (according to HPLC, Chiracel IA), demonstrating that no racemization had occurred during the deprotection and cyclization steps (Figure 17).

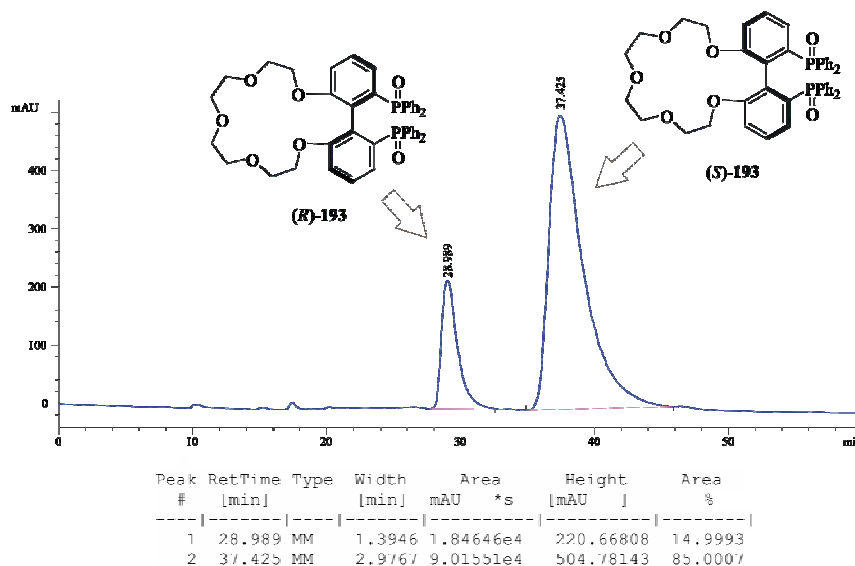


**Figure 17.** HPLC chromatogram of the enantiomerically enriched isolated crown ether (*S*)-**193**.

Seeking to develop alternative routes to resolving (*R*)- and (*S*)-**193**, and considering the ease with which they had been separated on analytical HPLC, we decided to try semipreparative HPLC. Thus, (*S*)-**193** (75 mg, 70% ee) was resolved by semipreparative HPLC on a Chiracel IA chiral chromatography column ([Chiral Technologies], 25 x 1 cm, 80:20 EtOH/H<sub>2</sub>O, 0.200 mL/min,  $\lambda$  = 216 nm,  $t_R(R)$  29.0 min,  $t_R(S)$  37.4 min.) to afford pure (*R*)-**193** (11.0 mg, > 99% ee according to HPLC) and (*S*)-**193** (61.6 mg, > 99% ee according to HPLC) (Figure 18).

<sup>28</sup> Benniston, A. C.; Harriman, A.; Patel, P. V.; Sams, C. A. *Eur. J. Org. Chem.* **2005**, 4680-4686. and references therein.

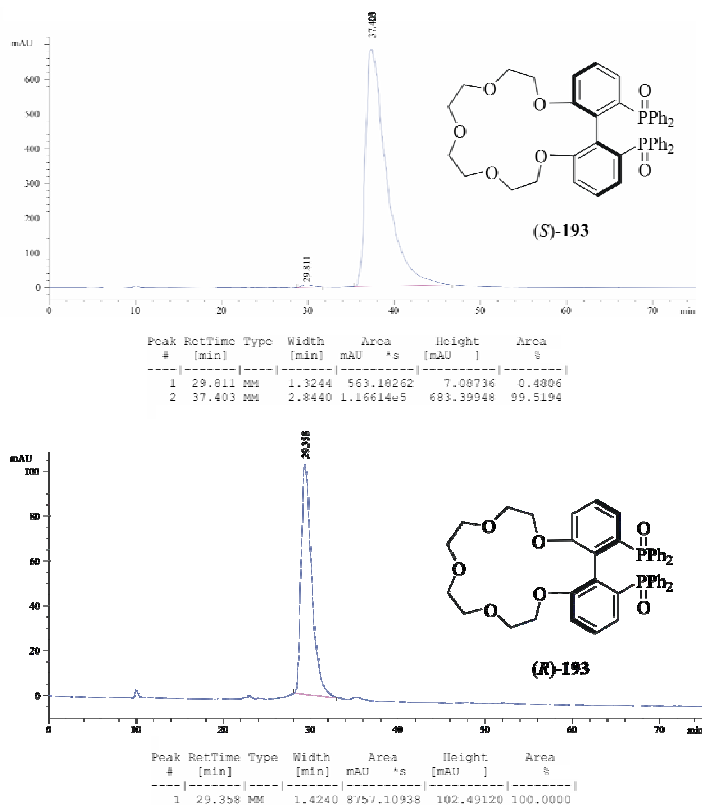
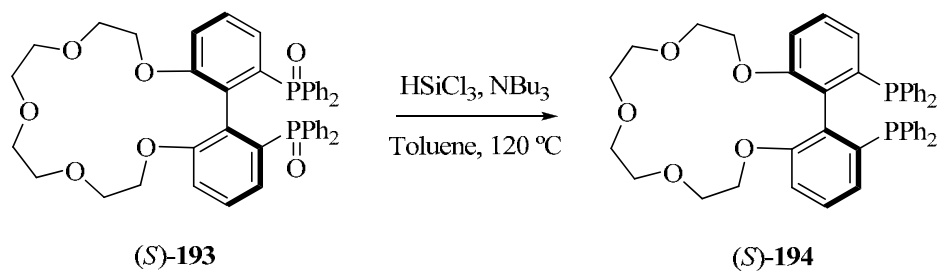


**Figure 18.** Enantiomerically pure (*R*)- and (*S*)-**193** resolved by semipreparative HPLC.

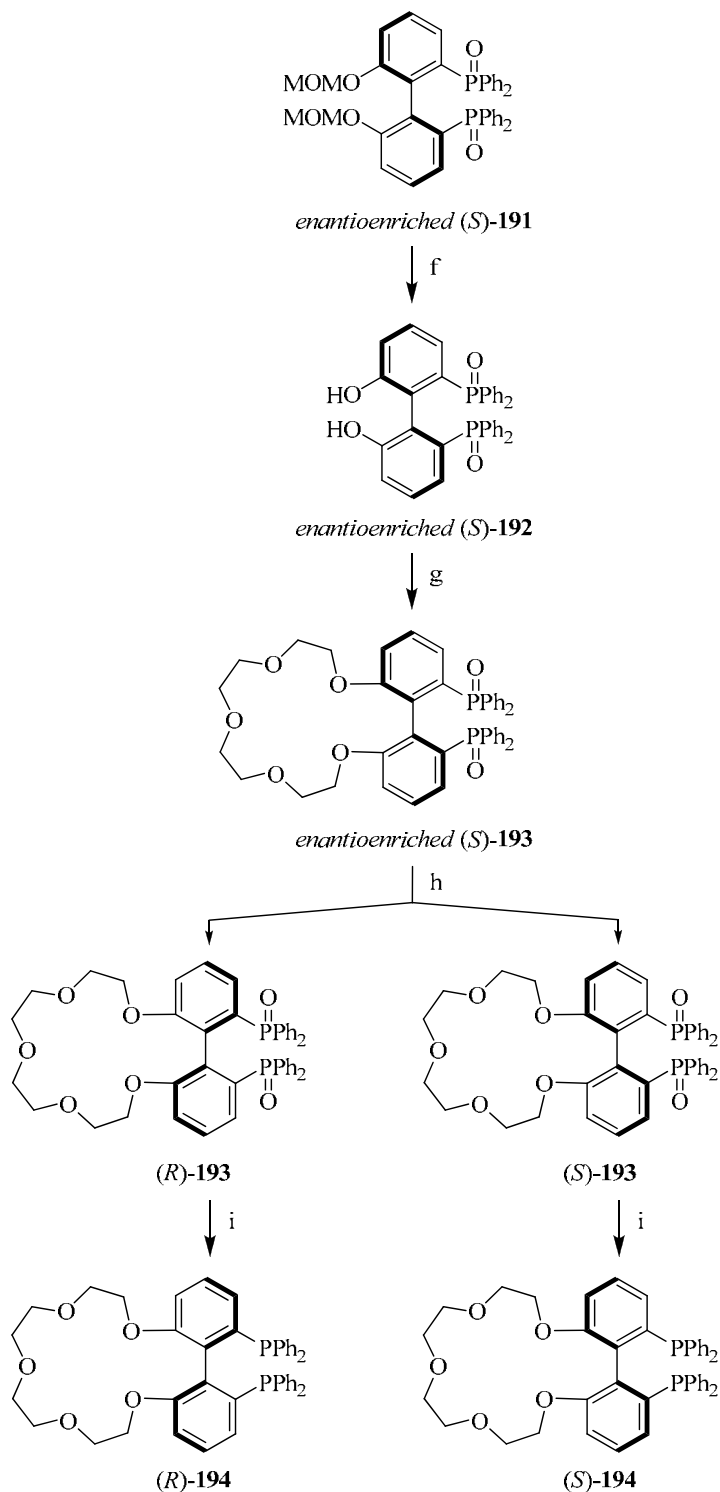
The final step in the synthesis of biaryl derivatives **194** was the reduction of diphosphine oxide **193**. Having isolated the enantiomerically pure crown ether (*S*)-**193**, we proceeded with the reduction, using excess  $\text{HSiCl}_3$ , and tributylamine in toluene (Scheme 10).<sup>21a</sup> A long reaction time (4 days) was necessary for full deprotection of the phosphine oxide. The target enantiomerically pure diphosphine (*S*)-**194** was isolated in 52% isolated yield.



**Scheme 10.** Reduction of phosphine oxide (*S*)-**193**.

In conclusion, we have developed a route to the new class of diphosphines **194**, which feature a crown ether as an allosteric site that, through ion-dipole interactions, might alter active site geometry, and consequently, the catalytic activity. We synthesized enantiomerically enriched (*S*)-**194** in nine steps starting from 3-bromophenol (Schemes 5 and 11). Moreover, we resolved (*S*)-**194** and (*R*)-**194** (> 99% ee each) by semipreparative HPLC.

*Preliminary Investigations into Bio-inspired Supramolecular Strategies for  
Asymmetric Catalysis: Results and Discussion*



<sup>a</sup> Reaction conditions: (f) HCl (6M), CH<sub>2</sub>Cl<sub>2</sub>, EtOH, 60 °C to rt; (g) Cs<sub>2</sub>CO<sub>3</sub>, tetraethylene glycol ditosylate, 60 °C to rt; (h) Semipreparative HPLC (Chiracel 1A); (i) HSiCl<sub>3</sub>, NBu<sub>3</sub>, toluene, 120 °C.

**Scheme 11.** Final steps in the synthesis of the crown ether diphosphines (*R*)- and (*S*)-194.

#### 2.2.4. Future outlook

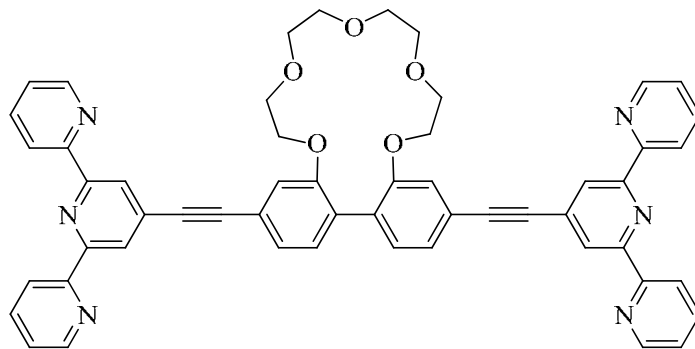
Unfortunately, we were unable to perform any catalytic studies on the diphosphines **194**; therefore, it remains to be seen whether allosteric modulation of their catalytic activity (in asymmetric transformations) is indeed possible. Thanks to the synthetic methodology described in this thesis for **194**, the preparation of more quantities of enantiomerically pure **194** and the subsequent catalytic studies are already ongoing in the group.

Benniston *et al.* have described a set of detailed molecular dynamics simulations on the related crown ether systems **195**, alone as well as in the presence of added cations ( $H^+$ ,  $Li^+$ ,  $Na^+$ ,  $K^+$ ,  $Rb^+$  or  $NH_4^+$ ). They reported a good correlation between the calculated biphenylene torsion angles and the Pauling cation radius (Table 2).<sup>29</sup>

---

<sup>29</sup> Benniston, A. C.; Li, P.; Sams, C. *Tetrahedron Lett.* **2003**, *44*, 3947-3949.

**Table 2.** Dihedral angles in the biphenyl unit of crown ether system **195**.



**195**

Cation	Dihedral angle <sup>a</sup> (deg)	Variation in dihedral angle <sup>b</sup> (deg)	Pauling cation radius (Å)
None	142.59	76.7-159	-
H <sup>+</sup>	59.86	22.9-98.0	-
Li <sup>+</sup>	50.89	25.5-95.1	0.60
Na <sup>+</sup>	61.95	30.8-104	0.95
K <sup>+</sup>	79.81	34.3-156	1.33
Rb <sup>+</sup>	83.29	49.5-146	1.48
NH <sub>4</sub> <sup>+</sup>	81.32	39.7-142	1.48

<sup>a</sup> Dihedral angle taken from the energy-minimized structure.

<sup>b</sup> Taken from molecular dynamics simulations.

These studies on **195** clearly indicate that ion-dipole interactions are capable of inducing conformational changes in a biaryl unit, thereby corroborating the concept that in the biaryl diphosphine system **194** binding forces could potentially generate changes in the active site geometry.

## **EXPERIMENTAL PROCEDURE**

UNIVERSITAT ROVIRA I VIRGLI

TOWARDS HIGHLY EFFICIENT LIGANDS FOR ASYMMETRIC HYDROGENATIONS: A COVALENT MODULAR APPROACH AND  
INVESTIGATIONS INTO BIOINSPIRED SUPRAMOLECULAR STRATEGIES

Héctor Fernández Pérez

ISBN:978-84-693-3385-3 /DL:T.994-2010



## 2.3. EXPERIMENTAL PROCEDURE

### 2.3.1. General remarks

All manipulations and reactions were performed under inert atmosphere of dry argon, either in a Braun glovebox or with standard Schlenk-type techniques. Glassware was dried before use with a hot gun. All solvents were dried and deoxygenated by using a Solvent Purification System (SPS). Diisopropylamine and tributylamine were distilled from  $\text{CaH}_2$ . Silica gel 60 (230-400 mesh) was used for column chromatography. NMR spectra were recorded on Bruker Avance 400 and 500 Ultrashield spectrometers in  $\text{CDCl}_3$  unless otherwise cited. Chemical shifts ( $\delta$ ) were given in ppm and were referenced to residual solvent peaks ( $^1\text{H}$ -NMR,  $^{13}\text{C}\{^1\text{H}\}$ -NMR) or to an external standard (85%  $\text{H}_3\text{PO}_4$ ,  $^{31}\text{P}\{^1\text{H}\}$ -NMR). ESI mass spectra were obtained on a Waters LCT Premier mass spectrometer. Optical rotations were measured on a Jasco P-1030 polarimeter. Melting points were determined in open capillaries on a Büchi B-540 instrument. Enantiomeric excesses were determined by HPLC on Agilent 1100 Series chromatograph with a UV detector. Semipreparative HPLC was carried out on Waters Delta 600 chromatograph with a UV detector and a Gilson FC 203B fraction collector.

Crystal structure determination was carried out using a Bruker-Nonius diffractometer equipped with APPEX 2 4K CCD area detector, a FR591 rotating anode with  $\text{MoK}\alpha$  radiation, Montel mirrors as monochromator and a Kryoflex low temperature device ( $T = 100\text{K}$ ). Fullsphere data was collected using omega and phi scans. Apex2 V. 1.0-22 (Bruker-Nonius 2004) for the data reduction and SADABS V. 2.10 (2003) for the absorption correction. Crystal structure was achieved using direct methods as implemented in SHELXTL Version 6.10 (Sheldrick, Universität Göttingen (Germany), 2000). Least-squares refinement on F2 using all measured intensities was carried out using the program SHELXTL Version 6.10 (Sheldrick, Universität Göttingen (Germany), 2000).

*Preliminary Investigations into Bio-inspired Supramolecular Strategies for  
Asymmetric Catalysis: Experimental Procedure*

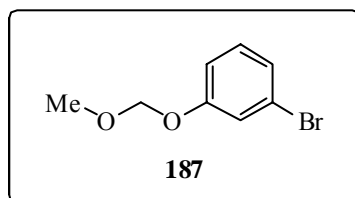
---

All non hydrogen atoms were refined including anisotropic displacement parameters.

### 2.3.2. Experimental procedures and characterization

*2.3.2.1. Synthesis and general physical and spectroscopic data of the intermediates in the synthesis of rac-(6,6'-bis(methoxymethoxy)biphenyl-2,2'-diyl)bis(diphenylphosphine oxide) (rac)-191*

**1-bromo-3-(methoxymethoxy)benzene (187).** A 500 ml three-necked flask was charged with sodium hydride (4.80 g, 120 mmol, 60 % oil dispersion). The sodium hydride was washed twice with hexane

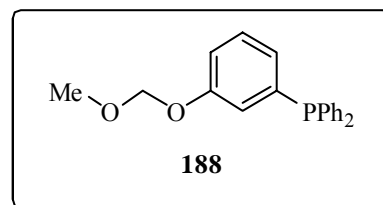


(30.0 mL) before DMF (180.0 mL) was added. The suspension was cooled to 0 °C and a solution of 3-bromophenol (17.302 g, 100 mmol) in DMF (50.0 ml ) was added slowly. After the generation of hydrogen stopped the yellow solution was stirred at room temperature for 45 min. Then, MOMO-Cl (9.1 ml, 120 mmol) in DMF (20.0 ml) was added slowly via syringe to the cooled solution (0 °C), and the reaction mixture was stirred for 60 min at room temperature. After addition of ice water (100.0 ml) and additional stirring for 5 min the mixture was transferred into a separator funnel. The mixture was extracted with methyl *tert*-butyl ether (3 x 200.0 ml). The combined organic layers were washed with saturated NaHCO<sub>3</sub> solution (200.0 ml), water and brine and dried over MgSO<sub>4</sub>. After filtration through a short pad of silica, the solvent was removed under reduced pressure to give **187** (21.3 g, 98% yield) as a pale oil. <sup>1</sup>H-NMR (400MHz, CDCl<sub>3</sub>) δ 7.22 (bs, 1H, H<sub>arom</sub>), 7.21-7.13 (m, 2H, H<sub>arom</sub>), 6.98-6.95 (m, 1H, H<sub>arom</sub>), 5.15 (s, 2H, O-CH<sub>2</sub>-OCH<sub>3</sub>), 3.47 (s, 3H, O-CH<sub>2</sub>-OCH<sub>3</sub>); <sup>13</sup>C{<sup>1</sup>H}-NMR (100MHz, CDCl<sub>3</sub>) δ 157.8 (C<sub>q</sub> arom, C-O), 130.4 (CH<sub>arom</sub>), 124.9 (CH<sub>arom</sub>), 122.6 (C<sub>q</sub> arom, C-Br), 119.5 (CH<sub>arom</sub>), 115.0 (CH<sub>arom</sub>), 94.4 (O-CH<sub>2</sub>-OCH<sub>3</sub>), 56.1

(O-CH<sub>2</sub>-OCH<sub>3</sub>); MS HR-ESI [found 215.9786; C<sub>8</sub>H<sub>9</sub>O<sub>2</sub>Br (M)<sup>+</sup> requires 215.9785].

### (3-(methoxymethoxy)phenyl)diphenylphosphine

**(188)**. A 100 mL flask was charged with compound **187** (6.328 g, 29.15 mmol) and dissolved in THF (18.0 mL). This solution was



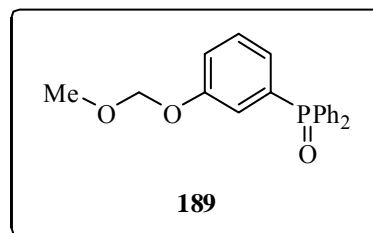
cooled at -78 °C and *n*-BuLi (12.1 mL, 2.50M in hexanes, 30.32 mmol) was added dropwise during 45 min. Then, the resulting solution was stirred for an additional 1.5 h at -78 °C. After this, freshly distilled chlorodiphenylphosphine (6.0 mL, 32.07 mmol) was slowly transferred via cannula to this latter solution at this temperature and the reaction mixture was allowed to reach 0 °C within 2h. The reaction mixture was quenched with saturated NH<sub>4</sub>Cl solution (25.0 mL) at 0 °C. Then, the mixture was extracted with AcOEt (3 x 25.0 mL) and the combined organic phases were washed with saturated NaCl solution (2 x 25.0 mL), dried over MgSO<sub>4</sub>, filtered and concentrated *in vacuo*. The resulting residue was purified by flash chromatography on SiO<sub>2</sub> using hexane/AcOEt (100:0-20:80) as eluent to give the target product **188** (4.872 g, 52% yield) as a colorless oil. <sup>1</sup>H-NMR (400MHz, CDCl<sub>3</sub>) δ 7.36-7.24 (m, 11H, *H*<sub>arom</sub>), 7.04-6.92 (m, 3H, *H*<sub>arom</sub>), 5.10 (s, 2H, O-CH<sub>2</sub>-OCH<sub>3</sub>), 3.43 (s, 3H, O-CH<sub>2</sub>-OCH<sub>3</sub>); <sup>13</sup>C{<sup>1</sup>H}-NMR (100MHz, CDCl<sub>3</sub>) δ 157.4 (d, <sup>3</sup>*J*<sub>C-P</sub> = 8.3 Hz, *C*<sub>q arom</sub>, C-OMOM), 139.0 (d, <sup>1</sup>*J*<sub>C-P</sub> = 11.6 Hz, *C*<sub>q arom</sub>, C-PPh<sub>2</sub>), 137.1 (d, <sup>1</sup>*J*<sub>C-P</sub> = 10.8 Hz, *C*<sub>q arom</sub>, PPh<sub>2</sub>), 133.9 (d, <sup>2</sup>*J*<sub>C-P</sub> = 19.5 Hz, CH<sub>o arom</sub>, PPh<sub>2</sub>), 129.6 (d, <sup>2</sup>*J*<sub>C-P</sub> = 7.4 Hz, CH<sub>arom</sub>), 128.9 (CH<sub>p arom</sub>, PPh<sub>2</sub>), 128.6 (d, <sup>3</sup>*J*<sub>C-P</sub> = 6.9 Hz, CH<sub>m arom</sub>, PPh<sub>2</sub>), 127.3 (d, <sup>2</sup>*J*<sub>C-P</sub> = 18.4 Hz, CH<sub>arom</sub>), 121.9 (d, <sup>2</sup>*J*<sub>C-P</sub> = 21.2 Hz, CH<sub>arom</sub>), 116.5 (CH<sub>arom</sub>), 94.7 (O-CH<sub>2</sub>-OCH<sub>3</sub>), 56.1 (O-CH<sub>2</sub>-OCH<sub>3</sub>); <sup>31</sup>P{<sup>1</sup>H}-NMR (162MHz, CDCl<sub>3</sub>) δ -1.6 (s, PPh<sub>2</sub>); MS HR-ESI [found 323.1205; C<sub>20</sub>H<sub>20</sub>O<sub>2</sub>P (M+H)<sup>+</sup> requires 323.1201].

*Preliminary Investigations into Bio-inspired Supramolecular Strategies for  
Asymmetric Catalysis: Experimental Procedure*

---

**(3-(methoxymethoxy)phenyl)diphenylphosphine**

**oxide (189)**. In a 100 mL flask with a suspension of **188** (4.872 g, 15.11 mmol) in MeOH (20.0 mL) was added dropwise at  $\leq 40$  °C 35% aqueous H<sub>2</sub>O<sub>2</sub> solution (1.5 mL, 16.62 mmol). The resulting clear

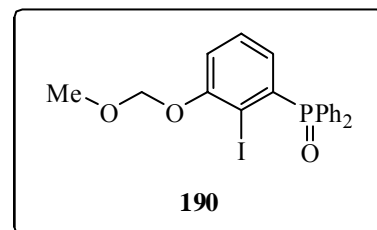


solution was stirred at room temperature for 1h. Then, the reaction mixture was treated during 1h with saturated Na<sub>2</sub>SO<sub>3</sub> solution (5.0 mL) and 1.0M HCl solution (3.5 mL). After evaporating the methanol, the resulting aqueous solution was extracted with dichloromethane (3 x 15.0 mL) and the combined organic layers were dried over MgSO<sub>4</sub>, filtered and concentrated under reduced pressure to give, without further purification, pure compound **189** (5.006 g, 97% yield) as a white solid. <sup>1</sup>H-NMR (400MHz, CDCl<sub>3</sub>)  $\delta$  7.70-7.65 (m, 4H, *H*<sub>o</sub> arom, POPh<sub>2</sub>), 7.56-7.52 (m, 2H, *H*<sub>p</sub> arom, POPh<sub>2</sub>), 7.48-7.44 (m, 4H, *H*<sub>m</sub> arom, POPh<sub>2</sub>), 7.40-7.33 (m, 2H, *H*<sub>arom</sub>), 7.28-7.20 (m, 2H, *H*<sub>arom</sub>), 5.15 (s, 2H, O-CH<sub>2</sub>-OCH<sub>3</sub>), 3.44 (s, 3H, O-CH<sub>2</sub>-OCH<sub>3</sub>); <sup>13</sup>C{<sup>1</sup>H}-NMR (100MHz, CDCl<sub>3</sub>)  $\delta$  157.3 (d, <sup>3</sup>J<sub>C-P</sub>= 15.2 Hz, C<sub>q</sub> arom, C-OMOM), 134.1 (d, <sup>1</sup>J<sub>C-P</sub>= 102.5 Hz, C<sub>q</sub> arom, C-POPh<sub>2</sub>), 132.5 (d, <sup>1</sup>J<sub>C-P</sub>= 103.5 Hz, C<sub>q</sub> arom, POPh<sub>2</sub>), 132.2 (d, <sup>2</sup>J<sub>C-P</sub>= 9.7 Hz, CH<sub>o</sub> arom, POPh<sub>2</sub>), 132.0 (d, <sup>4</sup>J<sub>C-P</sub>= 2.8 Hz, CH<sub>p</sub> arom, POPh<sub>2</sub>), 129.9 (d, <sup>2</sup>J<sub>C-P</sub>= 13.9 Hz, CH<sub>arom</sub>), 128.6 (d, <sup>3</sup>J<sub>C-P</sub>= 12.2 Hz, CH<sub>m</sub> arom, POPh<sub>2</sub>), 125.6 (d, <sup>3</sup>J<sub>C-P</sub>= 9.7 Hz, CH<sub>arom</sub>), 120.2 (d, <sup>2</sup>J<sub>C-P</sub>= 10.2 Hz, CH<sub>arom</sub>), 119.7 (d, <sup>4</sup>J<sub>C-P</sub>= 2.5 Hz, CH<sub>arom</sub>), 94.6 (O-CH<sub>2</sub>-OCH<sub>3</sub>), 56.2 (O-CH<sub>2</sub>-OCH<sub>3</sub>); <sup>31</sup>P{<sup>1</sup>H}-NMR (162MHz, CDCl<sub>3</sub>)  $\delta$  32.0 (s, POPh<sub>2</sub>); MS HR-ESI [found 361.0965; C<sub>20</sub>H<sub>19</sub>O<sub>3</sub>PNa (M+Na)<sup>+</sup> requires 361.0970]. M.p. 87.7-90.0 °C.

### (2-iodo-3-

### (methoxymethoxy)phenyl)diphenylphosphine

**oxide (190)**. To a solution of diisopropylamine (3.2 mL, 22.76 mmol) in THF (18.0 mL) was added, at low temperature (-78 °C), *n*-BuLi solution (7.0 mL,

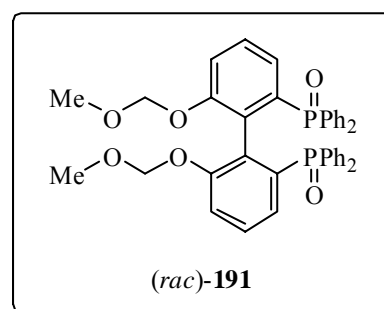


2.5M in hexanes, 20.19 mmol). After stirring for 30 min at -78 to -40 °C, the LDA solution was cooled again at -78 °C and was added dropwise via cannula to a flask containing a cooled solution (-78°C) of compound **189** (6.210 g, 18.35 mmol) in THF (37.0 mL). During the addition, the reaction mixture turned reddish-brown, and eventually a beige suspension formed. After stirring 3h at -78 °C, this solution was slowly transferred via cannula to a cooled solution (-78°C) of iodine (5.124 g, 20.19 mmol) in THF (18.0 mL) and the resulting solution was stirred overnight allowing to reach room temperature. Finally, the mixture was quenched by addition of aqueous Na<sub>2</sub>S<sub>2</sub>O<sub>3</sub> solution (1.37 g in 15.0 mL of H<sub>2</sub>O) and then it was concentrated *in vacuo* to remove THF. The resulting residue was dissolved in dichloromethane (50.0 mL) and the organic and aqueous phases were separated. The aqueous phase was extracted again with dichloromethane (2 x 25.0 mL) and finally, the combined organic fragments were dried over MgSO<sub>4</sub>, filtered and concentrated under reduced pressure to yield a brown paste. The desired product **190** was precipitated from methyl *tert*-butyl ether (35.0 mL) at reflux temperature. After standing at room temperature overnight, the solid was collected by filtration, washed with methyl *tert*-butyl ether (12.0 mL) and dried *in vacuo* (oil pump) to provide spectroscopically pure **190** (6.255 g, 73% yield) as a pale powder. <sup>1</sup>H-NMR (400MHz, CDCl<sub>3</sub>) δ 7.73-7.68 (m, 4H, *H*<sub>o</sub> arom, POPh<sub>2</sub>), 7.59-7.54 (m, 2H, *H*<sub>p</sub> arom, POPh<sub>2</sub>), 7.50-7.46 (m, 4H, *H*<sub>m</sub> arom, POPh<sub>2</sub>), 7.27-7.20 (m, 2H, *H*<sub>arom</sub>), 6.79 (m, 1H, *H*<sub>arom</sub>), 5.26 (s, 2H, O-CH<sub>2</sub>-OCH<sub>3</sub>), 3.50 (s, 3H, O-CH<sub>2</sub>-OCH<sub>3</sub>); <sup>13</sup>C{<sup>1</sup>H}-NMR (100MHz, CDCl<sub>3</sub>) δ 157.1 (d, <sup>3</sup>*J*<sub>C-P</sub>= 12.5 Hz, C<sub>q</sub> arom, C-OMOM), 137.7 (d, <sup>1</sup>*J*<sub>C-P</sub>= 105.1 Hz, C<sub>q</sub> arom, C-POPh<sub>2</sub>), 132.4 (d, <sup>2</sup>*J*<sub>C-P</sub>= 9.8 Hz, CH<sub>o</sub> arom, POPh<sub>2</sub>), 132.1 (d, <sup>4</sup>*J*<sub>C-P</sub>= 2.7 Hz, CH<sub>p</sub> arom, POPh<sub>2</sub>), 131.6

(d,  $^1J_{C-P}$  = 106.6 Hz,  $C_{q\text{ arom}}$ ,  $\text{POPh}_2$ ), 129.7 (d,  $^2J_{C-P}$  = 11.9 Hz,  $\text{CH}_{\text{arom}}$ ), 129.0 (d,  $^3J_{C-P}$  = 13.7 Hz,  $\text{CH}_{\text{arom}}$ ), 118.1 (d,  $^4J_{C-P}$  = 2.2 Hz,  $\text{CH}_{\text{arom}}$ ), 95.3 (O- $\text{CH}_2$ - $\text{OCH}_3$ ), 93.8 (d,  $^3J_{C-P}$  = 7.2 Hz,  $C_{q\text{ arom}}$ , C-I), 56.7 (O- $\text{CH}_2$ - $\text{OCH}_3$ );  $^{31}\text{P}\{^1\text{H}\}$ -NMR (162MHz,  $\text{CDCl}_3$ )  $\delta$  36.9 (s,  $\text{POPh}_2$ ); MS HR-ESI [found 465.0114;  $\text{C}_{20}\text{H}_{19}\text{O}_3\text{PI}$  (M+H) $^+$  requires 465.0117].

**(rac)-(6,6'-bis(methoxymethoxy)biphenyl-2,2'-**

**diyl)bis(diphenylphosphine oxide) (rac-191).** In a 50 ml two-necked flask, a mixture of compound **190** (6.162 g, 13.28 mmol) and activated Cu powder (2.530 g, 39.82 mmol)<sup>30</sup> in DMF (25.0 mL) was stirred at 140 °C (oil-bath temperature)



for 3h. After this, the cold mixture was evaporated to dryness. The resulting residue was treated for a few minutes with hot dichloromethane (25.0 mL). After filtration, the solution was washed with saturated  $\text{NH}_4\text{Cl}$  solution (2 x 25.0 mL), dried over  $\text{MgSO}_4$ , filtered and evaporated. The solid residue was treated with hot hexane (6 x 50.0 mL) and dried *in vacuo* (oil pump) to afford (rac)-**191** (2.08 g, 92% purity, 43% yield) as a beige powder.  $^1\text{H}$ -NMR (500MHz,  $\text{CDCl}_3$ )  $\delta$  7.66-7.57 (m, 8H,  $H_{o\text{ arom}}$ ,  $\text{POPh}_2$ ), 7.49-7.46 (m, 2H,  $H_{p\text{ arom}}$ ,  $\text{POPh}_2$ ), 7.42-7.36 (m, 6H,  $H_{m,p\text{ arom}}$ ,  $\text{POPh}_2$ ), 7.30-7.27 (m, 4H,  $H_{m\text{ arom}}$ ,  $\text{POPh}_2$ ), 7.24-7.20 (m, 4H,  $H_{\text{arom}}$ ), 6.88-6.83 (m, 2H,  $H_{\text{arom}}$ ), 4.63 (d,  $^2J_{H-H}$  = 7.0 Hz, 2H, O- $\text{CHH}$ - $\text{OCH}_3$ ), 4.16 (d,  $^2J_{H-H}$  = 7.0 Hz, 2H, O- $\text{CHH}$ - $\text{OCH}_3$ ), 3.08 (s, 6H, O- $\text{CH}_2$ - $\text{OCH}_3$ );  $^{13}\text{C}\{^1\text{H}\}$ -NMR (125MHz,  $\text{CDCl}_3$ )  $\delta$  155.8 (d,  $^3J_{C-P}$  = 14.1 Hz,  $C_{q\text{ arom}}$ , C-OMOM), 135.4 (d,  $^1J_{C-P}$  = 104.4 Hz,  $C_{q\text{ arom}}$ , C- $\text{POPh}_2$ ), 134.2 (d,  $^1J_{C-P}$  = 101.4 Hz,  $C_{q\text{ arom}}$ ,  $\text{POPh}_2$ ), 132.6 (d,  $^2J_{C-P}$  = 10.0 Hz,  $\text{CH}_{o\text{ arom}}$ ,  $\text{POPh}_2$ ), 132.4 (d,  $^2J_{C-P}$  = 9.1 Hz,  $\text{CH}_{o\text{ arom}}$ ,  $\text{POPh}_2$ ), 132.0 (d,  $^1J_{C-P}$  = 102.1 Hz,  $C_{q\text{ arom}}$ ,  $\text{POPh}_2$ ), 131.4 (d,  $^2J_{C-P}$  = 7.1 Hz,  $C_{q\text{ arom}}$ ), 131.3 (d,  $^2J_{C-P}$  = 7.1 Hz,  $C_{q\text{ arom}}$ ), 131.1 (d,  $^4J_{C-P}$  = 2.4 Hz,  $\text{CH}_{p\text{ arom}}$ ,  $\text{POPh}_2$ ), 131.1 (d,  $^4J_{C-P}$  = 2.0 Hz,  $\text{CH}_{p\text{ arom}}$ ,  $\text{POPh}_2$ ), 128.1 (d,  $^3J_{C-P}$  = 12.4 Hz,  $\text{CH}_{m\text{ arom}}$ ,

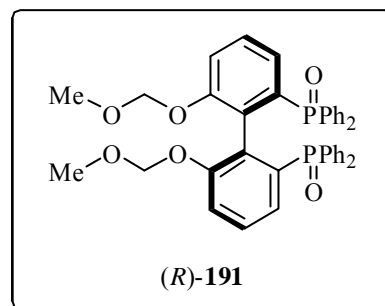
<sup>30</sup> Vogel's Textbook of Practical Organic Chemistry, 5th edn, Eds. Furniss, B. S.; Hannaford, A. J.; Smith, P. W. G.; Tatchell, A. R., Lomgmann, London, 1989, p. 426.

POPh<sub>2</sub>), 128.0 (d, <sup>3</sup>J<sub>C-P</sub>= 12.0 Hz, CH<sub>m arom</sub>, POPh<sub>2</sub>), 127.9 (d, <sup>3</sup>J<sub>C-P</sub>= 15.1 Hz, CH<sub>arom</sub>), 126.7 (d, <sup>2</sup>J<sub>C-P</sub>= 12.2 Hz, CH<sub>arom</sub>), 116.9 (d, <sup>4</sup>J<sub>C-P</sub>= 1.9 Hz, CH<sub>arom</sub>), 94.3 (O-CH<sub>2</sub>-OCH<sub>3</sub>), 55.3 (O-CH<sub>2</sub>-OCH<sub>3</sub>); <sup>31</sup>P{<sup>1</sup>H}-NMR (202MHz, CDCl<sub>3</sub>) δ 32.3 (s, POPh<sub>2</sub>); MS HR-ESI [found 675.2072; C<sub>40</sub>H<sub>37</sub>O<sub>6</sub>P<sub>2</sub> (M+H)<sup>+</sup> requires 675.2065].

2.3.2.2. Experimental procedure for the optical resolution of (*rac*)-(6,6'-bis(methoxymethoxy)biphenyl-2,2'-diyl)bis(diphenylphosphine oxide) **191**.

**(R)**-(6,6'-bis(methoxymethoxy)biphenyl-2,2'-diyl)bis(diphenylphosphine oxide) (**(R)**-**191**).

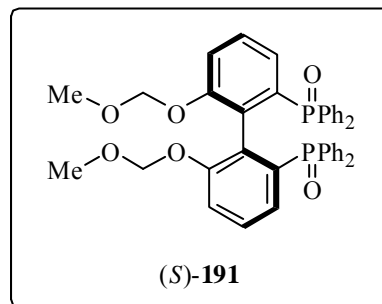
(*rac*)-**191** (1.000 g, 92% purity, 1.36 mmol) was dissolved in boiling dichloromethane (5.0 mL). To this solution was added, in one portion, a hot (50 °C) solution of (–)-(2*R*,3*R*)-2,3-*O*-dibenzoyltartaric acid (–)-DBTA (0.668 g, 1.83 mmol) in ethyl acetate (6.0 mL). The solution



was stirred overnight while the temperature reached room temperature. After this, the solution was kept in the fridge (5 °C) and complex (*R*)-**191**/(-)-DBTA precipitated. The solid was collected by filtration, washed with a cool dichloromethane/AcOEt (5.0/6.0 mL) mixture and dried *in vacuo* to provide the 1:1 complex (*R*)-**191**/(-)-DBTA (0.460 g, 65% of theory based on *rac*-**191**) as white crystals. (Mother liquors were stored for the preparation of enantiomerically enriched (*S*)-**191**). The complex (*R*)-**191**/(-)-DBTA was stirred with dichloromethane (5.5 mL) and 2M NaOH aqueous solution (2.0 mL), until the solid had completely dissolved. Then, the organic phase was separated, washed with 2M NaOH solution (2.0 mL) and H<sub>2</sub>O (2 x 2.5 mL), dried over MgSO<sub>4</sub>, filtered and dried *in vacuo* to provide desired (*R*)-**191** (0.257 g, 56% based on (*rac*)-**191**) as white solid. This compound was enantiomerically enriched (94% ee) according to HPLC on a Chiracel IA column (isopropanol:H<sub>2</sub>O 75:25, 0.200 mL/min, λ = 216 nm, t<sub>R</sub>(*R*) 28.8 min, t<sub>R</sub>(*S*) 34.7

min).  $^1\text{H-NMR}$ ,  $^{13}\text{C}\{^1\text{H}\}\text{-NMR}$ ,  $^{31}\text{P}\{^1\text{H}\}\text{-NMR}$ , HRMS: identical to the corresponding spectra of (*rac*)-**191**.  $[\alpha]_{\text{D}}^{25} = +40.0$  ( $c = 1.00$  g/100 mL, THF); M.p. 272.6-274.1 °C.

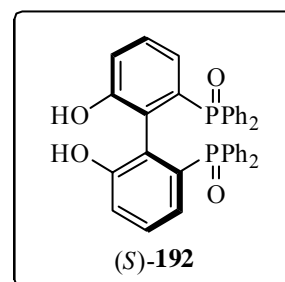
**Enantiomerically enriched (*S*)-(6,6'-bis(methoxymethoxy)biphenyl-2,2'-diyl)bis(diphenylphosphine oxide) ((*S*)-**191**).**



The residue obtained from the combined mother liquors of the (*R*)-**191** resolution was treated with dichloromethane (5.5 mL) and 2M NaOH solution (2.0 mL) until clear two-layer system resulted. The organic layer was separated and washed with 2M NaOH solution (2.0 mL) and H<sub>2</sub>O (2 x 2.5 mL), dried over MgSO<sub>4</sub>, filtered and evaporated. The solid residue (0.426 g), analyzed by HPLC, was a mixture 30:70 of (*R*)-**191**/*S*)-**191** enantiomers.

*2.3.2.3. Synthesis and general physical and spectroscopic data of the intermediates in the synthesis of enantiomerically enriched biaryl diphosphine ligands (194)*

**Enantiomerically enriched (*S*)-6,6'-bis(diphenylphosphino oxide)biphenyl-2,2'-diol ((*S*)-**192**).**



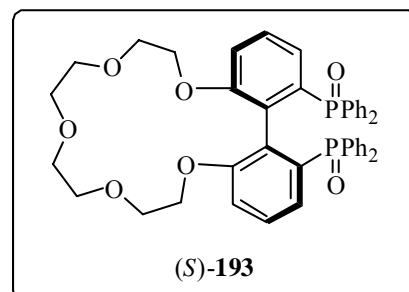
To a stirred solution of enantiomerically enriched compound (*S*)-**191** (0.426 g, 0.63 mmol) in dichloromethane (5.0 mL) were added ethanol (30.0 mL) and hydrochloric acid (2.1 mL, 6 M, 12.62 mmol).

Under nitrogen, the mixture was refluxed at 60 °C for 8 h. After the mixture was cooled to room temperature, the organic phase was separated and saturated NaHCO<sub>3</sub> solution (40.0 mL) was added to the aqueous layer up to pH = 7-8. The aqueous phase was extracted with dichloromethane (3 x 30.0 mL), and the combined organic phases were washed with water (25.0 mL) and then dried over



MgSO<sub>4</sub>, filtered and concentrated under reduced pressure. The resulting residue was redissolved in dichloromethane (8.0 mL) and the desired product was precipitated by addition of hexane (40.0 mL). The solid was collected by filtration and washed with hexane (2 x 15.0 mL) to provide enantiomerically enriched (*S*)-**192** (0.306 g, 83% yield) as a white powder. <sup>1</sup>H-NMR (400MHz, CD<sub>3</sub>OD) δ 7.63-7.29 (m, 20H, *H*<sub>arom</sub>, POPh<sub>2</sub>), 7.09-7.04 (m, 2H, *H*<sub>arom</sub>), 6.80-6.73 (m, 4H, *H*<sub>arom</sub>); <sup>31</sup>P{<sup>1</sup>H}-NMR (162MHz, CD<sub>3</sub>OD) δ 36.0 (s, POPh<sub>2</sub>); MS HR-ESI [found 586.1439; C<sub>36</sub>H<sub>28</sub>O<sub>4</sub>P<sub>2</sub> (M)<sup>+</sup> requires 586.1463].

**Enantiomerically enriched (*S*)-1,21-bis(diphenylphosphino oxide)-6,7,9,10,12,13,15,16-octahydrodibenzo[*n,p*][1,4,7,10,13]pentaoxacycloheptadecine ((*S*)-**193**).**

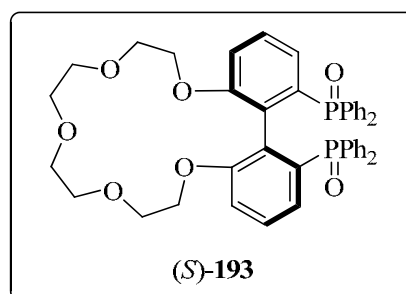
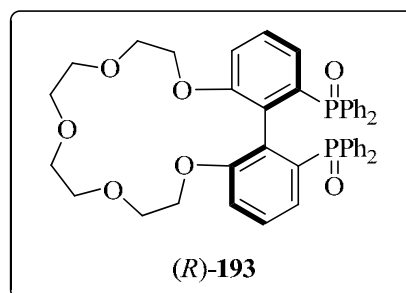


In a 250 ml two-necked flask, a solution of optically enriched compound (*S*)-**192** (0.296 g, 0.50 mmol), Cs<sub>2</sub>CO<sub>3</sub> (1.659 g, 5.04 mmol) and DMF (60.0 mL) was stirred for 2h at 60 °C. Then, a solution of tetraethylene glycol ditosylate (0.261 g, 0.50 mmol) was added over a period of 12h under argon. The reaction mixture was stirred at 60 °C overnight. After this, the mixture was quenched with water (30.0 mL) and concentrated at the rotary-evaporator at 50 °C. The resulting aqueous solution was extracted with AcOEt (3 x 75.0 mL) and the combined organic fragments were dried over MgSO<sub>4</sub>, filtered and evaporated. The resulting residue was purified by flash chromatography on SiO<sub>2</sub> using chloroform/acetone (100:0-50:50) as eluent to give enantiomerically enriched (*S*)-**193** (0.151 g, 40% yield) as a pale yellow oil. <sup>1</sup>H-NMR (400MHz, CDCl<sub>3</sub>) δ 7.69-7.61 (m, 8H, *H*<sub>o arom</sub>, POPh<sub>2</sub>), 7.49-7.27 (m, 12H, *H*<sub>m,p arom</sub>, POPh<sub>2</sub>), 7.19 (ddd, <sup>3</sup>*J*<sub>H-H</sub>= <sup>3</sup>*J*<sub>H-H</sub>= 7.8 Hz, <sup>4</sup>*J*<sub>H-P</sub>= 3.6 Hz, 2H, *H*<sub>arom</sub>), 6.88 (d, <sup>3</sup>*J*<sub>H-H</sub>= 7.8 Hz, 2H, *H*<sub>arom</sub>), 6.81 (dd, <sup>3</sup>*J*<sub>H-P</sub>= 13.4 Hz, <sup>3</sup>*J*<sub>H-H</sub>= 7.8 Hz, 2H, *H*<sub>arom</sub>), 3.86-3.80 (m, 2H, tetraethylene glycol), 3.46-3.00 (m, 14H, tetraethylene glycol); <sup>13</sup>C{<sup>1</sup>H}-NMR (100MHz, CDCl<sub>3</sub>) δ 156.8 (d, <sup>3</sup>*J*<sub>C-P</sub>= 14.2 Hz, C<sub>q arom</sub>, C-O, tetraethylene glycol),

135.4 (d,  $^1J_{C-P}$  = 104.5 Hz,  $C_{q\text{ arom}}$ , C-POPh<sub>2</sub>), 134.0 (d,  $^1J_{C-P}$  = 101.5 Hz,  $C_{q\text{ arom}}$ , POPh<sub>2</sub>), 132.6 (d,  $^2J_{C-P}$  = 10.0 Hz,  $CH_{o\text{ arom}}$ , POPh<sub>2</sub>), 132.4 (d,  $^2J_{C-P}$  = 9.1 Hz,  $CH_{o\text{ arom}}$ , POPh<sub>2</sub>), 132.4 (d,  $^1J_{C-P}$  = 103.7 Hz,  $C_{q\text{ arom}}$ , POPh<sub>2</sub>), 131.1 (d,  $^4J_{C-P}$  = 2.2 Hz,  $CH_{p\text{ arom}}$ , POPh<sub>2</sub>), 131.0 (d,  $^4J_{C-P}$  = 2.4 Hz,  $CH_{p\text{ arom}}$ , POPh<sub>2</sub>), 130.9 (d,  $^2J_{C-P}$  = 7.6 Hz,  $C_{q\text{ arom}}$ ), 130.8 (d,  $^2J_{C-P}$  = 7.2 Hz,  $C_{q\text{ arom}}$ ), 128.1 (d,  $^3J_{C-P}$  = 12.2 Hz,  $CH_{m\text{ arom}}$ , POPh<sub>2</sub>), 128.0 (d,  $^3J_{C-P}$  = 11.7 Hz,  $CH_{m\text{ arom}}$ , POPh<sub>2</sub>), 127.7 (d,  $^3J_{C-P}$  = 15.2 Hz,  $CH_{arom}$ ), 125.2 (d,  $^2J_{C-P}$  = 12.3 Hz,  $CH_{arom}$ ), 113.9 (d,  $^4J_{C-P}$  = 2.4 Hz,  $CH_{arom}$ ), 71.5 ( $CH_2$ , tetraethylene glycol), 71.3 ( $CH_2$ , tetraethylene glycol), 68.8 ( $CH_2$ , tetraethylene glycol), 67.8 ( $CH_2$ , tetraethylene glycol);  $^{31}P\{^1H\}$ -NMR (162MHz, CDCl<sub>3</sub>)  $\delta$  31.8 (s, POPh<sub>2</sub>); MS HR-ESI [found 745.2481; C<sub>44</sub>H<sub>43</sub>O<sub>7</sub>P<sub>2</sub> (M+H)<sup>+</sup> requires 745.2479].

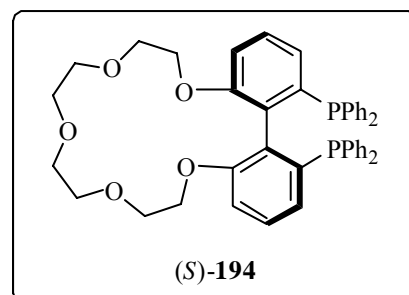
### Resolution of enantiomerically pure (*R*)- and (*S*)-**193** by semipreparative HPLC.

The conformationally enriched compound (*S*)-**193** was resolved by semipreparative HPLC on chiral chromatography column Chiracel IA (EtOH:H<sub>2</sub>O 80:20, 0.200 mL/min,  $\lambda$  = 216 nm,  $t_R$ (*R*) 29.0 min,  $t_R$ (*S*) 37.4 min.) to give both conformationally pure (*R*)-**193** and (*S*)-**193** (> 99% ee according to HPLC) as colorless oils. (*R*)-**193**:  $^1H$ -NMR,  $^{13}C\{^1H\}$ -NMR,  $^{31}P\{^1H\}$ -NMR, HRMS: identical to the corresponding



spectra of enantiomerically enriched (*S*)-**193**,  $[\alpha]_D^{25}$  = +31.5 (c = 0.08 g/100 mL, THF); (*S*)-**193**:  $^1H$ -NMR,  $^{13}C\{^1H\}$ -NMR,  $^{31}P\{^1H\}$ -NMR, HRMS: identical to the corresponding spectra of enantiomerically enriched (*S*)-**193**,  $[\alpha]_D^{25}$  = -18.6 (c = 0.08 g/100 mL, THF).

**(S)-1,21-bis(diphenylphosphino)-  
6,7,9,10,12,13,15,16-  
octahydrodibenzo[*n,p*][1,4,7,10,13]pentaoxacy  
cloheptadecine ((S)-194).** A 10-mL two-necked  
flask fitted with a magnetic stirring bar and a  
reflux condenser was charged with



enantiomerically pure (S)-193 (0.056 g, 0.08 mmol, > 99% ee) and toluene (1.5 mL). Tributylamine (1.8 mL, 7.47 mmol) and trichlorosilane (0.8 mL, 7.47 mmol) were syringed into the flask. The mixture was refluxed for 4 days. After this, the solution was cooled to 0 °C and a degassed 30% aqueous NaOH solution (2.2 mL) was carefully added. The mixture was then stirred at 60 °C until the organic and aqueous phases become clear. The organic product was extracted with toluene (3 x 5.0 mL), and the combined organic extracts were washed successively with degassed water (1 x 5.0 mL), saturated NaCl solution (2 x 10.0 mL) and dried over anhydrous Na<sub>2</sub>SO<sub>4</sub>. The organic layer was concentrated under reduced pressure, the residue was washed with hexane (3 x 5.0 mL) and (S)-194 was isolated pure as a white solid (0.028 g, 52% yield). <sup>1</sup>H-NMR (400MHz, CDCl<sub>3</sub>) δ 7.29-7.22 (m, 22H, H<sub>arom</sub>), 6.76-6.74 (m, 4H, H<sub>arom</sub>), 3.87-3.81 (m, 2H, tetraethylene glycol), 3.57-3.37 (m, 10H, tetraethylene glycol), 3.31-3.25 (m, 2H, tetraethylene glycol), 3.14-3.10 (m, 2H, tetraethylene glycol); <sup>13</sup>C{<sup>1</sup>H}-NMR (100MHz, CDCl<sub>3</sub>) δ 157.1 (d, <sup>3</sup>J<sub>C-P</sub>= 5.8 Hz, C<sub>q</sub> arom, C-O, tetraethylene glycol), 157.0 (d, <sup>3</sup>J<sub>C-P</sub>= 5.8 Hz, C<sub>q</sub> arom, C-O, tetraethylene glycol), 139.3 (d, <sup>1</sup>J<sub>C-P</sub>= 2.8 Hz, C<sub>q</sub> arom, C-PPh<sub>2</sub>), 139.2 (d, <sup>1</sup>J<sub>C-P</sub>= 2.8 Hz, C<sub>q</sub> arom, C-PPh<sub>2</sub>), 139.1 (d, <sup>1</sup>J<sub>C-P</sub>= 6.9 Hz, C<sub>q</sub> arom, PPh<sub>2</sub>), 139.0 (d, <sup>1</sup>J<sub>C-P</sub>= 7.0 Hz, C<sub>q</sub> arom, PPh<sub>2</sub>), 137.6 (d, <sup>1</sup>J<sub>C-P</sub>= 6.2 Hz, C<sub>q</sub> arom, PPh<sub>2</sub>), 137.5 (d, <sup>1</sup>J<sub>C-P</sub>= 6.2 Hz, C<sub>q</sub> arom, PPh<sub>2</sub>), 134.8 (d, <sup>2</sup>J<sub>C-P</sub>= 10.8 Hz, CH<sub>o</sub> arom, PPh<sub>2</sub>), 134.7 (d, <sup>2</sup>J<sub>C-P</sub>= 10.7 Hz, CH<sub>o</sub> arom, PPh<sub>2</sub>), 133.4 (d, <sup>2</sup>J<sub>C-P</sub>= 10.2 Hz, CH<sub>o</sub> arom, PPh<sub>2</sub>), 133.2 (d, <sup>2</sup>J<sub>C-P</sub>= 10.2 Hz, CH<sub>o</sub> arom, PPh<sub>2</sub>), 133.0 (d, <sup>2</sup>J<sub>C-P</sub>= 19.9 Hz, C<sub>q</sub> arom), 132.8 (d, <sup>2</sup>J<sub>C-P</sub>= 19.8 Hz, C<sub>q</sub> arom), 128.6 (CH<sub>p</sub> arom, PPh<sub>2</sub>), 128.3 (d, <sup>3</sup>J<sub>C-P</sub>= 9.4 Hz, CH<sub>m</sub> arom, PPh<sub>2</sub>), 128.2 (d, <sup>3</sup>J<sub>C-P</sub>= 4.8 Hz, CH<sub>arom</sub>), 128.0 (d, <sup>2</sup>J<sub>C-P</sub>= 6.9 Hz, CH<sub>arom</sub>), 127.9 (d, <sup>3</sup>J<sub>C-P</sub>= 10.1 Hz, CH<sub>m</sub>

*Preliminary Investigations into Bio-inspired Supramolecular Strategies for  
Asymmetric Catalysis: Experimental Procedure*

---

arom, PPh<sub>2</sub>), 126.0 (CH<sub>arom</sub>), 111.5 (CH<sub>arom</sub>), 71.4 (CH<sub>2</sub>, tetraethylene glycol), 71.4 (CH<sub>2</sub>, tetraethylene glycol), 69.9 (CH<sub>2</sub>, tetraethylene glycol), 67.6 (CH<sub>2</sub>, tetraethylene glycol); <sup>31</sup>P{<sup>1</sup>H}-NMR (162MHz, CDCl<sub>3</sub>) δ -10.8 (s, PPh<sub>2</sub>); MS HR-ESI [found 713.2560; C<sub>44</sub>H<sub>43</sub>O<sub>5</sub>P<sub>2</sub> (M+H)<sup>+</sup> requires 713.2586]; [α]<sub>D</sub><sup>25</sup> = -9.3 (c= 0.22 g/100 mL, THF).

UNIVERSITAT ROVIRA I VIRGLI

TOWARDS HIGHLY EFFICIENT LIGANDS FOR ASYMMETRIC HYDROGENATIONS: A COVALENT MODULAR APPROACH AND  
INVESTIGATIONS INTO BIOINSPIRED SUPRAMOLECULAR STRATEGIES

Héctor Fernández Pérez

ISBN:978-84-693-3385-3 /DL:T.994-2010

## **CONCLUSIONS**

UNIVERSITAT ROVIRA I VIRGLI

TOWARDS HIGHLY EFFICIENT LIGANDS FOR ASYMMETRIC HYDROGENATIONS: A COVALENT MODULAR APPROACH AND  
INVESTIGATIONS INTO BIOINSPIRED SUPRAMOLECULAR STRATEGIES

Héctor Fernández Pérez

ISBN:978-84-693-3385-3 /DL:T.994-2010

### 3.1. CONCLUSIONS

1. We have designed and developed a methodology for synthesizing new chiral *P-OP* ligands (phosphine-phosphinites and phosphine-phosphites) comprising two steps: ring-opening of an epoxide with a trivalent nucleophilic phosphorus reagent, and *O*-phosphorylation of the resulting phosphino-alcohols with an appropriate trivalent electrophilic phosphorus derivative.

The modular design of our target *P-OP* ligands enables incorporation of up to six molecular fragments, modification of the stereoelectronics of the phosphorus functionalities, and control over the stereogenic centers between the phosphorus groups.

2. We validated our approach by preparing 21 diverse ligands: six phosphino alcohols, four phosphine-phosphinites and eleven phosphine-phosphites, all obtained in good yields. These ligands derive exclusively from Sharpless epoxyethers and reflect diverse levels of steric congestion in the CH<sub>2</sub>OR group. For the phosphine functionality, diaryl- and dialkyl-substituted phosphino groups were introduced in the epoxide-derived chiral skeleton. Several phosphinite groups were readily incorporated into the *P-OP* ligands by using electronically diverse chlorophosphines. Various phosphite groups were bound to the *P-OH* derivatives obtained from epoxide ring-opening. The phosphite groups span extremes of conformational behavior, from conformationally dynamic biaryl derivatives (BIPOL derivatives) to configurationally stable biaryl compounds (BINOL derivatives). Lastly, alkyl phosphites were also synthesized.
3. We studied the complexation of our *P-OH* and *P-OP* ligands to Rhodium precursors, and then assessed the catalytic activity of the resulting complexes in asymmetric hydrogenations of functionalized olefins. Of all the Rhodium complexes formed from the enantiomerically pure *P-OP* ligands, those

derived from phosphine-phosphites **125** provided the highest rates of conversion and the best enantioselectivities. The Rhodium pre-catalysts derived from *P-OH* derivatives and from phosphine-phosphinites **124** displayed lower enantioselectivities.

4. The best catalyst of the series (ligand **125k**), incorporating an (*S*)-BINOL fragment in the phosphite moiety, performs well for a broad spectrum of diversely substituted prochiral functionalized alkenes (eighteen substrates): dehydroaryl alanines, dehydro leucines, itaconates, enamides and enol derivatives. This catalyst has comparable activities to those of certain *milestone-ligands* in Rhodium-mediated asymmetric hydrogenation, such as JOSIPHOS or BINAP.

The remarkable performance and modular nature of our catalysts make them very attractive for future applications. We are currently endeavoring to develop new catalysts for challenging chirogenic transformations.

5. The modular strategy that we describe in this thesis for the development of new chiral catalysts—tuning of the catalyst through modification of the stereoelectronics of its modules—is based on a solid premise: the different parts of a given catalyst can be optimized separately, and therefore, high enantioselectivities can ultimately be obtained even when starting from a mediocre ligand.
6. We have developed a practical route to chiral diphosphine ligands with supramolecular motifs, which we prepared for future catalytic studies. This work comprised synthesis of a diphosphine ligand containing a crown ether, encompassing three key steps: first, homocoupling of an iodoaryl phosphine oxide; second, subsequent optical resolution of the resulting racemic biaryl derivative, using a tartaric acid derivative as resolving agent; and third, formation of the crown ether, using an ethylene glycol derivative and base.



**APPENDIX: SELECTION OF  
NMR SPECTRA AND  
X-RAY STRUCTURES**

UNIVERSITAT ROVIRA I VIRGLI

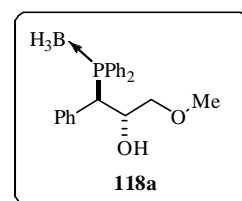
TOWARDS HIGHLY EFFICIENT LIGANDS FOR ASYMMETRIC HYDROGENATIONS: A COVALENT MODULAR APPROACH AND  
INVESTIGATIONS INTO BIOINSPIRED SUPRAMOLECULAR STRATEGIES

Héctor Fernández Pérez

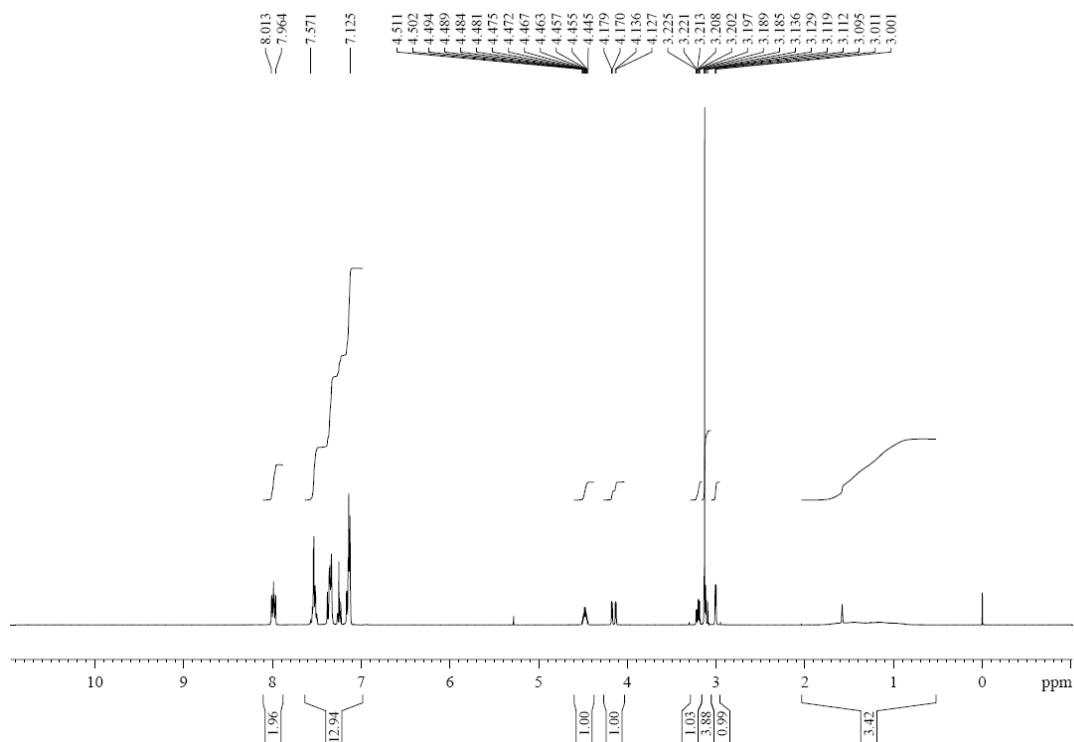
ISBN:978-84-693-3385-3 /DL:T.994-2010

## I. SELECTED NMR-SPECTRA

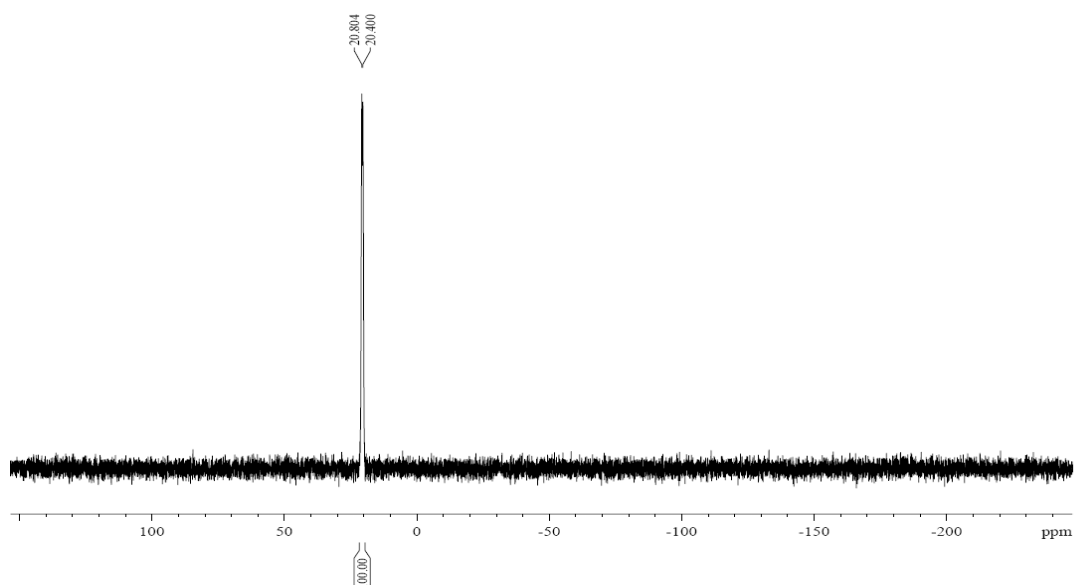
**(1*R*,2*S*)-1-(diphenylphosphino borane)-3-methoxy-1-phenylpropan-2-ol (118a).**



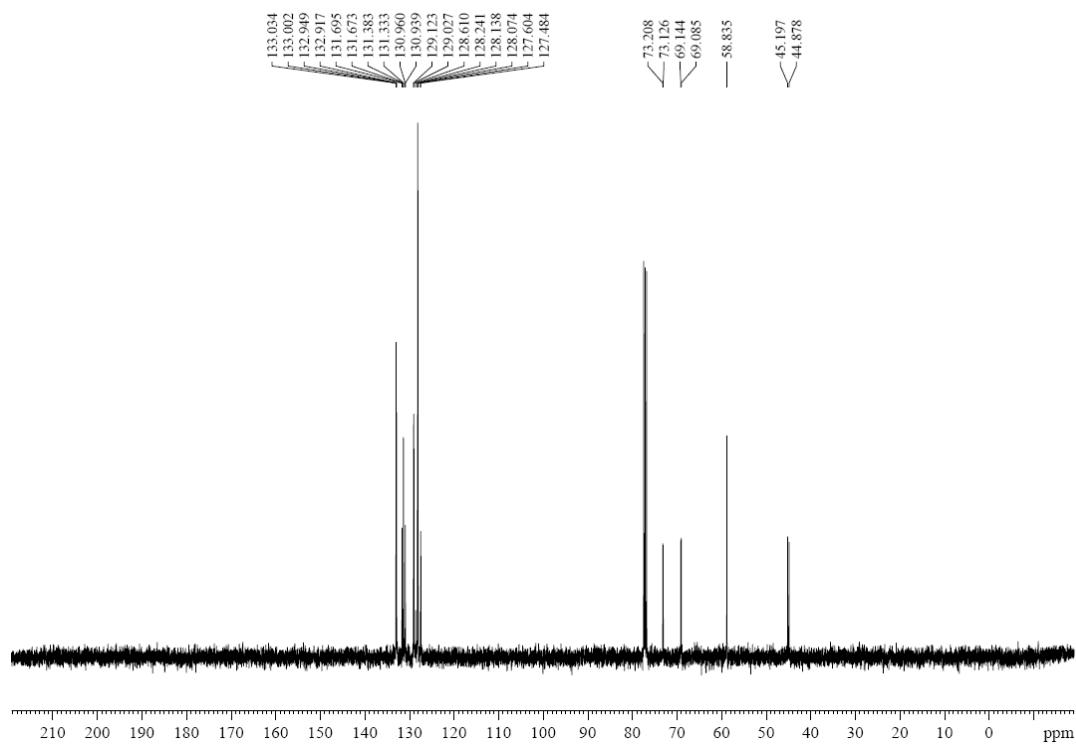
**<sup>1</sup>H-NMR (400MHZ, CDCl<sub>3</sub>)**



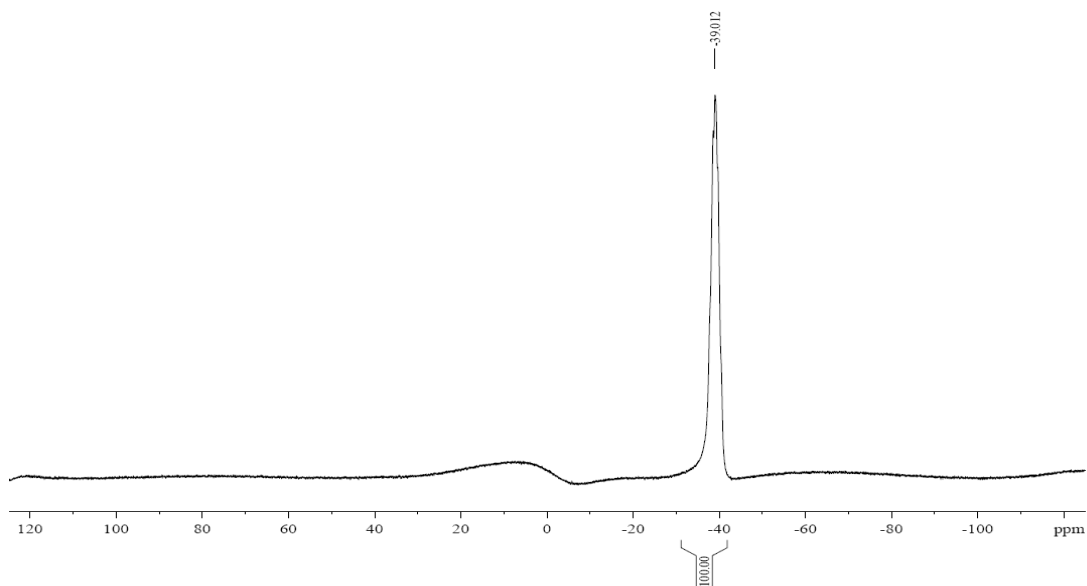
**<sup>31</sup>P{<sup>1</sup>H}-NMR (162MHZ, CDCl<sub>3</sub>)**



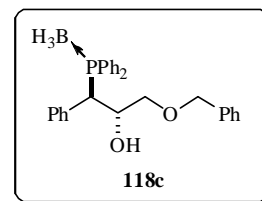
$^{13}\text{C}\{^1\text{H}\}$ -NMR (100MHZ,  $\text{CDCl}_3$ )



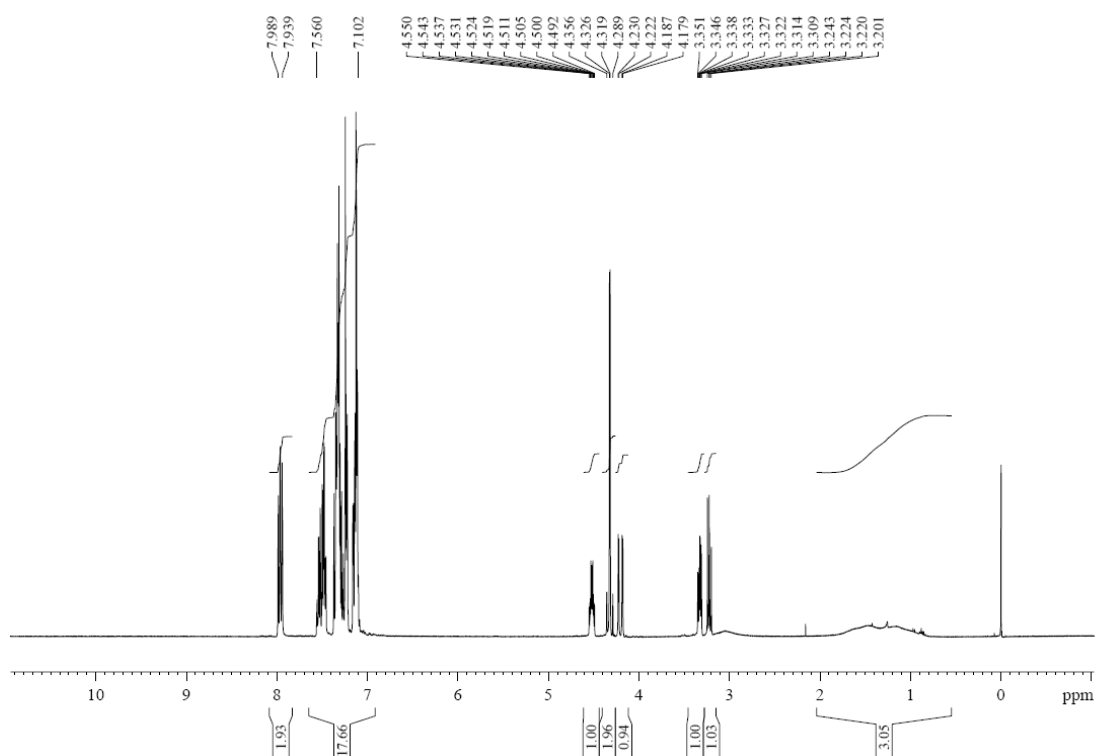
$^{11}\text{B}$ -NMR (128MHZ,  $\text{CDCl}_3$ )



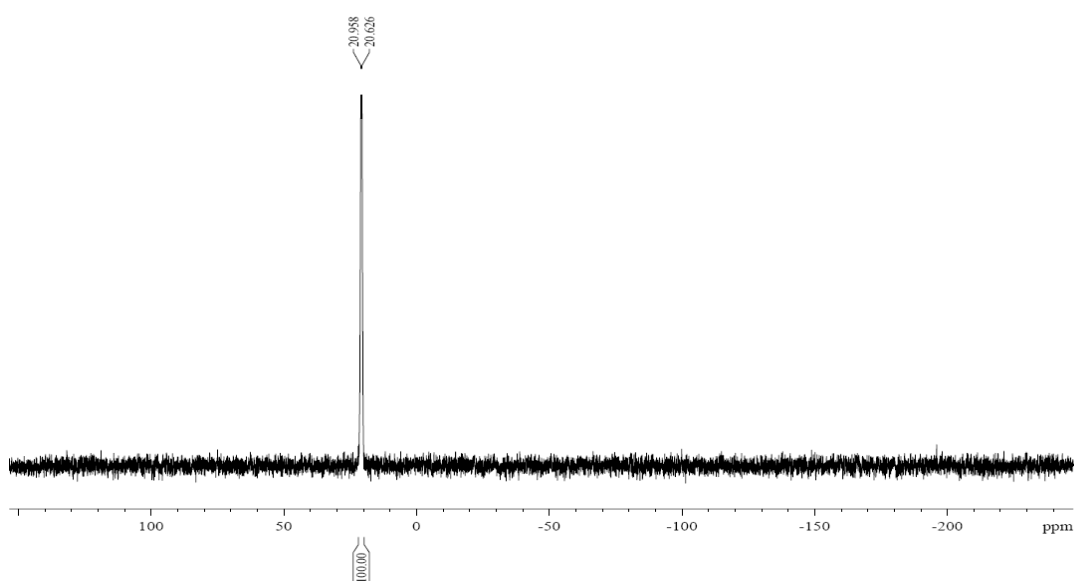
**(1*R*,2*S*)-3-(benzyloxy)-1-(diphenylphosphino borane)-1-phenylpropan-2-ol (118c).**



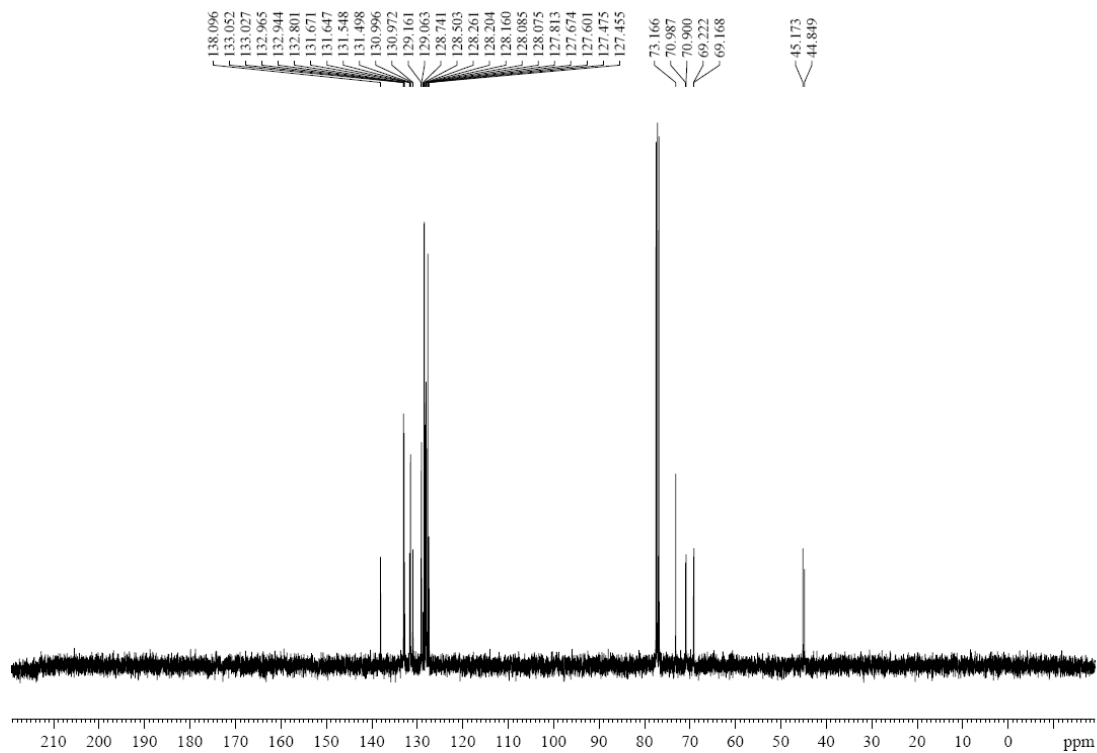
**<sup>1</sup>H-NMR (400MHZ, CDCl<sub>3</sub>)**



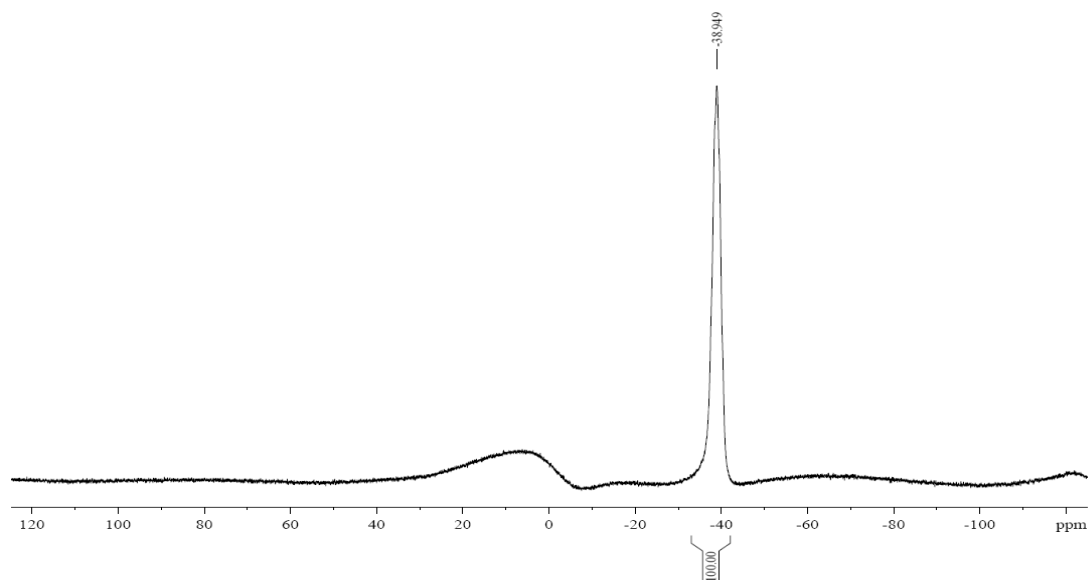
**<sup>31</sup>P{<sup>1</sup>H}-NMR (162MHZ, CDCl<sub>3</sub>)**



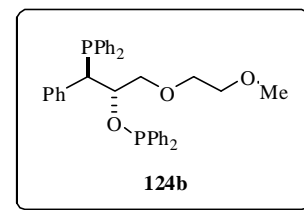
### $^{13}\text{C}\{^1\text{H}\}$ -NMR (100MHZ, $\text{CDCl}_3$ )



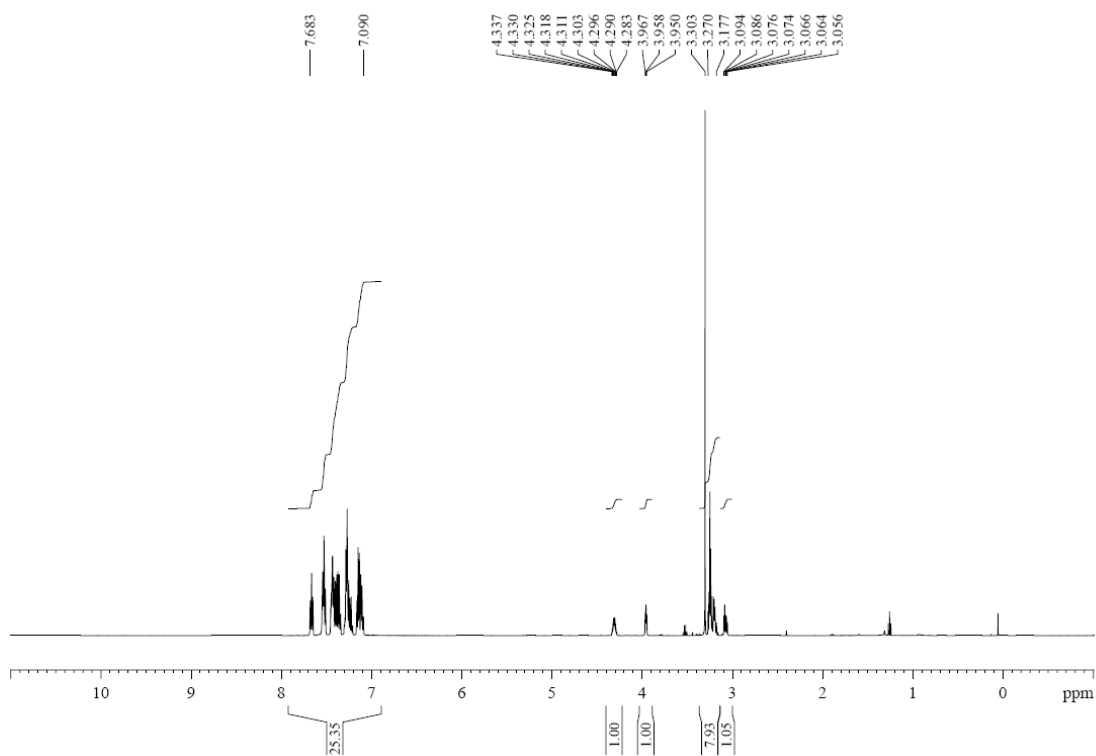
### $^{11}\text{B}$ -NMR (128MHZ, $\text{CDCl}_3$ )



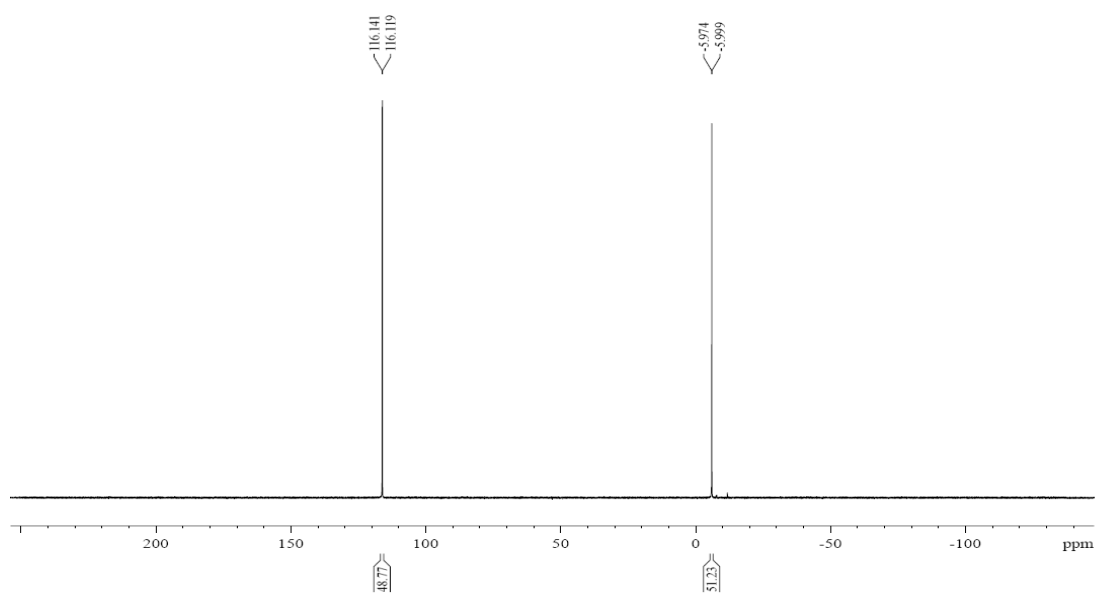
**(S)-3-((R)-(diphenylphosphino)(phenyl)methyl)-1,1-diphenyl-2,5,8-trioxa-1-phosphanone (124b).**

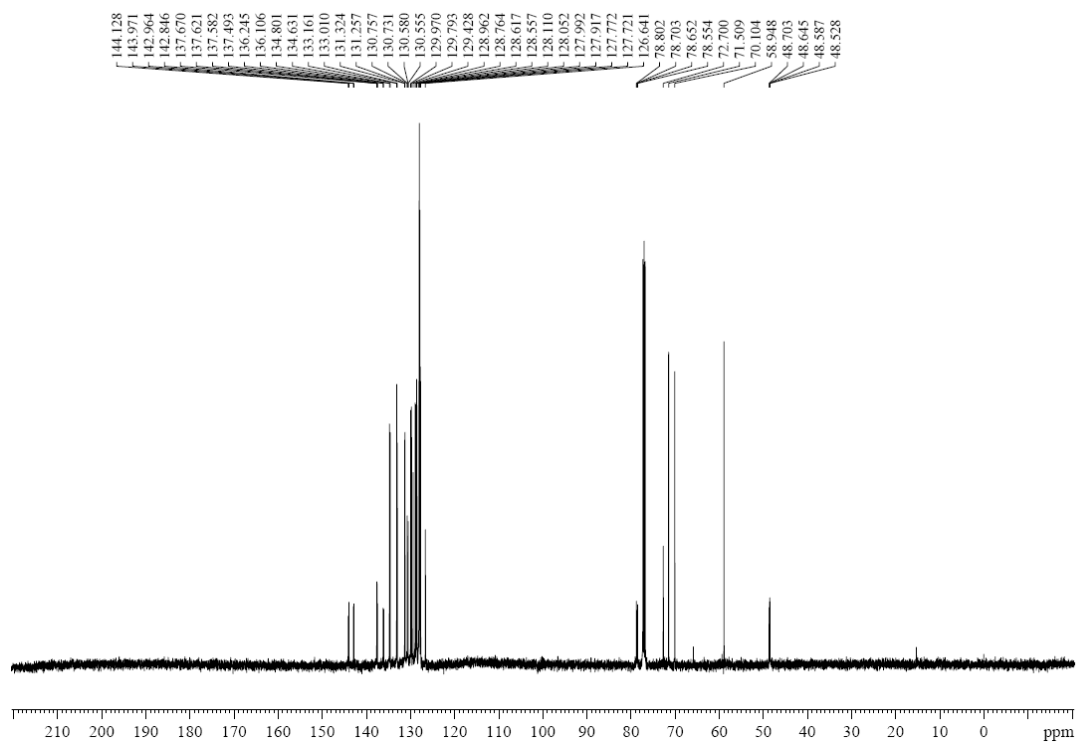


**$^1\text{H-NMR}$  (500MHZ,  $\text{CDCl}_3$ )**



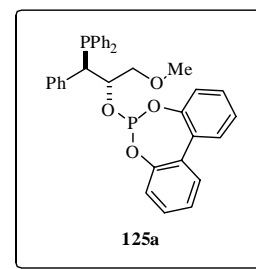
**$^{31}\text{P}\{^1\text{H}\}$ -NMR (202MHZ,  $\text{CDCl}_3$ )**



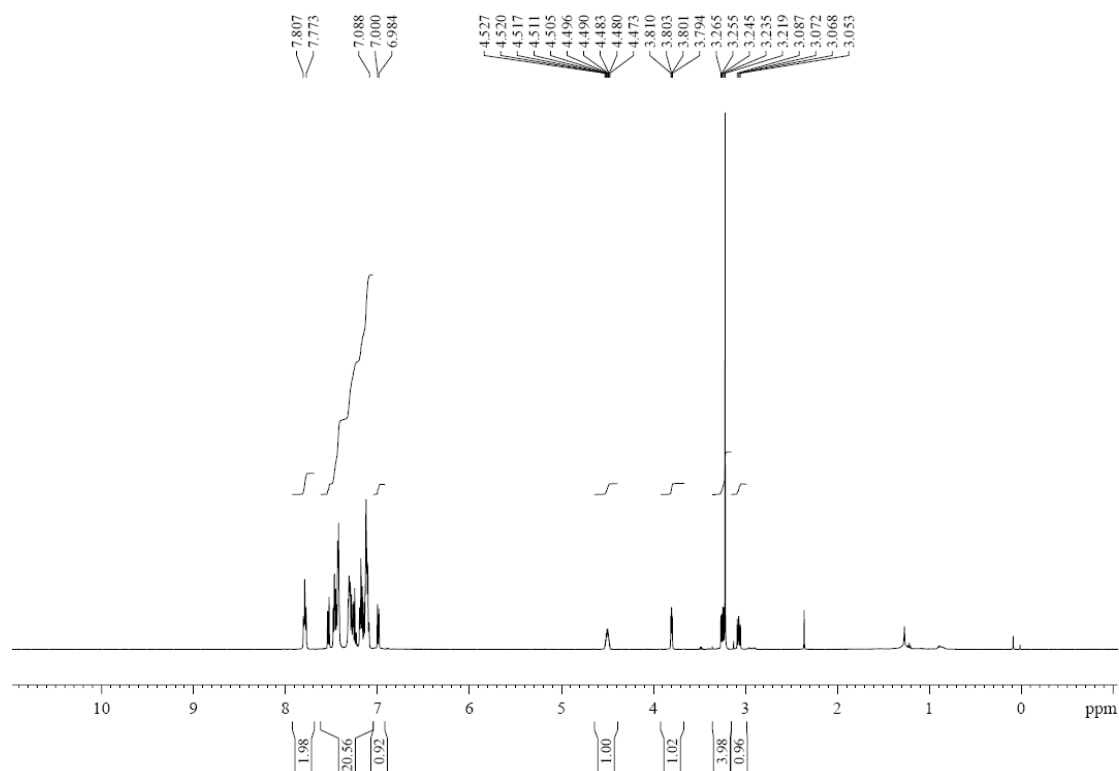
$^{13}\text{C}\{^1\text{H}\}$ -NMR (125MHZ,  $\text{CDCl}_3$ )



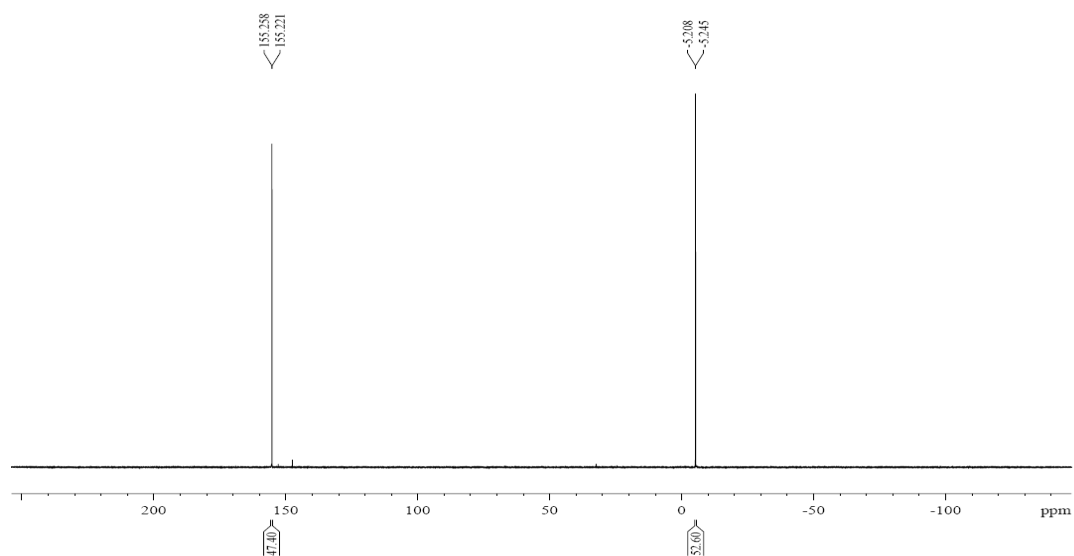
**6-((1*R*,2*S*)-1-(diphenylphosphino)-3-methoxy-1-phenylpropen-2-yloxy)dibenzo[*d,f*][1,3,2]dioxaphosphepine (125a).**

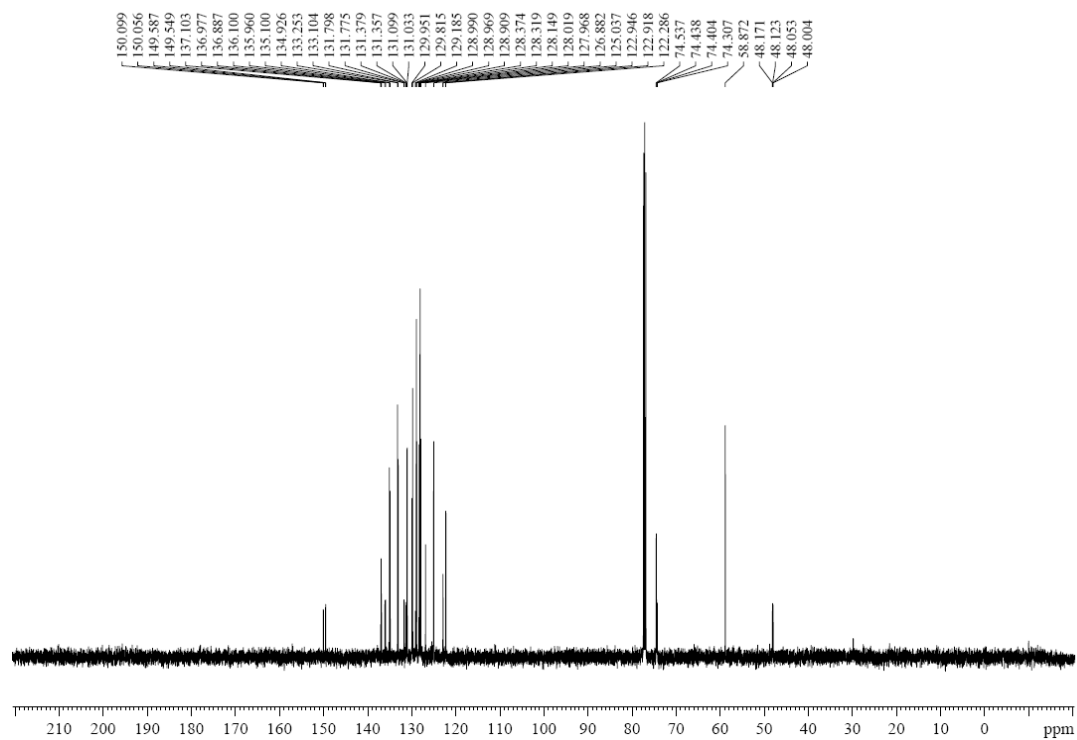


$^1\text{H-NMR}$  (500MHZ,  $\text{CDCl}_3$ )

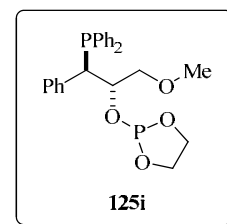


$^{31}\text{P}\{^1\text{H}\}$ -NMR (202MHZ,  $\text{CDCl}_3$ )

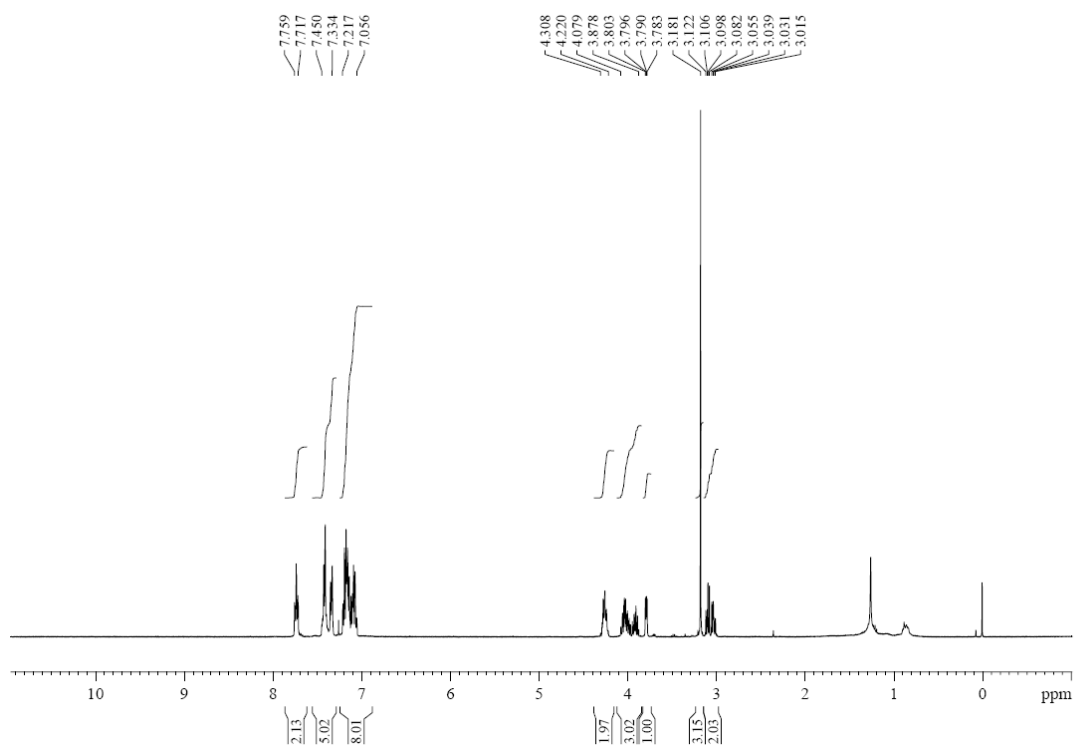


$^{13}\text{C}\{^1\text{H}\}$ -NMR (125MHZ,  $\text{CDCl}_3$ )

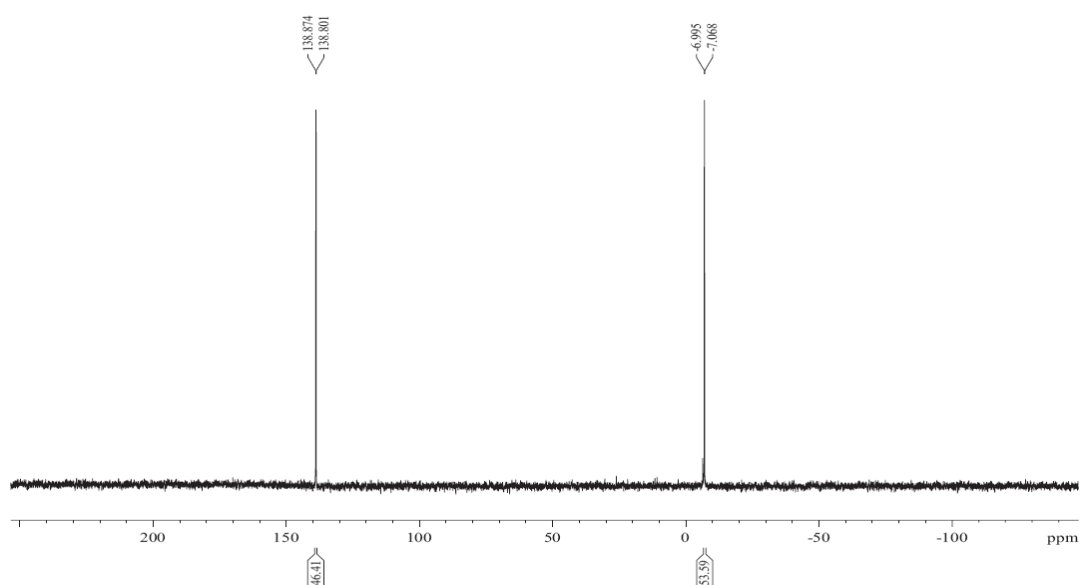
**2-((1*R*,2*S*)-1-(diphenylphosphino)-3-methoxy-1-phenylpropen-2-yloxy)-1,3,2-dioxaphospholane (125i).**

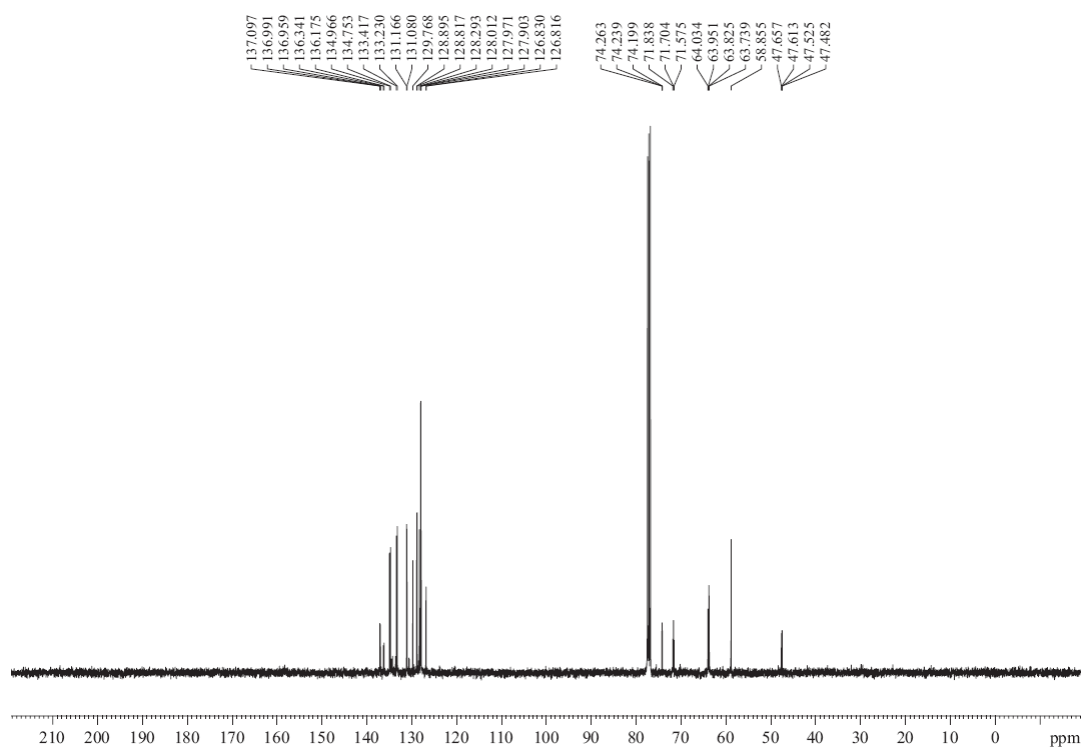


**$^1\text{H-NMR}$  (500MHz,  $\text{CDCl}_3$ )**

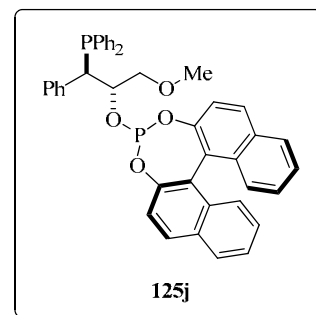


**$^{31}\text{P}\{^1\text{H}\}$ -NMR (202MHz,  $\text{CDCl}_3$ )**

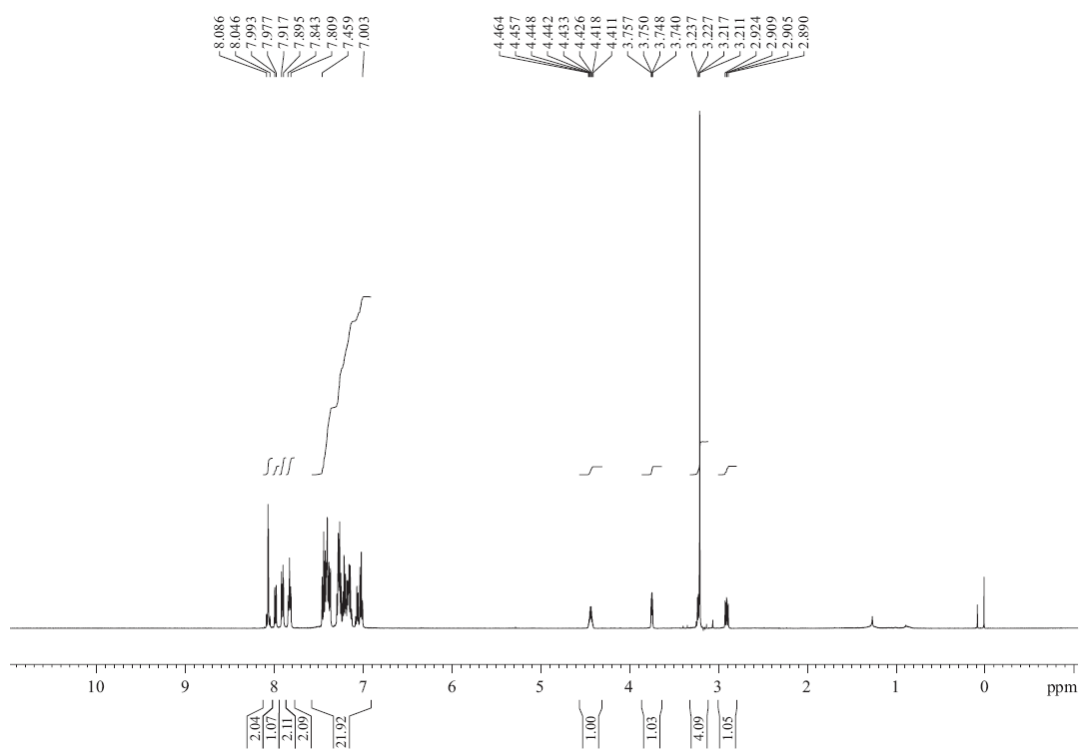


$^{13}\text{C}\{^1\text{H}\}$ -NMR (125MHz,  $\text{CDCl}_3$ )

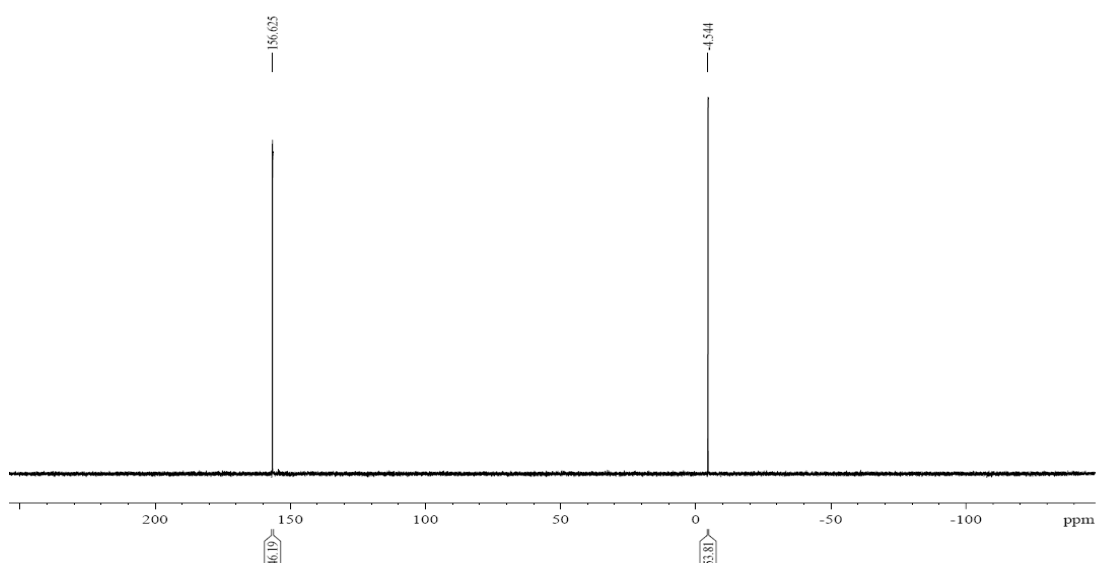
**(11bR)-4-((1R,2S)-1-(diphenylphosphino)-3-methoxy-1-phenylpropan-2-yloxy)dinaphtho[2,1-d:1',2'-f][1,3,2]dioxaphosphepine (125j).**

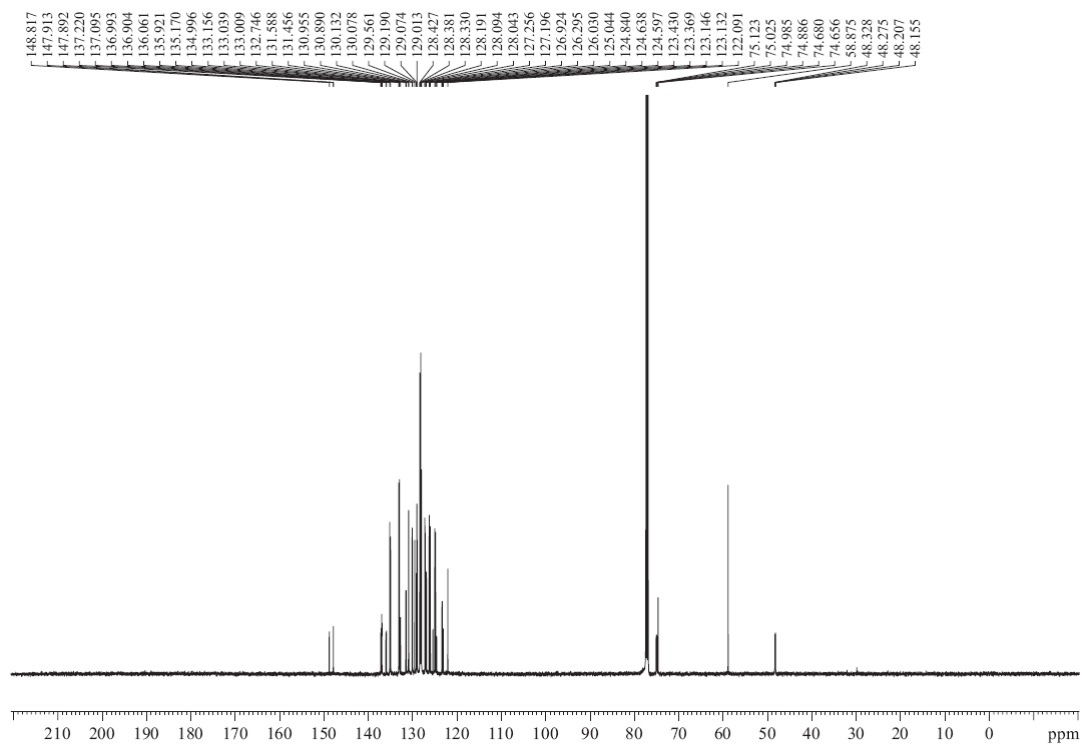


$^1\text{H-NMR}$  (500MHz,  $\text{CDCl}_3$ )

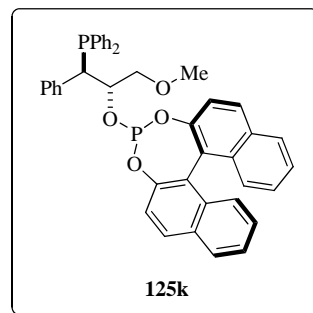


$^{31}\text{P}\{^1\text{H}\}$ -NMR (202MHz,  $\text{CDCl}_3$ )

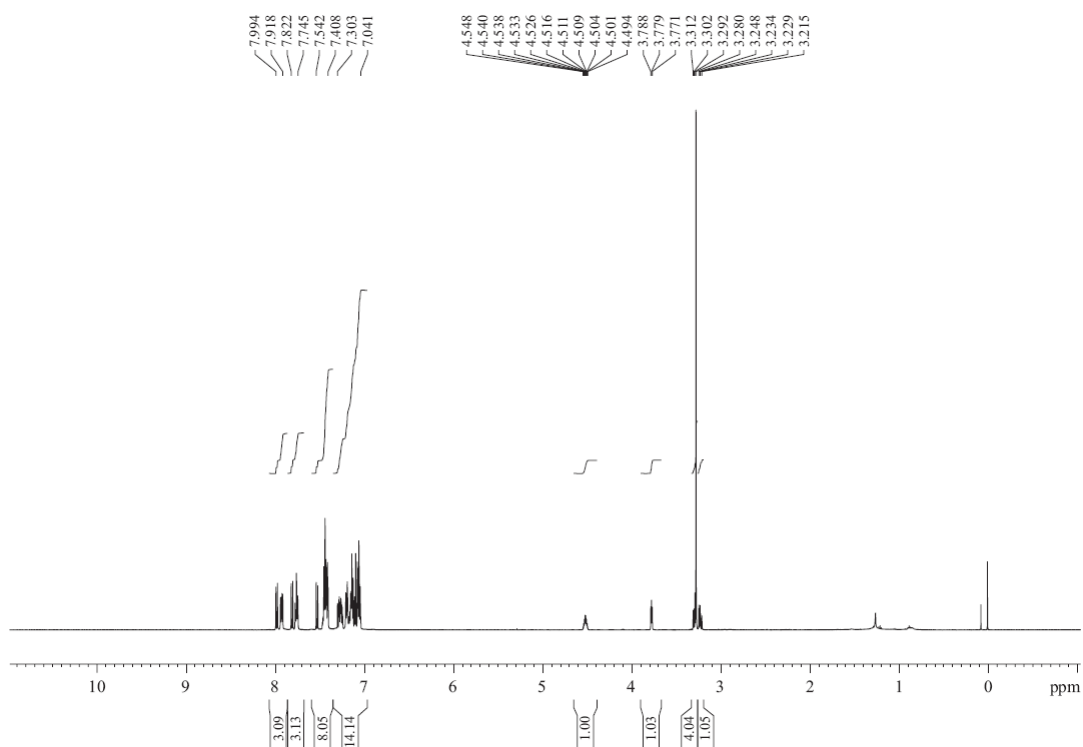


$^{13}\text{C}\{^1\text{H}\}$ -NMR (125MHz,  $\text{CDCl}_3$ )

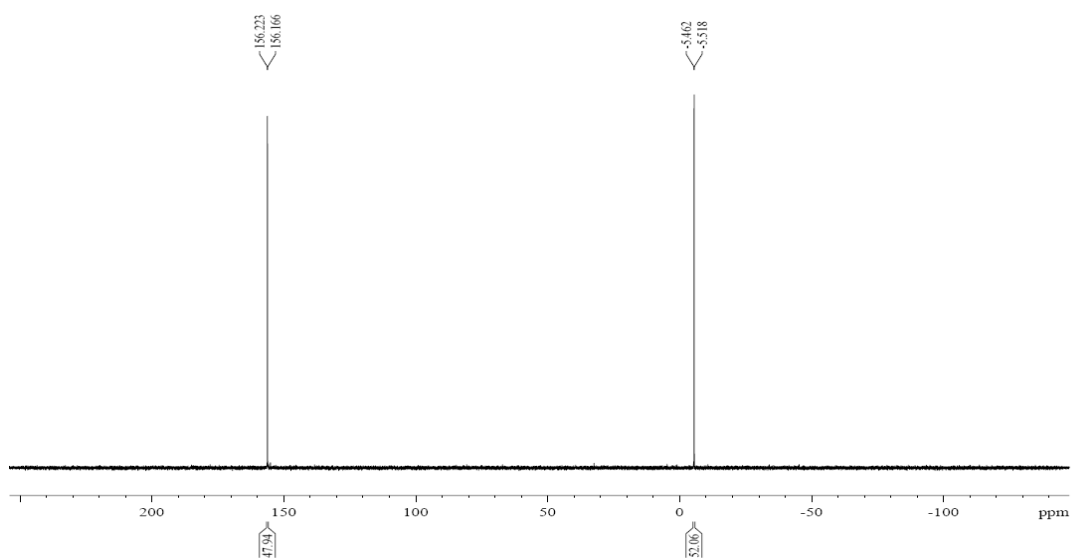
**(11bS)-4-((1R,2S)-1-(diphenylphosphino)-3-methoxy-1-phenylpropan-2-yloxy)dinaphtho[2,1-d:1',2'-f][1,3,2]dioxaphosphepine (125k).**

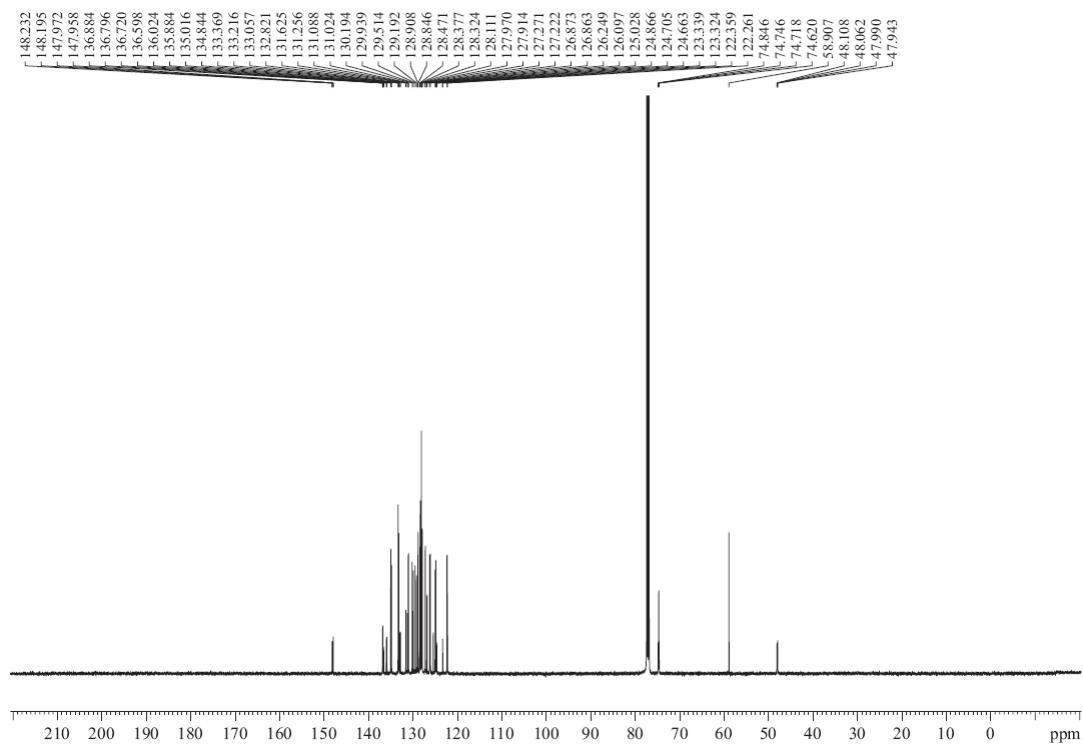


**$^1\text{H-NMR}$  (500MHz,  $\text{CDCl}_3$ )**

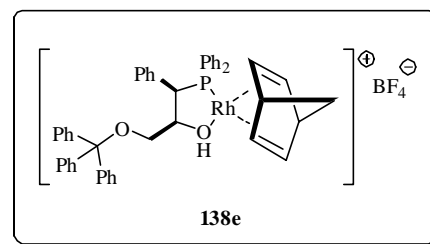
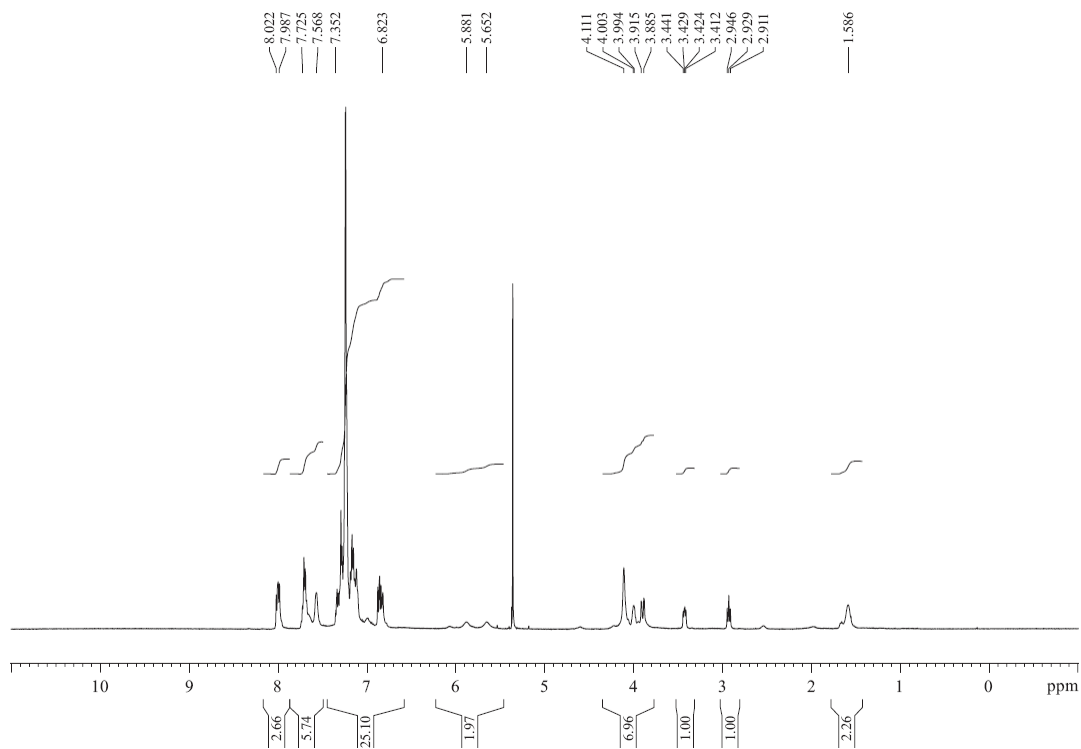
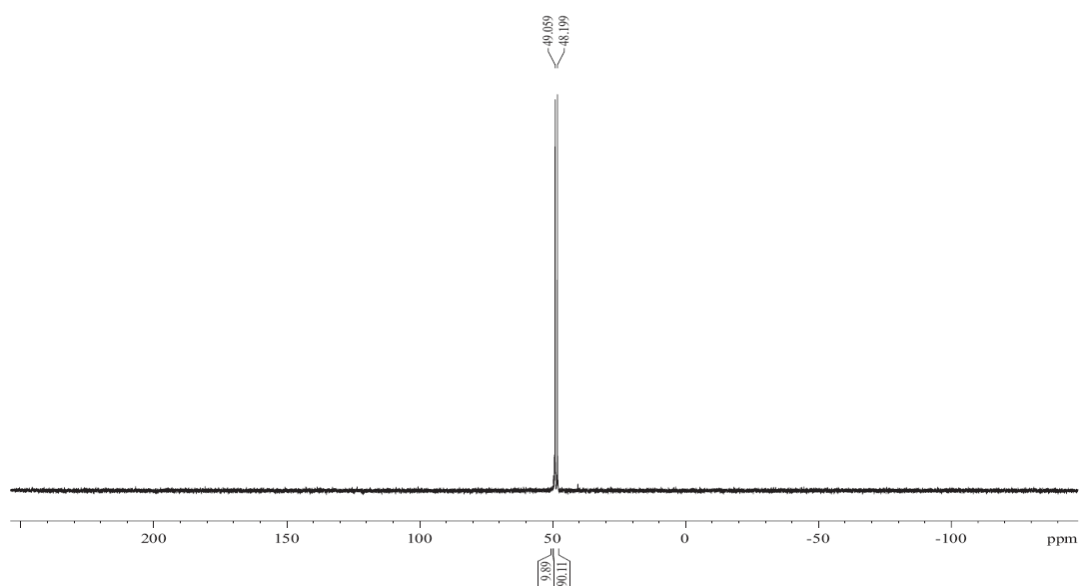


**$^{31}\text{P}\{^1\text{H}\}$ -NMR (202MHz,  $\text{CDCl}_3$ )**

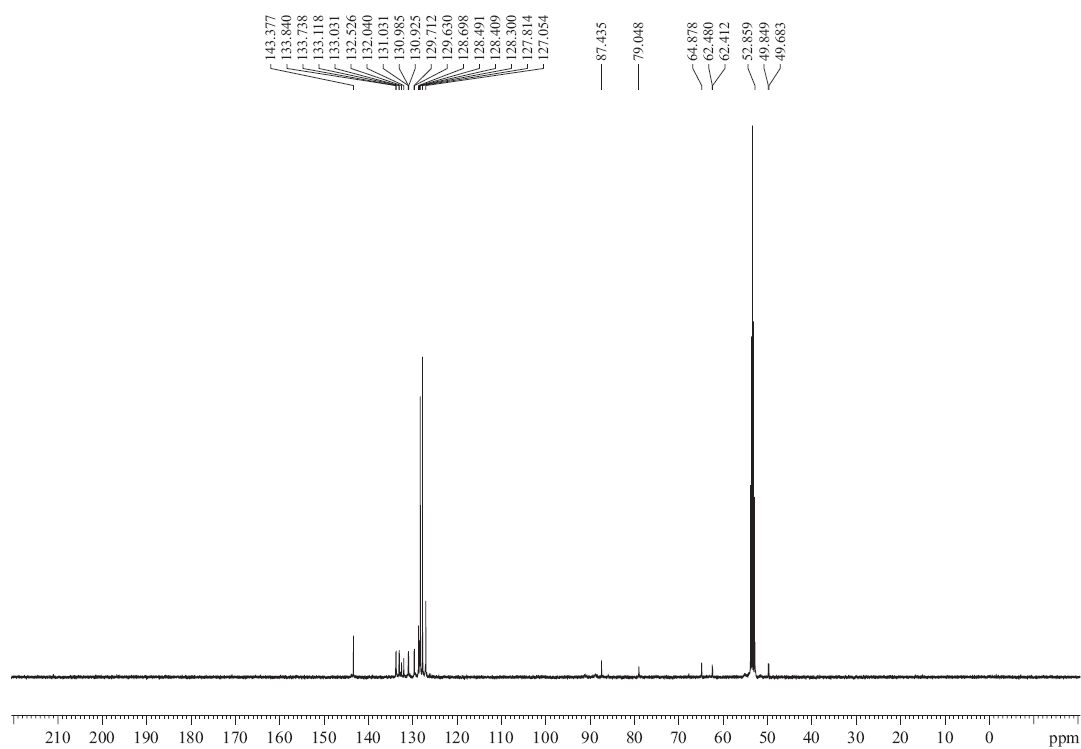


$^{13}\text{C}\{^1\text{H}\}$ -NMR (125MHz,  $\text{CDCl}_3$ )

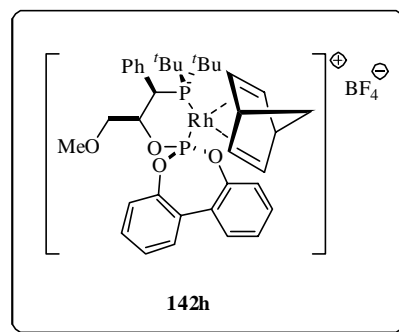


**[Rh(*P-OH*)(nbd)]BF<sub>4</sub> complex (138e).****<sup>1</sup>H-NMR (500MHz, CD<sub>2</sub>Cl<sub>2</sub>)****<sup>31</sup>P{<sup>1</sup>H}-NMR (202MHz, CD<sub>2</sub>Cl<sub>2</sub>)**

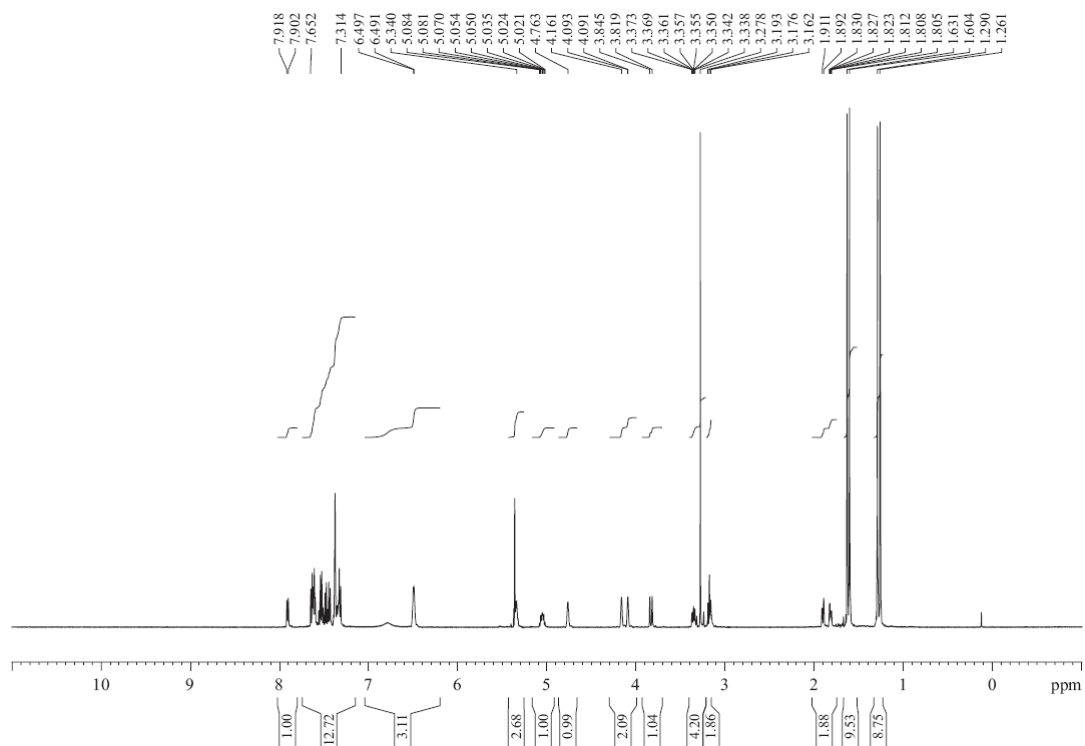
$^{13}\text{C}\{^1\text{H}\}$ -NMR (125MHz,  $\text{CD}_2\text{Cl}_2$ )



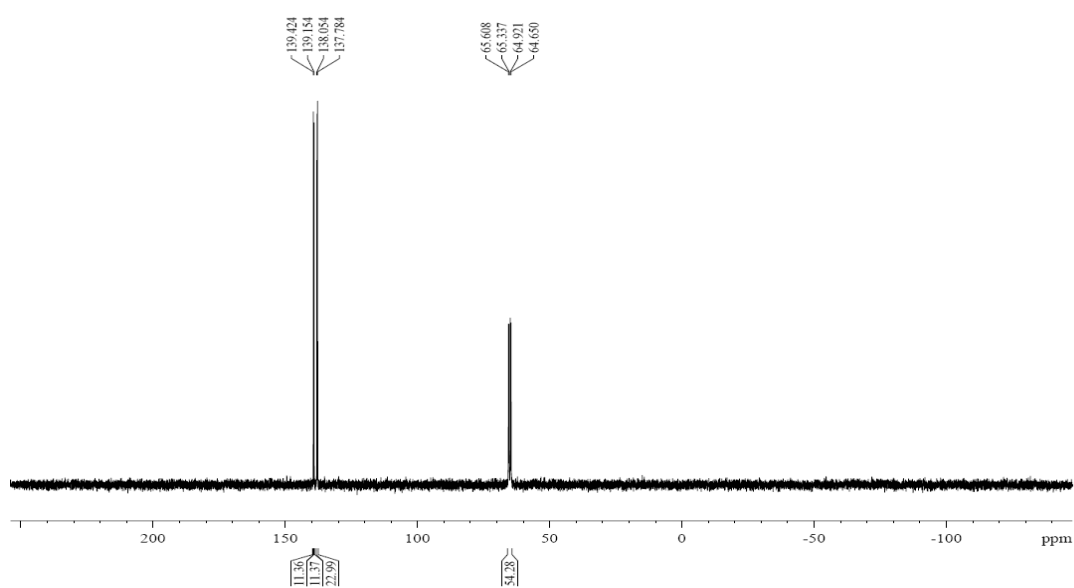
**[Rh(*P-OP*)(nbd)]BF<sub>4</sub> (142h).**



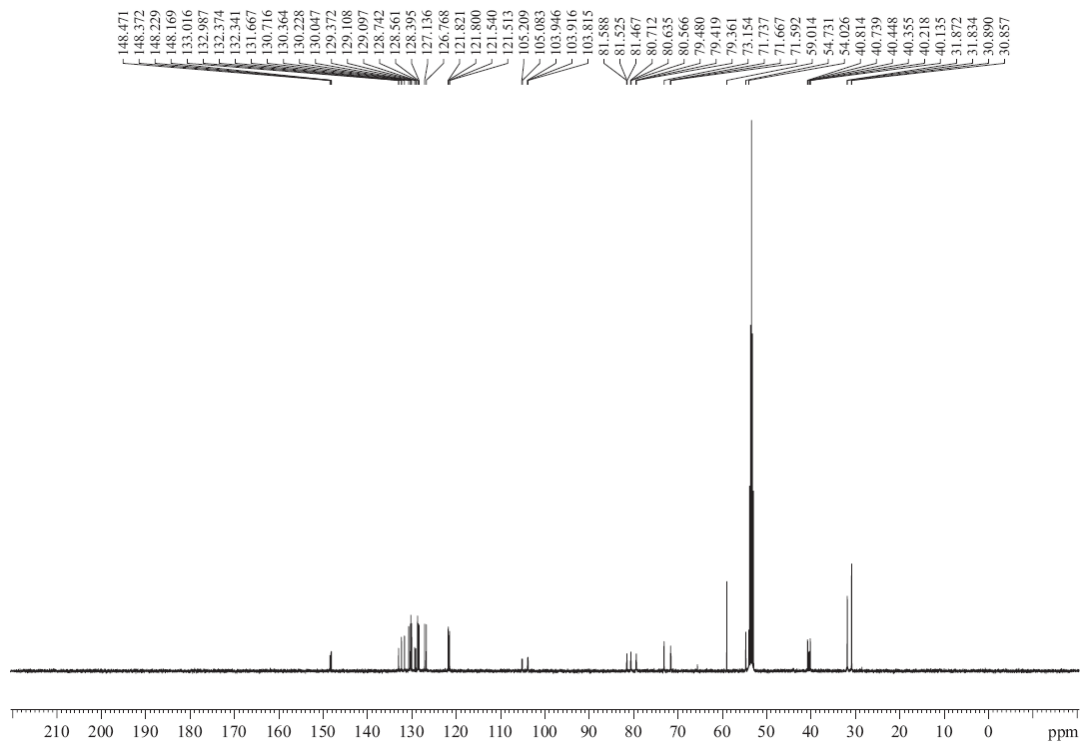
**<sup>1</sup>H-NMR (500MHz, CD<sub>2</sub>Cl<sub>2</sub>)**



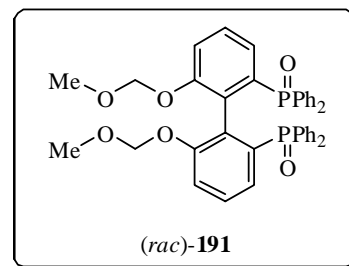
**<sup>31</sup>P{<sup>1</sup>H}-NMR (202MHz, CD<sub>2</sub>Cl<sub>2</sub>)**



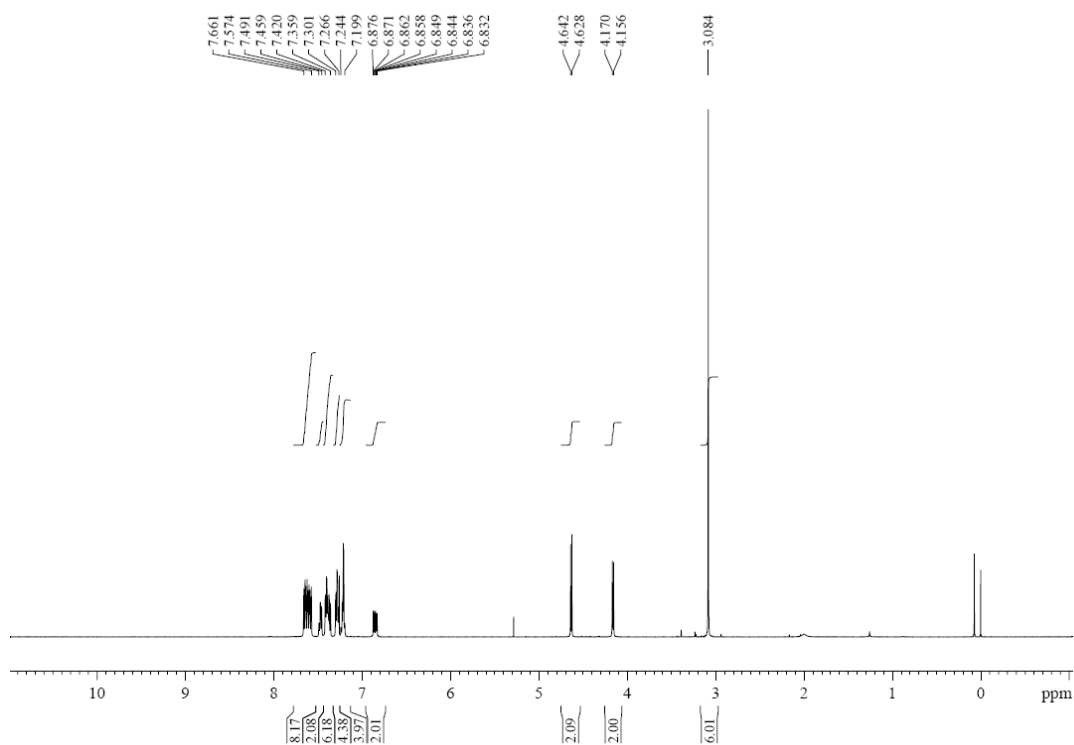
### $^{13}\text{C}\{^1\text{H}\}$ -NMR (125MHz, $\text{CD}_2\text{Cl}_2$ )



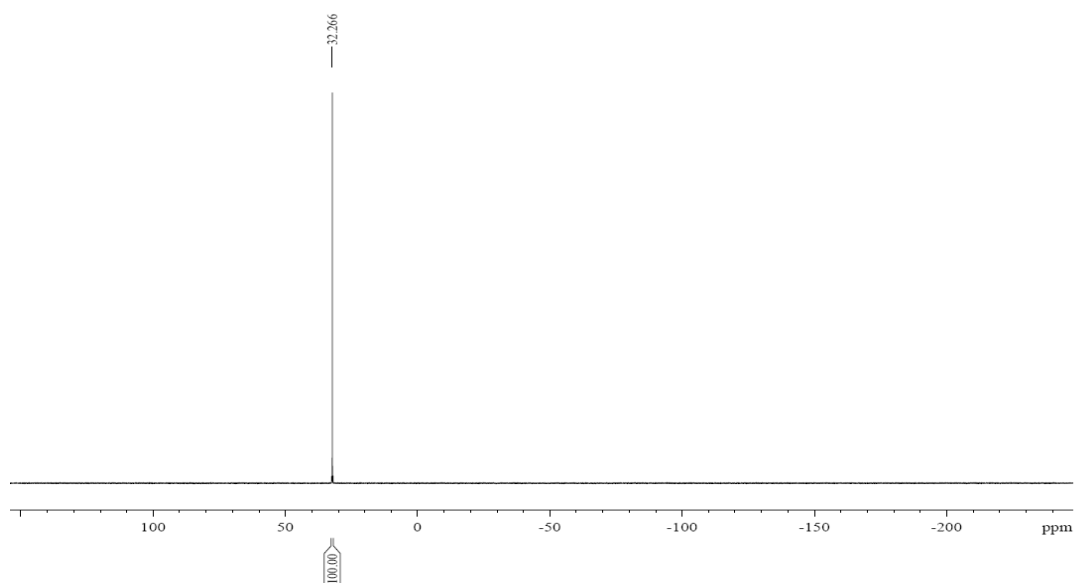
**(rac)-(6,6'-bis(methoxymethoxy)biphenyl-2,2'-diyl)bis(diphenylphosphine oxide) (rac-191).**



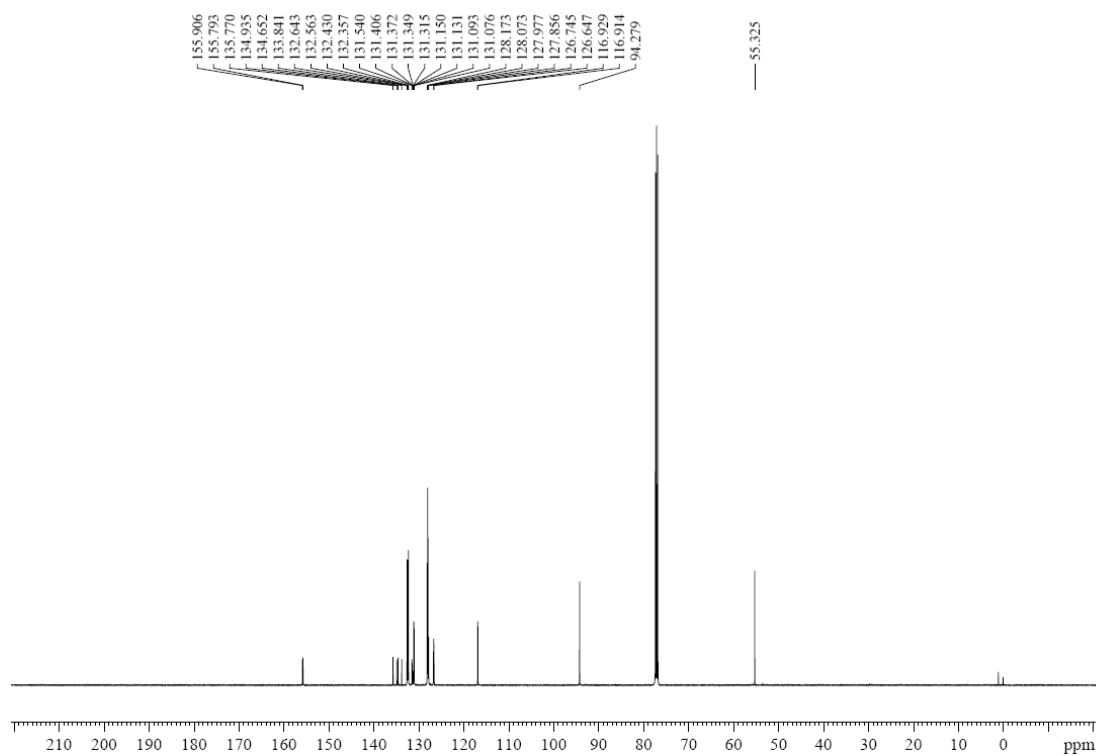
**$^1\text{H-NMR}$  (400MHz,  $\text{CDCl}_3$ )**



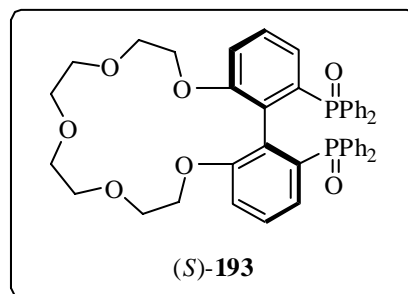
**$^{31}\text{P}\{^1\text{H}\}$ -NMR (162MHz,  $\text{CDCl}_3$ )**



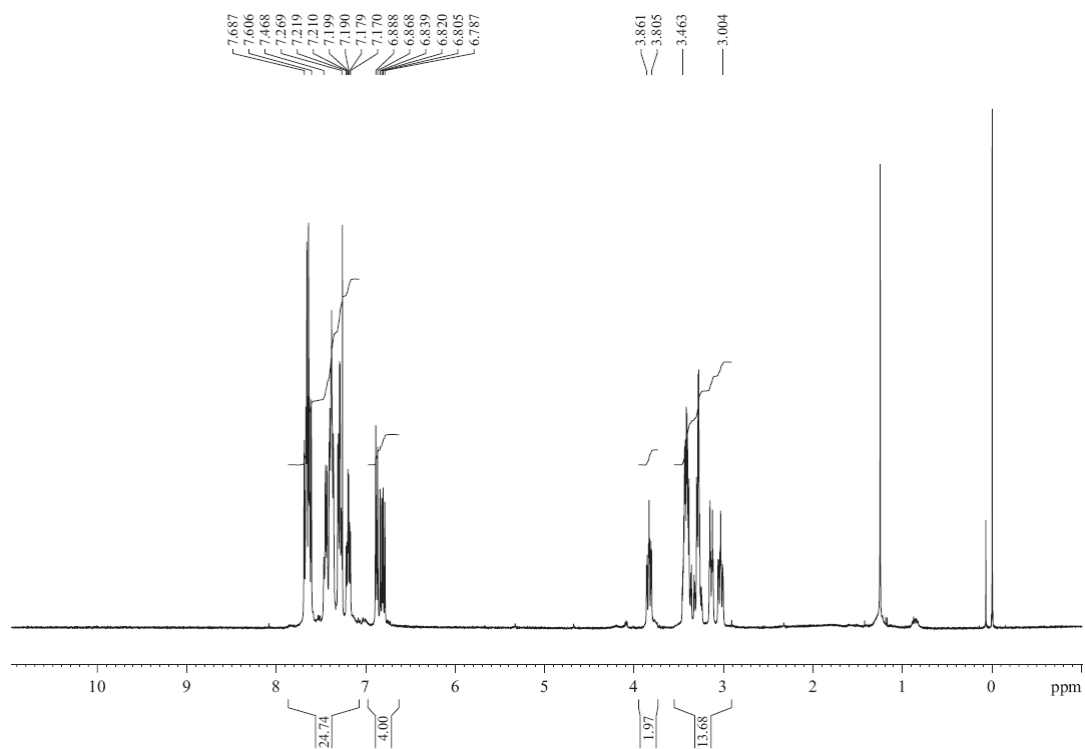
### $^{13}\text{C}\{^1\text{H}\}$ -NMR (100MHz, $\text{CDCl}_3$ )



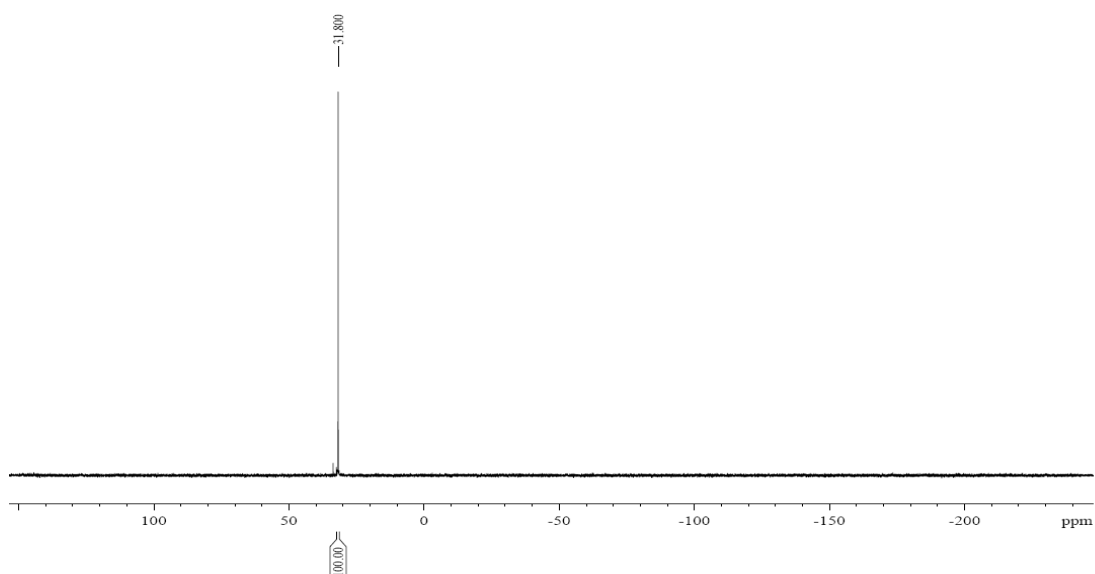
**(S)-1,21-bis(diphenylphosphino oxide)-  
6,7,9,10,12,13,15,16-  
octahydrodibenzo[*n,p*][1,4,7,10,13]pentaoxacy  
cloheptadecine ((S)-193).**

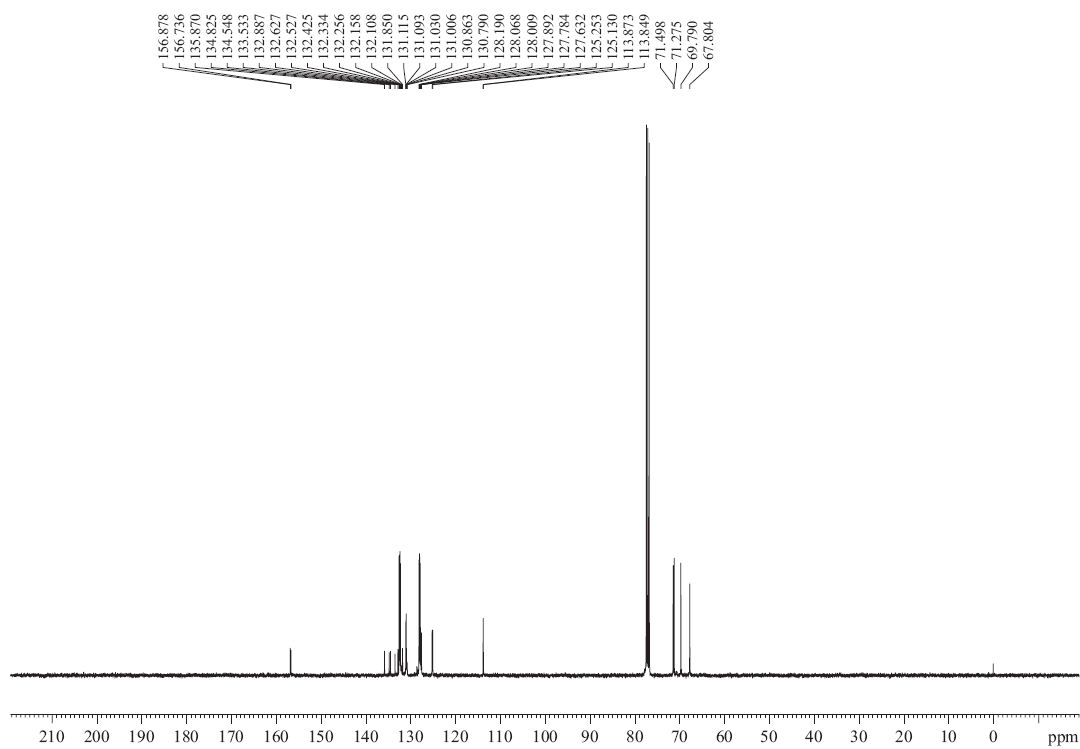


**<sup>1</sup>H-NMR (400MHz, CDCl<sub>3</sub>)**



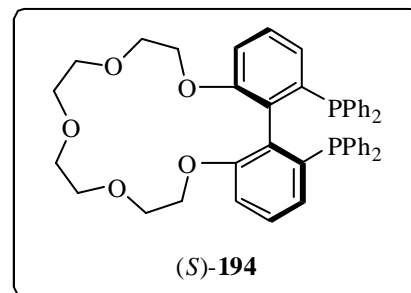
**<sup>31</sup>P{<sup>1</sup>H}-NMR (162MHz, CDCl<sub>3</sub>)**



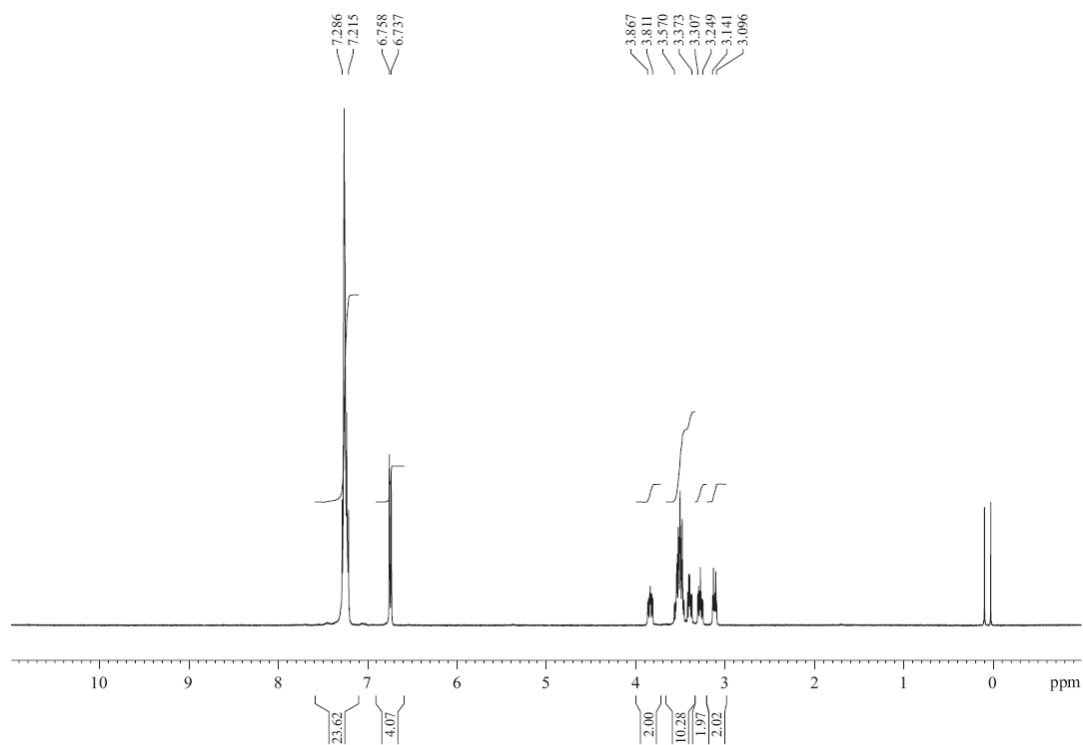
$^{13}\text{C}\{^1\text{H}\}$ -NMR (100MHz,  $\text{CDCl}_3$ )



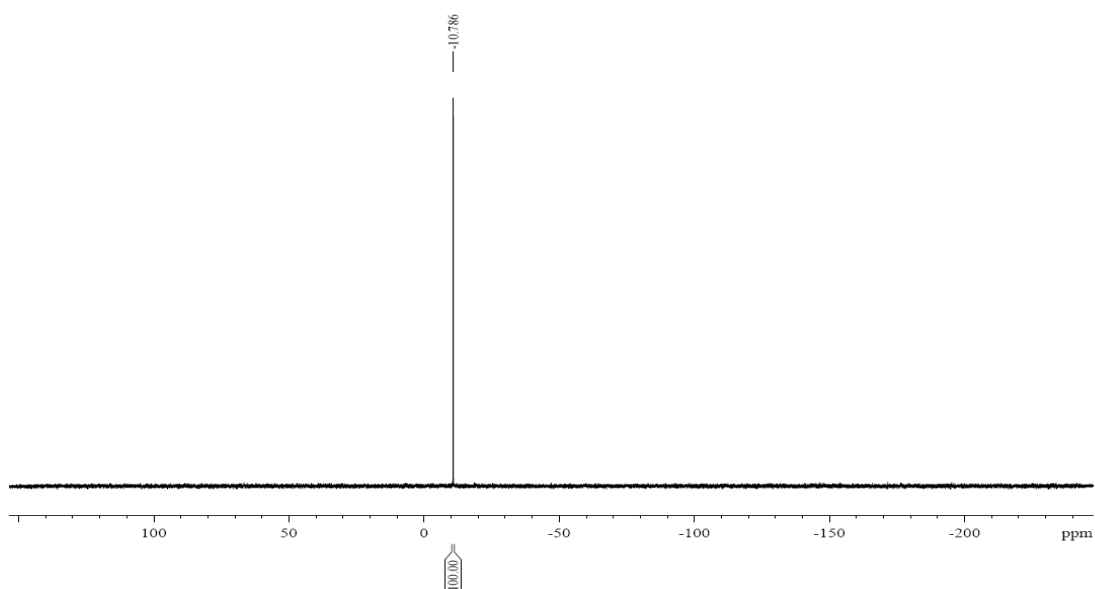
**(S)-1,21-bis(diphenylphosphino)-  
6,7,9,10,12,13,15,16-  
octahydrodibenzo[*n,p*][1,4,7,10,13]pentaoxacy  
cloheptadecine ((S)-194).**

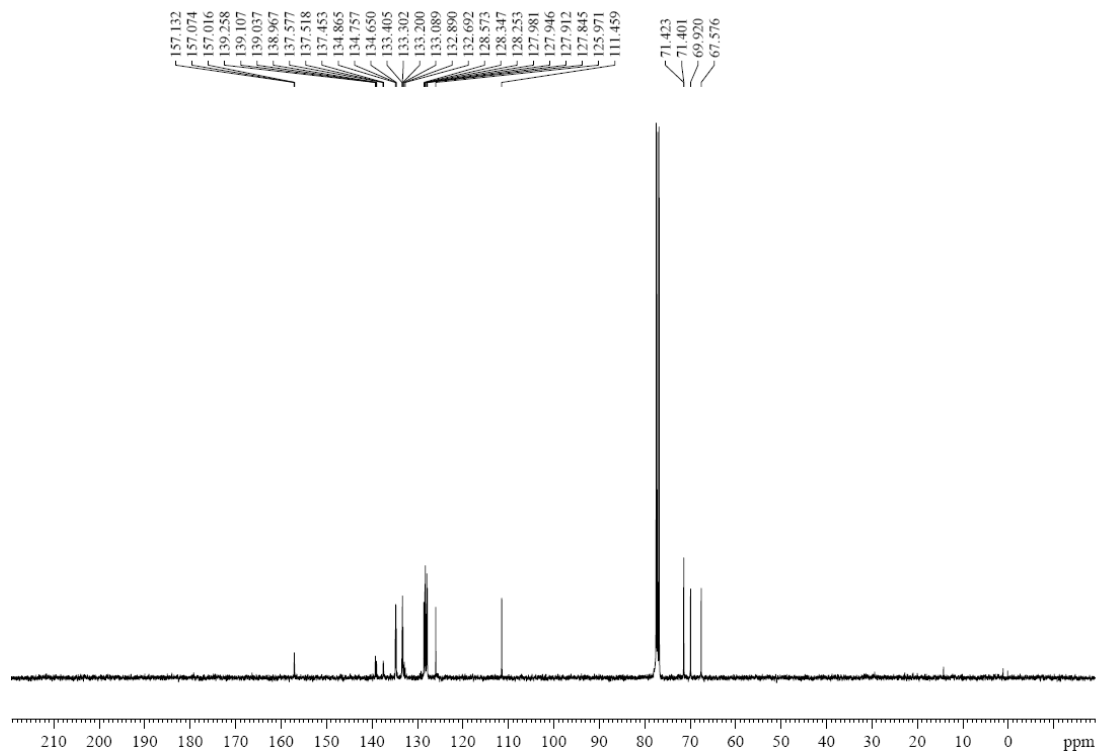


**$^1\text{H-NMR}$  (400MHz,  $\text{CDCl}_3$ )**



**$^{31}\text{P}\{^1\text{H}\}\text{-NMR}$  (162MHz,  $\text{CDCl}_3$ )**



$^{13}\text{C}\{^1\text{H}\}$ -NMR (100MHz,  $\text{CDCl}_3$ )

## II. X-RAY STRUCTURE FOR 118e

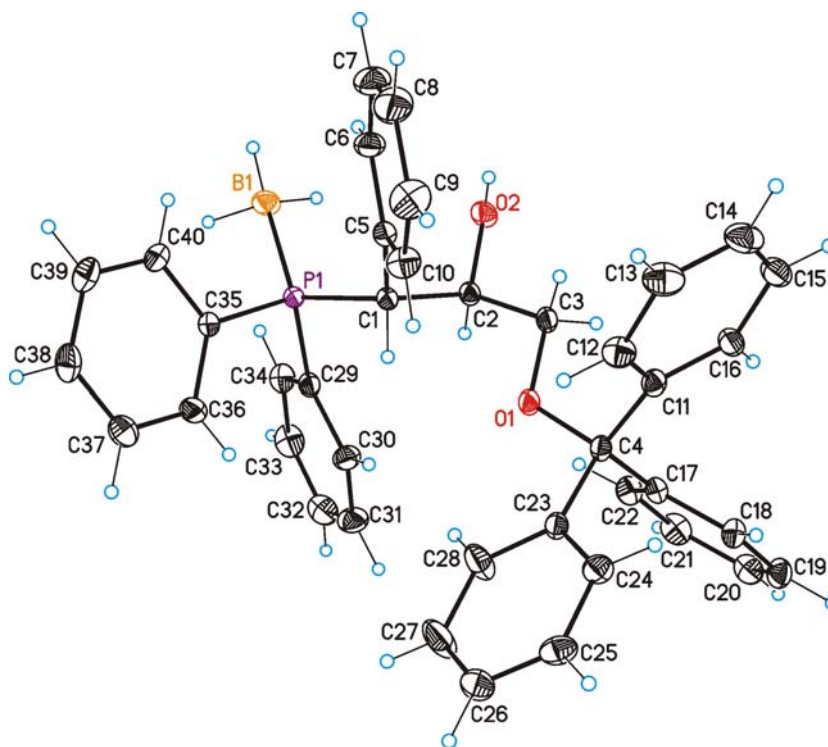


Table 1. Crystal data and structure refinement for **118e**.

Identification code	<b>118e</b>	
Empirical formula	$C_{40}H_{38}BO_2P$	
Formula weight	592.48	
Temperature	100(2) K	
Wavelength	0.71073 Å	
Crystal system	Monoclinic	
Space group	P2(1)	
Unit cell dimensions	$a = 9.3054(7)$ Å	$\alpha = 90^\circ$ .
	$b = 14.8098(11)$ Å	$\beta = 102.361(2)^\circ$ .
	$c = 12.0301(9)$ Å	$\gamma = 90^\circ$ .
Volume	$1619.4(2)$ Å <sup>3</sup>	
Z	2	
Density (calculated)	$1.215$ Mg/m <sup>3</sup>	
Absorption coefficient	$0.119$ mm <sup>-1</sup>	
F(000)	628	
Crystal size	$0.40 \times 0.40 \times 0.20$ mm <sup>3</sup>	
Theta range for data collection	2.75 to 39.29°.	

Index ranges	-14<=h<=16, -26<=k<=26, -21<=l<=14
Reflections collected	32945
Independent reflections	14877 [R(int) = 0.0271]
Completeness to theta = 39.29°	92.5 %
Absorption correction	SADABS (Bruker-Nonius)
Max. and min. transmission	0.9765 and 0.9539
Refinement method	Full-matrix least-squares on F <sup>2</sup>
Data / restraints / parameters	14877 / 1 / 413
Goodness-of-fit on F <sup>2</sup>	1.043
Final R indices [I>2sigma(I)]	R1 = 0.0396, wR2 = 0.1002
R indices (all data)	R1 = 0.0455, wR2 = 0.1051
Absolute structure parameter	-0.04(3)
Largest diff. peak and hole	0.489 and -0.278 e.Å <sup>-3</sup>

Table 2. Bond lengths [Å] and angles [°] for **118e**.

P(1)-C(35)	1.8181(8)
P(1)-C(29)	1.8209(8)
P(1)-C(1)	1.8430(9)
P(1)-B(1)	1.9282(10)
O(1)-C(3)	1.4206(9)
O(1)-C(4)	1.4468(11)
C(1)-C(5)	1.5092(11)
C(1)-C(2)	1.5427(11)
O(2)-C(2)	1.4216(9)
C(2)-C(3)	1.5242(13)
C(4)-C(11)	1.5298(12)
C(4)-C(23)	1.5344(10)
C(4)-C(17)	1.5349(12)
C(5)-C(10)	1.3909(13)
C(5)-C(6)	1.3965(12)
C(6)-C(7)	1.3927(14)
C(7)-C(8)	1.3822(19)
C(8)-C(9)	1.3880(18)
C(9)-C(10)	1.3881(14)
C(11)-C(16)	1.3936(13)
C(11)-C(12)	1.3991(13)

C(12)-C(13)	1.3916(15)
C(13)-C(14)	1.3879(19)
C(14)-C(15)	1.3876(17)
C(15)-C(16)	1.3949(13)
C(17)-C(18)	1.3935(14)
C(17)-C(22)	1.3961(12)
C(18)-C(19)	1.3882(13)
C(19)-C(20)	1.3955(15)
C(20)-C(21)	1.3798(18)
C(21)-C(22)	1.3985(15)
C(23)-C(28)	1.3862(14)
C(23)-C(24)	1.3923(12)
C(24)-C(25)	1.3953(13)
C(25)-C(26)	1.3791(18)
C(26)-C(27)	1.3852(18)
C(27)-C(28)	1.3933(14)
C(29)-C(30)	1.3992(13)
C(29)-C(34)	1.4006(13)
C(30)-C(31)	1.3936(13)
C(31)-C(32)	1.3850(17)
C(32)-C(33)	1.3858(18)
C(33)-C(34)	1.3938(14)
C(35)-C(40)	1.3938(13)
C(35)-C(36)	1.3985(11)
C(36)-C(37)	1.3904(13)
C(37)-C(38)	1.3879(16)
C(38)-C(39)	1.3877(15)
C(39)-C(40)	1.3927(14)
C(35)-P(1)-C(29)	107.43(4)
C(35)-P(1)-C(1)	100.86(4)
C(29)-P(1)-C(1)	103.62(4)
C(35)-P(1)-B(1)	111.50(5)
C(29)-P(1)-B(1)	110.46(5)
C(1)-P(1)-B(1)	121.78(4)
C(3)-O(1)-C(4)	117.18(7)
C(5)-C(1)-C(2)	111.94(7)
C(5)-C(1)-P(1)	113.86(6)

Appendix: NMR spectra and X-ray structures

C(2)-C(1)-P(1)	114.11(6)
O(2)-C(2)-C(3)	108.95(7)
O(2)-C(2)-C(1)	113.25(7)
C(3)-C(2)-C(1)	111.12(6)
O(1)-C(3)-C(2)	107.42(7)
O(1)-C(4)-C(11)	109.13(7)
O(1)-C(4)-C(23)	104.20(7)
C(11)-C(4)-C(23)	113.87(6)
O(1)-C(4)-C(17)	110.29(6)
C(11)-C(4)-C(17)	112.89(7)
C(23)-C(4)-C(17)	106.09(6)
C(10)-C(5)-C(6)	118.52(8)
C(10)-C(5)-C(1)	118.61(8)
C(6)-C(5)-C(1)	122.77(8)
C(7)-C(6)-C(5)	120.27(10)
C(8)-C(7)-C(6)	120.73(10)
C(7)-C(8)-C(9)	119.21(10)
C(8)-C(9)-C(10)	120.28(11)
C(9)-C(10)-C(5)	120.93(9)
C(16)-C(11)-C(12)	118.29(8)
C(16)-C(11)-C(4)	121.30(7)
C(12)-C(11)-C(4)	119.97(8)
C(13)-C(12)-C(11)	120.83(10)
C(14)-C(13)-C(12)	120.32(10)
C(15)-C(14)-C(13)	119.43(9)
C(14)-C(15)-C(16)	120.28(10)
C(11)-C(16)-C(15)	120.85(9)
C(18)-C(17)-C(22)	118.88(8)
C(18)-C(17)-C(4)	119.83(7)
C(22)-C(17)-C(4)	121.16(9)
C(19)-C(18)-C(17)	120.90(8)
C(18)-C(19)-C(20)	119.94(10)
C(21)-C(20)-C(19)	119.60(9)
C(20)-C(21)-C(22)	120.59(9)
C(17)-C(22)-C(21)	120.07(10)
C(28)-C(23)-C(24)	118.40(8)
C(28)-C(23)-C(4)	119.87(8)
C(24)-C(23)-C(4)	121.43(8)

---

C(23)-C(24)-C(25)	120.57(9)
C(26)-C(25)-C(24)	120.36(9)
C(25)-C(26)-C(27)	119.64(9)
C(26)-C(27)-C(28)	119.87(12)
C(23)-C(28)-C(27)	121.15(10)
C(30)-C(29)-C(34)	118.70(8)
C(30)-C(29)-P(1)	122.71(7)
C(34)-C(29)-P(1)	118.58(7)
C(31)-C(30)-C(29)	120.57(10)
C(32)-C(31)-C(30)	120.21(10)
C(31)-C(32)-C(33)	119.75(10)
C(32)-C(33)-C(34)	120.52(10)
C(33)-C(34)-C(29)	120.20(10)
C(40)-C(35)-C(36)	119.06(8)
C(40)-C(35)-P(1)	118.50(6)
C(36)-C(35)-P(1)	122.39(7)
C(37)-C(36)-C(35)	120.28(9)
C(38)-C(37)-C(36)	120.15(9)
C(39)-C(38)-C(37)	120.04(9)
C(38)-C(39)-C(40)	119.91(10)
C(39)-C(40)-C(35)	120.53(9)

---

Symmetry transformations used to generate equivalent atoms:

Table 3. Torsion angles [°] for **118e**.

---

C(35)-P(1)-C(1)-C(5)	-60.04(6)
C(29)-P(1)-C(1)-C(5)	-171.15(5)
B(1)-P(1)-C(1)-C(5)	63.87(7)
C(35)-P(1)-C(1)-C(2)	169.76(6)
C(29)-P(1)-C(1)-C(2)	58.64(6)
B(1)-P(1)-C(1)-C(2)	-66.34(8)
C(5)-C(1)-C(2)-O(2)	-58.36(9)
P(1)-C(1)-C(2)-O(2)	72.79(8)
C(5)-C(1)-C(2)-C(3)	64.66(9)
P(1)-C(1)-C(2)-C(3)	-164.19(5)
C(4)-O(1)-C(3)-C(2)	172.58(7)

Appendix: NMR spectra and X-ray structures

O(2)-C(2)-C(3)-O(1)	177.59(7)
C(1)-C(2)-C(3)-O(1)	52.13(9)
C(3)-O(1)-C(4)-C(11)	43.65(9)
C(3)-O(1)-C(4)-C(23)	165.63(7)
C(3)-O(1)-C(4)-C(17)	-80.90(8)
C(2)-C(1)-C(5)-C(10)	-99.71(9)
P(1)-C(1)-C(5)-C(10)	129.01(8)
C(2)-C(1)-C(5)-C(6)	76.62(11)
P(1)-C(1)-C(5)-C(6)	-54.65(11)
C(10)-C(5)-C(6)-C(7)	-0.23(16)
C(1)-C(5)-C(6)-C(7)	-176.57(10)
C(5)-C(6)-C(7)-C(8)	1.8(2)
C(6)-C(7)-C(8)-C(9)	-1.3(2)
C(7)-C(8)-C(9)-C(10)	-0.8(2)
C(8)-C(9)-C(10)-C(5)	2.38(19)
C(6)-C(5)-C(10)-C(9)	-1.84(16)
C(1)-C(5)-C(10)-C(9)	174.65(10)
O(1)-C(4)-C(11)-C(16)	-98.42(10)
C(23)-C(4)-C(11)-C(16)	145.64(9)
C(17)-C(4)-C(11)-C(16)	24.59(11)
O(1)-C(4)-C(11)-C(12)	73.92(9)
C(23)-C(4)-C(11)-C(12)	-42.02(12)
C(17)-C(4)-C(11)-C(12)	-163.07(8)
C(16)-C(11)-C(12)-C(13)	0.33(15)
C(4)-C(11)-C(12)-C(13)	-172.24(10)
C(11)-C(12)-C(13)-C(14)	0.12(18)
C(12)-C(13)-C(14)-C(15)	-0.70(19)
C(13)-C(14)-C(15)-C(16)	0.84(17)
C(12)-C(11)-C(16)-C(15)	-0.19(15)
C(4)-C(11)-C(16)-C(15)	172.28(9)
C(14)-C(15)-C(16)-C(11)	-0.40(16)
O(1)-C(4)-C(17)-C(18)	175.45(7)
C(11)-C(4)-C(17)-C(18)	53.08(10)
C(23)-C(4)-C(17)-C(18)	-72.29(9)
O(1)-C(4)-C(17)-C(22)	-8.77(10)
C(11)-C(4)-C(17)-C(22)	-131.14(8)
C(23)-C(4)-C(17)-C(22)	103.49(9)
C(22)-C(17)-C(18)-C(19)	0.76(13)



C(4)-C(17)-C(18)-C(19)	176.63(8)
C(17)-C(18)-C(19)-C(20)	0.43(14)
C(18)-C(19)-C(20)-C(21)	-0.75(15)
C(19)-C(20)-C(21)-C(22)	-0.11(15)
C(18)-C(17)-C(22)-C(21)	-1.62(13)
C(4)-C(17)-C(22)-C(21)	-177.44(8)
C(20)-C(21)-C(22)-C(17)	1.31(14)
O(1)-C(4)-C(23)-C(28)	31.79(12)
C(11)-C(4)-C(23)-C(28)	150.58(11)
C(17)-C(4)-C(23)-C(28)	-84.65(12)
O(1)-C(4)-C(23)-C(24)	-154.67(8)
C(11)-C(4)-C(23)-C(24)	-35.88(12)
C(17)-C(4)-C(23)-C(24)	88.89(10)
C(28)-C(23)-C(24)-C(25)	-0.81(16)
C(4)-C(23)-C(24)-C(25)	-174.44(9)
C(23)-C(24)-C(25)-C(26)	0.00(16)
C(24)-C(25)-C(26)-C(27)	0.4(2)
C(25)-C(26)-C(27)-C(28)	0.1(2)
C(24)-C(23)-C(28)-C(27)	1.3(2)
C(4)-C(23)-C(28)-C(27)	175.02(14)
C(26)-C(27)-C(28)-C(23)	-0.9(3)
C(35)-P(1)-C(29)-C(30)	-72.21(9)
C(1)-P(1)-C(29)-C(30)	34.01(8)
B(1)-P(1)-C(29)-C(30)	165.98(8)
C(35)-P(1)-C(29)-C(34)	106.67(8)
C(1)-P(1)-C(29)-C(34)	-147.12(7)
B(1)-P(1)-C(29)-C(34)	-15.14(9)
C(34)-C(29)-C(30)-C(31)	-1.79(14)
P(1)-C(29)-C(30)-C(31)	177.09(8)
C(29)-C(30)-C(31)-C(32)	-0.18(16)
C(30)-C(31)-C(32)-C(33)	1.73(17)
C(31)-C(32)-C(33)-C(34)	-1.27(17)
C(32)-C(33)-C(34)-C(29)	-0.73(16)
C(30)-C(29)-C(34)-C(33)	2.24(14)
P(1)-C(29)-C(34)-C(33)	-176.68(8)
C(29)-P(1)-C(35)-C(40)	-152.70(8)
C(1)-P(1)-C(35)-C(40)	99.15(8)
B(1)-P(1)-C(35)-C(40)	-31.53(9)

*Appendix: NMR spectra and X-ray structures*

---

C(29)-P(1)-C(35)-C(36)	29.80(9)
C(1)-P(1)-C(35)-C(36)	-78.35(8)
B(1)-P(1)-C(35)-C(36)	150.96(8)
C(40)-C(35)-C(36)-C(37)	1.67(15)
P(1)-C(35)-C(36)-C(37)	179.15(9)
C(35)-C(36)-C(37)-C(38)	-1.14(17)
C(36)-C(37)-C(38)-C(39)	-0.09(18)
C(37)-C(38)-C(39)-C(40)	0.77(18)
C(38)-C(39)-C(40)-C(35)	-0.23(17)
C(36)-C(35)-C(40)-C(39)	-0.98(16)
P(1)-C(35)-C(40)-C(39)	-178.57(9)

---

Symmetry transformations used to generate equivalent atoms:

### III. X-RAY STRUCTURE FOR 118f

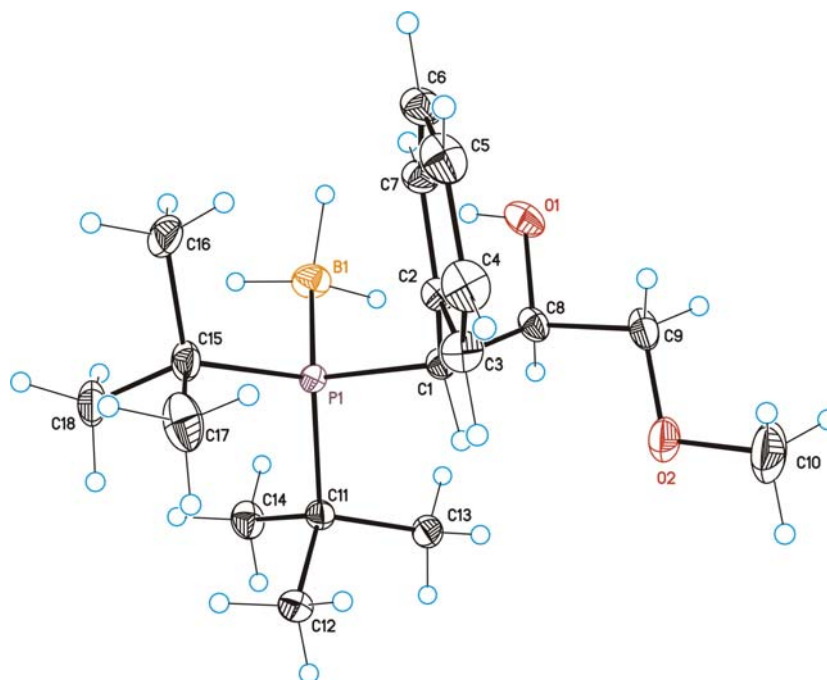


Table 1. Crystal data and structure refinement for **118f**.

Identification code	<b>118f</b>	
Empirical formula	$C_{18}H_{34}BO_2P$	
Formula weight	324.23	
Temperature	100(2) K	
Wavelength	0.71073 Å	
Crystal system	Monoclinic	
Space group	P2(1)	
Unit cell dimensions	$a = 8.6678(3)$ Å	$\alpha = 90^\circ$ .
	$b = 11.6108(5)$ Å	$\beta = 110.811(2)^\circ$ .
	$c = 10.4449(4)$ Å	$\gamma = 90^\circ$ .
Volume	$982.59(7)$ Å <sup>3</sup>	
Z	2	
Density (calculated)	$1.096$ Mg/m <sup>3</sup>	
Absorption coefficient	$0.144$ mm <sup>-1</sup>	
F(000)	356	
Crystal size	0.20 x 0.20 x 0.20 mm <sup>3</sup>	
Theta range for data collection	3.17 to 39.24°.	
Index ranges	-14 ≤ h ≤ 14, -13 ≤ k ≤ 20, -13 ≤ l ≤ 18	
Reflections collected	11836	

Independent reflections	7759 [R(int) = 0.0318]
Completeness to theta = 39.24°	85.3 %
Absorption correction	(SADABS, Bruker-Nonius)
Max. and min. transmission	0.9717 and 0.9717
Refinement method	Full-matrix least-squares on F <sup>2</sup>
Data / restraints / parameters	7759 / 1 / 219
Goodness-of-fit on F <sup>2</sup>	1.074
Final R indices [I > 2sigma(I)]	R1 = 0.0283, wR2 = 0.0753
R indices (all data)	R1 = 0.0290, wR2 = 0.0761
Absolute structure parameter	0.03(3)
Largest diff. peak and hole	0.424 and -0.169 e.Å <sup>-3</sup>

Table 2. Bond lengths [Å] and angles [°] for **118f**.

---

P(1)-C(1)	1.8809(5)
P(1)-C(15)	1.8854(7)
P(1)-C(11)	1.8896(7)
P(1)-B(1)	1.9349(9)
O(1)-C(8)	1.4161(10)
C(1)-C(2)	1.5171(7)
C(1)-C(8)	1.5597(9)
O(2)-C(9)	1.4122(12)
O(2)-C(10)	1.4161(10)
C(2)-C(7)	1.3938(10)
C(2)-C(3)	1.4009(9)
C(3)-C(4)	1.3944(9)
C(4)-C(5)	1.3867(14)
C(5)-C(6)	1.3922(12)
C(6)-C(7)	1.3969(9)
C(8)-C(9)	1.5225(9)
C(11)-C(12)	1.5298(11)
C(11)-C(13)	1.5364(10)
C(11)-C(14)	1.5425(8)
C(15)-C(17)	1.5332(13)
C(15)-C(16)	1.5338(13)
C(15)-C(18)	1.5401(9)

C(1)-P(1)-C(15)	110.99(3)
C(1)-P(1)-C(11)	104.62(3)
C(15)-P(1)-C(11)	110.41(3)
C(1)-P(1)-B(1)	111.31(3)
C(15)-P(1)-B(1)	109.83(4)
C(11)-P(1)-B(1)	109.57(3)
C(2)-C(1)-C(8)	110.14(5)
C(2)-C(1)-P(1)	117.72(4)
C(8)-C(1)-P(1)	112.02(4)
C(9)-O(2)-C(10)	112.03(8)
C(7)-C(2)-C(3)	118.65(5)
C(7)-C(2)-C(1)	123.22(5)
C(3)-C(2)-C(1)	117.99(6)
C(4)-C(3)-C(2)	120.62(8)
C(5)-C(4)-C(3)	120.25(7)
C(4)-C(5)-C(6)	119.64(6)
C(5)-C(6)-C(7)	120.16(8)
C(2)-C(7)-C(6)	120.63(6)
O(1)-C(8)-C(9)	104.73(6)
O(1)-C(8)-C(1)	114.85(6)
C(9)-C(8)-C(1)	110.53(5)
O(2)-C(9)-C(8)	108.61(6)
C(12)-C(11)-C(13)	108.32(6)
C(12)-C(11)-C(14)	109.96(6)
C(13)-C(11)-C(14)	106.12(5)
C(12)-C(11)-P(1)	113.30(4)
C(13)-C(11)-P(1)	109.24(5)
C(14)-C(11)-P(1)	109.63(5)
C(17)-C(15)-C(16)	109.67(7)
C(17)-C(15)-C(18)	108.70(8)
C(16)-C(15)-C(18)	106.28(7)
C(17)-C(15)-P(1)	115.15(6)
C(16)-C(15)-P(1)	108.32(6)
C(18)-C(15)-P(1)	108.35(5)

---

Symmetry transformations used to generate equivalent atoms:

Table 3. Torsion angles [°] for **118f**.

C(15)-P(1)-C(1)-C(2)	-24.10(6)
C(11)-P(1)-C(1)-C(2)	-143.19(5)
B(1)-P(1)-C(1)-C(2)	98.56(6)
C(15)-P(1)-C(1)-C(8)	-153.31(5)
C(11)-P(1)-C(1)-C(8)	87.61(5)
B(1)-P(1)-C(1)-C(8)	-30.64(6)
C(8)-C(1)-C(2)-C(7)	61.54(8)
P(1)-C(1)-C(2)-C(7)	-68.54(8)
C(8)-C(1)-C(2)-C(3)	-114.20(7)
P(1)-C(1)-C(2)-C(3)	115.72(6)
C(7)-C(2)-C(3)-C(4)	1.90(11)
C(1)-C(2)-C(3)-C(4)	177.83(6)
C(2)-C(3)-C(4)-C(5)	-0.17(11)
C(3)-C(4)-C(5)-C(6)	-1.20(12)
C(4)-C(5)-C(6)-C(7)	0.81(12)
C(3)-C(2)-C(7)-C(6)	-2.28(10)
C(1)-C(2)-C(7)-C(6)	-177.99(6)
C(5)-C(6)-C(7)-C(2)	0.95(11)
C(2)-C(1)-C(8)-O(1)	-62.43(6)
P(1)-C(1)-C(8)-O(1)	70.63(6)
C(2)-C(1)-C(8)-C(9)	55.78(7)
P(1)-C(1)-C(8)-C(9)	-171.16(5)
C(10)-O(2)-C(9)-C(8)	-174.92(8)
O(1)-C(8)-C(9)-O(2)	-177.10(6)
C(1)-C(8)-C(9)-O(2)	58.68(7)
C(1)-P(1)-C(11)-C(12)	74.24(5)
C(15)-P(1)-C(11)-C(12)	-45.24(6)
B(1)-P(1)-C(11)-C(12)	-166.33(5)
C(1)-P(1)-C(11)-C(13)	-46.61(5)
C(15)-P(1)-C(11)-C(13)	-166.09(4)
B(1)-P(1)-C(11)-C(13)	72.82(5)
C(1)-P(1)-C(11)-C(14)	-162.51(5)
C(15)-P(1)-C(11)-C(14)	78.01(6)
B(1)-P(1)-C(11)-C(14)	-43.08(6)
C(1)-P(1)-C(15)-C(17)	-43.16(7)
C(11)-P(1)-C(15)-C(17)	72.38(6)

B(1)-P(1)-C(15)-C(17)	-166.68(6)
C(1)-P(1)-C(15)-C(16)	80.01(6)
C(11)-P(1)-C(15)-C(16)	-164.45(5)
B(1)-P(1)-C(15)-C(16)	-43.51(6)
C(1)-P(1)-C(15)-C(18)	-165.10(6)
C(11)-P(1)-C(15)-C(18)	-49.55(7)
B(1)-P(1)-C(15)-C(18)	71.38(7)

---

Symmetry transformations used to generate equivalent atoms:

## IV. X-RAY STRUCTURE FOR 142a

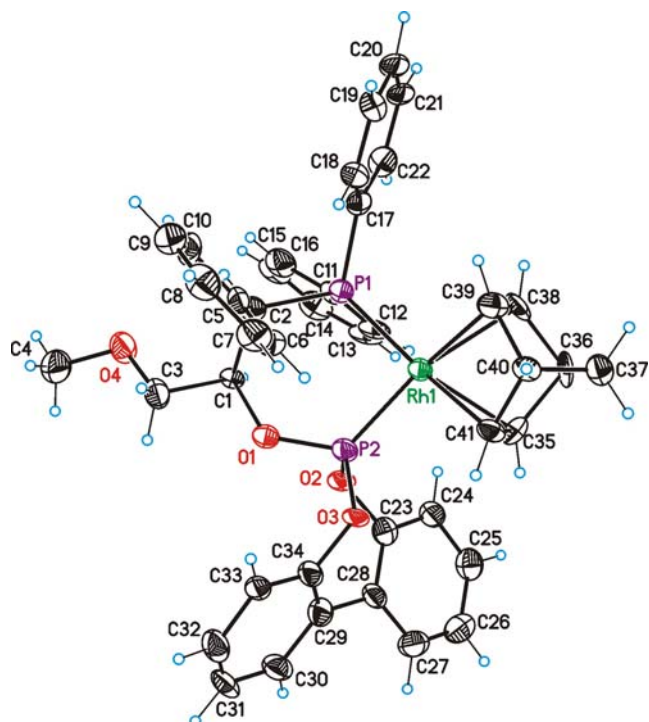


Table 1. Crystal data and structure refinement for **142a**.

Identification code	<b>142a</b>	
Empirical formula	$C_{41}H_{38}BF_4O_4P_2Rh$	
Formula weight	846.37	
Temperature	100(2) K	
Wavelength	0.71073 Å	
Crystal system	Orthorhombic	
Space group	P2(1)2(1)2(1)	
Unit cell dimensions	$a = 13.202(8)$ Å	$\alpha = 90^\circ$ .
	$b = 14.621(8)$ Å	$\beta = 90^\circ$ .
	$c = 19.929(15)$ Å	$\gamma = 90^\circ$ .
Volume	$3847(4)$ Å <sup>3</sup>	
Z	4	
Density (calculated)	$1.461$ Mg/m <sup>3</sup>	
Absorption coefficient	$0.587$ mm <sup>-1</sup>	
F(000)	1728	
Crystal size	$0.20 \times 0.02 \times 0.02$ mm <sup>3</sup>	
Theta range for data collection	2.56 to 26.03°.	
Index ranges	$-16 \leq h \leq 10$ , $-17 \leq k \leq 18$ , $-24 \leq l \leq 23$	



Reflections collected	32822
Independent reflections	7363 [R(int) = 0.1436]
Completeness to theta = 26.03°	96.8 %
Absorption correction	SADABS (Bruker-Nonius)
Max. and min. transmission	0.9912 and 0.8916
Refinement method	Full-matrix least-squares on F <sup>2</sup>
Data / restraints / parameters	7363 / 60 / 507
Goodness-of-fit on F <sup>2</sup>	1.056
Final R indices [I>2sigma(I)]	R1 = 0.0725, wR2 = 0.1649
R indices (all data)	R1 = 0.1081, wR2 = 0.1904
Absolute structure parameter	0.05(5)
Largest diff. peak and hole	2.338 and -1.909 e.Å <sup>-3</sup>

Table 2. Bond lengths [Å] and angles [°] for **142a**.

---

Rh(1)-C(41)	2.201(9)
Rh(1)-C(35)	2.207(7)
Rh(1)-P(2)	2.208(2)
Rh(1)-C(39)	2.249(8)
Rh(1)-C(38)	2.275(8)
Rh(1)-P(1)	2.298(2)
O(1)-C(1)	1.461(10)
O(1)-P(2)	1.600(6)
P(1)-C(17)	1.820(10)
P(1)-C(11)	1.835(9)
P(1)-C(2)	1.869(9)
C(1)-C(3)	1.531(11)
C(1)-C(2)	1.559(12)
P(2)-O(3)	1.600(6)
P(2)-O(2)	1.627(6)
O(2)-C(23)	1.414(10)
C(2)-C(5)	1.522(12)
O(3)-C(34)	1.418(11)
C(3)-O(4)	1.418(12)
O(4)-C(4)	1.418(11)
C(5)-C(10)	1.395(11)
C(5)-C(6)	1.403(14)

Appendix: NMR spectra and X-ray structures

C(6)-C(7)	1.390(13)
C(7)-C(8)	1.386(13)
C(8)-C(9)	1.388(16)
C(9)-C(10)	1.398(14)
C(11)-C(12)	1.378(12)
C(11)-C(16)	1.398(13)
C(12)-C(13)	1.399(14)
C(13)-C(14)	1.414(15)
C(14)-C(15)	1.371(15)
C(15)-C(16)	1.413(14)
C(17)-C(22)	1.389(14)
C(17)-C(18)	1.408(13)
C(18)-C(19)	1.374(14)
C(19)-C(20)	1.399(15)
C(20)-C(21)	1.379(14)
C(21)-C(22)	1.406(14)
C(23)-C(28)	1.398(13)
C(23)-C(24)	1.416(13)
C(24)-C(25)	1.404(13)
C(25)-C(26)	1.412(17)
C(26)-C(27)	1.368(16)
C(27)-C(28)	1.385(12)
C(28)-C(29)	1.494(13)
C(29)-C(34)	1.382(12)
C(29)-C(30)	1.412(14)
C(30)-C(31)	1.404(15)
C(31)-C(32)	1.373(14)
C(32)-C(33)	1.387(14)
C(33)-C(34)	1.406(14)
C(35)-C(41)	1.364(12)
C(35)-C(36)	1.558(13)
C(36)-C(37)	1.529(11)
C(36)-C(38)	1.536(13)
C(37)-C(40)	1.554(12)
C(38)-C(39)	1.353(14)
C(39)-C(40)	1.548(13)
C(40)-C(41)	1.535(11)
B(1)-F(1')	1.335(17)

B(1)-F(3)	1.352(17)
B(1)-F(4)	1.369(11)
B(1)-F(2)	1.38(3)
B(1)-F(2')	1.393(19)
B(1)-F(3')	1.481(16)
B(1)-F(1)	1.50(2)
C(41)-Rh(1)-C(35)	36.1(3)
C(41)-Rh(1)-P(2)	96.9(2)
C(35)-Rh(1)-P(2)	100.1(3)
C(41)-Rh(1)-C(39)	64.9(3)
C(35)-Rh(1)-C(39)	76.9(3)
P(2)-Rh(1)-C(39)	153.5(3)
C(41)-Rh(1)-C(38)	76.0(4)
C(35)-Rh(1)-C(38)	65.6(4)
P(2)-Rh(1)-C(38)	163.8(2)
C(39)-Rh(1)-C(38)	34.8(3)
C(41)-Rh(1)-P(1)	159.5(2)
C(35)-Rh(1)-P(1)	160.9(3)
P(2)-Rh(1)-P(1)	89.37(9)
C(39)-Rh(1)-P(1)	101.8(3)
C(38)-Rh(1)-P(1)	102.3(3)
C(1)-O(1)-P(2)	121.9(5)
C(17)-P(1)-C(11)	105.1(4)
C(17)-P(1)-C(2)	106.8(4)
C(11)-P(1)-C(2)	102.0(4)
C(17)-P(1)-Rh(1)	116.2(3)
C(11)-P(1)-Rh(1)	111.5(3)
C(2)-P(1)-Rh(1)	114.0(3)
O(1)-C(1)-C(3)	103.9(7)
O(1)-C(1)-C(2)	113.2(6)
C(3)-C(1)-C(2)	112.2(7)
O(3)-P(2)-O(1)	99.7(3)
O(3)-P(2)-O(2)	102.0(3)
O(1)-P(2)-O(2)	100.6(3)
O(3)-P(2)-Rh(1)	112.7(2)
O(1)-P(2)-Rh(1)	119.7(2)
O(2)-P(2)-Rh(1)	119.1(3)

Appendix: NMR spectra and X-ray structures

---

C(23)-O(2)-P(2)	119.3(5)
C(5)-C(2)-C(1)	114.9(7)
C(5)-C(2)-P(1)	114.3(6)
C(1)-C(2)-P(1)	108.3(5)
C(34)-O(3)-P(2)	118.7(5)
O(4)-C(3)-C(1)	106.8(8)
C(3)-O(4)-C(4)	111.3(8)
C(10)-C(5)-C(6)	118.0(8)
C(10)-C(5)-C(2)	119.1(8)
C(6)-C(5)-C(2)	122.9(7)
C(7)-C(6)-C(5)	120.9(8)
C(8)-C(7)-C(6)	120.5(9)
C(7)-C(8)-C(9)	119.4(9)
C(8)-C(9)-C(10)	120.1(8)
C(5)-C(10)-C(9)	121.0(9)
C(12)-C(11)-C(16)	120.2(8)
C(12)-C(11)-P(1)	118.6(7)
C(16)-C(11)-P(1)	121.0(7)
C(11)-C(12)-C(13)	120.8(9)
C(12)-C(13)-C(14)	119.7(9)
C(15)-C(14)-C(13)	119.0(9)
C(14)-C(15)-C(16)	121.6(10)
C(11)-C(16)-C(15)	118.8(9)
C(22)-C(17)-C(18)	118.4(9)
C(22)-C(17)-P(1)	120.0(7)
C(18)-C(17)-P(1)	121.4(8)
C(19)-C(18)-C(17)	120.9(10)
C(18)-C(19)-C(20)	119.7(9)
C(21)-C(20)-C(19)	120.9(9)
C(20)-C(21)-C(22)	118.7(10)
C(17)-C(22)-C(21)	121.3(9)
C(28)-C(23)-O(2)	119.7(7)
C(28)-C(23)-C(24)	123.6(8)
O(2)-C(23)-C(24)	116.5(9)
C(25)-C(24)-C(23)	116.3(10)
C(24)-C(25)-C(26)	120.5(9)
C(27)-C(26)-C(25)	120.5(9)
C(26)-C(27)-C(28)	121.7(11)

C(27)-C(28)-C(23)	117.4(9)
C(27)-C(28)-C(29)	122.2(10)
C(23)-C(28)-C(29)	120.4(8)
C(34)-C(29)-C(30)	117.7(9)
C(34)-C(29)-C(28)	121.4(8)
C(30)-C(29)-C(28)	120.9(8)
C(31)-C(30)-C(29)	119.4(9)
C(32)-C(31)-C(30)	120.8(9)
C(31)-C(32)-C(33)	121.5(9)
C(32)-C(33)-C(34)	117.0(9)
C(29)-C(34)-C(33)	123.6(8)
C(29)-C(34)-O(3)	118.6(8)
C(33)-C(34)-O(3)	117.8(7)
C(41)-C(35)-C(36)	104.4(7)
C(41)-C(35)-Rh(1)	71.7(5)
C(36)-C(35)-Rh(1)	96.4(5)
C(37)-C(36)-C(38)	100.4(7)
C(37)-C(36)-C(35)	101.3(7)
C(38)-C(36)-C(35)	103.4(6)
C(36)-C(37)-C(40)	93.0(6)
C(39)-C(38)-C(36)	106.3(9)
C(39)-C(38)-Rh(1)	71.6(5)
C(36)-C(38)-Rh(1)	94.4(5)
C(38)-C(39)-C(40)	107.0(7)
C(38)-C(39)-Rh(1)	73.6(5)
C(40)-C(39)-Rh(1)	95.4(5)
C(41)-C(40)-C(39)	101.6(6)
C(41)-C(40)-C(37)	99.8(6)
C(39)-C(40)-C(37)	99.5(7)
C(35)-C(41)-C(40)	108.4(8)
C(35)-C(41)-Rh(1)	72.2(5)
C(40)-C(41)-Rh(1)	97.8(6)
F(1')-B(1)-F(3)	78.0(12)
F(1')-B(1)-F(4)	112.4(10)
F(3)-B(1)-F(4)	118.2(10)
F(1')-B(1)-F(2)	127.2(13)
F(3)-B(1)-F(2)	107.5(14)
F(4)-B(1)-F(2)	110.1(13)

F(1')-B(1)-F(2')	113.6(10)
F(3)-B(1)-F(2')	115.7(12)
F(4)-B(1)-F(2')	114.0(10)
F(2)-B(1)-F(2')	16.1(11)
F(1')-B(1)-F(3')	108.2(12)
F(3)-B(1)-F(3')	30.9(8)
F(4)-B(1)-F(3')	99.8(9)
F(2)-B(1)-F(3')	93.7(13)
F(2')-B(1)-F(3')	107.8(11)
F(1')-B(1)-F(1)	28.3(8)
F(3)-B(1)-F(1)	105.8(13)
F(4)-B(1)-F(1)	103.1(10)
F(2)-B(1)-F(1)	112.0(13)
F(2')-B(1)-F(1)	96.0(11)
F(3')-B(1)-F(1)	136.4(13)

---

Symmetry transformations used to generate equivalent atoms:

Table 3. Torsion angles [°] for **142a**.

---

C(41)-Rh(1)-P(1)-C(17)	55.6(8)
C(35)-Rh(1)-P(1)-C(17)	-76.1(8)
P(2)-Rh(1)-P(1)-C(17)	163.9(3)
C(39)-Rh(1)-P(1)-C(17)	8.1(4)
C(38)-Rh(1)-P(1)-C(17)	-27.5(4)
C(41)-Rh(1)-P(1)-C(11)	176.0(7)
C(35)-Rh(1)-P(1)-C(11)	44.4(8)
P(2)-Rh(1)-P(1)-C(11)	-75.7(3)
C(39)-Rh(1)-P(1)-C(11)	128.5(4)
C(38)-Rh(1)-P(1)-C(11)	92.9(4)
C(41)-Rh(1)-P(1)-C(2)	-69.3(8)
C(35)-Rh(1)-P(1)-C(2)	159.1(8)
P(2)-Rh(1)-P(1)-C(2)	39.1(3)
C(39)-Rh(1)-P(1)-C(2)	-116.7(4)
C(38)-Rh(1)-P(1)-C(2)	-152.3(4)
P(2)-O(1)-C(1)-C(3)	167.4(5)
P(2)-O(1)-C(1)-C(2)	-70.6(8)

C(1)-O(1)-P(2)-O(3)	176.9(5)
C(1)-O(1)-P(2)-O(2)	-78.8(6)
C(1)-O(1)-P(2)-Rh(1)	53.7(6)
C(41)-Rh(1)-P(2)-O(3)	9.6(3)
C(35)-Rh(1)-P(2)-O(3)	45.9(3)
C(39)-Rh(1)-P(2)-O(3)	-34.9(6)
C(38)-Rh(1)-P(2)-O(3)	72.7(10)
P(1)-Rh(1)-P(2)-O(3)	-150.8(2)
C(41)-Rh(1)-P(2)-O(1)	126.2(4)
C(35)-Rh(1)-P(2)-O(1)	162.5(4)
C(39)-Rh(1)-P(2)-O(1)	81.7(6)
C(38)-Rh(1)-P(2)-O(1)	-170.8(10)
P(1)-Rh(1)-P(2)-O(1)	-34.3(3)
C(41)-Rh(1)-P(2)-O(2)	-109.9(3)
C(35)-Rh(1)-P(2)-O(2)	-73.5(4)
C(39)-Rh(1)-P(2)-O(2)	-154.3(6)
C(38)-Rh(1)-P(2)-O(2)	-46.8(10)
P(1)-Rh(1)-P(2)-O(2)	89.7(3)
O(3)-P(2)-O(2)-C(23)	-41.0(7)
O(1)-P(2)-O(2)-C(23)	-143.4(6)
Rh(1)-P(2)-O(2)-C(23)	83.8(7)
O(1)-C(1)-C(2)-C(5)	-58.5(9)
C(3)-C(1)-C(2)-C(5)	58.7(10)
O(1)-C(1)-C(2)-P(1)	70.7(7)
C(3)-C(1)-C(2)-P(1)	-172.1(6)
C(17)-P(1)-C(2)-C(5)	-61.1(7)
C(11)-P(1)-C(2)-C(5)	-171.1(7)
Rh(1)-P(1)-C(2)-C(5)	68.7(7)
C(17)-P(1)-C(2)-C(1)	169.4(6)
C(11)-P(1)-C(2)-C(1)	59.4(7)
Rh(1)-P(1)-C(2)-C(1)	-60.8(6)
O(1)-P(2)-O(3)-C(34)	52.4(6)
O(2)-P(2)-O(3)-C(34)	-50.7(6)
Rh(1)-P(2)-O(3)-C(34)	-179.7(5)
O(1)-C(1)-C(3)-O(4)	-168.1(6)
C(2)-C(1)-C(3)-O(4)	69.2(9)
C(1)-C(3)-O(4)-C(4)	166.7(7)
C(1)-C(2)-C(5)-C(10)	-115.9(9)

Appendix: NMR spectra and X-ray structures

P(1)-C(2)-C(5)-C(10)	118.0(7)
C(1)-C(2)-C(5)-C(6)	62.1(10)
P(1)-C(2)-C(5)-C(6)	-64.1(10)
C(10)-C(5)-C(6)-C(7)	0.3(13)
C(2)-C(5)-C(6)-C(7)	-177.6(8)
C(5)-C(6)-C(7)-C(8)	-0.1(14)
C(6)-C(7)-C(8)-C(9)	-0.1(14)
C(7)-C(8)-C(9)-C(10)	0.1(15)
C(6)-C(5)-C(10)-C(9)	-0.3(13)
C(2)-C(5)-C(10)-C(9)	177.7(8)
C(8)-C(9)-C(10)-C(5)	0.1(14)
C(17)-P(1)-C(11)-C(12)	118.2(7)
C(2)-P(1)-C(11)-C(12)	-130.5(7)
Rh(1)-P(1)-C(11)-C(12)	-8.5(8)
C(17)-P(1)-C(11)-C(16)	-67.4(8)
C(2)-P(1)-C(11)-C(16)	43.8(9)
Rh(1)-P(1)-C(11)-C(16)	165.8(7)
C(16)-C(11)-C(12)-C(13)	1.6(13)
P(1)-C(11)-C(12)-C(13)	175.9(7)
C(11)-C(12)-C(13)-C(14)	-2.6(14)
C(12)-C(13)-C(14)-C(15)	2.7(15)
C(13)-C(14)-C(15)-C(16)	-1.9(16)
C(12)-C(11)-C(16)-C(15)	-0.7(14)
P(1)-C(11)-C(16)-C(15)	-174.9(8)
C(14)-C(15)-C(16)-C(11)	0.8(15)
C(11)-P(1)-C(17)-C(22)	-20.5(8)
C(2)-P(1)-C(17)-C(22)	-128.3(7)
Rh(1)-P(1)-C(17)-C(22)	103.3(7)
C(11)-P(1)-C(17)-C(18)	165.8(7)
C(2)-P(1)-C(17)-C(18)	58.0(8)
Rh(1)-P(1)-C(17)-C(18)	-70.4(7)
C(22)-C(17)-C(18)-C(19)	2.0(12)
P(1)-C(17)-C(18)-C(19)	175.8(7)
C(17)-C(18)-C(19)-C(20)	1.1(13)
C(18)-C(19)-C(20)-C(21)	-4.0(14)
C(19)-C(20)-C(21)-C(22)	3.7(13)
C(18)-C(17)-C(22)-C(21)	-2.3(13)
P(1)-C(17)-C(22)-C(21)	-176.2(7)



C(20)-C(21)-C(22)-C(17)	-0.5(13)
P(2)-O(2)-C(23)-C(28)	75.1(8)
P(2)-O(2)-C(23)-C(24)	-111.0(7)
C(28)-C(23)-C(24)-C(25)	-0.4(12)
O(2)-C(23)-C(24)-C(25)	-174.0(7)
C(23)-C(24)-C(25)-C(26)	1.4(12)
C(24)-C(25)-C(26)-C(27)	-1.5(14)
C(25)-C(26)-C(27)-C(28)	0.5(13)
C(26)-C(27)-C(28)-C(23)	0.5(12)
C(26)-C(27)-C(28)-C(29)	179.6(8)
O(2)-C(23)-C(28)-C(27)	172.9(7)
C(24)-C(23)-C(28)-C(27)	-0.6(11)
O(2)-C(23)-C(28)-C(29)	-6.3(11)
C(24)-C(23)-C(28)-C(29)	-179.7(7)
C(27)-C(28)-C(29)-C(34)	135.5(9)
C(23)-C(28)-C(29)-C(34)	-45.4(12)
C(27)-C(28)-C(29)-C(30)	-43.4(13)
C(23)-C(28)-C(29)-C(30)	135.7(9)
C(34)-C(29)-C(30)-C(31)	-0.3(14)
C(28)-C(29)-C(30)-C(31)	178.7(9)
C(29)-C(30)-C(31)-C(32)	-0.8(15)
C(30)-C(31)-C(32)-C(33)	2.0(15)
C(31)-C(32)-C(33)-C(34)	-1.9(14)
C(30)-C(29)-C(34)-C(33)	0.3(14)
C(28)-C(29)-C(34)-C(33)	-178.6(9)
C(30)-C(29)-C(34)-O(3)	178.4(8)
C(28)-C(29)-C(34)-O(3)	-0.6(13)
C(32)-C(33)-C(34)-C(29)	0.8(14)
C(32)-C(33)-C(34)-O(3)	-177.3(8)
P(2)-O(3)-C(34)-C(29)	76.7(9)
P(2)-O(3)-C(34)-C(33)	-105.1(8)
P(2)-Rh(1)-C(35)-C(41)	-88.0(5)
C(39)-Rh(1)-C(35)-C(41)	65.1(5)
C(38)-Rh(1)-C(35)-C(41)	100.0(6)
P(1)-Rh(1)-C(35)-C(41)	153.6(6)
C(41)-Rh(1)-C(35)-C(36)	-103.1(7)
P(2)-Rh(1)-C(35)-C(36)	169.0(4)
C(39)-Rh(1)-C(35)-C(36)	-38.0(5)

C(38)-Rh(1)-C(35)-C(36)	-3.1(5)
P(1)-Rh(1)-C(35)-C(36)	50.5(10)
C(41)-C(35)-C(36)-C(37)	35.2(8)
Rh(1)-C(35)-C(36)-C(37)	108.0(6)
C(41)-C(35)-C(36)-C(38)	-68.5(8)
Rh(1)-C(35)-C(36)-C(38)	4.3(6)
C(38)-C(36)-C(37)-C(40)	53.3(7)
C(35)-C(36)-C(37)-C(40)	-52.7(7)
C(37)-C(36)-C(38)-C(39)	-36.4(8)
C(35)-C(36)-C(38)-C(39)	67.9(8)
C(37)-C(36)-C(38)-Rh(1)	-108.5(6)
C(35)-C(36)-C(38)-Rh(1)	-4.1(6)
C(41)-Rh(1)-C(38)-C(39)	-65.9(6)
C(35)-Rh(1)-C(38)-C(39)	-102.6(7)
P(2)-Rh(1)-C(38)-C(39)	-131.7(8)
P(1)-Rh(1)-C(38)-C(39)	93.1(6)
C(41)-Rh(1)-C(38)-C(36)	39.8(5)
C(35)-Rh(1)-C(38)-C(36)	3.1(5)
P(2)-Rh(1)-C(38)-C(36)	-26.0(13)
C(39)-Rh(1)-C(38)-C(36)	105.7(8)
P(1)-Rh(1)-C(38)-C(36)	-161.2(5)
C(36)-C(38)-C(39)-C(40)	1.5(9)
Rh(1)-C(38)-C(39)-C(40)	90.7(6)
C(36)-C(38)-C(39)-Rh(1)	-89.2(6)
C(41)-Rh(1)-C(39)-C(38)	102.0(6)
C(35)-Rh(1)-C(39)-C(38)	65.8(6)
P(2)-Rh(1)-C(39)-C(38)	152.1(5)
P(1)-Rh(1)-C(39)-C(38)	-94.6(6)
C(41)-Rh(1)-C(39)-C(40)	-4.2(5)
C(35)-Rh(1)-C(39)-C(40)	-40.3(5)
P(2)-Rh(1)-C(39)-C(40)	46.0(8)
C(38)-Rh(1)-C(39)-C(40)	-106.2(7)
P(1)-Rh(1)-C(39)-C(40)	159.2(4)
C(38)-C(39)-C(40)-C(41)	-68.9(8)
Rh(1)-C(39)-C(40)-C(41)	5.6(6)
C(38)-C(39)-C(40)-C(37)	33.2(8)
Rh(1)-C(39)-C(40)-C(37)	107.7(5)
C(36)-C(37)-C(40)-C(41)	51.7(8)

C(36)-C(37)-C(40)-C(39)	-51.9(7)
C(36)-C(35)-C(41)-C(40)	-0.3(9)
Rh(1)-C(35)-C(41)-C(40)	-92.5(6)
C(36)-C(35)-C(41)-Rh(1)	92.1(6)
C(39)-C(40)-C(41)-C(35)	68.1(8)
C(37)-C(40)-C(41)-C(35)	-33.9(9)
C(39)-C(40)-C(41)-Rh(1)	-5.7(6)
C(37)-C(40)-C(41)-Rh(1)	-107.6(6)
P(2)-Rh(1)-C(41)-C(35)	97.6(5)
C(39)-Rh(1)-C(41)-C(35)	-102.6(6)
C(38)-Rh(1)-C(41)-C(35)	-67.5(6)
P(1)-Rh(1)-C(41)-C(35)	-155.4(6)
C(35)-Rh(1)-C(41)-C(40)	106.9(7)
P(2)-Rh(1)-C(41)-C(40)	-155.5(5)
C(39)-Rh(1)-C(41)-C(40)	4.3(5)
C(38)-Rh(1)-C(41)-C(40)	39.4(5)
P(1)-Rh(1)-C(41)-C(40)	-48.5(10)

---

Symmetry transformations used to generate equivalent atoms:

## V. X-RAY STRUCTURE FOR 142h

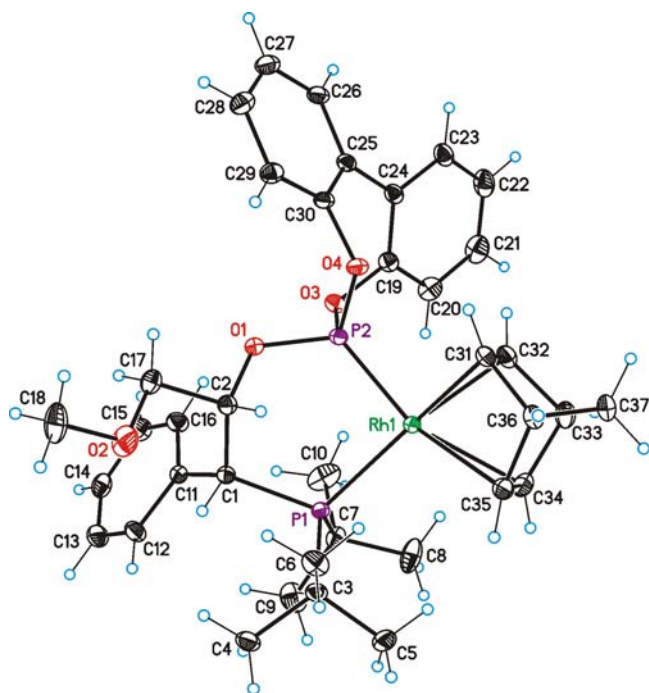


Table 1. Crystal data and structure refinement for **142h**.

Identification code	<b>142h</b>	
Empirical formula	$C_{37}H_{46}BF_4O_4P_2Rh$	
Formula weight	806.40	
Temperature	100(2) K	
Wavelength	0.71073 Å	
Crystal system	Orthorhombic	
Space group	P2(1)2(1)2(1)	
Unit cell dimensions	a = 12.5453(4) Å	$\alpha = 90^\circ$ .
	b = 13.1054(4) Å	$\beta = 90^\circ$ .
	c = 21.6798(7) Å	$\gamma = 90^\circ$ .
Volume	3564.40(19) Å <sup>3</sup>	
Z	4	
Density (calculated)	1.503 Mg/m <sup>3</sup>	
Absorption coefficient	0.629 mm <sup>-1</sup>	
F(000)	1664	
Crystal size	0.40 x 0.06 x 0.05 mm <sup>3</sup>	
Theta range for data collection	3.22 to 38.09°.	
Index ranges	-19 ≤ h ≤ 21, -22 ≤ k ≤ 10, -37 ≤ l ≤ 36	
Reflections collected	62932	

Independent reflections	19217 [R(int) = 0.0281]
Completeness to theta = 38.09°	98.5 %
Absorption correction	SADABS (Bruker-Nonius)
Max. and min. transmission	0.9692 and 0.7869
Refinement method	Full-matrix least-squares on F <sup>2</sup>
Data / restraints / parameters	19217 / 0 / 477
Goodness-of-fit on F <sup>2</sup>	1.030
Final R indices [I>2sigma(I)]	R1 = 0.0261, wR2 = 0.0615
R indices (all data)	R1 = 0.0285, wR2 = 0.0626
Absolute structure parameter	-0.008(9)
Largest diff. peak and hole	1.546 and -0.515 e.Å <sup>-3</sup>

Table 2. Bond lengths [Å] and angles [°] for **142h**.

Rh(1)-C(31)	2.1759(11)
Rh(1)-C(32)	2.1783(10)
Rh(1)-P(2)	2.1882(3)
Rh(1)-C(34)	2.3450(11)
Rh(1)-C(35)	2.3541(12)
Rh(1)-P(1)	2.4105(3)
P(1)-C(3)	1.8947(11)
P(1)-C(7)	1.8981(12)
P(1)-C(1)	1.9059(10)
C(1)-C(11)	1.5162(16)
C(1)-C(2)	1.5337(15)
O(1)-C(2)	1.4498(13)
O(1)-P(2)	1.5938(8)
P(2)-O(4)	1.6086(8)
P(2)-O(3)	1.6111(9)
C(2)-C(17)	1.5203(15)
O(2)-C(17)	1.4129(16)
O(2)-C(18)	1.4259(16)
C(3)-C(5)	1.5390(16)
C(3)-C(6)	1.5391(18)
C(3)-C(4)	1.5432(15)
O(3)-C(19)	1.4060(13)
O(4)-C(30)	1.4060(12)

Appendix: NMR spectra and X-ray structures

C(7)-C(9)	1.5329(18)
C(7)-C(10)	1.5330(19)
C(7)-C(8)	1.5371(17)
C(11)-C(12)	1.3983(15)
C(11)-C(16)	1.4000(16)
C(12)-C(13)	1.3917(19)
C(13)-C(14)	1.386(2)
C(14)-C(15)	1.3916(18)
C(15)-C(16)	1.3866(19)
C(19)-C(20)	1.3893(17)
C(19)-C(24)	1.4005(15)
C(20)-C(21)	1.3861(19)
C(21)-C(22)	1.390(2)
C(22)-C(23)	1.395(2)
C(23)-C(24)	1.4042(15)
C(24)-C(25)	1.4836(16)
C(25)-C(30)	1.3966(16)
C(25)-C(26)	1.4068(15)
C(26)-C(27)	1.3914(18)
C(27)-C(28)	1.3927(19)
C(28)-C(29)	1.3944(16)
C(29)-C(30)	1.3869(15)
C(31)-C(32)	1.3925(17)
C(31)-C(36)	1.5342(17)
C(32)-C(33)	1.5420(17)
C(33)-C(34)	1.5391(17)
C(33)-C(37)	1.5468(19)
C(34)-C(35)	1.3644(18)
C(35)-C(36)	1.5375(16)
C(36)-C(37)	1.5500(15)
F(1)-B(1)	1.371(2)
B(1)-F(4')	1.249(7)
B(1)-F(3)	1.292(5)
B(1)-F(2)	1.364(6)
B(1)-F(2')	1.406(9)
B(1)-F(4)	1.470(5)
B(1)-F(3')	1.573(7)

C(31)-Rh(1)-C(32)	37.30(4)
C(31)-Rh(1)-P(2)	93.00(3)
C(32)-Rh(1)-P(2)	93.55(3)
C(31)-Rh(1)-C(34)	75.31(4)
C(32)-Rh(1)-C(34)	64.17(4)
P(2)-Rh(1)-C(34)	155.70(3)
C(31)-Rh(1)-C(35)	63.94(4)
C(32)-Rh(1)-C(35)	75.52(4)
P(2)-Rh(1)-C(35)	154.02(3)
C(34)-Rh(1)-C(35)	33.76(4)
C(31)-Rh(1)-P(1)	157.91(3)
C(32)-Rh(1)-P(1)	163.58(3)
P(2)-Rh(1)-P(1)	91.330(10)
C(34)-Rh(1)-P(1)	107.57(3)
C(35)-Rh(1)-P(1)	105.82(3)
C(3)-P(1)-C(7)	111.68(5)
C(3)-P(1)-C(1)	98.74(5)
C(7)-P(1)-C(1)	112.11(5)
C(3)-P(1)-Rh(1)	112.95(4)
C(7)-P(1)-Rh(1)	108.43(4)
C(1)-P(1)-Rh(1)	112.77(3)
C(11)-C(1)-C(2)	115.94(9)
C(11)-C(1)-P(1)	119.17(8)
C(2)-C(1)-P(1)	109.51(7)
C(2)-O(1)-P(2)	116.78(7)
O(1)-P(2)-O(4)	105.12(4)
O(1)-P(2)-O(3)	94.80(5)
O(4)-P(2)-O(3)	101.48(4)
O(1)-P(2)-Rh(1)	120.86(3)
O(4)-P(2)-Rh(1)	109.75(3)
O(3)-P(2)-Rh(1)	121.98(3)
O(1)-C(2)-C(17)	106.75(9)
O(1)-C(2)-C(1)	111.44(9)
C(17)-C(2)-C(1)	113.06(9)
C(17)-O(2)-C(18)	113.16(11)
C(5)-C(3)-C(6)	109.94(10)
C(5)-C(3)-C(4)	107.82(9)
C(6)-C(3)-C(4)	107.02(9)

C(5)-C(3)-P(1)	109.92(8)
C(6)-C(3)-P(1)	106.59(7)
C(4)-C(3)-P(1)	115.47(8)
C(19)-O(3)-P(2)	119.77(8)
C(30)-O(4)-P(2)	121.43(8)
C(9)-C(7)-C(10)	109.84(13)
C(9)-C(7)-C(8)	108.14(11)
C(10)-C(7)-C(8)	105.64(12)
C(9)-C(7)-P(1)	115.23(9)
C(10)-C(7)-P(1)	109.20(8)
C(8)-C(7)-P(1)	108.34(9)
C(12)-C(11)-C(16)	117.34(11)
C(12)-C(11)-C(1)	117.97(10)
C(16)-C(11)-C(1)	124.68(10)
C(13)-C(12)-C(11)	121.71(12)
C(14)-C(13)-C(12)	120.00(11)
C(13)-C(14)-C(15)	119.01(12)
C(16)-C(15)-C(14)	120.83(12)
C(15)-C(16)-C(11)	120.94(11)
O(2)-C(17)-C(2)	105.18(9)
C(20)-C(19)-C(24)	122.62(10)
C(20)-C(19)-O(3)	117.68(10)
C(24)-C(19)-O(3)	119.60(10)
C(21)-C(20)-C(19)	119.10(12)
C(20)-C(21)-C(22)	120.16(12)
C(21)-C(22)-C(23)	120.03(11)
C(22)-C(23)-C(24)	121.27(12)
C(19)-C(24)-C(23)	116.80(11)
C(19)-C(24)-C(25)	121.74(9)
C(23)-C(24)-C(25)	121.44(10)
C(30)-C(25)-C(26)	116.81(10)
C(30)-C(25)-C(24)	121.82(9)
C(26)-C(25)-C(24)	121.33(10)
C(27)-C(26)-C(25)	121.20(11)
C(26)-C(27)-C(28)	120.09(11)
C(27)-C(28)-C(29)	120.12(11)
C(30)-C(29)-C(28)	118.65(11)
C(29)-C(30)-C(25)	123.08(9)



C(29)-C(30)-O(4)	117.50(10)
C(25)-C(30)-O(4)	119.26(9)
C(32)-C(31)-C(36)	106.63(9)
C(32)-C(31)-Rh(1)	71.44(7)
C(36)-C(31)-Rh(1)	100.03(7)
C(31)-C(32)-C(33)	106.16(10)
C(31)-C(32)-Rh(1)	71.26(6)
C(33)-C(32)-Rh(1)	99.67(7)
C(34)-C(33)-C(32)	102.73(8)
C(34)-C(33)-C(37)	99.84(10)
C(32)-C(33)-C(37)	99.52(10)
C(35)-C(34)-C(33)	107.17(10)
C(35)-C(34)-Rh(1)	73.49(7)
C(33)-C(34)-Rh(1)	93.04(7)
C(34)-C(35)-C(36)	106.71(10)
C(34)-C(35)-Rh(1)	72.75(7)
C(36)-C(35)-Rh(1)	92.74(7)
C(31)-C(36)-C(35)	102.96(9)
C(31)-C(36)-C(37)	99.62(9)
C(35)-C(36)-C(37)	99.93(9)
C(33)-C(37)-C(36)	93.78(9)
F(4')-B(1)-F(3)	82.5(6)
F(4')-B(1)-F(2)	120.7(4)
F(3)-B(1)-F(2)	102.1(4)
F(4')-B(1)-F(1)	119.3(6)
F(3)-B(1)-F(1)	120.5(5)
F(2)-B(1)-F(1)	108.7(3)
F(4')-B(1)-F(2')	109.6(6)
F(3)-B(1)-F(2')	112.1(8)
F(2)-B(1)-F(2')	15.0(8)
F(1)-B(1)-F(2')	110.2(4)
F(4')-B(1)-F(4)	23.9(7)
F(3)-B(1)-F(4)	106.1(3)
F(2)-B(1)-F(4)	117.1(4)
F(1)-B(1)-F(4)	103.1(2)
F(2')-B(1)-F(4)	102.8(7)
F(4')-B(1)-F(3')	105.4(5)
F(3)-B(1)-F(3')	28.5(2)

*Appendix: NMR spectra and X-ray structures*

---

F(2)-B(1)-F(3')	103.7(3)
F(1)-B(1)-F(3')	94.1(4)
F(2')-B(1)-F(3')	117.9(7)
F(4)-B(1)-F(3')	126.7(4)

---

Symmetry transformations used to generate equivalent atoms:

Table 3. Torsion angles [°] for **142h**.

---

C(31)-Rh(1)-P(1)-C(3)	-35.51(9)
C(32)-Rh(1)-P(1)-C(3)	115.86(12)
P(2)-Rh(1)-P(1)-C(3)	-136.82(4)
C(34)-Rh(1)-P(1)-C(3)	58.68(5)
C(35)-Rh(1)-P(1)-C(3)	23.43(5)
C(31)-Rh(1)-P(1)-C(7)	-159.84(8)
C(32)-Rh(1)-P(1)-C(7)	-8.47(12)
P(2)-Rh(1)-P(1)-C(7)	98.85(4)
C(34)-Rh(1)-P(1)-C(7)	-65.65(5)
C(35)-Rh(1)-P(1)-C(7)	-100.90(5)
C(31)-Rh(1)-P(1)-C(1)	75.40(9)
C(32)-Rh(1)-P(1)-C(1)	-133.24(12)
P(2)-Rh(1)-P(1)-C(1)	-25.92(4)
C(34)-Rh(1)-P(1)-C(1)	169.58(5)
C(35)-Rh(1)-P(1)-C(1)	134.33(5)
C(3)-P(1)-C(1)-C(11)	-117.01(8)
C(7)-P(1)-C(1)-C(11)	0.76(9)
Rh(1)-P(1)-C(1)-C(11)	123.49(7)
C(3)-P(1)-C(1)-C(2)	106.17(8)
C(7)-P(1)-C(1)-C(2)	-136.06(8)
Rh(1)-P(1)-C(1)-C(2)	-13.33(9)
C(2)-O(1)-P(2)-O(4)	-104.04(8)
C(2)-O(1)-P(2)-O(3)	152.68(8)
C(2)-O(1)-P(2)-Rh(1)	20.66(10)
C(31)-Rh(1)-P(2)-O(1)	-132.76(5)
C(32)-Rh(1)-P(2)-O(1)	-170.12(6)
C(34)-Rh(1)-P(2)-O(1)	167.32(8)
C(35)-Rh(1)-P(2)-O(1)	-106.52(8)
P(1)-Rh(1)-P(2)-O(1)	25.57(4)
C(31)-Rh(1)-P(2)-O(4)	-10.25(4)
C(32)-Rh(1)-P(2)-O(4)	-47.61(5)
C(34)-Rh(1)-P(2)-O(4)	-70.17(8)
C(35)-Rh(1)-P(2)-O(4)	15.99(7)
P(1)-Rh(1)-P(2)-O(4)	148.08(3)
C(31)-Rh(1)-P(2)-O(3)	108.02(5)
C(32)-Rh(1)-P(2)-O(3)	70.66(5)

Appendix: NMR spectra and X-ray structures

---

C(34)-Rh(1)-P(2)-O(3)	48.10(9)
C(35)-Rh(1)-P(2)-O(3)	134.26(7)
P(1)-Rh(1)-P(2)-O(3)	-93.65(4)
P(2)-O(1)-C(2)-C(17)	150.55(8)
P(2)-O(1)-C(2)-C(1)	-85.56(10)
C(11)-C(1)-C(2)-O(1)	-63.10(11)
P(1)-C(1)-C(2)-O(1)	75.26(10)
C(11)-C(1)-C(2)-C(17)	57.14(13)
P(1)-C(1)-C(2)-C(17)	-164.50(8)
C(7)-P(1)-C(3)-C(5)	51.92(9)
C(1)-P(1)-C(3)-C(5)	170.02(8)
Rh(1)-P(1)-C(3)-C(5)	-70.61(8)
C(7)-P(1)-C(3)-C(6)	171.02(7)
C(1)-P(1)-C(3)-C(6)	-70.88(8)
Rh(1)-P(1)-C(3)-C(6)	48.49(8)
C(7)-P(1)-C(3)-C(4)	-70.29(9)
C(1)-P(1)-C(3)-C(4)	47.81(9)
Rh(1)-P(1)-C(3)-C(4)	167.18(7)
O(1)-P(2)-O(3)-C(19)	155.86(8)
O(4)-P(2)-O(3)-C(19)	49.36(9)
Rh(1)-P(2)-O(3)-C(19)	-72.89(8)
O(1)-P(2)-O(4)-C(30)	-56.54(9)
O(3)-P(2)-O(4)-C(30)	41.70(8)
Rh(1)-P(2)-O(4)-C(30)	172.04(7)
C(3)-P(1)-C(7)-C(9)	44.46(11)
C(1)-P(1)-C(7)-C(9)	-65.31(11)
Rh(1)-P(1)-C(7)-C(9)	169.54(9)
C(3)-P(1)-C(7)-C(10)	168.60(9)
C(1)-P(1)-C(7)-C(10)	58.84(10)
Rh(1)-P(1)-C(7)-C(10)	-66.31(10)
C(3)-P(1)-C(7)-C(8)	-76.80(10)
C(1)-P(1)-C(7)-C(8)	173.43(9)
Rh(1)-P(1)-C(7)-C(8)	48.28(10)
C(2)-C(1)-C(11)-C(12)	-132.98(10)
P(1)-C(1)-C(11)-C(12)	92.85(11)
C(2)-C(1)-C(11)-C(16)	48.09(15)
P(1)-C(1)-C(11)-C(16)	-86.08(12)
C(16)-C(11)-C(12)-C(13)	3.99(18)

C(1)-C(11)-C(12)-C(13)	-175.02(11)
C(11)-C(12)-C(13)-C(14)	-0.7(2)
C(12)-C(13)-C(14)-C(15)	-2.38(19)
C(13)-C(14)-C(15)-C(16)	1.99(19)
C(14)-C(15)-C(16)-C(11)	1.5(2)
C(12)-C(11)-C(16)-C(15)	-4.36(18)
C(1)-C(11)-C(16)-C(15)	174.58(11)
C(18)-O(2)-C(17)-C(2)	168.16(12)
O(1)-C(2)-C(17)-O(2)	-177.06(11)
C(1)-C(2)-C(17)-O(2)	60.06(14)
P(2)-O(3)-C(19)-C(20)	107.71(12)
P(2)-O(3)-C(19)-C(24)	-75.84(13)
C(24)-C(19)-C(20)-C(21)	-0.9(2)
O(3)-C(19)-C(20)-C(21)	175.42(12)
C(19)-C(20)-C(21)-C(22)	-0.6(2)
C(20)-C(21)-C(22)-C(23)	1.4(2)
C(21)-C(22)-C(23)-C(24)	-0.7(2)
C(20)-C(19)-C(24)-C(23)	1.53(18)
O(3)-C(19)-C(24)-C(23)	-174.73(11)
C(20)-C(19)-C(24)-C(25)	179.97(12)
O(3)-C(19)-C(24)-C(25)	3.71(18)
C(22)-C(23)-C(24)-C(19)	-0.70(19)
C(22)-C(23)-C(24)-C(25)	-179.14(12)
C(19)-C(24)-C(25)-C(30)	39.57(17)
C(23)-C(24)-C(25)-C(30)	-142.07(12)
C(19)-C(24)-C(25)-C(26)	-138.28(12)
C(23)-C(24)-C(25)-C(26)	40.08(17)
C(30)-C(25)-C(26)-C(27)	-1.87(17)
C(24)-C(25)-C(26)-C(27)	176.09(11)
C(25)-C(26)-C(27)-C(28)	-0.12(19)
C(26)-C(27)-C(28)-C(29)	1.7(2)
C(27)-C(28)-C(29)-C(30)	-1.11(19)
C(28)-C(29)-C(30)-C(25)	-1.00(18)
C(28)-C(29)-C(30)-O(4)	174.33(11)
C(26)-C(25)-C(30)-C(29)	2.46(17)
C(24)-C(25)-C(30)-C(29)	-175.49(11)
C(26)-C(25)-C(30)-O(4)	-172.80(10)
C(24)-C(25)-C(30)-O(4)	9.26(16)

Appendix: NMR spectra and X-ray structures

---

P(2)-O(4)-C(30)-C(29)	108.12(10)
P(2)-O(4)-C(30)-C(25)	-76.36(11)
P(2)-Rh(1)-C(31)-C(32)	-91.92(6)
C(34)-Rh(1)-C(31)-C(32)	66.48(7)
C(35)-Rh(1)-C(31)-C(32)	100.53(7)
P(1)-Rh(1)-C(31)-C(32)	167.08(6)
C(32)-Rh(1)-C(31)-C(36)	-104.32(9)
P(2)-Rh(1)-C(31)-C(36)	163.76(6)
C(34)-Rh(1)-C(31)-C(36)	-37.84(7)
C(35)-Rh(1)-C(31)-C(36)	-3.79(6)
P(1)-Rh(1)-C(31)-C(36)	62.76(11)
C(36)-C(31)-C(32)-C(33)	0.29(11)
Rh(1)-C(31)-C(32)-C(33)	-94.96(8)
C(36)-C(31)-C(32)-Rh(1)	95.25(7)
P(2)-Rh(1)-C(32)-C(31)	90.29(6)
C(34)-Rh(1)-C(32)-C(31)	-99.81(8)
C(35)-Rh(1)-C(32)-C(31)	-65.81(7)
P(1)-Rh(1)-C(32)-C(31)	-162.70(9)
C(31)-Rh(1)-C(32)-C(33)	103.90(10)
P(2)-Rh(1)-C(32)-C(33)	-165.81(7)
C(34)-Rh(1)-C(32)-C(33)	4.09(7)
C(35)-Rh(1)-C(32)-C(33)	38.10(7)
P(1)-Rh(1)-C(32)-C(33)	-58.80(15)
C(31)-C(32)-C(33)-C(34)	67.39(11)
Rh(1)-C(32)-C(33)-C(34)	-5.75(10)
C(31)-C(32)-C(33)-C(37)	-35.06(11)
Rh(1)-C(32)-C(33)-C(37)	-108.20(8)
C(32)-C(33)-C(34)-C(35)	-68.38(12)
C(37)-C(33)-C(34)-C(35)	33.82(11)
C(32)-C(33)-C(34)-Rh(1)	5.28(9)
C(37)-C(33)-C(34)-Rh(1)	107.47(7)
C(31)-Rh(1)-C(34)-C(35)	64.85(7)
C(32)-Rh(1)-C(34)-C(35)	102.97(8)
P(2)-Rh(1)-C(34)-C(35)	128.14(8)
P(1)-Rh(1)-C(34)-C(35)	-92.34(7)
C(31)-Rh(1)-C(34)-C(33)	-42.17(7)
C(32)-Rh(1)-C(34)-C(33)	-4.04(7)
P(2)-Rh(1)-C(34)-C(33)	21.13(13)

C(35)-Rh(1)-C(34)-C(33)	-107.01(10)
P(1)-Rh(1)-C(34)-C(33)	160.65(6)
C(33)-C(34)-C(35)-C(36)	0.42(12)
Rh(1)-C(34)-C(35)-C(36)	-87.65(8)
C(33)-C(34)-C(35)-Rh(1)	88.07(8)
C(31)-Rh(1)-C(35)-C(34)	-102.92(8)
C(32)-Rh(1)-C(35)-C(34)	-64.94(7)
P(2)-Rh(1)-C(35)-C(34)	-132.36(7)
P(1)-Rh(1)-C(35)-C(34)	98.09(7)
C(31)-Rh(1)-C(35)-C(36)	3.73(6)
C(32)-Rh(1)-C(35)-C(36)	41.70(7)
P(2)-Rh(1)-C(35)-C(36)	-25.71(11)
C(34)-Rh(1)-C(35)-C(36)	106.65(9)
P(1)-Rh(1)-C(35)-C(36)	-155.26(6)
C(32)-C(31)-C(36)-C(35)	-68.12(10)
Rh(1)-C(31)-C(36)-C(35)	5.35(9)
C(32)-C(31)-C(36)-C(37)	34.50(11)
Rh(1)-C(31)-C(36)-C(37)	107.97(8)
C(34)-C(35)-C(36)-C(31)	67.94(11)
Rh(1)-C(35)-C(36)-C(31)	-4.87(8)
C(34)-C(35)-C(36)-C(37)	-34.44(12)
Rh(1)-C(35)-C(36)-C(37)	-107.25(8)
C(34)-C(33)-C(37)-C(36)	-51.56(10)
C(32)-C(33)-C(37)-C(36)	53.26(9)
C(31)-C(36)-C(37)-C(33)	-53.15(10)
C(35)-C(36)-C(37)-C(33)	51.95(10)

---

Symmetry transformations used to generate equivalent atoms:

## VI. X-RAY STRUCTURE FOR THE OPTICAL RESOLUTION OF (*rac*)-191

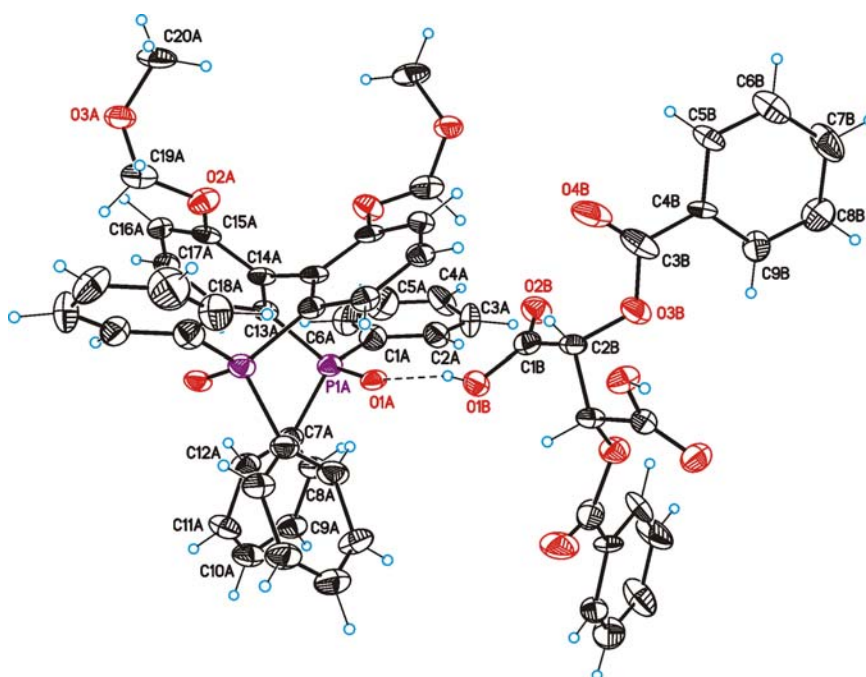


Table 1. Crystal data and structure refinement for (*R*)-**191**/(-)-DBTA.

Identification code	( <i>R</i> )- <b>191</b> /(-)-DBTA	
Empirical formula	C <sub>58</sub> H <sub>50</sub> O <sub>14</sub> P <sub>2</sub>	
Formula weight	1032.92	
Temperature	100(2) K	
Wavelength	0.71073 Å	
Crystal system	Orthorhombic	
Space group	P222(1)	
Unit cell dimensions	a = 9.6105(4) Å	α = 90°.
	b = 13.8851(5) Å	β = 90°.
	c = 19.0997(9) Å	γ = 90°.
Volume	2548.72(18) Å <sup>3</sup>	
Z	2	
Density (calculated)	1.346 Mg/m <sup>3</sup>	
Absorption coefficient	0.155 mm <sup>-1</sup>	
F(000)	1080	
Crystal size	0.40 x 0.20 x 0.05 mm <sup>3</sup>	
Theta range for data collection	2.79 to 25.74°.	
Index ranges	-11 ≤ h ≤ 10, -16 ≤ k ≤ 16, -19 ≤ l ≤ 22	



Reflections collected	13797
Independent reflections	4346 [R(int) = 0.0452]
Completeness to theta = 25.74°	90.4 %
Absorption correction	SADABS (Bruker-Nonius)
Refinement method	Full-matrix least-squares on F <sup>2</sup>
Data / restraints / parameters	4346 / 24 / 439
Goodness-of-fit on F <sup>2</sup>	1.218
Final R indices [I>2sigma(I)]	R1 = 0.0678, wR2 = 0.1717
R indices (all data)	R1 = 0.0742, wR2 = 0.1752
Absolute structure parameter	0.1(2)
Largest diff. peak and hole	0.647 and -0.339 e.Å <sup>-3</sup>

Table 2. Bond lengths [Å] and angles [°] for (*R*)-**191**/(-)-DBTA.

P(1A)-O(1A)	1.476(4)
P(1A)-C(1A)	1.798(6)
P(1A)-C(13A)	1.803(5)
P(1A)-C(7A)	1.841(5)
C(1A)-C(2A)	1.378(15)
C(1A)-C(6X)	1.39(2)
C(1A)-C(6A)	1.40(2)
C(1A)-C(2X)	1.418(16)
O(2A)-C(15A)	1.379(6)
O(2A)-C(19A)	1.403(7)
O(3A)-C(19A)	1.407(7)
O(3A)-C(20A)	1.425(6)
C(2A)-C(3A)	1.386(18)
C(3A)-C(4A)	1.37(3)
C(4A)-C(5A)	1.37(4)
C(5A)-C(6A)	1.26(4)
C(2X)-C(3X)	1.35(2)
C(3X)-C(4X)	1.40(3)
C(4X)-C(5X)	1.39(4)
C(5X)-C(6X)	1.44(3)
C(7A)-C(12A)	1.360(7)
C(7A)-C(8A)	1.383(7)
C(8A)-C(9A)	1.398(7)

C(9A)-C(10A)	1.362(8)
C(10A)-C(11A)	1.357(8)
C(11A)-C(12A)	1.414(7)
C(13A)-C(18A)	1.390(7)
C(13A)-C(14A)	1.422(7)
C(14A)-C(15A)	1.409(7)
C(14A)-C(14A)#1	1.470(11)
C(15A)-C(16A)	1.371(8)
C(16A)-C(17A)	1.397(7)
C(17A)-C(18A)	1.392(7)
C(1B)-O(2B)	1.201(6)
C(1B)-O(1B)	1.319(6)
C(1B)-C(2B)	1.508(8)
C(2B)-O(3B)	1.428(6)
C(2B)-C(2B)#2	1.522(9)
O(3B)-C(3B)	1.394(7)
C(3B)-O(4B)	1.183(7)
C(3B)-C(4B)	1.407(16)
C(3B)-C(4')	1.611(19)
C(4B)-C(9B)	1.369(17)
C(4B)-C(5B)	1.417(17)
C(5B)-C(6B)	1.364(18)
C(6B)-C(7B)	1.381(19)
C(7B)-C(8B)	1.440(17)
C(8B)-C(9B)	1.386(17)
C(4')-C(9')	1.33(2)
C(4')-C(5')	1.43(2)
C(5')-C(6')	1.38(2)
C(6')-C(7')	1.38(3)
C(7')-C(8')	1.39(2)
C(8')-C(9')	1.37(2)
O(1A)-P(1A)-C(1A)	110.8(2)
O(1A)-P(1A)-C(13A)	114.2(2)
C(1A)-P(1A)-C(13A)	110.7(2)
O(1A)-P(1A)-C(7A)	109.8(2)
C(1A)-P(1A)-C(7A)	106.1(2)
C(13A)-P(1A)-C(7A)	104.9(2)

C(2A)-C(1A)-C(6X)	113.2(11)
C(2A)-C(1A)-C(6A)	113.0(12)
C(6X)-C(1A)-C(6A)	15.3(11)
C(2A)-C(1A)-C(2X)	23.9(5)
C(6X)-C(1A)-C(2X)	121.7(12)
C(6A)-C(1A)-C(2X)	114.8(12)
C(2A)-C(1A)-P(1A)	121.7(7)
C(6X)-C(1A)-P(1A)	123.5(9)
C(6A)-C(1A)-P(1A)	125.3(10)
C(2X)-C(1A)-P(1A)	114.0(8)
C(15A)-O(2A)-C(19A)	117.4(4)
C(19A)-O(3A)-C(20A)	113.3(5)
C(1A)-C(2A)-C(3A)	125.2(13)
C(4A)-C(3A)-C(2A)	120.2(14)
C(5A)-C(4A)-C(3A)	109(2)
C(6A)-C(5A)-C(4A)	135(3)
C(5A)-C(6A)-C(1A)	117(2)
C(3X)-C(2X)-C(1A)	118.5(14)
C(2X)-C(3X)-C(4X)	119.3(16)
C(5X)-C(4X)-C(3X)	125.5(19)
C(4X)-C(5X)-C(6X)	114(2)
C(1A)-C(6X)-C(5X)	120.7(19)
C(12A)-C(7A)-C(8A)	121.8(4)
C(12A)-C(7A)-P(1A)	117.2(4)
C(8A)-C(7A)-P(1A)	120.2(4)
C(7A)-C(8A)-C(9A)	118.8(5)
C(10A)-C(9A)-C(8A)	119.9(5)
C(11A)-C(10A)-C(9A)	120.7(5)
C(10A)-C(11A)-C(12A)	120.7(5)
C(7A)-C(12A)-C(11A)	118.0(5)
C(18A)-C(13A)-C(14A)	120.5(5)
C(18A)-C(13A)-P(1A)	118.2(4)
C(14A)-C(13A)-P(1A)	121.2(4)
C(15A)-C(14A)-C(13A)	116.5(5)
C(15A)-C(14A)-C(14A)#1	117.9(5)
C(13A)-C(14A)-C(14A)#1	125.3(5)
C(16A)-C(15A)-O(2A)	123.5(4)
C(16A)-C(15A)-C(14A)	123.1(5)

O(2A)-C(15A)-C(14A)	113.4(5)
C(15A)-C(16A)-C(17A)	119.3(4)
C(18A)-C(17A)-C(16A)	119.7(5)
C(13A)-C(18A)-C(17A)	120.8(5)
O(2A)-C(19A)-O(3A)	113.2(4)
O(2B)-C(1B)-O(1B)	126.3(6)
O(2B)-C(1B)-C(2B)	124.8(5)
O(1B)-C(1B)-C(2B)	108.8(4)
O(3B)-C(2B)-C(1B)	111.9(4)
O(3B)-C(2B)-C(2B)#21	107.1(4)
C(1B)-C(2B)-C(2B)#21	112.0(5)
C(3B)-O(3B)-C(2B)	114.4(4)
O(4B)-C(3B)-O(3B)	122.8(5)
O(4B)-C(3B)-C(4B)	120.4(8)
O(3B)-C(3B)-C(4B)	116.6(8)
O(4B)-C(3B)-C(4')	136.1(8)
O(3B)-C(3B)-C(4')	100.0(8)
C(4B)-C(3B)-C(4')	21.8(5)
C(9B)-C(4B)-C(3B)	118.7(11)
C(9B)-C(4B)-C(5B)	120.7(13)
C(3B)-C(4B)-C(5B)	120.6(12)
C(6B)-C(5B)-C(4B)	119.1(14)
C(5B)-C(6B)-C(7B)	122.4(12)
C(6B)-C(7B)-C(8B)	117.6(11)
C(9B)-C(8B)-C(7B)	120.3(11)
C(4B)-C(9B)-C(8B)	119.8(13)
C(9')-C(4')-C(5')	119.2(15)
C(9')-C(4')-C(3B)	131.4(13)
C(5')-C(4')-C(3B)	109.3(13)
C(6')-C(5')-C(4')	119.0(15)
C(7')-C(6')-C(5')	120.9(13)
C(6')-C(7')-C(8')	118.2(14)
C(9')-C(8')-C(7')	121.1(16)
C(4')-C(9')-C(8')	121.5(15)

---

Symmetry transformations used to generate equivalent atoms:

#1 x,-y,-z+2 #2 -x+1,y,-z+5/2

Table 3. Torsion angles [°] for (*R*)-**191**/(-)-DBTA.

O(1A)-P(1A)-C(1A)-C(2A)	4.2(12)
C(13A)-P(1A)-C(1A)-C(2A)	131.8(12)
C(7A)-P(1A)-C(1A)-C(2A)	-114.9(12)
O(1A)-P(1A)-C(1A)-C(6X)	-160.3(12)
C(13A)-P(1A)-C(1A)-C(6X)	-32.7(12)
C(7A)-P(1A)-C(1A)-C(6X)	80.6(12)
O(1A)-P(1A)-C(1A)-C(6A)	-178.8(12)
C(13A)-P(1A)-C(1A)-C(6A)	-51.1(13)
C(7A)-P(1A)-C(1A)-C(6A)	62.2(13)
O(1A)-P(1A)-C(1A)-C(2X)	29.9(11)
C(13A)-P(1A)-C(1A)-C(2X)	157.5(10)
C(7A)-P(1A)-C(1A)-C(2X)	-89.2(10)
C(6X)-C(1A)-C(2A)-C(3A)	-19.9(18)
C(6A)-C(1A)-C(2A)-C(3A)	-3.3(18)
C(2X)-C(1A)-C(2A)-C(3A)	96(3)
P(1A)-C(1A)-C(2A)-C(3A)	174.1(11)
C(1A)-C(2A)-C(3A)-C(4A)	8(2)
C(2A)-C(3A)-C(4A)-C(5A)	-5(3)
C(3A)-C(4A)-C(5A)-C(6A)	-2(5)
C(4A)-C(5A)-C(6A)-C(1A)	7(6)
C(2A)-C(1A)-C(6A)-C(5A)	-3(3)
C(6X)-C(1A)-C(6A)-C(5A)	91(7)
C(2X)-C(1A)-C(6A)-C(5A)	-29(3)
P(1A)-C(1A)-C(6A)-C(5A)	179(2)
C(2A)-C(1A)-C(2X)-C(3X)	-76(3)
C(6X)-C(1A)-C(2X)-C(3X)	-0.6(18)
C(6A)-C(1A)-C(2X)-C(3X)	14.9(17)
P(1A)-C(1A)-C(2X)-C(3X)	169.4(10)
C(1A)-C(2X)-C(3X)-C(4X)	-3(2)
C(2X)-C(3X)-C(4X)-C(5X)	3(3)
C(3X)-C(4X)-C(5X)-C(6X)	0(4)
C(2A)-C(1A)-C(6X)-C(5X)	29(3)
C(6A)-C(1A)-C(6X)-C(5X)	-63(6)
C(2X)-C(1A)-C(6X)-C(5X)	4(3)
P(1A)-C(1A)-C(6X)-C(5X)	-165(2)
C(4X)-C(5X)-C(6X)-C(1A)	-4(4)

O(1A)-P(1A)-C(7A)-C(12A)	69.5(5)
C(1A)-P(1A)-C(7A)-C(12A)	-170.8(4)
C(13A)-P(1A)-C(7A)-C(12A)	-53.6(5)
O(1A)-P(1A)-C(7A)-C(8A)	-100.2(5)
C(1A)-P(1A)-C(7A)-C(8A)	19.5(5)
C(13A)-P(1A)-C(7A)-C(8A)	136.7(4)
C(12A)-C(7A)-C(8A)-C(9A)	-2.2(9)
P(1A)-C(7A)-C(8A)-C(9A)	167.1(4)
C(7A)-C(8A)-C(9A)-C(10A)	1.2(9)
C(8A)-C(9A)-C(10A)-C(11A)	-0.6(9)
C(9A)-C(10A)-C(11A)-C(12A)	1.0(10)
C(8A)-C(7A)-C(12A)-C(11A)	2.5(9)
P(1A)-C(7A)-C(12A)-C(11A)	-167.1(5)
C(10A)-C(11A)-C(12A)-C(7A)	-1.9(9)
O(1A)-P(1A)-C(13A)-C(18A)	-168.6(3)
C(1A)-P(1A)-C(13A)-C(18A)	65.6(5)
C(7A)-P(1A)-C(13A)-C(18A)	-48.3(4)
O(1A)-P(1A)-C(13A)-C(14A)	8.7(4)
C(1A)-P(1A)-C(13A)-C(14A)	-117.1(4)
C(7A)-P(1A)-C(13A)-C(14A)	129.0(4)
C(18A)-C(13A)-C(14A)-C(15A)	-1.1(6)
P(1A)-C(13A)-C(14A)-C(15A)	-178.3(3)
C(18A)-C(13A)-C(14A)-C(14A)#1	-175.2(4)
P(1A)-C(13A)-C(14A)-C(14A)#1	7.5(6)
C(19A)-O(2A)-C(15A)-C(16A)	21.0(6)
C(19A)-O(2A)-C(15A)-C(14A)	-158.5(4)
C(13A)-C(14A)-C(15A)-C(16A)	-1.0(6)
C(14A)#1-C(14A)-C(15A)-C(16A)	173.5(4)
C(13A)-C(14A)-C(15A)-O(2A)	178.5(4)
C(14A)#1-C(14A)-C(15A)-O(2A)	-6.9(6)
O(2A)-C(15A)-C(16A)-C(17A)	-177.7(4)
C(14A)-C(15A)-C(16A)-C(17A)	1.8(7)
C(15A)-C(16A)-C(17A)-C(18A)	-0.4(6)
C(14A)-C(13A)-C(18A)-C(17A)	2.5(7)
P(1A)-C(13A)-C(18A)-C(17A)	179.8(3)
C(16A)-C(17A)-C(18A)-C(13A)	-1.7(7)
C(15A)-O(2A)-C(19A)-O(3A)	-77.1(5)
C(20A)-O(3A)-C(19A)-O(2A)	-72.7(6)

O(2B)-C(1B)-C(2B)-O(3B)	-11.4(6)
O(1B)-C(1B)-C(2B)-O(3B)	170.2(4)
O(2B)-C(1B)-C(2B)-C(2B)#2	-131.8(4)
O(1B)-C(1B)-C(2B)-C(2B)#2	49.8(4)
C(1B)-C(2B)-O(3B)-C(3B)	99.0(5)
C(2B)#2-C(2B)-O(3B)-C(3B)	-137.8(5)
C(2B)-O(3B)-C(3B)-O(4B)	-9.1(8)
C(2B)-O(3B)-C(3B)-C(4B)	176.0(8)
C(2B)-O(3B)-C(3B)-C(4')	161.0(7)
O(4B)-C(3B)-C(4B)-C(9B)	176.9(11)
O(3B)-C(3B)-C(4B)-C(9B)	-8.0(16)
C(4')-C(3B)-C(4B)-C(9B)	35(2)
O(4B)-C(3B)-C(4B)-C(5B)	-3.3(17)
O(3B)-C(3B)-C(4B)-C(5B)	171.8(10)
C(4')-C(3B)-C(4B)-C(5B)	-145(4)
C(9B)-C(4B)-C(5B)-C(6B)	-3(2)
C(3B)-C(4B)-C(5B)-C(6B)	176.9(14)
C(4B)-C(5B)-C(6B)-C(7B)	4(2)
C(5B)-C(6B)-C(7B)-C(8B)	-3(3)
C(6B)-C(7B)-C(8B)-C(9B)	1(3)
C(3B)-C(4B)-C(9B)-C(8B)	-178.5(14)
C(5B)-C(4B)-C(9B)-C(8B)	2(2)
C(7B)-C(8B)-C(9B)-C(4B)	-1(2)
O(4B)-C(3B)-C(4')-C(9')	155.3(17)
O(3B)-C(3B)-C(4')-C(9')	-13(2)
C(4B)-C(3B)-C(4')-C(9')	-154(4)
O(4B)-C(3B)-C(4')-C(5')	-20.5(19)
O(3B)-C(3B)-C(4')-C(5')	171.6(11)
C(4B)-C(3B)-C(4')-C(5')	30(2)
C(9')-C(4')-C(5')-C(6')	1(3)
C(3B)-C(4')-C(5')-C(6')	177.1(14)
C(4')-C(5')-C(6')-C(7')	-3(3)
C(5')-C(6')-C(7')-C(8')	4(3)
C(6')-C(7')-C(8')-C(9')	-3(3)
C(5')-C(4')-C(9')-C(8')	1(3)
C(3B)-C(4')-C(9')-C(8')	-174.8(16)
C(7')-C(8')-C(9')-C(4')	0(3)

---

Symmetry transformations used to generate equivalent atoms:

#1  $x, -y, -z+2$  #2  $-x+1, y, -z+5/2$



## VII. X-RAY STRUCTURE FOR (*R*)-191

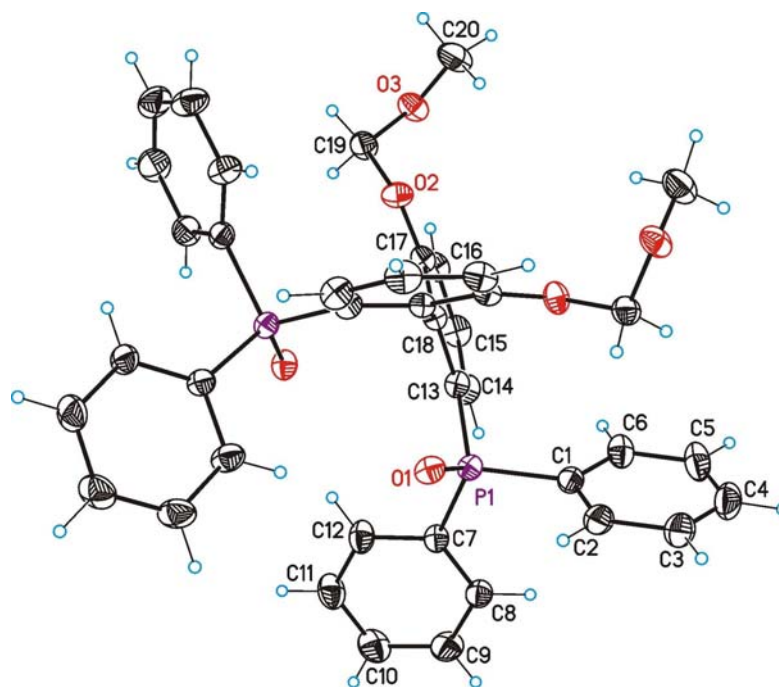


Table 1. Crystal data and structure refinement for (*R*)-191.

Identification code	<b>(<i>R</i>)-191</b>	
Empirical formula	<b>C<sub>40</sub>H<sub>36</sub>O<sub>6</sub>P<sub>2</sub></b>	
Formula weight	674.63	
Temperature	100(2) K	
Wavelength	0.71073 Å	
Crystal system	Orthorhombic	
Space group	Fdd2	
Unit cell dimensions	a = 26.0369(5) Å	α = 90°.
	b = 28.0120(6) Å	β = 90°.
	c = 9.3934(2) Å	γ = 90°.
Volume	6851.0(2) Å <sup>3</sup>	
Z	8	
Density (calculated)	1.308 Mg/m <sup>3</sup>	
Absorption coefficient	0.175 mm <sup>-1</sup>	
F(000)	2832	
Crystal size	0.40 x 0.30 x 0.20 mm <sup>3</sup>	
Theta range for data collection	3.28 to 39.88°.	
Index ranges	-45 ≤ h ≤ 46, -50 ≤ k ≤ 13, -10 ≤ l ≤ 16	
Reflections collected	27433	

Independent reflections	8116 [R(int) = 0.0226]
Completeness to theta = 39.88°	90.3 %
Absorption correction	SADABS (Bruker-Nonius)
Max. and min. transmission	0.9659 and 0.9333
Refinement method	Full-matrix least-squares on F <sup>2</sup>
Data / restraints / parameters	8116 / 1 / 218
Goodness-of-fit on F <sup>2</sup>	1.054
Final R indices [I > 2sigma(I)]	R1 = 0.0360, wR2 = 0.0960
R indices (all data)	R1 = 0.0401, wR2 = 0.0987
Absolute structure parameter	-0.05(4)
Largest diff. peak and hole	0.373 and -0.220 e.Å <sup>-3</sup>

Table 2. Bond lengths [Å] and angles [°] for (*R*)-**191**.

P(1)-O(1)	1.4846(6)
P(1)-C(7)	1.8052(9)
P(1)-C(13)	1.8065(9)
P(1)-C(1)	1.8075(9)
C(1)-C(6)	1.3964(15)
C(1)-C(2)	1.4009(13)
C(2)-C(3)	1.3992(17)
O(2)-C(17)	1.3722(11)
O(2)-C(19)	1.4168(11)
C(3)-C(4)	1.381(2)
O(3)-C(19)	1.3879(14)
O(3)-C(20)	1.4229(16)
C(4)-C(5)	1.395(2)
C(5)-C(6)	1.3920(15)
C(7)-C(8)	1.3933(12)
C(7)-C(12)	1.3991(13)
C(8)-C(9)	1.3914(16)
C(9)-C(10)	1.3907(19)
C(10)-C(11)	1.3947(18)
C(11)-C(12)	1.3902(17)
C(13)-C(18)	1.3945(11)
C(13)-C(14)	1.3991(10)
C(14)-C(15)	1.3848(14)

C(15)-C(16)	1.3849(15)
C(16)-C(17)	1.3903(10)
C(17)-C(18)	1.3975(11)
C(18)-C(18)#1	1.4879(13)
O(1)-P(1)-C(7)	111.01(5)
O(1)-P(1)-C(13)	115.53(4)
C(7)-P(1)-C(13)	103.77(4)
O(1)-P(1)-C(1)	111.18(4)
C(7)-P(1)-C(1)	108.29(4)
C(13)-P(1)-C(1)	106.57(4)
C(6)-C(1)-C(2)	119.57(9)
C(6)-C(1)-P(1)	123.70(7)
C(2)-C(1)-P(1)	116.66(8)
C(3)-C(2)-C(1)	119.87(12)
C(17)-O(2)-C(19)	117.09(7)
C(4)-C(3)-C(2)	120.07(11)
C(19)-O(3)-C(20)	111.98(8)
C(3)-C(4)-C(5)	120.43(11)
C(6)-C(5)-C(4)	119.81(12)
C(5)-C(6)-C(1)	120.23(10)
C(8)-C(7)-C(12)	120.01(9)
C(8)-C(7)-P(1)	124.44(7)
C(12)-C(7)-P(1)	115.39(7)
C(9)-C(8)-C(7)	119.88(10)
C(10)-C(9)-C(8)	120.12(10)
C(9)-C(10)-C(11)	120.07(11)
C(12)-C(11)-C(10)	119.99(11)
C(11)-C(12)-C(7)	119.84(9)
C(18)-C(13)-C(14)	120.20(8)
C(18)-C(13)-P(1)	120.97(5)
C(14)-C(13)-P(1)	118.76(7)
C(15)-C(14)-C(13)	120.28(9)
C(14)-C(15)-C(16)	120.06(7)
C(15)-C(16)-C(17)	119.63(8)
O(2)-C(17)-C(16)	123.91(8)
O(2)-C(17)-C(18)	114.91(6)
C(16)-C(17)-C(18)	121.18(8)

*Appendix: NMR spectra and X-ray structures*

---

C(13)-C(18)-C(17) 118.54(6)

C(13)-C(18)-C(18)#1123.05(7)

C(17)-C(18)-C(18)#1118.40(7)

O(3)-C(19)-O(2) 112.89(9)

---

Symmetry transformations used to generate equivalent atoms:

#1 -x+1/2,-y+1/2,z

Table 3. Torsion angles [°].for (*R*)-**191**

---

O(1)-P(1)-C(1)-C(6)	-152.75(8)
C(7)-P(1)-C(1)-C(6)	85.04(9)
C(13)-P(1)-C(1)-C(6)	-26.06(9)
O(1)-P(1)-C(1)-C(2)	24.19(10)
C(7)-P(1)-C(1)-C(2)	-98.02(8)
C(13)-P(1)-C(1)-C(2)	150.89(8)
C(6)-C(1)-C(2)-C(3)	-1.11(17)
P(1)-C(1)-C(2)-C(3)	-178.19(10)
C(1)-C(2)-C(3)-C(4)	-0.4(2)
C(2)-C(3)-C(4)-C(5)	1.4(2)
C(3)-C(4)-C(5)-C(6)	-0.9(2)
C(4)-C(5)-C(6)-C(1)	-0.57(18)
C(2)-C(1)-C(6)-C(5)	1.58(16)
P(1)-C(1)-C(6)-C(5)	178.44(9)
O(1)-P(1)-C(7)-C(8)	-118.30(8)
C(13)-P(1)-C(7)-C(8)	116.99(9)
C(1)-P(1)-C(7)-C(8)	4.02(10)
O(1)-P(1)-C(7)-C(12)	57.12(8)
C(13)-P(1)-C(7)-C(12)	-67.60(8)
C(1)-P(1)-C(7)-C(12)	179.43(8)
C(12)-C(7)-C(8)-C(9)	-1.57(15)
P(1)-C(7)-C(8)-C(9)	173.65(9)
C(7)-C(8)-C(9)-C(10)	-1.24(18)
C(8)-C(9)-C(10)-C(11)	2.7(2)
C(9)-C(10)-C(11)-C(12)	-1.4(2)
C(10)-C(11)-C(12)-C(7)	-1.40(18)
C(8)-C(7)-C(12)-C(11)	2.89(15)
P(1)-C(7)-C(12)-C(11)	-172.75(9)
O(1)-P(1)-C(13)-C(18)	20.70(9)
C(7)-P(1)-C(13)-C(18)	142.45(7)
C(1)-P(1)-C(13)-C(18)	-103.35(7)
O(1)-P(1)-C(13)-C(14)	-156.19(8)
C(7)-P(1)-C(13)-C(14)	-34.44(8)
C(1)-P(1)-C(13)-C(14)	79.76(8)
C(18)-C(13)-C(14)-C(15)	2.64(15)
P(1)-C(13)-C(14)-C(15)	179.55(8)

Appendix: NMR spectra and X-ray structures

---

C(13)-C(14)-C(15)-C(16)	-2.45(16)
C(14)-C(15)-C(16)-C(17)	-0.37(16)
C(19)-O(2)-C(17)-C(16)	19.00(13)
C(19)-O(2)-C(17)-C(18)	-160.56(8)
C(15)-C(16)-C(17)-O(2)	-176.49(9)
C(15)-C(16)-C(17)-C(18)	3.05(14)
C(14)-C(13)-C(18)-C(17)	-0.01(13)
P(1)-C(13)-C(18)-C(17)	-176.85(7)
C(14)-C(13)-C(18)-C(18)#1	179.58(8)
P(1)-C(13)-C(18)-C(18)#1	2.73(11)
O(2)-C(17)-C(18)-C(13)	176.74(8)
C(16)-C(17)-C(18)-C(13)	-2.84(13)
O(2)-C(17)-C(18)-C(18)#1	-2.86(11)
C(16)-C(17)-C(18)-C(18)#1	177.56(8)
C(20)-O(3)-C(19)-O(2)	-66.37(12)
C(17)-O(2)-C(19)-O(3)	-78.72(12)

---

Symmetry transformations used to generate equivalent atoms:

#1 -x+1/2,-y+1/2,z

## ABBREVIATIONS

Ac - Acetyl

acac - Acetylacetonato

AcOEt - Ethyl acetate

APIs - Active Pharmaceutical Ingredients

BINAP - 2,2'-Bis(diphenylphosphino)-1,1'-binaphthyl

BINAPHOS - (2-(Diphenylphosphino)-1,1'-binaphthalen-2'-yl)-(1,1'-binaphthalen-2,2'-yl)phosphite

BINOL - 1,1'-Binaphthyl-2,2'-diol

BIPHEMP - (6,6'-Dimethylbiphenyl-2,2'-diyl)bis(diphenylphosphine)

MeO-BIPHEP - (6,6'-Dimethoxybiphenyl-2,2'-diyl)bis(diphenylphosphine)

BIPNITE - (2'-(Diphenylphosphino)-1,1'-binaphthyl-2-yl)oxydiphenylphosphine

BIPPPOS - 2'-(Diphenylphosphino)-1,1'-binaphthyl-2-yl diphenyl phosphite

Bn - Benzyl

Boc - (*tert*-butoxy)carbonyl

BPE - 1,2-bis(2,5-Dialkylphospholan-1-yl)ethane

Bz - Benzoyl

Bzh - Benzhydryl

Cbz - Benzyloxycarbonyl

Cod - 1,5-Cyclooctadiene

Conv - Conversion

DABCO - 1,4-Diazabicyclo[2.2.2]octane

DBTA - 2,3-*O,O*-Dibenzoyl tartaric acid

DBU - 1,8-Diazabicyclo[5.4.0]undec-7-ene

DCM - Dichloromethane

DIOP - (2,2-Dimethyl-1,3-dioxolane-4,5-diyl)-bis-(methylene)-bis-(diphenylphosphine)

DIPAMP - 1,2-Bis((2-methoxyphenyl)(phenyl)phosphino)ethane

DMAP - 4-(*N,N*-Dimethylamino)pyridine  
DME – 1,2-Dimethoxyethane  
DMF - Dimethylformamide  
DMS - Dimethylsulfane  
DUPHOS - 1,2-Bis(2,5-dialkylphospholan-1-yl)benzene  
ESI - Electrospray Ionization  
ee- Enantiomeric excess  
FID - Flame Ionization Detector  
Fmoc - 9-Fluorenylmethoxycarbonyl  
GC- Gas Chromatography  
HPLC - High Performance Liquid Chromatography  
IR - Infrared  
JOSIPHOS - 1-[2-(diphenylphosphino)ferrocenyl]ethylcyclohexylphosphine  
L - Ligand  
LDA - Lithium diisopropylamide  
L-DOPA - (*S*)-2-acetamido-3-(4-acetoxy-3-methoxyphenyl)propanoic acid  
MAA - Methyl (*N*)-acetylaminoacrylate  
MOM - Methoxymethyl  
nbd - Norbornadiene  
*n*-BuLi - *n*-Butyllithium  
NMR - Nuclear Magnetic Resonance  
NOESY - Nuclear Overhauser Enhancement Spectroscopy  
ORTEP – Oak Ridge Thermal Ellipsoid Plot Program  
PHOX - Phosphinooxazoline  
Py – Pyridine  
RT – Room Temperature  
SPS - Solvent Purification System  
TADDOL – (2,2-Dimethyl-1,3-dioxolane-4,5-diyl)bis(diphenylmethanol)  
TBS - *tert*-Butyldimethylsilyl



THF - Tetrahydrofurane

TLC - Thin LayerChromatography

TMS - Trimethylsilyl

TMSN<sub>3</sub> - Trimethylsilyl azide

TOF - Turnover Frequency

TON - Turnver Number

Tr – Trityl

t<sub>R</sub> – Retention time

UV - Ultraviolet

WLA - Weak Link Approach

Z-MAC - Methyl (Z)-(N)-acetylaminocinnamate

UNIVERSITAT ROVIRA I VIRGLI

TOWARDS HIGHLY EFFICIENT LIGANDS FOR ASYMMETRIC HYDROGENATIONS: A COVALENT MODULAR APPROACH AND  
INVESTIGATIONS INTO BIOINSPIRED SUPRAMOLECULAR STRATEGIES

Héctor Fernández Pérez

ISBN:978-84-693-3385-3 /DL:T.994-2010